University of Alberta

Library Release Form

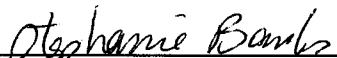**Name of Author:** Stephanie J. Banks

Title of Thesis: Mechanical Characteristics of Kaolin-Cement Mixture

Degree: Master of Science

Year this Degree Granted: 2001

Permission is hereby granted to the University of Alberta Library to reproduce single copies of this thesis and to lend or sell such copies for private, scholarly or scientific research purposes only.

The author reserves all other publication and other rights in association with the copyright in the thesis, and except as herein before provided, neither the thesis nor any substantial portion thereof may be printed or otherwise reproduced in any material form whatever without the author's prior written permission

Stephanie Banks
Stephanie J. Banks
90 Anchor Drive
Halifax, Nova Scotia
B3N 3E1

Date: _August 24, 2001_

University of Alberta

Mechanical Characteristics of Kaolin-Cement Mixture

by

Stephanie J. Banks

A thesis submitted to the Faculty of Graduate Studies and Research in partial
fulfillment of the requirements for the degree of Master of Science

in

Geotechnical Engineering

Civil and Environmental Engineering Department
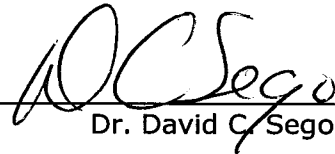
Edmonton, Alberta

Fall 2001

University of Alberta

Faculty of Graduate Studies and Research

The undersigned certify that they have read, and recommend to the Faculty of Graduate Studies and Research for acceptance, a thesis entitled "Mechanical characteristics of kaolin-cement mixture" submitted by Stephanie J. Banks in partial fulfillment of the requirements for the degree of Master of Science in Geotechnical Engineering.
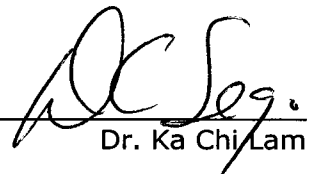
Dr. Dave H. Chan (Supervisor)

Dr. David C. Sego

Dr. Chong-Qing Ru

Dr. Ka Chi Lam

Date:_____24 / 08 / 2001_____

ABSTRACT

An extensive laboratory program was carried out to determine the mechanical characteristics of kaolin-cement, with some brief examination of the effects of curing environment. SEM analysis was also conducted. A proposed constitutive elastic-plastic model was tested.

Cement contents up to 10 percent were considered and water curing was employed. Results show that while cement increases strength, it also reduces axial strain required to achieve failure at low confining pressures under drained conditions. Furthermore, when the cement content is 5 percent or less, kaolin-cement may not improve after 28 to 56 days of curing; this may be due to softening during curing.

Addition of cement increases the degree of flocculation of the clay particles; this is associated with an increase in pH of the pore water.

More research is recommended in the area of soil-cement when water curing is employed, particularly with regards to the effect of age and cement content.

ACKNOWLEDGEMENTS

TABLE OF CONTENTS

APPENDICES

LIST OF TABLES

LIST OF FIGURES

LIST OF SYMBOLS AND TERMS

a'	t-intercept, from which effective cohesion is derived (kPa)
$\bar{A}$	overall pore pressure coefficient, $\dfrac{\Delta u}{(\sigma_1 - \sigma_3)}$
A_c	cement content, calculated as the dry mass of cement divided by the dry mass of soil (%)
A_C	sample area after consolidation, $A_o\left(1 - \dfrac{2}{3}\dfrac{\varepsilon_{vC}}{100}\right)$ (mm^2)
A_o	original area of sample (mm^2)
$\bar{B}$	overall pore pressure coefficient, $\left(\dfrac{\Delta u}{\Delta \sigma_1}\right)$
c	cohesion (kPa)
c'	effective cohesion (kPa)
c'_{peak}	effective cohesion at peak stress conditions (kPa)
c'_{fs}	effective cohesion at fully-softened stress conditions (kPa)
c_v	coefficient of consolidation for one-dimensional consolidation (m^2/year)
c_{vi}	coefficient of consolidation for isotropic consolidation (m^2/year)
C_C	compression index (slope of virgin compression curve)
C_s	swelling index (slope of consolidation rebound curve)
D_C	sample diameter after consolidation, $\sqrt{4A_C/\pi}$ (mm)
e	exponential function basis of natural logarithm
e	void ratio
e_C	void ratio of sample after consolidation
e_o	initial void ratio of sample prior to consolidation
e_1	void ratio at the beginning of consolidation stage
e_2	void ratio at the end of consolidation stage
δe	change in void ratio during stage of consolidation, $(e_1 - e_2)$
E_c	compressive modulus (MPa)
E_f	flexural modulus (MPa)
f	yield locus
f_b	modulus of rupture (kPa)
g	plastic potential

G_s	specific gravity
H_C	height of sample after consolidation, $H_o\left(1-\dfrac{1}{3}\dfrac{\Delta V}{V_o}\right)$ (mm)
H_o	initial height of sample prior to consolidation (mm)
$\overline{H}$	mean height (mm)
k_p	control parameter that describes bond degradation ratio between soil particles
L_C	height of sample after consolidation, $L_o\left(1-\dfrac{1}{3}\dfrac{\varepsilon_{vC}}{100}\right)$ (mm)
m	bonding stress ratio
m_v	coefficient of volume compressibility for one-dimensional consolidation (m^2/MN)
m_{vi}	coefficient of volume compressibility for isotropic consolidation (m^2/MN)
M	maturity (days, ^oC)
M	magnification
p	mean normal stress, $\left(\dfrac{\sigma_1+2\sigma_3}{3}\right)$ (kPa) (Cambridge stress field)
p'	effective mean normal stress, $\left(\dfrac{\sigma'_1+2\sigma'_3}{3}\right)$ (kPa)
p_c'	midpoint of yield locus along the mean normal effective stress axis p' (kPa)
p_C	consolidation yield stress (kPa)
p_C'	effective consolidation pressure (kPa)
p_{cs}'	effective mean normal stress at critical state (kPa)
p_o'	effective confining pressure (kPa)
p_1'	effective stress at beginning of consolidation stage (kPa)
p_2'	effective stress at end of consolidation stage (kPa)
$\delta p'$	effective stress increment during stage of isotropic consolidation, $(p_1'-p_2')$ (kPa)
P	axial force (N)
q	deviator stress, $(\sigma_1-\sigma_3)$ (kPa) (Cambridge stress field)
q'	effective deviator stress, $(\sigma'_1-\sigma'_3)$ (kPa)
q_{cs}	deviator stress at critical state conditions (kPa)

q_{fs}	deviator stress at fully-softened stress conditions (kPa)
q_{max}	maximum deviator stress (kPa)
q_u	unconfined compressive strength (kPa)
s	mean normal stress, $\left(\dfrac{\sigma_1+\sigma_3}{2}\right)$ (kPa) (MIT stress field)
s'	effective normal stress, $\left(\dfrac{\sigma'_1+\sigma'_3}{2}\right)$ (kPa)
S	degree of saturation (%)
S_T	split tensile strength (kPa)
t	deviator stress, $\left(\dfrac{\sigma_1-\sigma_3}{2}\right)$ (kPa) (MIT stress field)
t	curing temperature (°C)
t'	effective deviator stress, $\left(\dfrac{\sigma'_1-\sigma'_3}{2}\right)$ (kPa)
t_{50}	time to reach 50% consolidation, as determined from volume change vs. log time consolidation curves (min)
t_{90}	time to reach 90% consolidation, as determined from volume change vs. root time consolidation curves (min)
t_{100}	time to reach 100% consolidation, as determined from volume change vs. root time consolidation curves (min)
T_c	curing time (days)
u	pore pressure (kPa)
u_e	excess pore pressure (kPa)
V_C	volume of specimen after consolidation, $V_o - \Delta V_C$ (cm^3)
V_o	original volume of specimen prior to consolidation (cm^3)
ΔV	change in volume during shear (cm^3)
ΔV_C	change in volume during consolidation, which is cumulative in the case of isotropic consolidation tests (cm^3)
w	moisture content of kaolin prior to addition of dry cement (%)
w_c	moisture content of kaolin-cement after curing (%)
w_L	liquid limit (%)
w_P	plastic limit (%)
α'	angle of t-s' envelope, from which the effective friction angle is derived (°)

ε_a	axial strain (%)
ε_q	triaxial shear strain
ε_p^q	total plastic shear strain
ε_v	volumetric strain (%)
ε_{vC}	volumetric strain during consolidation, $\dfrac{\Delta V_C}{V_o}\times 100\%$ (%)
ε_{vf}	volumetric strain at failure (%)
Γ	intercept of critical state line in (υ-ln p') plane
η	stress ratio, q/p'
η_{cs}	stress ratio at critical state conditions
η_{max}	maximum stress ratio
ϕ	angle of internal friction (°)
ϕ'	effective angle of internal friction (°)
ϕ'_{cs}	effective angle of internal friction at critical state conditions (°)
ϕ'_{fs}	effective angle of internal friction at fully-softened stress conditions (°)
ϕ'_{peak}	effective angle of internal friction at peak stress conditions (°)
κ	gradient of swelling line in the (e, ln p') plot
λ	a dimensionless coefficient used to calculate c_{vi} for triaxial tests, the value of which depends on drainage conditions
λ	gradient of normal consolidation line in (e, ln p') space
λ'	gradient of normal consolidation line in (e, ln p') space, which changes with p'; determined through regression of the ICL
λ_c	slope of critical state line
μ	Poisson ratio
M	slope of critical state line in (q, p') space
N	specific volume of an isotropic normally consolidated soil at $p'=1.0$ kPa; intercept of isotropic consolidation line in (υ, ln p') plane
N_o	specific volume of a one-dimensional normally consolidated soil at $p'=1.0$ kPa
υ	specific volume (1+e)
υ_{cs}	specific volume at critical state
υ_κ	specific volume of an isotropically over-consolidated soil at $p'=1.0$ kPa

υ_{ko}	specific volume of a one-dimensionally over-consolidated soil at $p'=1.0$ kPa
ρ_b	bulk density (g/cm^3)
ρ_d	dry density (g/cm^3)
σ	normal stress (kPa)
σ'	normal effective stress, σ-u (kPa)
σ_1, σ_3	principal stresses (kPa)
σ_1', σ_3'	principal effective stresses (kPa)
$\Delta\sigma'$	change in effective stress during consolidation, which is the equivalent to the change in pore pressure during consolidation, since total stress remains constant (kPa)

CDM	cement deep mixing
CID	consolidated isotropic drained triaxial test
CIU	consolidated isotropic undrained triaxial test
CSL	critical state line
DJM	dry jet mixing
DLM	deep lime mixing
DM	deep mixing
DRE	dry-rotary-end
IC	isotropic consolidation
ICL	isotropic compression (consolidation) line
NCL	normal compression (consolidation) line
LCM	lime column method
OCR	over-consolidation ratio
OED	oedometer
PI	plasticity index
SEM	Scanning Electron Microscope
SLC	Swedish Lime Column
UC	unconfined compression
URL	unloading reloading line
VOC	volatile organic compounds

1. INTRODUCTION

1.1 Project Background

With continuous development of urban and metropolitan centres and decreasing availability of suitable land for development, ground improvement is becoming an extremely popular and necessary industry worldwide. The cost of land in highly populated areas has risen dramatically in recent years in many countries, making sites with poor soil conditions attractive for development (Porbaha, 1998) due to their comparatively reduced purchase value and the effective and economic ground improvement techniques now available.

Development on soft clay deposits, typical of marine and coastal environments, is necessary to sustain a healthy economy associated with expanding ports and harbours. These developments are particularly rapid in Southeast Asia, where the strengthening economy is directly linked to the export of products via the major port cities and especially high and dense populations require that land use be efficient. Soft clay is highly compressible, therefore, where deposits are thick, construction on soft clay can only take place by installing costly deep foundations or by altering the in situ soil conditions to improve the bearing capacity and reduce the compressibility of the unfavourable foundation material. Often deep foundations made of piles or drilled piers are uneconomical, making ground improvement via the Deep Mixing (DM) method one of the most viable options currently available for improvement of soft and deep clay deposits.

In general terms, the Deep Mixing method is the process of mixing lime or cement with soft soils to allow deep stabilization of soft deposits by improving the soil properties (Bergado *et al.*, 1996). This technology has been used for several decades, with extensive research on modern applications starting in Japan in the late 1970s. The Deep Mixing method was originally developed to stabilize foundations related to near shore marine structures, but is now commonly used to improve foundations below structures on land such as embankments, buildings and storage tanks.

There are many Deep Mixing methods available to improve the stability of soft clay so that it is suitable for development. Type of stabiliser

and machinery can vary depending on the soil type, desired improvements and local experience and practice. One relatively new method mixes dry cement in situ with the wet clay, forming deep columns of stable clay-cement mixture. With the proper design and implementation of the method, the cured mixture can be a suitable foundation for any size structure. This dry mixing method has many advantages over the more traditional method, whereby the cement is added as a wet slurry, as it does not displace the in situ material and can be used for particularly soft deposits with a high moisture content.

This ground improvement technique of cement stabilization via DM with dry cement is gaining popularity, particularly in Japan and other parts of Southeast Asia and in Scandinavia. However, the strength/deformation behaviour and resulting soil structure of the clay-cement mixture is presently not well understood; this is with respect to both dry mix and wet mix methods.

1.2   Objective of Current Research

Currently, empirical formulas relating in situ moisture content with desired bearing capacity, settlement tolerances and cement requirements are being used in applications of DM methods. However, these relationships are generally conservative and do not accurately predict the long term behaviour of the clay-cement mixture. Furthermore, often the unconfined compressive strength is the strength value used for design purposes as it can easily be obtained in the laboratory and allows for quick confirmation of the in situ strength of the improved soil (Kohata *et al.*, 1997). Various reduction factors are applied in design so that the quality of stabilized material in the field as compared with that of ideal laboratory samples is considered. The unconfined compression test, however, does not consider the undrained behaviour nor the effect of confining pressure, which have both been shown to greatly affect the mechanical behaviour. Furthermore, the unconfined compressive behaviour is typically brittle and tests yield negligible residual strength (Tatsuoka and Kobayashi, 1983) so that design based only on results of

unconfined compression tests may be extremely conservative (and therefore expensive).

Little work prior to 1995 has been done to research the behaviour of clay-cement beyond the unconfined compressive strength. Of the recent published studies reviewed where more elaborate laboratory programs were employed, it was found that most triaxial tests were performed on samples cured for 1 month or less whereby the cement was mixed as a wet slurry. Furthermore, sample preparation and curing methods were often vaguely reported, making it difficult to assess the relevancy of the results to field applications.

The scope of the current project, reported herein, is to collect high-quality laboratory results from a series of undrained and drained isotropically consolidated triaxial compression tests, unconfined compression tests and oedometer and isotropic consolidation tests. The laboratory tests were conducted on samples with moisture contents of 70 and 100 percent, cement contents of 2, 5 and 10 percent and curing periods of 7, 28, 56 and 112 days. Confining pressures for triaxial tests were 50, 100 and 400 kPa. All laboratory tests were conduced at the City University of Hong Kong between June 2000 and July 2001. A lot of effort was spent in establishing a procedure for preparation of high-quality samples. The goal was to produce homogeneous samples with minimum air voids, and to produce a group of samples for each mix type having the same physical properties.

A constitutive elastic-plastic stress-strain model is being developed at the University of Alberta to more accurately predict the long-term behaviour of clay-cement in a critical state framework. From the laboratory data, the critical state parameters have been derived, as well as parameters for the constitutive elastic-plastic stress-strain model. Using the derived parameters, the proposed constitutive model was tested to confirm it's accuracy and reliability.

Images captured using a Scanning Electron Microscope (SEM) have been analysed to increase the understanding of how the structure of the clay-cement mixture contributes to its strength/deformation characteristics. The effects of age, moisture content and cement content on the structure of the soil were considered.

This research lays the framework for future study in this area which may include laboratory tests on a wider variety of soil types with more combinations of moisture contents and cement contents, as well as field tests. In particular, laboratory tests on samples with greater cement contents and at higher confining pressures are recommended.

2. DEEP MIXING METHODS AND DRY MIXING METHODS

2.1 Deep Mixing Methods

Based on available literature, it is clear that the majority of research in the area of soil improvement through DM methods over the last 10 to 15 years has taken place in Japan and Scandinavia, where the technology is most popular. Unfortunately, literature on DM technology and research has been mostly published in the form of technical reports of research institutes and therefore, it is not widely accessible and furthermore, articles are not often published in English (Porbaha, 1998). Fortunately, some authors (i.e. Porbaha, 1998; Kohata *et al.,* 1997; Babasaki *et al.,* 1997) have attempted in recent years to review and summarize literature that may be difficult to access and/or may not published in English.

In 1996, the Second International Conference on Ground Improvement Geosystems, focusing on grouting and deep mixing, took place in Tokyo. In 1999, an International Conference on Dry Mix Methods took place in Stockholm. The proceedings from these conferences provide much of the information summarized here and referred to in future chapters.

2.1.1 Description

Deep Mixing (DM) is a soil modification technique used to improve deep deposits of soft soil. In this context, the term "soft soil" refers to soil that is cohesive with a high moisture content, or soil that is fine, granular, saturated and in a loose state (Porbaha, 1998).

Masses of stabilized soil, in the shape of columns, walls, grids or blocks are formed by DM (Fig. 2.1) (Kamon, 1997). The method mixes a reagent, which can be either cementitious (i.e. cement, lime, fly ash, etc.), chemical or biological, in the form of a wet slurry or dry powder, with the soft in situ material. Mixing is done using hollow, rotating shafts with cutting tools, mixing paddles and/or augers attached to penetrate to varying distances beyond the tip of the shaft (Fig. 2.2) (Bruce *et al.,* 1998). The soil is penetrated to the desired depth and mixing is normally done mechanically during withdrawal of the tool (Fig. 2.3).

WALL TYPE   GRID TYPE   BLOCK TYPE   AREA TYPE
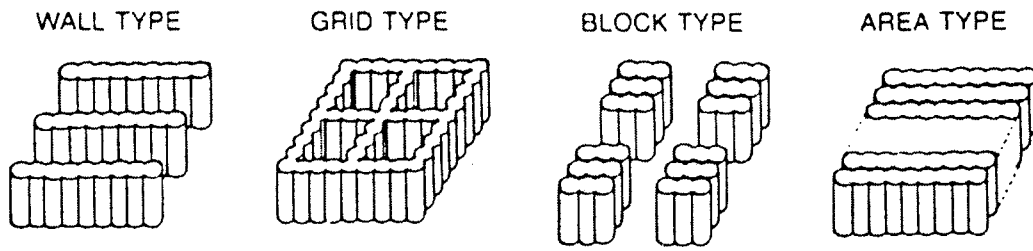
Figure 2.1. Basic soil improvement patterns using DM (Yang and Takeshima, 1994).
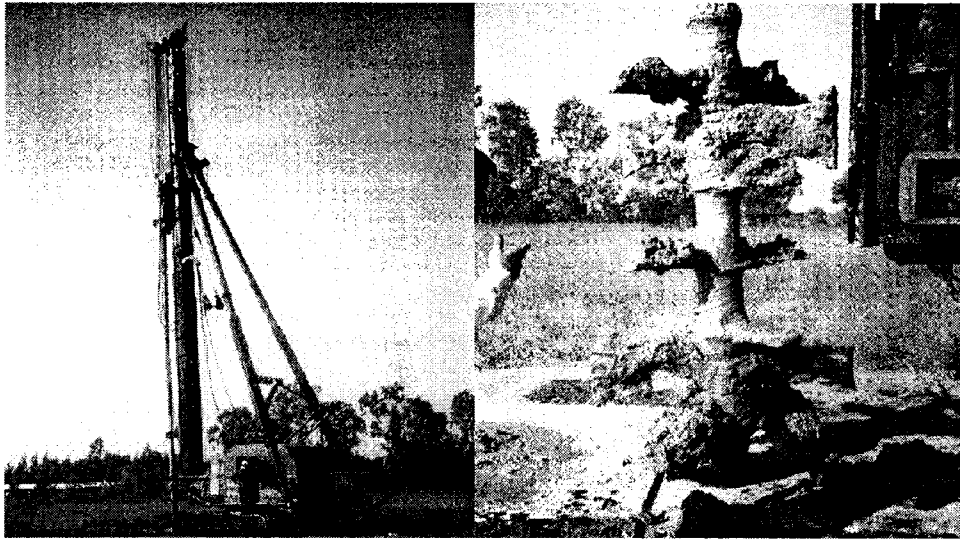
Figure 2.2. Installation of cement piles using DM method (Bergado *et al.*, 1996).

(a) slurry state   (b) dry powder state
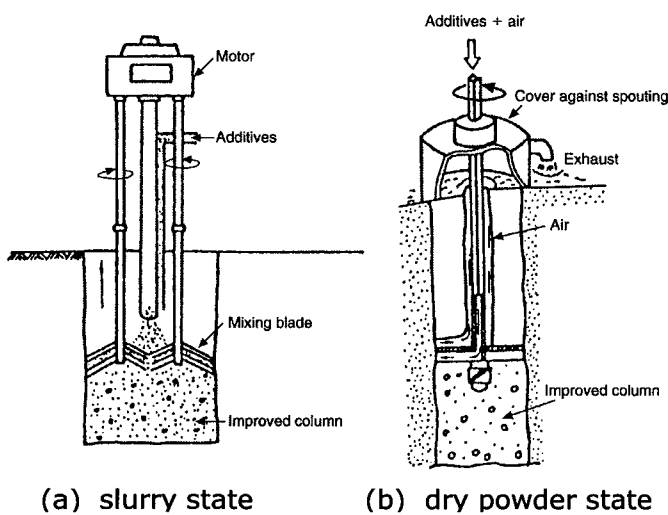
Figure 2.3. Mechanical mixing methods for DM (Porbaha, 1998)

The types of improvements achieved by DM can be classified into three general categories (Kamon, 1997).

1) *Mechanical properties*: These include increased bearing capacity, prevention of deformation, reduction of earth pressure and improvement of slope stability.

2) *Liquefaction and hydrological properties*: Prevention of liquefaction and erosion caused by drainage and running water fall into this category.

3) *Environmental properties*: Included here are environmental preservation and waste management.

A more elaborate summary of DM applications is provided in Figure 2.4.
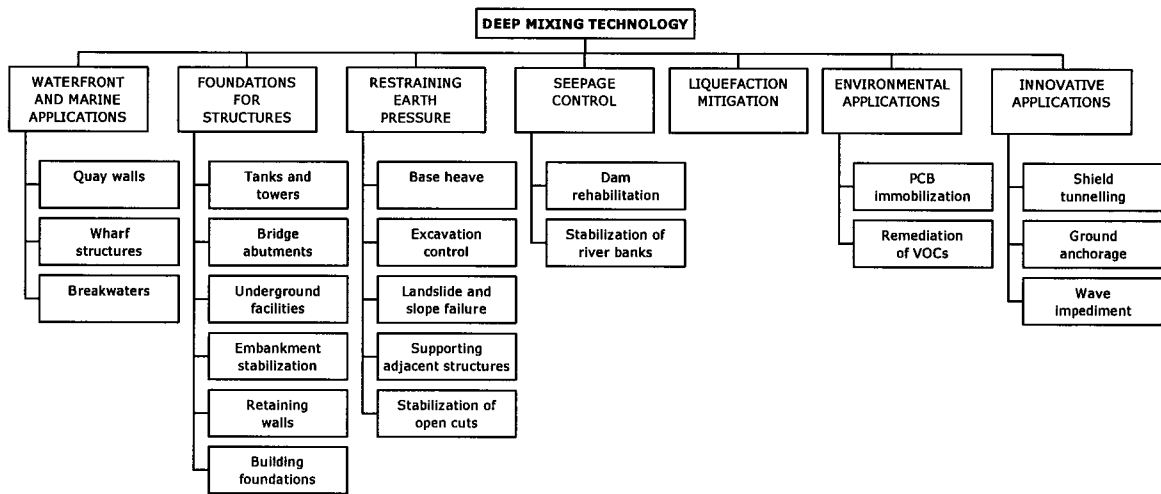
Figure 2.4. Flowchart of various applications of Deep Mixing (DM) technology (Porbaha *et al.*, 1998).

There are several systems used to classify DM methods; ECO Geosystem Inc. devised one of the more useful and popular classification systems to identify and distinguish between the different DM methods (Holm, 1999). According to this system, there are 24 unique DM methods, classified based on the state of binder (wet vs. dry), the penetration/mixing method (rotary vs. jet) and the location of mixing action (shaft vs. end). For example, DRE describes the DM method that uses a dry binder and a rotary

mixing method at the end of the shaft. Other classification systems are based on the geometry of the treated mass, construction technique and type of stabilizing agent (Porbaha, 1998).

2.1.2 History

Deep Mixing methods were originally developed to improve the conditions of soft ground for construction of port and harbour developments (Bergado *et al.*, 1996). Bruce *et al.* (1998) report that the original idea of DM was developed in the United States in 1954 but that the techniques for DM were developed in Japan and Scandinavia in the 1970s. The general consensus in literature is that Japan has lead the way in development of DM technology since the 1960s (Porbaha, 1998). Okumura (1997) states that in Japan, the Deep Lime Mixing (DLM) method was developed in the 1960s and brought into practice in 1974. Deep Lime Mixing is considered to be a dry mix method as the lime is mixed in a dry granular state. In 1975, the practical use of slurry mix methods was developed; the first method developed was called Cement Deep Mixing (CDM). Between 1977 and 1993, approximately 23.6 million m^3 of soil was stabilized by DM methods in Japan; this includes both land and sea projects (Porbaha, 1998). Roughly 300 DM projects per year have been recently carried out in Japan. China began formal research in the area of DM technology in the late 1970s; the total amount of soil treated by DM in China is over 1 million m^3.

Sweden and Finland have also been investing heavily in research and development of DM methods since the late 1960s. In 1967, the Swedish Lime Column (SLC) method was developed by the Swedish Geotechnical Institute.

Even as DM methods became popular and widely accepted in Southeast Asia and Scandinavia through the 1970s and 1980s, the United States was hesitant to continue extensive research and development of DM methods as they felt it was not a cost-effective technology (Porbaha, 1998). However, after success in Southeast Asia and Scandinavia, DM methods were introduced in the United States in 1986 and have been used primarily in New England (Boston and New York), the Salt Lake City area and in California. The first application in the United States was to protect a structure from soil liquefaction during earthquakes. The largest DM project in the United States

took place in Boston, MA and involved 600,000 m³ of stabilized soil (Bruce *et al.*, 1999).

In 1996, the Second International Conference on Ground Improvement Geosystems was held in Tokyo, with its focus on grouting and deep mixing. This was the first opportunity for experts from around the world to congregate and present the state-of-the-art technology currently being researched and applied internationally. The event was attended by many American representatives who have since made great progress with bringing techniques developed in Japan and Scandinavia to North America. There has been much research and subsequent publications on the topic of DM methods, particularly in the United States, who was initially reluctant to implement DM methods.

2.1.3 Empirical Design

The most important properties necessary for design of stabilized ground are strength (compressive, shear and tensile), modulus, permeability, compressibility and dynamically measured properties such as shear modulus and damping at different strain levels (Porbaha *et al.*, 2000). Generally, empirical formulas are used in the design of DM based on the unconfined compressive strength, q_u. Some typical empirical formulas are provided below (Mitchell, 1981):

cohesion:	$c = 60 + 0.29\, q_u$	(2.1)
angle of internal friction:	$25° < \varphi < 35°$	(2.2)
compressive modulus:	$E_c = 70 + 0.124\, q_u$	(2.3)
	(MPa, at 100 kPa confining pressure)	
flexural modulus:	$E_f = 4.6\, f_b - 950$ (MPa)	(2.4)
modulus of rupture:	$f_b \approx 0.25\, q_u$ (kPa)	(2.5)
split tensile strength:	$S_T \approx 0.13\, q_u$ (kPa)	(2.6)
Poisson's ratio:	$\mu \approx 0.1$	(2.7)

Mitchell *et al.* (1974) also proposed a formula to calculate the unknown unconfined compressive strength at a given curing time based on

the known unconfined compressive strength (expressed in kPa) at T_o (expressed in days) and cement content, A_c.

$$q_u (T_c) = q_u (T_o) + K \log (T_c/T_o) \qquad (2.8)$$

Where $q_u (T_c)$ = unconfined compressive strength after T_c days of curing (kPa)

$q_u (T_o)$ = unconfined compressive strength after T_o days of curing (kPa)

$K = 480\ A_c$ (for granular soils)

$K = 70\ A_c$ (for fine-grained soils)

This relationship implies a linear increase in unconfined compressive strength with cement content, which was later found by Tatsuoka and Kabayashi (1983) to be untrue.

The unconfined compressive strength can also be expressed as a function of the soil type, sample maturity (M), curing time (T_c), and curing temperature (t). The following expression was suggested by Babasaki *et al.* (1997).

$$q_u = A \log M + B \qquad (2.9)$$

Where A and B are functions of the soil type and M is the maturity which is defined by the following formula.

$$M = \int_0^{T_c} 2 \cdot \exp\left(\frac{t+10}{10}\right) dT_c \qquad (2.10)$$

There also exist functions to relate the unconfined compressive strength in the lab to that in the field (i.e. Babasaki *et al.*, 1997).

Kézdi (1979) provides guidelines, including various tables and charts, which may be used to design soil-cement mixtures for road stabilization applications. The proposed design is primarily based on grain size distribution and maximum density of the soil to be improved. Kézdi recommends that 10 to 14 percent cement is suitable for stabilization of clay; this is greater than

that suggested for silty or sandy soils. Furthermore, the finer the soil being stabilized, the less suitable the soil is as a sub-grade below pavement.

2.1.4 Environmental Impacts of DM

Soil mixing has found increased use for remediation of contaminated soils and sludges. Treating ground through DM allows contaminated sites to be closed safely and/or developed (Kamon, 1997). Excavation, shoring and dewatering are not required with DM and therefore, remediation costs are greatly reduced when DM is applied and the exposure of waste to the surface environment is reduced. Furthermore, heat induced by the reaction of quicklime powder in clay deposits can actually cause volatile organic compounds (VOCs) to evaporate and be safely and easily removed (Fig. 2.5).

While DM has numerous positive environmental impacts, there also exist several important negative environmental impacts when DM is used. Cement and lime stabilizers may cause leaching of alkaline into the groundwater (Kamon, 1997). Clay, fortunately, has a natural buffering capacity allowing toxic leachate to be absorbed and neutralized. Sands, however, have a comparatively low alkaline restraint ability. Therefore, sandy soils stabilized with cement or lime should not come into direct contact with the groundwater.

Another more serious problem is groundwater contamination due to migration of grouting chemicals (Kamon, 1997). In Japan, strict guidelines were put in place after some accidents occurred whereby humans were exposed to contaminated drinking water. Use of grouts such as clay, cement and waterglass is the current practice in Japan.
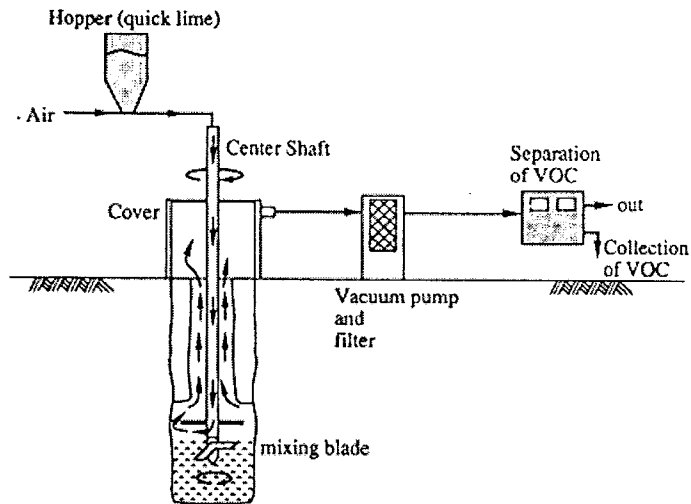
Figure 2.5. Remediation of VOCs by DM (Kamon, 1997).

2.2 Dry Deep Mixing Methods

2.2.1 Description

Dry DM methods mix the stabilizing binder as a dry powder with the in situ material, which typically has a high moisture content. There are three unique dry DM methods; all are classified as DRE (dry-rotary-end) by the ECO Geosystem Inc. (Holm, 1999). The three unique dry DM methods are used in three separate geographic locations, and have essentially been developed independently of one another to meet the specific needs and soil conditions encountered in each region. Lime cement columns are installed in Scandinavia (Nordic countries), Dry Jet Mixing (DJM and the Dry Jet Mixing Association) are present in Japan, and Italy uses a technology they have termed Trevimix.

Similar principles apply to dry DM methods as wet DM methods except the binder is mixed in situ with the soft soil in a dry state using slightly different machinery. Because of this difference, the method is suitable for soils with a high moisture content (above 60 percent) and does not displace any soil creating the need to dispose of spoil. Spoil disposal can be a large economic burden, particularly if the material is contaminated. In fact, with dry DM methods, treatment of contaminated soil is possible in situ;

12   *Mechanical Characteristics of Kaolin-Cement Mixture*

contaminants are immobilized and therefore, excavation disposal is not necessary. Dry DM methods cause little to no heave and therefore, negligible movement of nearby buildings, which is a problem commonly associated with wet mix methods. Furthermore, vibrations and noise associated with construction of DM is almost non-existent for dry DM methods. The DJM Association in Japan believes that an additional advantage of dry DM methods is that the strength gain is faster than that of wet methods, in all soil types.

The choice to add the stabilizer wet (in a slurry) or dry (as a powder) depends on the specific project. Site conditions, soil type, local experience/practice and the nature of the project will determine which method is most appropriate and ultimately selected. In general, wet DM methods are mechanically and logistically simpler, particularly in awkward geographic locations (Bruce et al., 1999). This is primarily due to the more advanced development of wet DM techniques and greater amount of experience and case histories available.

2.2.2 History

In 1967, research began in the form of laboratory tests in Japan on the treatment of soft marine soils using dry lime powder to develop a technique later termed Deep Lime Mixing (DLM) (Bruce et al., 1999). Sweden was also conducting similar research simultaneously to develop what they call the Lime Column Method (LCM). By 1974, DLM was being used commercially in Japan and elsewhere in Southeast Asia and by 1975, LCM was being used commercially in Sweden. In 1976, Japan began research on Dry Jet Mixing (DJM) using dry cement (or quick-lime, which was less common) and began using DJM commercially in 1980 (Bruce et al., 1999). At the same time, the practice of DLM was discontinued in Japan (Okumura, 1997). By 1980, dry mixing methods were also being used in China.

The DJM Association was formed in Japan in the early 1980s (Bruce et al., 1999). Throughout the 1980s, the popularity of dry DM methods increased significantly in both Japan and Scandinavia (Holm, 1999).

In 1996, lime cement columns were installed commercially in the United States for the first time. The application of this dry DM method is mostly for settlement reduction and liquefaction mitigation. Dry DM methods

are being used today throughout many European countries. Currently, still more countries are conducting initial laboratory programs with regards to dry DM methods and it is predicted that dry DM methods will see use in many more countries in the future (Holm, 1999).

In 1999 the International Conference on Dry Mix Methods For Deep Soil Stabilisation was held in Stockholm. The proceedings cover a full range of subjects on this topic, such as applications, properties of binders and stabilized soils, design methods and behaviour of stabilized soils, case histories, predictions and performance, quality control of dry mix methods and equipment for dry DM methods for deep soil stabilization.

2.2.3 Applications of Dry DM Methods

The applications of dry DM methods are many and can be summarized as follows (Holm, 1999).

- *Settlement control.* Rows of single columns can be installed below embankments to reduce settlement.
- *Slope stability.* Single elements are installed beneath the slope crest and overlapping columns forming walls are installed perpendicular to the road alignment under the slope to improve its stability.
- *Improvement of bearing capacity.*
- *Prevention of sliding failure.*
- *Protection of structures located near large excavations.*
- *Vibration reduction.*
- *Mitigation of liquefaction.* A lattice-type structure is installed to reinforce liquefiable soil and reduce pore pressure.
- *Soil remediation.* Contaminants are fixated so that excavation of contaminated material is avoided.

2.2.4 Estimated Market of Dry Mix Methods

Between 1980 and 1996, Japan treated approximately 16 million m^3 of soil using DJM, on 2345 separate projects with an average annual volume of

approximately 2 million m^3 (Bruce *et al.*, 1999). It is estimated that the value of the annual DJM market in Japan is roughly $150 million (US).

Currently, it is estimated that Sweden installs about 4 million lineal metres of LCM per year. An additional 1.5 million lineal metres of LCM are installed in Finland and about 0.5 million lineal metres of LCM in Norway. The total annual market in all of Scandinavia is estimated to be between $45 and $60 million (US). Due to the wide variety of engineering applications as compared with other DM methods, the dry DM method has become the most frequently used DM method for large budget infrastructure projects in Sweden and Finland in the 1990s (Holm, 1999).

In 1999, it was estimated that the annual American market for dry DM methods is approximately $5 million (US); this is roughly 10 percent of the total annual DM market in the United States (Bruce *et al.*, 1999).

2.2.5 Use of Dry Mix Methods in Japan vs. Scandinavia

Dry mixing methods were developed simultaneously in Japan and Sweden in the 1970s (Bergado *et al.*, 1999). Japan uses the Deep Jet Method (DJM), which most commonly mixes cement as the binding agent, and Scandinavia uses the Lime Column Method (LCM). In Sweden, only lime and cement are used as binding agents. In Norway, however, alternative materials such as by-products of the steel industry are being used as binding agents, in addition to the standard lime and cement. Japan tends to not use lime very often because cement is cheaper than lime and unslaked lime is difficult to store in the hot and humid environment that exists in Japan. Furthermore, greater strength can be achieved with cement whereas there is a limit to the strength which can be achieved with lime (Bergado *et al.*, 1996).

The Japanese tend to use large scale equipment for DJM, treating relatively coarser soils to depths over 30 m to achieve an unconfined compressive strength above 0.5 MPa. Dry Jet Mixing (DJM) is typically used for settlement control and slope stability applications under both static and seismic conditions. In Scandinavia, however, the soil improvement problems solved by dry mix methods are less severe than in Japan, so that smaller, lighter equipment can be used and an unconfined compressive strength above 0.2 MPa is rarely required. Typical applications of LCM in Scandinavia are for

settlement control, with an estimated 80 percent being related to road and railway work (Bruce *et al.*, 1999).

In Scandinavia, semi-hard columns are the design of choice for most dry mix projects. This is because they are less brittle than high-strength columns and therefore, are able to interact with the surrounding untreated soft soil. The use of semi-hard columns allows for a cost-effective and competitive ground improvement system (Holm, 1999).

2.2.6 Typical Specifications for Dry Mix Methods

Göran Holm of the Swedish Geotechnical Institute presented a keynote lecture on the Applications of Dry Mix Methods for Deep Soil Stabilization at the Stockholm conference (1999). Holm provides a tidy summary of some typical specifications used in dry DM methods worldwide. Depending on the machinery used, either 1 or 2 shafts are mixed at a time. Each column has a diameter of 0.5 to 1.2 m (typically 0.6 to 1.0 m) and extends to a depth of 18 to 33 m. Common binders include quick lime, quick lime and cement together, standard Portland cement and slag cement. The amount of binder is typically between 80 and 240 kg/m^3 of stabilized soil to achieve an unconfined compressive strength between 100 and 1500 kPa. The area ratio (stabilized area to unstabilized area) ranges from 0.1 to 0.3 in Scandinavia and is typically 0.5 in Japan.

2.2.7 Recent Applications of Dry Mix Methods

New additives, such as blast furnace slag, fly ash, and other waste products are being mixed with cement and/or lime in DM projects as an effective means of waste disposal. Other benefits such as slowing the curing process, thereby lowering the ground temperature during hydration, have been realized through the use of some waste products (Esrig, 1999). Increasing the soil pH by mixing products other than cement and lime in situ increase the degree of flocculation, so that, in some cases, less stabilizer is required to achieve satisfactory ground improvement leading to substantially reduced DM project costs.

A new technique called mass stabilization has been developed recently for the treatment of shallow organic deposits (Holm, 1999). The entire mass of soil is stabilized (as opposed to only treating columns) using a special mixing tool which moves both vertically and horizontally. The maximum depth that can presently be stabilized by mass stabilization is 5 m. The binding material is often quick lime and cement, or cement and blast furnace slag. Typically, between 200 and 400 kg of binder is mixed with 1 m^3 of soil to achieve an unconfined compressive strength between 50 and 100 kPa.

3. PROPERTIES OF SOIL-CEMENT

3.1 Cement as a Soil Stabiliser

Cement, as well as lime and other hardening agents, can be used to stabilize soft soil. The choice not only depends on what material is most readily available, but also on local practice and the desired improved soil conditions to be achieved. Dozens of hardening agents are available on the market; some of the newer additives have been developed for use when moisture or organic contents are particularly high (Babasaki et al., 1997). In some cases, construction conditions require that the rate of improvement be controlled; specific stabilizers are available for this purpose.

Cement may be the most popular soil stabilizer; experience and research has proven its effectiveness over the past decades. When mixed with the pore fluid in soil, the hydration of the cement causes the cement particles to bond with the soil particles, thereby increasing the soil strength and reducing the potential settlement. Hydration also causes the stabilized material to become more brittle. Due to the nature of the curing process of cement, the strength and deformation characteristics of the treated soil are expected to improve over time. The reactions that cause the increase in bond strength can last for months or years following the initial hydration of the cement particles.

3.1.1 Soil-Cement Reactions

Type I Portland Cement is normally the cement of choice in deep mixing ground improvement applications (Bergado et al., 1999). Type I Portland cement is heterogeneous and contains four primary strength-producing compounds (Lea, 1970).

- Tricalcium silicate (C_3S),
- Dicalcium silicate (C_2S),
- Tricalcium aluminate (C_3A), and
- a solid solution called tetracalcium aluminofarrite (C_4AF).

Hydration of the cement occurs quickly once the cement is exposed to water, either from the slurry or the pore water of the soil. The major hydration (primary cementitious) products are hydrated calcium silicates (C_2SH_x, $C_3S_2H_x$) and hydrated calcium aluminates (C_3AH_x, C_4AH_x). Hydrated lime ($Ca(OH)_2$) is also a product of the hydration and is deposited as a separate crystalline solid phase; the dissociation of hydrated lime results in an increase in pH level during hydration of cement. Adjacent cement particles are bonded together by the hydration products to form a hardened skeleton matrix which encloses soil particles which remain unaltered.

The strong basic (high pH) solution caused by the dissociation of hydrated lime dissolves the acidic silica and alumina from the clay minerals and the amorphous materials on the surface of the clay particles; this reaction is similar to that between a strong base and a weak acid. The new solution of dissolved silica and alumina reacts with the calcium liberated by the hydrolysis of cement over time, causing a pozzolanic (secondary) reaction. This reaction produces insoluble compounds, which are the secondary cementitious products. These compounds harden when cured, thereby stabilizing the soil. It is the pozzolanic reaction that causes a gradual increase in shear strength with time (Porbaha *et al.*, 2000).

Following the addition of water, the compounds in Portland cement will transform by the chemical equations below (Bergado *et al.*, 1996).

$$2(3CaO.SiO_2) + 6H_2O = 3CaO.2SiO_2.3H_2O + 3Ca(OH)_2 \qquad (3.1)$$
(tricalcium silicate) (water)   (tobermorite gel) (calcium hydroxide)

$$2(2CaO.SiO_2) + 4H_2O = 3CaO.2SiO_2.3H_2O + Ca(OH)_2 \qquad (3.2)$$
(bicalcium silicate)   (tobermorite gel)   (calcium hydroxide)

$$4CaO.Al_2O_3.FeO_3 + 10H_2O + 2Ca(OH)_2 = 6CaO.Al_2O3.Fe_2O_3.12H_2O \qquad (3.3)$$
(tetracalciumaluminoferite)   (calcium aluminoferrite hydrate)

$$3CaO.Al_2O_3 + 12H_2O + Ca(OH)_2 = 3CaO.Al_2O_3.Ca(OH)_2.12H_2O \qquad (3.4)$$
(tricalcium aluminate)   (tetracalcium aluminate hydrate)

$$3CaO.Al_2O_3 + 10H_2O + CaSO_4.2H_2O = 3CaO.Al_2O_3.Ca(OH)_2.12H_2O \qquad (3.5)$$
(tricalcium aluminate) (gypsum) (calcium monosulfoaluminate)

Equations 3.1 and 3.2 illustrate the hydration of the two calcium types which constitute 75 percent of Portland cement. Of the compounds resulting from these reactions, tobermorite gel governs the bondage, strength and volume change of Portland cement. The most important constituent in Portland cement is tricalcium silicate (C_3S). In soil-cement, the following reactions involving tricalcium silicate take place during stabilisation (Bergado *et al.*, 1996).

$$C_3S \quad + \quad H_2O \quad \rightarrow \quad C_3S_2H_x \quad + \quad Ca(OH)_2 \qquad (3.6)$$
$$\text{(hydrated gel)}$$
$$\text{(primary cementitious products)}$$

$$Ca(OH)_2 \quad \rightarrow \quad Ca^{++} \quad + \quad 2(OH)^- \qquad (3.7)$$

$$Ca^{++} \quad + \quad 2(OH)^- \quad + \quad SiO_2 \quad \rightarrow \quad CSH \qquad (3.8)$$
$$\text{(soil silica)} \quad \text{(secondary cementitious product)}$$

$$Ca^{++} \quad + \quad 2(OH)^- \quad + \quad Al_2O_3 \quad \rightarrow \quad CAH \qquad (3.9)$$
$$\text{(soil alumina)} \quad \text{(secondary cementitious product)}$$
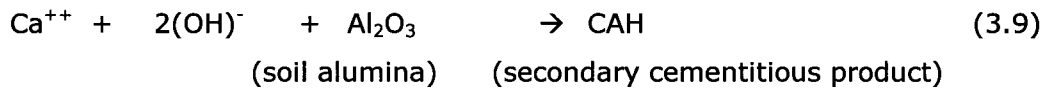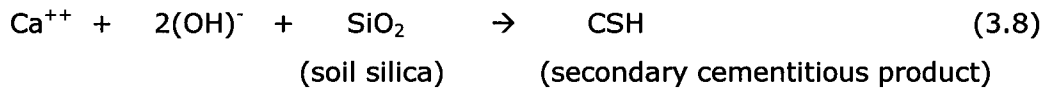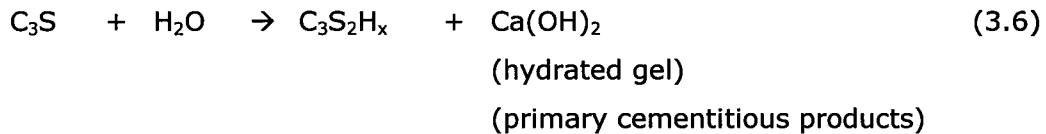
when pH>12.6, the following reaction occurs:

$$C_3S_2H_x \quad \rightarrow \quad C_2S_2H_x \quad + \quad Ca(OH)_2 \qquad (3.10)$$
$$\text{(hydrated gel)}$$
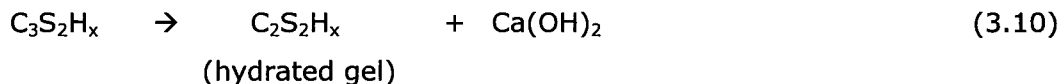
In soil-cement containing clay particles, both primary and secondary cementitious products are formed. The strength gained during the primary reaction is far more than that gained during the secondary reaction. The hardening of the primary products allow them to become high-strength additives in the soil and therefore, differ from those produced during hydration of normal cement in concrete. The hardening of the secondary products increases the strength and durability of the soil-cement as additional

cementing substances are produced and the bond strength between particles is improved.

Kézdi (1979) conducted experiments to help understand the interaction between clay and cement in clay-cement. Due to the relatively large size of cement particles relative to clay particles, it is suspected that upon mixing, the cement will form a skeleton and the clay a matrix. Within each cement skeleton, layers of modified clay are added to a core of hydrated cement gel. As hydration of the cement proceeds, so does the pozzolanic reaction which leads to cementation and the formation of bonds between adjacent clay particles. Aggregates form around the cement grains and modified clay fills the voids between individual particles. This description leads to the conclusion that the new structure is a function of the grain size of the bonded material and hence, the specific surface. Kézdi (1979) states that the larger the specific surface of the stabilized soil, the more cement is required to achieve the desired increase in strength of the original soil. This means that clay, for example, requires more cement than sand, due to its comparatively larger specific surface.

Figure 3.1 illustrates schematically the structure of cement-improved cohesive soil. In Figure 3.1a, the condition of the soil immediately following addition of a cement is shown. It can be seen that the clay particles form clusters, which are surrounded by cement, even when the soil and cement are mixed thoroughly. After curing, a hardened body is formed (Fig. 3.1b) by the pozzolanic reaction between the clay and the hydrated lime ($Ca(OH)_2$) produced by cement hydration.

(a) [ ] Cement Slurry
     [ ] Cluster of Clay Particles

(b) [ ] Hardened Cement Bodies
     [ ] Hardened Soil Bodies
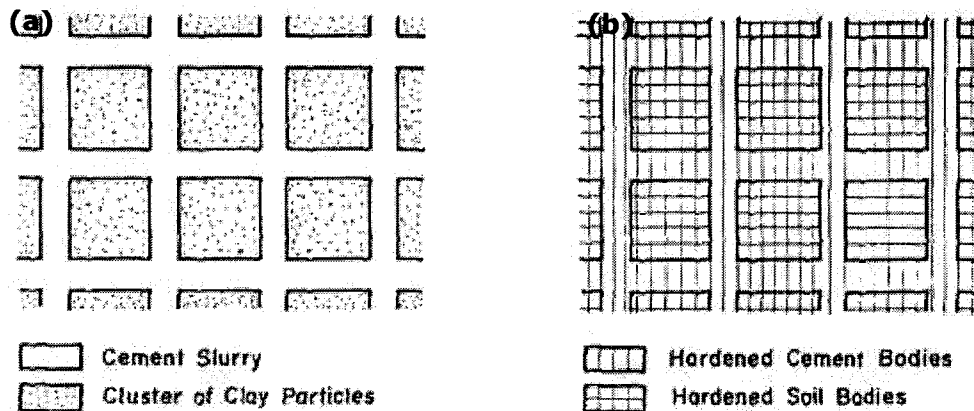
Figure 3.1. Schematic illustrations of improved soil (a) immediately after mixing; (b) after hardening. (Saitoh *et al.*, 1985 from Bergado *et al.*, 1996)

3.1.2 Factors Contributing to the Strengthening Characteristics of Cement in Clay-Cement

Bergado *et al.* (1996) described seven factors that control the hardening characteristics of cement-treated clay. These are summarized below.

1) *Type of Cement*. While Type III Portland cement has proven to be more effective in stabilizing soft clay deposits, Type I Portland cement is the most commonly used as it is cheap and readily available, as compared to other types.

2) *Cement Content*. As the cement content increases, it is expected that the strength of the stabilized soil will also increase.

3) *Curing Time*. Similar to concrete, it is expected that as the curing time increases, so does the strength of the cement-treated clay. The rate of increase in strength is generally most rapid during the initial curing period, and the strength increases more rapidly for cement-treated clay than for lime treated clay.

4) *Soil Type*. As the soil moisture content increases, the effectiveness of the cement decreases. Furthermore, an increase in plasticity index will also lead to a decrease in effectiveness (Broms, 1984). Organic content also has a negative effect on the improvement of soil with cement; however, cement is more effective as a stabilizer than lime when organics are present. Marine soils, which naturally have a flocculated structure, experience little increase in

strength due to the flocculation caused by additives as there is no significant change in structure.

5) *Curing Temperature*. The chemical reactions leading to strength increase following the addition of cement will be accelerated when the curing temperature increases. An increase in curing temperature also increases the solubility of the silicates and aluminates. Curing temperature has a greater influence upon the unconfined compressive strength during the initial curing period and has less influence as curing time increases (Kawasaki *et al.*, 1984). The process of hydration raises the actual curing temperature; this temperature change is governed by the type of hardening agent, thermal properties of the stabilized soil, and boundary conditions of the improved soil such as size and shape of the soil mass (Babasaki *et al.*, 1997).

6) *Soil Minerals*. Depending on the minerals present, soils will either have a low or high pozzolanic reactivity. If the reactivity is low, the strength characteristics of the hardened soil bodies will govern the strength characteristics of the treated soil. For soils with a high pozzolanic reactivity, the strength characteristics of the hardened cement bodies will control the strength characteristics of the treated soil (Saitoh *et al.*, 1985, from Bergado *et al.*, 1996). This means that if all other conditions are equal, soils with a higher pozzolanic reactivity will yield greater strength. Montmorillonitic and kaolinitic clays have a higher pozzolanic reactivity than illitic, chloritic or vermiculitic clays (Hilt and Davidson, 1960 from Bergado *et al.*, 1996).

7) *Soil pH*. High pH values (basic solutions) lead to an increased solubility of the silicates and aluminates of the clay particles and therefore, lead to longer pozzolanic reactions. When the pH of the treated clay is less than 12.6, a weaker cementitious material, CSH, is produced instead of $C_3S_2H_x$. This results in a weaker treated material than when the pH is greater than 12.6. Kawasaki *et al.* (1984) found that the effectiveness of cement stabilization deteriorates when the pH drops below 4.5 to 6.0. A report by Babasaki *et al.* (1997) states that soils with a pH less than 5 show little increase in strength compared to soils with a pH above 5 when mixed with the same amount and type of hardening agent.

3.2   Previous Research

The fundamental strength and deformation characteristics of cement-treated soils are not well understood (Kohata *et al.*, 1997). For this reason, a large amount of research has been dedicated to the area of soil-cement, particularly over the last decade. A number of authors from different countries have conducted research on the properties of soil-cement; their work has involved a variety of laboratory tests, including isotropically consolidated triaxial tests (drained and undrained), oedometer tests, unconfined compression tests, constant stress ratio tests and Brazilian tensile tests.

Since much research has been conducted in Asia, particularly in Japan, many of the most relevant publications are not in English. Fortunately, Kohata *et al.* (1997) summarize in English their review of 290 papers published in Japan between 1986 and 1996 on studies of DM cement-treated soil properties. Furthermore, Babasaki *et al.* (1997) published a similar article reviewing literature from the same time period on the improvement effects and influential factors on non-compacted improved soils. These two papers provide great insight into the Japanese practice of DM methods and the improved soil properties for those readers who do not have access to Japanese literature.

Table 3.1 on the following page briefly describes the laboratory programs conducted by a number of researchers, including the program reported herein. What follows is a summary of some of the significant findings of each author that can later be compared with the findings of the current study. Some of the conclusions made by others may seem obvious, but are stated here regardless for those readers who may lack the background to understand the intuitive behaviour of soil-cement. It should also be noted that the conclusions made are only for the range of testing conditions considered by each author and therefore, do not necessarily apply under all circumstances.

Table 3.1. Summary of soil-cement laboratory programs

	Current Study (2001)	Ahnberg (1997)	Consoli et al. (1997)	Uddin (1995)	Kawasaki et al. (1984)	Tatsuoka et al. (1983)	Wissa and Ladd (1964)
Tests	CIU and CID, UCS, Oedometer & IC	CIU and CID, UCS & Oedometer	CID, UCS & Brazilian Tensile	CIU and CID, UCS, Oedometer & CSR	CIU and CID, UCS, Shear box & Simple tensile test	CIU and CID, UCS & IC	CIU & UCS
Material	Kaolin: 47.6% clay & 52.4% silt	clayey silt (18% clay), clay (68% clay) & clayey gyttja (65% clay)	residual soils: weathered sandstone and claystone	soft Bangkok clay: 69% clay, 28% silt & 3% sand	21 types of clay from Japan: 5-64% clay, 32-73% silt & 1-44% sand	33.0% clay, 63.1% silt & 3.9% sand	15% clay, 43% silt & 42% sand
Organic Content	-	<0.1, 1.3 & 7.7	-	5.6% (organic carbon=2.87)		-	0.20%
pH value	-	6.2, 7.4 & 5.5	-	6.1	3.4 to 7.8	-	-
Atterberg Limits	LL=77% & PL=47%	LL=30, 70 & 135%	LL=21 & 40% and PL=17 & 24%	LL=103% & PL=43%	LL=41.5-230% & PL=21.5-72.6%	LL=100% & PL=46%	LL=20.5% & PL=14.7%
Moisture Content	70 & 100%	29, 78 & 155%	18 & 26.3%	76 to 84%	54.4 to 305.1%	120%	14.2 to 16.4%
Cement Type	ordinary Portland cement	Portland cement	Type IV Portland cement	Type I Portland cement	Type I Portland cement	ordinary Portland cement	Type I Portland cement
Cement State	dry	dry		slurry	slurry	slurry	dry cement with dry soil
Cement Content	2, 5 & 10%	10%	1 to 17%	5 to 40%	5 to 30%	8 to 20%	3 & 5%
Curing Time	7, 28, 56 & 112 days	14 to 119 days	7 days	1 week to 6 months	up to 60 days	7 & 28 days	10, 21, 50 & 98 days
Loading Rate (%/min)	0.005(triaxial) & 1.0 (UCS)	0.017 (triaxial)	-	0.01267 (CIU), 0.0025 (CID) & 1.0 (UCS)	0.1 (triaxial) & 1.0 (UCS)	0.06 (triaxial) & 1.0 (UCS)	0.0167 (triaxial) & 0.5 (UCS)
Confining Pressure (kPa)	50, 100 & 400	20, 80 & 160	20, 60 & 100	50 to 2000	50 to 700	up to 700	up to 55.4 kg/cm^2 (~5500 kPa)

*This material was artificially bonded by heating the material at 500°C for 5 hours

3.2.1 Triaxial Test Results

Wissa and Ladd (1964) were among the first to conduct a thorough study on the mechanical behaviour of material stabilized with cement and lime and published a report entitled "Effective stress-strength behavior of compacted stabilized soils". Two materials were stabilized: sandy clayey silt (CL-ML) and clay (CH). However, the sandy clayey silt was the only material stabilized with cement so only the results of tests on the cement-stabilized samples will be discussed here. They concluded the following, based on results of drained and undrained triaxial tests.

- The failure envelope for the stabilized soils, based on undrained tests only, was linear; therefore, Mohr-Coulomb failure criteria applies to cement stabilized soils.

- Moulding water content does not affect the friction angle of the stabilized soil.

- Cohesion is a function of curing time; with an increase in curing time, cohesion increases at a decreasing rate.

- The increase in friction angle that is associated with a higher cement content may be due to an increase in the maximum particle size resulting from cementation of smaller soil particles in the stabilized soil.

- At large strains there is no cohesion in cement and lime-stabilized soils.

- An increase in curing time increases the tendency of stabilized samples to dilate during shear; this is because the strength of the cementation bonds increases, enabling the material to dilate instead of crush during shear.

- Generally, the effective stress paths at high consolidation pressures resemble that of normally consolidated soil and at low consolidation pressures resemble that of over-consolidated soil.

- The initial tangent modulus increases with increasing consolidation pressure and curing time during undrained shear.

- As long as premature brittle failure does not occur, the axial strain at peak stress conditions is independent of consolidation pressure and curing time.

- As cement content increases, the axial strain at failure decreases.

Tatsuoka and Kobayashi (1983) of Japan studied the difference in strength of cement stabilized clay when evaluated by unconfined compression tests vs. consolidated triaxial tests. They observed the following.

• Volume change during consolidation of the treated samples was small due to cementation and the consolidated density values are nearly equal, regardless of consolidation pressure. Subsequently, the volume change during shear of the drained tests was greater for cement-treated samples than for untreated samples.

• For the undrained tests, the positive excess pore water pressure induced during shear was greater for the treated samples due to a higher degree of contractibility. This resulted in very similar effective stress conditions at peak conditions, regardless of consolidation pressure.

• The peak strength for the drained condition increases with consolidation pressure, and the rate of increase is greater with decreasing cement content. Furthermore, the drained residual strength is more sensitive to the consolidation pressure than the peak strength. Based on the nearly negligible residual strength measured by the unconfined compression test, the implication can be made that a decrease in confining (consolidation) pressure leads to a more brittle behaviour for the drained condition.

• During undrained conditions, the residual stress is only 20 to 30 percent less than the corresponding peak stress, and both are insensitive to the consolidation pressure. From this it can be said that during undrained shearing, the material is not brittle.

• A critical consolidation pressure exists at which the residual drained and undrained strengths are the same. When the consolidation pressure is greater than the critical value, the undrained residual strength is less than the drained residual strength, and vice versa.

Kawasaki *et al.* (1984) covered a broad spectrum of topics with regards to deep mixing, including design and the improved soil behaviour. Their study included 21 types of clay found in Japan and an extensive laboratory program. They made the following conclusions.

• In general, the stress at failure increases with an increase in confining pressure. However, under undrained conditions and at a cement content of 15 percent, which is the maximum value considered, the stress at failure remains approximately constant, regardless of the confining pressure. This

peak value roughly corresponds with the unconfined compressive strength at failure.

• The stress-strain curves are approximately coincident until the deviator stress reaches the unconfined compressive strength when the cement content is 15 percent, regardless of confining pressure or drainage conditions. For the undrained tests, failure normally occurs at approximately the unconfined compressive strength; for the drained tests, the stress-strain curve bends down slightly at the unconfined compressive strength and continues to increase approximately linearly until failure.

• Volume decreases as axial strain increases for the drained tests. When the cement content is 15 percent, the rate of decrease becomes larger when the deviator stress reaches the unconfined compressive strength (corresponding with the bend in the stress-strain curve). Furthermore, at 15 percent cement, the change in volume corresponds to the change in axial strain prior to failure, regardless of the confining pressure.

• It is suggested that a confining pressure exists after which the quality of the improved soil is reduced. Therefore, it is suspected that if the confining pressure sufficiently high, the stress-strain relationship of an improved soil is the same, regardless of the cement content.

One of the more detailed and relevant reports on the properties of clay-cement was reported by Uddin (1995) in his D.Eng. dissertation thesis entitled "Strength and deformation characteristics of cement treated Bangkok clay". Laboratory tests were conducted on samples with a wide range of cement contents and curing times at the Asian Institute of Technology. His conclusions are too many to summarise here as he reported his findings in great detail but his thesis will be referred to where relevant in the upcoming chapters. Some of his key points with regards to triaxial tests can be summarised as follows.

• The failure envelope is curved, such that as the consolidation pressure increases, the effectiveness of the cement decreases.

• As cement content and curing time increases, the axial strain at failure decreases.

• When comparing the Mohr-Coulomb parameters based on the drained and undrained test results, the drained tests yielded larger values of cohesion and smaller values of effective friction angle than the undrained tests.

• The effective friction angle did not increase for all values of cement content during the first month based on the drained test results, whereas the undrained tests yielded a significant improvement in effective friction angle for all cement contents.

• An increase in effective friction angle is due to flocculation and rearrangement of particles, which is a function of the drainage condition; an increase in cohesion is due to cementation which is due to the pozzolanic reactions.

Undrained Triaxial Tests:

• At a cement content of 7.5 percent and less, there is little to no change in strength with curing time. Furthermore, there is no significant difference in strength of samples with 5 and 7.5 percent cement.

• At low confining pressures, maximum pore pressure is achieved prior to sample failure; at high confining pressures, the behaviour is the opposite. The axial strain at peak pore pressure increases with confining pressure.

• As curing time increases, samples have a greater tendency to develop negative pore pressure.

• Cement treatment above 5 percent causes the behaviour to change from normally consolidated to over-consolidated.

• The treated clay strain-softened after failure so that the residual conditions were near the critical state line of the untreated clay.

Drained Triaxial Tests:

• As cement content and curing time increase, the failure behaviour is brittle, especially at low consolidation pressures.

• As cement content increases and consolidation pressure decreases, the degree of dilation at residual conditions increases. This is because higher consolidation pressures will destroy cementation so that dilation is reduced or eliminated.

• Volumetric strain at failure decreases as cement content and curing time increase; at high consolidation pressures, volumetric strain at failure is not affected by cement content and curing time.

• Cohesion and angle of friction increase with cement content and curing time.

• Most of the drained tests did not reach the failure envelope of the untreated clay, even at large axial strains. A destructured envelope was defined on which the residual stresses generally lay.

Consoli *et al.* (1997) studied cement-treated residual soils and found the following based on results of drained triaxial tests.

• Behaviour is strongly influenced by cement content and confining pressure.

• At high confining pressures, the peak deviator stress approaches that of the corresponding uncemented sample at the same density.

• At high cement contents, the peak deviator stress from the drained tests approaches the unconfined compressive strength of the same mix, regardless of the confining pressure.

• The peak deviator stress at low confining pressures is of the same order of magnitude as the unconfined compressive strength.

• With an increase in confining pressure, the axial strain at failure increases slightly and the peak deviator stress also increases.

• The cohesion intercept and cement content are linearly related; as the cement content increases so does the cohesion. The residual cohesion intercept also increases with an increase in cement.

• The peak friction angle increases with an increase in cement content, while the residual friction angle decreases slightly (or stays the same) with an increase in cement content.

Åhnberg (1997) of the Swedish Geotechnical Institute studied the stress dependent parameters of three types of soils stabilized with both cement and lime. The following observations were made.

• Strength increases significantly during the first 28 days of curing; an increase in curing temperature causes a more rapid increase in strength.

• A decrease in pore pressure prior to failure was often noted in the undrained tests and was more pronounced at low confining pressures; this is an indication that the sample has a tendency to dilate at failure.

• An increase in confining pressure leads to an increase in deformation at failure for the drained tests.

• The friction angle, as determined from the drained tests, was approximately the same for peak and residual conditions and was calculated to be in the order of 34 to 44°.

• Deformation during consolidation decreases as the curing time increases.

3.2.2 Unconfined Compressive Strength

The unconfined compressive strength is a common index to measure the strength of cement-treated soils as it is easy, fast and therefore, inexpensive to determine. The strength of cement-treated soil varies greatly, depending on the soil and stabilizer type.

Uddin (1995) defined three zones describing the influence of cement content on the unconfined compressive strength. Figure 3.2 shows that the most significant increase in peak strength was observed when the cement content was between 5 and 25 percent, and that the peak unconfined compressive strength changed very little when the cement content was less than 5 percent or greater than 25 percent. Based on the unconfined compressive strength, Uddin concluded that 15 to 20 percent cement content and 1 to 2 months curing time were considered optimum.

Consoli et al. (1997) found that on average, the tensile strength is approximately 12 percent of the unconfined compressive strength. Furthermore, it was concluded that the unconfined compressive strength increases with cement content and that this relationship is not linear (the slope increases with an increase in cement content).

Kamon (1997) reports that the unconfined compressive strength determined in the lab is roughly 2 to 5 times the value which can be expected in the field. Larger values for unconfined compressive strength can be expected when the seafloor is stabilized due to the adiabatic temperature rise.
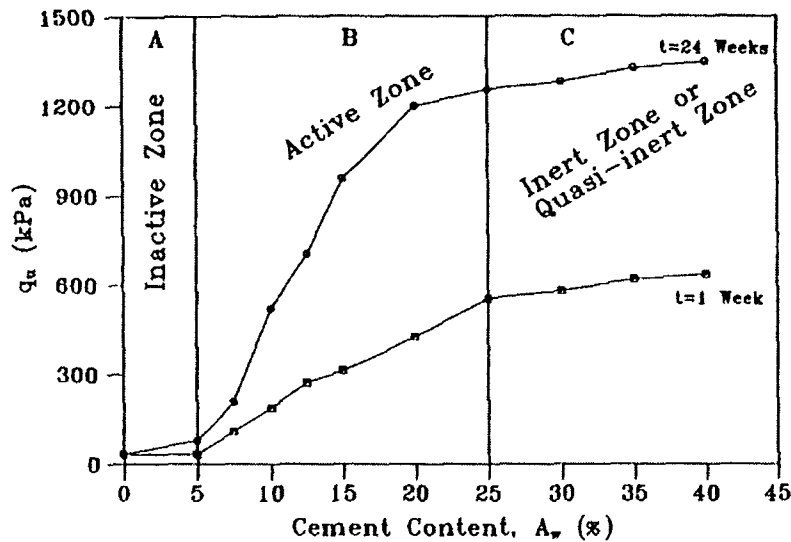
Figure 3.2. Influence of cement content on unconfined compressive strength (Uddin, 1995)

3.2.3 Deformation (Consolidation) Properties

Based on a series of oedometer tests, Uddin (1995) observed that as cement content increased so did the apparent pre-consolidation pressure and the coefficient of consolidation (c_v). As the consolidation pressure increased, the coefficient of consolidation decreased in an approximately linear manner. A significant reduction in the compression index (C_c) occurred when the cement content and/or the curing time increased; after 15 percent and 1 to 2 months, respectively, the reduction was minimal. At only 5 percent cement content, curing time did not significantly affect the consolidation properties brought about by hardening. Furthermore, it was concluded that cement content has a greater effect on sample hardening than curing time. Uddin determined an optimum cement content and curing time for the improvement in c_v and reduction of C_c of 15 percent and 1 to 2 months, respectively.

Uddin also conducted a number of isotropic consolidation tests and found that at low pressures, the isotropic consolidation lines resembled those of over-consolidated soil as they were curved. Yet at high pressures, the treated clay resembles normally consolidated material as the (e-ln p′) curve is flat and parallel to that of the untreated material.

Kawasaki *et al.* (1984) made similar conclusions to Uddin by stating that as the cement content increases, so does the consolidation yield stress.

3.2.4 Properties of Samples Cured Under Confining Pressure

Consoli *et al.* (2000) provide a good argument for the need to cure stabilized samples under confining pressure in order to accurately model the behaviour of such material in the field. They conducted drained triaxial tests on samples of weathered sandstone (classified as silty sand) with 3 percent cement. Preparation of samples was done following the method suggested by Ladd (1978, from Consoli *et al.*, 1997). Samples cured and tested at confining pressures of 50, 250 and 500 kPa were considered; the strain rate was 1.8 percent per hour. Equivalent tests were also conducted on samples cured under zero confining pressure. They made the following conclusions.

• Samples cured under stress exhibited less contraction and higher strength during shear than those cured under zero stress.

• The mechanical behaviour of the soil is greatly influenced by the stress state during curing.

• The friction angle increases when samples are cured under confining pressure as opposed to when cured under no confining pressure; the cohesion intercept remains unaffected by the confining pressure during curing.

• When the confining stress is applied (within the range tested), the stiffness is reduced as the mean effective stress increases for those samples cured under zero confining pressure; the opposite behaviour was observed for those samples cured under confining pressure.

4.   GENERAL DESCRIPTION OF LABORATORY PROGRAM

4.1   Kaolin Description

The soil used in the clay-cement samples for the laboratory tests was kaolin from Indonesia. The Atterberg Limits, grain size distribution, specific gravity and pH of the kaolin were determined in the laboratory; the grain size distribution was also provided by the manufacturer. The liquid limit and plastic limit of the kaolin was 77 and 40 percent, respectively; the plasticity index was 37 percent. The particle size distribution of the kaolin is illustrated in Figure 4.1. Under the Unified Classification system, the kaolin can be classified as high plasticity silt (MH), as it plots below the "A" line on the plasticity chart. The specific gravity (G_s) of the kaolin was determined with a pycnometer; at least 50 g of dry material was mixed with distilled water. The specific gravity of the kaolin was found to be 2.57; Das (1994) reports a value of 2.6. The soil pH was measured by mixing 10.0 g of dry soil with 40 ml of distilled water; the soil pH was 4.58.

The manufacturer's report provides the chemical analysis summarised in Table 4.1.
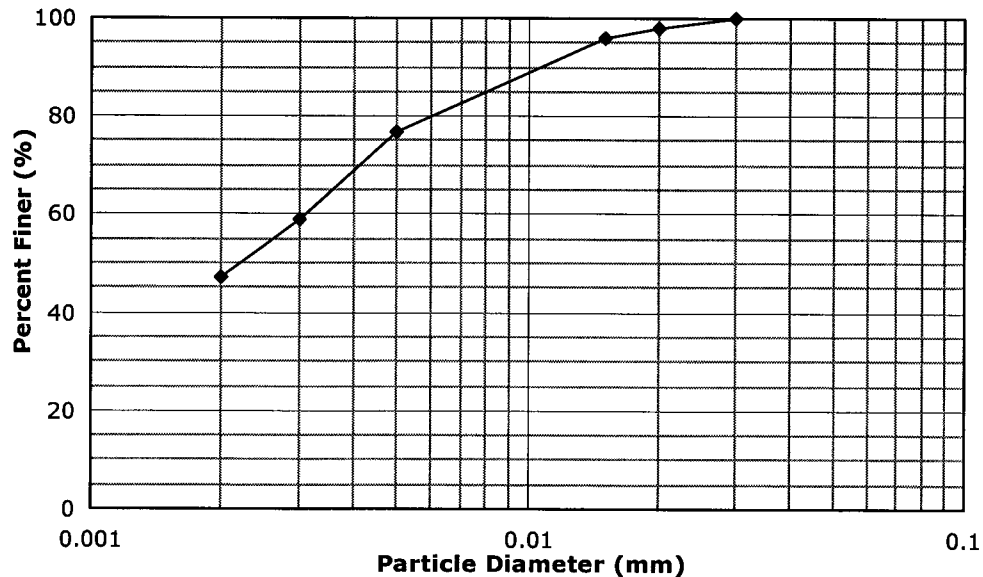
Figure 4.1. Grain size distribution curve for kaolin

Table 4.1. Chemical analysis of kaolin

Aluminium	34.54 %
Silica	49.70 %
Iron	0.55 %
Calcium	0.03 %
Magnesium	0.02 %
Kalium	0.60 %
Natrium	0.04 %
Titanium	0.21 %
Ignition Loss	14.19 %

4.2   Cement and Kaolin-Cement Description

Emerald brand Portland cement from Green Island Cement Company in Hong Kong was used as the stabilizing agent in all laboratory samples; this is equivalent to ordinary Portland cement. The chemical composition of the cement, as provided by the manufacturer, is summarized in Table 4.2.

Table 4.2. Chemical analysis of cement

Silicon dioxide	20.2 %
Iron (III) oxide	3.2 %
Aluminium oxide	6.2 %
Calcium oxide	65.6 %
Magnesium oxide	0.5 %
Sulphuric anhydride as SO_3	2.5 %
Acid soluble Alkali: Na_2O	0.1 %
Acid soluble Alkali: K_2O	0.4 %
Ignition Loss	1.6 %
Chloride content	0.005 %
Insolubles	0.1 %
Free lime	1.2 %

Atterberg limits were conducted on each mix of clay-cement considered in the laboratory program. Tests were conducted quickly so that the effects of curing were negligible. The specific gravity (G_s) was determined in the laboratory for pure cement, pure kaolin and kaolin with 10 percent cement. The values for kaolin with 2 and 5 percent cement were interpolated. Material pH was determined for the same mixes by adding the appropriate mass of dry cement to 10.0 g of dry kaolin and 40 ml of distilled water. These tests were done immediately and continued periodically for a period of 75 days to determine the change in pH with time. Concurrent with the laboratory program, moisture content after curing, initial void ratio, bulk density and dry density were calculated for sample.

Summarized in Table 4.3 are the properties of each mixture, based only on cement content. Table 4.4 includes physical property data calculated from samples prepared for the laboratory program. The effect of curing time on these properties is very small, especially when the cement content is 5 percent or less; only average values are provided here. The effects of curing time on the properties of kaolin-cement, including pH, are discussed in Appendix H.

Table 4.3. Atterberg Limits, specific gravity and pH for kaolin-cement

Cement content, A_c (%)	Atterberg Limits (%)			G_s	pH
	w_L	w_P	PI		
0	77.0	40.0	37.0	2.57	3.6
2	77.5	46.0	31.5	2.59*	12.3†
5	78.0	46.2	31.8	2.61*	12.7
10	79.0	46.5	32.5	2.66	12.9
100	-	-	-	3.39	13.7

*value is interpolated

†value is less than 12.6, therefore, cementitious material is weaker than when the pH is greater than 12.6 (Bergado *et al.*, 1996)

Table 4.4. Moisture content, void ratio and density of kaolin-cement mixtures.

Moisture content, w (%)	Cement content, A_c (%)	Average moisture content after curing, w_c (%)	Average initial void ratio, e_o	Average bulk density, ρ_b (g/cm^3)	Average dry density, ρ_d (g/cm^3)
40	0	38.5	1.02	1.77	1.28
70	2	68.5	1.82	1.55	0.92
	5	66.5	1.78	1.56	0.94
100	5	93.3	2.49	1.45	0.75
	10	88.3	2.43	1.46	0.78

4.3 Sample Preparation

4.3.1 Review of Literature on Sample Preparation and Curing Methods

The strength of soil-cement samples achieved in the laboratory is normally far greater than that achieved in the field for the same mix. Kamon (1997) suggests the unconfined strength of samples prepared in the laboratory is 2 to 5 times that of samples of the same mix obtained in the field. It is nearly impossible to mimic the exact field conditions in the laboratory, making it difficult to design efficient DM programs. Therefore, it is very important, when preparing laboratory samples, to match as best as possible the field conditions. Most importantly, this includes the state of the binder (i.e. dry vs. wet slurry) and the curing environment.

Very little information of sufficient detail was found in literature regarding sample preparation for triaxial or unconfined compression tests on cement-stabilized clay samples. Methods were often described but significant problems that are frequently encountered were not addressed so that when these methods were attempted for the current project, the results were unsatisfactory. Weak seams and trapped air pockets between lifts were the most common problems encountered, particularly for the samples prepared with only 70 percent moisture content.

All samples used for compression tests that were found in reviewed literature were cylindrical and had a length to diameter ratio of 2; this complies with both ASTM standards and British Standards (BS). In most cases, the triaxial and unconfined compression test samples had a diameter of 50 mm and a length of 100 mm. Uddin (1995) conducted unconfined compression tests and triaxial tests on samples that were 35.5 mm in diameter and 71 mm in height. Pousette *et al.* (1999) prepared stabilized peat samples and found that unconfined compressive strength results from larger samples (with a diameter of 68 mm) were less spread out and more reproducible. This may be due to the larger degree of heterogeneity found in peat and may not be true for stabilized clay that is well mixed prior to casting. Pousette *et al.* also found that the mixing time affected the structure of the peat but again, no literature was found to support this argument in the case of clays, except to state that mixing time should be kept to a minimum to prevent significant hydration of cement prior to casting of the samples.

One of the most thorough reports on sample preparation was provided by Edstam and Carlsten (1999) of the Swedish Deep Stabilization Research Centre. Their goal was to develop a standard technique to be used in Sweden when establishing the mechanical properties of stabilized soils so that the results were reliable and reproducible. They asked four separate laboratories in Sweden to prepare samples following conventional methods (which included mixing the material in a dough mixer and then compacting the soil into moulds in lifts) and then conduct unconfined compression tests on the cured samples after 7 days. The results showed good reproducibility of results within each individual laboratory, but the results between laboratories were not acceptably similar.

The new method developed by Edstam and Carlsten uses a special mixing tool, to be operated by hand, which fits directly into a relatively narrow cylinder. The soil is mixed by not only rotating the tool, but moving it up and down. The clay, generally at the liquid limit, is first mixed in the cylinder using the specially designed tool until the mixture is homogeneous. A plug of clay is removed from the full length of the cylinder and replaced with the appropriate mass of dry cement. Using the same tool, the cement is mixed with the wet clay until homogeneous. The sample tube is pushed

directly into the cylinder to remove the sample, and then placed in a climate controlled chamber for curing.

Unconfined compression test results from the same four laboratories, preparing samples following this new method, were in close agreement. However, nearly all unconfined compressive strength values were below the values obtained following the original traditional method. The purpose of this new method was to obtain reproducible results between different laboratories. This goal was achieved, however, the quality of the samples, as compared with the more traditionally prepared samples, was not discussed. Due to the lower strength test results, it is suspected that the sample quality following the new preparation method may be inferior to that following the traditional method.

Uddin (1995) conducted an experimental program to determine the best means to prepare samples of treated Bangkok clay. He adopted three sample preparation methods, using only lime as the hardening agent, and then performed unconfined compression tests on the cured samples. He established which method was most effective prior to the start of his full scale laboratory program, when he used both lime and cement as hardening agents. The three methods Uddin considered are summarised as follows:

Method A. Lime was added as a wet slurry to wet clay and mixed for 10 minutes by hand. It was found that the wet slurry was most workable when the water to dry lime ratio was 0.25. Once thoroughly mixed, the wet material was compacted into a steel mould in 5 equal lifts; each lift was compacted with 30 blows of a 25-mm diameter steel rod and a fall height of 200 mm. The moulds were waxed and placed in a humid room for curing. Following the required curing time, a sub-sample of the appropriate size was extruded from the mould for testing.

Method B. A cylindrical clay cake (250 mm diameter and 150 mm height) was obtained in the field using a mould, and a sample was extruded from the cake using a thin-walled tube (63.5 mm diameter). Dry lime powder was "sprinkled" onto the clay sub-sample in two portions, and mixing was carefully done with gloved hands following each addition until the mix was uniform, which usually took about 2 to 5 minutes. The mixed clay was then

placed back in the cylindrical void in the clay cake, in 5 lifts. Each lift was compacted in the same manner as in Method A, by 30 blows of a 25-mm steel rod and a fall height of 200 mm, so that two 'mini-lime columns' were formed in each cake. The mould was removed from the cake and the sample was sealed in wax and allowed to cure in a humid room for the desired time. Cutting wires were used to cut a sample of the appropriate size from the cake at the time of testing.

Method C. This method is identical to Method A, except the lime slurry was prepared so that the moisture content of the final mix is equivalent to the liquid limit of the clay.

Uddin chose to use Method A for preparing samples for the laboratory program as it provided samples with the highest strength and stiffest modulus characteristics. Furthermore, the results of the unconfined compression tests were most uniform and consistent for those samples prepared by Method A than by the other two methods considered.

Wissa and Ladd (1964) conducted a thorough study on the effective stress behaviour of stabilized soils, using both lime and cement as stabilizing agents to treat samples of clay and clayey silt. The moisture content of the soil stabilized with cement was relatively low at less than 20 percent. Between 3 and 5 percent of dry stabilizer was mixed with oven-dried soil. Water was added to the dry soil plus stabiliser and mixed by hand and the samples were immediately cast. For the samples with cement, no more than 15 minutes was allowed to pass between the introduction of water to the mix and final compaction and each sample was mixed and compacted individually. Wissa and Ladd used a two-end static compaction method whereby 400 psi (approximately 2750 kPa) of compactive effort was applied to each end using a hydraulic press. The pressure was sustained for approximately 1 minute. It is understood that the material was compacted all in one lift so that no laminations were present within the sample.

It was found that this method of static compaction produces samples which are not uniform in density. Wall friction during compaction leads to a lower dry density at the centre of the sample. However, the distribution of density is symmetrical across the middle of the sample, provided that the compaction load at either end is applied at the same rate.

Samples were extruded and then humid cured in a sealed glass dessicator, with water in its base, for the desired curing time. Stabilized samples were immersed in water for at least 24 hours prior to the start of saturation in the triaxial cell. Moisture content measurements taken after completion of curing found that samples compacted wet of optimum lost moisture during the curing process. Wissa and Ladd believe this is due to curing too many samples in one dessicator at a time. It was also observed that when samples both wet and dry of optimum were cured together, the samples dry of optimum gained moisture during curing.

Kohata *et al.* (1997) mention that Japan has standardized procedures for sample preparation which were developed in 1990. Details of this procedure were not found, however, it was stated that samples are air-sealed and cured at 20°±3°C, to take into account the undrained conditions present in the improved ground.

Curing method contributes a great deal to the subsequent strength properties of soil-cement. Three techniques have emerged from literature: humid curing, underwater curing and curing samples sealed in plastic. Kézdi reports on experiments conducted by Gáspár (1964 from Kézdi, 1979) whereby the strength of samples cured in both a humid environment and underwater were compared. The compressive strength was found to be 20 to 30 percent greater for the samples cured in a humid environment than for those cured underwater.

Consoli *et al.* (1997) prepared samples by compacting the material in lifts in a 50x100 mm tube, wrapping the tubes in plastic, and curing them in a humid environment for 7 days.

Tatsuoka and Kobayashi (1983) report that they filled split moulds in 3 layers, avoiding entrapment of air bubbles. After 24 hours of curing, the top of the sample was trimmed and the mould disassembled. The sample was then wrapped in plastic and submerged in water to avoid loss of water for the remainder of the curing period. Other samples were also prepared and cured under normally consolidated conditions. These samples were first cured under vacuum for 10 days and then cured under a normal stress for 10 days. They reported that all sample preparations and testing was performed in a

temperature and humidity controlled environment of 22°C and 60 percent, respectively.

4.3.2 Sample Mixing

Sample preparation for the current study was conducted twice a week; preparation of each series of samples took place over a two-day period. On the first day, oven-dried kaolin was mixed with the appropriate mass of distilled water to obtain the desired moisture content. Both the kaolin and water were at room temperature when mixed. Mixing was done using a large electric mixer fitted with a paddle type mixing blade (Fig. 4.2) until a homogeneous consistency was achieved throughout. The wet clay was sealed in plastic and allowed to soak at room temperature for approximately 24 hours. This allowed moisture to penetrate any small clumps of dry clay minerals and for any physical changes in the clay caused by the addition of water (such as swelling) to occur prior to casting the samples.

On the second day, following the soaking period, the appropriate mass of dry cement required to achieve the desired cement content was measured and added to the wet clay. Immediately, the material was mixed thoroughly using the same electric mixer (or an equivalent smaller model) until a homogeneous mixture was achieved. This second mixing stage took less than ten minutes and was monitored closely, with some hand-mixing required, to ensure a uniform mix within a minimum time period. The exact mixing time was not considered to be a critical factor contributing to the quality of the samples, however it was kept to a minimum. The material was then immediately cast in the moulds.[1]

---

[1] Six to nine samples were normally cast from each mixture. When the moisture content of the mixture was 100 percent, casting of all samples in one batch took less than ten minutes. However, the material with a moisture content of 70 percent was much more time consuming, and often took as long as ten minutes per sample. During the initial casting of these samples, all samples from each batch were cast at once and therefore, it often took upwards of an hour to cast a full batch of samples. However, due to the unknown influence of time on the sample quality, the batches were reduced and mixed in a smaller mixing bowl so that only three to four samples were cast from each batch, considerably reducing the maximum time between mixing and casting for each sample.
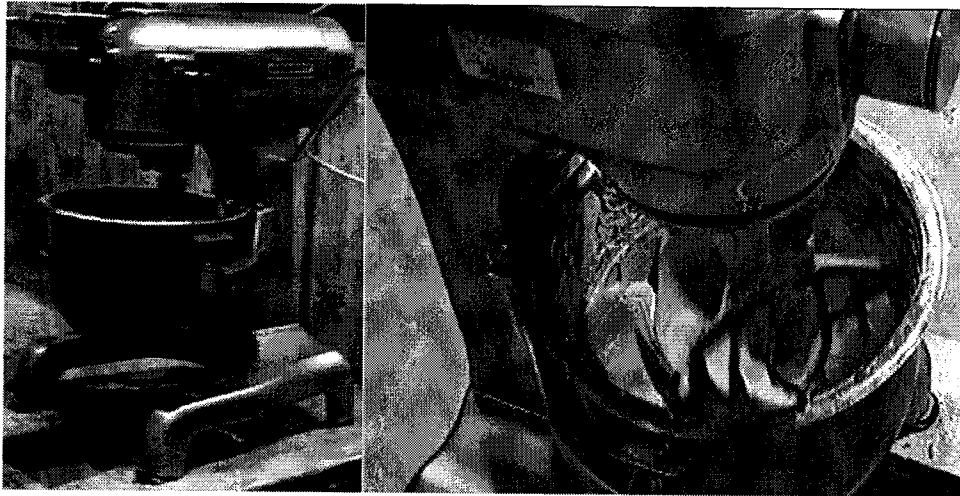
Figure 4.2. Sample mixing apparatus.

4.3.3 Sample Casting

The moulds used for preparation of samples consisted of high-density plastic tubes, with a 50 mm internal diameter and a length of approximately 150 mm (Fig. 4.3). The tubes were lined with PVC to reduce friction between the sample and the mould during casting and extrusion.
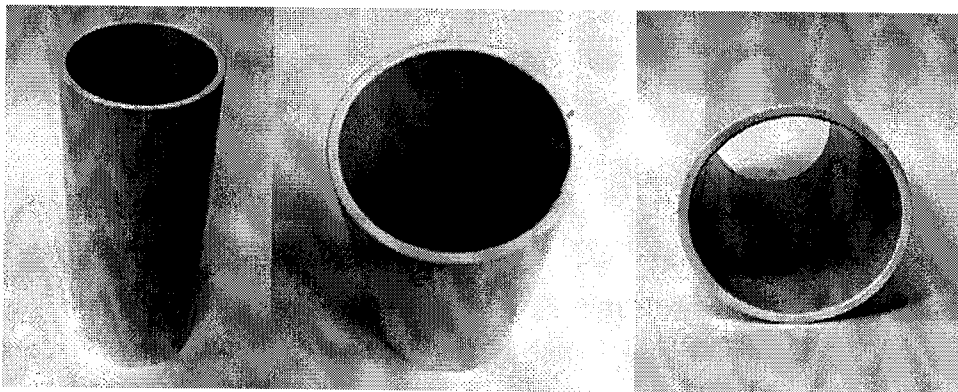

Figure 4.3. Plastic mould used for casting kaolin-cement samples for laboratory strength tests

Casting of the material in the mould was done following one of two methods, depending on the moisture content and hence the sample consistency.

4.3.3.1   Method 1: w=100%

When the moisture content of the kaolin was 100 percent, the consistency of the material was extremely soft. When vibrated at a high frequency on a vibrating table used for casting concrete samples, the material liquefied. Therefore, to prepare high quality samples with a moisture content of 100 percent, the moulds were placed vertically on a vibrating table and held firmly against a flat rigid plastic plate. With the vibrating table switched on, the material was quickly scooped into the mould using a large metal spatula. As the mould vibrated with the table, the soft material easily slid down the inside of the mould, creating a high quality sample with minimum voids and constant bulk density throughout.

Occasionally, problems were encountered when large air voids formed at the bottom of the mould, working their way upwards causing a bubbling effect on the surface of the sample. It is suspected that this air entered the sample at the base of the mould between the plastic plate and the mould, and occurred more frequently towards the end of the batch (when the mixture became slightly stiffer and the technician holding the mould firmly against the plate more tired). This problem was alleviated by working quickly and relieving fatigued technicians during the process.

Following this method, it took less than fifteen minutes to prepare a batch of six to nine samples with a moisture content of 100 percent. This meant the total time between the addition of cement and casting of each sample was 25 minutes or less.

4.3.3.2   Method 2: w=70%

Material with a moisture content of only 70 percent was much stiffer than the material with a moisture content of 100 percent.   Therefore, sample preparation using material with a moisture content of 70 percent was more laborious and therefore, it was more difficult to prepare high quality samples. Material was usually mixed in small batches to minimize the curing of the cement prior to completion of casting of the samples in the mould. Several different methods were attempted before arriving at a final decision on how these samples should be prepared; each method is described below.

Method A: An attempt was made to mimic the method used by Wissa and Ladd (1964) to prepare cement-treated samples. The material stabilized by Wissa and Ladd had a moisture content below 20 percent; they used a hydraulic press to achieve two-end static compaction. For the current study, an aluminium piston attached to a heavy duty C-clamp was used to compact the soil-cement. The piston fit exactly the inside diameter of the mould and was pushed into the mould manually by screwing the C-clamp, until refusal was reached. The mould was filled with approximately 10 to 12 equal lifts of material. It was originally thought that this method would produce a sample with a constant density throughout in little time and with little effort. However, there was no means for the air to escape and therefore, upon extruding initial trial samples, voids were found around the perimeter of the sample between lifts.

Method B: Small amounts of material were first kneaded into a ball and then firmly tossed into the bottom of the mould so that the material adhered to the underlying material prior to tamping. Tamping was done using a cylindrical wooden rammer. The use of other rammers such as a steel rod and a steel rod covered with PVC was attempted, but the material was very sticky and only the wooden rammer provided satisfactory results. Tamping was done in such as way as to result in a more-or-less consistent density throughout the sample and between samples of the same mix.

Method C: Kneading a large amount of sample at once and attempting to squeeze it into the mould was also attempted; this method was also unsatisfactory due to the resulting large trapped air voids.

Method B was the only sample preparation method which provided satisfactory results; this method was employed to prepare all samples at 70 percent moisture content. Some samples were also prepared without cement at 40 and 70 percent moisture content following this method. Preparation of these samples was the same as for the cement-stabilized samples, except curing was not necessary and therefore, laboratory tests were conducted immediately following sample casting.

4.3.4 Sample Curing

Once the material was compacted in the mould, the ends were covered with heavy plastic and held tightly in place with thick rubber bands. The moulds were placed vertically in a constant temperature (20°C) and constant humidity (65 percent) room for 24 hours. After this period, the plastic was replaced with porous fabric (Fig. 4.4) and the samples were submerged vertically in a distilled water bath at 20°C for the remainder of the curing period (Fig. 4.5). Water curing simulates typical field conditions, where the water table is normally high. The samples were in the constant temperature and constant humidity room for the duration of their curing period. Due to the high moisture content of the samples prepared for this study, extruding the samples prior to curing was not possible as the material was too soft.

Preparation of the oedometer samples was done in a similar manner. Material was cast in small, PVC-lined steel cylindrical moulds, slightly larger than the diameter of the consolidation ring. After casting, the top of the mould was covered with plastic for the initial 24-hour curing period. After this time, the steel base-plate was removed, and both ends were tightly covered with fabric and the sample was submerged upright in the bath of distilled water for the remainder of the curing period.

At the start of the sample preparation program, the intent was to seal the ends of all sample tubes in wax (Fig. 4.6), and allow them to cure upright in the moisture and humidity controlled room. This practice was followed initially, however, after only 7 days of curing some shrinkage and desiccation (horizontal hairline cracking) was observed following extrusion, and therefore, the wax curing method was abandoned for future samples and the 7-day wax-sealed samples were discarded. However, out of interest, some 112-day samples with a moisture content of 100 percent were cured in wax for the full curing time. When extruded, the moisture content of these samples was 3 to 6 percent below that of the same samples, cured for 112 days in water. All laboratory tests were carried out on the 112-day samples to compare curing methods and the results are somewhat surprising. The unconfined strength of the water-cured samples was 30 to 50 percent greater than that of the wax-cured samples yet the water-cured samples were slightly stiffer. Failure was very brittle in both cases. For the triaxial tests, however, the results

were nearly the same for both the water-cured and wax-cured samples, particularly at high confining pressures. The results are presented in Appendix H and described in greater detail.

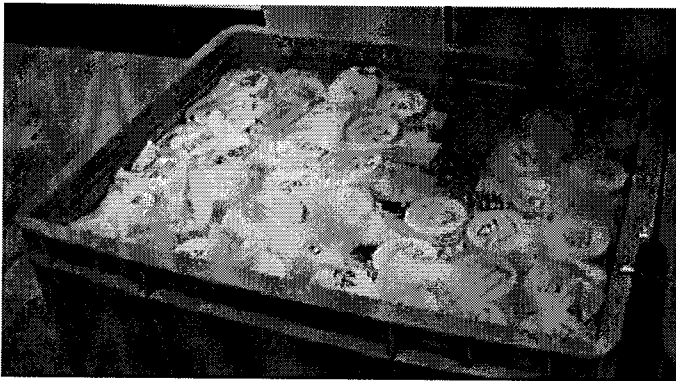Figure 4.4. Kaolin-cement samples and mould with fabric on ends.

Figure 4.5. Kaolin-cement samples submerged in water bath for curing.

Figure 4.6. Wax-cured samples.

4.4   Triaxial Tests

Consolidated isotropic undrained (CIU) and consolidated isotropic drained (CID) triaxial compression tests were performed. All tests were conducted following the British Standard method of testing using new ELE machines (Fig. 4.7). A diagram of the triaxial cell is provided in Figure 4.8. Determination of the moisture content was done before and after each test, using sample trimmings and the actual failed sample, respectively.

The triaxial apparatus used for all triaxial experiments consisted of six cells and three loading machines. Normally, at any given time, three samples were saturating or consolidating and three samples were shearing. In this way, six triaxial tests were in progress at any one time (including one isotropic consolidation test).

The capacity of the compressor was 700 kPa. This allowed for a maximum back pressure of 650, 600 and 300 kPa when the effective confining pressure was 50, 100 and 400 kPa, respectively.

Prior to each test, each transducer was set to zero. The change in axial load, volume, pore pressure and axial displacement were measured and recorded automatically using a computerized data acquisition system. Raw data was downloaded upon the completion of each test; the necessary corrections were made to the data and appropriate plots were generated using MS Excel.

Table 4.5 summarizes the triaxial tests conducted at various moisture contents and cement contents. For each mix type, both drained and undrained tests were performed on samples that had cured for 7, 28, 56 and 112 days. The drained triaxial tests were performed at an effective confining stress of 50, 100 and 400 kPa; the undrained tests were conducted at an effective confining stress of 100 and 400 kPa, only. A series of triaxial tests were also conducted on uncemented samples at 40 percent moisture content. Samples prepared with a moisture content of 70 percent and a cement content of zero percent were prepared but were not stable once extruded from the mould; therefore, these tests were abandoned. Similarly, samples prepared with 70 percent moisture and 10 percent cement were also abandoned due to difficulty in preparing high quality samples with such a stiff

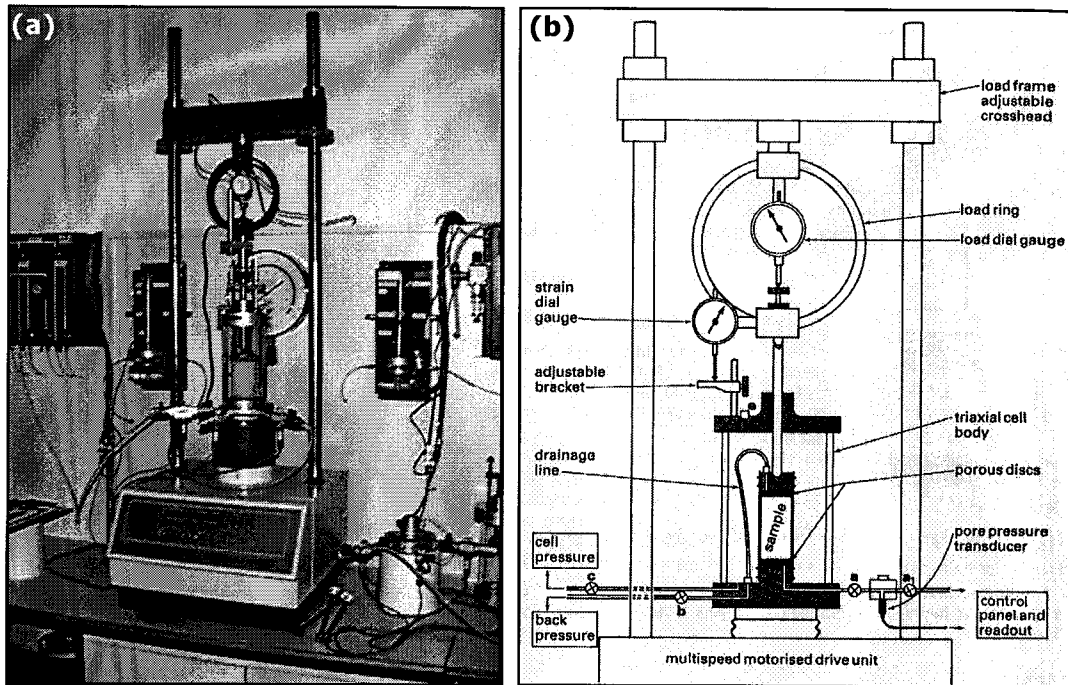material. Large voids were present and clear seams or "joints" developed between lifts.

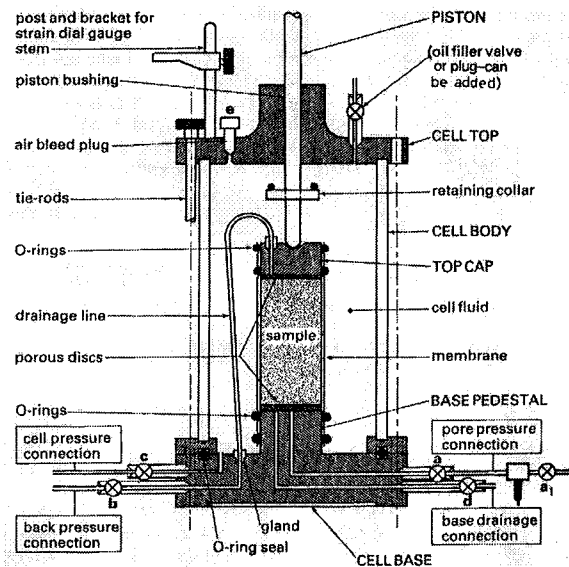Figure 4.7. Triaxial apparatus (a) photo from laboratory; (b) diagram from Head (1998).

Figure 4.8. Details of a typical triaxial cell (the oil filter plug is not normally fitted to commercially available cells) (Head, 1998).

Table 4.5. Summary of triaxial tests performed

Moisture Content, w (%)	Cement Content, A_c (%)
40	0
70	2
70	5
100	5
100	10

The strain rate for all tests (both drained and undrained) was set at a constant 0.005 mm/min or 0.3 percent/hour. The actual strain rate was often slightly less than this, due to the resistance caused by the sample.

It should be noted that saturation of samples began one day prior to the final curing date of the sample. For example, for 7-day samples, saturation began on the 6th day. In this way, consolidation began at the end of the 7th day and shearing began at the beginning of the 8th day.

Prior to the start of each shearing phase, the piston was manually adjusted to almost touch the loading cap and the axial displacement and axial load were reset to zero. In most cases, the piston was intentionally not seated prior to shear to avoid premature loading. Therefore, some corrections were made to the data so that only the measurements recorded following seating of the load were considered. For this reason, the load at zero strain was often greater than zero. Occasionally, the exact time when the piston was seated was difficult to determine. This was especially true for the tests with an effective confining pressure of 400 kPa, which often resulted in samples having an axis that was not perfectly vertical following consolidation. The best attempt was made to establish exactly when the piston was seated, based on examination of the shear data. When ambiguous, it was assumed that the piston was seated when the pore pressure began to increase significantly (during the CIU tests) or when the volume began to change significantly (during the CID tests). It should also be noted here that the friction between the piston and the top of the cell was never measured, but the corrections described above should allow the piston friction to be ignored, as any stress measured prior to contact between the piston and the loading cap would have been considered as zero load.

4.4.1 Sample Set-up

Prior to the start of preparing each sample for the test apparatus, each cell was inspected and all lines were flushed with de-aired water to remove any air bubbles present. The cells providing the cell pressure and back pressure were also inspected to ensure that the air bladder was not overfull and to remove any trapped air pockets in the water. Porous stones were de-aired and saturated by first placing the stones in a bath of distilled water and vibrating the water at a high frequency for 30 minutes to remove any trapped soil from the stones. The stones were then submerged in clean distilled water and placed in a vacuumed dessicator for approximately 20 minutes to de-air completely. Water used in the triaxial cells and to saturate the samples was de-aired by boiling it under high pressure for approximately 30 minutes.

With the cells prepared, samples were carefully extruded using a hydraulic extruder. At this time, the sample quality was judged. Samples with large voids around the perimeter were discarded. Where occasional small (shallow) voids were present, careful patch work was done without disturbing the intact material. Voids on the surface that were up to approximately 2 mm in diameter were considered acceptable for mending; if larger than this, the sample was not used. Samples were then wrapped in a single layer of waxed paper and placed inside a steel split mould (Fig. 4.9). By trimming the ends of the sample to be flush with the mould, the sample was made to be exactly 100 mm long. Trimming was done using thin violin wire and a sharp steel straight-edge. Further inspection of the sample quality was done during trimming by examining the cross-section and samples were discarded if the quality was in doubt. For nearly all mix types, there was at least one spare sample prepared for each proposed test so that discarded samples could be easily replaced with a suitable identical sample.

The sample, waxed paper and mould were then weighed, and the mould and wax paper removed from the sample. The wax paper and mould were re-weighed so that the wet mass of the sample could be back-calculated. A saturated and de-aired porous stone was placed on the cell pedestal, followed by a saturated piece of filter paper, trimmed to the exact diameter of the sample. The sample was placed upright on the cell pedestal so that it was directly in contact with the filter paper, with no trapped air. A

second piece of saturated filter paper, followed by a second saturated and de-aired porous stone were placed on top of the sample. Radial filter paper was wrapped around the sample so that the filter paper ran vertically and approximately half of the vertical surface area of the sample was covered with filter paper (Fig. 4.10). For the drained tests, the radial filter paper was allowed to be in contact with both the top and bottom porous stones because the change in pore pressure was not relevant. However, for the undrained tests, the radial filter paper was cut to a shorter length so that it was not in contact with the bottom porous stone, and therefore, not influencing the pore pressure.

A thin smear of silicone grease was applied to the vertical surfaces of the pedestal and loading cap to enable a good seal between the rubber membrane and the steel. Using a membrane "stretcher", a thin rubber membrane was placed around the sample, followed by 2 to 3 rubber "O"-rings, both above and below the sample. The piston was raised as high as possible, and the triaxial cell placed over the sample and tightly screwed into place. The cell was filled with de-aired water until the cell was full with no trapped air pockets.

The sample was photographed prior to application of the radial filter paper so that the quality of the sample was well documented; a photograph was also taken of the sample following shearing. These photographs are provided in Appendix G.
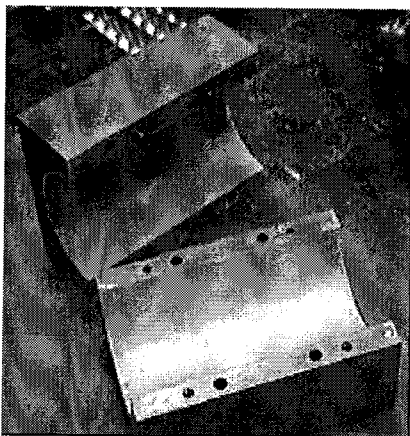

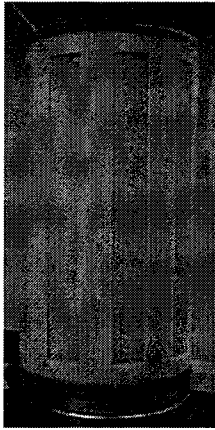Figure 4.9. Steel split-mould used to trim triaxial samples.

Figure 4.10. Triaxial sample with radial filter paper.

4.4.2 Sample Saturation

A review of literature in Japan (Kohata *et al.*, 1997) revealed that the standard practice for saturating triaxial samples of stabilized soil is to achieve a B-value of 0.95 or greater. Since it is difficult to saturate cement-treated soils (particularly at high cement contents), the dry-setting method is often employed, as well as the percolation of either carbon dioxide or de-aired water into the specimen by applying negative pressure. Back pressures between 1 to 4 kgf/cm^2 (approximately 100 to 400 kPa) are normally applied during saturation.

For the present study, saturation of the sample took place over a period of approximately 36 hours. A minimum final back pressure of 300 kPa was applied to all tests. A B-test was conducted initially with the back pressure valve shut and the cell pressure set at 50 kPa. The initial saturation stage was implemented once the pore pressure equalized; during this stage the cell pressure was maintained at 50 kPa and the back pressure at 40 kPa. Each subsequent B-test and saturation stage was done by increasing the cell pressure 40 kPa (for the B-test) and then increasing the cell pressure an additional 10 kPa and increasing the back pressure 50 kPa for the saturation stage. The cell and back pressure were increased in this manner, with pressure increments of 50 kPa, until a B-value of at least 0.8 was obtained. After which, for the tests where the confining pressure was at least 100 kPa, the pressure increments were increased to 100 kPa, as recommended by Head (1998), until a B-value near 1.0 and the desired stress levels were

achieved. For the tests with a confining stress of only 50 kPa, the stress increments were limited to 50 kPa only, so that more increments were required than for those tests at greater confining pressures. Pressure increments proceeded until the cell pressure reached 700 kPa; the back pressure was such that the desired confining pressure was achieved. A final B-test was conducted to confirm adequate saturation.

Throughout saturation, the B-value and degree of saturation (based on the volume change during the saturation stages and the initial moisture content and specific gravity) were calculated. Prior to the final back pressure increment and final B-value test, the B-value and degree of saturation were checked to ensure that they were above 0.95 and 99 percent, respectively. Occasionally, particularly for samples with 10 percent cement content, this criteria was not met and the B-value was sometimes below 0.9. Wissa and Ladd (1964) found that the B-value decreased as consolidation pressure and curing time increased and suggest that a B-value less than 1.0 for cement stabilized soil is due to the high rigidity of the soil skeleton and not the presence of air within the system.

4.4.3 Sample Consolidation

Isotropic consolidation was commenced by opening the back pressure valve and took place over a roughly 12 to 14 hour period, after which time primary consolidation was completed.

Plots were generated of change in volume vs. time. The coefficient of consolidation (c_{vi}) and coefficient of volume compressibility (m_{vi}) were calculated based on the isotropic consolidation triaxial data using the following equations (Head, 1998).

$$c_{vi} = \frac{0.5256\pi D_C^2}{\lambda t_{100}} \text{ (m}^2\text{/year)} \tag{4.1}$$

$$m_{vi} = \frac{\Delta V_C}{V_o} \times \frac{1000}{\Delta \sigma'} \text{ (m}^2\text{/MN)} \tag{4.2}$$

For drainage at both ends as well as radial drainage, Head (1998) recommends a λ of 100.

It is important to note here that Head warns against calculating c_{vi} in this way when making consolidation or permeability calculations, as the value can be misleading when side drains are used. The primary function of deriving c_{vi} in this way is to estimate the rate of strain for triaxial tests. For more accurate evaluation of c_{vi}, side drains should be omitted. The coefficient of consolidation was also calculated based on the isotropic consolidation and oedometer test results. Therefore, any error in the calculation of c_{vi} from the triaxial data is acceptable.

4.4.4 Sample Shearing

Following isotropic consolidation, the cell and back pressure valves were shut, the triaxial cell was placed in the loading apparatus and the cell and back pressure adjusted as needed (due to the height difference from the saturation pedestal which was below that of the loading apparatus). The cell and back pressure valves were opened and the pedestal was raised until the loading device was seated on the piston and the piston was approximately 1 mm above the loading cap. The valves were left open to allow all pressures to equalize (change in pressure during this equalization was normally on the order of 2 kPa or less). Once the pressures had equalized, the back pressure valve was shut for the undrained tests. The axial displacement and load transducers were set to zero, and the shearing phase of the triaxial test was commenced.

The strain rate for all tests was set to 0.005 mm/min (0.005 percent/minute=0.3 percent/hour). Kohata *et al.* (1997) indicate that the normal practice in Japan is to apply a strain rate of 0.04 to 0.5 percent/min for triaxial tests. However, at larger strain rates, the excess pore pressure generated for the drained tests was considered to be too high. Shear tests were normally allowed to run until at least 25 percent strain or until the deviator stress remained approximately constant with increasing strain, whichever occurred first. Often, when time permitted, tests were allowed to run to nearly 30 percent strain, particularly for the drained tests, when the

axial strains at peak conditions were higher than those for the undrained tests.

The intention prior to the testing program was to achieve residual conditions for all triaxial tests. The residual condition is unique for clay and is defined as the condition when all particles are reoriented and the soil has a minimum strength; high strains are required to reach residual conditions. Under drained conditions, for a given set of stress conditions, soils at the residual condition will have the same final moisture content and void ratio, regardless of the initial state (Mitchell, 1993). Residual conditions can also be achieved for undrained tests. However, in the case of structured material, the bonding effects make it very difficult to reach the true residual state. Axial strain was often allowed to exceed 25 percent in an attempt to achieve residual conditions; normally at this time, lateral deformation was significant and accurate stresses could no longer be calculated. It is not believed that residual conditions were achieved for the current triaxial tests. Therefore, the term "fully-softened" condition is introduced, and will be used in future discussions; Mitchell (1993) also makes use of this term. The fully-softened condition is the condition when the deviator stress remains constant with axial strain. The residual condition has been discussed previously with reference to the work of other authors (i.e. Tatsuoka and Kobayashi, 1983; Consoli et al., 1997) on cement-treated soil. It is not clear how these authors define the residual condition in their discussions and if their interpretation of residual condition is the same as the fully-softened condition defined here.

The deviator stress was calculated based on the applied load and the sample area, with some corrections made to account for the change in area during shear. The following equations were applied (Head, 1998).

Drained tests:
$$(\sigma_1 - \sigma_3) = \frac{P}{A_C} \times \frac{100 - \varepsilon_a}{100} \times \frac{1000}{\left(1 - \frac{\Delta V}{V_C}\right)} \text{ (kPa)} \qquad (4.3)$$

Undrained tests:
$$(\sigma_1 - \sigma_3) = \frac{P}{A_C} \times 10(100 - \varepsilon_a) \text{ (kPa)} \qquad (4.4)$$

For each test, stress-strain (q vs. ε_a) curves and stress paths (q vs. p′) were plotted, as well as the volumetric strain or excess pore water pressure vs. axial strain for the drained and undrained tests, respectively. For the undrained tests, the overall pore pressure coefficient, $\overline{A}$, (based on Skempton's A value) was also calculated. This coefficient relates the pore pressure developed during shear to the applied stress difference; if it is positive then the sample is contracting, if it is negative, then the sample is dilating.

All triaxial samples were photographed after shearing; these photographs are provided in Appendix G.

4.4.5 Data Acquisition System

An ELE Autonomous Data-acquisition Unit (ADU) linked to a PC was used to automatically record all relevant data from six triaxial cells and three loading machines. A diagram illustrating the layout of the ADU and triaxial set-up is provided in Figure 4.11.
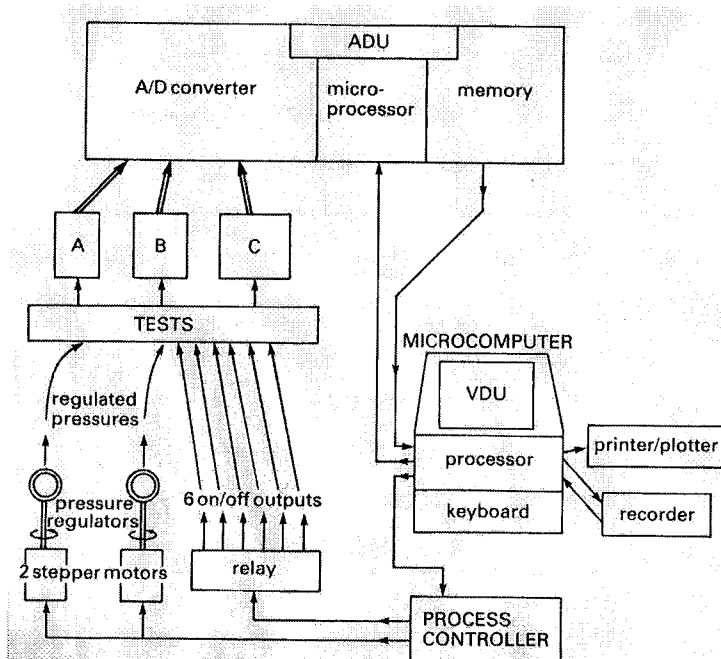
Figure 4.11. Schematic layout using ADU for automatic control of laboratory tests (Head, 1998).

4.4.6 Data Correction

Head (1998) suggests correcting the sample area during shear to account for barrelling of the sample. However, based on the sample size and the relative stiffness of the material, the reduction in deviator stress due to barrelling would be 2 kPa or less and is not simple to accurately calculate. These corrections were not applied to the triaxial shear data.

Due to the radial side drains, the filter paper restricts initial straining of the sample slightly so a correction was made to accommodate this initial restraint. This correction is only necessary up to an axial strain of 2 percent. For a 50 mm diameter specimen, Head (1998) suggests a total correction of 7 kPa be made to the deviator stress. This correction is applied in a linear manner such that the total reduction in deviator stress is proportional to the axial strain. Therefore, at 0, 1 and 2 percent axial strain, the correction is 0, 3.5 and 7 kPa, respectively. In retrospect, there were other errors at low strains due to sample seating that could not be corrected and therefore, correcting for restraint caused by the radial filter papers is almost a moot point and not necessary since the corrections are so small relative to the peak loads.

All other corrections suggested by Head (1998), including membrane corrections, single-plane slip corrections and volume change corrections were considered negligible.

Once the test was completed, the shear data required some corrections to account for such things as friction in the piston and load seating. Typically, the piston was lowered so that there was a barely visible space between the piston and loading cap. The axial load measured through this distance was taken as the piston friction, and was generally constant (as expected) and near or equal to zero. Furthermore, the top of the piston was firmly seated against the proving ring so that a zero load at the start of each test included the force of the cell pressure against the piston.

The axial strain was adjusted to account for the seating of the piston on the loading cap. Often following consolidation the axis of the sample was not entirely vertical, so that the piston was not perfectly centred over the loading cap at the start of shear. Therefore, the initial strain was due to the seating of the piston in the loading cap, and not the axial strain in the

sample. The load was considered to be fully seated (i.e. axial strain was adjusted to 0 percent) when a significant increase in pore pressure was noted (in the case of the undrained triaxial tests) or a significant change in volume was measured (in the case of the drained triaxial tests). Normally, seating occurred within a few tenths of a mm of vertical strain; when the consolidation was 400 kPa, sometimes seating did not occur until up to 1 mm or more of vertical strain. The data recorded for each test was considered individually in making these corrections and the best possible care and judgement was taken to ensure that the corrections were done with accuracy. However, data at low strains (<0.5 percent) may not be exact.

Kohata *et al.* (1997) suggest that bedding errors are significant when performing compression tests on cement-treated soils when the conventional method of measuring strain by displacement of the loading cap is used. Because of bedding error, the sample stiffness may be underestimated considerably. It is suggested that bedding error at the top and bottom of the sample can be caused by three main factors:

a)   a thin loose layer formed during specimen preparation;

b)   imperfect contact between specimen and rigid loading cap and pedestal;

c)   compression of lubrication layer when used.

For the current study, strain *was* measured by determining the displacement of the loading cap and any obvious bedding errors were corrected by simply adjusting the stress-strain curve. The best practice to eliminate bedding errors is to measure the sample strain using a separate LVDT attached directly onto the sample. This was not done for the current study and the effect of bedding error is not known, but is likely small based on the relatively large sample size.

4.5   Isotropic Consolidation Tests

Isotropic consolidation (IC) tests were conducted on one sample from every mix considered for the triaxial testing program, including 40 percent moisture content with no cement. With the exception of tests on samples with no cement, the size of the IC samples was 50 mm diameter and 50 mm high (1:1 ratio). The size was reduced from the triaxial samples to minimize the time required to reach secondary consolidation for each load phase. A second steel split-mould was machined to aid in the preparation of the IC samples. Samples with no cement were the same size as the triaxial samples.

Similar to the triaxial compression tests, saturation of the IC samples was done over a 36-hour period so that the final back pressure was 300 kPa and no stress increment was greater than 50 kPa. Following saturation, the consolidation phases were implemented in the following effective stress sequence: 50, 100, 200, 400, 200, 100, 50 and 10 kPa. Normally, each consolidation phase was 10 to 14 hours long. Between each phase, the back pressure valve was shut and the cell pressure increased (or decreased, as appropriate) and the pore pressure allowed to equalize before commencing the subsequent consolidation phase.

Effective stress, volume, and pore pressure were measured automatically using the computerized data acquisition system. The raw data was downloaded and appropriate plots were later generated using MS Excel.

For each isotropic consolidation phase, the coefficient of consolidation (c_{vi}) and coefficient of volume compressibility (m_{vi}) were calculated based on data extrapolated from the void ratio vs. pressure (e-ln p′) curves. Because radial drainage was not necessary for the IC tests, the equation for calculating c_{vi} is somewhat different than that used for consolidation of the triaxial samples. The equation for m_{vi} is essentially the same as that used for consolidation of triaxial samples. Based on Head (1998), the following equations were applied.

$$c_{vi} = \frac{0.199\overline{H}^2}{t_{50}} \quad (\text{m}^2/\text{year}) \qquad (4.5)$$

$$m_{vi} = \frac{\delta e}{\delta p'} \times \frac{1000}{1+e_1} \quad (m^2/MN)$$

<div align="right">(4.6)</div>

The consolidation yield stress (p_C), compression index (C_C) and swell index (C_s) were extracted from the consolidation curves. Often the unloading data was very poor and an accurate rebound curve could not be plotted. The poor data is likely because the cement bonds often failed during consolidation so that the volume change during unloading as compared with loading is very small.

All isotropic consolidation samples were photographed after the test was completed; these photographs are included in Appendix G.

4.6   Unconfined compression tests

Unconfined compression (UC) tests were conducted on all mixes and curing times considered for the triaxial tests, including samples with 40 and 50 percent moisture content and no cement. Tests were conducted using a standard CBR loading apparatus set for the British Standard loading rate of 1 mm/min. Tests were conducted on samples 50 mm in diameter by 100 mm in height; hence the strain rate was 1 percent/minute. The capacity of the proving ring on the loading apparatus was 2.0 kN.

Samples were prepared as per the triaxial tests, using the same steel split-mould and wax paper to aid in the trimming. In some cases where the quality of the sample was not adequate for triaxial tests, the sample was used for a UC test instead. When this was the case, the inferior sample quality was noted; voids indicating poor sample quality can be seen on the outside of some UC samples in the photographs included in Appendix G. Multiple tests were conducted on each mix and poor results were ignored.

All measurements were recorded by hand at appropriate displacement intervals so that a clear stress-strain plot could be produced showing the initial modulus as well as the peak and residual stresses.

During the tests, the samples were exposed to the air with no measures taken to prevent evaporation. Moisture contents were measured before (using sample trimmings) and after (using the entire failed sample)

the test to confirm that evaporation during the test was negligible (usually less than 1.5 percent). The majority of tests failed at an axial strain of less than 4.5 percent.

All UC samples were photographed at the end of the test; these photographs are included in Appendix G.

4.7 Oedometer Tests

Consolidation tests in the oedometer apparatus (one-dimensional consolidation) were conducted on one sample of every mix considered for the triaxial tests, as well as samples at moisture contents of 40, 50 and 70 percent, with no cement.

The oedometer apparatus consisted of two new ELE machines (Fig. 4.12). Samples were approximately 75 mm in diameter and 20 mm high. With the exception of the zero percent cement samples, all samples were prepared by simultaneously trimming the material and slowly and carefully pushing a lubricated consolidation ring horizontally into the cast sample, prepared as described in Section 4.3. A thin smear of silicone grease was used as a lubricant. Trimming of the sample was done using a combination of thin violin wire and a steel straight-edge to ensure a flat and relatively undisturbed surface. For the samples with no cement, the remoulded clay was compacted directly in the consolidation ring to minimize trimming and sample disturbance.

Each test took approximately two weeks. This allowed two tests to run concurrently as one test commenced each week. Both the top and bottom of the sample were fitted with filter paper and de-aired and saturated porous stones. The samples were submerged in distilled water in the consolidation cell. Normal loads were applied in the following sequence: 50, 100, 200, 400, 800, 1600, 3200, 800, 200, 50 and 10 kPa. Each load was applied for a minimum of approximately 24 hours to ensure completion of primary consolidation.

Prior to the start of the oedometer testing program, the two machines were calibrated separately to measure the natural bend in the lever arm when loaded with the appropriate mass. This displacement was subtracted from

the measured displacement during each consolidation phase when calculating the sample height (and hence void ratio) at the end of each load stage.

For each phase, plots of displacement vs. log time and displacement vs. root time were generated; from these, the coefficient of consolidation (c_v) was calculated following both the Casagrande and Taylor methods, respectively. Occasionally during the initial loading stage and for some unloading stages, the displacement vs. log time curves provided inadequate information at low time increments and it was impossible to calculate c_v following the Casagrande method.

For samples which have porous stones at the top and bottom, as is the case for the tests considered here, the following equations may be used to determine the coefficient of consolidation (c_v) and the coefficient of volume compressibility (m_v) of one-dimensional consolidation. Note that the expression for m_v is the same as that of m_{vi} for isotropic consolidation.

$$c_v = \frac{0.112\overline{H}^2}{t_{90}} \text{ (m}^2/\text{yr)} \qquad \text{(Taylor method)} \qquad (4.7)$$

$$c_v = \frac{0.026\overline{H}^2}{t_{50}} \text{ (m}^2/\text{yr)} \qquad \text{(Casagrande method)} \qquad (4.8)$$

$$m_v = \frac{\delta e}{\delta p'} \times \frac{1000}{1+e_1} \text{ (m}^2/\text{MN)} \qquad (4.9)$$

The consolidation yield stress (p_C), compression index (C_C) and swell index (C_s) were determined from the consolidation curves. Occasionally, as with the isotropic consolidation tests, the unloading data was poor and an accurate rebound curve could not be plotted.
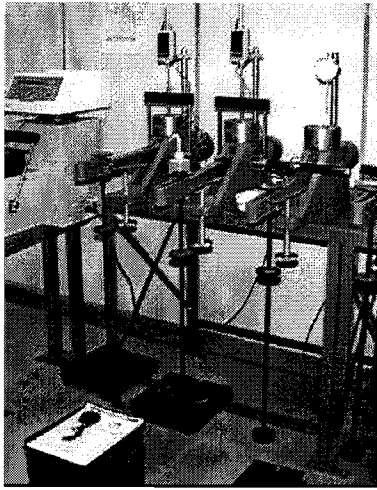
Figure 4.12.   Oedometer apparatus.

5.   KAOLIN AND KAOLIN-CEMENT STRENGTH CHARACTERISTICS

5.1   General

The discussion below considers both the isotropic consolidated triaxial drained and undrained (CID and CIU) compression test results as well as the unconfined compression (UC) test results. To examine the effects of excess pore water pressure, the stress ratio, η (q/p′) is considered for the case of the triaxial tests, which is particularly useful with respect to the undrained triaxial test results, where the excess pore water pressure is significant.

For the current series of triaxial tests, only two different cement contents were considered for each of two different moisture contents. This results in a total of four combinations of cement contents and moisture contents.   Due to the limited combinations considered, the cement to moisture content ratio will often be considered. Of the four mix combinations tested, two are considered to have a relatively low cement to moisture content ratio and two are considered to have a relatively intermediate cement to moisture content ratio. Mixes with a low cement to moisture content ratio include 2 percent cement and 70 percent moisture content as well as 5 percent cement and 100 percent moisture content; the cement to moisture content ratios for these mixes are 0.03 and 0.05, respectively. Mixes with an intermediate cement to moisture content ratio include 5 percent cement and 70 percent moisture content as well as 10 percent cement and 100 percent moisture content; the cement to moisture content ratios for these mixes are 0.07 and 0.1, respectively. It should be emphasised that these terms are intended to be meaningful only within the context of this report and are not meant to reflect the current practice outside the scope of this discussion. Babasaki *et al.* (1997) also suggest use of the cement to moisture content ratio as a meaningful index to compare soil-cement mixes.

Triaxial and unconfined compression tests were also conducted on samples of pure kaolin at 40 percent moisture content, with no cement. These results will be compared to those of the cement-treated samples.

For all triaxial tests, graphs of deviator stress (q) and stress ratio (η) were plotted against axial strain; stress path plots (q vs. p′) were also constructed. Axial strain was plotted against volumetric strain and excess

pore water pressure for the drained and undrained triaxial tests, respectively. Plots were compared to understand the independent effects of curing time, cement and moisture content and confining pressure. While some test results may be unreasonable due to poor sample preparation or sample disturbance, clear general trends were illustrated.

Cohesion and friction angle were determined from stress path plots (t vs. s') for the drained triaxial test results. Peak conditions were interpreted as the point where σ_1'/σ_3' was a maximum; this corresponds to the maximum stress ratio, η_{max}, and is the interpretation generally accepted in practice. An alternative to this approach is to take the peak conditions as the axial strain when the maximum deviator stress, q_{max}, is achieved. For more than half of the tests, these two points are coincident. However, occasionally q_{max} occurred at a different axial strain than η_{max}. When this occurred, it was most often during the undrained tests and normally q_{max} was reached before η_{max}, which usually corresponded to peak excess pore water pressure.

It is not believed that residual conditions were achieved during the triaxial tests due to the bonding effects and the extremely high strains required. The fully-softened condition, which occurs following peak when the deviator stress is approximately constant, is considered instead. In many cases, the trends in the fully-softened stress are vague or difficult to interpret; this is likely due to inaccurate stress calculations at large strains, when lateral deformations are significant.

Results of the triaxial tests are also briefly discussed within a critical state framework in Chapter 8.

5.2   Consolidated Drained Triaxial Test Results

The following discussion is an interpretation of the results of the isotropically consolidated drained (CID) triaxial compression tests. Graphs generated for these tests can be found in Appendix A. The effects of curing time are illustrated in Figures A.1 to A.12. Figures A.13 to A.24 show the effects cement and moisture content. The effects of confining pressure are illustrated in Figures A.25 to A.40. Stress path plots used to derive Mohr-Coulomb failure parameters are provided in Figures A.41 to A.56.

5.2.1 Deviator Stress and Stress Ratio

The peak deviator stress and peak stress ratio for each drained triaxial test was plotted against curing time for all mixes considered (Fig. 5.1). Fully-softened values were also plotted (Fig. 5.2). For all drained triaxial tests performed, the maximum peak deviator stress was 1425 kPa; this was achieved when the cement and moisture content were 10 and 100 percent, respectively, at a confining pressure of 400 kPa and curing times of 28 days or more. The maximum peak deviator stress for the pure kaolin at 40 percent moisture content and 400 kPa confining pressure was approximately 660 kPa.

5.2.1.1   Effect of Curing Time

Based on the test results, the patterns in peak stress with curing time are most clearly interpreted at greater cement contents. Furthermore, the trends are more easily recognizable at low confining pressures as opposed to high confining pressures, as confining pressure greatly influences the results.

The peak deviator stress and the peak stress ratio are expected to increase with curing time, at a decreasing rate. However, the results presented herein show that this is not always the case (Fig. 5.1), and frequently, the peak strength was found to decrease following 28 days or 56 days of curing. This reduction in strength was most common at low cement contents and/or low moisture contents (i.e. 70 percent). For the samples with 70 percent moisture content, compacting the samples in lifts, which was not the case for the samples with 100 percent moisture content, may be an influencing factor. At high cement contents, there was typically no further gain in strength following 56 days of curing.

When examining only the fully-softened values, there is no predictable pattern in the fully-softened strength with curing time (Fig. 5.2); this is likely due to significant lateral deformation at large strains. However, when examining the stress-strain curves for tests on the same mix at the same confining pressure, each curve seems to *approach* a common value at fully-softened conditions, regardless of curing time (Fig. 5.3). This is particularly true at higher confining pressures when cement bonds have failed during

consolidation. Therefore, it is concluded that curing time does not influence the fully-softened strength.

5.2.1.2   Effect of Cement Content and Moisture Content

As expected, an increase in the cement to moisture content ratio leads to an increase in peak deviator stress and peak stress ratio (Fig. 5.1). The only test when this was not the case is at 400 kPa confining pressure for the sample with a moisture content of 70 percent, cement content of 5 percent and curing time of 56 days; poor test results are likely the reason for this anomaly. An increase in strength with cement content is a general concept of soil-cement and has been proven in literature by many (i.e. Uddin, 1995) and is seen in the current study.

In general, the fully-softened deviator stress and fully-softened stress ratio are a function of cement content. When the confining pressure is low, the fully-softened strength usually increases with cement content (Fig. 5.4a). However, at a confining pressure of 400 kPa, many of the cement bonds have failed during consolidation and the kaolin-cement behaves more like an un-bonded material, particularly at high strains, when the fully-softened stress is roughly the same for all cement contents (Fig. 5.4b). Based on the limited test results, it is suggested that the moisture content does not influence the fully-softened strength.

Results of tests on pure kaolin are also included in Figures 5.1, 5.2 and 5.4. As illustrated, without cement, the peak deviator stress of kaolin is significantly less than with cement. However, the fully-softened strength at 2 percent cement is very close to the strength without cement.
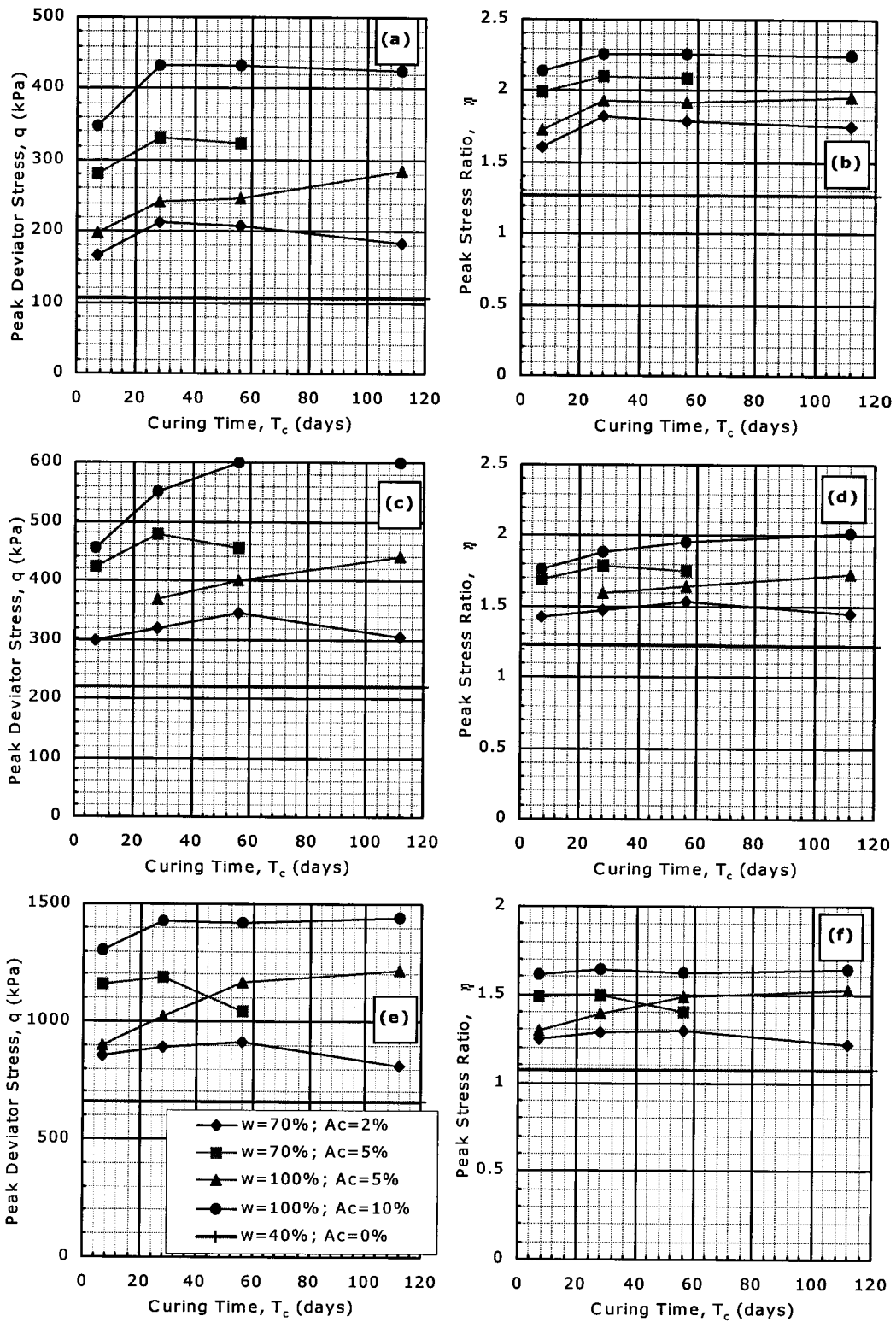
Figure 5.1. Peak deviator stress and stress ratio vs. curing time for CID triaxial tests at confining pressures of (a) & (b) 50 kPa; (c) & (d) 100 kPa; (e) & (f) 400 kPa.
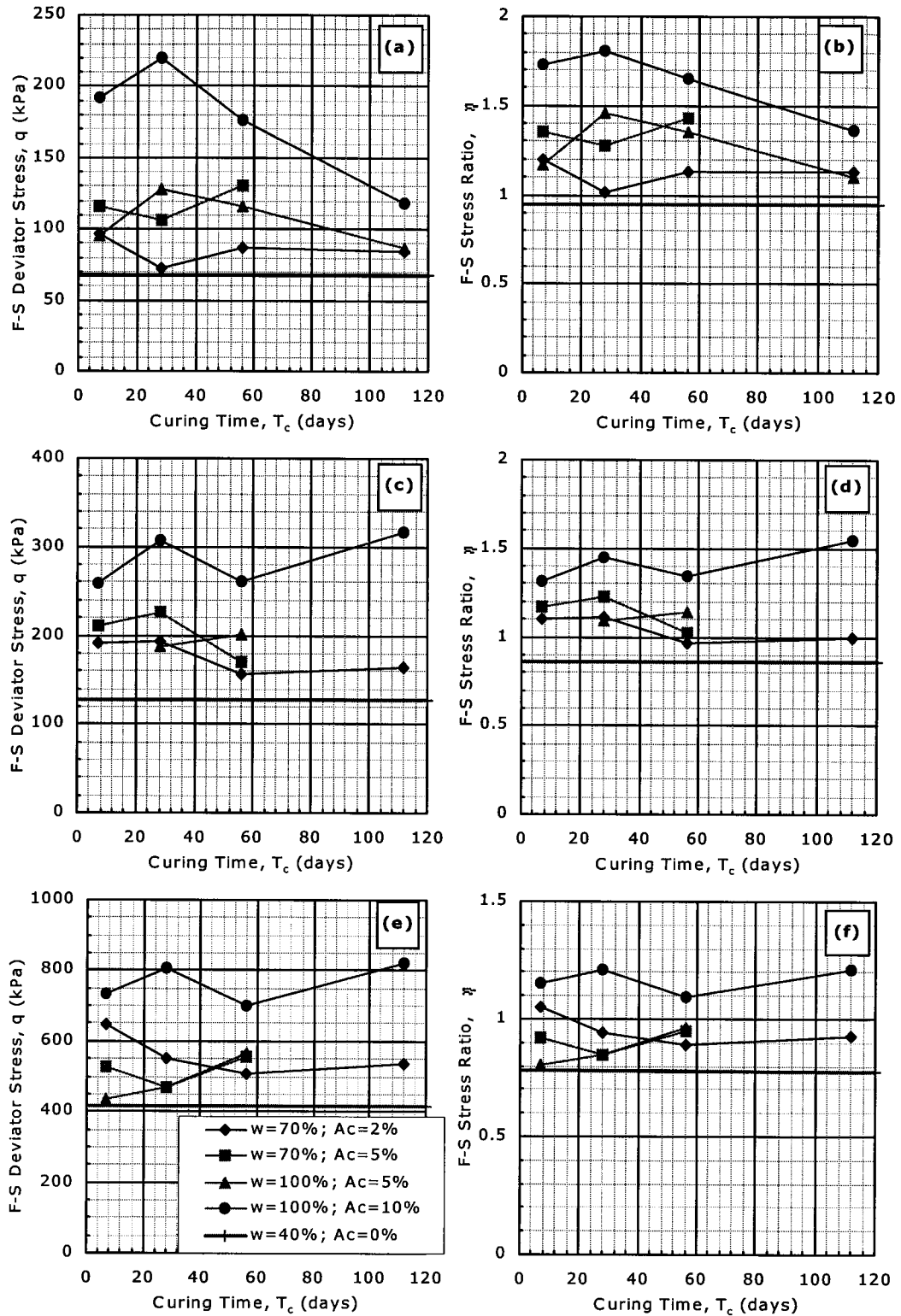
Figure 5.2. Fully-softened deviator stress and stress ratio vs. curing time for CID triaxial tests at confining pressures of (a) & (b) 50 kPa; (c) & (d) 100 kPa; (e) & (f) 400 kPa.
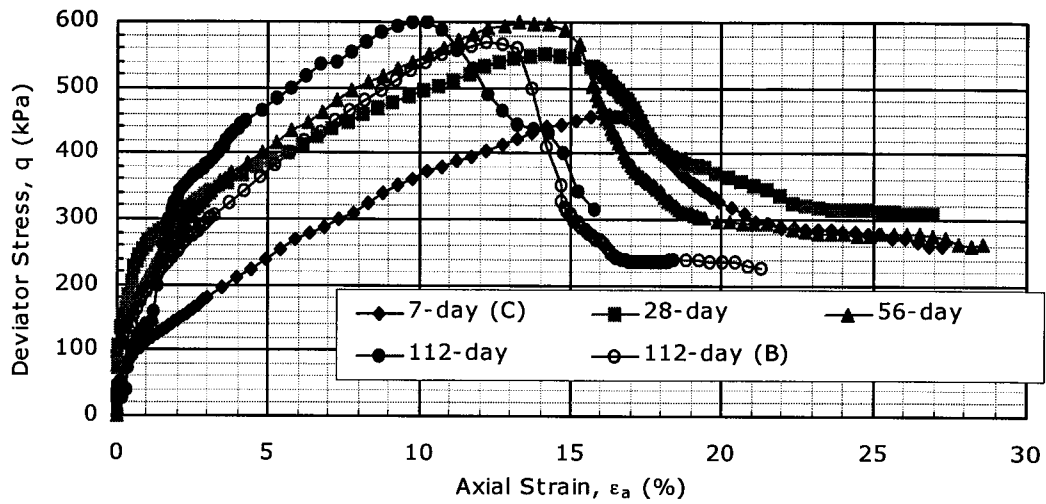
Figure 5.3. q vs. ε_a for w=100%, A_c=10% & $p_o{'}$=100 kPa (CID).

Figure 5.4. q vs. ε_a for T_c=56 days (CID) (a) $p_o{'}$=50 kPa; (b) $p_o{'}$=400 kPa.

Mechanical Characteristics of Kaolin-Cement Mixture   71
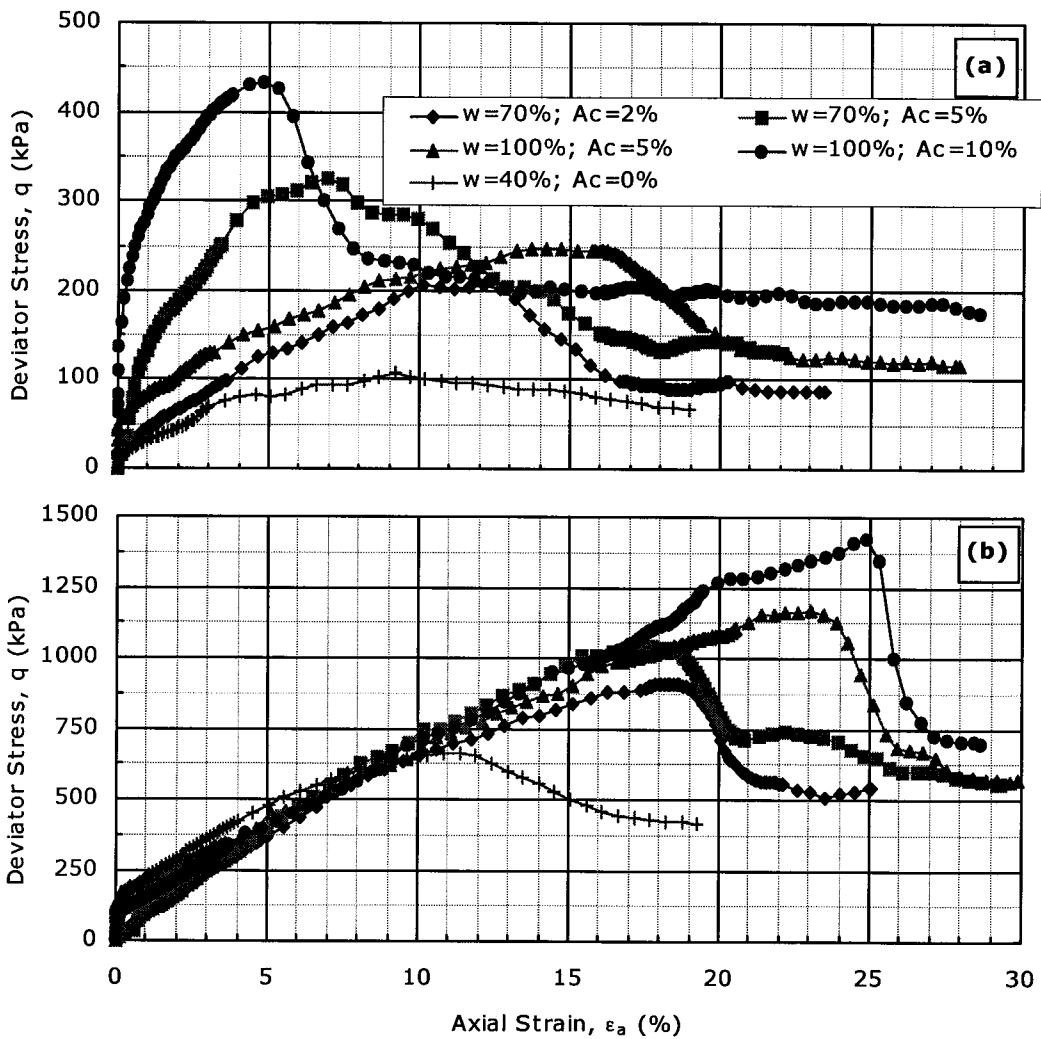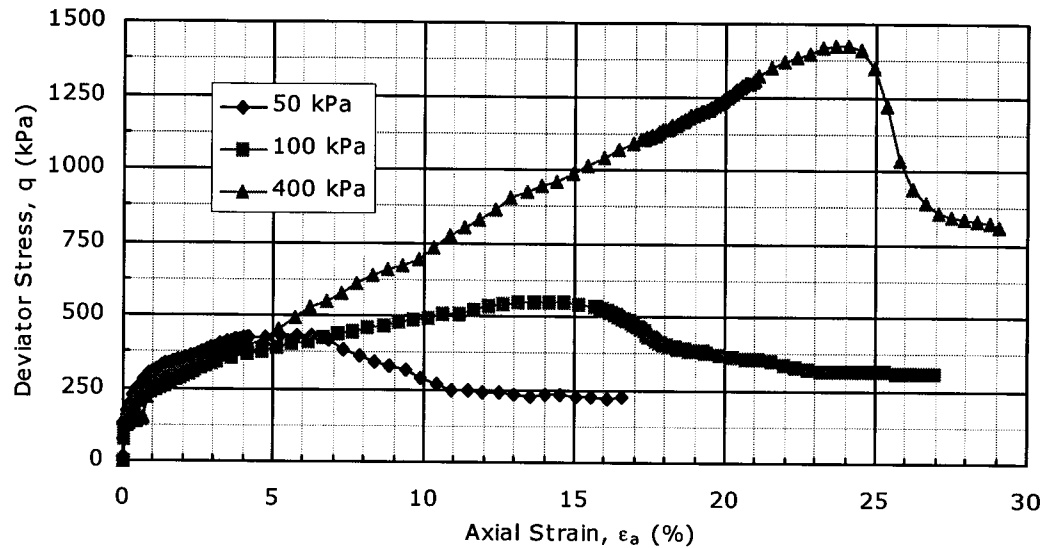
Figure 5.5. q vs. ε_a for w=100%, A_c=10% & T_c=28 days (CID).

5.2.1.3 Effect of Confining Pressure

It has been reported by several authors (i.e. Tatsuoka and Kobayashi, 1983; Kawasaki et al., 1984) that as confining pressure increases, the peak deviator stress increases (Fig. 5.5) and the peak stress ratio decreases. This was found to be true for all cases considered herein, including pure kaolin without cement. The same trend was observed in the fully-softened values.

5.2.2 Axial Strain at Peak Conditions and Material Consistency

The axial strain at peak conditions for the drained triaxial tests ranges between roughly 4 and 25 percent. It is interesting to note that both the minimum and maximum values were from tests on the samples with the maximum cement content considered of 10 percent, and only the confining pressure is different. Note that the shear data was corrected to account for initial straining during seating of the load; therefore, often the load is positive at zero strain.

5.2.2.1 Effect of Curing Time

At low confining pressures (i.e. 50 and 100 kPa), the axial strain corresponding to peak conditions decreases with an increase in curing time (Fig. 5.3). However, the opposite is true at high confining pressures (i.e. 400 kPa), when the axial strain corresponding to peak conditions *increases* with curing time, up to at least 56 days (Fig. 5.6). The first observation is an indication of an increase in the material stiffness with curing time. However, at higher confining pressures, the material stiffness is governed by the confining pressure and is independent of curing time. Therefore, the axial strain is directly related to the material strength, which sometimes deteriorates with curing time. Furthermore, the axial strain at peak stress conditions is directly related to the corresponding volumetric strain, and the volumetric strain during drained shear is a function of the volume change during consolidation. At high confining pressures, cement bonds can fail during consolidation. Therefore, as the cement bonds strengthen with curing time, the volume change during consolidation under high pressures decreases and the capacity of the material to strain during shear increases.
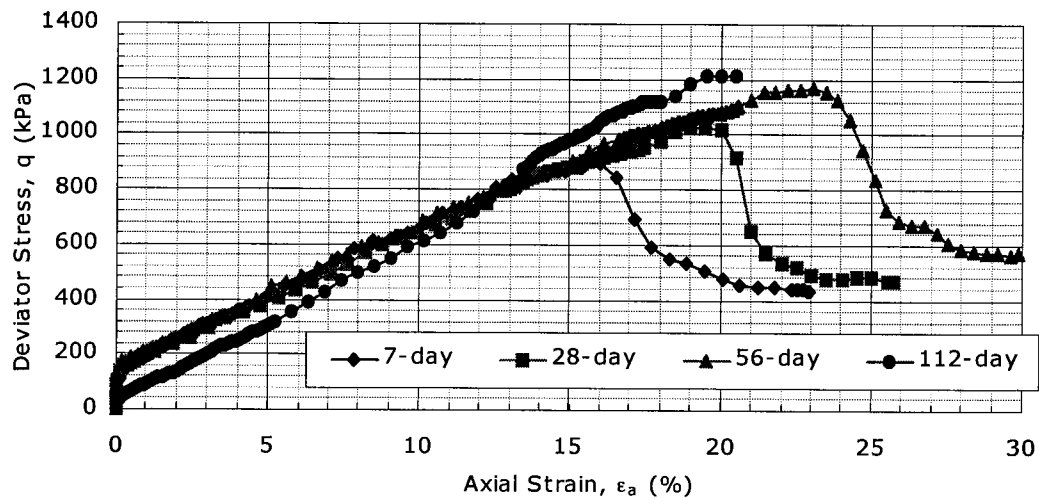
Figure 5.6. q vs. ε_a for w=100%, A_c=5% & $p_o{'}$=400 (CID).

5.2.2.2 Effect of Cement Content and Moisture Content

Just as curing time increases the material's stiffness, so does the cement to moisture content ratio; the trends in the axial strain at peak stress conditions

are exactly the same. At 50 kPa confining pressure, the axial strain at peak conditions decreases with an increase in the cement to moisture content ratio (Fig. 5.4a); this is an indication of an increase in the material's stiffness. As confining pressure increases to 400 kPa, the opposite trend occurs; the axial strain is directly related to the material's strength and the material's stiffness is governed by confining pressure (Fig. 5.4b). When pure kaolin is considered, cementation effects are irrelevant and the behaviour is only a function of the moisture content. At 400 kPa confining pressure, pure kaolin has the same stiffness as the cemented material but fails at a much lower axial strain due to its reduced strength (Fig. 5.4b).

5.2.2.3   Effect of Confining Pressure

An increase in confining pressure reduces the material's stiffness and therefore, the axial strain at peak stress conditions always increases with an increase in confining pressure (Fig. 5.5). This trend is more apparent as the cement to moisture content ratio increases. Without cement, the axial strain at peak stress conditions increases only very slightly with an increase in confining pressure.

5.2.3 Volumetric Strain

The volumetric strain during drained shear is expressed as a percentage relative to the volume of the sample following consolidation. Furthermore, it is a function of the volume change during consolidation and is therefore strongly influenced by the confining pressure. For the drained triaxial tests on kaolin-cement, the volumetric strain is always negative and following peak stress conditions, behaviour is usually slightly dilative, more-so at high cement contents and lower confining pressures. While the stress-strain curves may indicate over-consolidated behaviour due to the clear peak and strain-softening behaviour, the volumetric strain curves indicate primarily contractive behaviour, with some tests at sufficiently high cement to moisture content ratios exhibiting slightly dilative behaviour. Furthermore, different from the behaviour of over-consolidated clay, dilation of kaolin-cement does not occur until peak stress conditions are achieved, at relatively large axial

strains. These are important observations on the behaviour of kaolin-cement which make it fundamentally different from typical over-consolidated clay. Kohata *et al.* (1997) report that cement-treated soil does behave as an over-consolidated material, and found positive dilatancy from the early stages of shearing. However most of the tests reported by Kohata *et al.* were on cement-treated sand, which may explain the discrepancies from the current data.

The volumetric strain was calculated to be as great as 20 percent for some tests at 100 percent moisture content and 400 kPa confining pressure. When pure kaolin with a moisture content of 40 percent is considered, the volumetric strain becomes positive after peak stress conditions at a confining pressure of 50 kPa, indicating over-consolidated behaviour. Most kaolin-cement samples dilated slightly following peak stress conditions; without cement, dilation was much greater and normally began prior to peak. The difference in behaviour between kaolin-cement and pure kaolin may be a function of the curing environment; pure kaolin samples were tested immediately following casting.

5.2.3.1   Effect of Curing Time

It is observed that curing time has only a small effect on the volumetric strain of the drained triaxial tests, particularly at high confining pressures. In general, as curing time increases, the volumetric stain during shear decreases. This trend is most clear at 50 kPa confining pressure and 100 percent moisture content (Fig. 5.7). Occasionally the trend is somewhat reversed and the volume change is greatest after at least 56 days of curing; this phenomenon is likely due to a weakening of the cementation effects after a particular curing time. When this was observed, greater volume change is often, but not always, associated with a reduction in strength.

Most samples dilated slightly following peak stress conditions; samples cured for greater curing times tended to dilate more. This is because as the strength of the cement bonds increases, the material is able to dilate instead of crush during shear (Wissa and Ladd, 1964). Occasionally, when the curing time was only 7 days, some samples continued to contract following peak but at a slower rate than prior to peak, while samples of the same mixture but

greater curing times dilated once peak had occurred. Contraction also continued following peak stress conditions for the occasional sample with a curing time greater than 7 days. In these cases, premature brittle failure may have occurred, or it may simply be an indication of normally consolidated behaviour.
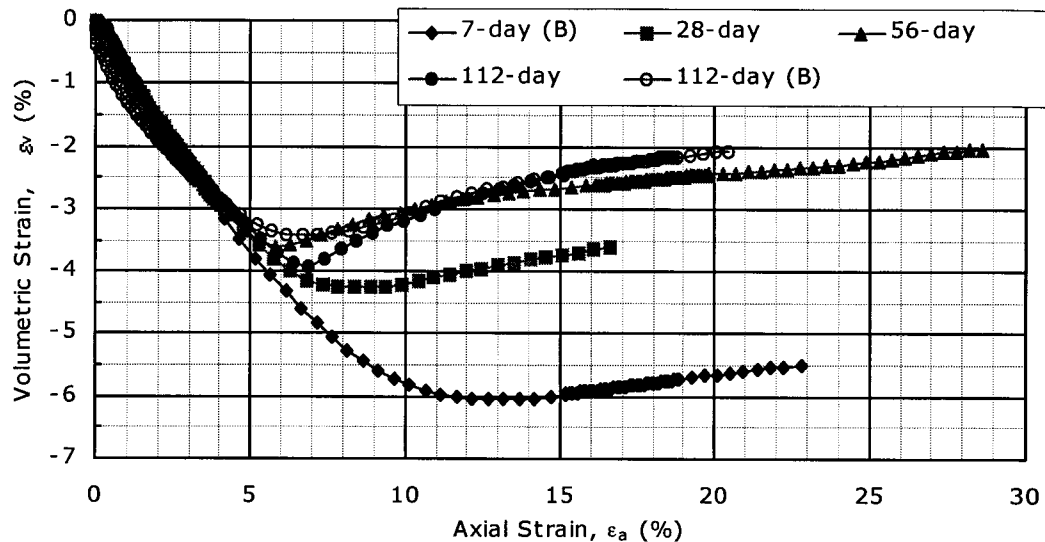
Figure 5.7. ε_v vs. ε_a for w=100%, A_c=10% & $p_o{}'$=50 kPa (CID).

5.2.3.2   Effect of Cement Content and Moisture Content

Based on the test results, it is observed that the volumetric strain is not a function of the cement to moisture content ratio, but instead, a function of the cement and moisture content, individually. Regardless of the confining pressure, greater volumetric strain is associated with greater moisture contents. The relationship between cement content and volumetric strain, however, is not so simple. Confining pressure has significant control over the volume change during shear, and so the effect of cement content on the volumetric strain is a function of confining pressure.

At a confining pressure of only 50 kPa, the volumetric strain decreases with an increase in cement content (Fig. 5.8a). This result is expected since a greater amount of cement will result in stronger and/or more frequent bonds and hence, less deformation occurs during shear. However, at 100 and 400 kPa confining pressure, the opposite is true: the volumetric strain *increases* with an increase in cement content (Fig. 5.8b). To understand this

phenomenon the volume change during consolidation must be considered, as well as the degree/strength of cementation. Volume change during consolidation is greater at low cement contents and high moisture contents (i.e. low cement to moisture content ratios), and can be significantly greater when the consolidation pressure is high enough to cause bonds to fail in very weakly cemented material. Furthermore, volume change during consolidation is directly related to the consolidation pressure, and when significant volume change occurs during consolidation, there is less potential for volume change during shear. Therefore, more volume change can be expected during shear as the cement content increases and the moisture content decreases, particularly at high confining pressures.

When no cement is present and the moisture content is 40 percent, volumetric strain during consolidation *and* shear is smaller than when cement is present at higher moisture contents. This pattern, however, is mostly due to the lower void ratio associated with a lower moisture content. It is difficult to make an accurate comparison between samples with and without cement when the moisture content is different. However, effective cementation will reduce the volume change during consolidation, thereby increasing the potential for volume change during shear.

As shown in the volumetric strain vs. axial strain plots in Appendix A, all samples with cement contract up to an axial strain either coincident or slightly beyond that corresponding to the peak stress. When cement is not present, contraction continues up to an axial strain slightly less than that corresponding to peak stress. The majority of samples dilated following peak stress conditions; the degree of dilation is generally greatest at 50 kPa confining pressure and high cement contents. These samples exhibited the smallest amount of volume change during shear. When no cement is present and the moisture content is 40 percent, dilation begins just prior to peak stress conditions, and at a confining pressure of 50 kPa, it continues until the volumetric strain is positive. It can be said that cement retards the change from contraction to dilation during drained shear tests.
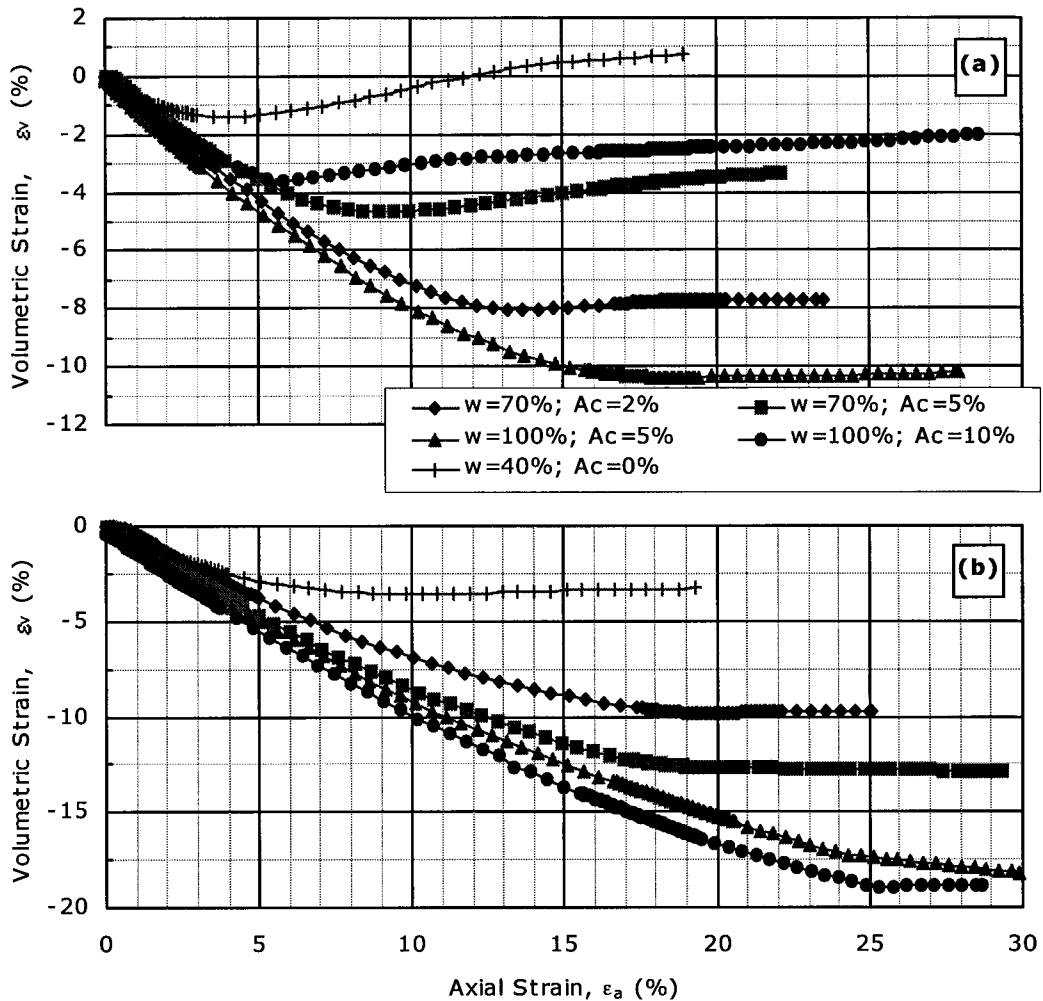
Figure 5.8. ε_v vs. ε_a for T_c=56 days (CID) (a) $p_o{}'$=50 kPa; (b) $p_o{}'$=400 kPa.

5.2.3.3 Effect of Confining Pressure

Confining pressure has the greatest influence over volumetric strain out of all the factors discussed. It is clear that as confining pressure increases, so does the volumetric strain (Fig. 5.9). Other authors (i.e. Uddin, 1995; Porbaha *et al.*, 2000) support these findings, stating that there is greater contraction at failure with increasing confining pressure.

Low confining pressures also increase the tendency for the sample to dilate following shear. In most cases, when contraction continued following peak deviator stress, the confining pressure was 400 kPa. When this trend was observed at only 100 kPa confining pressure, the contraction following peak conditions was very slight.
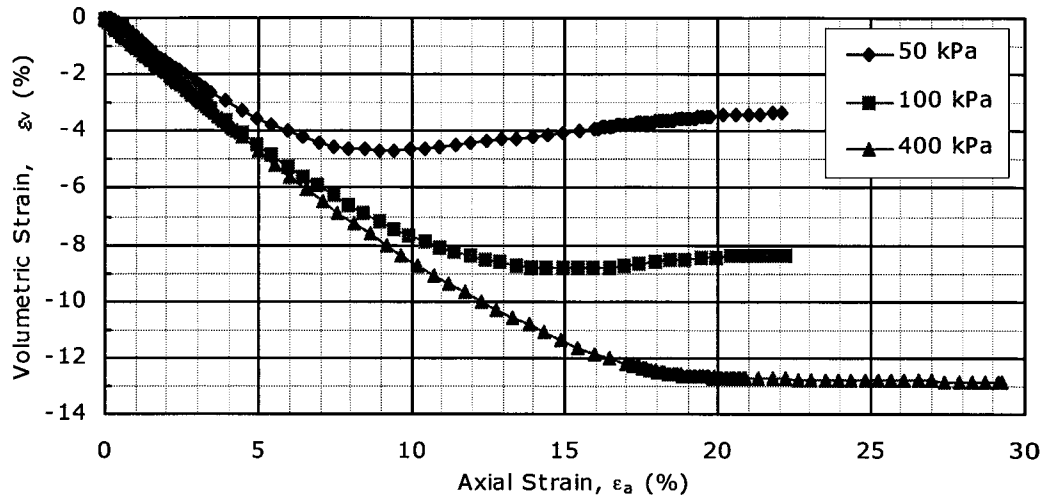
Figure 5.9. ε_v vs. ε_a for w=70%, A_c=5% & T_c=56 kPa (CID).

5.2.4 Mohr-Coulomb Failure Criteria: Cohesion and Friction Angle

Kohata *et al.* (1997) state that the Mohr-Coulomb failure criterion is applicable to cement-treated soil and verified that effective stress analysis is appropriate. Wissa and Ladd (1964) found that the effective friction angle was constant up to at least 55 kg/cm^2 ($\approx$5500 kPa). Authors such as Uddin (1995), however, found the failure envelope to be slightly curved so that as confining pressure increased, the effectiveness of the cementation was reduced; such a failure envelope is often applied to soft rock. Based on the range of confining pressures considered for the current study, a linear failure envelope, with a constant cohesion and friction angle, was found to be most appropriate when considering the drained test results (Fig. 5.10). However, due to some unreasonable trends which will be discussed in the following sub-sections, it may be that that the failure envelope *is* curved, but within the low and narrow range of confining pressures considered, it only *appears* linear. This means that under some circumstances, cohesion and friction angle will influence one another, and the friction angle will be lower and the cohesion higher than they would be at higher confining pressures since they are being measured from the initial and curved portion of the failure envelope.

The cohesion and friction angle (peak and fully-softened values) for each mixture considered were derived from the drained effective stress path

plots (i.e. t and s′, describing the MIT stress field). These effective stress path plots are provided in Appendix A (Figs. A.41 to A.56).

The following equations were used to calculate effective cohesion, c′, and effective friction angle, φ′, from the t-intercept, a′, and the angle of the t-s′ envelope, α′.

$$\phi' = \sin^{-1}(\tan \alpha')$$ (5.1)

$$c' = \frac{a'}{\cos \phi'}$$ (5.2)
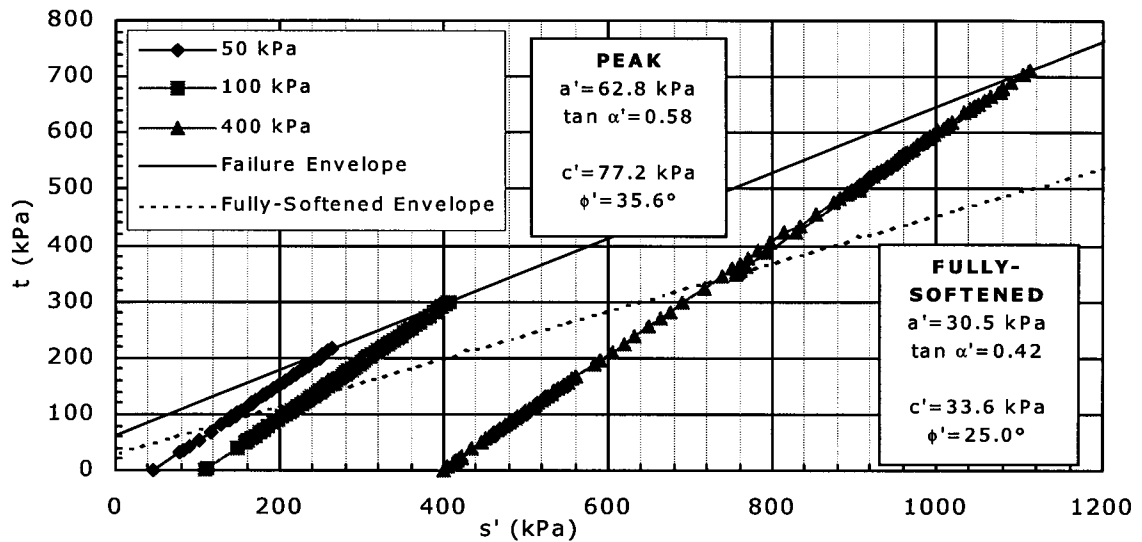
Figure 5.10. t-s' plot for w=100%, A_c=10% & T_c=56 days.

5.2.4.1   Effect of Curing Time

Based on the behaviour of concrete and reports by other authors (i.e. Uddin, 1995), the peak cohesion of soil-cement is expected to increase with curing time at a decreasing rate. Uddin found that peak friction angle also increases with curing time, however, this may be related to a humid curing environment; Wissa and Ladd (1964) reported peak friction angle and curing time to be independent of one another.

For the current study, at intermediate cement to moisture content ratios, an increase in curing time up to at least 56 days caused an increase in

peak cohesion, at a decreasing rate (Fig. 5.11a), and a decrease in peak friction angle (Fig. 5.12a); after 56 days of curing, the trends reversed when the cement content was 10 percent[2] indicating some deterioration in strength. Furthermore, when the cement content was at least 5 percent, a sharp decrease in peak cohesion is usually associated with a sharp increase in peak friction angle. These observations lead to the suggestion that cohesion and friction angle influence one another and the failure envelope may actually be curved. Uddin found that a curved failure envelope was most appropriate based on results of drained triaxial tests up to a maximum confining pressure of 2000 kPa. The failure envelope *appears* linear over the relatively narrow range of confining pressures considered, however, with a maximum confining pressure of only 400 kPa, the failure envelope may actually represent a small portion of a curved failure envelope. This suggestion is based on very limited test results.

When the cement content is only 2 percent, the majority of the improvement in cohesion occurs between 28 and 56 days of curing and the peak friction angle is nearly constant until it deteriorates following 112 days of curing. These trends are not reasonable as compared with the results at higher cement contents. An increase in cohesion is a result of cementation (Sivapullaiah *et al.*, 2000); it is concluded that when the cement content is low (i.e. 2 percent), there is very little cementation and most of the cohesion is a result of the clay particles. Furthermore, there is very little improvement with curing time. It is appropriate to note here the low pH measured for the material with only 2 percent cement; the initial pH was only 12.3. According to Bergado *et al.*, (1996), when the pH is less than 12.6, cementation is weaker than when the pH is above this value. This is because of the favoured production of CSH, a weaker cementitious material than the more typical $C_2S_2H_x$, when the pH is low.

In general, the cement to moisture content ratios considered in the current study are relatively low compared to those considered by other authors and the mixes used in DM design. Furthermore, the stabilized material, kaolin, is a manufactured soil containing no coarse-grained material. These two conditions contribute to a reduced improvement from cement

---

[2] Data not available for w=70% and A_c=5% after 112 days of curing.

treatment. Furthermore, the curing environment also contributes to the properties of the cured material. Uddin (1995) suggests that the reduction in moisture content that occurs during curing in a humid environment is a possible explanation for the particle flocculation and the resulting improvement in strength with curing. However, for the current study, samples were cured in water and the moisture content actually increased slightly up to 56 days of curing or stayed approximately the same with curing time (Fig. 5.13). Therefore, according to Uddin's theory, particle flocculation and the resulting increase in strength may be less when the samples are cured in water. In fact, based on the decreasing pH of the pore water with curing (Fig. 5.14), which is typical of aging soils (Mitchell, 1993), the soil structure is expected to become *less* flocculated with curing. This theory is supported by a slight increase in void ratio with curing time (Fig. 5.15). Sivapullaiah *et al.* (2000) state that the peak friction angle is directly related to the degree of flocculation. The reduction in friction angle with curing time, may, therefore, be due to a reduction in flocculation associated with decreasing pH and void ratio.

The fully-softened Mohr-Coulomb parameters are illustrated in Figures 5.11b and 5.12b. While cohesion is destroyed at residual conditions so that the residual strength is purely frictional (Uddin, 1995), the test results suggest that cohesion is not entirely destroyed at fully-softened conditions. In general, the fully-softened cohesion increases slightly initially and then decreases after 28 days so that the value after 56 days is almost the same as that after 7 days. Therefore, it is concluded that the fully-softened cohesion does not change with curing time. The same observation was made of the fully-softened deviator stress. There is no clear trend in the fully-softened friction angle with curing time; between 7 and 112 days of curing, the fully-softened friction angle did not change more than 4° for any mixture. After 56 days of curing, the fully-softened friction angle for all mixtures was roughly the same, at between 22° and 25°. As noted in the discussion of fully-softened stress, significant lateral deformation at large strains makes it difficult to accurately calculate the fully-softened stress so that the fully-softened Mohr-Coulomb parameters may also be inaccurate.
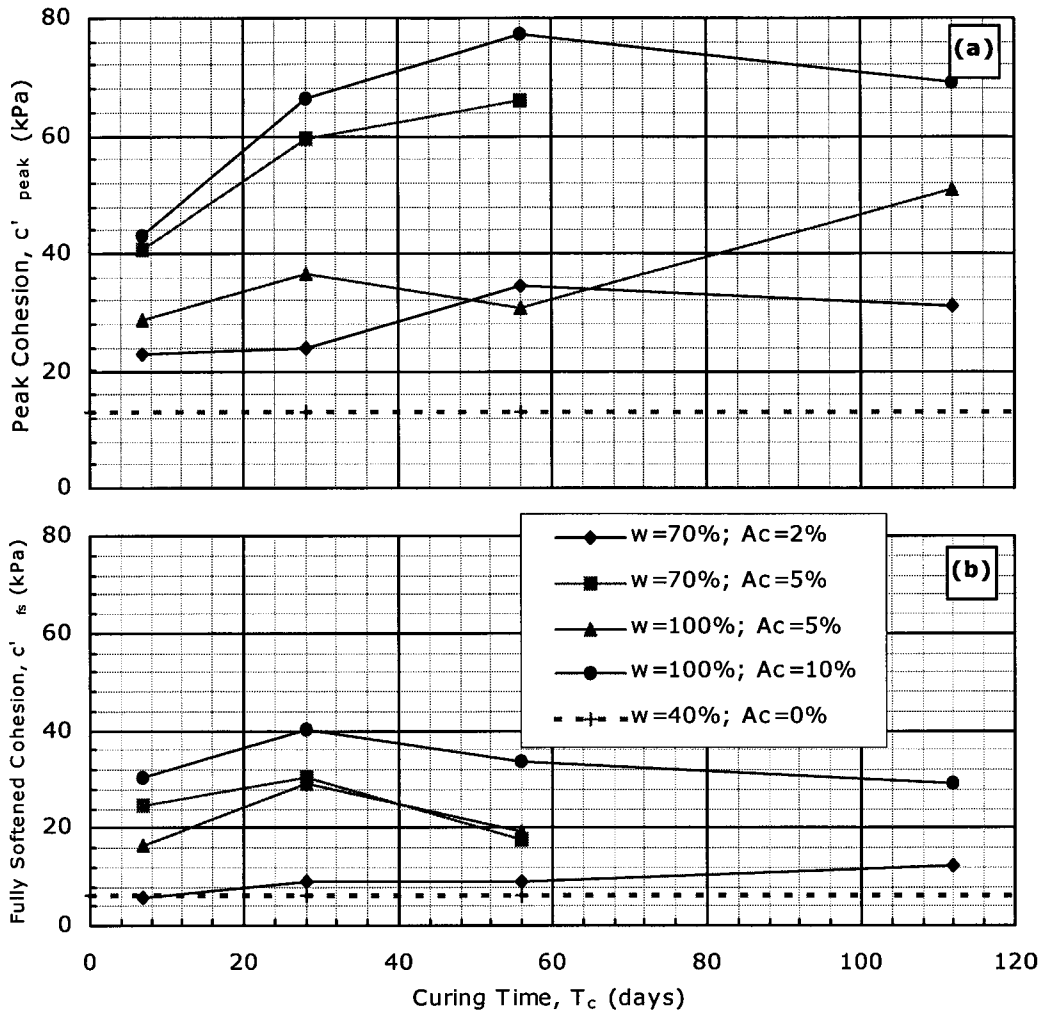
Figure 5.11. Effective cohesion vs. curing time (a) peak; (b) fully-softened.

5.2.4.2 Effect of Cement Content and Moisture Content

Wissa and Ladd (1964) found that moisture content does not affect friction angle. Kézdi (1979) also observed that there exists a cement content beyond which the peak cohesion will not continue to increase; this maximum value depends on the soil type. The increase in cohesion with cement content is due to increased cementation. The increase in friction angle is due to the increased flocculation that accompanies the addition of cement.

For the current study, as the cement to moisture content ratio increased, so did the peak cohesion and peak friction angle (Fig. 5.11a and 5.12a); this agrees with reports in literature (i.e. Uddin, 1995; Kézdi, 1979). An anomaly occurs after 56 days for the material with 100 percent moisture

content and 5 percent content whereby a sharp decrease in peak cohesion is associated with a sharp increase in peak friction angle. As discussed previously, it is suspected that the failure envelope may actually be curved over the relatively low and narrow range of confining pressures considered. Therefore, cohesion and friction angle influence one another. For the case just mentioned, the peak friction angle increased at the expense of peak cohesion.

The fully-softened cohesion typically increased with cement content and was independent of moisture content (Fig. 5.11b). The same observations were made of the fully-softened deviator stress.

Contrary to the trend in peak friction angle, the fully-softened friction angle does not increase with the cement to moisture content ratio (Fig. 5.12b). The mixture with the lowest cement to moisture content ratio has nearly the same fully-softened friction angle as that of the mixture with the highest cement to moisture content ratio. Similar to the fully-softened cohesion, the fully-softened friction angle is nearly the same for both mixtures with 5 percent cement content, regardless of the moisture content. As already discussed, significant lateral deformation at large strains makes it difficult to accurately calculate fully-softened values.

It is interesting to note the difference between the Mohr-Coulomb parameters for the cemented materials to those of the pure kaolin at 40 percent moisture content. Obviously, cement is not a factor so the cohesion and friction angle are influenced only by the clay particles. The peak cohesion of the pure kaolin is roughly half that of the kaolin-cement with only 2 percent cement. However, the fully-softened cohesion is nearly the same for these two mixtures, suggesting that at very low cement contents, cementation is destroyed when the fully-softened condition is achieved.
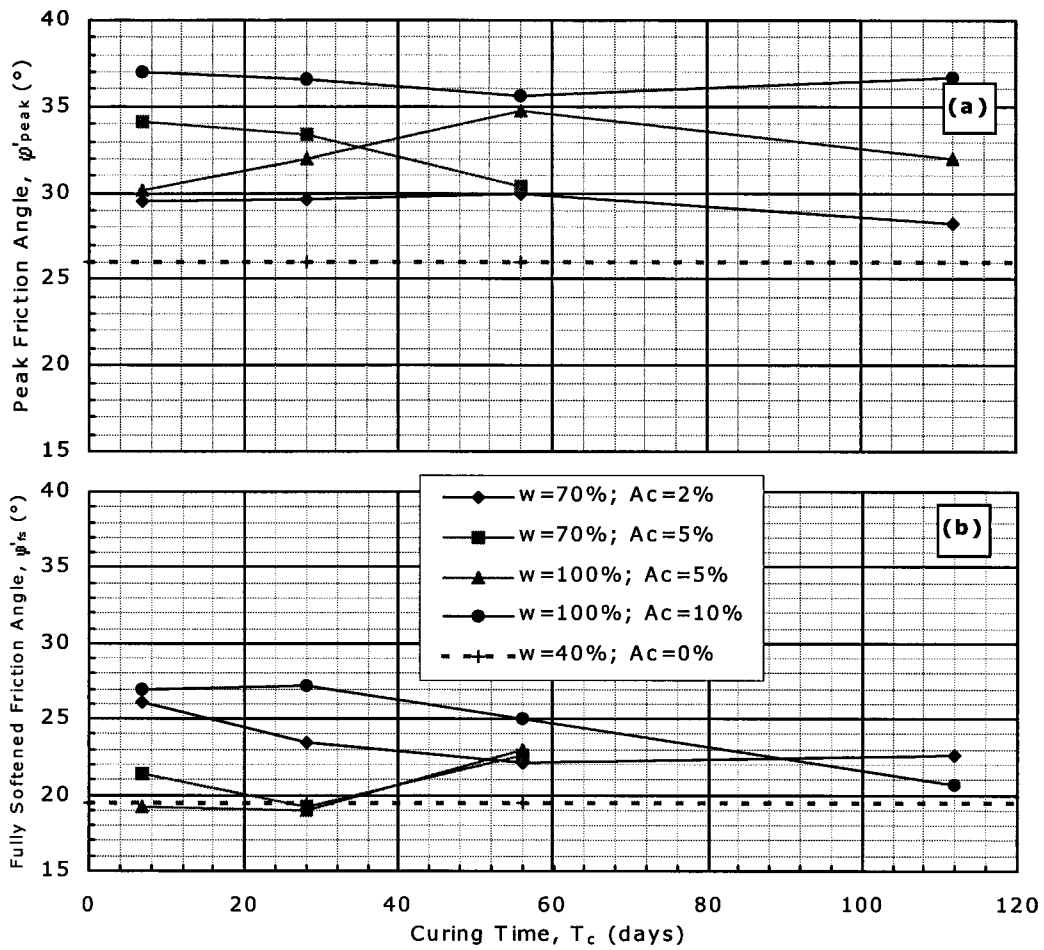
Figure 5.12.   Effective friction angle vs. curing time (a) peak; (b) fully-softened.
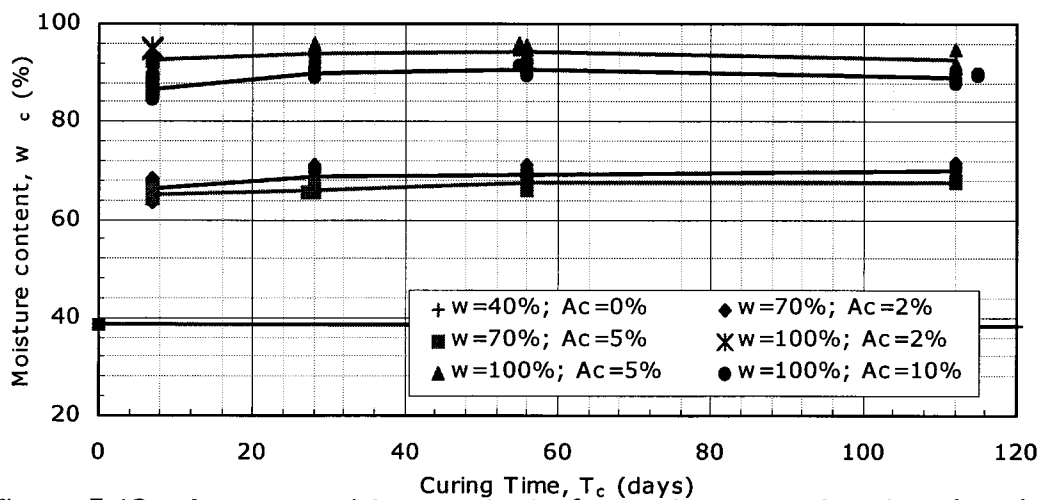
Figure 5.13.   Average moisture content after curing vs. curing time (results include all successful laboratory tests).
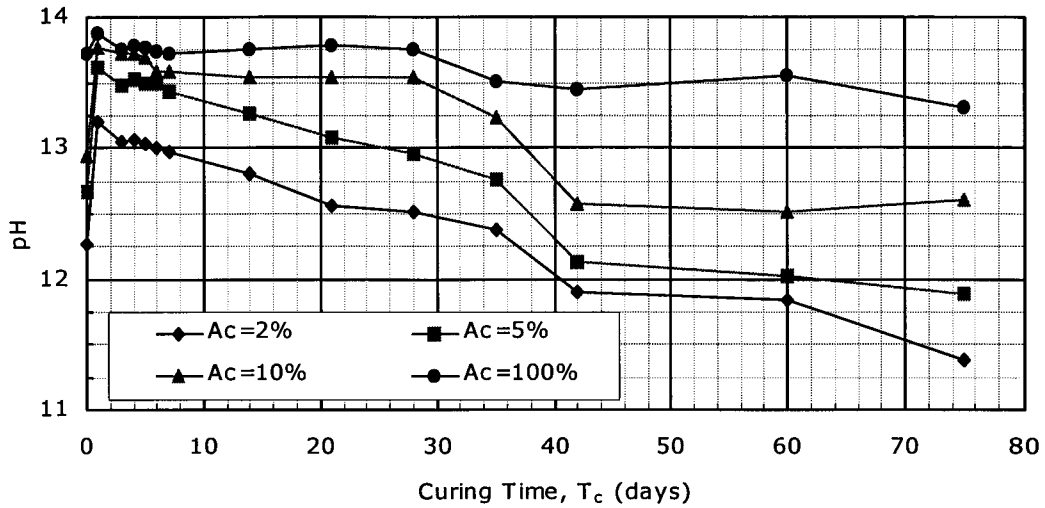
Figure 5.14. pH vs. curing time.
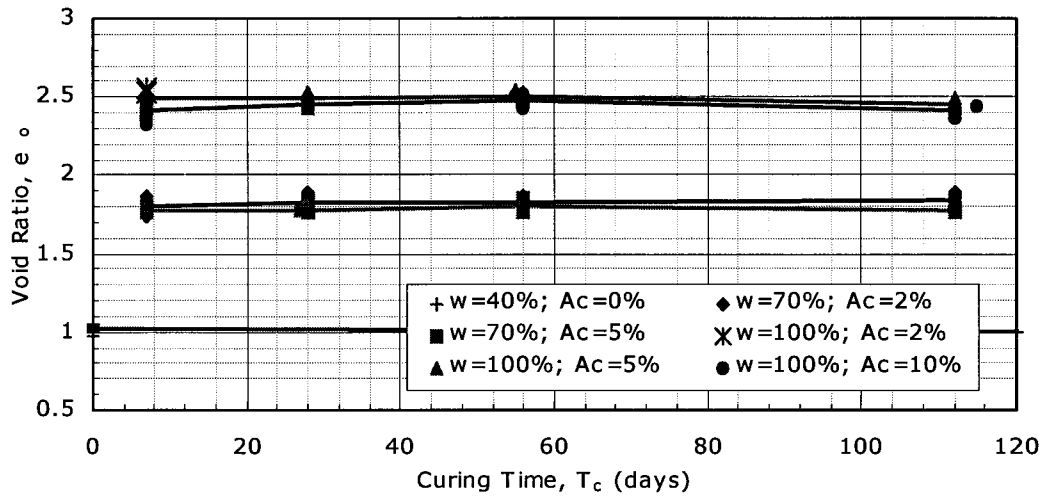
Figure 5.15. Average void ratio vs. curing time (results include all successful laboratory tests).

5.2.5 Failure Behaviour

The failure behaviour of the drained triaxial tests can be interpreted from the deviator stress and stress ratio vs. axial strain curves provided in Appendix A. Furthermore, photographs of the samples following failure, which yield some information regarding failure behaviour, are included in Appendix G.

In general, the failure behaviour was brittle and strain-softening, particularly at low confining pressures. An increase in the cement to moisture

content ratio and curing time caused the failure to be more brittle. Porbaha *et al.* (2000) notes that as confining pressure increases from zero, failure becomes less brittle.

Based on the volumetric strain data, most samples changed from contracting to dilating at peak stress conditions, which is interpreted as failure. However, in some cases, usually when curing time was only 7 days, samples continued to contract after failure, which is often an indication of crushing.

Figure 5.16 shows three CID samples after failure; Figures 5.16a and 5.16b are more typical. Normally, some sample barrelling occurred and a clear failure plane was formed during shear; the failure plane was normally about 30° from the vertical axis of the sample. Porbaha *et al.* (2000) comment that a failure plane form even at low confining pressures and is due to the plastic shearing at failure that occurs under triaxial conditions. Typically, this failure plane ran from the top to the bottom of the sample, dividing the sample into two, nearly equal, portions. As the cement to moisture content ratio and curing time increased, less sample disturbance near the failure plane occurred (Fig. 5.16b). In many cases, small shallow tension cracks occurred around the outside of the sample as deformation following failure proceeded. In some cases (i.e. Fig. 5.16c), more than one failure plane was formed simultaneously so that the top of the sample remained intact, with the exception of barrelling, and the two shear planes formed an approximately symmetric V-shape at the bottom of the sample.
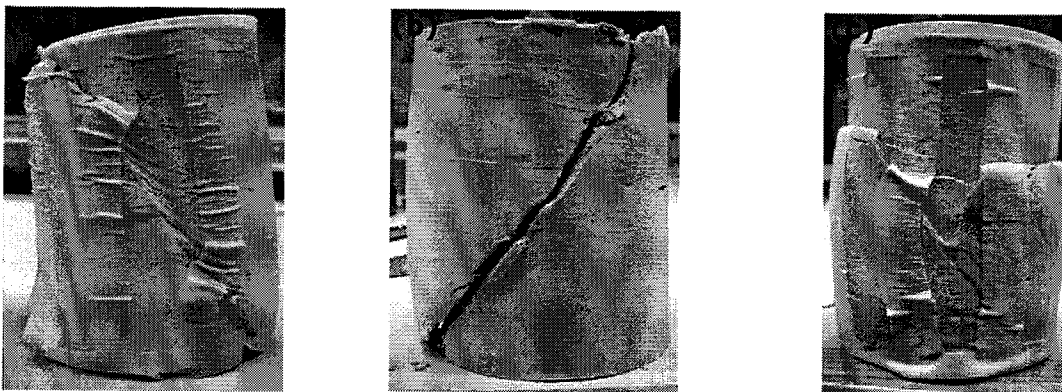
Figure 5.16. CID triaxial samples after failure. (a) w=70%, A_c=2%, $p_o{}'$=50 kPa & T_c=7 days; (b) w=100%, A_c=10%, $p_o{}'$=400 kPa & T_c=28 days; (c) w=70%, A_c=2%, $p_o{}'$=400 kPa & T_c=7 days.

5.3   Consolidated Undrained Triaxial Test Results

The following discussion is an interpretation of the results of the isotropically consolidated undrained (CIU) triaxial compression tests.   Graphs generated for these tests can be found in Appendix B.   The effects of curing time are illustrated in Figures B.1 to B.8.   Figures B.9 to B.16 show the effects cement and moisture content. The effects of confining pressure are illustrated in Figures B.17 to B.32.

5.3.1   Deviator Stress and Stress Ratio

It is appropriate to note here the often large difference in the shape of the deviator stress plots as opposed to the stress ratio plots for the undrained triaxial tests (Fig. 5.17).   The stress ratio considers both the deviator stress, q, and the effective mean normal stress, p'.   Inherent in the determination of the effective mean normal stress is the excess pore water pressure.   The effect of pore water pressure causes the peak deviator stress to be far less when the conditions are undrained than for the drained tests.   During undrained shear, the excess pore water pressure is significant and therefore, considering the stress ratio instead of only the deviator stress smoothes the stress-strain curve and makes it easier to interpret trends in the test results; trends in the deviator stress are sometimes erratic and misleading.   The following discussion will focus more on the stress ratio than the deviator stress.

Figure 5.18 illustrates the peak deviator stress and peak stress ratio for each mix, curing time and confining pressure considered; the fully-softened values are plotted in Figure 5.19.   Trends in the undrained test results are very difficult to interpret, particularly at high confining pressures when the excess pore water pressure is very high.   For all undrained triaxial tests conducted, the maximum peak deviator stress is around 540 kPa and was for the sample with 100 percent moisture content, 10 percent cement content, a confining pressure of 400 kPa and curing time of 7 days.   For pure kaolin at 40 percent moisture content, the maximum peak deviator stress at a confining pressure of 400 kPa was roughly 455 kPa; this is greater than most cases with cement.   However, the excess pore water when cement is present

is far greater than when no cement is present, so that improvement with cement is indicated by the stress ratio.

5.3.1.1 Effect of Curing Time

As indicated in the discussion of the drained test results, it is expected that curing time should increase the sample strength. However, as seen for the drained tests, this is not always the case. In fact, for the undrained tests presented herein, this theory is rarely true, particularly beyond 28 days of curing and at 400 kPa confining pressure.

It is very difficult to establish trends in the peak stress ratio for the undrained triaxial tests based on curing time. With the exception of two tests at 400 kPa confining pressure, the peak stress ratio increased between 7 and 28 days of curing, as expected (Fig. 5.18). For roughly half of the tests, however, the peak stress ratio decreased between 28 and 56 days of curing.
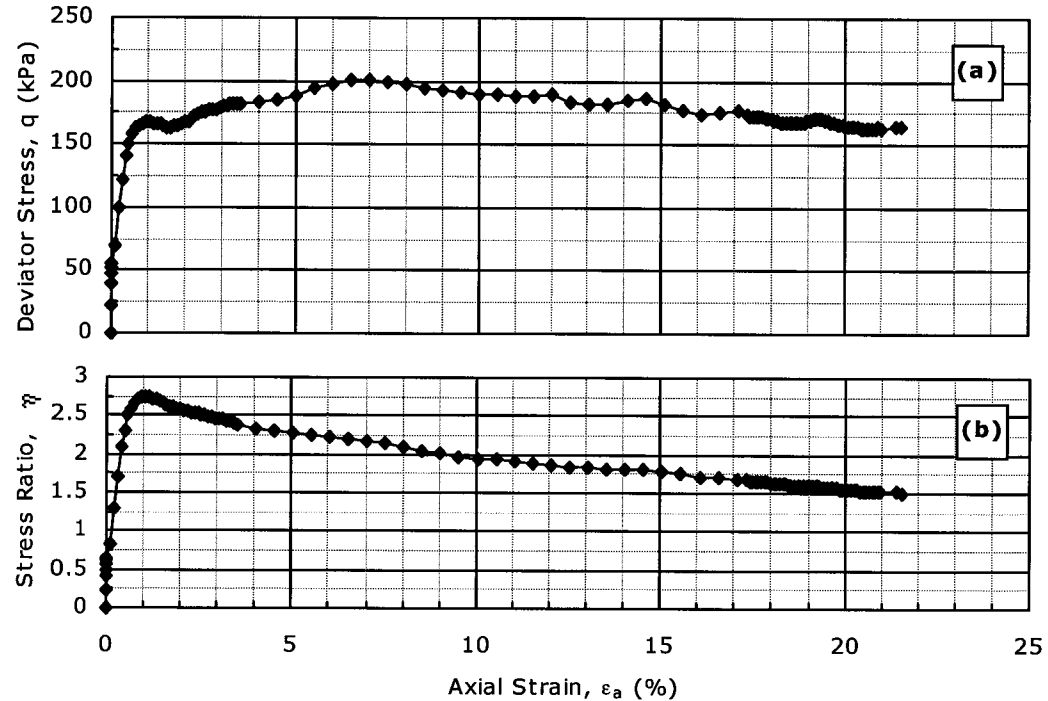
Figure 5.17. w=70%, A_c=5%, p_o'=100 kPa & T_c=7 days (CIU) (a) q vs. ε_a; (b) η vs. ε_a.
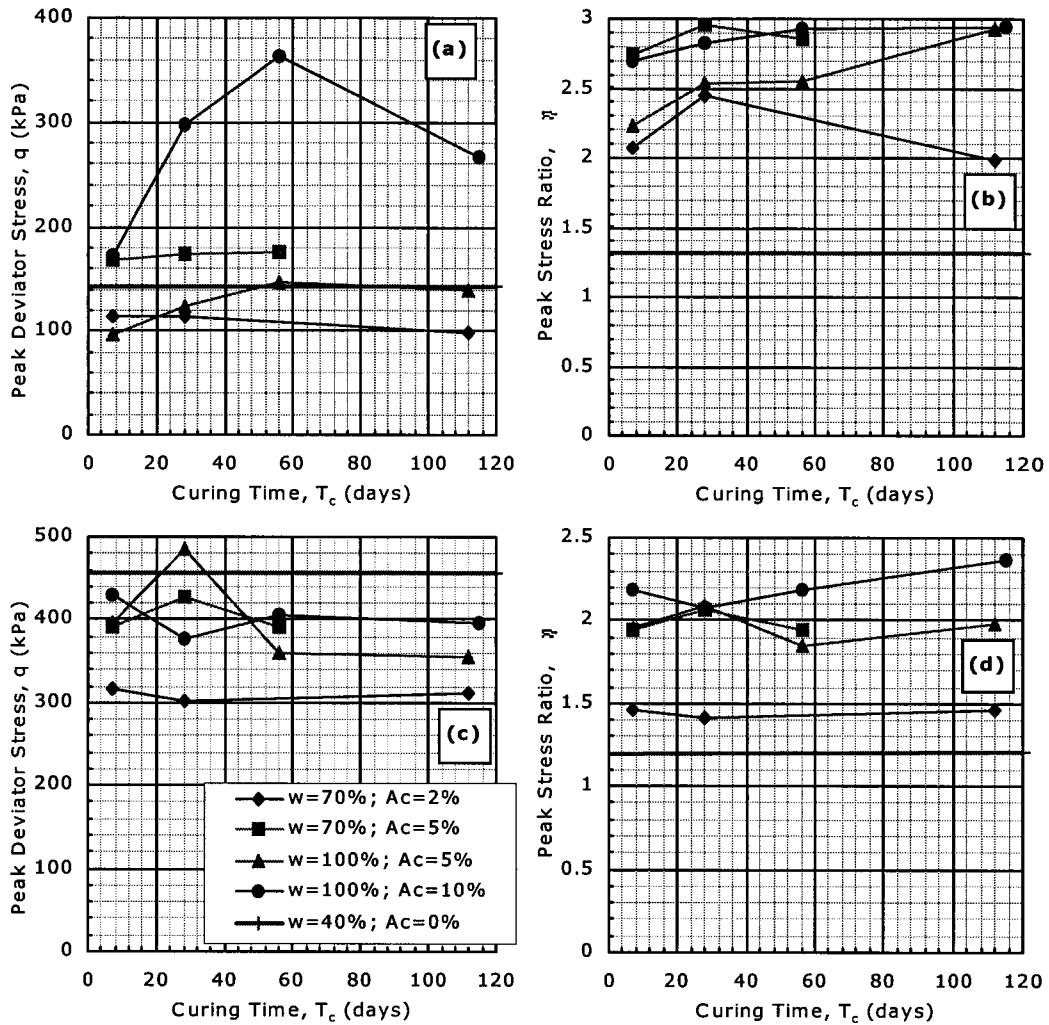
Figure 5.18. Peak deviator stress and peak stress ratio vs. curing time for CIU triaxial tests at confining pressures of (a) & (b) 100 kPa; (c) & (d) 400 kPa.

In some cases, the fully-softened deviator stress and fully-softened stress ratio appear unaffected by curing time and the stress-strain plots converge to a single value (Fig. 5.20); this was also observed in the drained test results. However, other cases show no clear relationship between fully-softened stress ratio and curing time. Significant lateral deformation at high strains makes it difficult to accurately calculate fully-softened values.
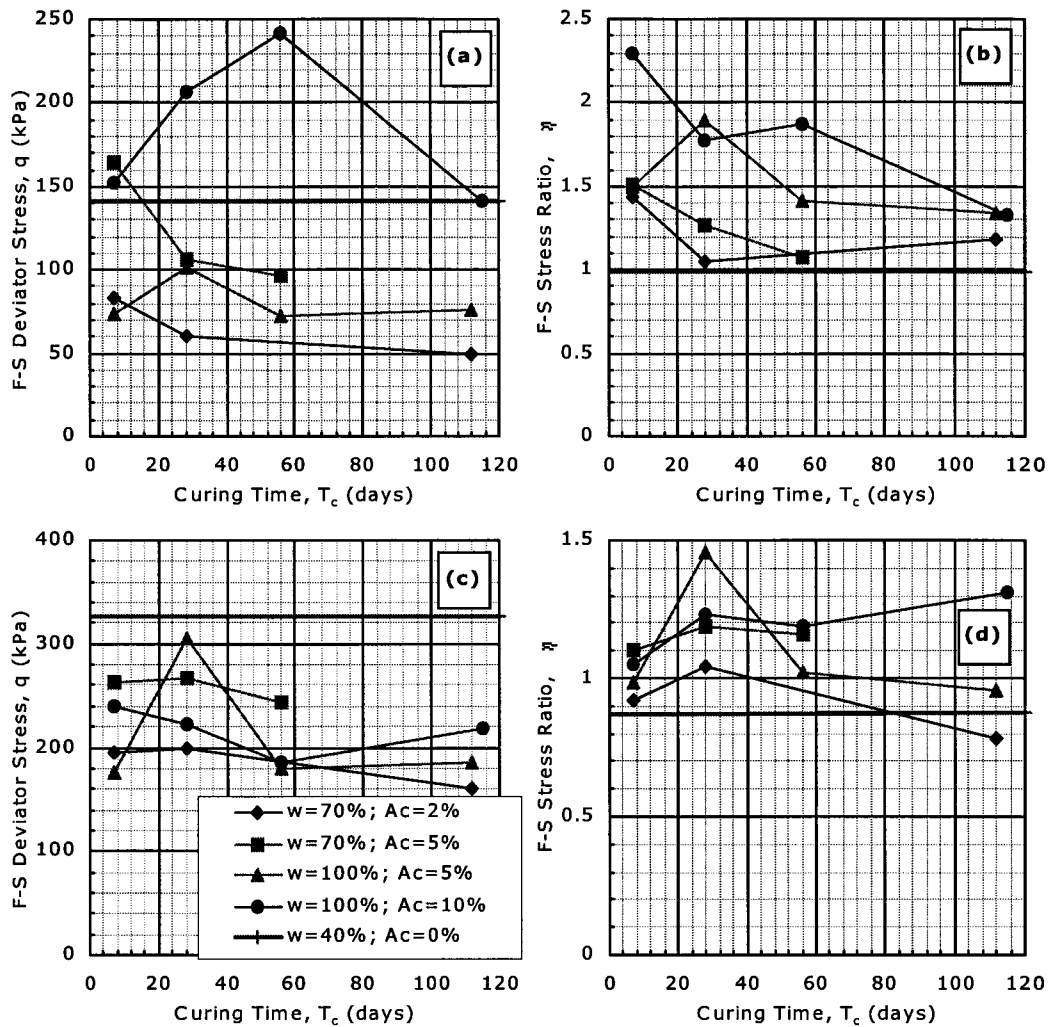
Figure 5.19. Fully-softened stress and peak stress ratio vs. curing time for CIU triaxial tests at confining pressures of (a) & (b) 100 kPa; (c) & (d) 400 kPa.

5.3.1.2 Effect of Cement Content and Moisture Content

The general trend is for the peak deviator stress and peak stress ratio to increase with increasing cement to moisture content ratio (Fig. 5.18). However, often the peak values for the two mixtures with an intermediate ratio are very similar so that either one may have a slightly higher peak for any series of tests. The samples with only 2 percent cement content and 70 percent moisture content have a noticeably lower peak strength than the other three cases at 400 kPa confining pressure.

Similar to curing time, it is very difficult to find a relationship between the cement and moisture content and the fully-softened strength, except when the cement content is only 2 percent and the fully-softened values are very low.

5.3.1.3   Effect of Confining Pressure

As expected, there is a clear change in both the peak and fully-softened deviator stress and stress ratio when the confining pressure is altered.   An increase in the confining pressure causes the peak deviator stress to increase (Fig. 5.21a) and the peak stress ratio to decrease (Fig. 5.21b).   The same was true for the drained triaxial tests.   Of all variables considered, confining pressure has the most influence on the undrained strength of kaolin-cement; this is because confining pressure has such a strong influence on the excess pore water pressure (Fig. 5.21c).

Confining pressure has the same effect on the fully-softened deviator stress as on the peak deviator stress; an increase in confining pressure results in an increase in the fully-softened deviator stress (Fig. 5.21a). However, the same cannot be said for the fully-softened stress ratio.   At intermediate cement to moisture content ratios and curing times of 28 days or greater, the fully-softened stress ratio is approximately the same for both confining pressures considered (Fig. 5.21b).

5.3.2 Axial Strain at Peak Conditions and Material Consistency

The axial strain at peak conditions for the undrained triaxial test varies considerably and is highly dependent on the confining pressure and the stiffness of the sample. At a confining pressure of 100 kPa, the axial strain at peak conditions is roughly 1 percent when the cement to moisture content is intermediate (Fig. 5.20).   When the confining pressure is 400 kPa and the cement to moisture content ratio is low, the axial strain at peak conditions is on the order of 7 or 8 percent.   Note that the shear data was corrected to account for initial straining during seating of the load; therefore, often the load is positive at zero strain.

5.3.2.1 Effect of Curing Time

An increase in curing time causes a small reduction in the axial strain at peak conditions (Fig. 5.20). The same observation was made by Uddin (1995) and of the drained tests at low confining pressures. However, it is often the case that the axial strain at peak is approximately the same for each curing time considered within each mixture; this is more true at 100 kPa confining pressure than at 400 kPa confining pressure.
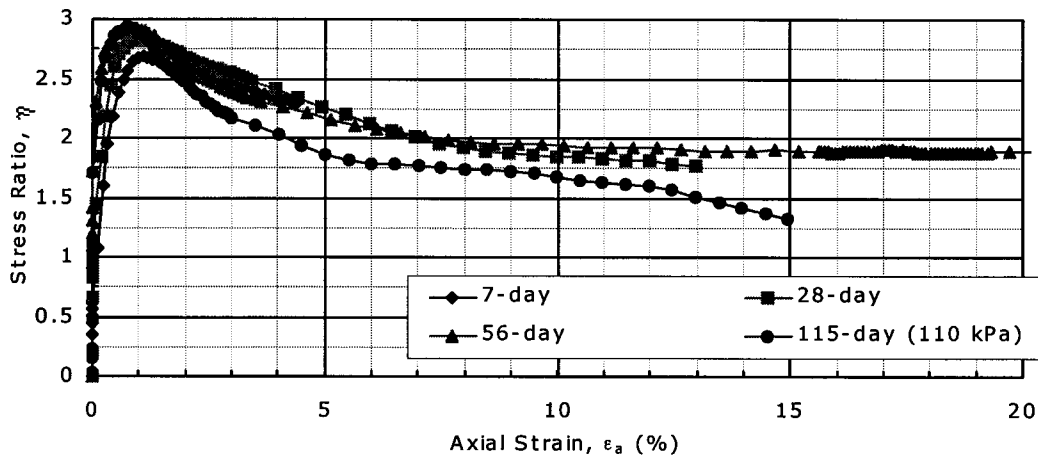
Figure 5.20. η vs. ε_a for $w=100\%$, $A_c=10\%$ and $p_o{}'=100$ kPa (CIU).

5.3.2.2 Effect of Cement Content and Moisture Content

An increase in the cement to moisture content ratio has the same effect as an increase in curing time and causes the axial strain at peak conditions to decrease (Fig. 5.22a). When pure kaolin at 40 percent moisture content is considered, the axial strain at failure is higher than when cement is present and the moisture content is greater. This is the same as the drained test results at low confining pressures and is due to the increased stiffness associated with greater cement to moisture content ratios. The stiffness is further increased with undrained conditions which is why failure occurs much sooner and at a lower stress level than when conditions are drained.
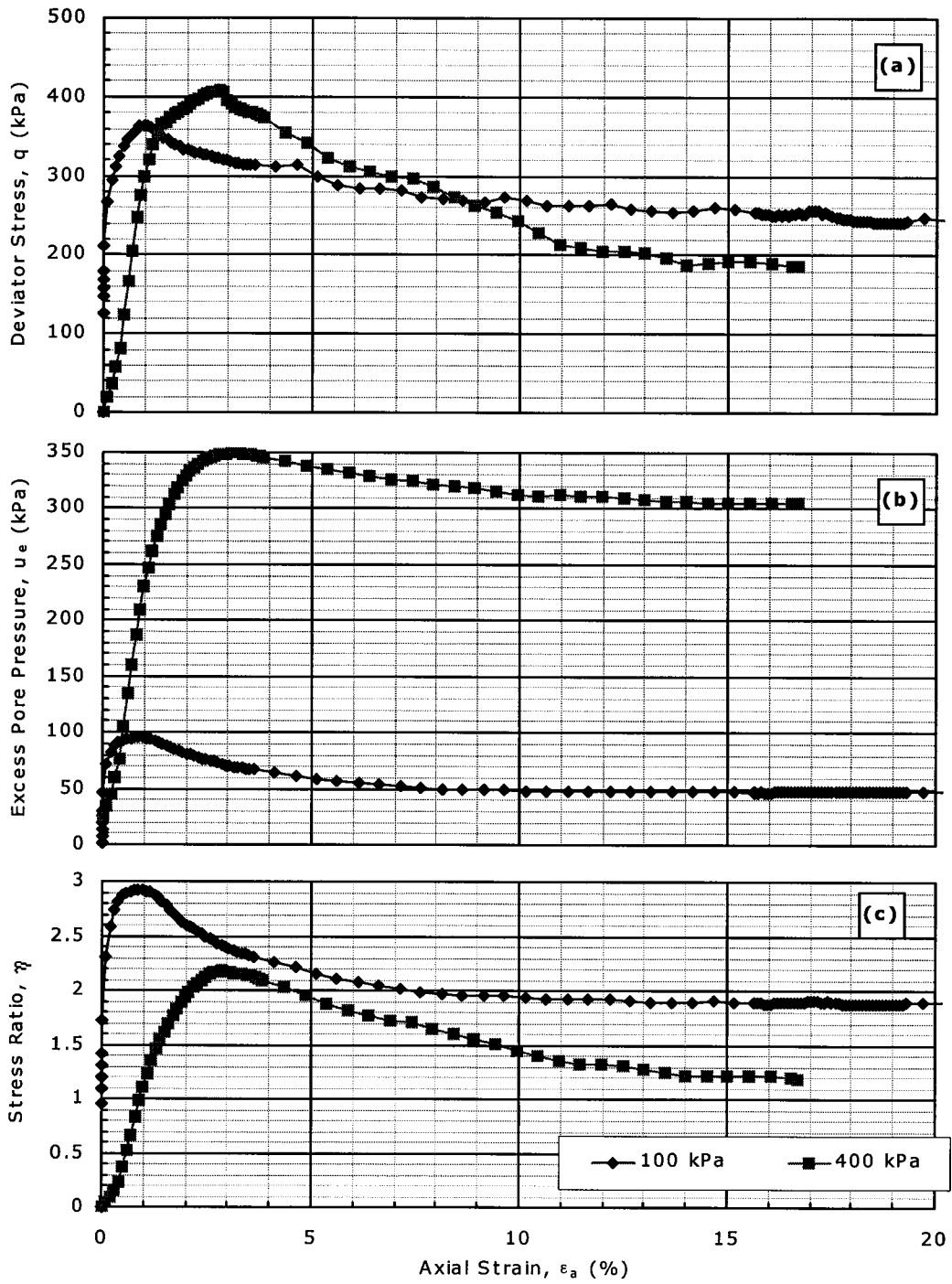
Figure 5.21. w=100%, A_c=10% & T_c=56 days (CIU) (a) q vs. ε_a; (b) η vs. ε_a; (c) u_e vs. ε_a.
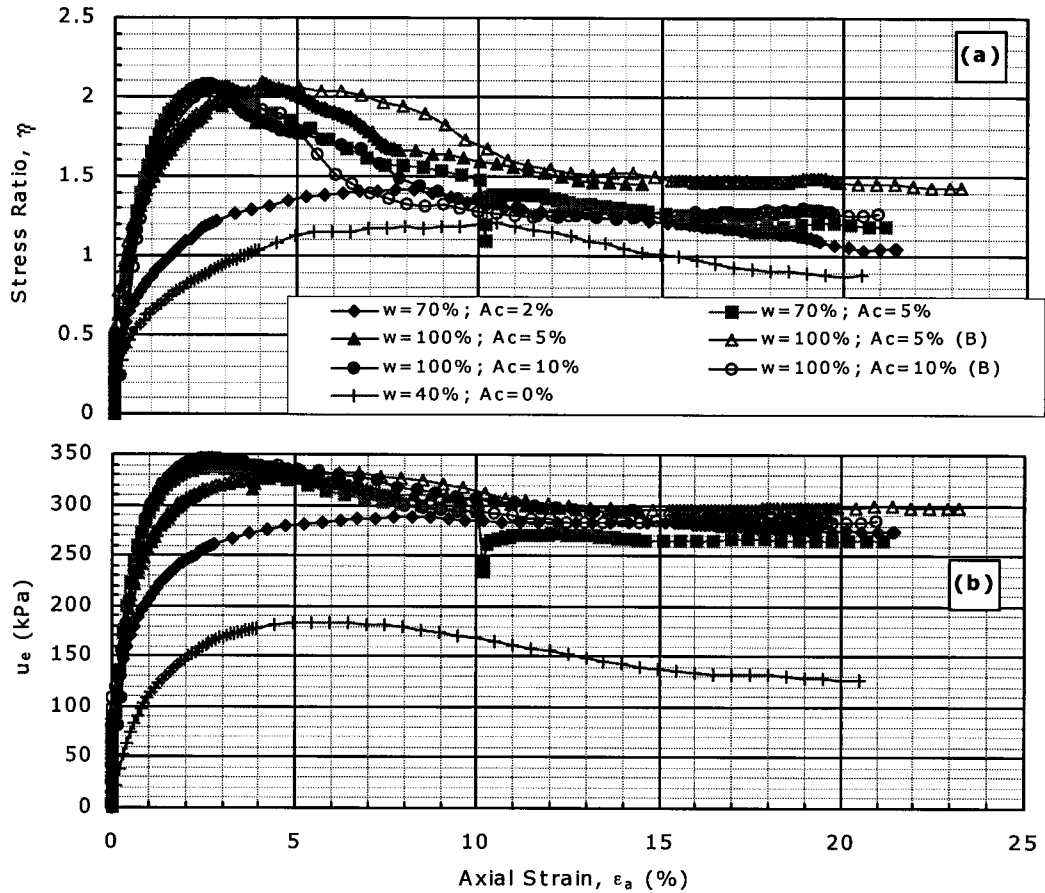
Figure 5.22. $p_o'=400$ kPa & $T_c=28$ days (CIU). (a) η vs. ε_a; (b) u_e vs. ε_a.

5.3.2.3   Effect of Confining Pressure

It is clear that as confining pressure increases, the axial strain at peak conditions also increases (Fig. 5.21b). As was observed from the drained test results, an increase in confining pressure leads to a reduction in the stiffness of the material. When the cement content is zero, the material is very soft and the confining pressure has very little effect on the axial strain at failure.

5.3.3 Excess Pore Water Pressure

For all undrained triaxial tests on kaolin-cement, the excess pore water pressure remained positive throughout the test.   The excess pore water pressure always increased up to an axial strain roughly coincident with peak conditions, and then decreased, while remaining positive (Fig. 5.22). Similar

to the drained test results, trends in excess pore water pressure indicate contraction to peak stress conditions, followed by some dilation. This is an indication of normally consolidated to slightly over-consolidated behaviour, while the stress-strain behaviour clearly resembles that of over-consolidated material.

When pure kaolin at 40 percent moisture content was tested, the excess pore water pressure was slightly negative at the end of the test when the confining pressure was only 100 kPa. Furthermore, samples of pure kaolin began to dilate before peak stress conditions were achieved. This behaviour is that of over-consolidated material. The difference in behaviour between kaolin-cement and pure kaolin may be a function of the curing environment as well as cementation; pure kaolin samples were tested immediately following casting.

5.3.3.1   Effect of Curing Time

In general, the maximum excess pore water pressure increased with curing time (Fig. 5.23). Just like the peak stress ratio, however, for about half of the cases, the peak excess pore water pressure is slightly greater after 28 days than after 56 days of curing. This often corresponds to a peak strength that is also slightly greater after 28 days than after 56 days.

Following peak stress conditions, dilation occurred and the excess pore water pressure is approximately the same for all curing times when fully-softened stress conditions are achieved (Fig. 5.23).
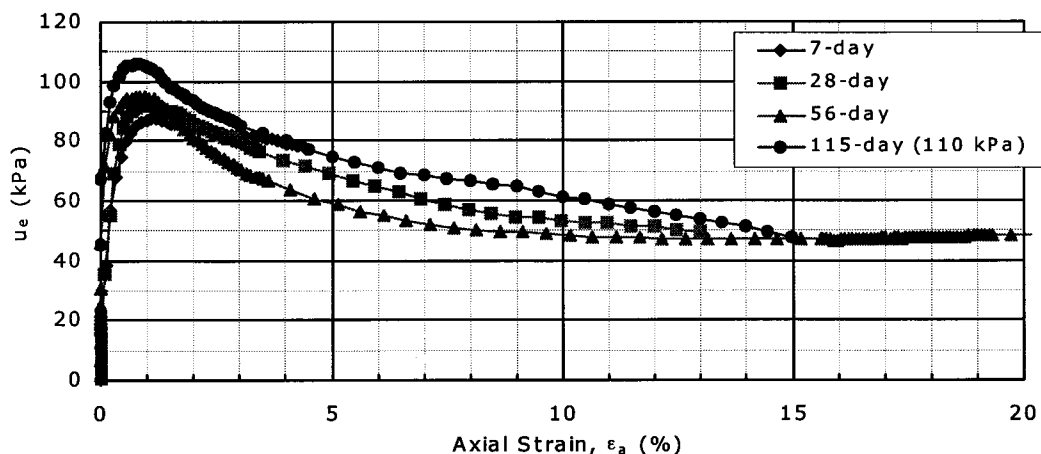
Figure 5.23. u_e vs. ε_a for w=100%, A_c=10% & $p_o{}'$=100 kPa (CIU).

5.3.3.2   Effect of Cement and Moisture Content

As the cement to moisture content ratio increases, so does the peak excess pore water pressure (Fig. 5.22b).   When no cement is present, the peak excess pore water pressure is very low, and at a confining pressure of 100 kPa, becomes slightly negative at the end of the test.

For all tests on kaolin-cement, dilation began at an axial strain approximately coincident with peak stress conditions.   Following peak conditions and at a confining pressure of 100 kPa, dilation was far greater at intermediate cement to moisture content ratios than at low ratios (Fig. 5.24). At 400 kPa confining pressure, sample dilation was such that the excess pore water pressure at fully-softened stress conditions was approximately the same for all mixes with cement (Fig. 5.22b).   The pure kaolin at 40 percent moisture content began to dilate prior to peak stress conditions (Fig. 5.22); it can be said that cement retards the change from contraction to dilation during undrained shear tests.   The same statement was made for drained tests.

5.3.3.3   Effect of Confining Pressure

As confining pressure increases, so does the excess pore water pressure. This is true at both peak and fully-softened conditions (Fig. 5.21c).   Of all factors discussed, confining pressure has the greatest influence on the excess pore water pressure.
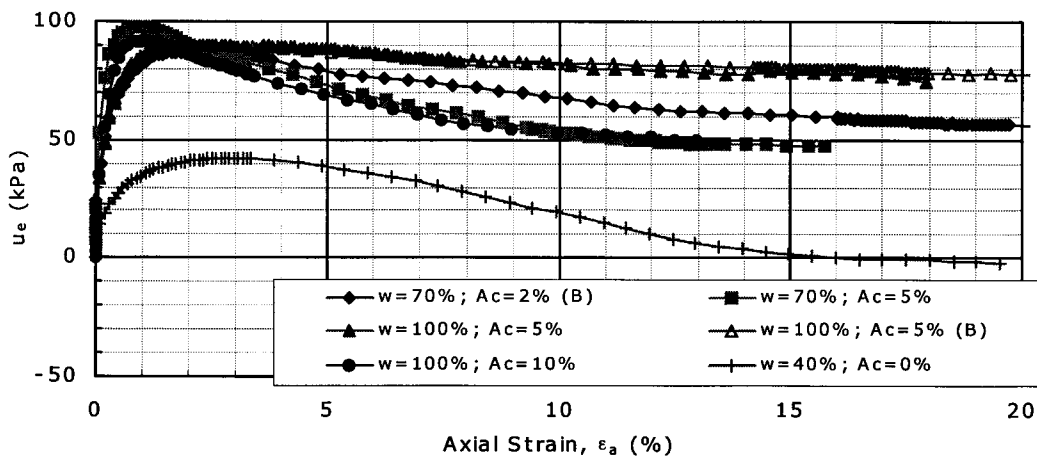
Figure 5.24. u_e vs. ε_a for $p_o{}' = 100$ kPa & $T_c = 28$ days (CIU).

5.3.4 Failure Behaviour

The failure behaviour of the undrained triaxial tests can be interpreted from the deviator stress and stress ratio vs. axial strain curves provided in Appendix B. Furthermore, photographs of the samples following failure, which yield some information regarding failure behaviour, are included in Appendix G.

In general, the failure behaviour was strain-softening. Although the material under undrained conditions was more stiff, as indicated by the relatively low axial strain at peak, failure was not brittle, as it was for the drained triaxial tests.

Figure 5.25 shows a variety of CIU samples after failure with the sample shown in Figure 5.25a being the most typical. A clear failure plane, roughly 30° from the vertical axis of the sample, developed during shear; this was also the case for most CID tests. Failure often occurred more through the lower portion of the sample so that following shear, the top piece was larger than the bottom piece. As the cement to moisture content ratio and curing time increased, less sample disturbance near the failure plane occurred. In one test, two clear failure planes developed simultaneously (Fig. 5.25b). Similar to the CID tests, more sample disturbance near the shear plane occurred at lower cement to moisture content ratios. As for the CID tests, barrelling occurred, but to a slightly greater degree.

Where a shear plane did not form, failure is believed to be by crushing. This mode of failure caused the top portion of the sample to punch through the bottom portion of the sample, so that the bottom portion of the sample was greatly disturbed and it's diameter was far greater than the diameter of the top portion. This type of failure rarely occurred, and was exhibited in the undrained triaxial tests only (Fig. 5.25c).
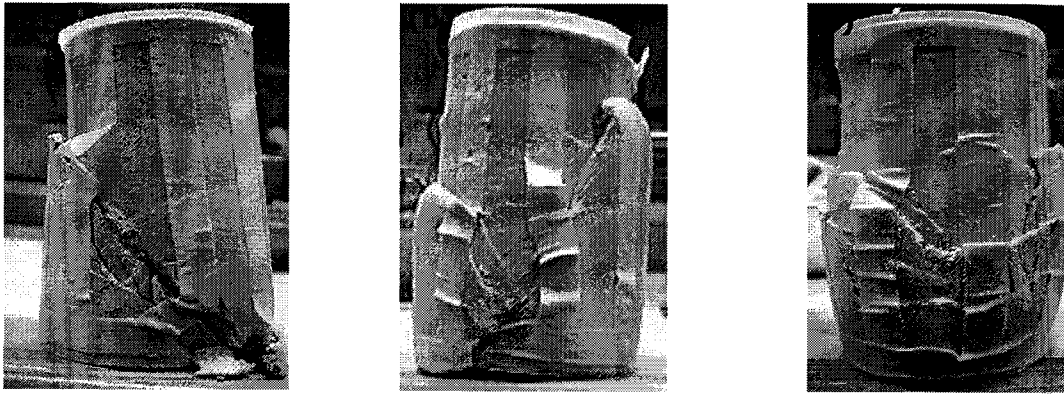
Figure 5.25. CIU triaxial samples after failure. (a) w=100%, A_c=10%, $p_o{'}$=400 kPa & T_c=56 days; (b) w=70%, A_c=2%, $p_o{'}$=400 kPa & T_c=28 days; (c) w=100%, A_c=5%, $p_o{'}$=100 kPa & T_c=28 days.

5.3.5 Effective Stress Paths

Effective stress paths generated during triaxial tests reveal a great amount of information about the sample behaviour. Wissa and Ladd (1964) describe three distinct stress path shapes in q-p$'$ space (Fig. 5.26) which they found to occur most frequently during their study of undrained cemented soil behaviour. The characteristics associated with each of these shapes is summarised in Table 5.1.
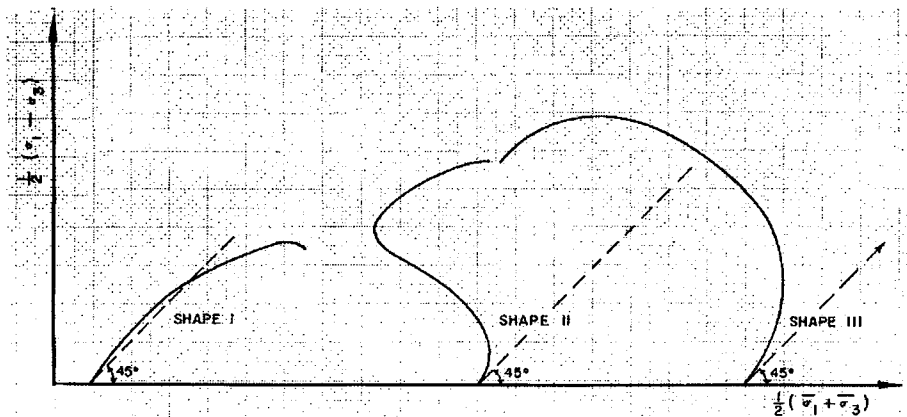
Figure 5.26. Classification of effective stress path according to shape (Wissa and Ladd, 1964).

Table 5.1. Soil characteristics associated with shape of effective stress path

Characteristic	Shape I	Shape II	Shape III
Consolidation	Heavily over-consolidated clays and dense sands.	Slightly over-consolidated clays and loose sands.	Normally consolidated clays which are not very sensitive and very loose sands.
Trend of excess pore pressure	Begins to decrease early in test so that it is negative.	At low axial strains, behaviour is like that of shape III; at high axial strains, the behaviour is like that of shape I.	Increases continuously at a decreasing rate until failure is reached.
Dilation vs. contraction	Soil skeleton wants to dilate during shear.		Skeleton contracts during shear.

Several authors (i.e. Kohata *et al.*, 1997) report that cement treatment causes the stabilized material to behave as an over-consolidated clay. However, the current study suggests otherwise, with findings indicating primarily normally consolidated behaviour. Most of the stress paths plotted by Uddin (1995) at confining pressures of 600 kPa or below are similar to Shapes I and II; Uddin conducted CIU tests on samples of Bangkok clay with cement contents of 5 to 15 percent.

For the current study, however, most of the CIU tests yielded stress paths similar to Shape III (Fig. 5.27), although with a much better defined peak, exhibiting normally consolidated behaviour. This indicates that the apparent consolidation yield stress resulting from the cementation is equal to or less than the consolidation pressure applied during the test. Only when the cement to moisture content ratio was intermediate and the confining pressure 100 kPa did the undrained stress paths resemble Shape II, indicating slightly over-consolidated behaviour. This shows that as the degree of hardening increases, the apparent consolidation yield stress also increases to a value above 100 kPa but less than 400 kPa. This theory is confirmed in Chapter 6 when the results of the consolidation tests are discussed.

Shape II was also found to apply when the cement content was zero, suggesting that the pressure exerted on the material during hand tamping was greater than 400 kPa. However, the same hand tamping was used to compact the samples with 70 percent moisture content and these samples have an apparent consolidation yield stress *less than* 400 kPa. These observations suggest that when exposed to water during curing, the apparent consolidation yield stress may actually be reduced instead of increased.

Uddin (1995) notes that for Bangkok clay, cement contents of 5 percent or less do not change the apparent consolidation characteristics of the untreated material. Therefore, the cement contents considered for the current study, combined with kaolin, which contains no coarse-grained particles, may be too low to have a significant effect on some characteristics of the stabilized material. Furthermore, when cured in water, the consolidation characteristics may actually deteriorate, as shown by the reduction in the apparent consolidation yield stress, for those samples which were compacted by hand tamping. Consolidation characteristics of soil-cement will be discussed further and in more detail in Chapter 6.
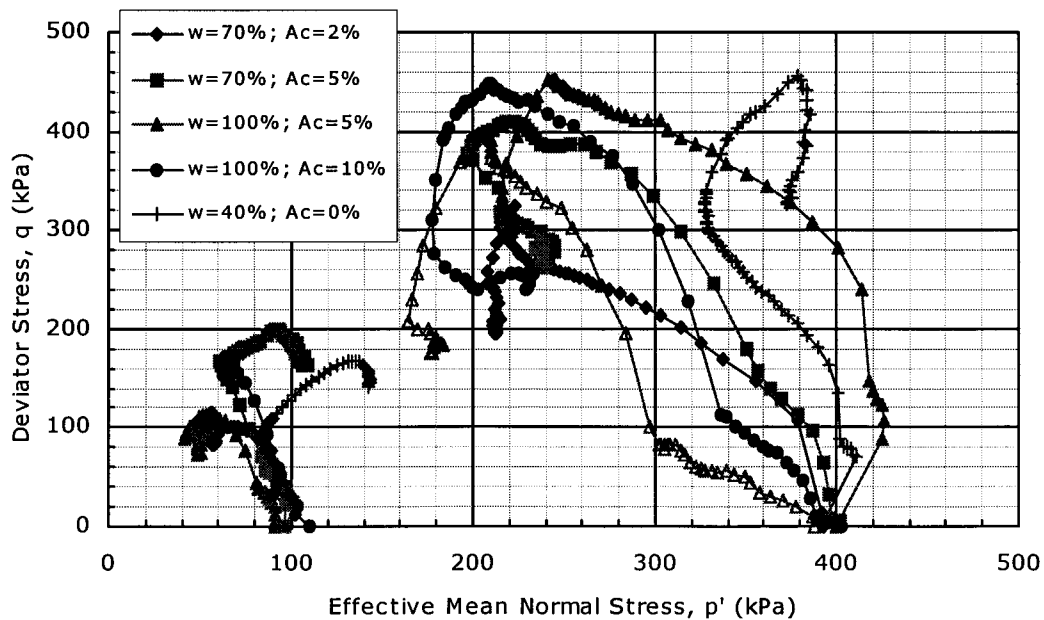
Figure 5.27. CIU stress path plots (p' vs. q) for $T_c=7$ days.

5.4   Unconfined Compressive Strength

The unconfined compressive (UC) strength is the most common criteria used in design of deep mixing ground improvement applications (Porbaha *et al.*, 2000). It is a simple yet crude test which provides one with an approximation of the compressive strength behaviour of a given material. However, in no way does it attempt to simulate the actual field conditions, especially at depth where confining stresses are significant. For this reason, it is regarded as insufficient if an efficient and effective ground improvement strategy is to be designed at depth. Based on data collected in Japan, the unconfined compressive strength measured on laboratory samples is 2 to 5 times that in the field.

For the current laboratory program, two to five UC tests were conducted on each mix; it was found that the UC strength varied considerably. Samples with 2 percent cement and 100 percent moisture content were also tested after only 7 days of curing. In some cases, samples of insufficient quality for triaxial tests were tested in the UC apparatus so the UC strength of these samples may be low. The sample quality was judged based on the voids and cracks observed on the surface; photos of each sample are provided in Appendix G. When interpreting the UC test results and defining trends in the UC tests, only the maximum strength within a group of tests from the same mixture was considered. While this process may bias the results slightly by ignoring poor test results, it also allows samples of inferior quality to be identified so that trends in peak strength are more clear.

For samples with 10 percent cement, the UC strength increased from 150 to 335 kPa between 7 and 112 days of curing; this mix yielded the greatest strength of all mixes considered. The poorest strength was found in the samples with only 2 percent cement and 70 percent moisture content; the UC strength for these samples ranged from 25 to 52 kPa between 7 and 28 days, and then deteriorated in strength following 28 days. Samples of pure kaolin and a moisture content of 40 percent were also tested. The UC strength of this material was over 150 kPa; this is greater than any of the kaolin-cement mixes considered after only 7 days of curing, suggesting that curing in water causes some softening. The stress-strain results of the UC

tests are plotted in Appendix C. Figures C.1 to C.4 illustrate the effect of curing time; Figures C.5 to C.8 illustrate the effects of cement and moisture content.

5.4.1 Effect of Curing Time

The peak UC strength is plotted against curing time for each mixture in Figure 5.28; stress-strain plots are provided in Figure 5.29. The change in the UC strength with curing time is a function of the cement content. For all samples, the UC strength approximately doubles between 7 and 28 days of curing. After this time, the UC strength of samples with at least 5 percent continues to increase slightly up to at least 112 days of curing. When the cement content is only 2 percent, the UC strength begins to deteriorate noticeably after 56 days of curing. Porbaha *et al.* (2000) include UC test results on marine clay from Tokyo Bay at 100 percent moisture content stabilized with 5 to 20 percent cement. At 10 percent cement and less, the improvement in strength with curing time is small. In fact, when the cement content is only 5 percent, the UC strength decreases slightly after roughly 80 days of curing. The curing environment for the samples tested is not known.

The axial strain at peak stress conditions generally decreased with curing time up to at least 56 days (Fig. 5.29), indicating that the material becomes more stiff with curing. After 56 days of curing, the reduction in strength for the case with only 2 percent cement is associated with a greater axial strain at failure, indicating that the sample softened. As the cement to moisture content ratio increased, the material stiffness became more uniform for all mixes and the axial strain at failure did not change considerably with age.

Where samples did not fail completely so that the load went to zero, the stress-strain curves converged after failure so that the fully-softened stress was the same, regardless of curing time.
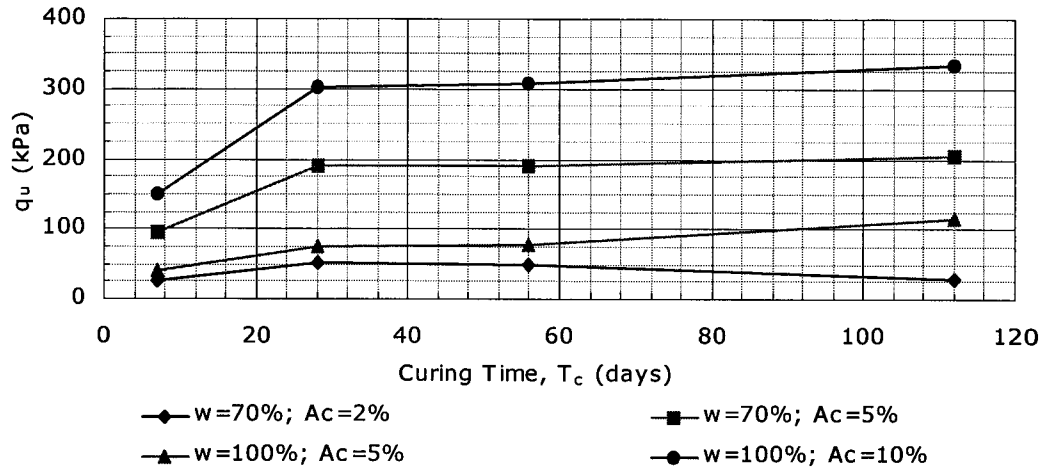
Figure 5.28. UC strength vs. curing time.

5.4.2 Effect of Cement Content and Moisture Content

As seen in the triaxial test results, the UC test results indicate that as the cement to moisture content ratio increased, so did the strength (Fig. 5.28). The stiffness of the material also increased with cement to moisture content ratio, as seen by a reduction in axial strain at failure (Fig. 5.30).

Uddin (1995) found that there was very little to no improvement in the UC strength when 5 percent cement or less was used to stabilize Bangkok clay. Although an initial increase in strength is observed up to 28 days for all mixes considered in the current study, when 5 percent cement or less is used to stabilize kaolin, a reduction in strength was observed with curing time.

Samples with no cement and a moisture content of 40 percent were also prepared and tested in the UC apparatus. The peak UC strength of the material without cement is greater than any of the kaolin-cement mixes considered after only 7 days of curing. Furthermore, the material was much softer as it failed at an axial strain above 10 percent; with cement, the axial strain at failure is always less than 5 percent. Cementation increases sample stiffness and moisture content reduces the strength. Following 7 days of curing, only samples with an intermediate cement to moisture content ratio were stronger than the material without cement, giving evidence to the theory that curing in water causes the material to soften.
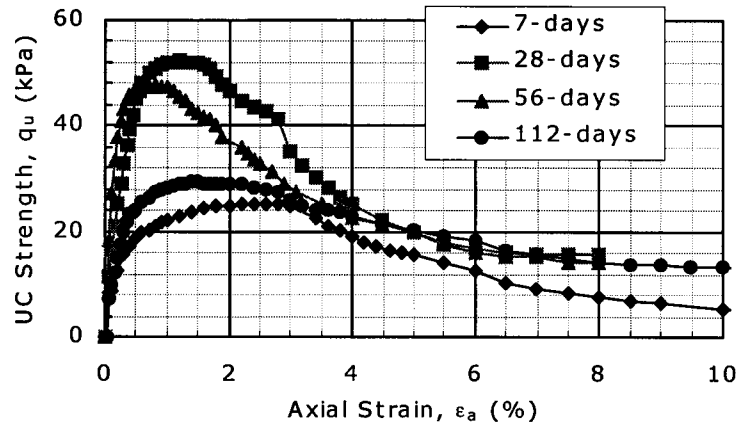
Figure 5.29. UC stress-strain curve for w=70% & A_c=2%.
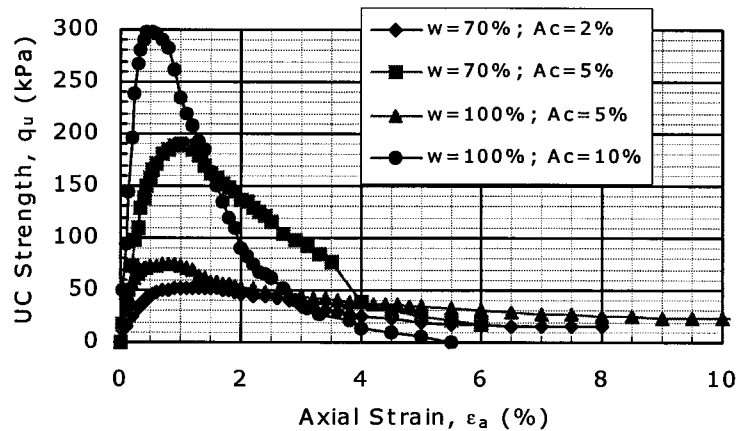
Figure 5.30. UC stress-strain curve for T_c=28 days.

5.4.3 Failure Behaviour

Under unconfined conditions, failure is brittle and by crushing (Porbaha *et al.*, 2000), particularly at greater curing times. The top of the sample normally remained intact and nearly vertical tension cracks formed in the bottom of the sample (Fig. 5.31a); crushing proceeded once samples failed in tension. Occasionally, the opposite is true so that the bottom of the sample remained intact (Fig. 5.31b). Spalling is also seen from time to time (Fig. 5.31b). Oblique fractures sometimes occurred, separating the sample into two nearly equal pieces (Fig. 5.31c), as was the case for most of the triaxial tests. The failure behaviour can be observed in stress vs. strain plots and in the photographs of the UC samples after failure; these photographs are provided in Appendix G.
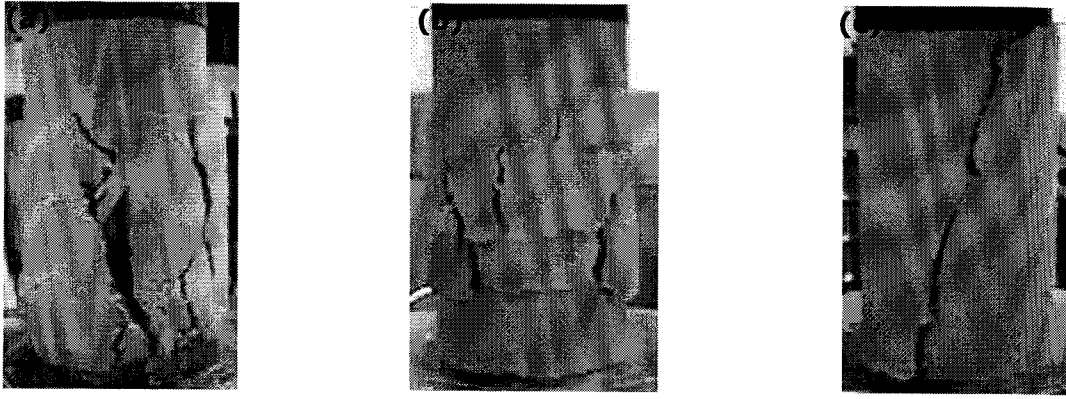
Figure 5.31. Unconfined compression samples after failure. (a) w=70%, A_c=2% & T_c=28 days; (b) w=70%, A_c=5% & T_c=56 days; (c) w=100%, A_c=10% & T_c=7 days.

5.5 Summary and Conclusions

Some of the significant concepts observed from the triaxial and unconfined compression tests on pure kaolin and kaolin-cement are summarized below. Note that conclusions are based on somewhat limited test results and are not intended to characterize conditions not considered in the current study.

5.5.1 Strength Properties

• The strength of soil-cement, as determined from the triaxial results, increases with the cement to moisture content ratio and curing time. However, when the cement was 5 percent or less and/or the moisture content only 70 percent, the peak stress and peak cohesion sometimes decreased following 28 or 56 days of curing. Some factors contributing to the loss of strength include insufficient cement and/or too much moisture, , and lack of coarse-grained particles in the stabilized material. Furthermore, curing in water may lead to softening over time or may cause leaching of cement out of the stabilized material. Different compaction methods may have contributed to the loss of strength in the samples with 70 percent moisture content. More research is required to understand exactly what phenomena lead to this observed reduction in strength with curing time.

- The UC strength increased consistently with curing time when the cement content was at least 5 percent; the increase was small following 28 days of curing. At only 2 percent cement, the UC strength deteriorated following 56 days of curing. These results show better improvement as compared with the triaxial test results. The reason is likely related to the lack of consolidation for the UC tests; consolidation causes weakly cemented bonds to fail prior to shear.

- The drained tests yield greater and more consistent peak stress results than the undrained tests. The poor undrained test results are due to significant excess pore water pressures that develop during shear; the stress ratio should be considered instead of the deviator stress when interpreting trends in the undrained test results.

- A linear failure envelope, with a constant cohesion and friction angle, was found to be most appropriate based on the results of the drained tests, for the range of confining pressures considered. The same conclusion was made by Wissa and Ladd (1964) who considered confining pressures up to approximately 5500 kPa. However, peak cohesion and peak friction angle were found to be inversely related when the cement content was at least 5 percent; as one increased the other decreased. This leads to the conclusion that the failure envelope may actually be curved when greater confining pressures are considered. Uddin (1995), who considered a maximum confining pressure of 2000 kPa, found the failure envelope to be curved, similar to the behaviour of soft rock.

- Typically, at intermediate cement to moisture content ratios, peak cohesion increased with curing time and peak friction angle decreased with curing time, up to 56 days. A reduction in cohesion following 28 days of curing for the case of 100 percent moisture and 5 percent cement is associated with an increase in friction angle. Wissa and Ladd (1964) concluded that at low cement contents there is no change in friction angle with curing time. Sivapullaiah et al. (2000) report that friction angle is directly related to the degree of flocculation, and Uddin (1995) states that flocculation (and hence friction angle) increase with curing time due to the reduction in moisture content associated with humid curing. However, curing for the current study was done in water and a reduction in pH with curing

time should lead to a reduced degree of flocculation and therefore, a slight decrease in the angle of friction with curing time.

• At low cement contents (i.e. 2 percent), there is very little cementation and most of measured cohesion is due to the clay particles. This may be a function of the low pH, resulting in production of a weaker cementitious material than when the pH is greater.

• The fully-softened drained strength and cohesion is a function of cement content and confining pressure and is not influenced by moisture content. With only 2 percent cement, the fully-softened cohesion was only marginally above that of pure kaolin. For all triaxial tests, significant lateral deformation at large strains made it difficult to accurately determine the fully-softened values.

• For all triaxial tests, an increase in confining pressure leads to an increase in the peak deviator stress and a decrease in the peak stress ratio; the same trends were observed in the fully-softened values. However, the undrained fully-softened stress ratio is not affected by confining pressure when the cement to moisture content ratio is intermediate and the curing time is 28 days or more.

• For the undrained triaxial tests, the confining pressure had the most influence over the strength properties of all factors considered; this is because excess pore water pressure and confining pressure are so strongly related.

5.5.2 Axial Strain at Peak Stress Conditions and Material Consistency

• The axial strain at peak stress conditions is a function of both confining pressure and the material consistency. At low confining pressures (i.e. 50 and 100 kPa) for drained triaxial tests and for all undrained tests, the axial strain corresponding to peak conditions decreased with curing time and cement to moisture content ratio. However, the opposite is true for drained tests at high confining pressures (i.e. 400 kPa), when the axial strain corresponding to peak conditions *increases* with curing time and cement to moisture content ratio. The latter trend is due to failure of weak cement bonding during consolidation at high pressures, causing significant volume change, thereby increasing the stiffness of the sample prior to shear.

- The material becomes more stiff with curing time, cement to moisture content ratio and a reduction in confining pressure. During drained conditions at 400 kPa, the material stiffness is governed only by confining pressure and is independent of curing time and cement to moisture content ratio.

- The axial strain at failure is directly related to the maximum volume change during drained triaxial tests.

- Softening sometimes occurs following 28 or 56 days of curing and is especially clear in the UC test results. When softening occurs, it is associated with a reduction in UC strength, and is likely due to the curing environment. The degree of softening is a function of curing time and the cement and moisture contents. It may also be a function of the compaction method used during sample preparation.

- The undrained tests reach peak stress conditions at a much lower strain than the drained tests; this is because undrained conditions significantly increase the material's rigidity.

5.5.3 Volumetric Strain During Drained Conditions

- For the kaolin-cement, volumetric strain remained negative throughout shear and only a small amount of dilation occurred, if at all, at an axial strain roughly coincident with peak stress conditions. While the stress-strain behaviour resembles that of over-consolidated material, the volumetric strain behaviour is usually more similar to that of normally-consolidated clays. For the pure kaolin at low confining pressures, the volumetric strain was positive after peak stress conditions, indicating over-consolidated behaviour; this difference in behaviour from the kaolin-cement may be a function of curing environment as well as cementation effects.

- In general, as curing time increases, the volumetric strain during shear decreases. This trend is the opposite to that of peak stress and is most clear at low (i.e. 50 kPa) confining pressures and at large cement to moisture content ratios. A reduction in strength is normally associated with a reduction in the maximum volumetric strain.

- Maximum volumetric strain is directly related to the axial strain at peak conditions.

- Nearly all samples contracted up to an axial strain slightly beyond peak conditions; this contraction occurs at a nearly constant rate. Most samples dilated at or soon after peak stress conditions; the degree of dilation increased with cement content and curing time. Occasionally, the sample continued to contract following failure; usually this occurred at low cement contents or low curing times and may be due to premature brittle failure.

- When no cement was present, the sample began to dilate prior to failure. Cement retards to the change from contraction to dilation during drained shear.

- Volumetric strain during shear increases with moisture content.

- The effect of cement content and curing time on volumetric strain is a function of confining pressure because volume change also occurs during consolidation. At low confining pressures (i.e. 50 kPa), an increase in cement content and/or curing time lead to a decrease in volume change during shear, as expected; however, the opposite is true at high confining pressures (i.e. 400 kPa). This trend is directly related to the volume change during consolidation, which is significantly greater for weakly cemented materials at high consolidation pressures. When a large volume change occurs during consolidation due to failure of cement bonds, the volume change during drained shear is reduced. Therefore, at 400 kPa confining pressure, an increase in cement content and/or curing time results in an *increase* in volume change during shear.

- As confining pressure increases, so does the volumetric strain. Low confining pressures increase the tendency for the sample to dilate following peak.

5.5.4 Excess Pore Water Pressure During Undrained Conditions

- The excess pore water pressure remained positive throughout all undrained triaxial tests on kaolin-cement, with some dilation beginning at an axial strain roughly corresponding to peak stress conditions. Similar to the drained test results, this behaviour resembles that of normally-consolidated to slightly over-consolidated clay.

- For pure kaolin, the sample began to dilate before peak stress conditions were achieved. Furthermore, the excess pore water pressure was negative at

fully-softened stress conditions when the confining pressure was only 100 kPa; this indicates over-consolidated behaviour. Without cement, the change from contraction to dilation occurs sooner.

• The degree of sample dilation following peak stress conditions increased with cement to moisture content ratio and decreased with confining pressure.

• As the confining pressure increased, so did the excess pore water pressure. Of all factors considered, confining pressure has the most significant influence on the excess pore water pressure and the overall undrained behaviour of kaolin-cement.

• The peak excess pore water pressure increased with curing time and cement content, although the strong influence of confining pressure often minimized the effects of these variables.

5.5.5 Failure Behaviour

• All of the triaxial tests exhibited strain-softening behaviour; failure for the drained tests was brittle. The degree of brittleness increased with cement content and curing time (stiffness) and decreased with confining pressure.

• More sample disturbance near the failure plane is associated with lower cement to moisture content ratios and lower curing times.

• A clear shear plane roughly 30° from the vertical axis develops during failure for all of the triaxial tests due to plastic shearing; sometimes two shear planes develop simultaneously. Occasionally, for the undrained tests only, no shear plane developed and it is believed that failure was by crushing.

• For the drained tests, some samples continued to contract following failure. This may be due to premature brittle failure and subsequent crushing of the sample.

• Under unconfined conditions, failure is brittle; samples fail in tension followed by crushing. Normally, nearly vertical tension cracks formed during shear; sometimes spalling was observed.

5.5.6 Overall Conclusions

• When the cement content of kaolin-cement is 5 percent or less and curing is done in water, the strength of the material may deteriorate after 28 to 56

days of curing. This is partly because of the relatively large amount of cement required for effective stabilization of clay particles due to their high specific surface.

• Curing environment has a significant influence on the strength properties of kaolin-cement. These results indicate that under some circumstances, kaolin-cement cured in water may begin to soften over time. Softening leads to a reduced strength and apparent consolidation yield stress. Leaching of cementitious material out of the kaolin-cement during curing may also contribute towards the apparent loss of strength with time. More research is required to understand and define the circumstances which lead to sample softening.

• Cement stabilization has been reported to cause an apparently over-consolidated behaviour (Kohata *et al.*, 1997) and to increase the apparent consolidation yield stress of the material being stabilized. While stress-strain curves show strain softening, similar to over-consolidated behaviour, trends in volumetric strain and excess pore water pressure during drained and undrained tests, respectively, as well as undrained stress paths, indicate that the behaviour more closely resembles that of normally consolidated clay. This may be a fundamental concept of cement-stabilized clay. Pure kaolin at sufficiently low confining pressures behaved as an over-consolidated material.

• Undrained stress paths from triaxial tests on kaolin-cement and pure kaolin reveal that, under some circumstances, kaolin-cement actually has a *lower* apparent consolidation yield stress than pure kaolin. This theory will be studied in more detail in the following chapter on the consolidation characteristics of kaolin-cement.

6. KAOLIN-CEMENT CONSOLIDATION CHARACTERISTICS

6.1 General

It has been reported by others (i.e. Kohata *et al.*, 1997) that the deformation characteristics of cement-treated soils are similar to those of over-consolidated clay in that a well-defined yield point is present. Similar to ordinary clay, the strength of cement-treated soil increases as consolidation progresses. However, due to the cement, the consolidation characteristics of clay-cement mixtures can be compared to those of natural clays with soil structure, which describes the presence of fabric and bonding.

Based on the results of the current study, it is proposed that the apparent consolidation yield stress (p_c) derived from the consolidation data is equivalent to the point at which the cement bonds begin to fail during consolidation. While this value is extracted from the consolidation curve, it does not provide information about the stress history of the soil. Based on the consolidation data, as well as the triaxial shear data discussed in Chapter 5, it is suggested that the behaviour of kaolin-cement is more similar to that of normally consolidated to only slightly over-consolidated clay (when the cement to moisture content ratio is sufficiently high), contrary to conclusions drawn by others. Furthermore, when exposed to water during curing, the apparent consolidation yield stress or bond strength may actually *decrease* with curing time under some circumstances.

Besides recording data during consolidation of the triaxial tests, both oedometer tests and isotropic consolidation (IC) tests were performed to assess the consolidation characteristics of the kaolin-cement and pure kaolin mixtures. A maximum normal load of 3200 kPa was applied to the oedometer samples; a maximum isotropic pressure of 400 kPa was applied to the IC samples. A back pressure of 300 kPa was used for saturating the IC samples as the limit of the compressor used in the triaxial apparatus was 700 kPa. The complete laboratory procedures for the oedometer and IC tests are described in Sections 4.7 and 4.5, respectively.

For all tests, the apparent consolidation yield stress (p_c), compression index (C_c) and swelling index (C_s) were calculated. In addition, the coefficient of consolidation (c_v) and coefficient of volume compressibility (m_v) were

determined for each load phase. The following subsections describe each consolidation characteristic considered, and the effect of curing time, cement and moisture content on each characteristic. Furthermore, the differences observed between the characteristics obtained from one-dimensional consolidation (i.e. oedometer test) and those obtained from isotropic consolidation will be described. However, consolidation properties determined by each test are often different for the same mix simply because of the difference in maximum load. The maximum load for the IC tests was only 400 kPa, which is often not much greater than the apparent consolidation yield stress. Therefore, unlike the oedometer results, the curve for the IC tests does not always extend into the so-called over-consolidated range. Oedometer test results are therefore considered to be more accurate. Appendix D includes plots of specific volume, coefficient of consolidation and coefficient of volume compressibility against load for each mix. The oedometer, IC and triaxial consolidation data are plotted together to compare the results provided by each test in Figures D.1 to D.17. Figures D.18 to D.21 illustrate the effect of curing time and Figures D.22 to D.25 illustrate the effect of cement and moisture content on the consolidation characteristics. Often only the oedometer data is plotted in Appendix D since these tests cover a considerably wider range of consolidation pressures than the IC data.

Table 6.1 summarizes some of the consolidation test results for the sample mixes and curing times considered. It is appropriate to note here the relatively large value of C_c/C_s for the oedometer tests on kaolin-cement samples; values range from roughly 4 to 25. These large values are due to the bonding characteristics and open structure of kaolin-cement, and can be compared to those of quick clays. Further discussion of the structure of soil-cement is included in Chapter 7.

Table 6.1. Summary of consolidation test results

Moisture content, w (%)	Cement content, Ac (%)	Curing time, Tc (days)	OEDOMETER TEST RESULTS			ISOTROPIC CONSOLIDATION TEST RESULTS		
			pc (kPa)	Cc	Cs	pc (kPa)	Cc	Cs
40	0	-	118	0.23	0.111	≤50	0.18	0.096
70	2	7	≤50	0.57	0.117	≤50	0.45	0.045
		28		0.59	0.129		0.52	0.071
		56	110	0.61	0.116	116	0.53	0.058
		112	≤50	0.60	0.150	≤50	0.49	0.072
	5	7	240	0.65	0.055	138	0.55	0.008
		28	282	0.68	0.062	240	0.54	0.017
		56	278			252	0.50	0.032
		112	322	0.71	0.051	-	-	
100	5	7	≤50	0.87	0.085	≤50	0.92	0.023
		28	118	0.96	0.082	114	0.87	0.048
		56	126	1.03	0.077		0.85	0.051
		112	157	0.95	0.046	120	0.73	0.036
	10	7	242	1.04	0.053	246	0.84	0.013
		28	265	1.10	0.059	273	0.70	
		56	271	1.11	0.062	282	0.66	0.032
		112	332	0.97	0.038	344	0.45	

6.2   Apparent Consolidation Yield Stress

Traditionally, the consolidation yield stress, p_c, is the maximum pressure which the material has experienced in the past and is determined from the consolidation curve. For cement-treated soils, an apparent consolidation yield stress is derived since it is not actually a function of the soil-cement's stress history. It is proposed that the apparent consolidation yield stress is the pressure at which the cement bonds begin to fail during consolidation. For this study, the term "consolidation yield stress" was deemed to be more appropriate than the "pre-consolidation pressure", however, traditionally in the case of clays, the two terms are equivalent. While the following discussion implies that the kaolin-cement consolidates similar to clay, it is proposed that the majority of the consolidation is merely collapse of the cement bonds.

For the current study, the apparent consolidation yield stress was determined for both the oedometer and IC tests following Casagrande's

method. The general trend is for the consolidation curve to resemble that of an over-consolidated material, similar to what was concluded by Kohata *et al.* (1997). However, when the kaolin-cement is weakly bonded at low cement to moisture content ratios, the apparent consolidation yield stress was very small (< 50 kPa) and so the consolidation curve resembled that of a normally consolidated material. Furthermore, the volumetric strain and excess pore water pressure generated during drained and undrained triaxial tests, respectively, suggest that the true behaviour of kaolin-cement is more similar to that of a normally consolidated material. Due to the cement bonds, the consolidation curves may falsely lead us to believe otherwise.

A plot of the apparent consolidation yield stress against curing time is provided in Figure 6.1. As seen, the oedometer tests sometimes yield a greater value due to the larger applied loads. Note that apparent consolidation yield stresses below 50 kPa could not be measured.
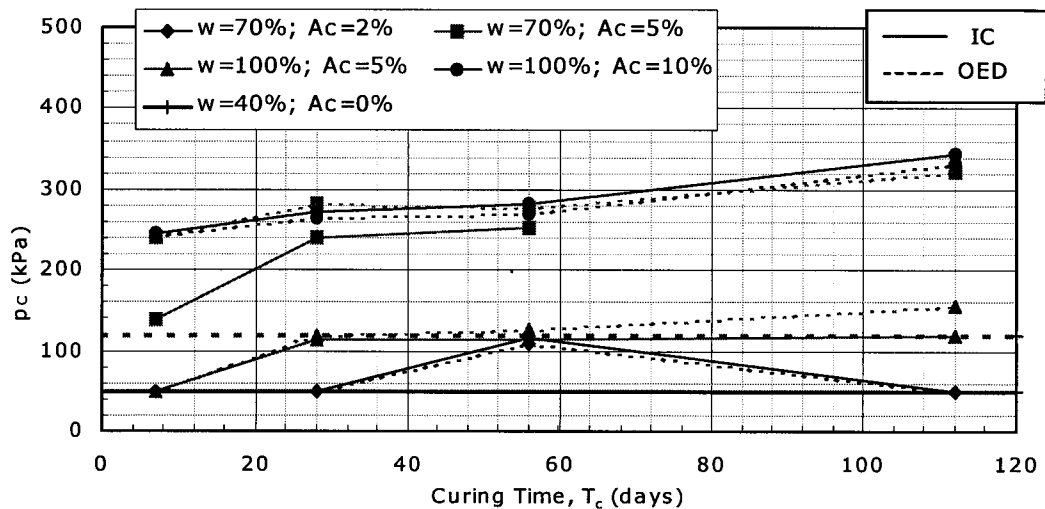
Figure 6.1. Apparent consolidation yield stress vs. curing time.

6.2.1 Effect of Curing Time

It is clear from Figure 6.1 that the apparent consolidation yield stress and therefore, the apparent over-consolidation ratio, increased with curing time up to at least 56 days, as determined from both the oedometer and IC tests. When the cement content is only 2 percent, however, the apparent consolidation yield stress decreased after 56 days of curing so that after 112 days, the apparent consolidation yield stress was roughly the same as after

116   *Mechanical Characteristics of Kaolin-Cement Mixture*

only 7 days of curing (≤50 kPa). The same deterioration was seen in the results of the strength tests; with so little cement and curing in water, softening may have occurred during curing.

Similar to the trends observed for the strength tests, the change in the apparent consolidation yield stress is generally greatest between 7 and 28 days of curing. This indicates that the increase in strength with curing time is directly linked to the apparent consolidation that progresses with curing.

6.2.2 Effect of Cement Content and Moisture Content

The apparent consolidation yield stress increases with cement to moisture content ratio (Fig. 6.1). Results show that values at intermediate cement to moisture content ratios are very similar to one another, as are values at low ratios. Furthermore, when the cement content is very low (i.e. 2 percent), the apparent consolidation yield stress *decreases* after 56 days of curing. These same general trends were also seen in the strength data; an increase in apparent consolidation yield stress often corresponds to an increase in strength, and vice versa.

When no cement is present, there is obviously no apparent consolidation due to cementation. Therefore, the apparent consolidation yield stress is mainly a function of the compaction method. Samples with 40 percent moisture were compacted by hand tamping and the apparent consolidation yield stress for these samples is roughly 120 kPa, based on the oedometer test results. This is *greater* than that of the samples with a low cement to moisture content ratio. These results indicate that curing in water may reduce the apparent consolidation yield stress for weakly cemented soils. The same observation was made when interpreting the stress paths for the undrained triaxial tests.

6.3   Compression Index

The compression index, C_c, is the slope of the virgin compression curve and is a measure of the volume change that can be expected once the apparent consolidation yield stress is exceeded. For each oedometer and IC test, the

compression index was calculated using linear regression through the linear portion of the virgin compression curve.

Figure 6.2 shows the change in the compression index with curing time for each mix considered. There is a consistent difference in the compression index for the two types of tests; the oedometer test always yields a greater value. This is because the back pressure applied during the IC tests will reduce compression and hence the compression index.
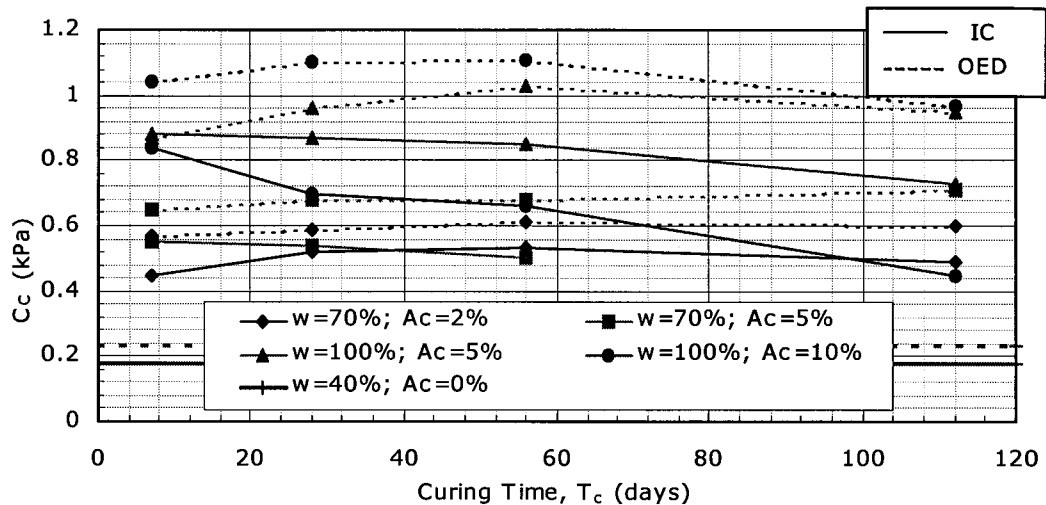
Figure 6.2. Compression index vs. curing time.

6.3.1 Effect of Curing Time

For the oedometer tests, the compression index increased slightly with curing time (Fig. 6.2); often the rate was approximately constant. Typically, the opposite trend was observed in the IC test results; the compression index *decreased* with curing time. Furthermore, the compression index was almost always greater for the oedometer tests than for the IC tests.

For a bonded material, an increase in sample deformation with curing time, as seen in the oedometer test results, suggests an increase in void ratio with curing time and failure of cement bonds during consolidation. An increase in void ratio over time would result from deflocculation of the clay particles, which is expected due to the reduction in pH of the pore water with time. Results from all laboratory tests show that the void ratio does increase very slightly with curing time up to 56 days (Fig. 6.3). A maximum load of 3200 kPa for the oedometer tests would be sufficient to break the cement

bonds for the cement contents considered, therefore, an increase in compression with curing time is expected for these tests.

The pattern in the IC test results is different because loads were not great enough to cause failure of the bonds, except when the cement content was very low at 2 percent. Therefore, a *reduction* in compression with curing time is seen. The same trend was observed by Uddin (1995) from oedometer tests on stabilized Bangkok clay with 5 to 10 percent cement. Uddin cured samples in a humid environment and some coarse-grained material was present in the stabilized material. Therefore, the cement bonds likely did not fail during consolidation as was the case for the current study. Uddin did not observe any significant changes in the consolidation properties with curing time at cement contents less than 5 percent.
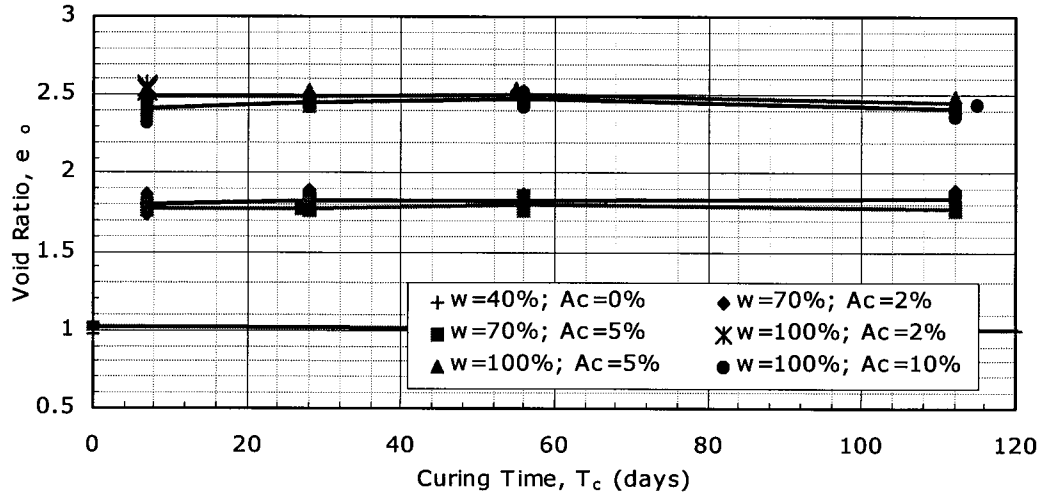
Figure 6.3. Average void ratio vs. curing time (results include all successful laboratory tests).

6.3.2 Effect of Cement Content and Moisture Content

Based on the findings, the compression index is affected primarily by moisture content; as moisture content increases, so does the compression index (Fig. 6.2). This trend is expected and is true for non-cemented clays also.

It is also expected that the compression index will decrease with cement content; this was the conclusion made by Uddin (1995) who considered up to 25 percent cement. However, except for the IC tests at 100

percent moisture content, the compression index nearly always *increased* slightly with cement content. This increase is very small and usually not detectable when the slopes of each curve are visually examined. Because the bonds have failed at pressures where the compression index is calculated, the compression index should be independent of cement content. Some increase in the compression index with cement content is seen only because the bonds begin to fail at a slightly lower pressure for the mixes with a lower cement content yet the same moisture content. Therefore, these curves are slightly steeper at lower pressures, but the difference is not significant.

6.4   Swelling Index

The swelling index, C_s, is the slope of the rebound (or expansion) curve, which is plotted when the sample is unloaded. Figure 6.4 shows the change in the swelling index with curing time for each mix considered. For each oedometer and IC test, the swelling index was calculated using linear regression through the rebound curve.   In general, the swelling index decreased with cement content and increased with curing time. Due to the significantly larger loads applied during the oedometer tests and the high likelihood that cement bonds failed during consolidation, the resulting degree of swelling is noticeably higher than that from the IC tests. The same observation was made for the compression index, as the two properties are directly related.
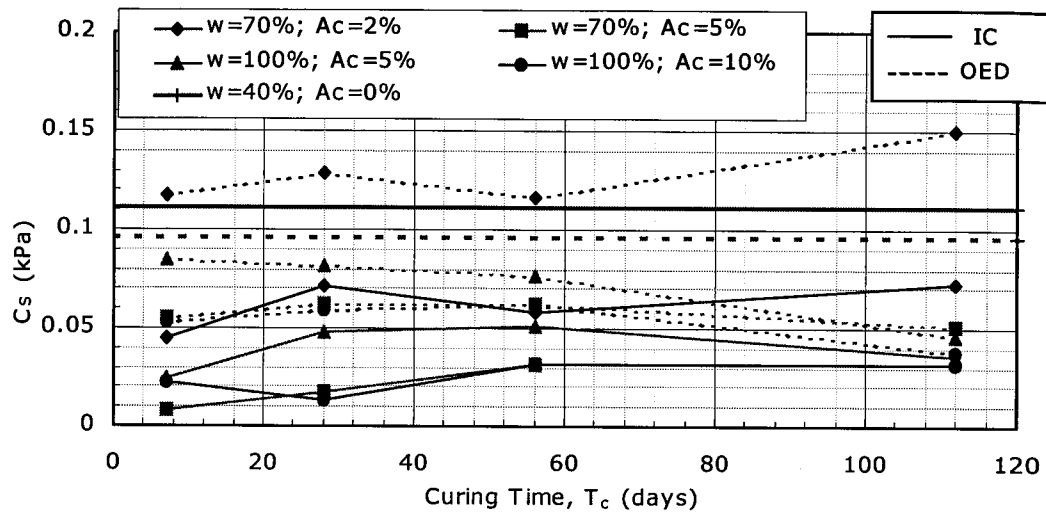
Figure 6.4. Swelling index vs. curing time.

6.4.1 Effect of Curing Time

A general increase in the swelling index with curing time was observed (Fig. 6.4) and corresponds to the trend in the compression index with curing time. All changes in the swelling index due to curing time were very small. At only 2 percent cement, the change in the swelling index is very erratic for both the oedometer and IC tests. This material is very weakly bonded and the bonds fail during consolidation; this may influence the swelling in an unpredictable manner.

6.4.2 Effect of Cement Content and Moisture Content

An increase in the cement to moisture content ratio leads to a reduction in the swelling index (Fig. 6.4), for all cases considered. For the two mixes with an intermediate cement to moisture content ratio, the swelling index is nearly identical at all curing times.

The change in swelling index due to moisture content corresponds to the change in compression index; as compression increases during loading, so does swelling during unloading. However, cement causes more permanent deformation so that swelling is reduced significantly as cement content increases. As loading progresses, the cemented particles become interlocked and simple unloading does not reverse this process. A comparison of

Mechanical Characteristics of Kaolin-Cement Mixture   121

consolidation curves with and without cement is illustrated in Figure 6.5. When no cement is present, the material rebounds to a void ratio only slightly less than what it was prior to consolidation. However, the cemented material rebounds a much lesser degree due to permanent deformation and damaged/failed bonds.

6.5   Coefficient of Consolidation

The coefficient of consolidation, c_v, was calculated for each stage of both the oedometer tests and IC tests, as well as for the consolidation stage of each triaxial test. The coefficient of consolidation ranged from values on the order of 1 to almost 1000 m^2/year.

Due to the judgement required to calculate the coefficient of consolidation, the results vary considerably and should not be taken as exact. Often, but not always, the coefficient of consolidation was greater for the IC tests than for the oedometer tests.
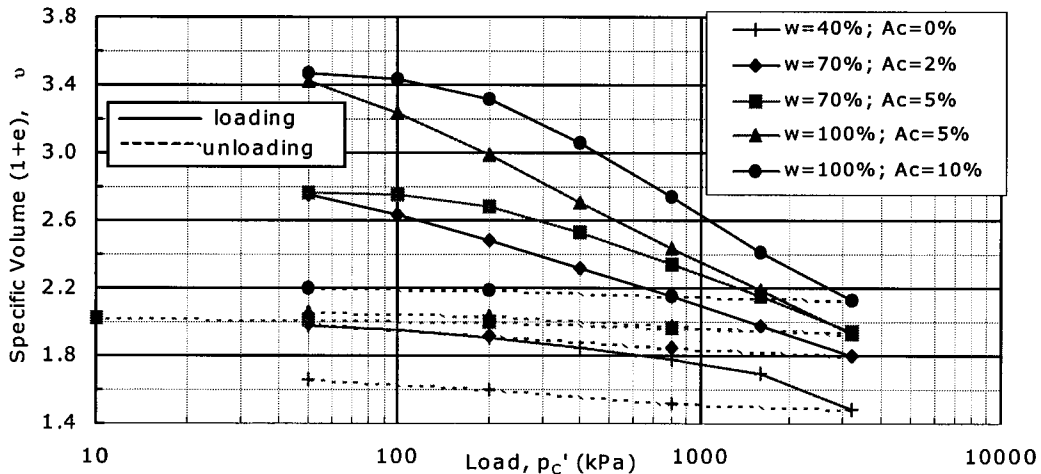
Figure 6.5. Consolidation curves for $T_c=7$ days (oedometer tests).

6.5.1   Effect of Curing Time

While it is difficult to see this trend, up to a given consolidation pressure, which depends on the sample mixture, the coefficient of consolidation generally increased with curing time (Fig. 6.6). This is the desired effect and

the same observation was made by Uddin (1995) at all pressures. However, at high consolidation pressures for the current study, the coefficient of consolidation actually *decreased* with curing time. It is suggested that this reversal occurs at approximately the apparent consolidation yield stress and is due to failure of cement bonds and subsequent collapse of structure during consolidation. Patterns observed in the apparent consolidation yield stress and compression index also support this theory.
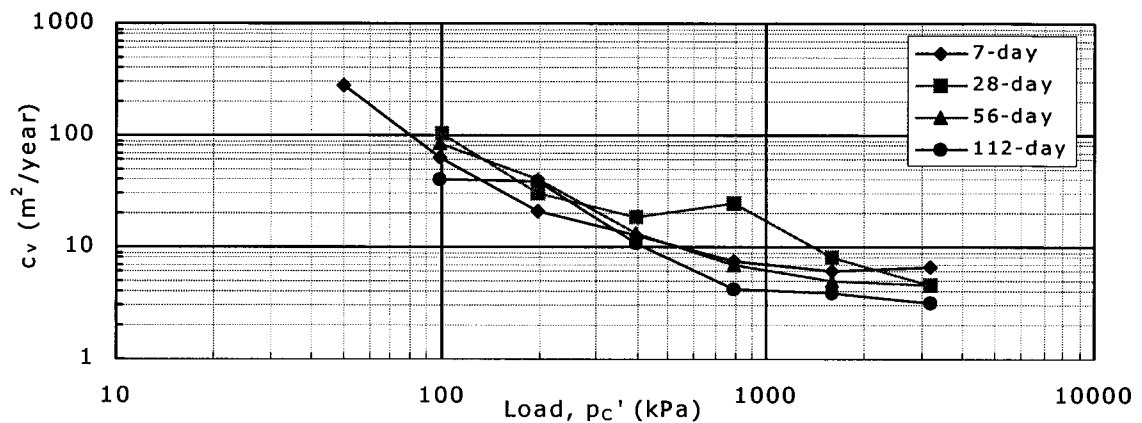
Figure 6.6. Coefficient of consolidation vs. load for w=100% & A_c=10% (oedometer tests, loading only).

6.5.2 Effect of Cement Content and Moisture Content

Uddin (1995) concluded that cement treatment increases the coefficient of consolidation. For the current study, a clear trend emerged that supports this theory only at low consolidation pressures, while the cement bonds are still intact. The effects of an increased cement to moisture content ratio are similar to that of curing time. At low consolidation pressures, the coefficient of consolidation increased with an increase in the cement to moisture content ratio. However, at high consolidation pressures, the trend is the exact opposite (Fig. 6.7). Note that for the sample with only 2 percent cement, the coefficient of consolidation changes very little with load.

Uddin (1995) found the coefficient of consolidation decreased as the load increased. Based on the current consolidation test results, as consolidation pressure increases, the coefficient of consolidation decreases significantly initially, and then changes very little or increases slightly (Fig. 6.7). This again supports the theory that after some consolidation pressure, the cement bonds failed.

Once unloading begins, the material is over-consolidated again and, following an initial rise in the coefficient of consolidation after the first unloading stage, c_v decreases with a reduction in consolidation pressure.
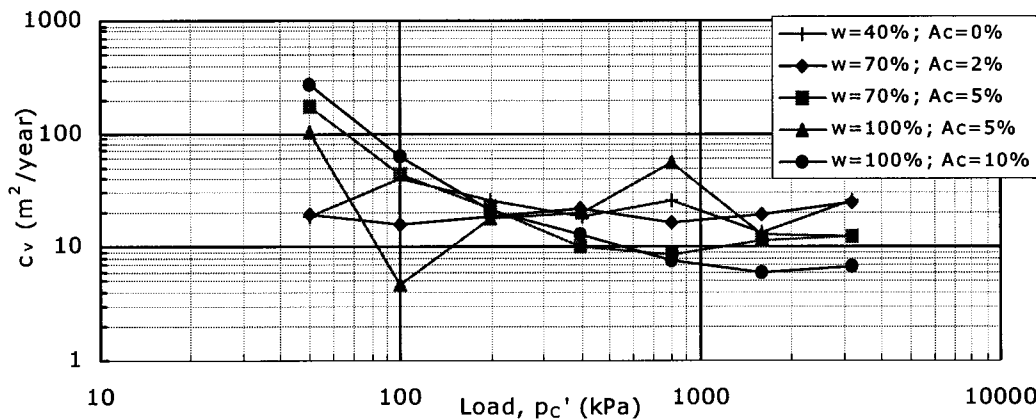
Figure 6.7. Coefficient of consolidation vs. load for T_c=7 days (oedometer tests, loading only).

6.6 Coefficient of Volume Compressibility

The coefficient of volume compressibility, m_v, describes the rate of volume change and was calculated for each loading stage of both the oedometer tests and IC tests, and for the consolidation stage of the triaxial tests. The coefficient of volume compressibility ranges from near 0 to approximately 1.5 m^2/MN; lower values are associated with stiffer material.

Typically, but not always, the coefficient of volume compressibility is greater for the oedometer tests than for the IC tests. This is partially due to back pressure applied to the IC tests, which reduced compressibility.

6.6.1 Effect of Curing Time

An increase in curing time, up to at least 56 days, generally leads to a decrease in the coefficient of volume compressibility during loading (Fig. 6.8), except when the cement content is 2 percent or occasionally during the initial loading stage for the oedometer tests. This indicates that as curing proceeds, the material becomes more stiff and less consolidation occurs for the same load. At high loads when cement bonds have failed and during unloading, the change in the coefficient of volume compressibility with curing time was small to negligible. At 2 percent cement and in some cases, beyond approximately 56 days of curing, softening may have occurred with curing time due to insufficient cementation. The large values in the coefficient of volume compressibility that are sometimes calculated for the initial stage of the oedometer tests are likely due to seating of the oedometer cap. Consolidation occurred at such a fast rate for this initial stage that it was difficult to take accurate measurements.
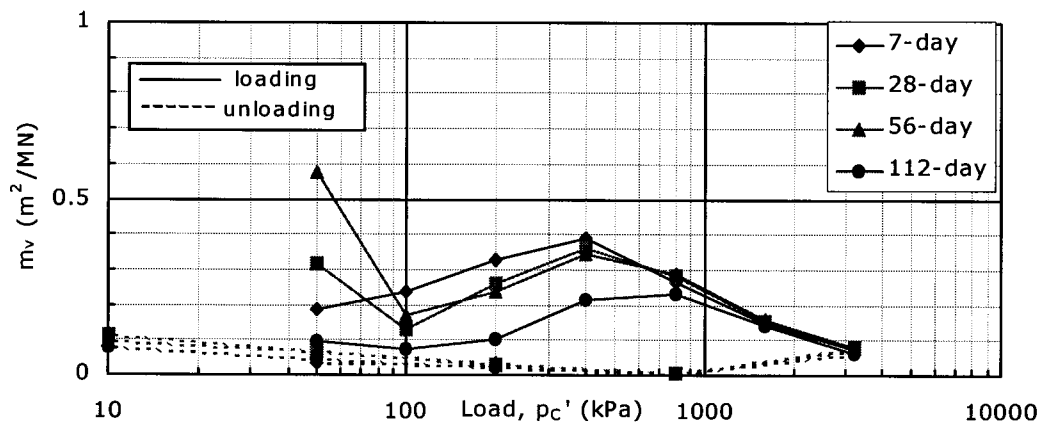
Figure 6.8.   Coefficient of volume compressibility vs. load for w=100% & A$_c$=10% (oedometer tests).

6.6.2 Effect of Cement Content and Moisture Content

Prior to the apparent consolidation yield stress, the coefficient of volume compressibility increases with a decrease in the cement to moisture content ratio (Fig. 6.9). Once the apparent consolidation yield stress is achieved, the trend reverses and is a function of void ratio. At high loads, the coefficient of

volume compressibility is the same for each moisture content, regardless of cement content; eventually all samples have the same coefficient of volume compressibility. These trends give evidence to the previous suggestion that the cement bonds are broken at approximately the consolidation yield stress and eventually, the structure collapses.

6.6.3 Effect of Consolidation Pressure

In general, during loading, there is an initial increase in the coefficient of volume compressibility at low pressures, when the cement bonds are intact (Figs. 6.8 and 6.9). This is followed by a distinct *decrease* up to the maximum load, when the cement bonds are failing. As the cement to moisture content ratio and curing time increase, the material becomes more stiff and the pressure at which the trend changes from increasing to decreasing becomes greater.
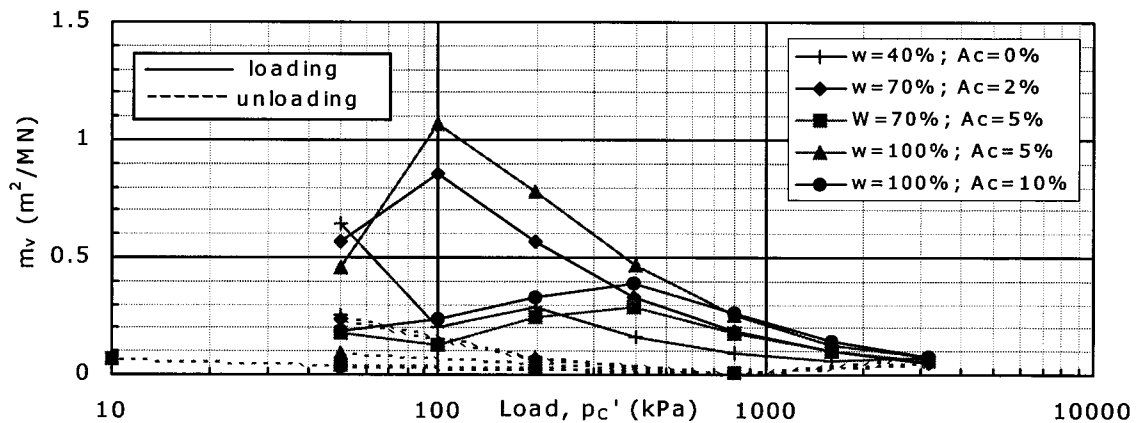
Figure 6.9. Coefficient of volume compressibility vs. load for $T_c=7$ days (oedometer tests).

6.7 Summary and Conclusions

Some of the significant concepts observed from the oedometer and IC tests on pure kaolin and kaolin-cement are summarized below. Note that conclusions are based on somewhat limited test results and are not intended to characterize conditions not considered in the current study.

6.7.1 Apparent Consolidation Yield Stress

- When the cement content is sufficiently high, the consolidation behaviour of kaolin-cement resembles that of an over-consolidated clay in that an apparent consolidation yield stress can be determined from the consolidation curve. However, in no way does this apparent consolidation yield stress provide information about the stress history of the kaolin-cement. Furthermore, volumetric strain and excess pore water pressure data obtained from drained and undrained triaxial tests, respectively, suggests that kaolin-cement behaves as a normally consolidated to slightly over-consolidated material.

- The apparent consolidation yield stress is roughly equivalent to the pressure at which the cement bonds begin to fail during consolidation.

- The apparent consolidation yield stress increases with cement to moisture content ratio and curing time, up to at least 56 days. However, when the cement content is sufficiently low, a reduction in the apparent consolidation yield stress was observed following 56 days of curing. This indicates deterioration of the kaolin-cement with time; the same observation was made of the strength test results.

- When exposed to water during curing, the apparent consolidation yield stress of weakly cemented materials may decrease due to softening. Leaching of cementitious material during water curing may also lead to this behaviour.

6.7.2 Compression and Swelling Indices

- The values of C_c/C_s from oedometer tests are on the order of roughly 4 to 25 for kaolin-cement; these are relatively large and can be compared to those of quick clays.

- The compression index increases with moisture content but is relatively independent of cement content. This is because the cement bonds have failed at the consolidation pressures at which the compression index was calculated.

- The results of the oedometer and IC results were typically different; usually, this was because the oedometer tests were consolidated further

beyond the apparent consolidation yield stress. However, back pressure applied during isotropic consolidation reduces compression; this was indicated by a decrease in the compression index and the coefficient of volume compressibility of the IC test results, as compared with the oedometer test results.

• Void ratio may increase very slightly with curing time, up to at least 56 days. It is suggested that this may be due to some deflocculation of clay particles resulting from a reduction in pore water pH. Furthermore, when cement contents are sufficiently small and consolidation pressure sufficiently high, cement bonds will fail during consolidation. Therefore, an increase in compression was observed with curing time at high pressures and relatively low cement contents.

• The trends in the swelling index are very similar to those in the compression index, except the swelling index is a function of cement content. This may be because cemented particles interlock during consolidation, causing permanent deformation, which is a function of the degree of cementation.

6.7.3 Coefficient of Consolidation

• Based on limited data, it was observed that the coefficient of consolidation generally increased with curing time and cement content up to a pressure roughly corresponding to the apparent consolidation yield stress, when the trend was reversed. When the cement to moisture content is low, there is very little change in the coefficient of consolidation with consolidation pressure.

6.7.4 Coefficient of Volume Compressibility

• Based on limited data, it was observed that the coefficient of volume compressibility increased as the material stiffness decreased at consolidation pressures less than the apparent consolidation yield stress. Once the apparent consolidation yield stress was reached and the cement bonds failed, the trend reversed and was a function of void ratio.

- The consolidation pressure at which the maximum coefficient of volume compressibility was achieved increases with cement to moisture content ratio.

- At high loads and during unloading, the structure has collapsed and the coefficient of volume compressibility is approximately the same for all mixes and curing times.

- Usually, the IC tests yielded lower coefficients of volume compressibility than the oedometer tests; this is likely due to the applied back pressure, which reduces the compressibility.

7.   MICRO-STRUCTURE OF KAOLIN-CEMENT

7.1   General

The mechanical behaviour of soil is strongly influenced by the shape, size and surface characteristics of the soil particles (Mitchell, 1993). Furthermore, the soil structure, which is also a function of the individual particle properties, heavily influences the soil's behaviour. Sufficient detail of the particle properties can only be observed with the aid of a Scanning Electron Microscope (SEM).

When cement is added to clay, the hydrogen bonds that normally exist between clay particles in the presence of water are strengthened by a chemical change in the pore water and the soil structure becomes more flocculated; this phenomenon is generally accepted in literature (i.e. Porbaha *et al.*, 2000). The bonded structure controls the yield behaviour of bonded materials, which can be independent of its stress history (Malandraki *et al.*, 2000). Therefore, to better understand the mechanical behaviour of kaolin-cement, and the affect of moisture content, cement content and curing time, it is useful to study the soil structure.

When describing the soil structure of clay, the following four terms must first be understood (van Olphen, 1963):

1.   *Dispersed*. No face-to-face association of clay particles.
2.   *Aggregated*. Face-to-face association of several clay particles.
3.   *Flocculated*.   Edge-to-edge or edge-to-face association of aggregates
4.   *Deflocculated*. No association between aggregates.

Figure 7.1 on the following page illustrates the 7 modes of particle associations in clay suspensions using the above terminology. These modes will be used to describe the structure of kaolin and kaolin-cement in future sub-sections.

Scanning Electron Microscope images were taken of each mixture considered for the laboratory tests; the procedure and results are described in

the following sub-sections. All images at reasonable magnifications are included in Appendix E.
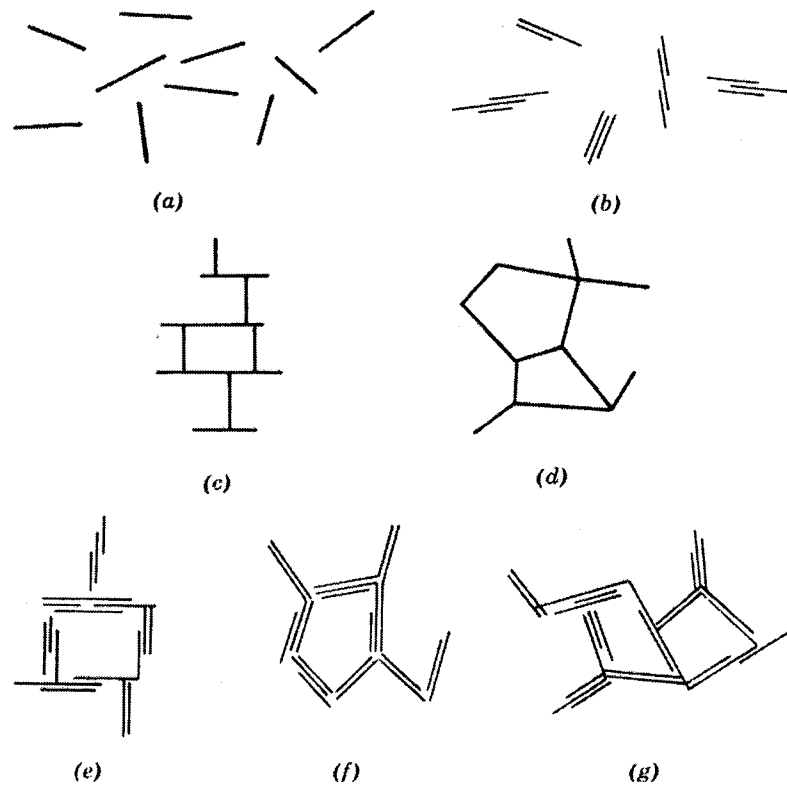
Figure 7.1. Modes of particle associations in clay suspensions and terminology (van Olphen, 1963).

(a) dispersed and deflocculated. (b) Aggregated but deflocculated (face-to-face association, or parallel or oriented aggregation). (c) Edge-to-face flocculated but dispersed. (d) Edge-to-edge flocculated but dispersed. (e) Edge-to-face flocculated and aggregated. (f) Edge-to-edge flocculated and aggregated. (g) Edge-to-face and edge-to-edge flocculated and aggregated.

7.2   Sample Preparation for Scanning Electron Microscope Tests

Scanning Electron Microscope photomicrographs were taken at the University of Alberta. Prior to sample preparation, the pore water must be either removed, replaced or frozen. This is very difficult to do without disturbing the structure of the sample and there is some debate as to what method is most suitable for different types of soils. Mitchell (1993) reports that air drying may be appropriate for very stiff soils, or soils that will not shrink significantly. However, because of the time required for air drying, some

particle rearrangement may occur and therefore, for soft soils with a high moisture content, oven-drying may be more appropriate. However, Shi *et al.* (1999) report that both air-drying and oven-drying soils with high moisture contents results in significant shrinkage leading to important changes in the soil's microstructure.

Shi *et al.* suggest a freeze-cut-drying method to minimize changes in the microstructure of the soil. This method involves dipping a sample at its natural moisture content into liquid freon and then cooling the sample with liquid nitrogen. The rapid freezing prevents volume change since non-crystal ice is formed, and therefore, no disturbance to the soil microstructure results. A fresh fracture surface is made with a cool sharp knife, and the sample is dried using a vacuum set-up and dry ice. Not only is this sample preparation method complex, but the sample must be maintained at a very low temperature during scanning. Due to the change in structure that comes with aging of soil-cement, sample preparation would have had to have taken place frequently and simultaneously with the other laboratory tests; this method was not considered to be reasonable for the current study. For the current study, samples were oven-dried and traditional sample preparation and SEM analysis was performed.

Undisturbed trimmings from laboratory samples were oven-dried and then prepared so that freshly fractured surfaces were exposed for scanning. Sample preparation was done by gently breaking off a small piece of dry material, which was very brittle and the consistency of weak chalk, to expose a relatively flat, freshly-fractured surface. This surface was not touched so that it remained clean. Using silver paint as glue, the sub-sample was placed on a small round metal stub, with the fractured surface facing upwards. Because the sample was so porous, the silver paint aided in filling the exposed voids on the surfaces which were not going to be scanned. Using silver increased the conductivity of the sample, making it easier to get a good image with the microscope. The vertical edge of the sample was completely coated with silver paint so that the only portion of the sample exposed to the atmosphere was the horizontal fracture surface. A thin line or "seatbelt" of silver paint was also placed across the top of the sample, connecting to the paint on the sides of the sample. This reduced the undesirable charging near the "seatbelt" and images were normally taken in this area. Once the silver

paint was sufficiently dry, the exposed fracture surface was gently cleaned with a shot of compressed air to remove any loose particles. The sample was then coated with gold, following the "sputter" method, using argon gas at a low pressure to attract gold to the sample surface. Immediately following this final stage, the sample was placed in the SEM; the quality of the images were best when the gold was fresh. Six samples were placed in the machine at one time. Images were captured at magnifications of 1000, 3000 and 10,000 times.

Scanning Electron Microscope images were taken at all moisture contents, cement contents and curing times considered for the laboratory program. In addition, images were taken of pure kaolin at 40 and 70 percent moisture content, without cement.

7.3   Soil Structure of Kaolin

Kaolin has a 1:1 silica to alumina structure (Fig. 7.2). That is, kaolin is composed of alternating sheets of silica tetrahedrons (Fig. 7.3) and alumina octahedrons (Fig. 7.4). These sheets are held together tightly by hydrogen bonding, and some weak van der Waals forces. The surface of kaolin minerals is made up of a layer of either oxygen or hydroxyls; strong hydrogen bonding occurs when the positive corners of water molecules are attracted to the oxygen and the negative corners are attracted to the hydroxyls. Van der Waals bonds are weaker than hydrogen bonds and are due to the attraction between oppositely charged electrons.

A single kaolin particle may consist of over one hundred stacks of silica and alumina minerals (Craig, 1992) to form well-crystallized six-sided plate structures (Mitchell, 1993) (Fig. 7.5). The lateral dimensions of these structures range from about 0.1 to 4 μm and their thickness ranges from 0.05 to 2 μm. The specific surface area of kaolin is about 10 to 20 m^2/g of dry clay. When poorly crystallized, the hexagonal kaolin structures are less distinct and the particle size is usually smaller than for well-crystallized structures.

Figures 7.6a and 7.6b illustrate the structure of oven-dried kaolin that, prior to oven-drying, had a moisture content of 40 and 70 percent,

respectively. Both mixes show large aggregates of kaolin particles, consisting of several adjacent stacks. The particle arrangement can be described as edge-to-face and edge-to-edge flocculated and aggregated. There is no obvious difference in the structure of the samples due to the moisture content, although the void ratio prior to drying is obviously greater for the sample with a moisture content of 70 percent. Sample drying may have caused sufficient shrinkage so that the change in void ratio is not seen.
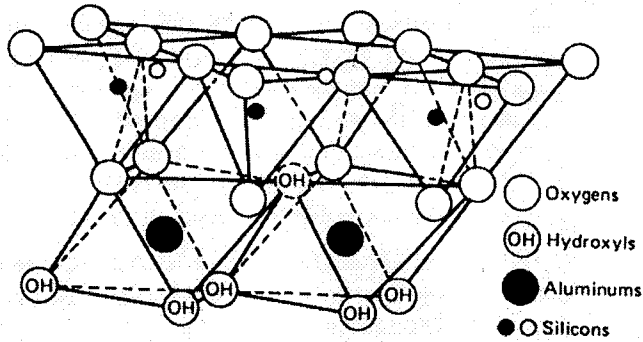
Figure 7.2. Diagrammatic sketch of kaolin structure (Mitchell, 1993).
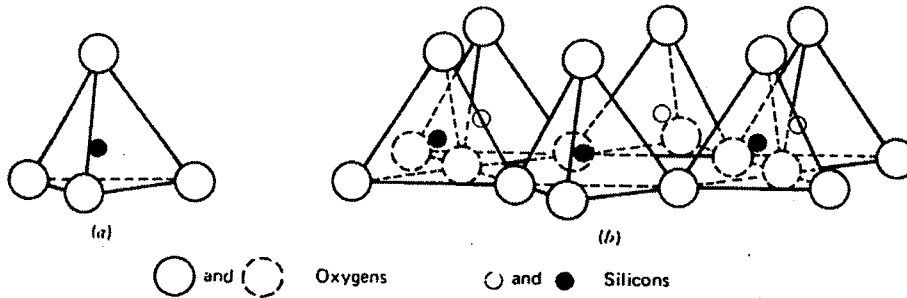
Figure 7.3. Silicon tetrahedron and silica tetrahedra arranged in a hexagonal network (Mitchell, 1993).
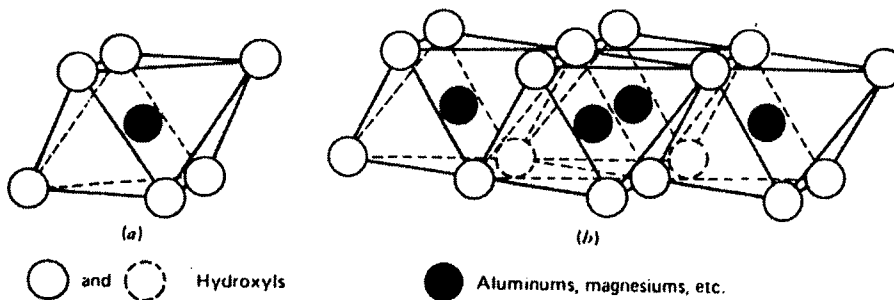
Figure 7.4. Octrahedral unit and sheet structure of octrahedral units (Mitchell, 1993).
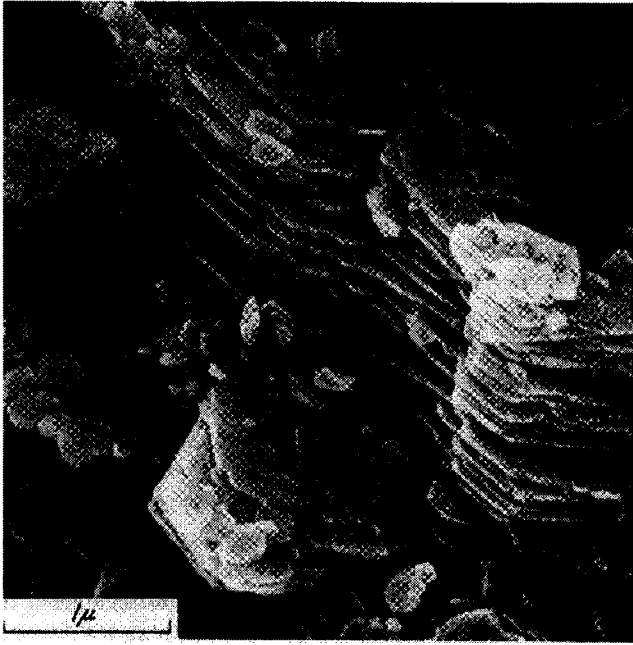
Figure 7.5. Photomicrograph of kaolin (Terzaghi *et al.*, 1996).
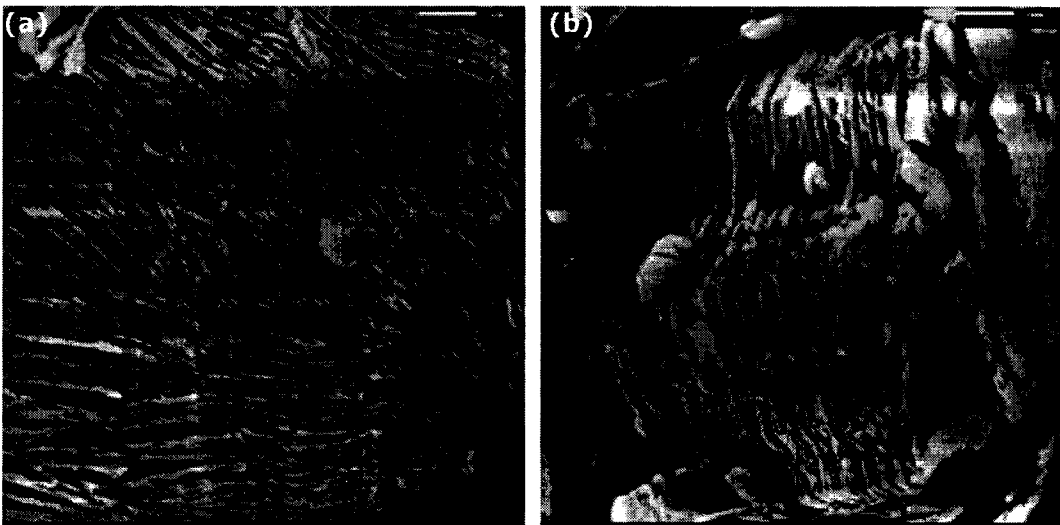
Figure 7.6. Photomicrographs of oven-dried kaolin at M≈7500X. (a) w=40%; (b) w=70%.

7.4   Soil Structure of Kaolin-Cement

7.4.1   Cement Characteristics

When viewed with the SEM, cementitious material appears as needles or cobwebs attached to both the edges and faces of the kaolin particles. When the cement content is 10 percent, the presence of cementitious material is obvious; cementitious material is seen throughout the image (Fig. 7.7a), particularly at higher magnifications. However, at 5 percent cement, it is sometimes difficult to find the cementitious material (Fig. 7.7b and 7.8a) and at 2 percent cement, no cementitious material can be seen (Fig. 7.8b). This agrees with the observations made of the laboratory test results; when 2 and 5 percent cement are considered, the cementation effects on the mechanical properties of kaolin-cement are sometimes difficult to detect. Porbaha *et al.* (2000) state that even when cement and clay are thoroughly mixed, clusters of clay particles surrounded by cementitious material are still expected so that not all clay particles will be cemented. Furthermore, Bergado *et al.* (1996) state that at low pH values (less than 12.6), a different and weaker cementitious material (CSH) is produced than at higher pH values, when the cementitious material is stronger ($C_3S_2H_x$). This concept may explain why the cementitious material cannot be seen at low cement contents (and therefore low pH values) as there is a different cementitious material present altogether. Initially, the pH of a solution with only 2 percent cement was only 12.3.

For the mixture with 10 percent cement content and 100 percent moisture content, a new cement structure, seen in no other mixes, was occasionally found with the SEM (Fig. 7.9). This new structure appeared as small spherical particles. It is hypothesized that this structure represents clumps of cement that did not mix with the kaolin prior to hydration. These clumps may have been present in the cement prior to mixing, or may have formed during mixing/hydration.
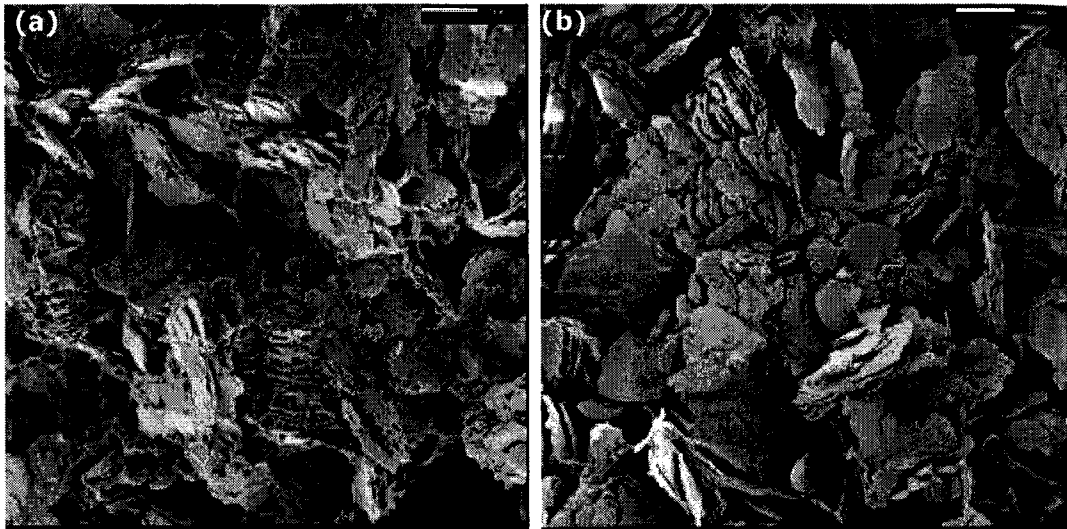
Figure 7.7. Photomicrographs of kaolin-cement at w=100%, T_c=28 days and M$\approx$7500X, illustrating how cement appears in the SEM. (a) A_c=10%; (b) A_c=5%.
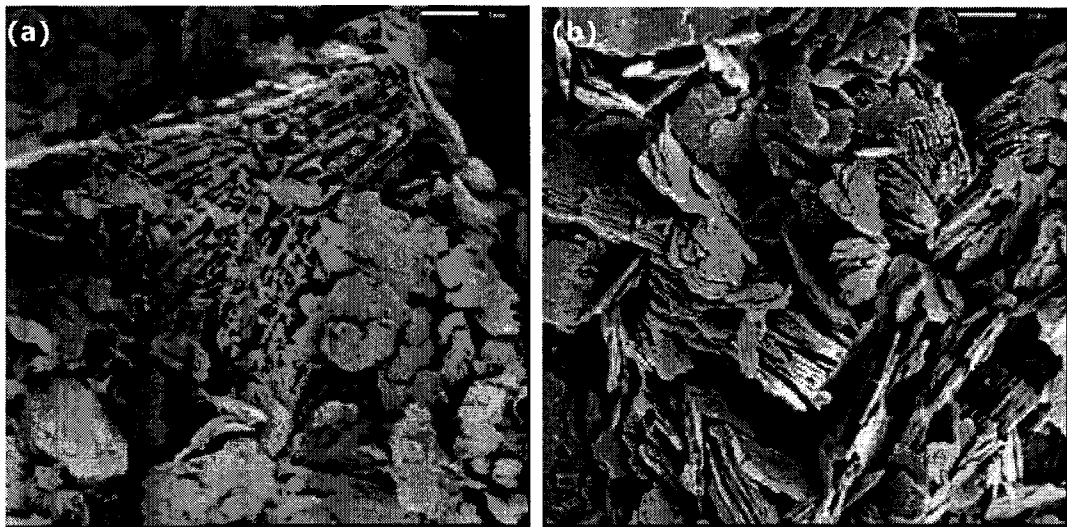
Figure 7.8. Photomicrographs of kaolin-cement at w=70%, T_c=28 days and M$\approx$7500X, illustrating how cement appears in the SEM. (a) A_c=5%; (b) A_c=2%.
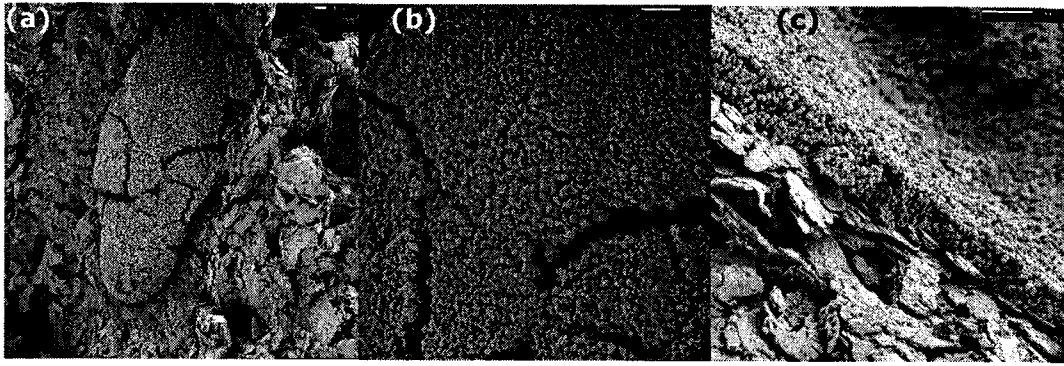
Figure 7.9. Photomicrographs of cement clumps in kaolin-cement with w=100% and A_c=10%. (a) M≈1520X; (b) M≈5055X; (c) M≈6575X.

7.4.2 Kaolin-Cement Characteristics

Scanning Electron Microscope images of kaolin-cement are included in Appendix E (Figs. E.3 to E.16).

The edges of kaolin particles have a negative charge when in a basic (high pH) environment and a positive charge when in an acidic (low pH) environment (Mitchell, 1993). When only kaolin is present, the pH was measured to be roughly 3.6 to 4.0, so that the edges are positively charged. However, when at least 2 percent cement is added to kaolin, the pH of the pore water increases to above 13 after only one day of curing, and is very near the pH of 100 percent cement, which approaches 14. This increase in pH is due to an increase in the electrolytic concentration of the pore water that results from dissociation of calcium hydroxide ($Ca(OH)_2$) (Porbaha et al., 2000). Therefore, Ca cations are attracted to the negatively charged clay particles and the clay particles become flocculated. As curing proceeds, the pH gradually decreases, but remains basic; the decrease is greatest for lower cement contents (Fig. 7.10). Therefore, the clay particles in kaolin-cement should become slightly less flocculated with curing time; this argument is difficult to prove but is supported by a small increase in void ratio with curing time (Fig. 7.11).

The SEM images show that the edge-to-edge flocculation and aggregation is actually *greater* when no cement is present; the aggregates are larger and consist of several adjacent stacks when the cement content is zero (Fig. 7.6) as compared with the aggregates in the samples with cement

(Fig. 7.7 and 7.8), which typically consist of only a single stack. This is an indication of the open structure resulting from the addition of cement, and is supported by the relatively large values of C_c/C_s calculated from the oedometer test results. However, without cement (Fig. 7.12a), it is easier to distinguish individual kaolin particles than when cement is present (Fig. 7.12b), indicating greater overall flocculation with cement, as expected. This is true even when the cement content is only 2 percent and is not visible in the SEM images.

Friction angle and the degree of flocculation are directly related according to Sivapullaiah *et al.*, (2000); as flocculation increases, so does the friction angle. The majority of test results show a slight decreasing trend in friction angle with curing time. This agrees with a reduction in flocculation associated with a decreasing pH and increasing curing time. However, other authors (i.e. Uddin, 1995) expect friction angle to *increase* with curing time, which contradicts the current findings. Uddin suggests that flocculation of the cement particles is a result of the decreasing moisture content that is associated with humid curing. However, when cured in water, the current study shows that the moisture content does not change significantly with curing. Therefore, when curing is done in water, the degree of flocculation may not be as great and because the moisture content does not decrease, flocculation will not increase with curing time.

Calculations show that the void ratio decreases slightly with an increase in cement content (Fig. 7.11); this is partially due to increased flocculation with cement. However, based on the SEM images, it appears that the void ratio actually *increases* with an increase in the cement to moisture content ratio as the structure is more open. It is possible that as the cement to moisture content ratio increases, there is less shrinkage during drying of the material. Therefore, the void ratio cannot be interpreted accurately from the SEM images. Furthermore, it is difficult to detect a change in the degree of flocculation with curing time and cement content due to shrinkage during drying.
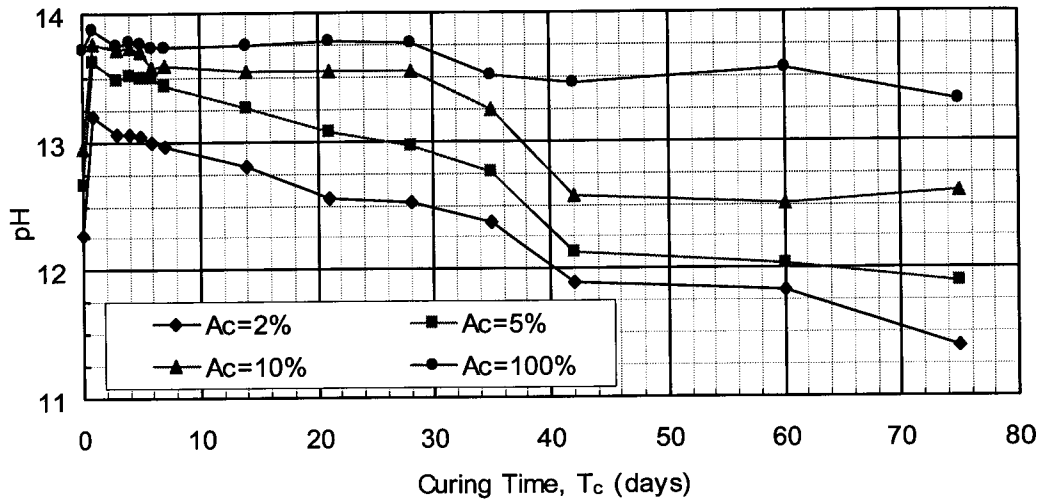
Figure 7.10. pH vs. curing time of kaolin-cement.
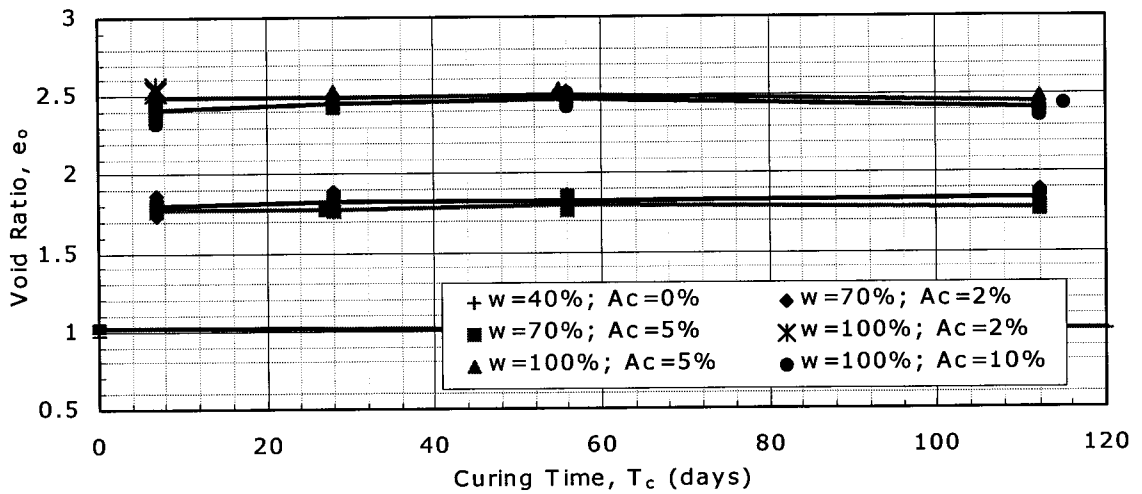
Figure 7.11. Average void ratio vs. curing time (results include all successful laboratory tests).
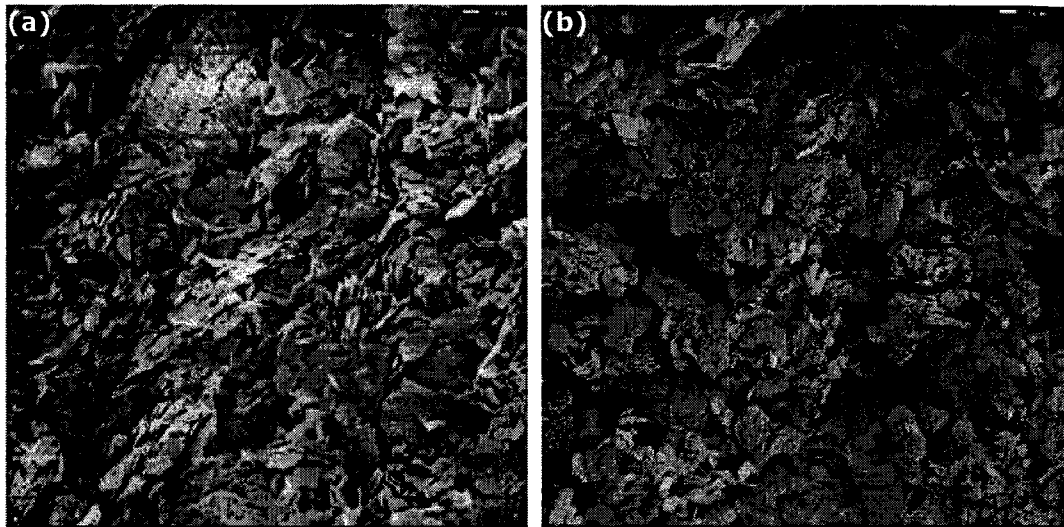
Figure 7.12. Photomicrographs of kaolin-cement at M≈2250X. (a) w=70% & A_c=0%; (b) w=100%, A_c=10% & T_c=7 days.

7.5   Summary and Conclusions

Below is a summary of the observations and conclusions made following analysis of the SEM images.

• Kaolin generally has an aggregated and edge-to-face and edge-to-edge flocculated structure.

• The addition of cement causes the kaolin to be less aggregated but more flocculated with a more open structure, as compared with pure kaolin with no cement. The relatively large C_c/C_s values calculated from oedometer test results also indicate that kaolin-cement has an open structure.

• At only 2 percent cement, the cementitious material could not be seen in the SEM photomicrographs, yet the particle structure was still affected by the cement. At 5 percent cement, the cementitious material was seen only sometimes indicating that not all kaolin particles are cemented. At 10 percent cement, the presence of cementitious material was clear throughout the material. These observations agree with those made of the laboratory test results; with 5 percent cement or less, the mechanical properties of the stabilized material are difficult to detect or do not change significantly with curing time. Furthermore, low cement contents lead to reduced pH values,

which may result in production of a weaker (and different) cementitious material than at higher cement contents.

• Flocculation decreases with an increase in curing time, as indicated by a slight increase in void ratio, and is due to a reduction in pH with curing time. This observation corresponds to a slight reduction in friction angle with curing time, which is directly related to the degree of flocculation. Other authors (i.e. Uddin, 1995) observe an increase in the friction angle with curing time, but this may be due to an increase in flocculation that is associated with a loss of moisture during humid curing.

• Some shrinkage occurs during oven-drying of the samples prior to SEM analysis. Therefore, the void ratio cannot be interpreted accurately from the SEM images.

• It is not known if shrinkage during drying was significant enough to damage the microstructure of the kaolin and kaolin-cement; it is believed that any damage was relative so that the comparisons made are still relevant.

• More research is required with respect to SEM images of kaolin-cement. It is recommended that triaxial tests be halted at different axial strains and samples obtained for SEM imaging so that the rearrangement of particles with strain can be studied.

• New SEMs are now available for environmental purposes which allow wet samples to be scanned, but with relatively poor resolution; such a device was not available for the current study.

8. CONSTITUTIVE ELASTIC-PLASTIC MODEL OF CEMENT-STABILIZED CLAY

8.1 General

Constitutive models can be used to predict the mechanical behaviour of engineering materials by defining the relationship between stress and strain; they are particularly useful in geotechnical engineering to predict the behaviour of soil. A constitutive model describes the ideal material response using various mathematical equations and controlling parameters. It is desirable to keep such models simple, and therefore, all aspects of the soil behaviour may not be included in the model. Complex models should be avoided as they can be full of the potential for hidden inaccuracies, numerical instabilities, lack of unique solutions and other errors (Wroth and Houlsby, 1985).

There are different types of soil behaviour that can be modelled; elastic-plastic theory most closely matches the true behaviour of soil. An elastic-plastic model assumes the presence of a yield surface. Yielding is a law which defines the limit of elasticity under any combination of stresses known as a yield criterion. Yielding occurs when plastic deformation begins; therefore, the yield surface is a boundary in 3-dimensional stress space. When the stress conditions are within the boundary, deformation is elastic (recoverable). Once the boundary is exceeded, then deformation is plastic *and* elastic and the yield surface expands due to plastic deformation. To define a constitutive elastic-plastic model, the nature of the plastic deformations, the magnitudes and relative magnitudes of various components of plastic deformation and the link between these magnitudes and the changing size of the yield surface must be determined (Muir Wood, 1990).

The Modified Cam-Clay model is an example of an elastic-plastic model based on the critical state concept. The first Cam Clay model was developed by Roscoe and Schofield in 1963 (Muir Wood, 1990) and later modified by Roscoe and Burland in 1968 to become the Modified Cam Clay model. It is a specific elastic-plastic model which can be described as a volumetric hardening model.

Cement-treated soil differs from soil modelled by the Modified Cam Clay model in that bonds exist between soil particles; these bonds control the yield behaviour. Furthermore, the consolidation behaviour is a function of the cement bonding and does not reflect the stress history of the soil-cement. Based on the consolidation curve of cement-treated soil, the material often appears as though it is over-consolidated, however, it is only failure of the cement bonds during consolidation that causes the formation of the virgin compression curve.

The behaviour of cemented soil is influenced by many factors; it is impossible to construct functions based on these parameters to predict the mechanical properties of cemented soil. Therefore, the use of experimental data obtained through laboratory tests is critical to model the soil behaviour. For the current study, triaxial compression tests and oedometer and isotropic consolidation tests were used to collect data to develop and verify the proposed model. Therefore, constitutive elastic-plastic models, and particularly the proposed model, will be discussed with respect to the findings of these tests.

8.2 Review of Critical State Soil Mechanics and the Modified Cam-Clay Model

Critical state is the condition of perfect plasticity and is achieved following continued loading, either drained or undrained, whereby plastic hardening, expansion of the yield surface, and increase of stress ratio (η) occur until the effective stress state is at the top of the current yield surface, and no further change in stress or volume change occurs (Muir Wood, 1990). The attainment of a critical state can be expressed as follows.

$$\frac{\partial p'}{\partial \varepsilon_q} = \frac{\partial q}{\partial \varepsilon_q} = \frac{\partial v}{\partial \varepsilon_q} = 0 \qquad (8.1)$$

The effective stress ratio when the critical state is achieved is defined by M.

$$\frac{q_{cs}}{p'_{cs}} = \eta_{cs} = M \qquad (8.2)$$

M can also be expressed in terms of the friction angle, φ.

$$M = \frac{6\sin\left(\frac{\pi\phi}{180}\right)}{3 - \sin\left(\frac{\pi\phi}{180}\right)} \qquad (8.3)$$

When drained or undrained triaxial tests are performed on normally consolidated (or slightly over-consolidated) soil, yielding will first occur when η<M. As loading continues and plastic hardening occurs, the yield surface dilates until the critical state is reached. When the soil is heavily over-consolidated, yielding will first occur when η>M, but as deformation continues due to strain softening, the yield surface will contract and η will decrease until η=M.

The critical state line (CSL) exists in 3-dimensional space defined by q, p' and υ, and is the line joining each yield surface at η=M (Fig. 8.1a). Therefore, to locate the critical state line, the yield surfaces (or yield loci) must be defined for each p' considered; as p' increases, so does the yield surface.

The position, shape and size of each yield locus is a function of the stress history of the soil. To define the yield locus mathematically, the behaviour of the soil under compression must be examined. The typical response of a soil under isotropic compression is shown in Figure 8.1. The equation of the isotropic normal compression (consolidation) line (NCL) can be expressed as follows.

$$\upsilon = N - \lambda \ln p' \qquad (8.4)$$

and the equation of the isotropic swelling line can be expressed as follows.

$$\upsilon = \upsilon_\kappa - \kappa \ln p' \qquad (8.5)$$

The critical state line is parallel to the NCL and can be expressed as follows

$$\upsilon_{cs} = \Gamma - \lambda \ln p_{cs}{}' \tag{8.6}$$

where

$$\Gamma = N - (\lambda-\kappa) \ln2 \tag{8.7}$$

The soil constants λ, N and κ, must be determined by laboratory tests, such as isotropic consolidation tests. For one-dimensional consolidation, the slope of the normal consolidation and swelling lines are the same as for isotropic consolidation, but the intercepts at $p'=1.0$ are slightly different. The equations to define the lines for one-dimensional consolidation tests are as follows.

$$\upsilon = N_o - \lambda \ln p' \tag{8.8}$$

$$\upsilon = \upsilon_{\kappa o} - \kappa \ln p' \tag{8.9}$$

Schofield and Wroth (1968) report the values of the soil constants describing the critical state line for various soils, including kaolin (Table 8.1).

Table 8.1. Values of critical state constants for kaolin.

λ	0.26
κ	0.05
Γ	3.77
M	1.02
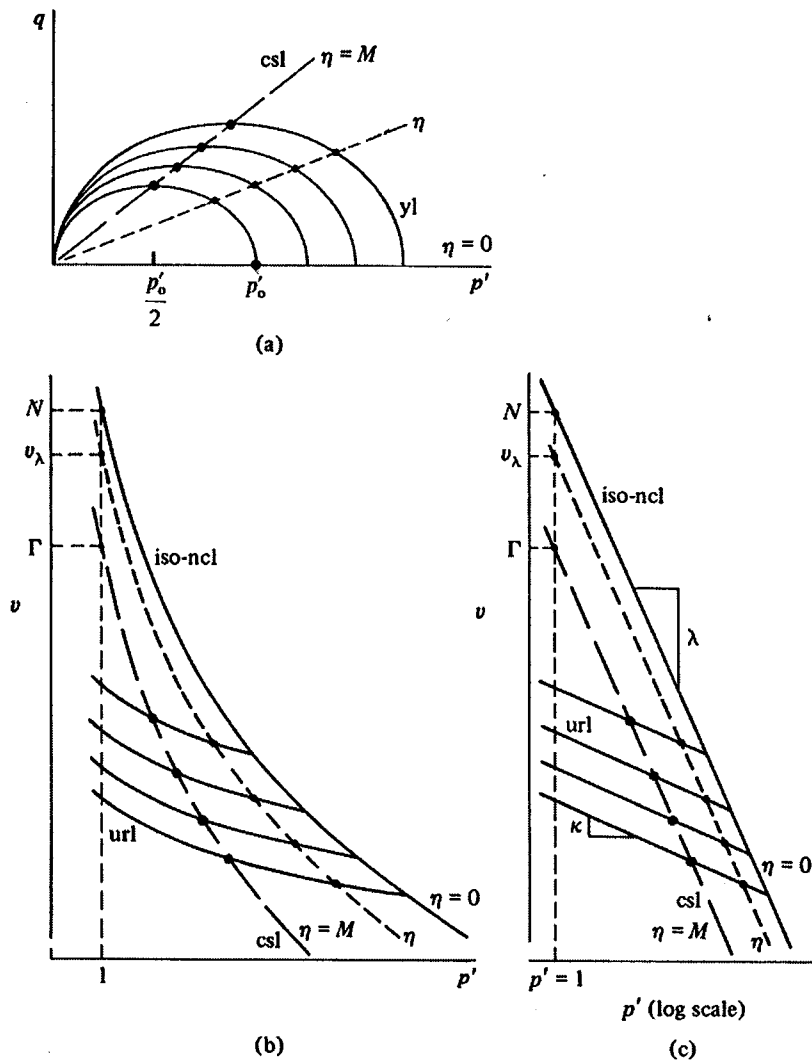
Figure 8.1. Critical state line (CSL) and intersection of yield loci with line q/p'=η (Muir Wood, 1990).

8.3 Results of Laboratory Tests in a Critical State Framework

For all mixes and curing times, critical state constants were determined based on a combination of the isotropic consolidation and oedometer test results. Due to bonding effects, this was not such an easy task and the effective stress paths from the triaxial tests were also used to verify that the derived critical state constants were reasonable; minor adjustments were made where necessary. Effective stress paths were then plotted with both the critical state line (CSL) and the isotropic normal compression line (NCL) to interpret the soil behaviour with respect to bonding. The table below provides the

Mechanical Characteristics of Kaolin-Cement Mixture 147

critical state soil constants for the various mixes of kaolin-cement based on the laboratory data. Figure 8.2 illustrates a typical series of stress paths at 10 percent cement after 56 days of curing. A complete set of these figures are included in Appendix F.

Table 8.2. Values of critical state soil constants for kaolin-cement.

w (%)	A_c (%)	T_c (days)	λ	κ	Γ	M
70	2	7	0.24	0.046	3.59	1.05
		28	0.25	0.031	3.68	0.96
		56	0.22	0.05	3.52	0.90
		112	0.22	0.065	3.52	0.92
	5	7	0.27	0.024	3.86	0.92
		28	0.22	0.025	3.66	1.24
		56	0.26	0.025	3.89	0.96
		112	-	-	-	-
100	5	7	0.41	0.037	4.87	0.81
		28	0.39	0.036	4.80	0.85
		56	0.43	0.033	5.00	0.96
		112	0.36	0.037	4.75	1.10
	10	7	0.49	0.053	5.45	1.18
		28	0.49	0.026	5.65	1.21
		56	0.45	0.027	5.48	1.09
		112	0.38	0.027	4.95	0.95

The critical state framework allows the presence of bonding to be interpreted in clays. This is particularly useful for natural structured clays, but can also be used in the case of artificially bonded (i.e. cement-treated) clays. Generally, when the stress path lies above the ICL (NCL) in υ-p' space, this is an indication of bonding. For the current study, the drained stress path at a confining pressure of 400 kPa nearly always showed some bonding and at lower confining pressures, the presence of bonding was only sometimes apparent. However, at higher confining pressures, the cement bonds often failed during consolidation and before shear so bonding should have been more apparent at lower confining pressures. Based on these observations it is shown that the critical state framework does not apply

perfectly to artificially cemented soils as it is very difficult to achieve critical state, and furthermore, that laboratory data is not perfect.
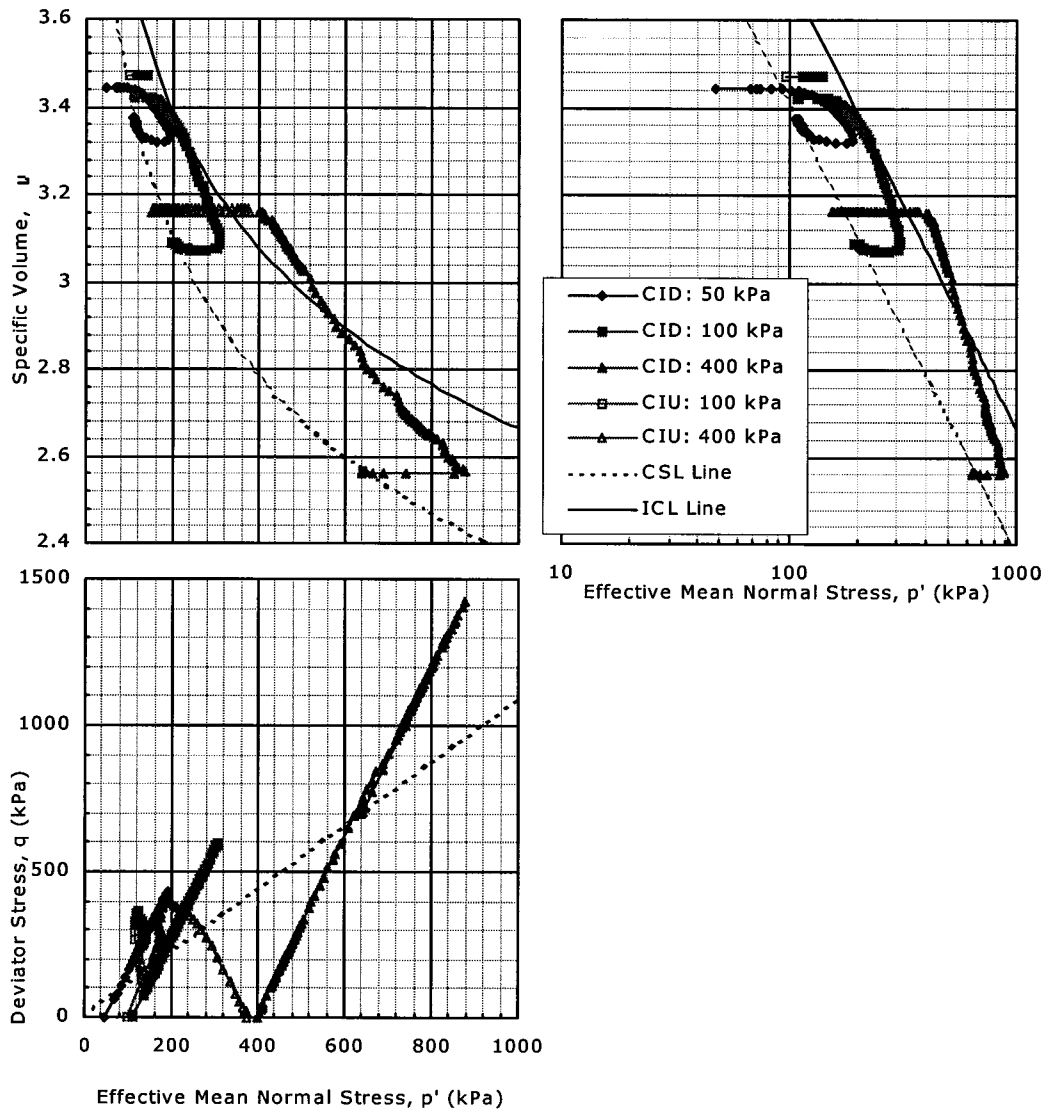
Figure 8.2. Stress path plots in a critical state framework for w=100%, A_c=10% and T_c=56 days.

8.4   Review of Model Proposed by Chan and Lee

Chan and Lee at the University of Alberta (not yet published) are currently working on a constitutive model for cement-treated clay based on the critical state framework. The primary objective of the proposed model is to capture the strength and volumetric behaviour of cement-treated soils. One of the

Mechanical Characteristics of Kaolin-Cement Mixture   149

fundamental characteristics of cement-treated soil, which was found in the triaxial test results, is that while the stress-strain curves are strain-softening and resemble those of over-consolidated material, the volumetric strain and excess pore water pressure data, for drained and undrained tests, respectively, resembles more closely that of normally consolidated to slightly over-consolidated clay.

The research conducted for the current project is intended to test and verify the proposed model. Only a review of the model is presented here; its development will not be discussed. The proposed model is based on the Modified Cam Clay model, with some exceptions made to account for the cement bonding effects and resulting change in classical soil behaviour. Besides a description of the proposed model, some of the most significant changes and new assumptions to the Modified Cam Clay model are summarised below.

Either naturally or artificially cemented soils fall under the umbrella of structured soils. That is, the size of the yield surface is a function of the void ratio as well as the strength of the bonds between particles. The proposed model assumes that the yield surface is elliptical; this is the same as for the Modified Cam Clay model. However, unlike the Modified Cam Clay model, the proposed model assumes that some tensile strength, c′, exists between particles. Therefore, the initial yield locus will cross the q-axis. As shear strain proceeds, the yield locus will shift and the tensile strength will decrease until the cement bonds are destroyed and both the tensile strength and cohesion are eliminated.

Besides cohesion and tensile strength, the bonding stress ratio, m, is introduced to account for the effects of cementation and bond breaking with shear strain. This means that instead of the traditional stress path method employed by the Modified Cam Clay model, the proposed model uses the strain increment method to predict the change in strength and volume during shear. In the proposed model, the bonding stress ratio, m, is expressed as follows.

$$m = M + \frac{c}{p_c{'}} e^{-k_p \varepsilon_q^p} \tag{8.10}$$

In the above equation, k_p is a parameter which controls the rate of bond degradation during shear and is a function of the confining pressure. Generally, bonds degrade at a greater rate when confining pressures are low.

The bonding stress ratio has two components (equation 8.10). The first term, the critical state stress ratio, is the same as that described for critical state soil mechanics and considers the frictional strength of un-bonded soils. The second term accounts for bonding between soil particles. As can be seen, when the cement bonds break during shear and cohesion is eliminated, the bonding stress ratio will be reduced to the critical state stress ratio.

In critical state soil mechanics, the slope of the critical state line in e-ln p' space is described by λ_c, prior to yield and λ, following yield. However, the proposed model assumes that the slope of the critical state line in e-ln p' space is changing continually so that it cannot be described by only λ_c or λ. Therefore, a 3rd order polynomial is fit to the isotropic consolidation line by regression so that the slope of the curve can be obtained for any e and p'. This changing slope is relabelled as the variable λ'.

It has been documented by others (i.e. Kohata *et al.*, 1997) that one of the most significant effects of cementation is that the cemented soil adopts the characteristics of an over-consolidated material. The current study suggests that this is not exactly the case and that trends in volumetric strain and excess pore water pressure, for drained and undrained triaxial tests, respectively, demonstrate normally consolidated to only slightly over-consolidated behaviour. Furthermore, the pressure at which the cement bonds fail is equivalent to the apparent consolidation yield stress, as determined from the consolidation curve. The term "apparent" is used here as the apparent consolidation yield stress does not reveal information regarding the stress history of the soil-cement. The Modified Cam Clay model assumes that the material deforms elastically at least until the consolidation yield stress is reached. However, for cemented material, the elastic domain is very small to non-existent even though the apparent consolidation yield stress can be high. Therefore, the Modified Cam Clay model will over-estimate the extent of the elastic domain. To correct the assumption of the Modified Cam Clay model, the proposed model assumes that cemented material behaves in an elasto-plastic manner as soon as shearing

commences. Traditional critical state soil mechanics describes the swelling behaviour with the variable κ; however, the proposed model uses λ' instead.

The associated flow rule is assumed to be valid for the proposed model. That is to say that the yield loci, f, and plastic potentials, g, are assumed to be equivalent (i.e. $g \equiv f$). The nature of the plastic deformation, also described as flow, is associated with the material's yield surface (Muir Wood, 1990); this theory is also termed normality. The assumption that the associated flow rule is valid simplifies the proposed model as it reduces the number of functions that describe the soil's plastic behaviour.

The yield function of the Modified Cam Clay model, for triaxial conditions, can be described as follows.

$$f = q^2 - M^2[p'(p_o' - p')] = 0 \tag{8.11}$$

The bonding effect is considered by introducing cohesion, c, and tensile strength, c′, to equation 8.11. The tensile strength is a function of the cumulative plastic shear strain, ε_p^q.

$$f = (p' - \beta)^2 (M\alpha)^2 + q^2 \alpha^2 - (M^2 \alpha^4) = 0 \tag{8.12}$$

where

$$\alpha = \frac{p_o' - c'}{2} \tag{8.13}$$

$$\beta = \frac{p_o' + c'}{2} \tag{8.14}$$

$$c' = \frac{c}{M} e^{-k_p \varepsilon_q^p} \tag{8.15}$$

Figure 8.3 shows the shape of the yield surface and illustrates many of the new variables described above. The bonds between soil particles govern the size of the yield surface which are controlled by the confining pressure, p_o' and cohesion, c.

The isotropic hardening rule controls the size and shifting of the yield surface and is implemented in the proposed model as a function of the tensile strength. Without tensile strength, the isotropic hardening rule is the same for the Modified Cam Clay model as it is for the proposed model.
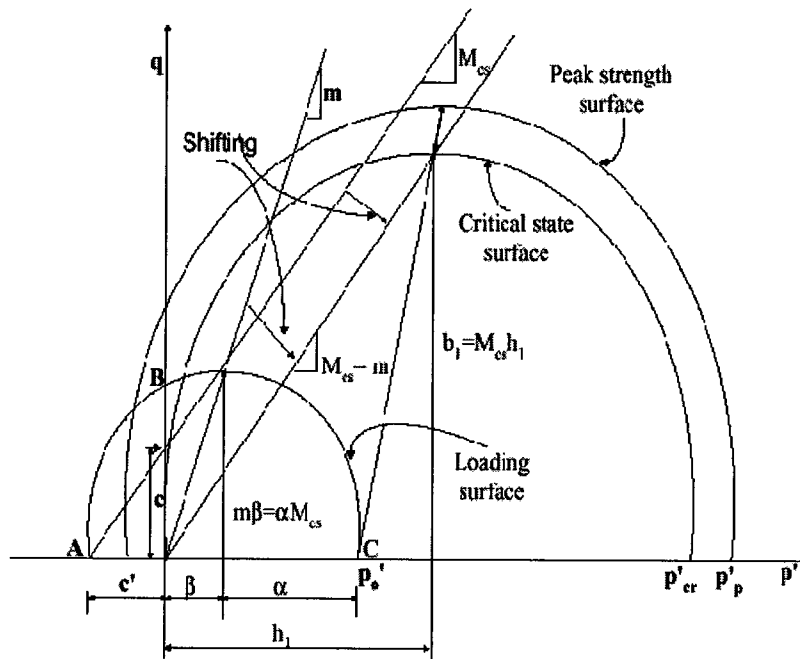
Figure 8.3. Yield surface for cement-treated clay

8.5   Sensitivity Study for Proposed Model

Prior to verifying the model with the laboratory data, a sensitivity study was conducted to understand the influence of each model parameter. Specifically, the sensitivity study examined the influence of cohesion (c), friction angle (ϕ), parameter controlling the rate of bond degradation (k_p) and confining pressure (p_o'). To keep the study simple, Poisson's ratio (μ), the gradient of the swelling line (κ) and the coefficients describing the gradient of the normal consolidation line (λ), were kept constant.

Figure 8.4 illustrates the influence of each parameter on the deviator stress and volumetric strain. The following statements can be made based on each plot.
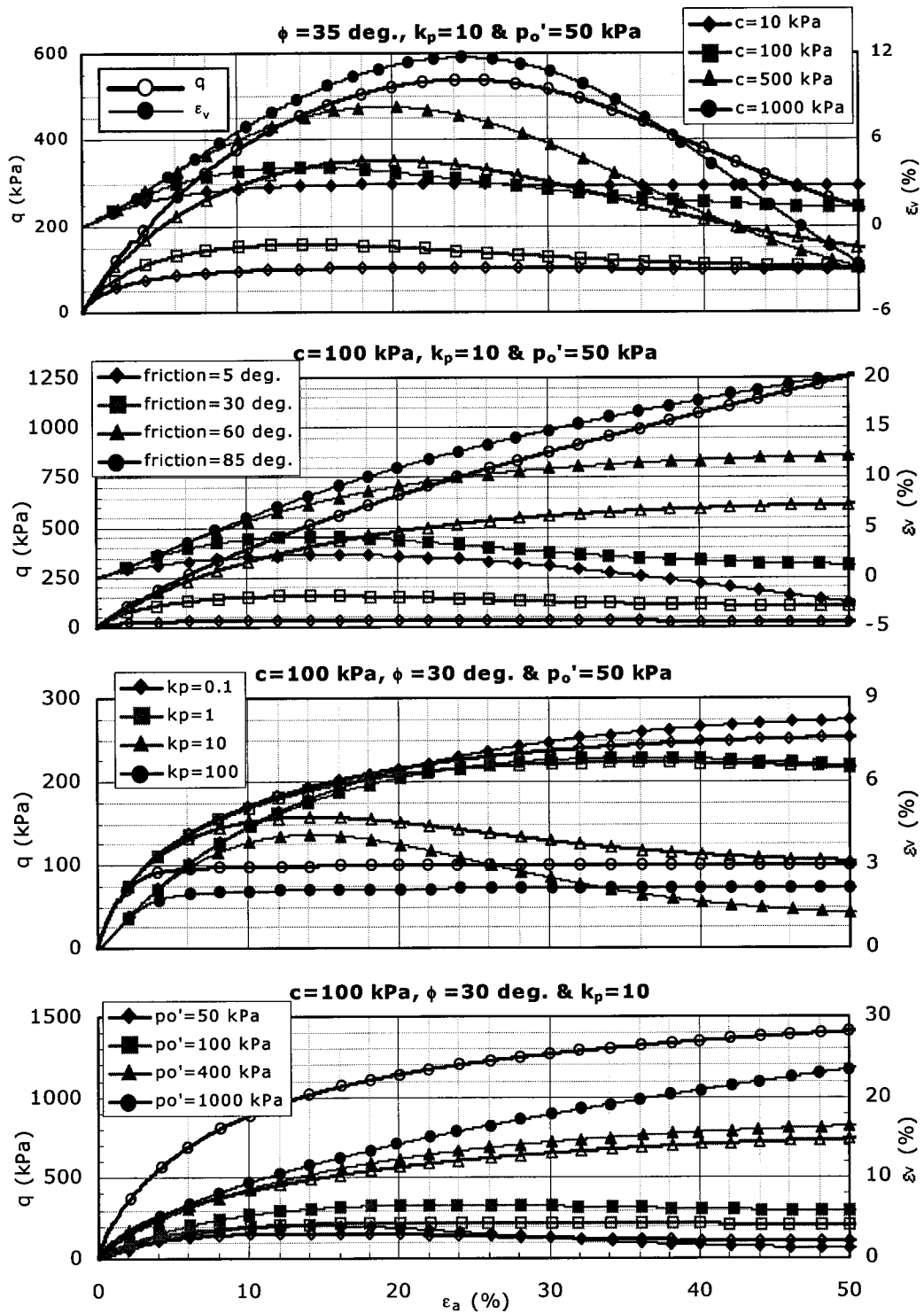
Figure 8.4. Effects of various parameters on the predicted deviator stress and volumetric strain.

Cohesion: Increases both the peak deviator stress and peak volumetric strain. Also increases the axial strain at peak conditions and the tendency towards dilation and strain softening at large axial strains.

Friction angle: Same effect as cohesion, except it *decreases* the tendency towards dilation at large axial strains. At large friction angles, behaviour is strain hardening and dilation does not occur.

Parameter controlling bond degradation: Reduces the peak deviator stress and corresponding axial strain; causes strain softening behaviour. However, there exists a certain minimum deviator stress which cannot be reached, regardless of k_p. That is, there is a k_p after which all behaviour is strain hardening; for the parameters considered here, a k_p of 100 results in low peak stress *and* strain hardening behaviour. For all values of k_p, a deviator stress less than 100 kPa could not be achieved following peak stress conditions.

Confining pressure: Increases peak deviator stress and corresponding axial strain. Causes behaviour to change from strain softening, at low values, to strain hardening, at higher values.

8.6   Verification of Proposed Model

The data used to test the model was from drained triaxial tests on samples with 100 percent moisture content, 10 percent cement and a curing time of 7 days. With a reasonably large amount of cement, this laboratory data is believed to best represent the behaviour of cement-stabilized clay, whereby any softening effects from water curing are small to none. For this case, both the isotropic consolidation data and the oedometer data obtained in the laboratory were used to model the isotropic consolidation behaviour; the isotropic consolidation data alone did not extend to a sufficiently high consolidation pressure. Figure 8.5 includes plots of both the oedometer and isotropic consolidation data, as well as the equivalent curve used in the model. The following equation describes the isotropic consolidation line.

$$v = a + bp_C'^2 + cp_C'^3 + dp_C'^4 \tag{8.16}$$
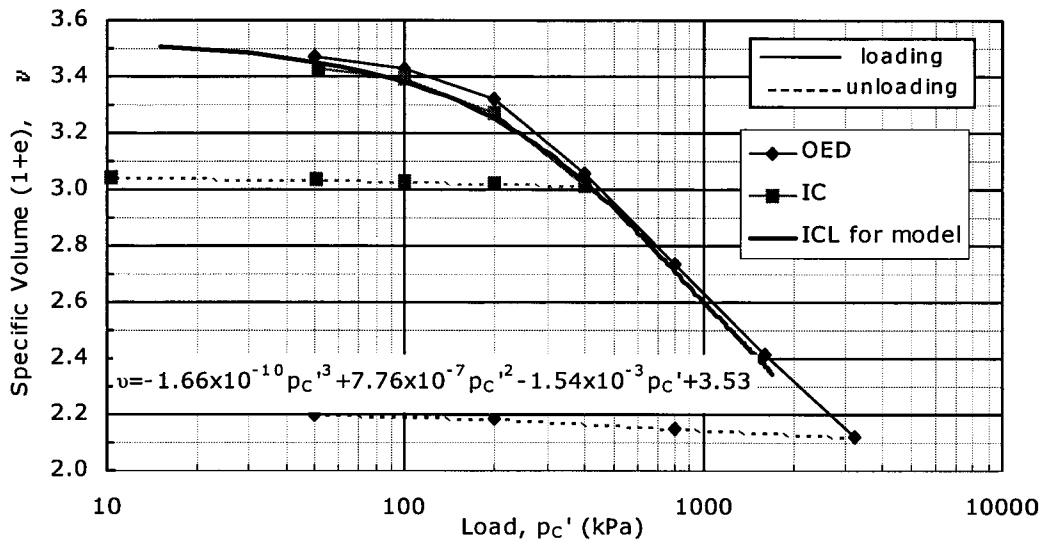
Figure 8.5. Consolidation curves for w=100%, A_c=10% and T_c=7 days.

Besides the 3rd order polynomial equation describing the isotropic consolidation curve, the proposed model requires the input of several other parameters including confining pressure ($p_o{}'$), cohesion (c) and friction angle (ϕ), swelling index (κ), Poisson's ratio (μ) and the parameter controlling the bond degradation rate (k_p). Confining pressures of 50, 100 and 400 kPa are tested to match those of the laboratory drained triaxial tests. Friction angle (taken at peak conditions) and swelling index are kept constant at 37° and 0.05, as per the results of the laboratory tests. Poisson's ratio is kept constant at 0.2. Cohesion and k_p are modified by trial and error for each test to approximately match the laboratory test results. It was extremely difficult to impossible to match both the deviator stress *and* volumetric strain data. Increasing cohesion increases deviator stress, corresponding axial strain and volume change. Increasing k_p, up to a limit, reduces deviator stress and causes more strain softening and dilative behaviour.

Table 8.3 is a summary of the input data for the model, at confining pressures of 50, 100 and 400 kPa. Figure 8.6 illustrates the comparison of the behaviour predicted by the model and the laboratory data.

Table 8.3. Input parameters for model verification at w=100%, A_c=10% and T_c=7 days.

p_o' (kPa)	c (kPa)	ϕ (°)	k_p	κ	a	b	c	d
50	1000	37	70	0.05	3.53	-1.54×10^{-3}	7.76×10^{-7}	-1.66×10^{-10}
100			40					
400			10					

It was necessary to assume a value for cohesion far greater than what was found for the laboratory tests. As the model was being adjusted, it was found that the parameters describing the isotropic consolidation line (a, b, c and d) and hence λ for each load have a large influence on the results.

Based on the cases considered in verifying the model, it can be said that the model captures the general behaviour of kaolin-cement. It is suggested that the model predicts stress behaviour best at low confining pressures (i.e. 50 kPa) and volume change behaviour best at high confining pressures (i.e. 400 kPa). The model did not predict the extent of brittle failure behaviour at confining pressures of 100 and 400 kPa. Following peak stress conditions at confining pressures of 50 and 100 kPa, the model shows more rapid dilation than the actual data suggests. Furthermore, the exact treatment of cohesion is not accurate as it was necessary to increase the value of peak cohesion, based on laboratory data, to a value that was unreasonably high.
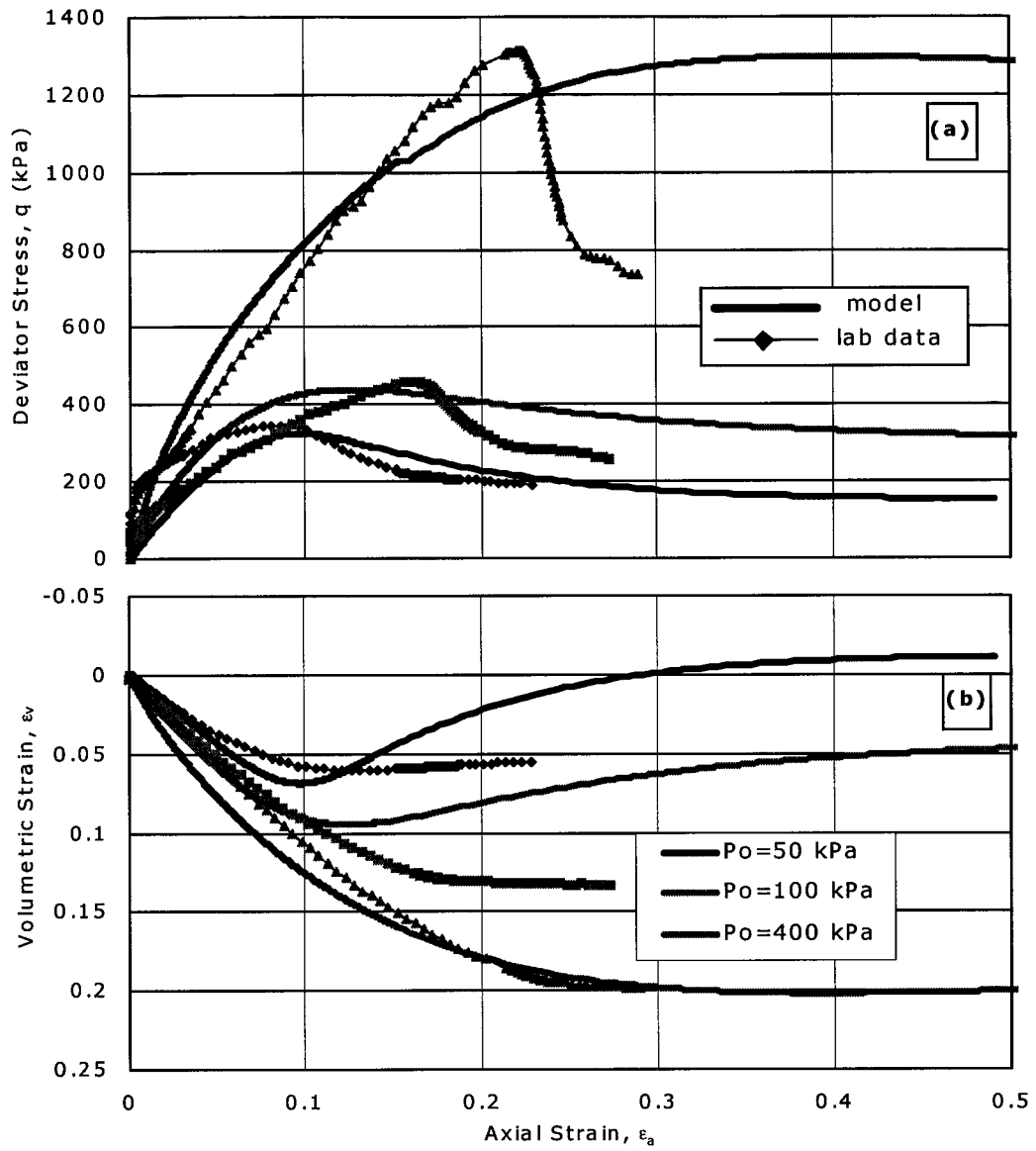
Figure 8.6. Figures illustrating real data for drained tests at w=100%, A_c=10% and T_c=7 days vs. data generated by the proposed model. (a) q vs. ε_a; (b) ε_v vs. ε_a.

8.7 Conclusions

Based on the attempts made to verify the proposed model, the following general conclusions can be made.

- The proposed constitutive elastic-plastic model by Chan and Lee captures the general behaviour of kaolin-cement, with respect to stress and volumetric strain.
- The proposed model can be used to predict the peak stress and corresponding axial strain conditions at relatively low confining pressures (i.e. 50 kPa). To do this, however, peak cohesion must be unreasonably high.
- If the peak friction angle is increased to a value above what is reasonable, the volume change behaviour at low confining pressures can be predicted by the model, however, the behaviour also becomes less stiff and failure is ductile instead of brittle.
- Calibration of the model is necessary to determine appropriate values for the parameter controlling the rate of bond degradation and peak cohesion.
- The degree of dilation is over-estimated by the model at low confining pressures (i.e. 50 and 100 kPa) when the strength behaviour is predicted correctly.
- Volumetric strain can be predicted accurately at high confining pressures (i.e. 400 kPa).
- The model does not predict the brittle failure behaviour and extent of strain softening at confining pressures of 100 kPa and greater.

9.   OVERALL CONCLUSIONS AND RECOMMENDATIONS FOR FURTHER RESEARCH

Based on the results of this study on the mechanical characteristics of kaolin-cement, some general overall conclusions can be made, as follows. Note that conclusions are based on somewhat limited test results and are not intended to characterize conditions not considered in the current study.

• Curing environment has a significant influence over the properties of soil-cement. Particularly at low cement contents, water cured samples have a much lower strength than humid cured samples, but they will be less stiff and possess more ductile failure behaviour. Furthermore, humid cured samples often lost significant amounts of moisture during curing so that after at least 28 days, some samples were damaged with cracks. Therefore, when developing a laboratory program for Deep Mixing (DM) projects, the curing environment must be considered carefully so that it simulates the field conditions as best as possible. Sites where DM is used typically have thick deposits of soft, wet clay. Therefore, water curing of laboratory samples is often more appropriate than humid curing when designing an effective and efficient DM program.

• Cement treatment of clay causes the clay particles to be more flocculated but less aggregated, resulting in a more open structure. This increase in the degree of flocculation is likely due to the rise in pH and hence the electrolytic concentration of the soil pore water due to the addition of cement. As the cement content increases, so does the pH and the degree of flocculation. This flocculation causes an increase in the peak friction angle of cement-treated clay. Furthermore, the pH of the pore water decreases as curing proceeds. It is suggested that the degree of flocculation and hence the friction angle may also decrease with curing time.

• At relatively low confining pressures, the failure envelope of kaolin-cement appears linear. However, trends in both peak cohesion and friction angle with curing time suggest that the two properties influence one another: when one increases, the other decreases, and vice versa. This observation leads to the suggestion that the failure envelope is actually curved, like that of soft rock.

However, over a narrow range of confining pressures, the failure envelope appears linear.

• While an increase in cement content does increase the peak strength of the treated soil, it also increases the stiffness thereby reducing the strain at which failure occurs. Furthermore, cement causes failure to be more brittle and therefore, catastrophic under drained conditions. This is a fundamental trade-off associated with cement-treated clays; while a gain in strength is desirable, a loss of ductility is not. Therefore, when designing a DM program, some intermediate cement content must be chosen to achieve adequate strength, but maintain some reduced stiffness and ductility if failure were to occur.

• When an insufficient amount of cement is used to stabilize fine-grained material, the mechanical properties may not improve with curing time. In fact, under some circumstances, the material may actually deteriorate with time. Based on the current study, cement contents of 5 percent or less are not sufficient to cause consistent and significant improvement in the mechanical properties of kaolin. It is suggested that softening of material or leaching of cementitious material out of the treated soil during water curing may explain the observed deterioration of cement-treated kaolin with curing time. The results of the current study are limited, however, and more research is required to confirm these observations and suggestions. Further triaxial tests at greater confining pressures and on samples with greater cement contents are recommended. The possibility of cement leaching can be examined further by sampling the water in which the treated samples are cured; this should be done over curing times far greater than 112 days.

• In the past, cement-treated clay has been described by some authors (i.e. Kohata *et al.*, 1997) as an over-consolidated material. Consolidation curves obtained from cement-treated clay do resemble that of an over-consolidated material, however, it is proposed that the apparent consolidation yield stress represents the pressure at which the cement bonds begin to fail and the virgin compression curve is formed when the structure collapses. Furthermore, while stress-strain curves are strain-softening, similar to over-consolidated material, trends in volumetric strain and excess pore water pressure during drained and undrained tests, respectively, indicate the shear behaviour is more similar to normally consolidated or only slightly over-

consolidated clay. This is a fundamental difference between cemented clay and uncemented clay. Triaxial tests on pure kaolin at low confining pressures exhibit over-consolidated behaviour. Samples of pure kaolin were not cured in water; this difference must also be considered.

- The constitutive elastic-plastic model proposed by Chan and Lee predicts the general behaviour of kaolin-cement. The model works well to predict the stress-strain behaviour of soil-cement at very low confining pressures (i.e. 50 kPa). While the maximum volumetric strain predicted by the model at very low confining pressures was roughly correct, the model overestimates the degree of dilation following peak stress conditions. At high confining pressures (i.e. 400 kPa), the model predicted volume change behaviour well, however it did not capture the brittle failure behaviour exhibited in the laboratory tests. A method for determining appropriate input values such as the parameter controlling the bond degradation rate and cohesion must be developed. At the moment, the cohesion required for the model to predict the peak stress found in the laboratory is unreasonably high.

- Many questions remain unanswered with regards to the properties of soil-cement, and how they change with curing time and cement content. More research is recommended as follow-up to the current study. This includes examination of the behaviour of kaolin-cement at greater cement contents, and triaxial tests at greater confining pressures. Furthermore, tests should be conducted beyond 112 days of curing, and at more frequent intervals in between. The possibility of softening and/or leaching of cement during water curing should be studied further.

10. REFERENCES

ÅHNBERG, H. 1997. Stress dependent parameters of cement and lime stabilised soil. *In* Grouting and deep mixing; Proceedings of 2nd international conference on ground improvement geosystems, Tokyo, May 14-17, 1996. Vol. 1. *Edited by* Yonekura, R., Terashi, M. and Shibazaki, M. A.A. Balkema, Rotterdam. pp. 387-392.

AZMAN, Md., Amin, Md., Bakar, I. and Hyde, A.F.L. 1995. Effect of initial consolidation on the undrained shear response of cement-treated soil. *In* Developments in deep foundations and ground improvement schemes; Proceedings symposia on geotextiles, geomembranes and other geosynthetics in ground improvement, Bangkok, 1994. *Edited by* Balasubramaniam, A.S., Bergado, D.T., Phien-Wej, N., Hong, S.W., Ashford, S.A. and Nutalaya, P. A.A. Balkema Rotterdam. pp. 161-173.

BABASAKI, R, Maekawa, A., Terashi, M., Kawamura, M., Suzuki, T. and Fukazawa, E. 1997. JGS TC Report: Factors influencing the strength of improved soil. *In* grouting and deep mixing; Proceedings of 2nd international conference on ground improvement geosystems, Tokyo, May 14-17, 1996. Vol. 2. *Edited by* Yonekura, R., Terashi, M. and Shibazaki, M. A.A. Balkema, Rotterdam. pp. 913-918.

BERGADO, D.T., Anderson, L.R., Miura, N. and Balasubramaniam, A.S. 1996. Soft ground improvement in lowland and other environments. ASCE, New York.

BERGADO, D.T., Ruenkrairergsa, T., Taesiri, Y. and Balasubramaniam, A.S. 1999. Deep soil mixing used to reduced embankment settlement. *Ground Improvement* 3: 145-162.

BROMS, B.B. 1984. Stabilization of soft clay with lime columns. Seminar on soil improvement and construction techniques in soft ground, Singapore, January 10-11, 1984. pp. 120-133.

BRUCE, D.A., Bruce, M.E.C. and DeMillio, A.F. 1998. Deep Mixing Method: A Global Perspective. *In* Soil improvement for big digs, Proceedings of sessions of geo-congress, Boston, October 18-21, 1998. *Edited by* Maher, A. and Yang, D.S. ASCE, Reston. pp. 1-26.

BRUCE, D.A., Bruce, M.E.C. and DeMillio, A.F. 1999. Dry Mix Methods: A brief overview of international practice. *In* Dry mix methods for deep soil stabilization, Proceedings of the international conference on dry mix methods for deep soil stabilization, Stockholm, October 13-15, 1999. *Edited by* Bredenberg, H., Holm, G. and. Broms, B.B. A.A. Balkema, Rotterdam. pp. 15-25.

BURLAND, J.B. 1990. On the compressibility and shear strength of natural clays. *Géotechnique* **40**: 329-378.

CONSOLI, N.C., Schnaid, F., and Rohlfes, J.A. 1997. Engineering properties of residual soil-cement mixtures. *In* Grouting and deep mixing; Proceedings of 2nd international conference on ground improvement geosystems, Tokyo, May 14-17, 1996. Vol. 1. *Edited by* Yonekura, R., Terashi, M. and Shibazaki, M. A.A. Balkema, Rotterdam. pp. 25-30.

CONSOLI, N.C., Rotta, G.V. and Prietto, P.D.M. 2000. Influence of curing under stress on the triaxial response of cemented soils (Technical note). *Géotechnique* **50**: 99-105.

CRAIG, R.F. 1992. Soil mechanics, 5th Ed., Chapman & Hall, New York.

DAS, B.M. 1994. Principles of geotechnical engineering, 3rd Ed., PWS Publishing Co., Boston.

EDSTAM, T. and Carlsten, P. 1999. A new method for laboratory preparation of stabilized clay. *In* Dry mix methods for deep soil stabilization, Proceedings of the international conference on dry mix methods for deep soil stabilization, Stockholm, October 13-15, 1999. *Edited by* Bredenberg, H., Holm, G. and. Broms, B.B. A.A. Balkema, Rotterdam. pp. 315-319.

ESRIG, M.I. 1999. Keynote lecture: Properties of binders and stabilized soils. *In* Dry mix methods for deep soil stabilization, Proceedings of the international conference on dry mix methods for deep soil stabilization, Stockholm, October 13-15, 1999. *Edited by* Bredenberg, H., Holm, G. and. Broms, B.B. A.A. Balkema, Rotterdam. pp. 67-72.

HEAD, K.H. 1998. Manual of soil laboratory testing, Volume 3: Effective stress tests, 2nd Ed., John Wiley & Sons, Chichester.

HOLM, G. 1999. Keynote lecture: Applications of Dry Mix Methods for deep soil stabilization. *In* Dry mix methods for deep soil stabilization, Proceedings of the international conference on dry mix methods for deep soil stabilization, Stockholm, October 13-15, 1999. *Edited by* Bredenberg, H., Holm, G. and. Broms, B.B. A.A. Balkema, Rotterdam. pp. 3-13.

KAMON, M. 1997. Effect of grouting and DMM on big construction projects in Japan and the 1995 Hyogoken-Nambu Earthquake. *In* Grouting and deep mixing; Proceedings of 2nd international conference on ground improvement geosystems, Tokyo, May 14-17, 1996. Vol. 2. *Edited by* Yonekura, R., Terashi, M. and Shibazaki, M. A.A. Balkema, Rotterdam. pp. 807-823.

KAWASAKI, T., Saitoh, S., Suzuki, Y. and Babasaki, R. 1984. Deep Mixing Method using cement slurry as hardening agent. Seminar on soil improvement and construction techniques in soft ground, Singapore, January 10-11, 1984. pp. 17-38.

KÉZDI, Á. 1979. Stabilized earth roads, developments in geotechnical engineering 19, Elsevier Scientific Publishing Company, New York.

KOHATA, Y., Muramoto, K., Yajima, J., Maekawa, H. and Babasaki, R. 1997. JGS TC Report: Deformation and strength properties of DM cement-treated soils. *In* Grouting and deep mixing; Proceedings of 2nd international conference on ground improvement geosystems, Tokyo, May 14-17, 1996. Vol. 2. *Edited by* Yonekura, R., Terashi, M. and Shibazaki, M. A.A. Balkema, Rotterdam. pp. 905-911.

LEA, F.M. 1970. The chemistry of cement and concrete, 3rd Ed., Edward Arnold Ltd., London.

MALANDRAKI, V. and Toll, D. 2000. Drained probing triaxial tests on a weakly bonded artificial soil. *Géotechnique* **50**: 141-151.

MITCHELL, J.K., Veng, T.S. and Monismith, C.L. 1974. Behaviour of stabilized soils under repeated loading, Department of Civil Engineering, University of California, Berkeley.

MITCHELL, J.K. 1981. Soil improvement methods and their applications in civil engineering, Department of Civil Engineering, North Carolina State University, Raleigh.

MITCHELL, J.K. 1993. Fundamentals of soil behavior, 2nd Ed., John Wiley & Sons, Inc., New York.

MUIR WOOD, D. 1990. Soil behaviour and critical state soil mechanics, Cambridge University Press, New York.

OKUMURA, T. 1997. Deep Mixing Method of Japan. *In* Grouting and deep mixing; Proceedings of 2nd international conference on ground improvement geosystems, Tokyo, May 14-17, 1996. Vol. 2. *Edited by* Yonekura, R., Terashi, M. and Shibazaki, M. A.A. Balkema, Rotterdam. pp. 879-887.

PORBAHA, A. 1998. State of the art in deep mixing technology. Part I: basic concepts and overview. *Ground Improvement* **2**: 81-92.

PORBAHA, A., Tanaka, H. and Kobayashi, M. 1998. State of the art in deep mixing technology. Part II: applications. *Ground Improvement* **2**: 125-139.

PORBAHA, A., Shibuya, S. and Kishida, T. 2000. State of the art in deep mixing technology. Part III: geomaterial characterization. *Ground Improvement* **3**: 91-110.

POUSETTE, K., Mácsik, J., Jacobsson, A., Andersson, R. and Lahtinen, P. 1999. Peat soil samples stabilized in laboratory – Experiences from manufacturing and testing. *In* Dry mix methods for deep soil stabilization, Proceedings of the international conference on dry mix methods for deep soil stabilization, Stockholm, October 13-15, 1999. *Edited by* Bredenberg, H., Holm, G. and. Broms, B.B. A.A. Balkema, Rotterdam. pp. 85-92.

SCHOFIELD, A.N. and Wroth, C.P. 1968. Critical state soil mechanics. McGraw-Hill Book Co., London.

SHI, B., Wu, Z, Inyang, H., Chen, J. and Wang, B. 1999. Preparation of soil specimens for SEM analysis using freeze-cut-drying. *Bull. Eng. Geol. Env.* **58**: 1-7.

SIVAPULLAIAH, P.V., Sridharan, A. and Bhaskar Raju, K.V. 2000. Role of amount and type of clay in the lime stabilization of soils. *Ground Improvement* **4**: 37-45.

TATSUOKA, F. and Kobayashi, A. 1983. Triaxial strength characteristics of cement-treated soft clay. *In* Improvement of ground; Proceedings of the 8th ECSMFE, Helsinki, May 23-26, 1983. Vol. 1. pp. 421-426.

TERZAGHI, K., Peck, R.B. and Mesri G. 1996. Soil mechanics in engineering practice, 3rd Ed., John Wiley & Sons, Inc., New York.

UDDIN, M.K. 1995. Strength and deformation characteristics of cement treated Bangkok clay, D. Eng. Dissertation No. GT-94-1, Asian Institute of Technology, Bangkok, Thailand.

VAN OLPHEN, H. 1963. Clay colloid chemistry for clay technologists, geologists, and soil scientists. John Wiley & Sons, New York.

WISSA, A.E.Z. and Ladd, C.C. 1964. Effective stress-strength behavior of compacted stabilized soils. Soil Mechanics Division, Department of Civil Engineering, Massachusetts Institute of Technology. Research report R64-32.

WROTH C.P. and Houlsby, G.T. 1985. Soil mechanics – Property characterization and analysis procedures. *In* Proceedings of 11th international conference on soil mechanics and foundation engineering, San Francisco, Vol. 1. A.A. Balkema, Rotterdam. pp. 1-55.

YANG, D.S. and Takeshima, S. 1994. Soil mix walls in difficult ground. *In* In-situ deep soil improvement; Proceedings of sessions sponsored by the Geotechnical Engineering Division of ASCE, Atlanta, October 9-13, 1994. Edited by Rollins, K.M. ASCE, New York. pp.106-120.

Mechanical Characteristics of Kaolin-Cement Mixture

APPENDIX A: CONSOLIDATED DRAINED TRIAXIAL TEST DATA

Isotropically consolidated drained triaxial (CID) compression tests were conducted at the City University of Hong Kong between June 2000 and July 2001. Tests were conducted on samples at 70 percent moisture content with 2 and 5 percent cement and samples at 100 percent moisture content with 5 and 10 percent cement. Samples were cured in distilled water at 20°C for 7, 28, 56 and 112 days. Tests were also done on samples of pure kaolin at 40 percent moisture content. Confining pressures of 50, 100 and 400 kPa were considered, with a back pressure of 650, 600 and 300 kPa, respectively. Chapter 5 describes and interprets the results of the triaxial tests.

Graphs of the shear data from the CID tests are included in this appendix. The data presented includes deviator stress (q), volumetric strain (ε_v) and stress ratio ($\eta=q/p'$) vs. axial strain (ε_a); these are found in plots a, b and c, respectively. Note that the shear data was corrected to account for initial straining during seating of the load; therefore, often the load is positive at zero strain.

Graphs appear in groups so that the effects of curing time, cement and moisture content and confining pressure can be interpretted. Therefore, data for each test appear several times. There are some tests which were considered to be unsuccessful due to problems during the test or poor sample quality; the results for these tests are not included. Plots of the effective stress paths (p' vs. q) were also generated for the drained triaxial tests and are included here and in Appendix F, as part of a presentation on critical state soil mechanics and bonded soil.

Tables A.1 to A.4 summarize the figures provided in this appendix.

Table A.1. Plots illustrating the effects of curing time. (a) q vs. ε_α; (b) ε_v vs. ε_a; (c) η vs. ε_a.

w (%)	A_c(%)	$p_o{}'$ (kPa)	Curing Time, T_c (days)			
			7	28	56	112
70	2	50	A.1			
		100	A.2			
		400	A.3			
	5	50	A.4			
		100	A.5			
		400	A.6			
100	5	50	A.7			
		100	A.8			
		400	A.9			
	10	50	A.10			
		100	A.11			
		400	A.12			

Table A.2. Plots illustrating the effects of cement and moisture content. (a) q vs. ε_α; (b) ε_v vs. ε_a; (c) η vs. ε_a.

T_c (days)	p_o' (kPa)	w=40%; A_c=0%*	w=70%; A_c=2%	w=70%; A_c=5%	w=100%; A_c=5%	w=100%; A_c=10%
7	50	A.13				
7	100	A.14†				
7	400	A.15				
28	50	■	A.16			
28	100	■	A.17			
28	400	■	A.18			
56	50	■	A.19			
56	100	■	A.20			
56	400	■	A.21			
112	50	■	A.22‡			
112	100	■	A.23‡			
112	400	■	A.24‡			

*samples tested immediately following casting; T_c=0 days.
† 7-day test unsuccessful for sample with w=100% and A_c=5%.
‡samples with w=70% and A_c=5% not tested after 112 days of curing.

Table A.4. Stress-path plots (t-s') deriving the Mohr-Coulomb parameters.

w (%)	A_c(%)	T_c (days)	Effective confining Pressure, p_o' (kPa)		
			50	100	400
40	0	0	A.41		
70	2	7	A.42		
		28	A.43		
		56	A.44		
		112	A.45		
	5	7	A.46		
		28	A.47		
		56	A.48		
		112	███████████████████		
100	5	7	A.49†		
		28	A.50		
		56	A.51		
		112	A.52		
	10	7	A.53		
		28	A.54		
		56	A.55		
		112	A.56		

† test unsuccessful at 100 kPa confining pressure.
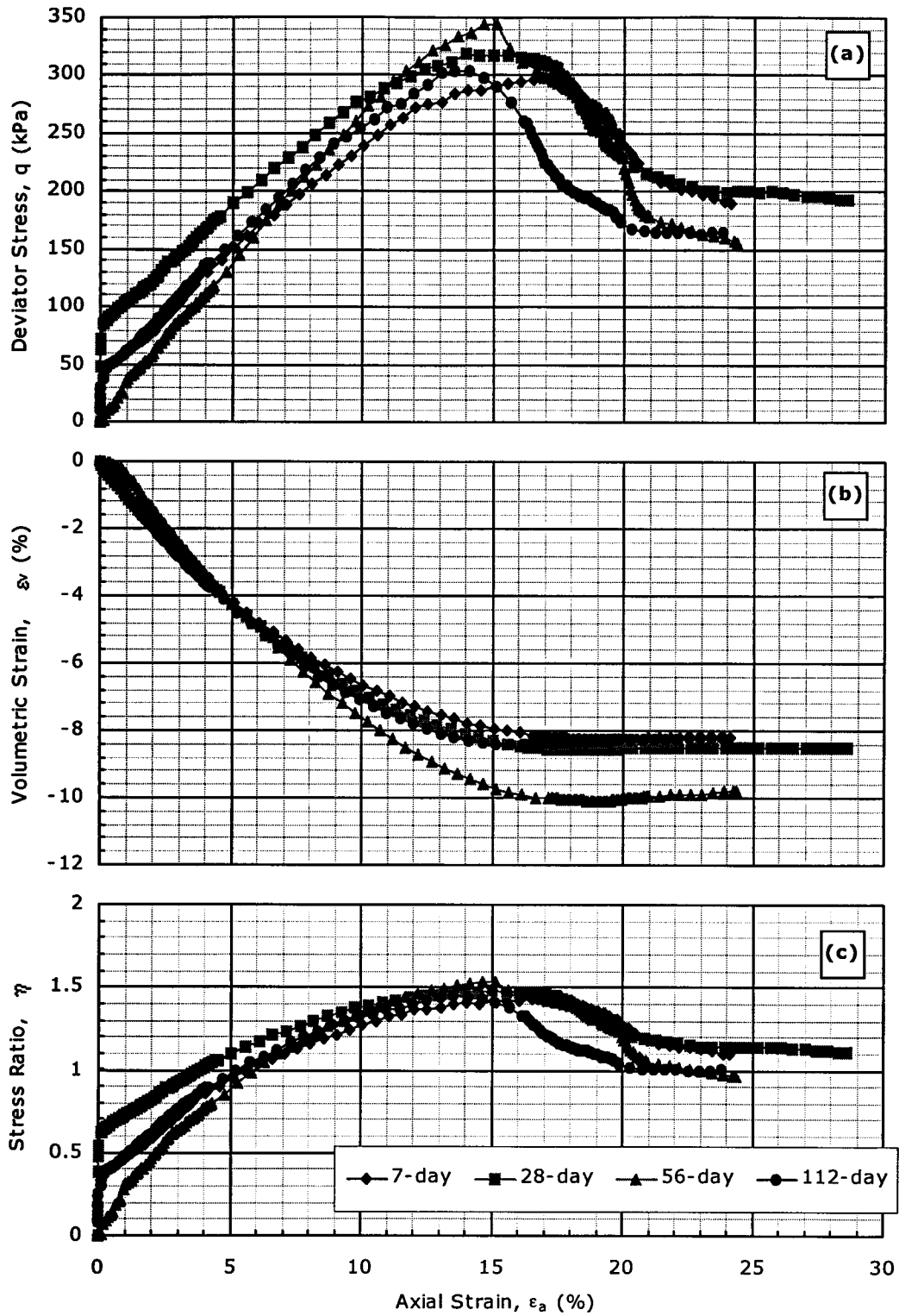
Figure A.2. CID data for w=70%; A_c=2% & $p_o{'}$=100 kPa. (a) q vs. ε_a; (b) ε_v vs. ε_a; (c) η vs. ε_a.
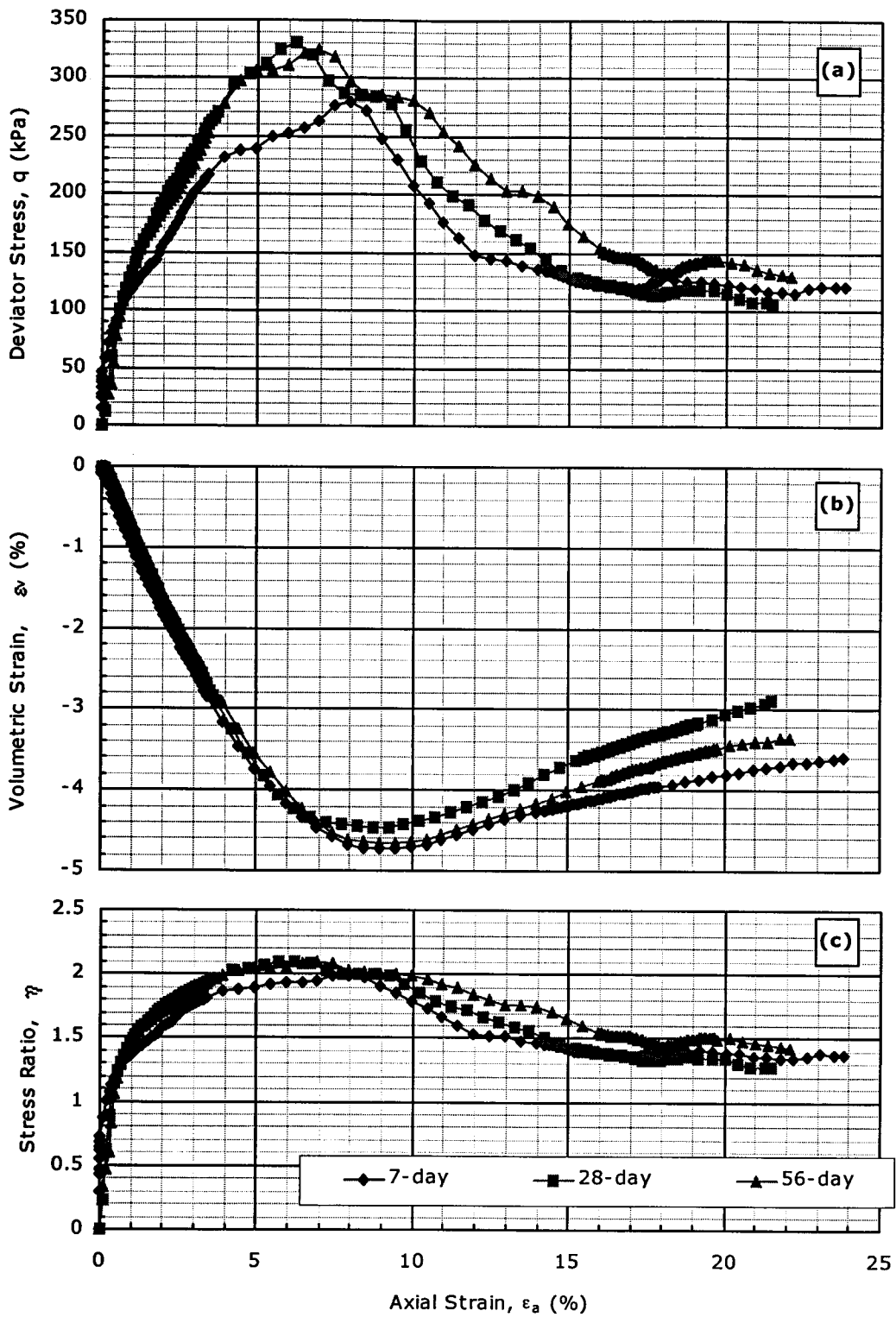
Figure A.4. CID data for w=70%; A_c=5% & $p_o{}'$=50 kPa. (a) q vs. ε_a; (b) ε_v vs. ε_a; (c) η vs. ε_a.

Mechanical Characteristics of Kaolin-Cement Mixture   177
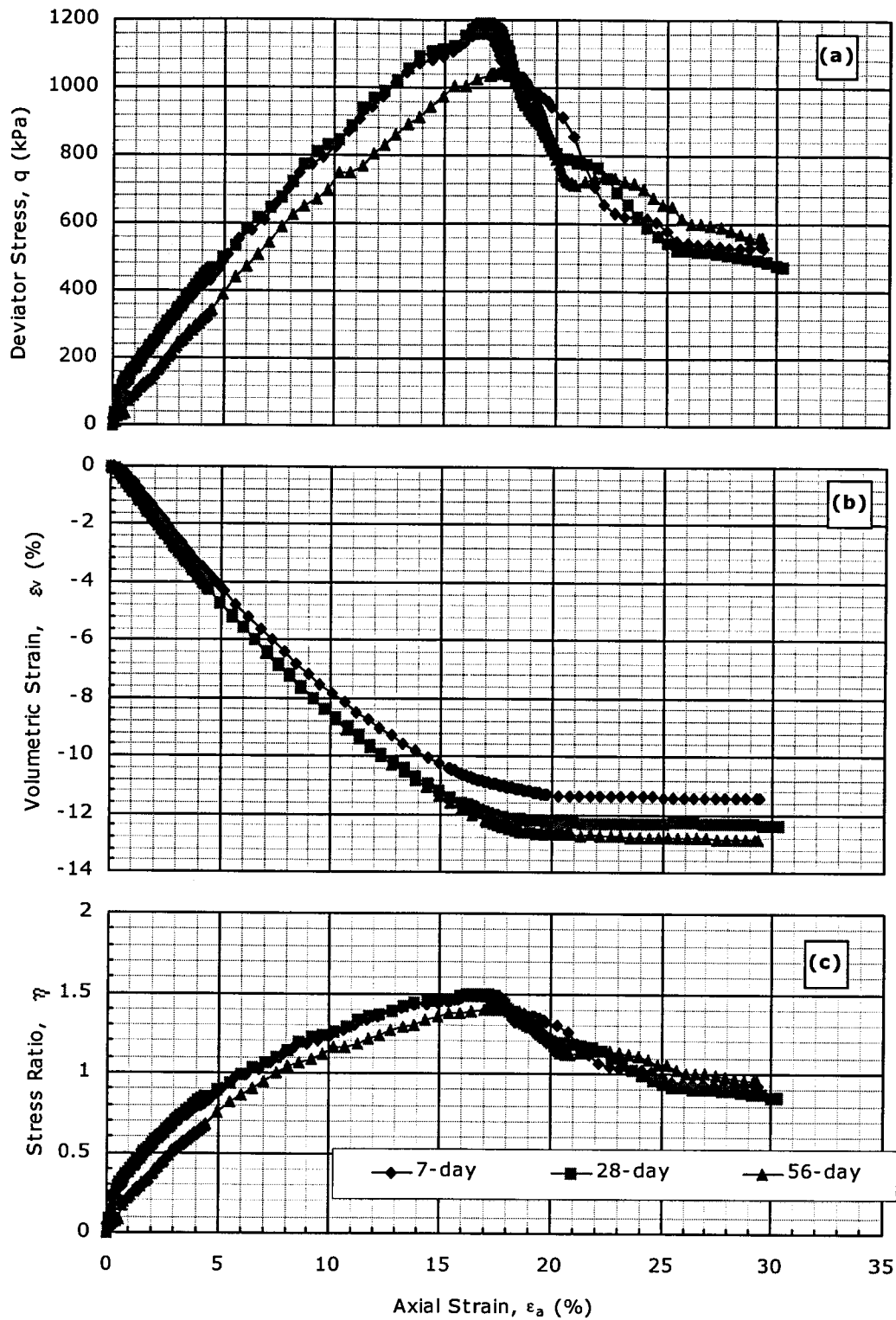
Figure A.6. CID data for w=70%; A_c=5% & $p_o{'}$=400 kPa. (a) q vs. ε_a; (b) ε_v vs. ε_a; (c) η vs. ε_a.
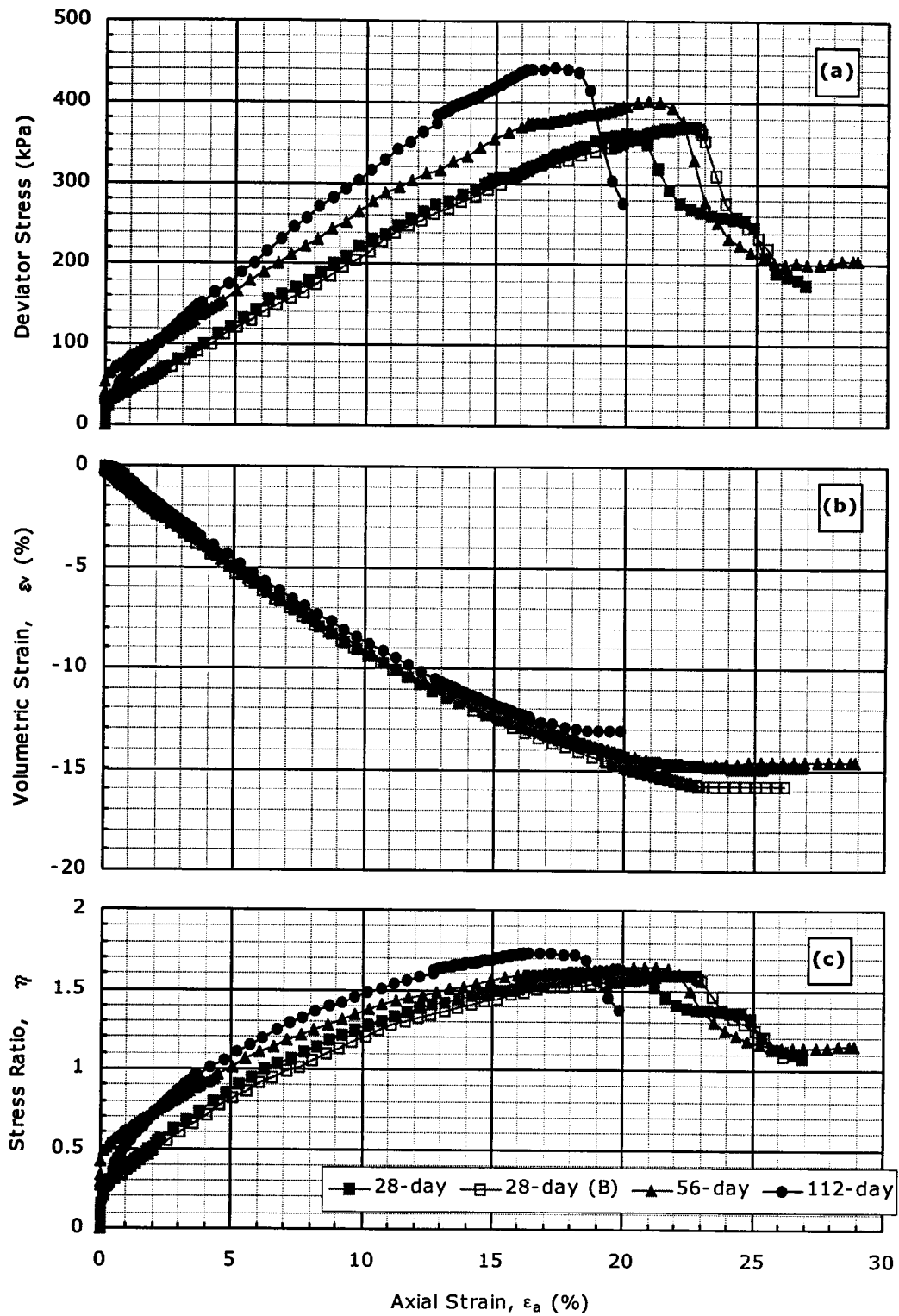
Figure A.8. CID data for w=100%; A_c=5% & $p_o{}'$=100 kPa. (a) q vs. ε_a; (b) ε_v vs. ε_a; (c) η vs. ε_a.

Mechanical Characteristics of Kaolin-Cement Mixture   181
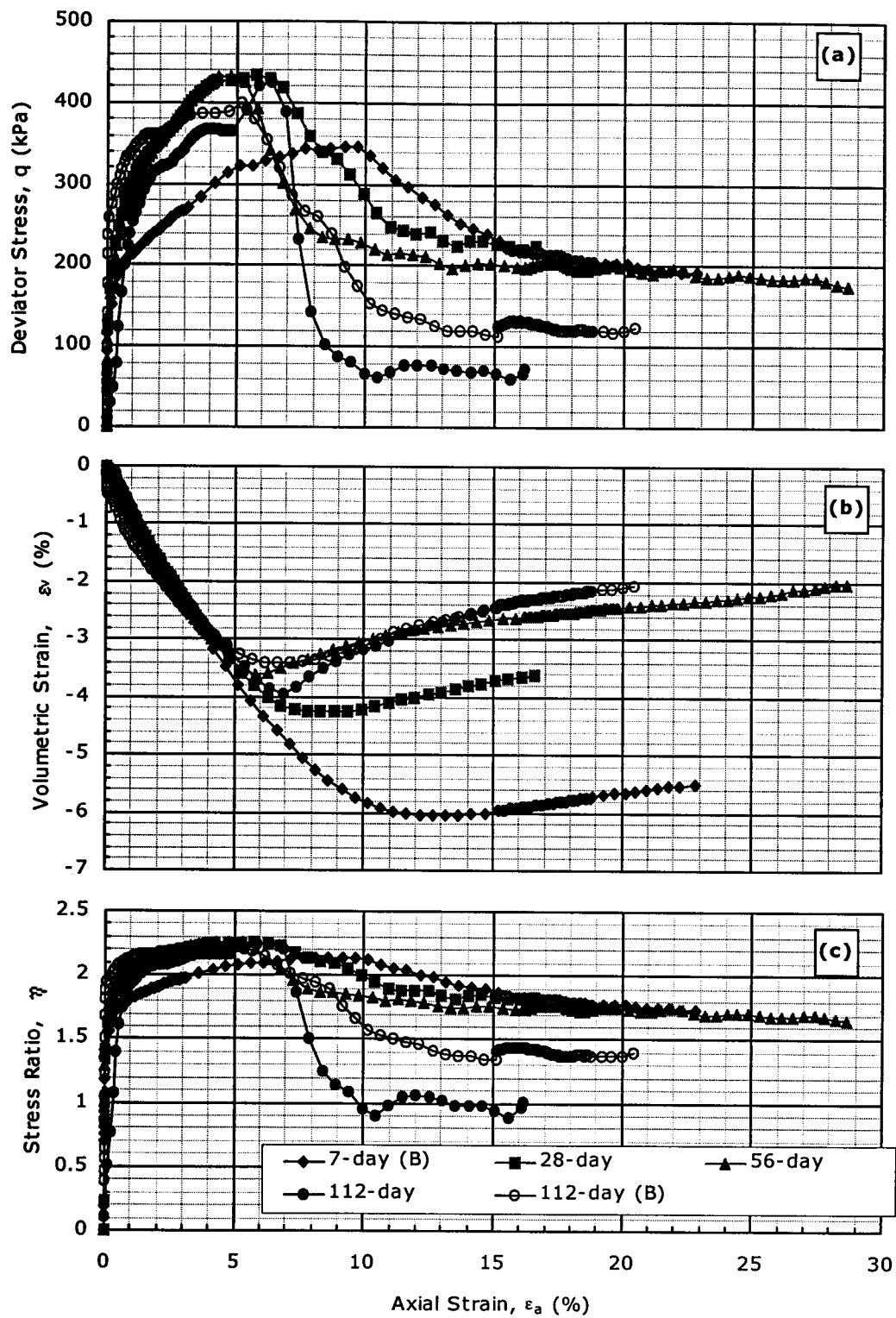
Figure A.10. CID data for w=100%; A_c=10% & $p_o{'}$=50 kPa. (a) q vs. ε_a; (b) ε_v vs. ε_a; (c) η vs. ε_a.

Mechanical Characteristics of Kaolin-Cement Mixture 183
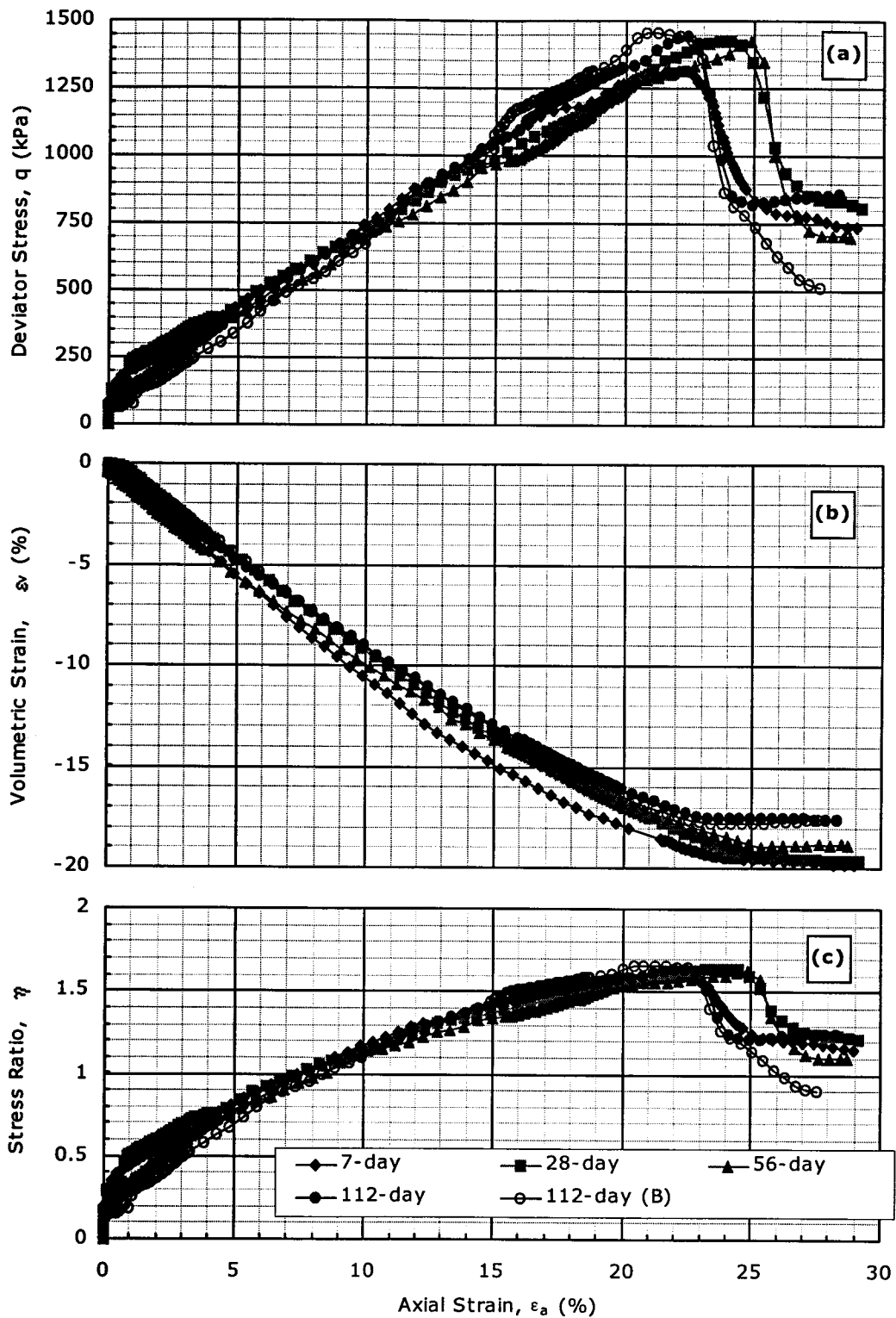
Figure A.12. CID data for w=100%; A_c=10% & p_o'=400 kPa. (a) q vs. ε_a; (b) ε_v vs. ε_a; (c) η vs. ε_a.

Mechanical Characteristics of Kaolin-Cement Mixture   185
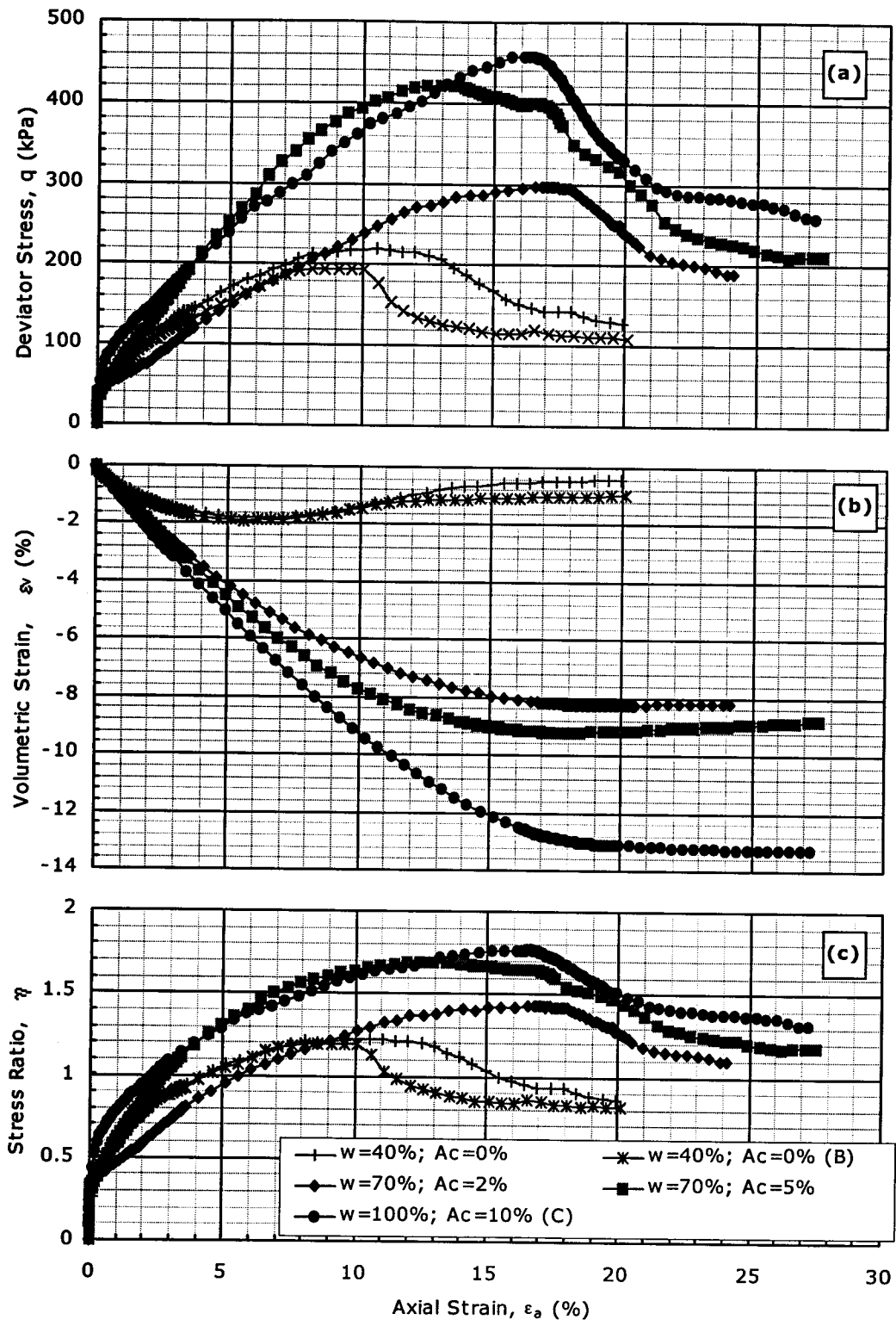
Figure A.14. CID data for $T_c=7$ days & $p_o{}'=100$ kPa. (a) q vs. ε_a; (b) ε_v vs. ε_a; (c) η vs. ε_a.
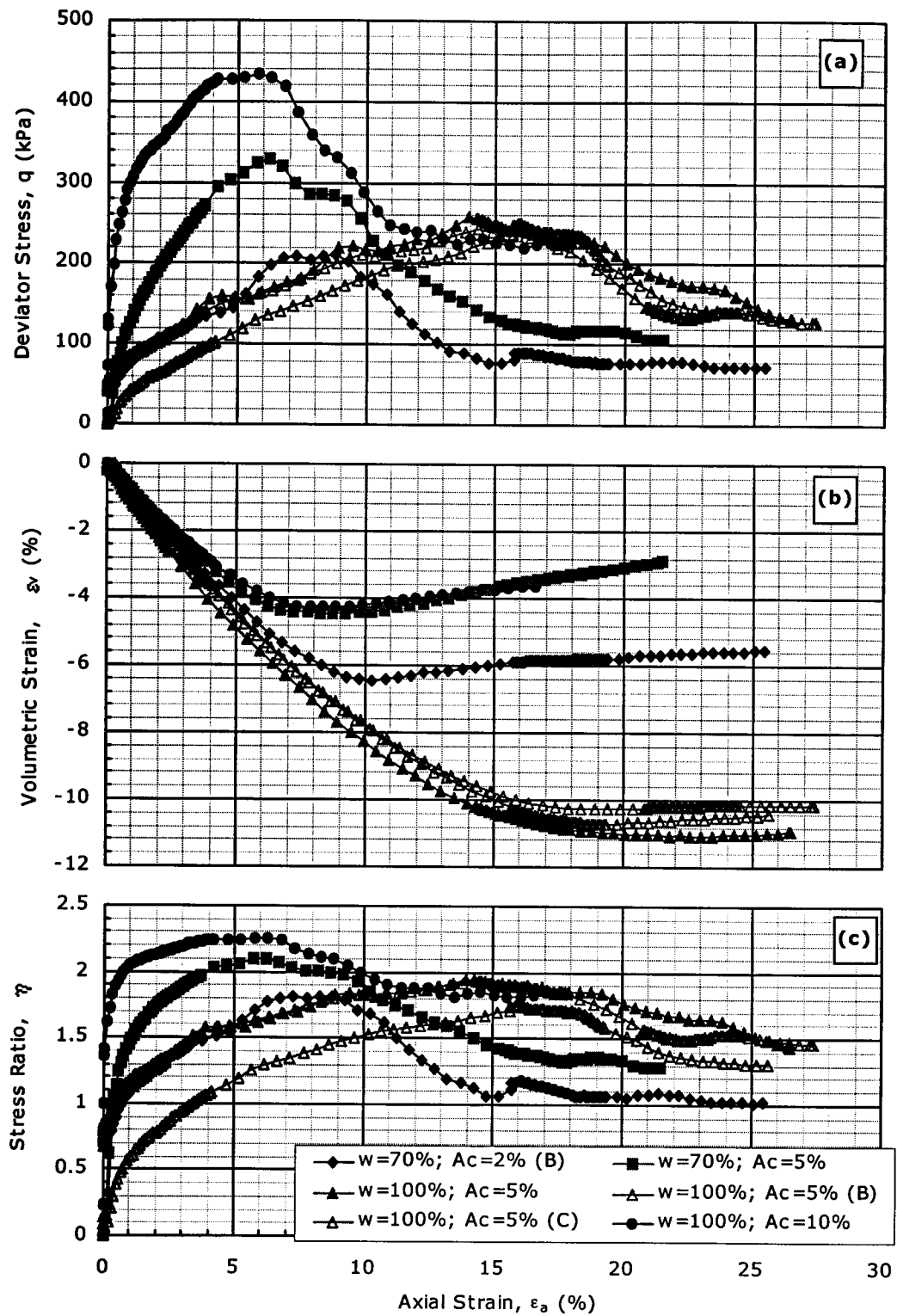
Figure A.16. CID data for T_c=28 days & $p_o{'}$=50 kPa. (a) q vs. ε_a; (b) ε_v vs. ε_a; (c) η vs. ε_a.

Mechanical Characteristics of Kaolin-Cement Mixture 189
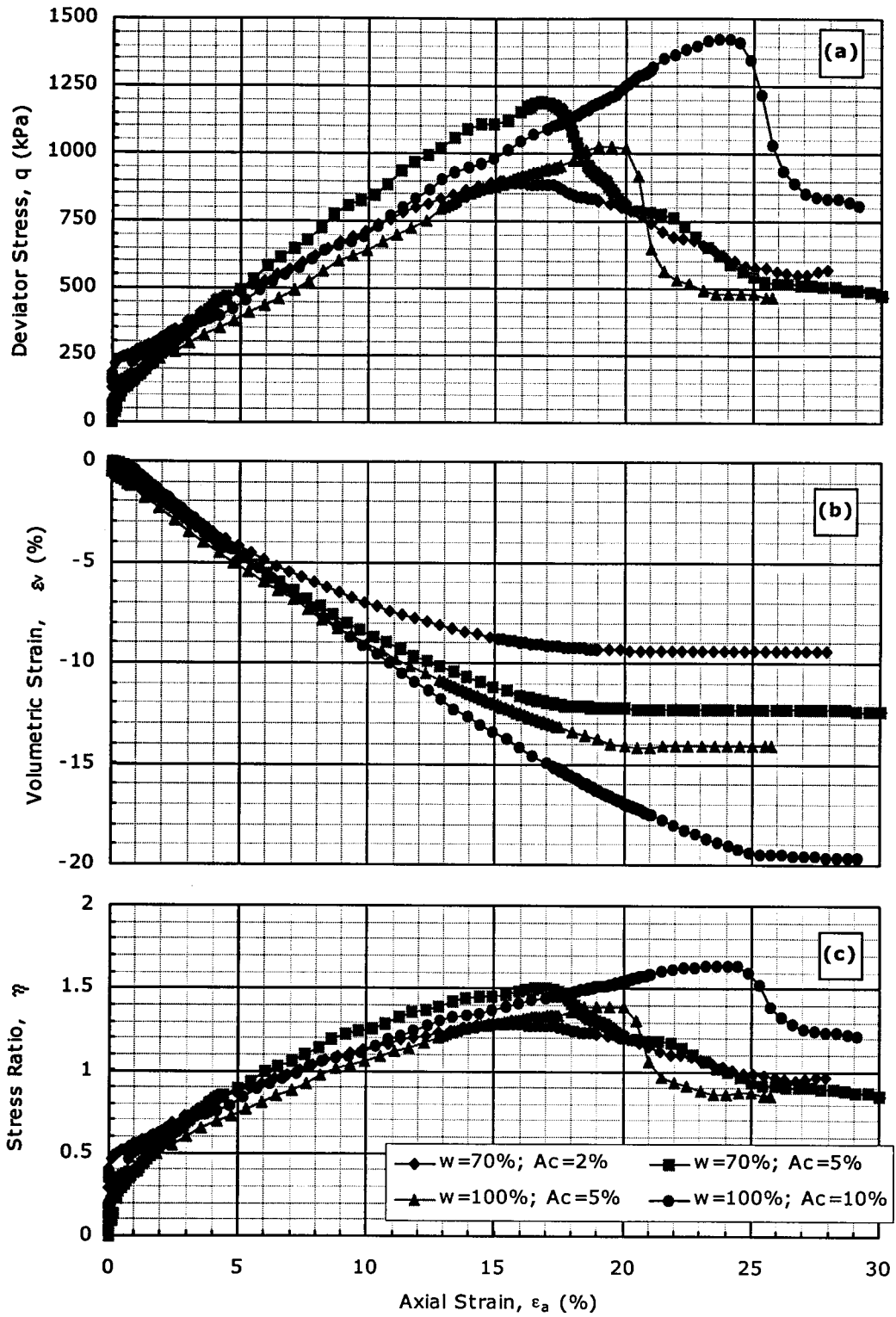
Figure A.18. CID data for T_c=28 days & $p_o{'}$=400 kPa. (a) q vs. ε_a; (b) ε_v vs. ε_a; (c) η vs. ε_a.
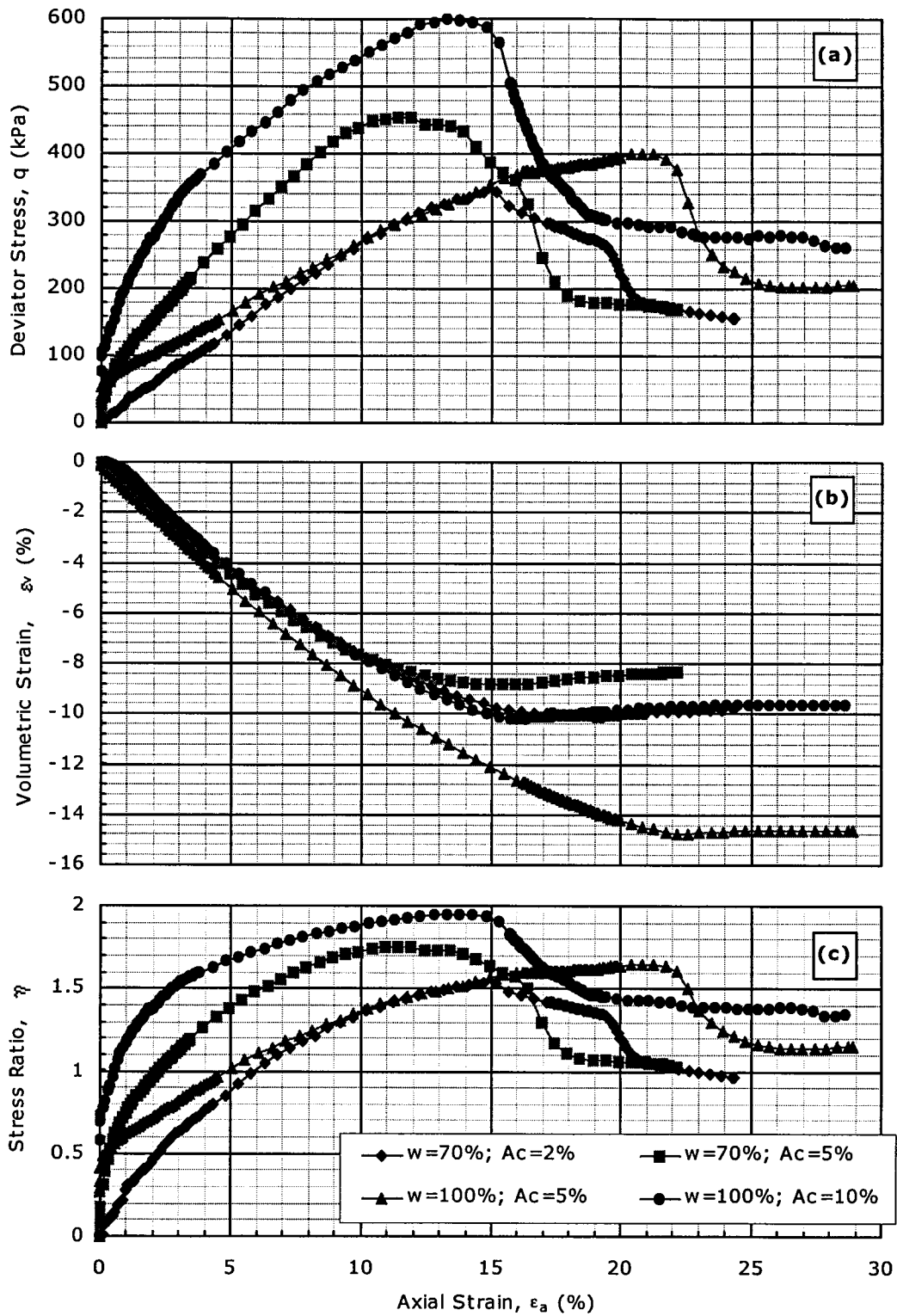
Figure A.20. CID data for T_c=56 days & p_o'=100 kPa. (a) q vs. ε_a; (b) ε_v vs. ε_a; (c) η vs. ε_a.

Mechanical Characteristics of Kaolin-Cement Mixture   193
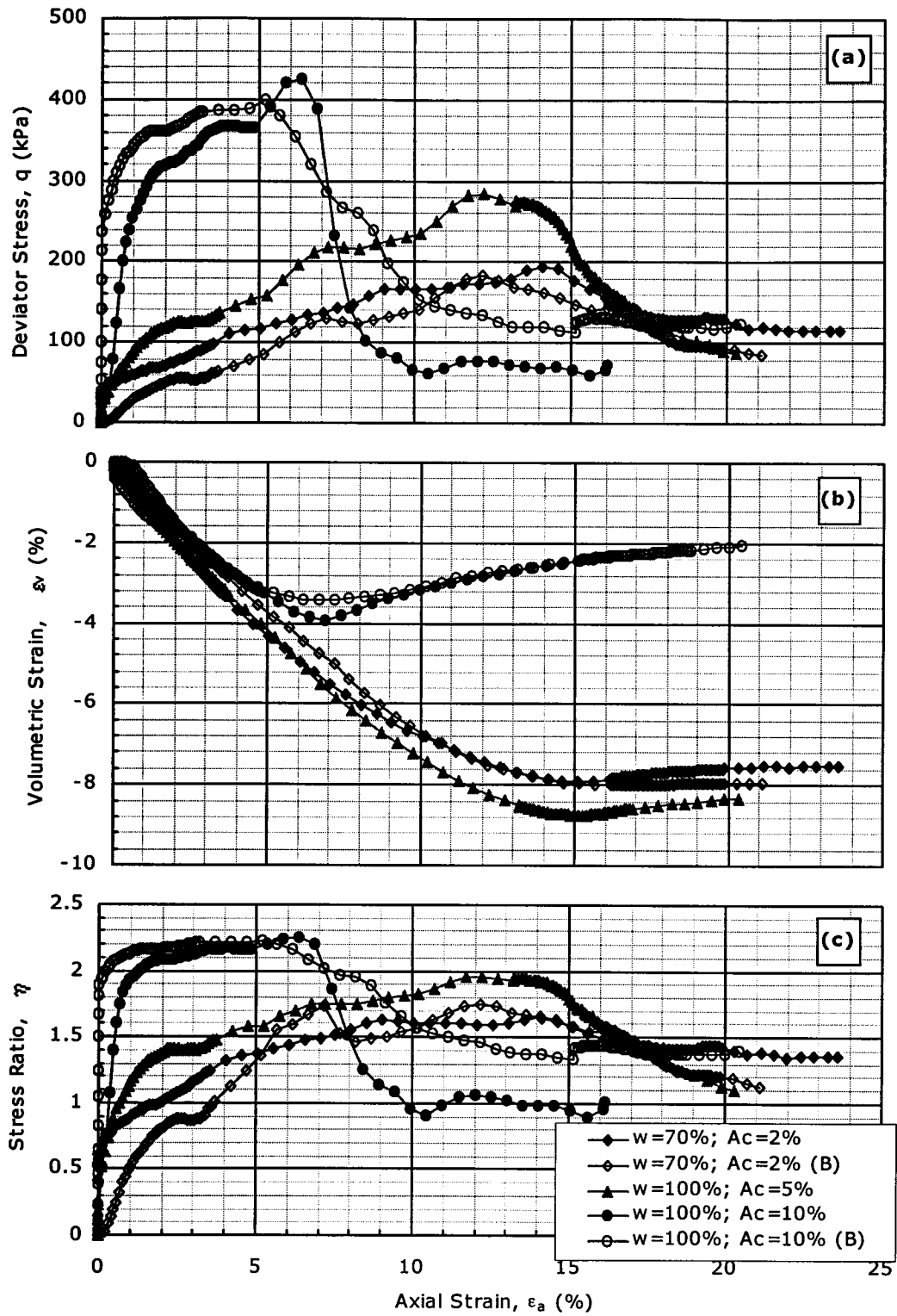
Figure A.22. CID data for T_c=112 days & p_o'=50 kPa. (a) q vs. ε_a; (b) ε_v vs. ε_a; (c) η vs. ε_a.
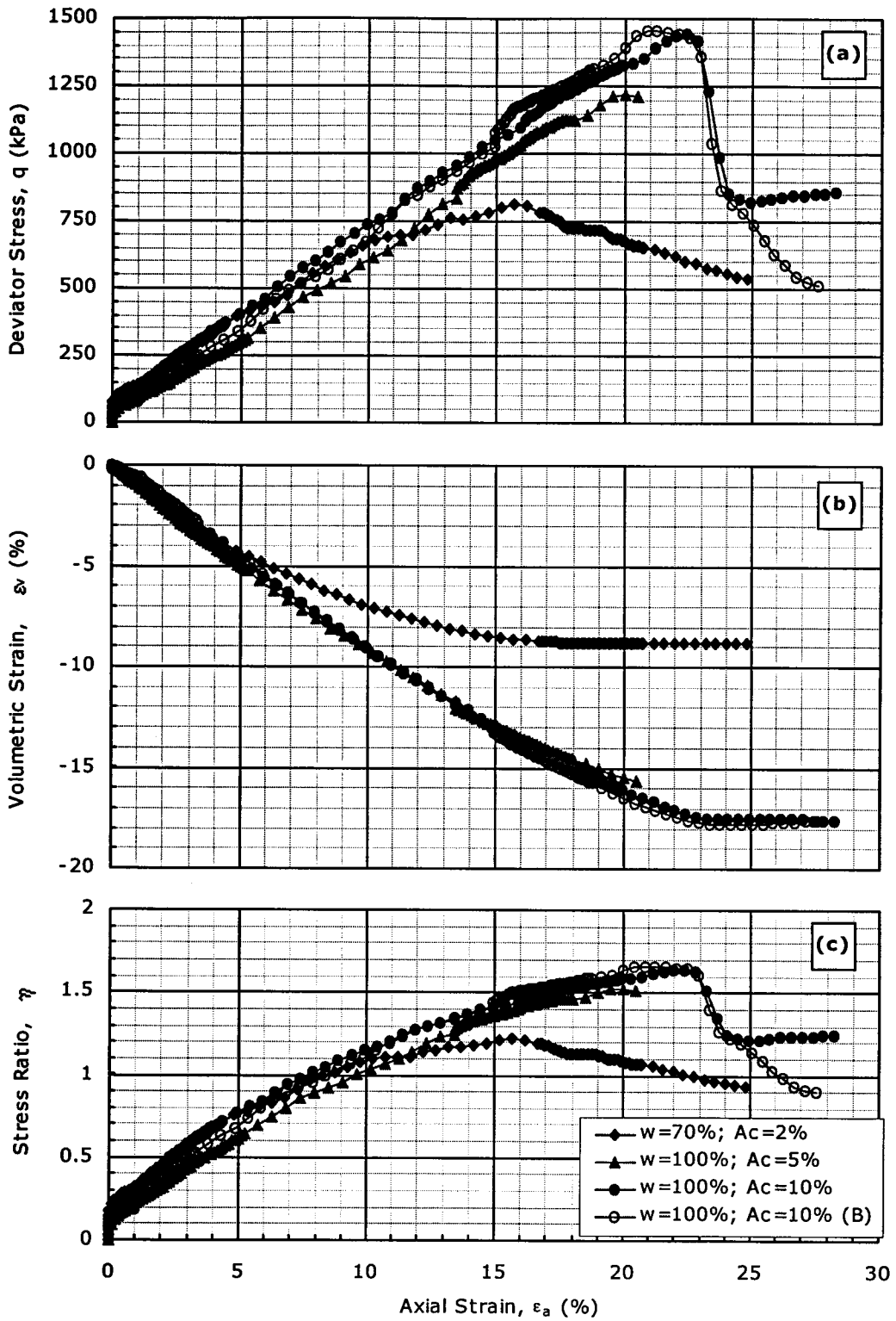
Figure A.24. CID data for $T_c=112$ days & $p_o'=400$ kPa. (a) q vs. ε_a; (b) ε_v vs. ε_a; (c) η vs. ε_a.

Mechanical Characteristics of Kaolin-Cement Mixture   197
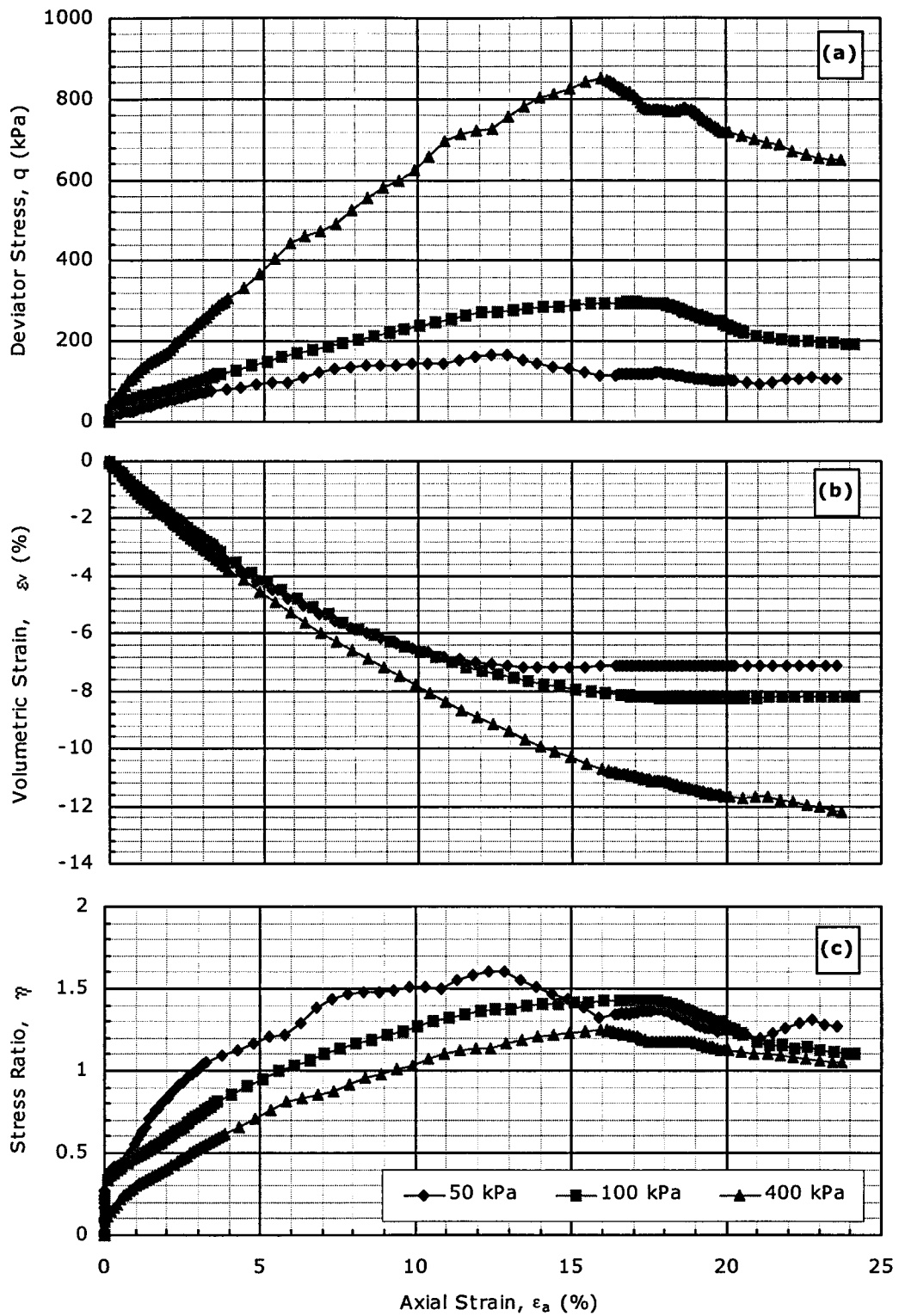
Figure A.26. CID data for w=70%; A_c=2% & T_c=7 days. (a) q vs. ε_a; (b) ε_v vs. ε_a; (c) η vs. ε_a.

Mechanical Characteristics of Kaolin-Cement Mixture 199
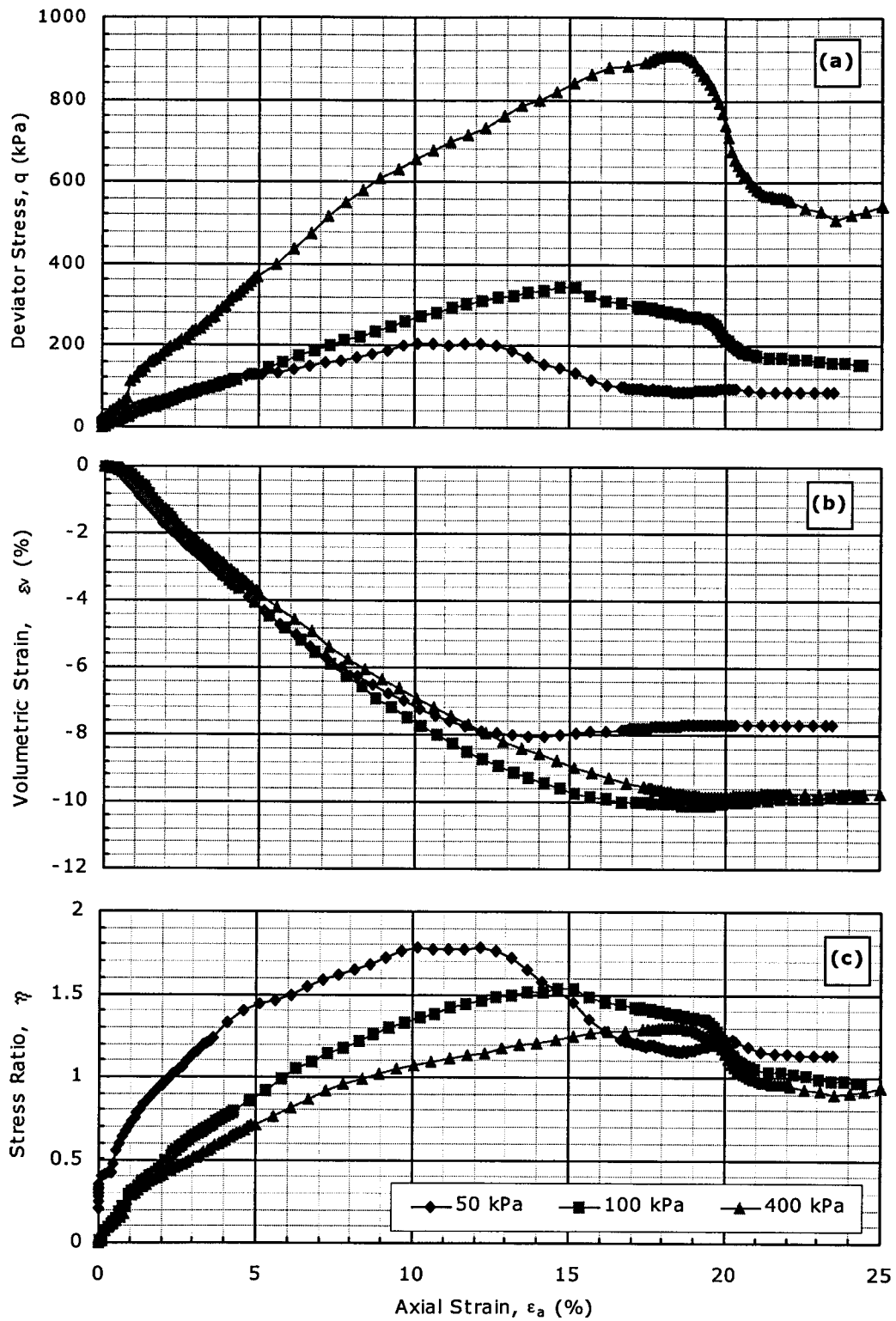
Figure A.28.   CID data for w=70%; A_c=2% & T_c=56 days.   (a) q vs. ε_a; (b) ε_v vs. ε_a; (c) η vs. ε_a.

Mechanical Characteristics of Kaolin-Cement Mixture 201
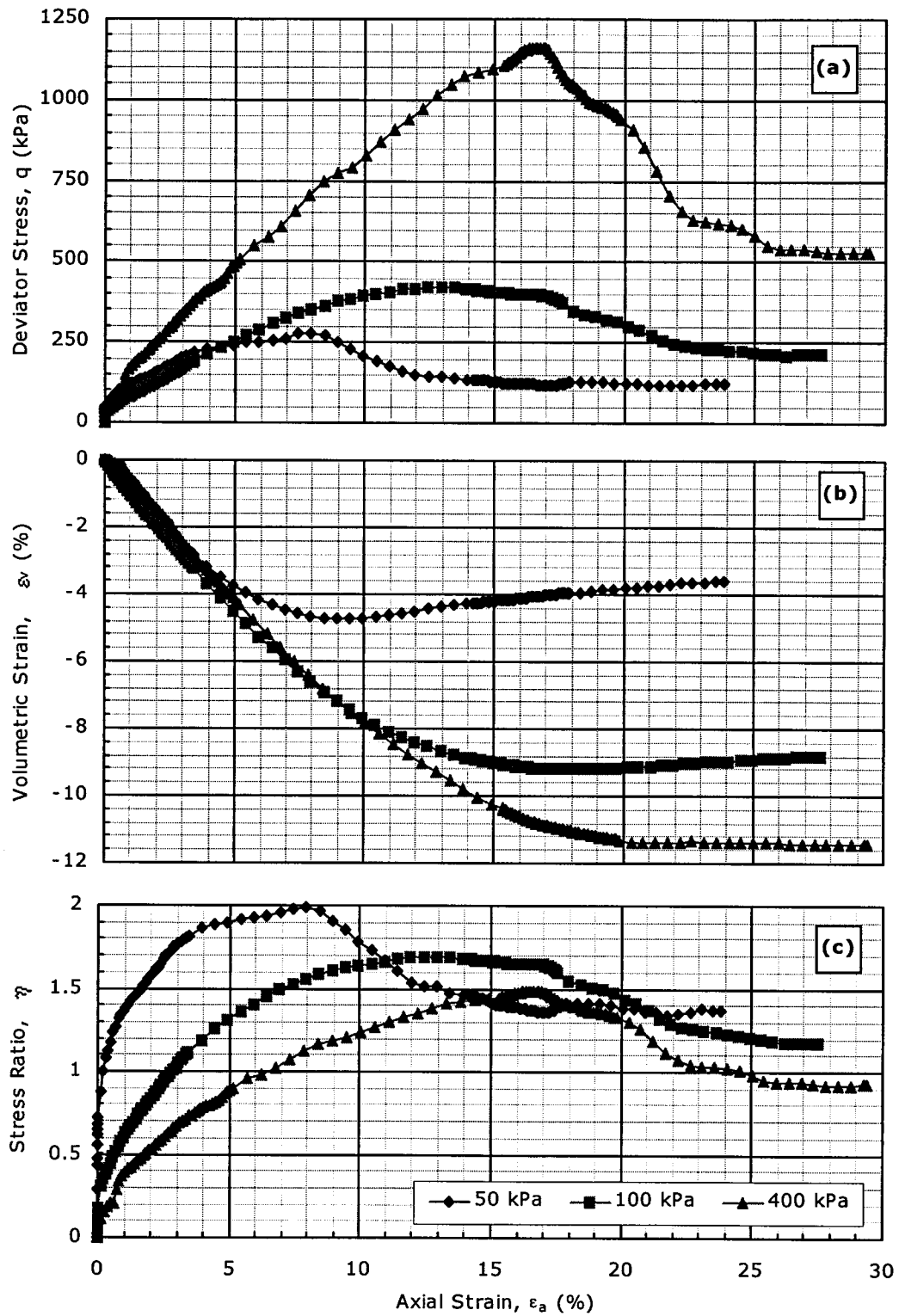
Figure A.30. CID data for w=70%; A_c=5% & T_c=7 days. (a) q vs. ε_a; (b) ε_v vs. ε_a; (c) η vs. ε_a.
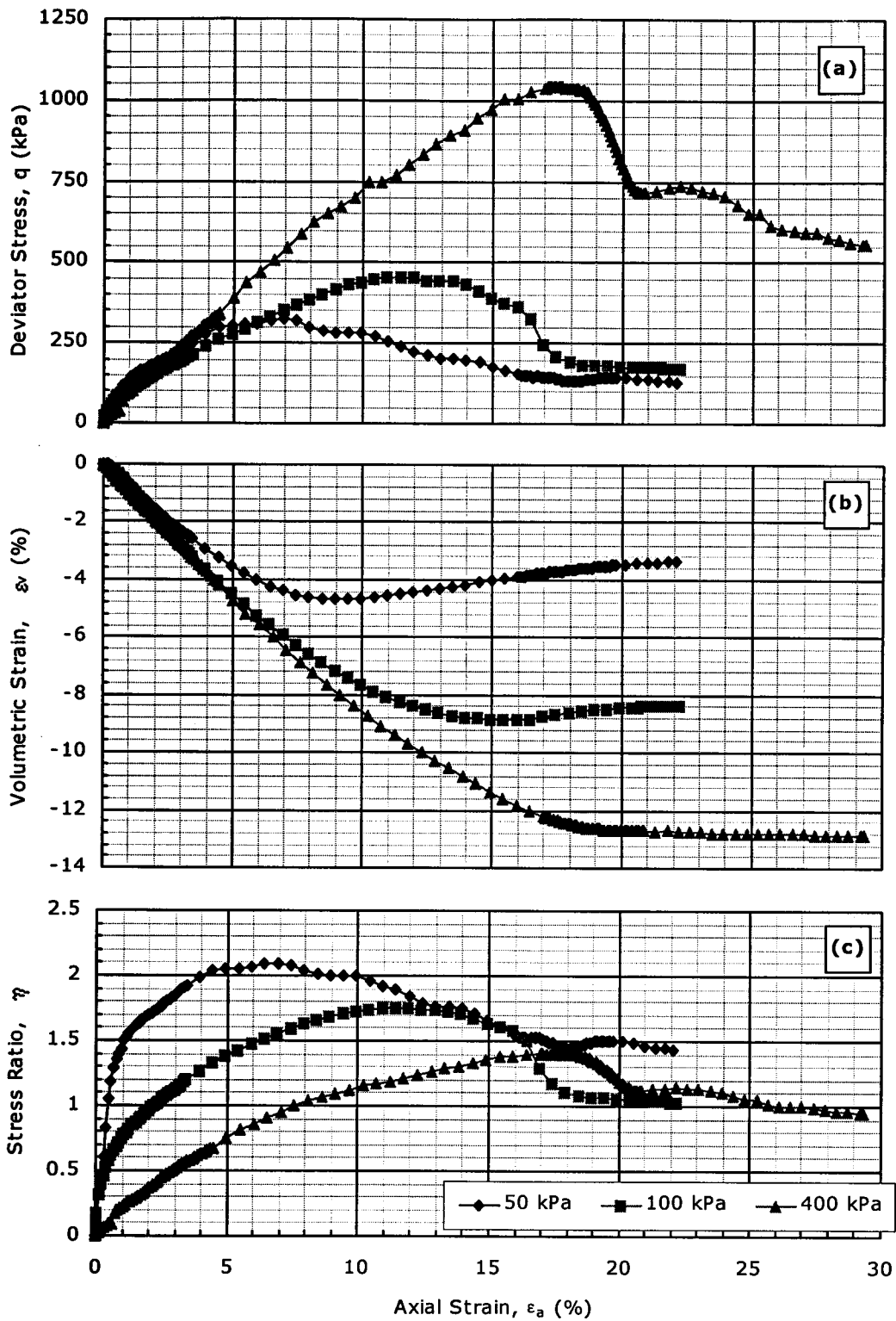
Figure A.32. CID data for w=70%; A_c=5% & T_c=56 days. (a) q vs. ε_a; (b) ε_v vs. ε_a; (c) η vs. ε_a.

Mechanical Characteristics of Kaolin-Cement Mixture   205
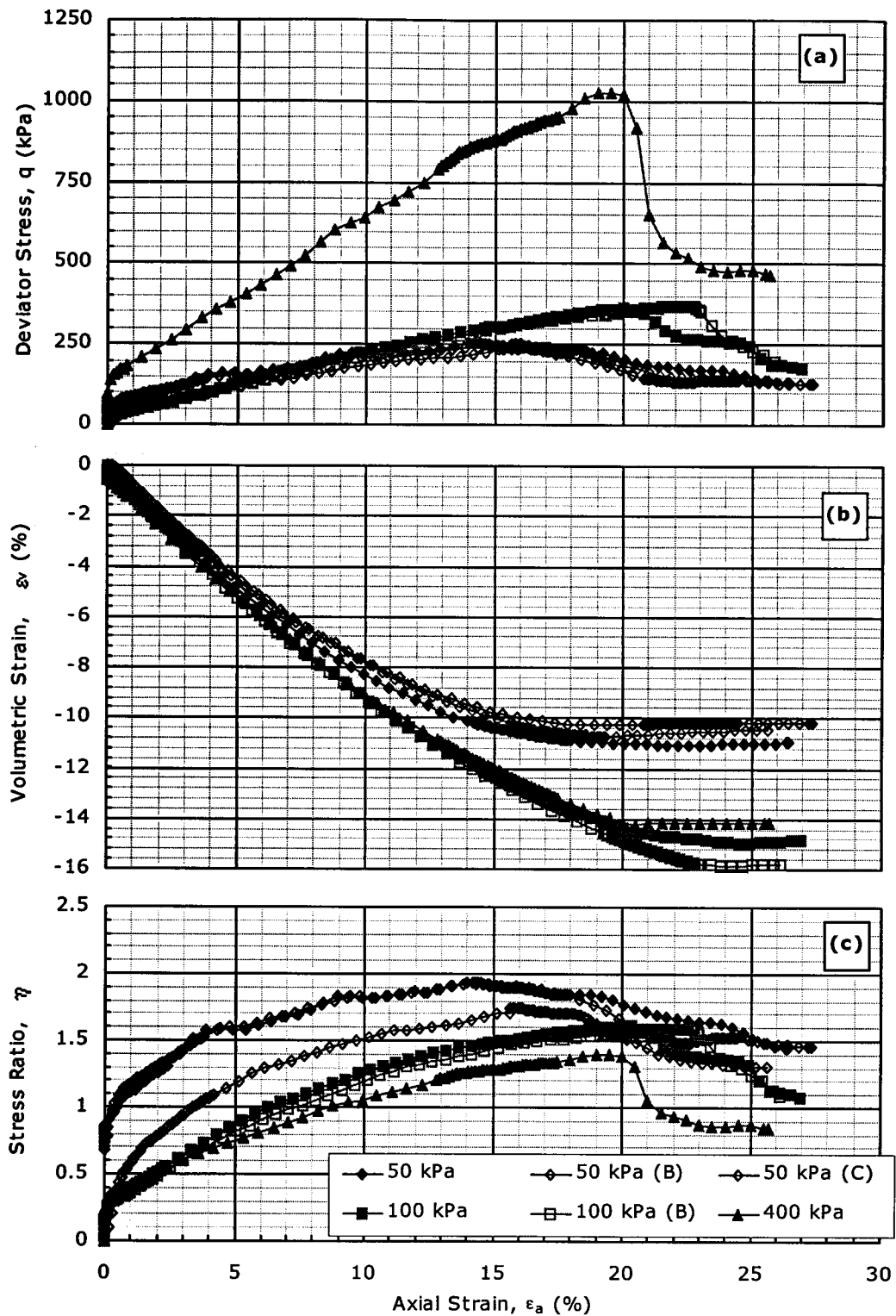
Figure A.34. CID data for w=100%; A_c=5% & T_c=28 days. (a) q vs. ε_a; (b) ε_v vs. ε_a; (c) η vs. ε_a.

Mechanical Characteristics of Kaolin-Cement Mixture 207
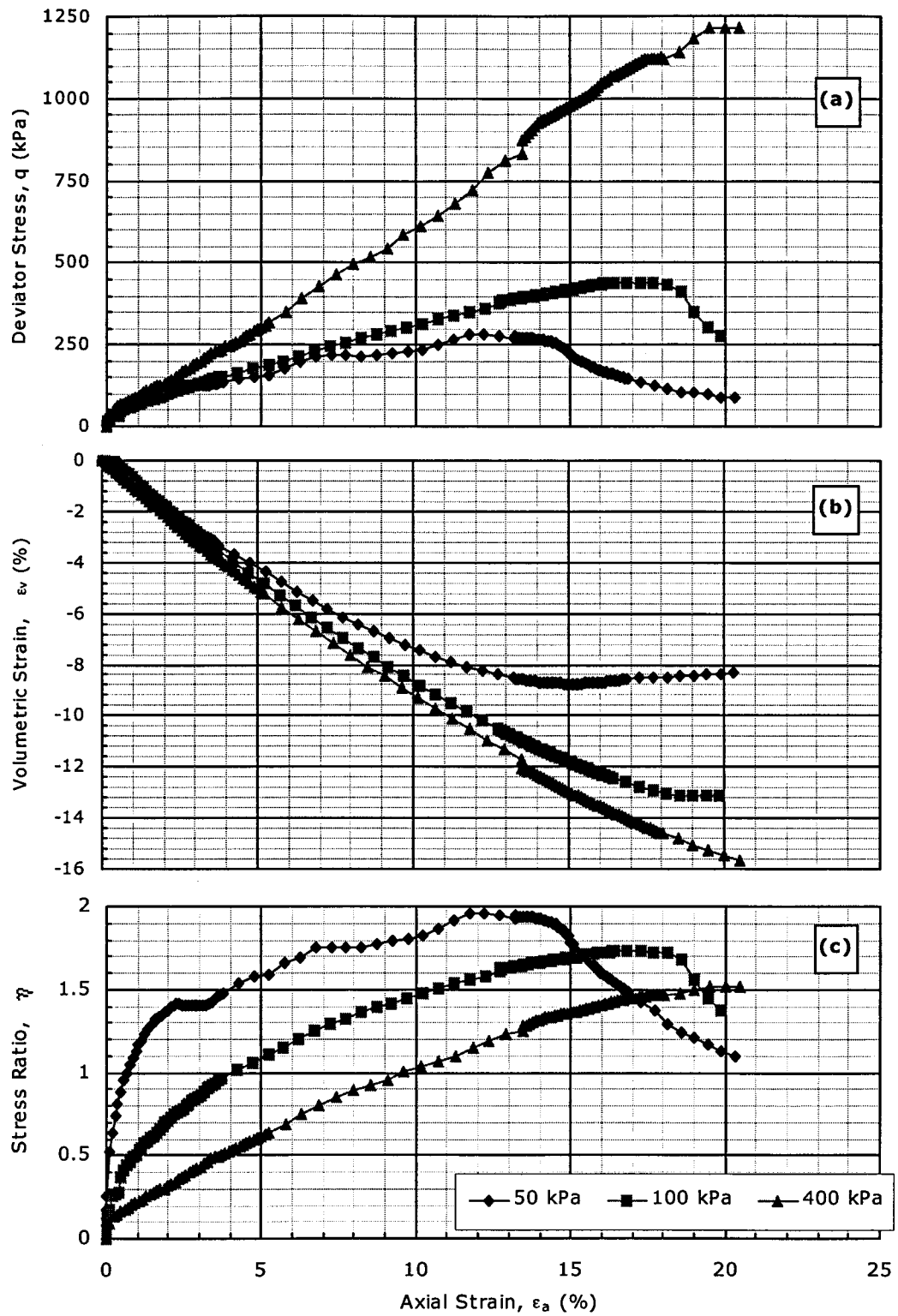
Figure A.36. CID data for w=100%; A_c=5% & T_c=112 days. (a) q vs. ε_a; (b) ε_v vs. ε_a; (c) η vs. ε_a.

Mechanical Characteristics of Kaolin-Cement Mixture   209
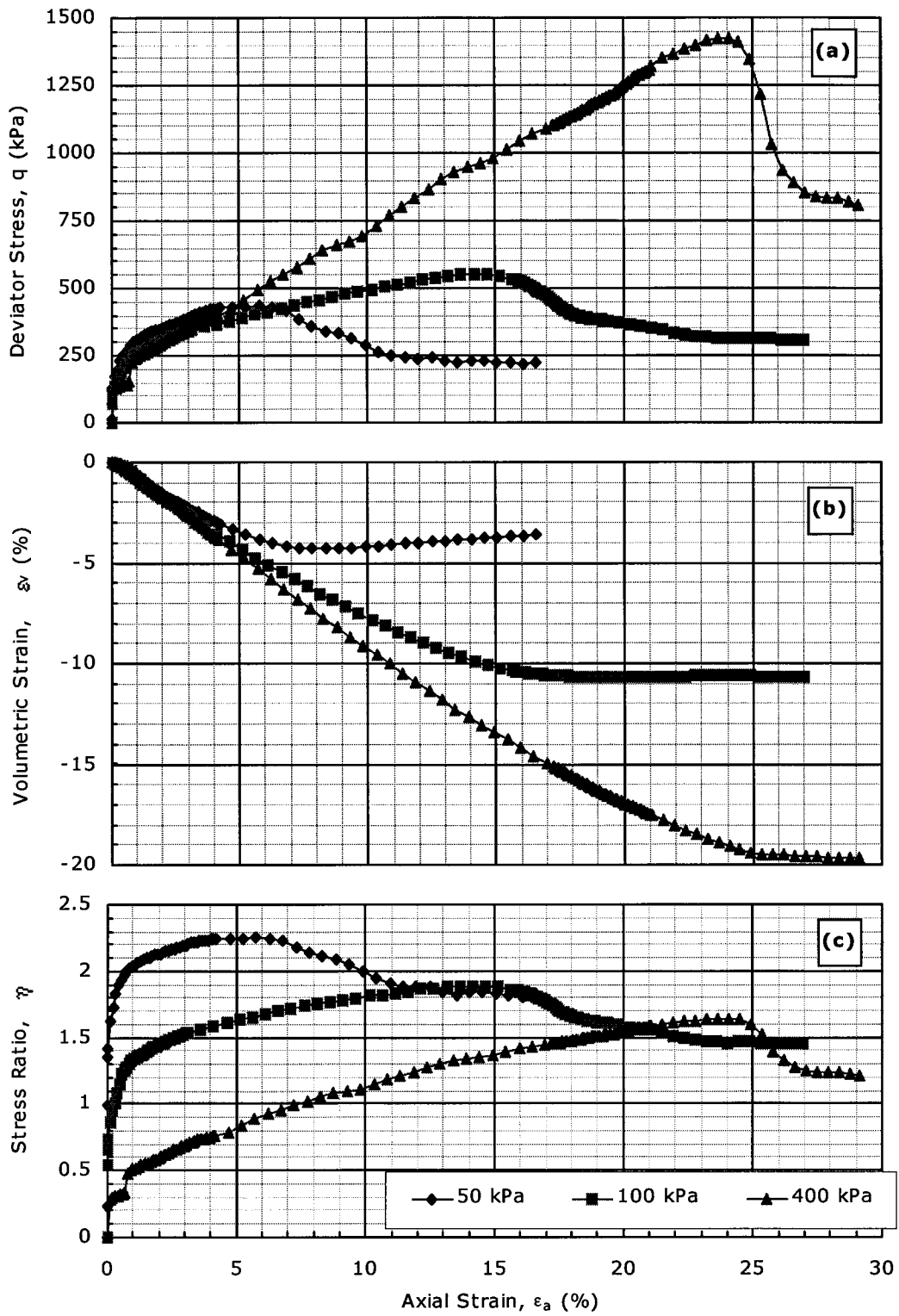
Figure A.38. CID data for w=100%; A_c=10% & T_c=28 days. (a) q vs. ε_a; (b) ε_v vs. ε_a; (c) η vs. ε_a.

Mechanical Characteristics of Kaolin-Cement Mixture   211
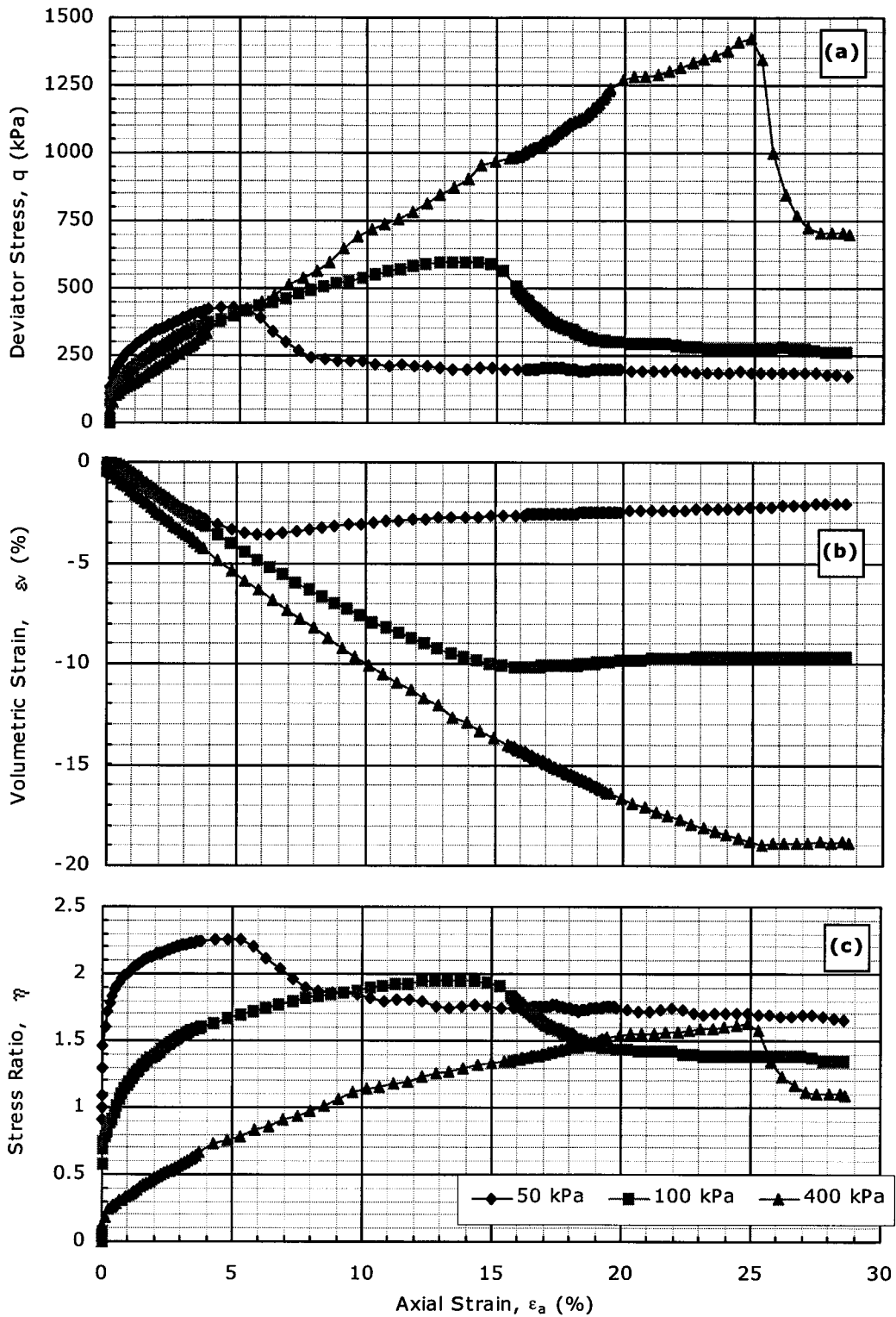
Figure A.39.   CID data for w=100%; A$_c$=10% & T$_c$=56 days.   (a) q vs. ε$_a$; (b) ε$_v$ vs. ε$_a$; (c) η vs. ε$_a$.
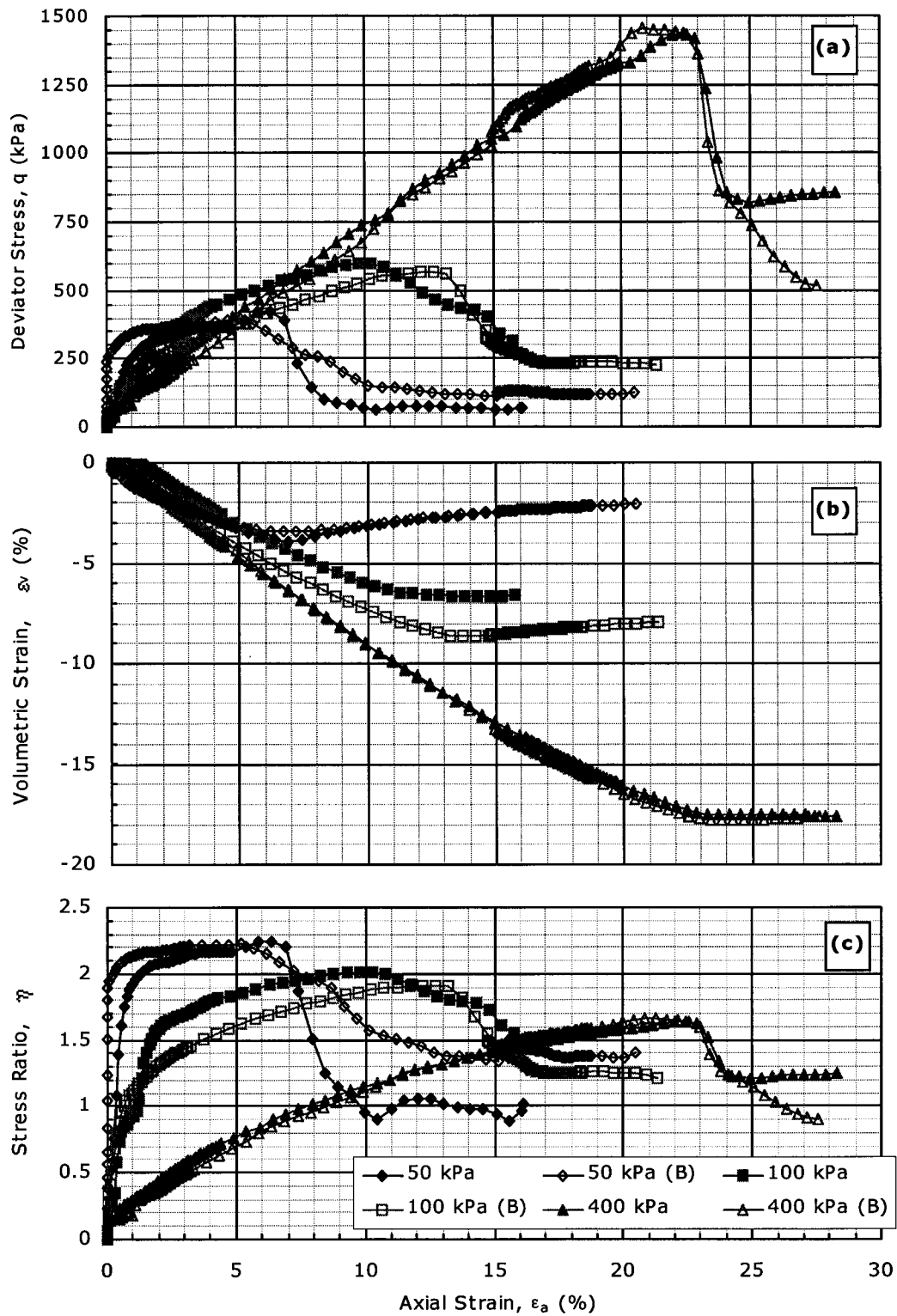
Figure A.40. CID data for w=100%; A_c=10% & T_c=112 days. (a) q vs. ε_a; (b) ε_v vs. ε_a; (c) η vs. ε_a.

Mechanical Characteristics of Kaolin-Cement Mixture   213
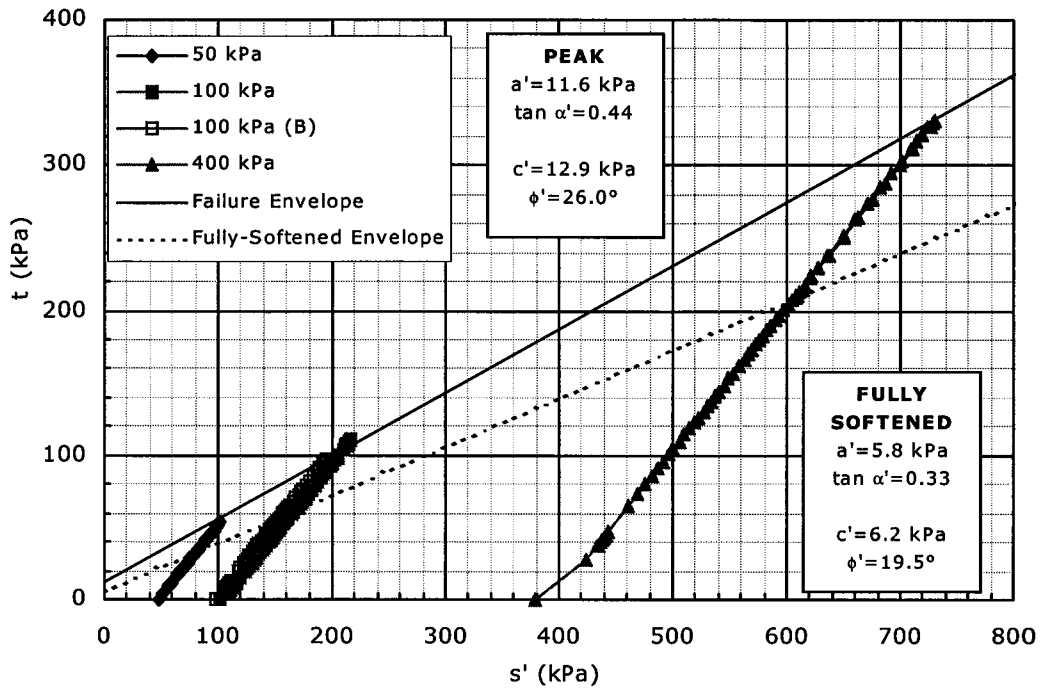
Figure A.41. t-s' plot for w=40% & A_c=0%.
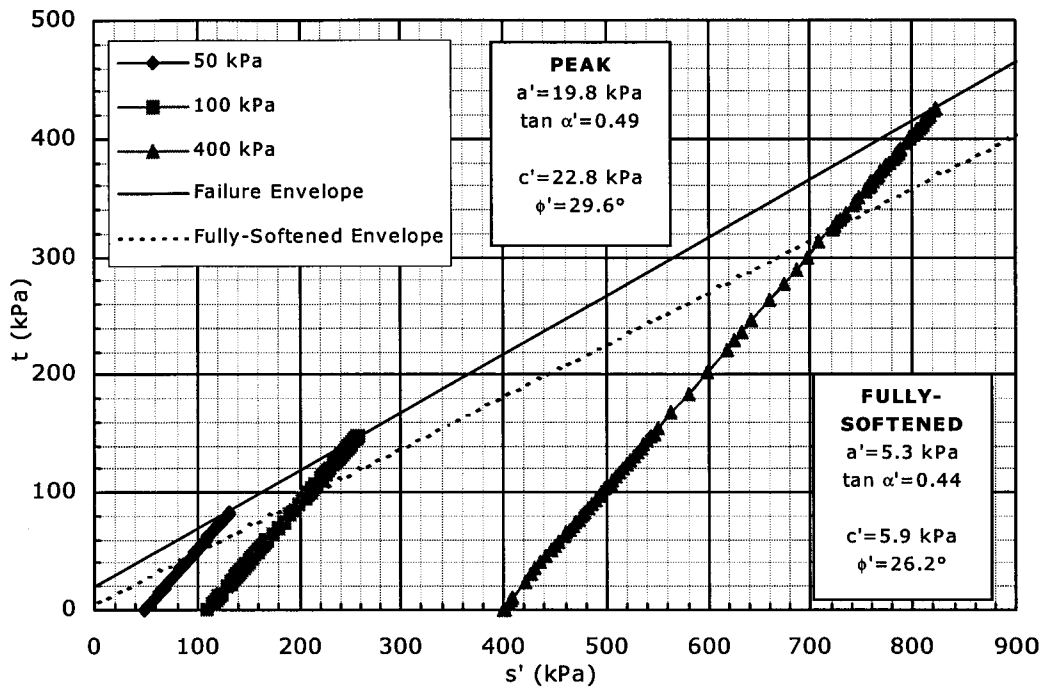
Figure A.42. t-s' plot for w=70%, A_c=2% & T_c=7 days.
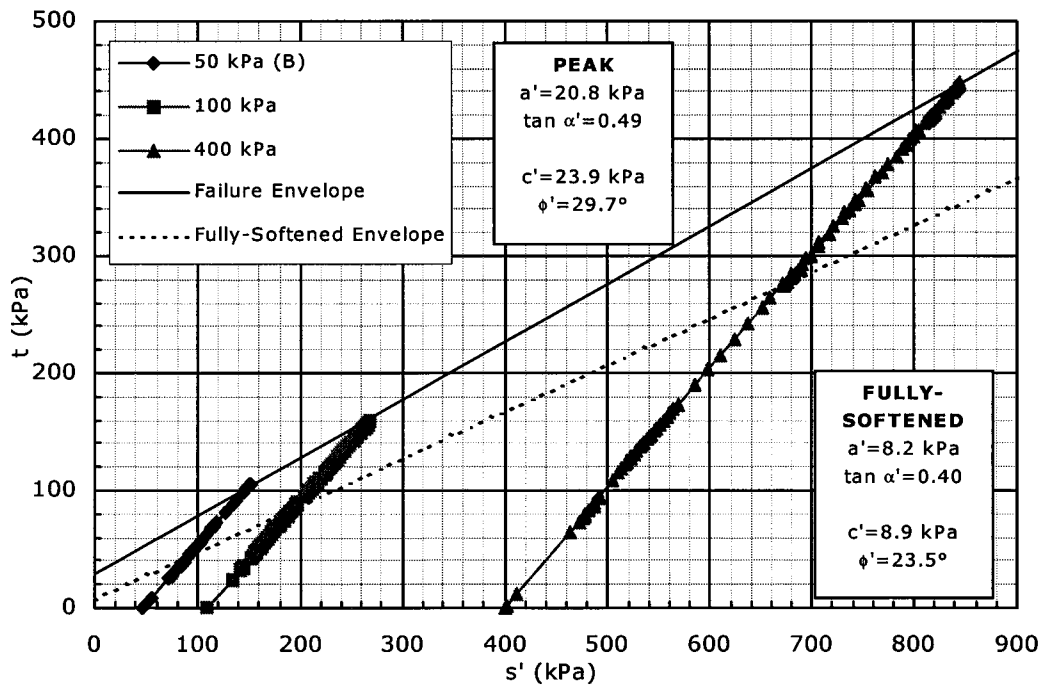
Figure A.43. t-s' plot for w=70%, A_c=2% & T_c=28 days.
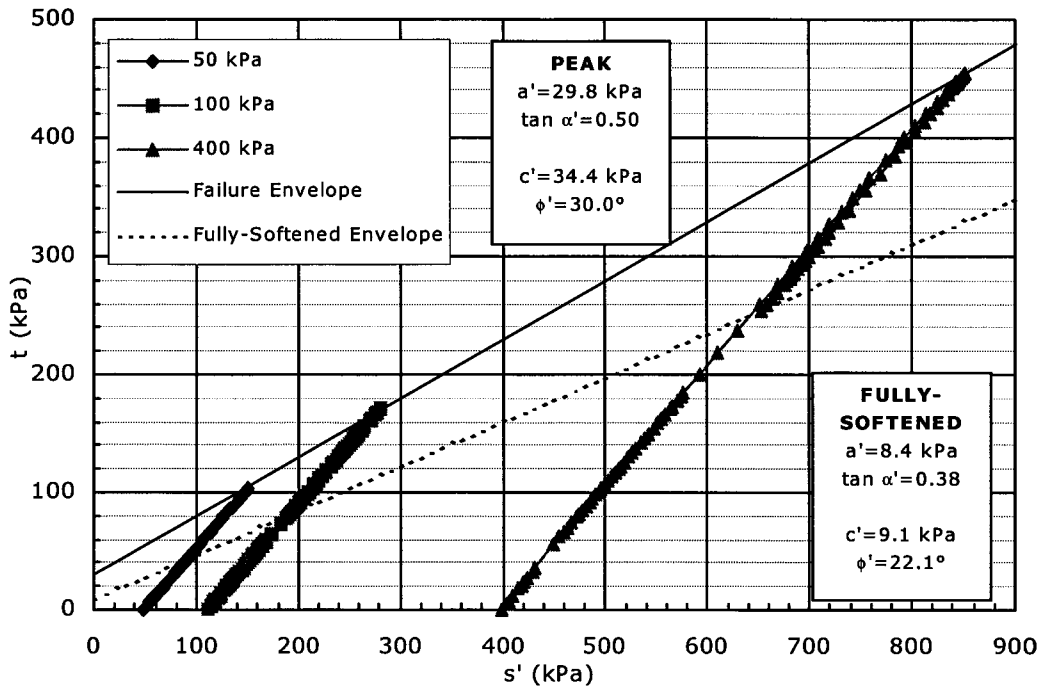
Figure A.44. t-s' plot for w=70%, A_c=2% & T_c=56 days.
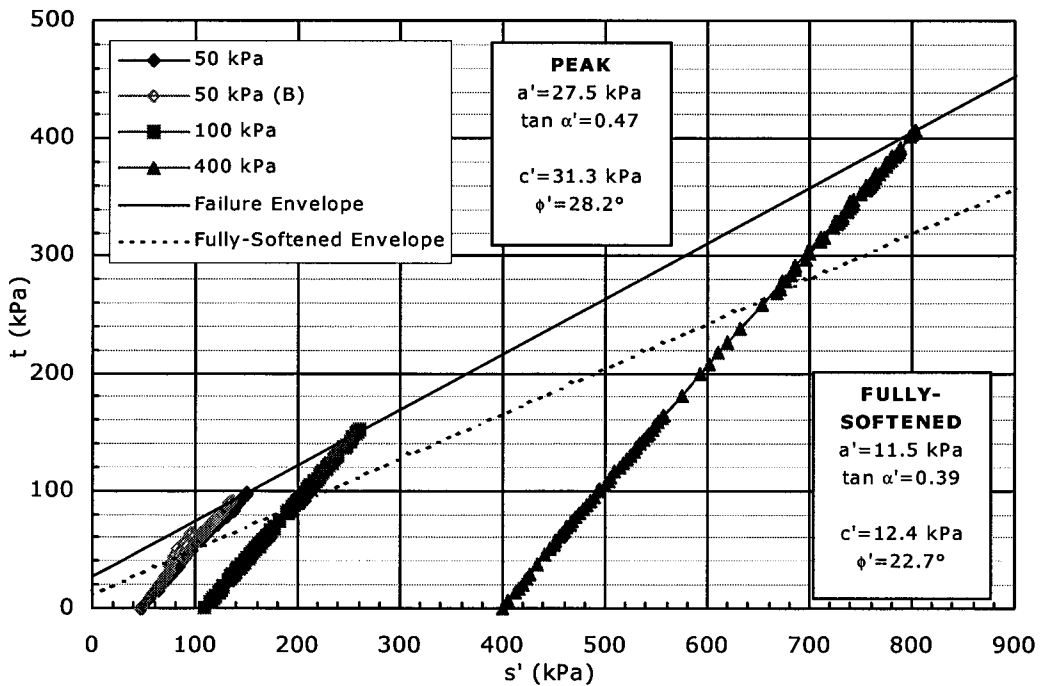
Figure A.45. t-s' plot for w=70%, A_c=2% & T_c=112 days.
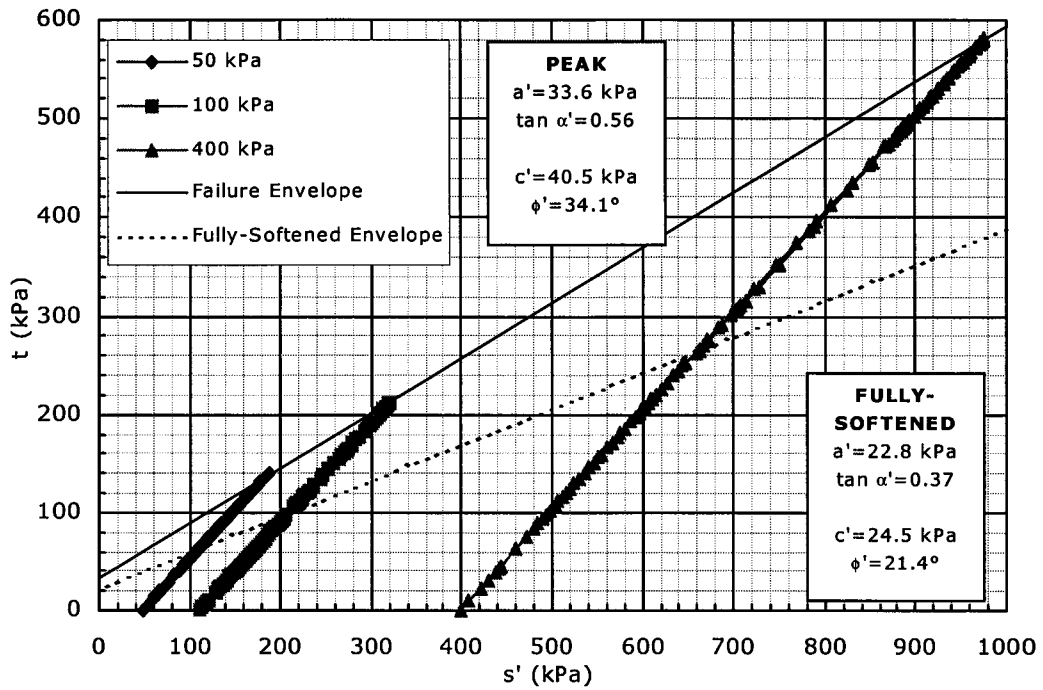
Figure A.46. t-s' plot for w=70%, A_c=5% & T_c=7 days.
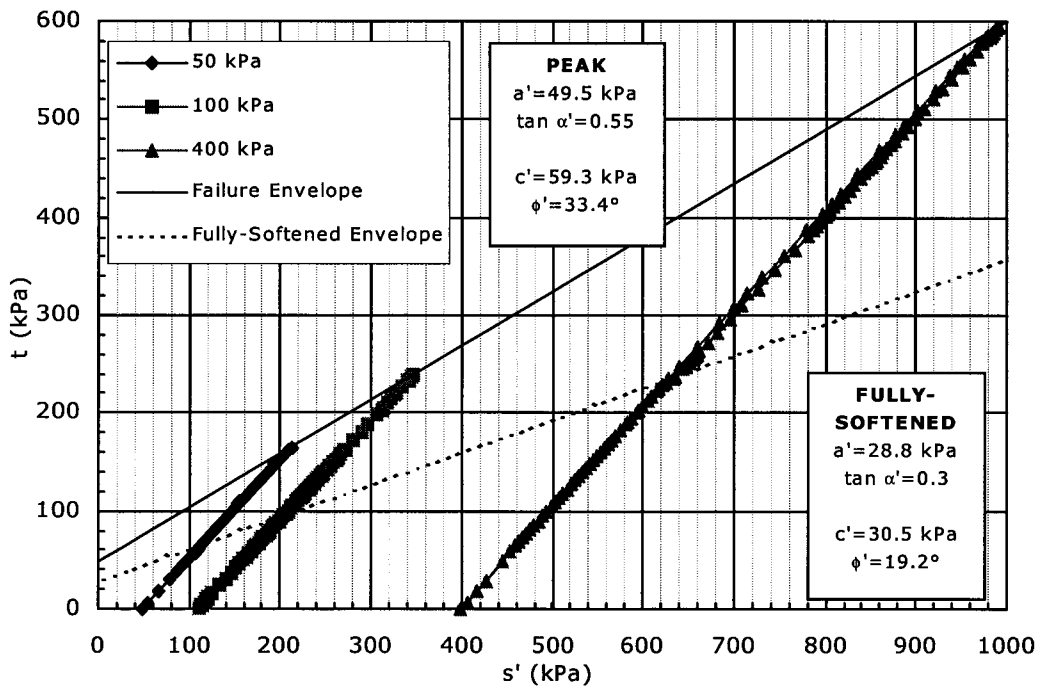
Figure A.47. t-s' plot for w=70%, A_c=5% & T_c=28 days.

Mechanical Characteristics of Kaolin-Cement Mixture   217
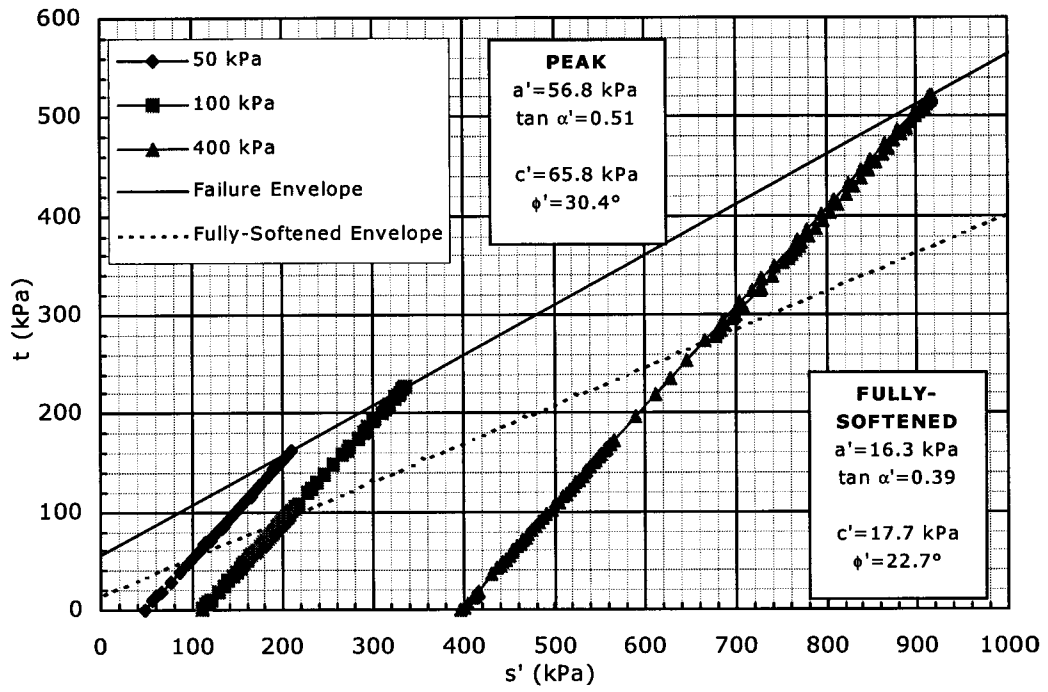
Figure A.48. t-s' plot for w=70%, A_c=5% & T_c=56 days.
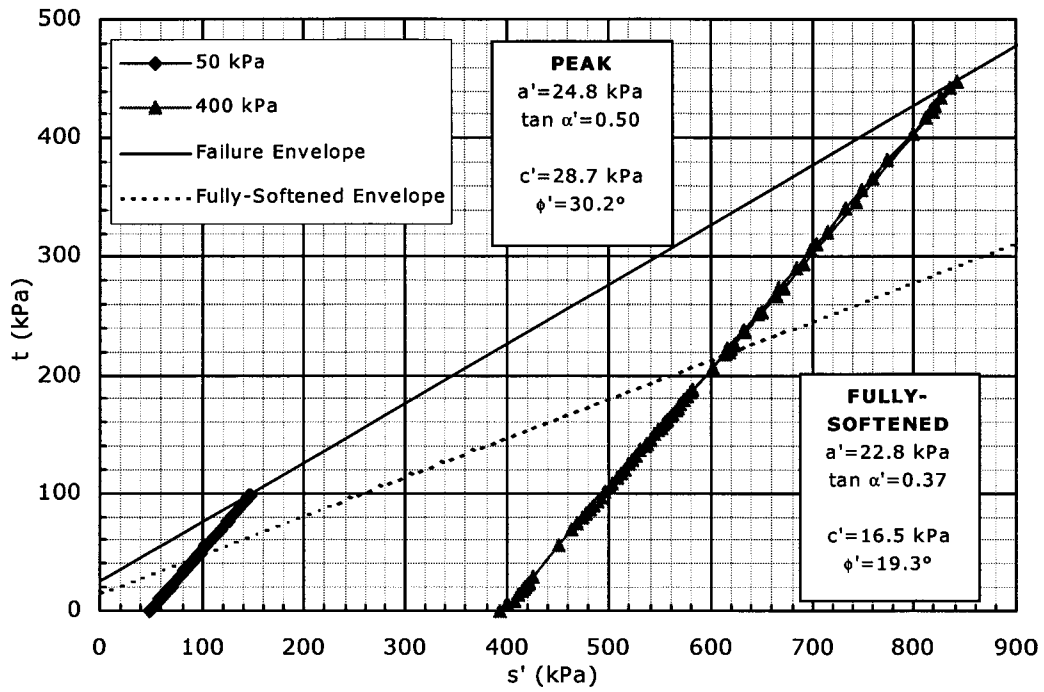
Figure A.49. t-s' plot for w=100%, A_c=5% & T_c=7 days.
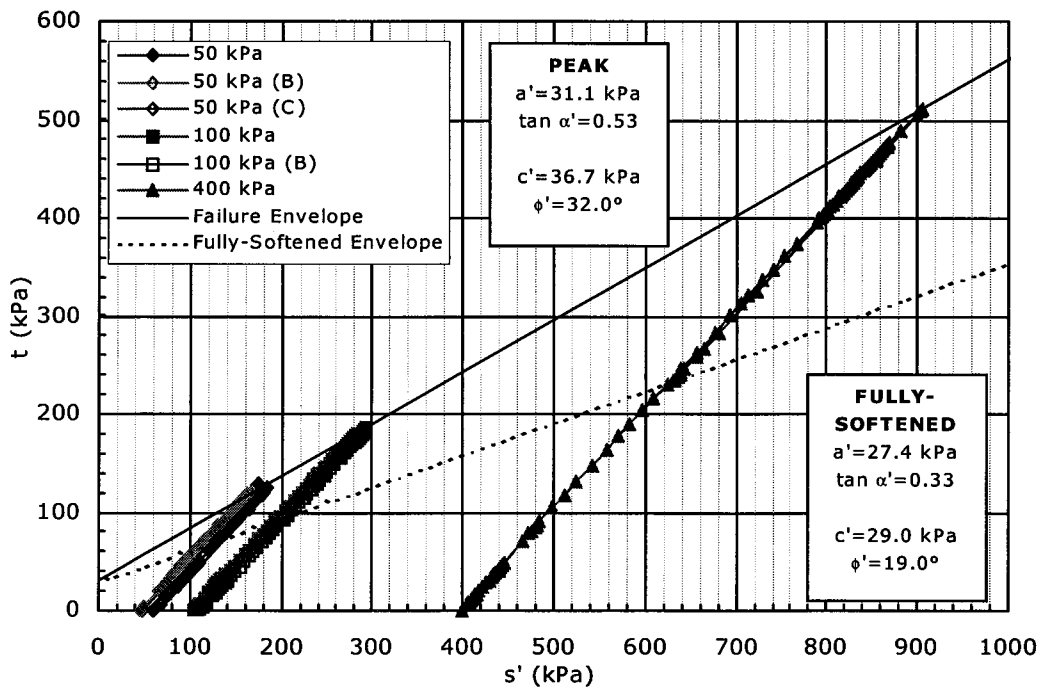
Figure A.50. t-s' plot for w=100%, A_c=5% & T_c=28 days.

Mechanical Characteristics of Kaolin-Cement Mixture   219
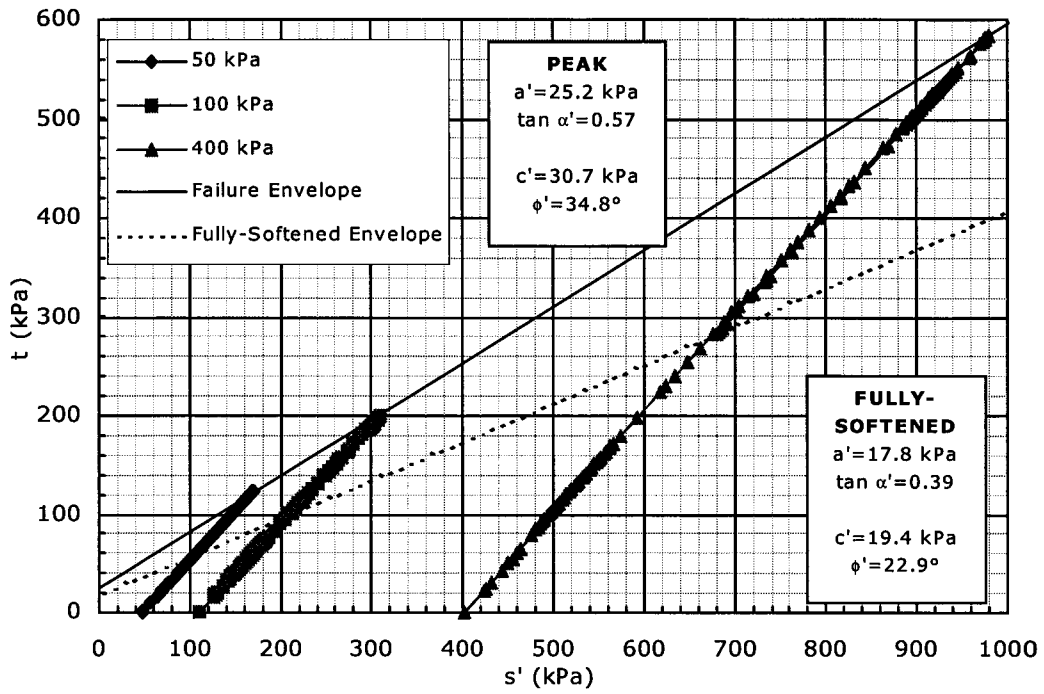
Figure A.51. t-s' plot for w=100%, A_c=5% & T_c=56 days.
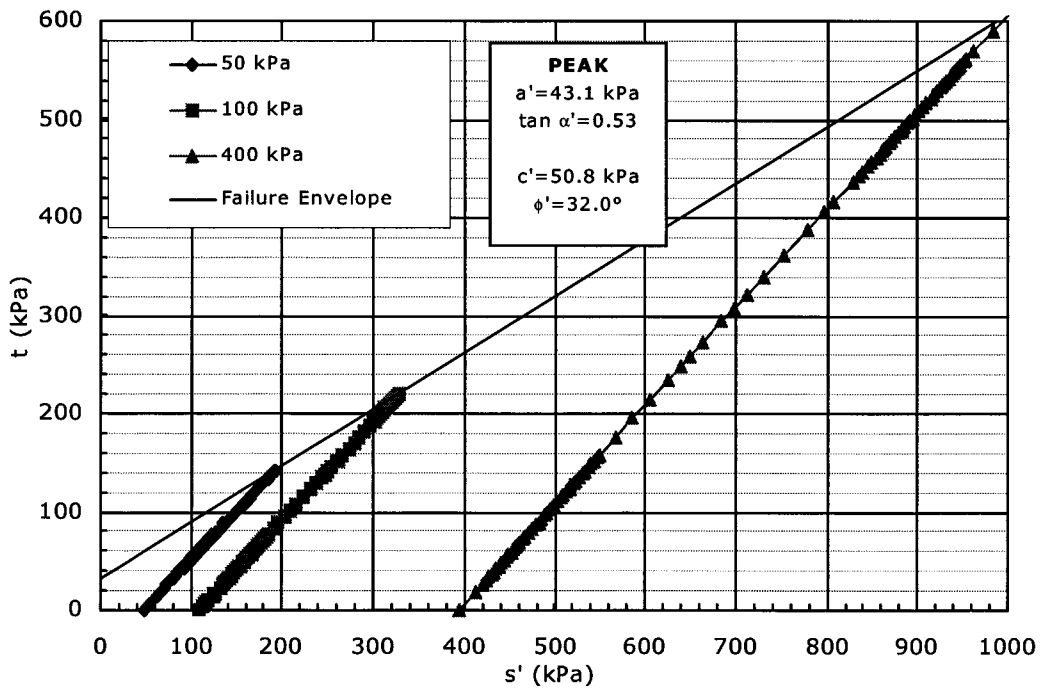
Figure A.52. t-s' plot for w=100%, A_c=5% & T_c=112 days.
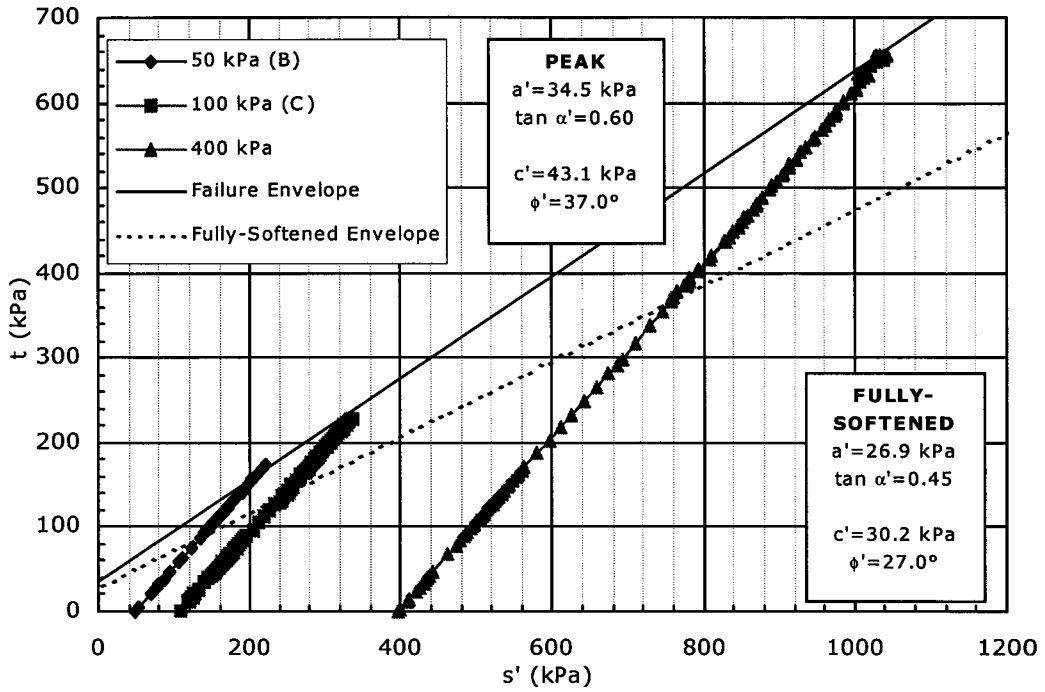
Figure A.53. t-s' plot for w=100%, A$_c$=10% & T$_c$=7 days.
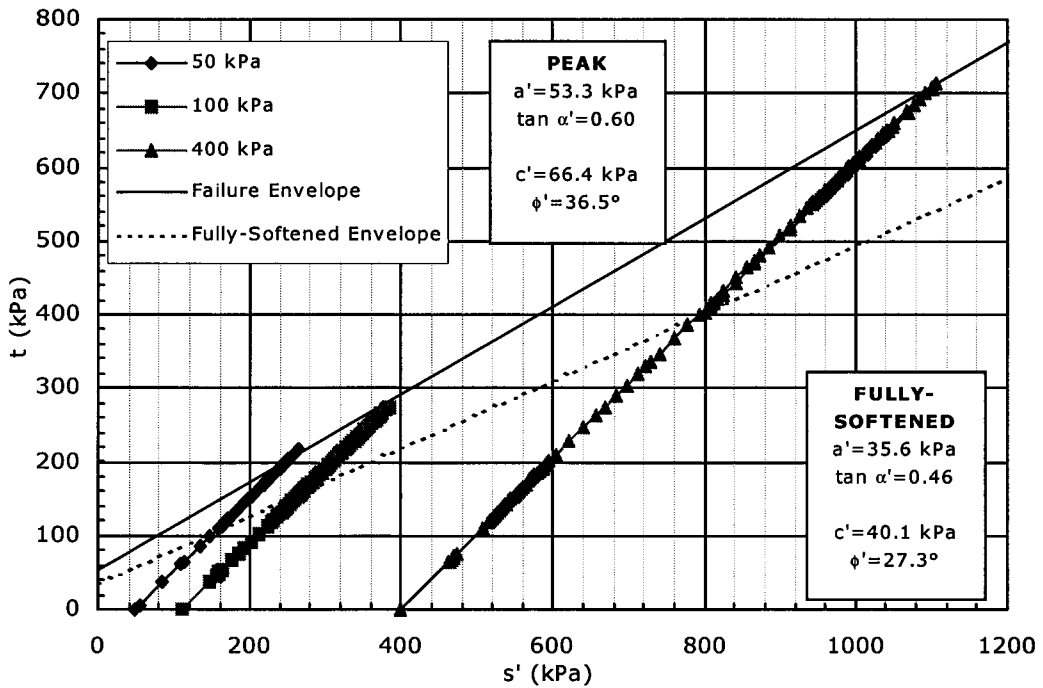
Figure A.54. t-s' plot for w=100%, A$_c$=10% & T$_c$=28 days.
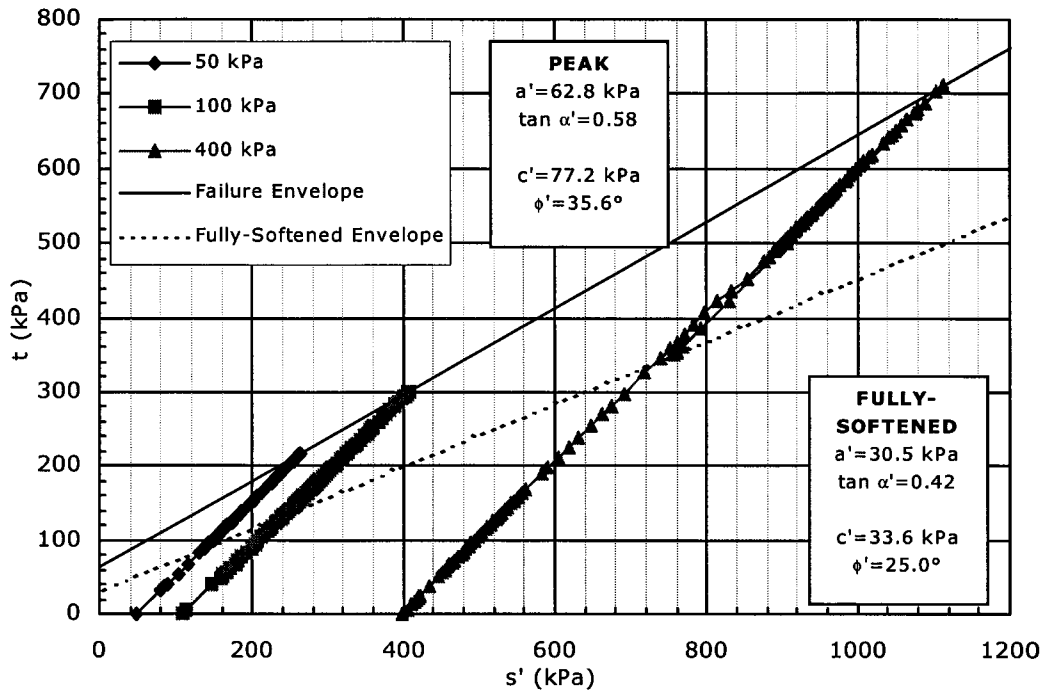
Figure A.55. t-s' plot for w=100%, A_c=10% & T_c=56 days.
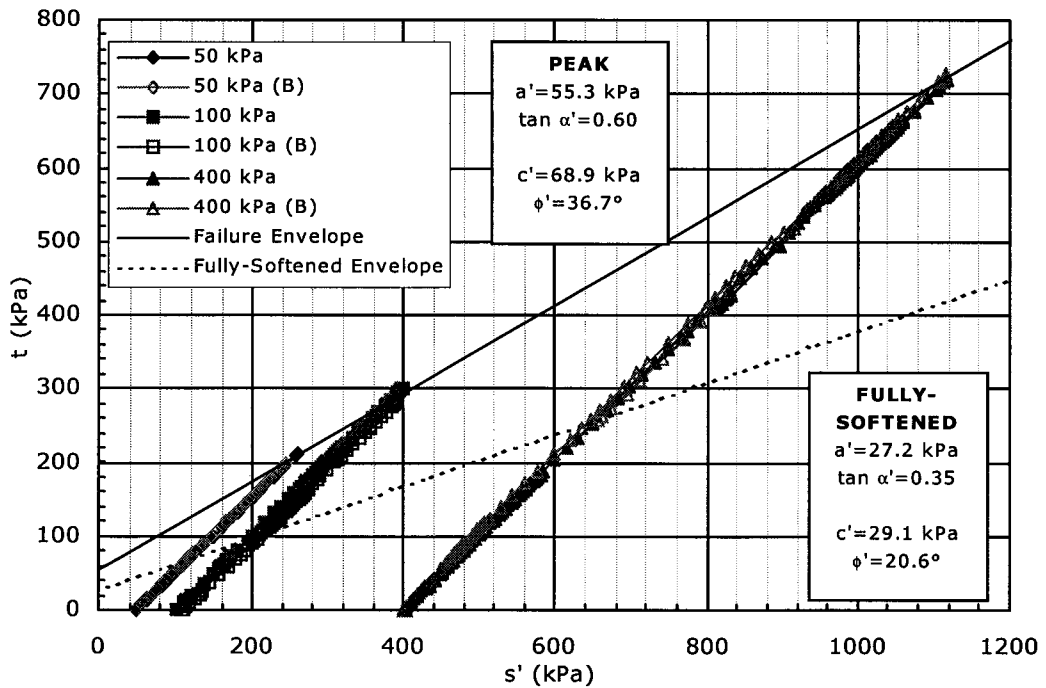
Figure A.56. t-s' plot for w=100%, A_c=10% & T_c=112 days.

APPENDIX B: CONSOLIDATED UNDRAINED TRIAXIAL TEST PLOTS

Isotropically consolidated undrained triaxial (CIU) compression tests were conducted at the City University of Hong Kong between June 2000 and July 2001. Tests were conducted on samples at 70 percent moisture content with 2 and 5 percent cement and samples at 100 percent moisture content with 5 and 10 percent cement. Samples were cured in distilled water at 20°C for 7, 28, 56 and 112 days. Tests were also done on samples of pure kaolin at 40 percent moisture content. Confining pressures of 100 and 400 kPa were considered, with a back pressure of 600 and 300 kPa, respectively. Chapter 5 describes and interprets the results of the triaxial tests.

Graphs of the shear data from the CIU tests are included in this appendix. The data presented includes deviator stress (q), excess pore water pressure (u_e) and stress ratio ($\eta = q/p'$) vs. axial strain (ε_a); these are found in plots a, b and c, respectively. Note that the shear data was corrected to account for initial straining during seating of the load; therefore, often the load is positive at zero strain.

Graphs appear in groups so that the effects of curing time, cement and moisture content and confining pressure can be interpretted. Therefore, data for each test appear several times. There are some tests which were considered to be unsuccessful due to problems during the test or poor sample quality; the results for these tests are not included. Plots of the effective stress paths (p' vs. q) were also generated and are included in Appendix F as part of a presentation on critical state soil mechanics and bonded soil.

Tables B.1 to B.3 summarize the figures provided in this appendix.

Table B.1. Plots illustrating the effects of curing time. (a) q vs. ε_a; (b) u_e vs. ε_a; (c) η vs. ε_a.

w (%)	A_c(%)	$p_o{'}$ (kPa)	Curing Time, T_c (days)			
			7	28	56	112
70	2	100	B.1			
		400	B.2			
	5	100	B.3			■
		400	B.4			■
100	5	100	B.5			
		400	B.6			
	10	100	B.7			
		400	B.8			

Table B.2. Plots illustrating the effects of cement and moisture content. (a) q vs. ε_a; (b) u_e vs. ε_a; (c) η vs. ε_a.

T_c (days)	$p_o{'}$ (kPa)	w=40%; A_c=0%*	w=70%; A_c=2%	w=70%; A_c=5%	w=100%; A_c=5%	w=100%; A_c=10%
7	100	B.9				
	400	B.10				
28	100	■	B.11			
	400	■	B.12			
56	100	■	B.13			
	400	■	B.14			
112	100	■	B.15†			
	400	■	B.16†			

*samples tested immediately following casting; T_c=0 days.
†samples with w=70% and A_c=5% not tested after 112 days of curing.

Table B.3. Plots illustrating the effects of confining pressure. (a) q vs. ε_α; (b) u_e vs. ε_a; (c) η vs. ε_a.

w (%)	A_c(%)	T_c (days)	Effective Confining Pressure, p_0' (kPa)	
			100	200
40	0	0	B.17	
70	2	7	B.18	
		28	B.19	
		56	B.20	
		112	B.21	
	5	7	B.22	
		28	B.23	
		56	B.24	
		112	███████████	
100	5	7	B.25	
		28	B.26	
		56	B.27	
		112	B.28	
	10	7	B.29	
		28	B.30	
		56	B.31	
		112	B.32	
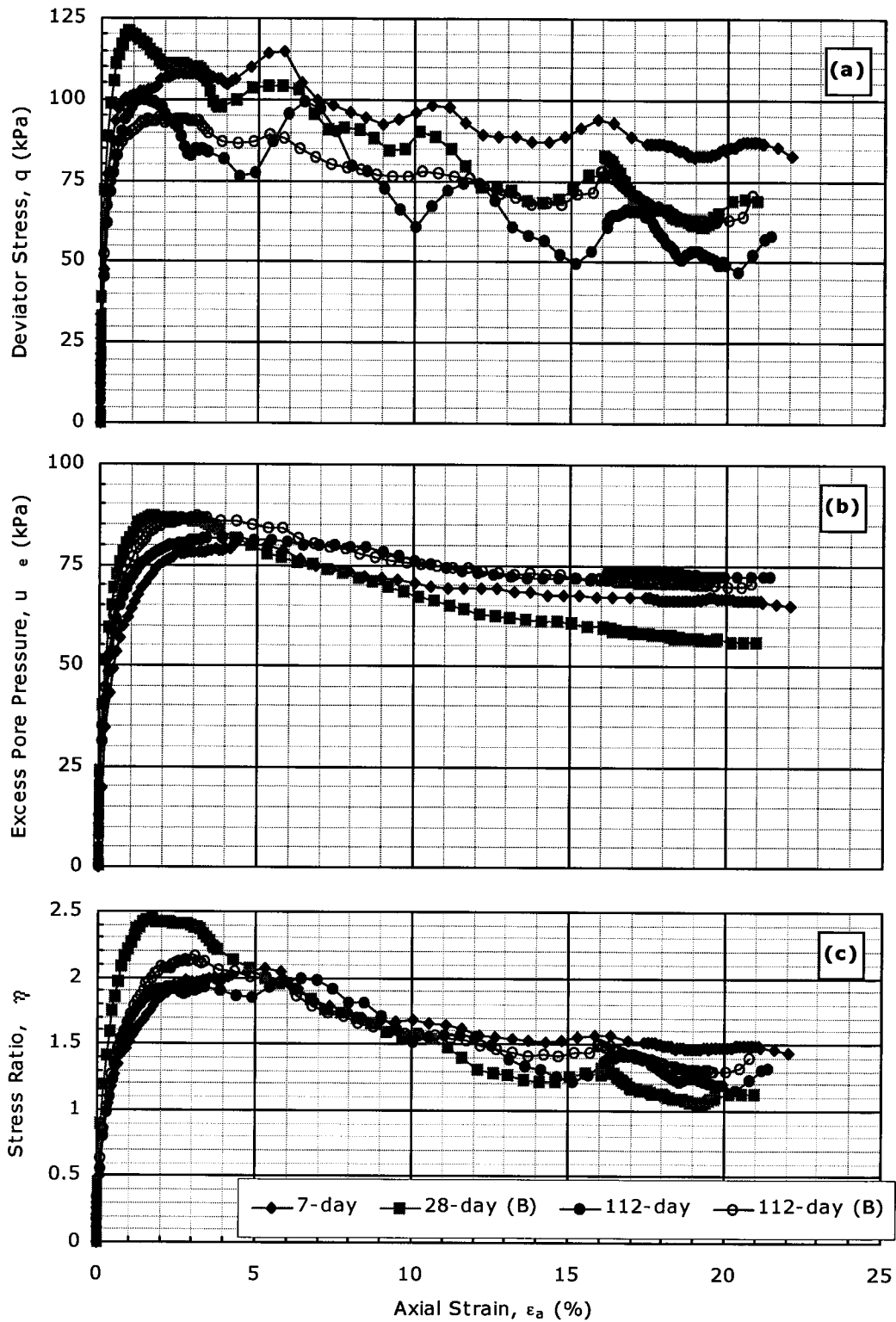
Figure B.1. CIU data for w=70%; A_c=2% & $p_o{'}$=100 kPa. (a) q vs. ε_a; (b) u_e vs. ε_a; (c) η vs. ε_a.
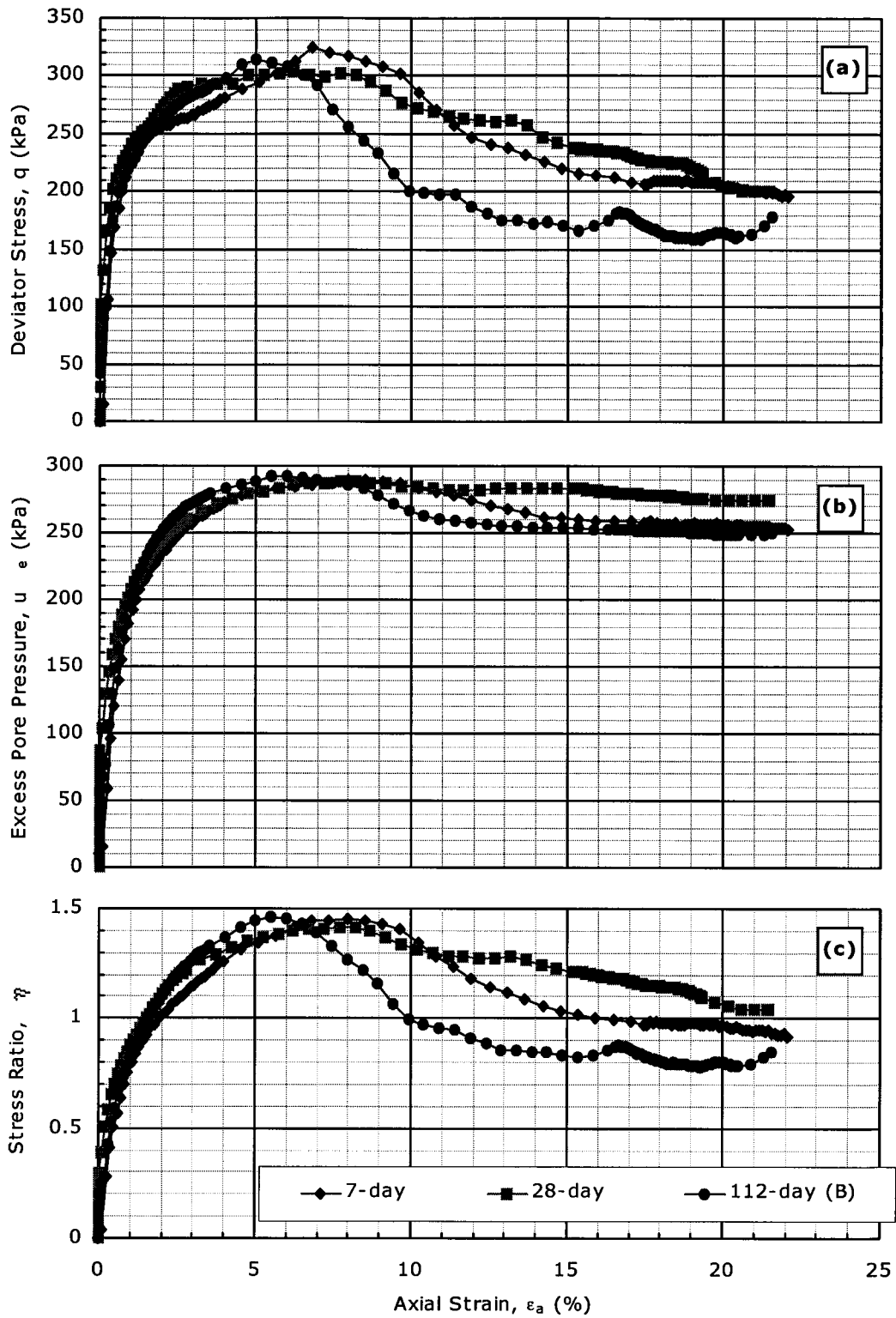
Figure B.2. CIU data for w=70%; A_c=2% & p_o'=400 kPa. (a) q vs. ε_a; (b) u_e vs. ε_a; (c) η vs. ε_a.

Mechanical Characteristics of Kaolin-Cement Mixture 227
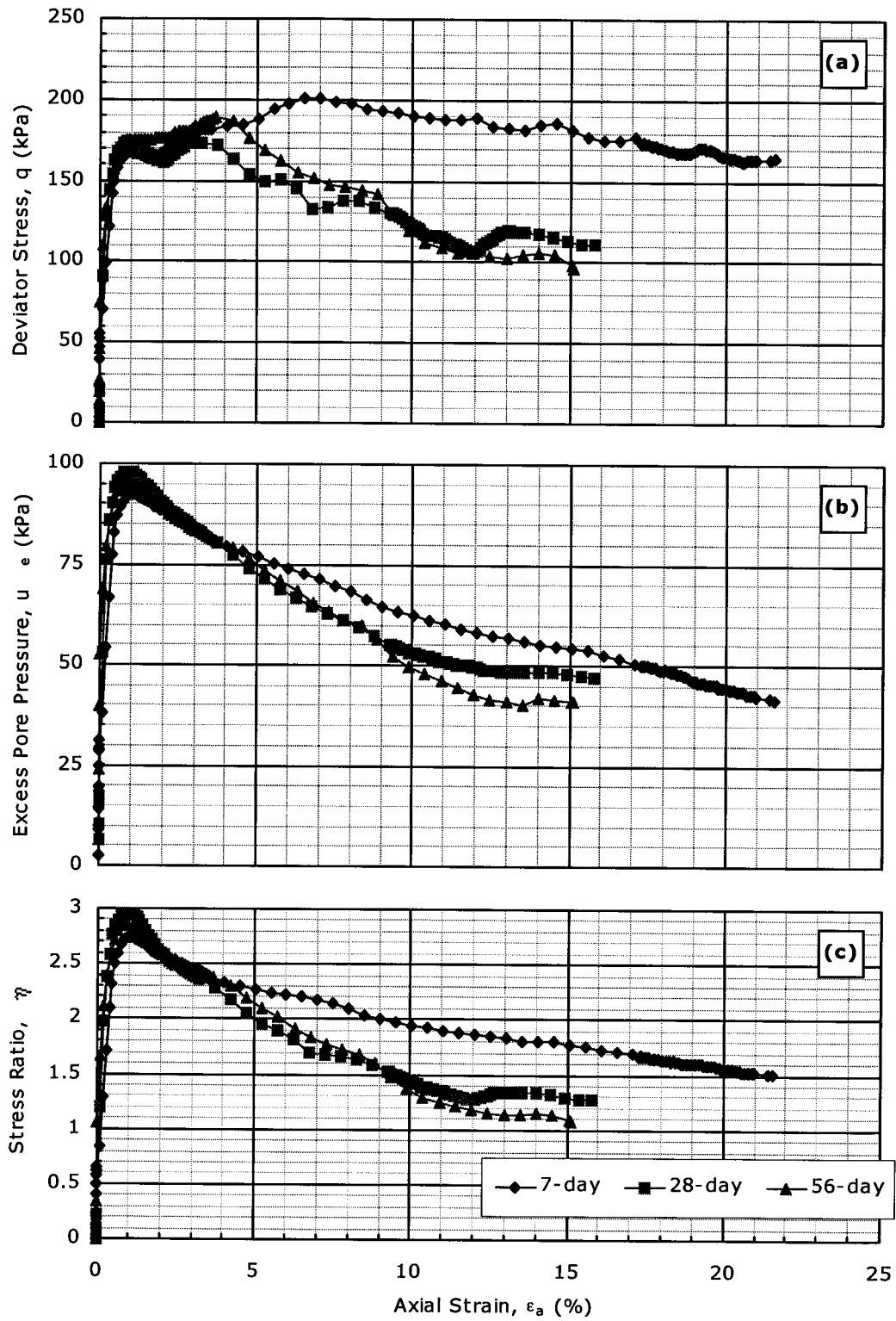
Figure B.3. CIU data for w=70%; A_c=5% & p_o'=100 kPa. (a) q vs. ε_a; (b) u_e vs. ε_a; (c) η vs. ε_a.
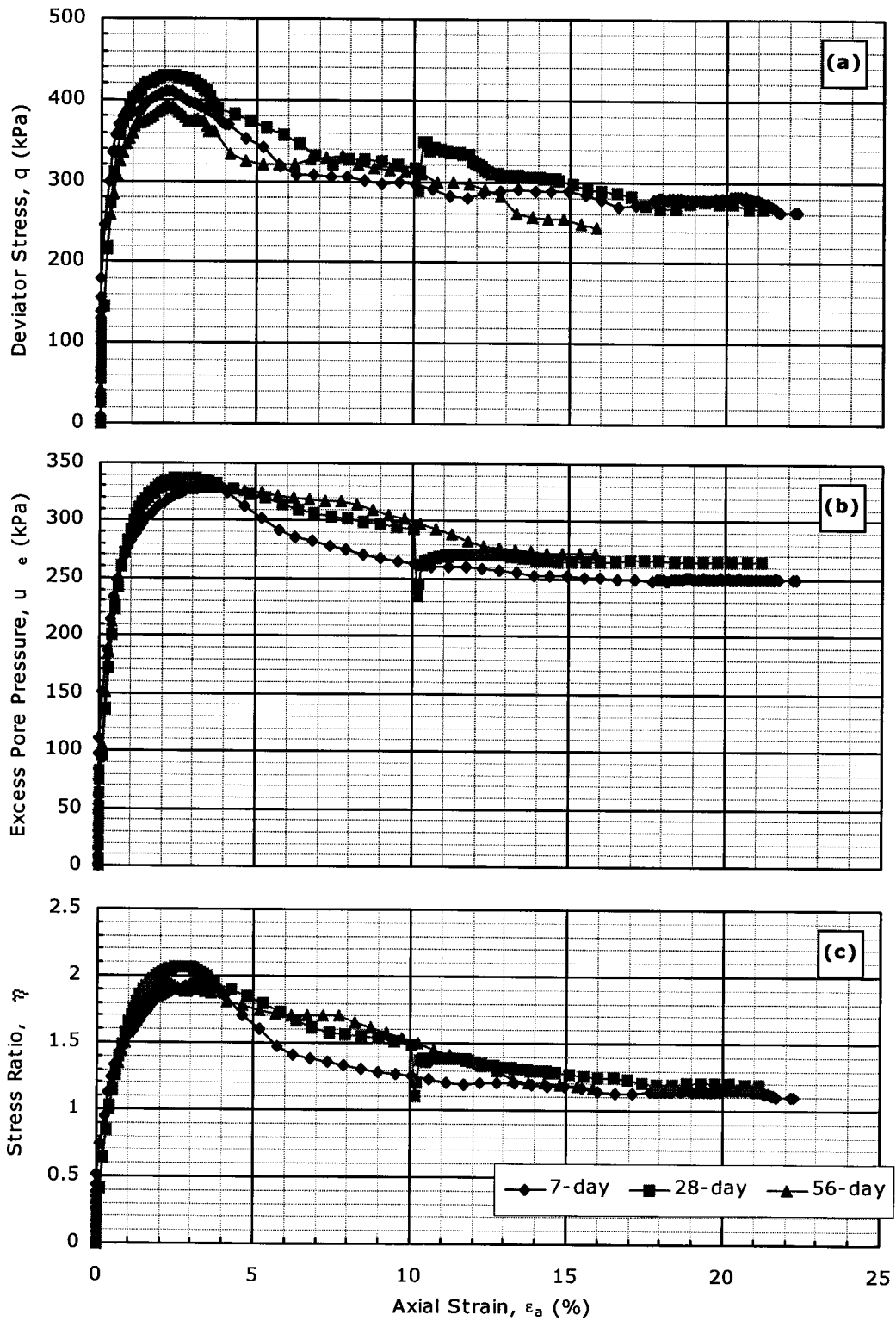
Figure B.4. CIU data for w=70%; A_c=5% & $p_o{'}$=400 kPa. (a) q vs. ε_a; (b) u_e vs. ε_a; (c) η vs. ε_a.

Mechanical Characteristics of Kaolin-Cement Mixture   229
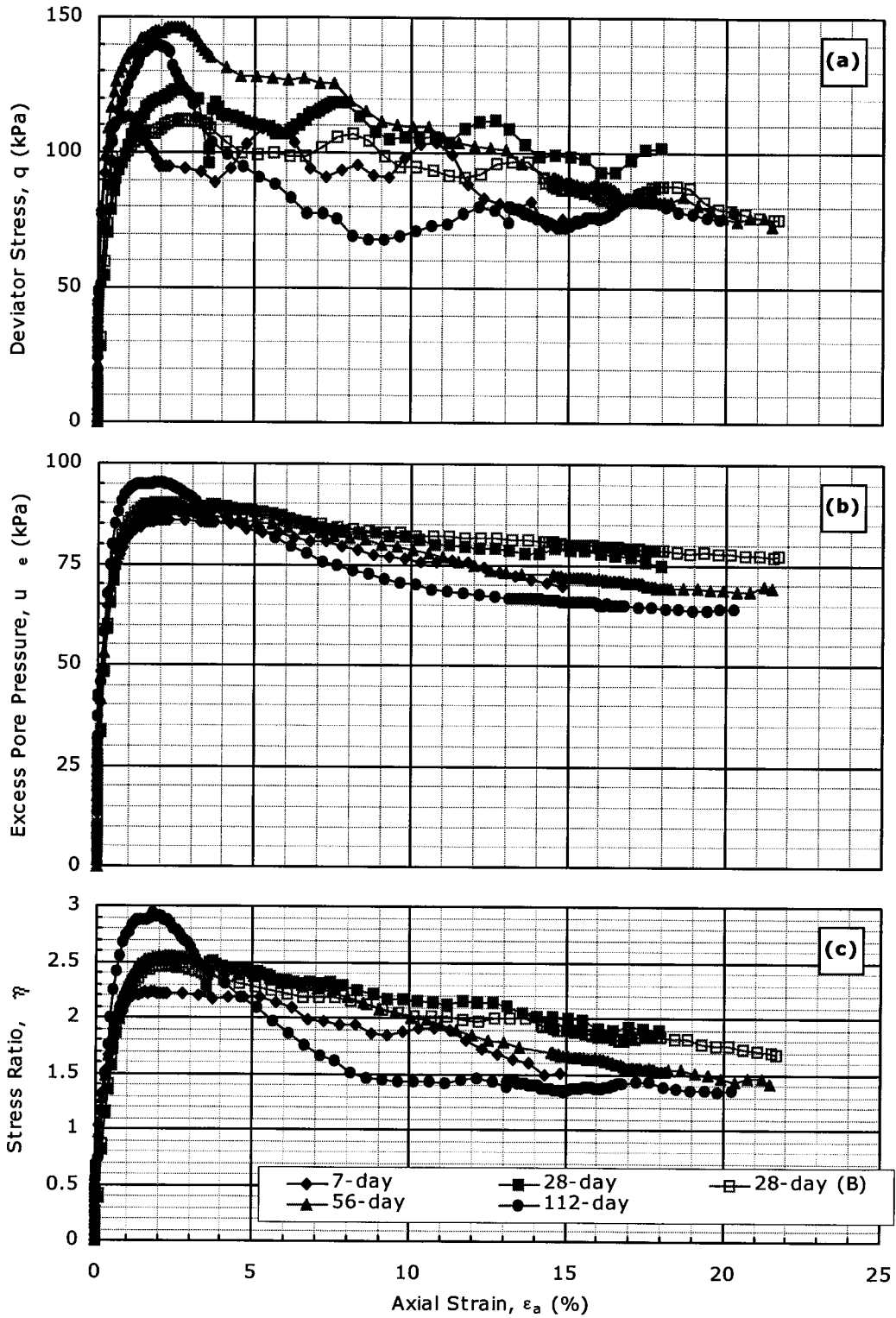
Figure B.5. CIU data for w=100%; A_c=5% & p_o'=100 kPa. (a) q vs. ε_a; (b) u_e vs. ε_a; (c) η vs. ε_a.
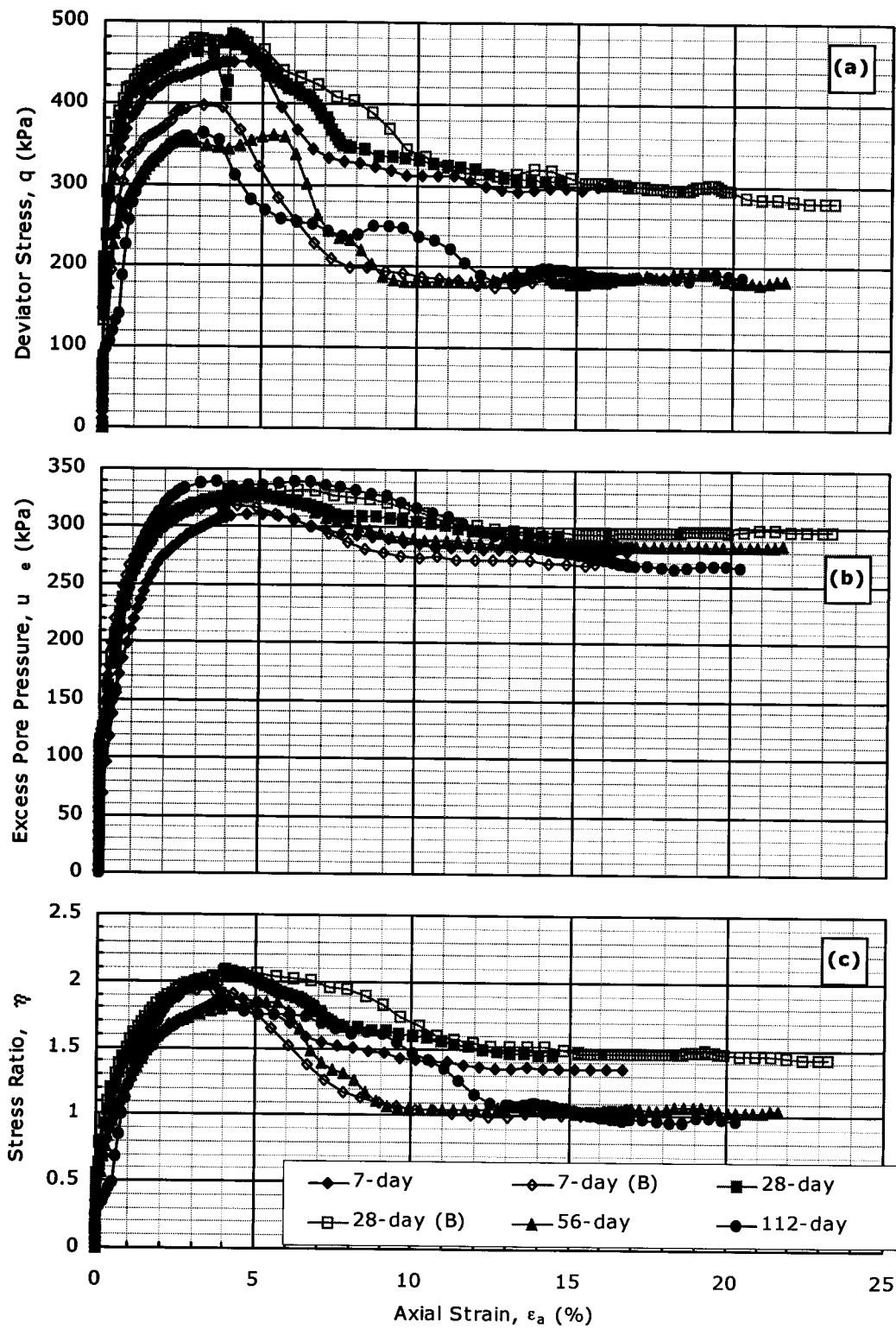
Figure B.6. CIU data for $w=100\%$; $A_c=5\%$ & $p_o{}'=400$ kPa. (a) q vs. ε_a; (b) u_e vs. ε_a; (c) η vs. ε_a.

Mechanical Characteristics of Kaolin-Cement Mixture 231
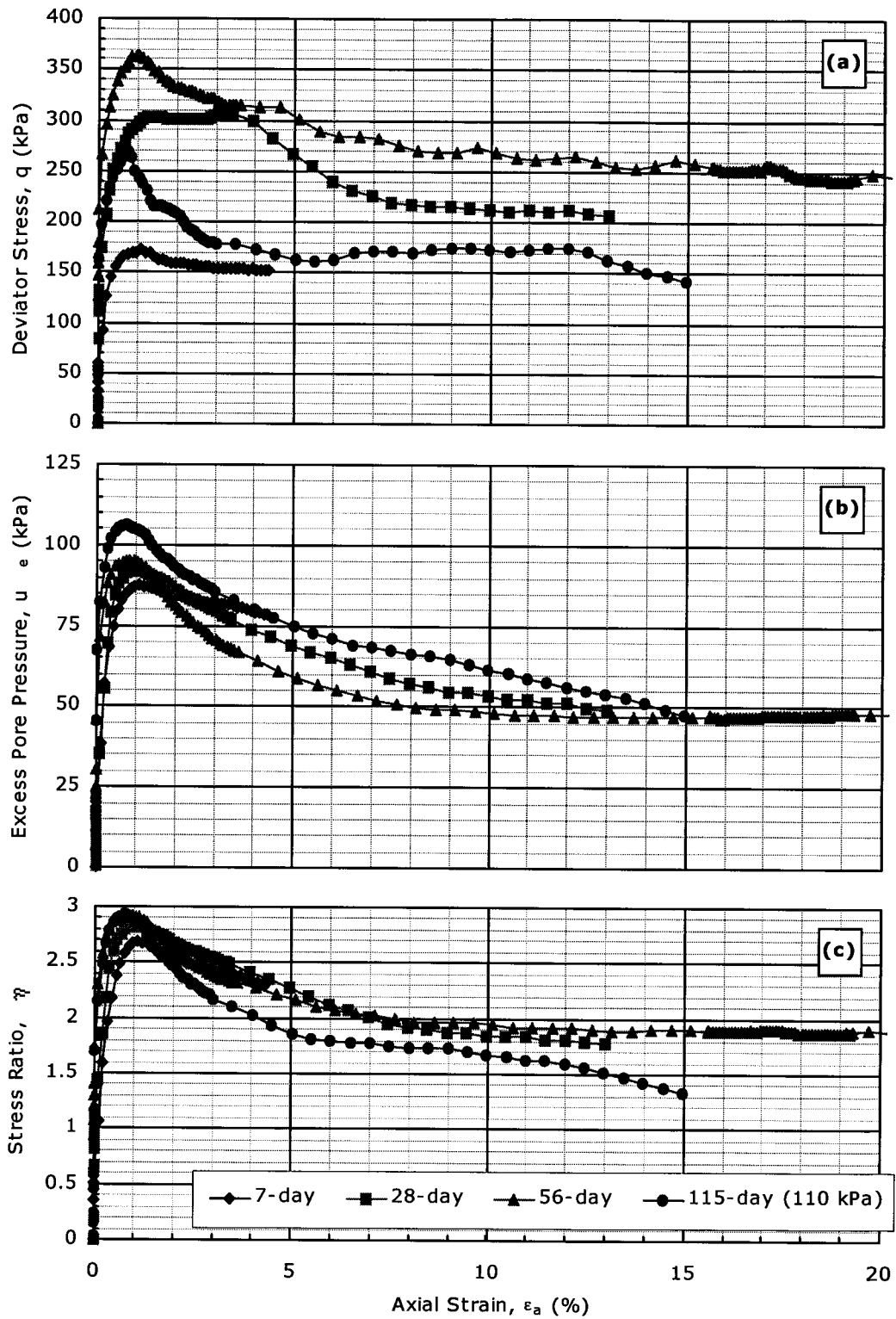
Figure B.7. CIU data for w=100%; A_c=10% & p_o'=100 kPa. (a) q vs. ε_a; (b) u_e vs. ε_a; (c) η vs. ε_a.
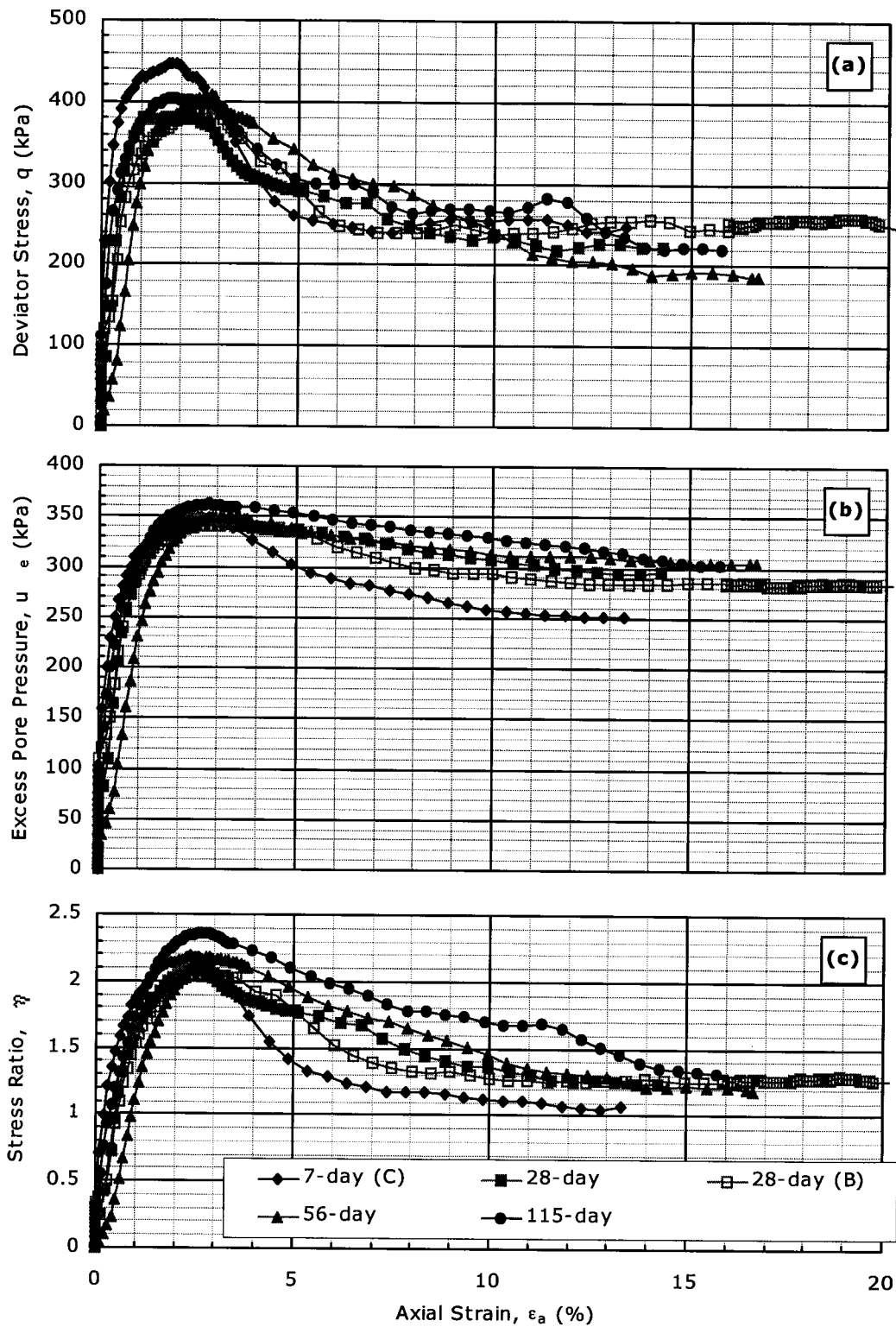
Figure B.8. CIU data for w=100%; A_c=10% & $p_o{'}$=400 kPa. (a) q vs. ε_a; (b) u_e vs. ε_a; (c) η vs. ε_a.

Mechanical Characteristics of Kaolin-Cement Mixture   233
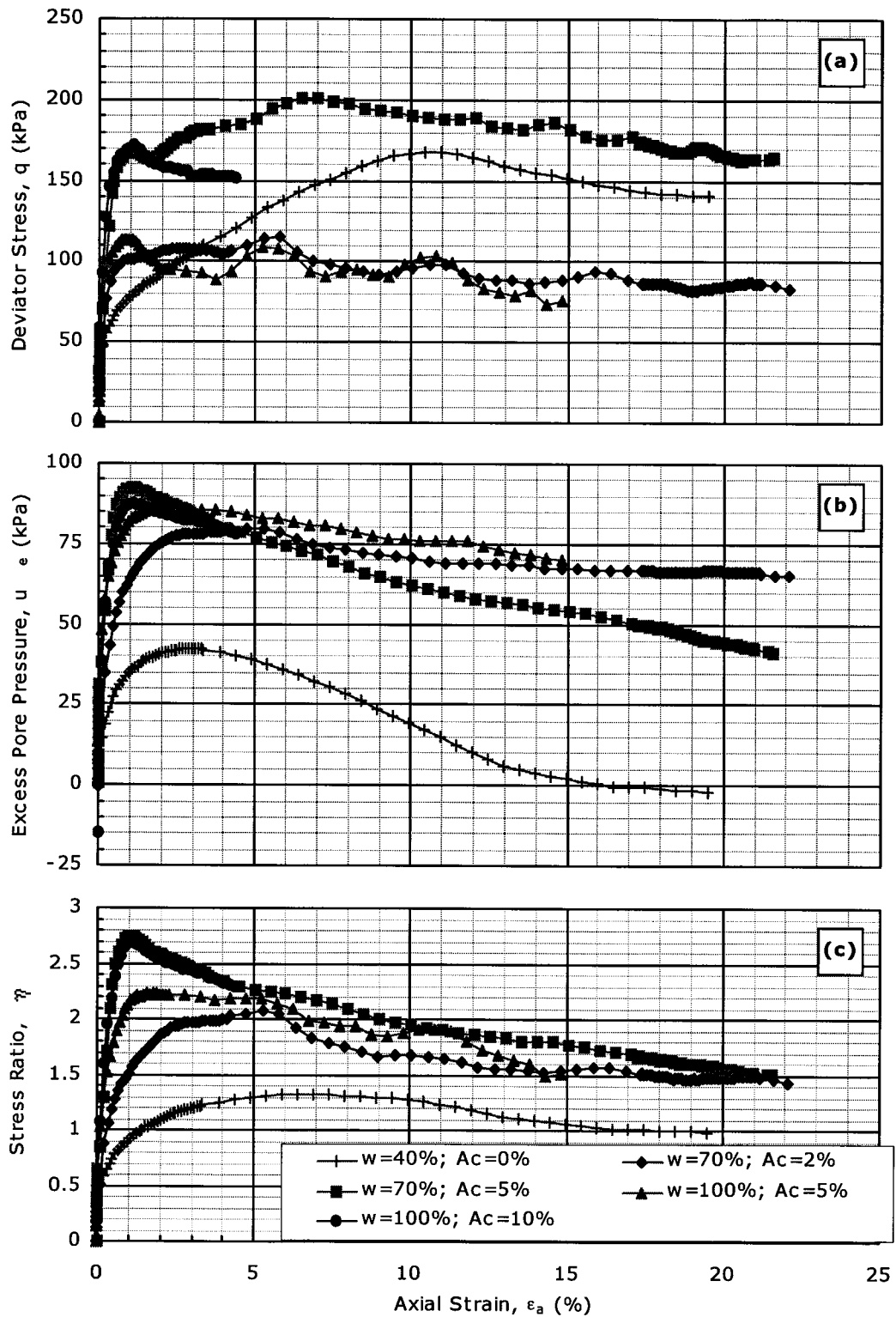
Figure B.9. CIU data for T_c=7 days & $p_o{}'$=100 kPa. (a) q vs. ε_a; (b) u_e vs. ε_a; (c) η vs. ε_a.
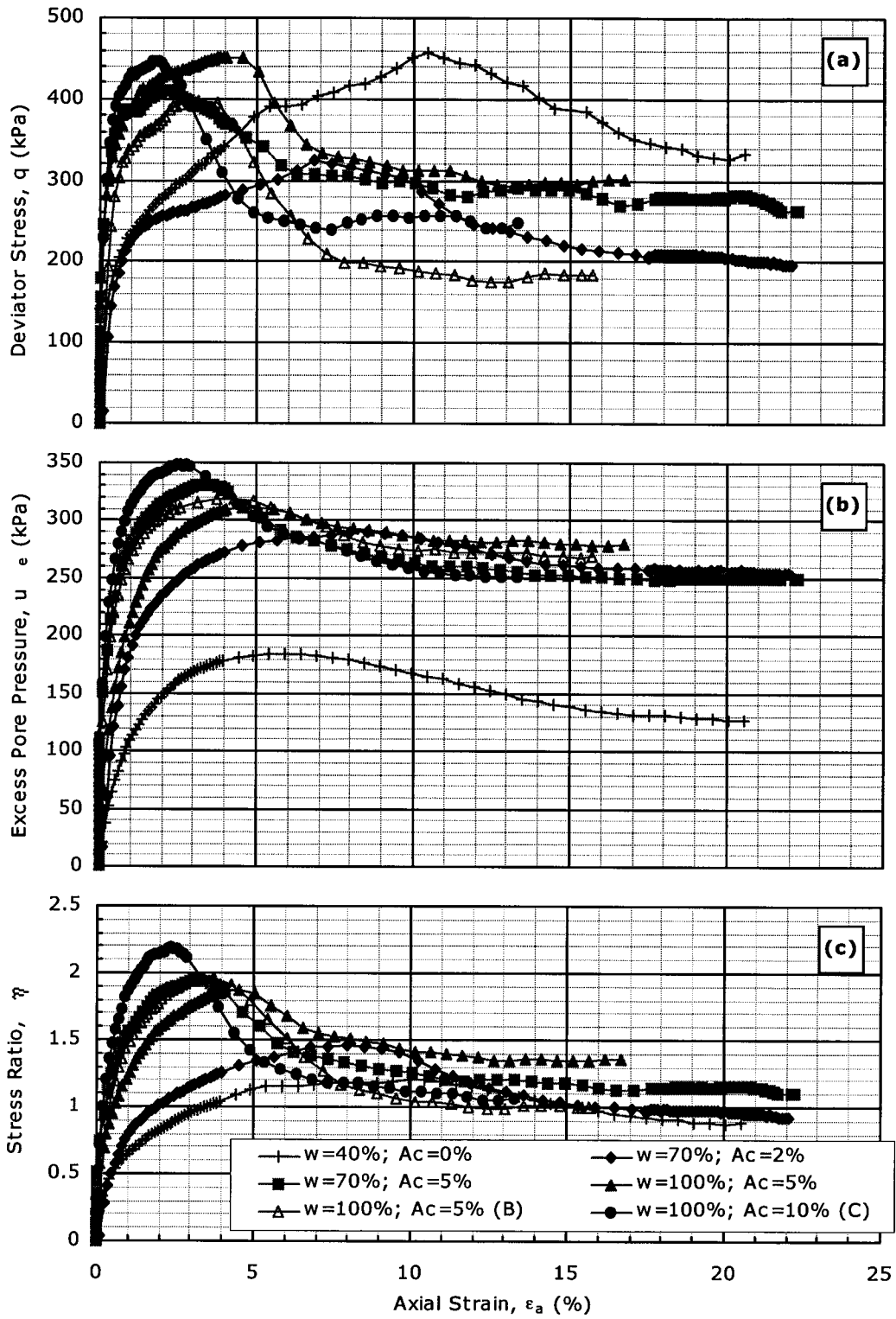
Figure B.10. CIU data for $T_c=7$ days & $p_o'=400$ kPa. (a) q vs. ε_a; (b) u_e vs. ε_a; (c) η vs. ε_a.

Mechanical Characteristics of Kaolin-Cement Mixture   235
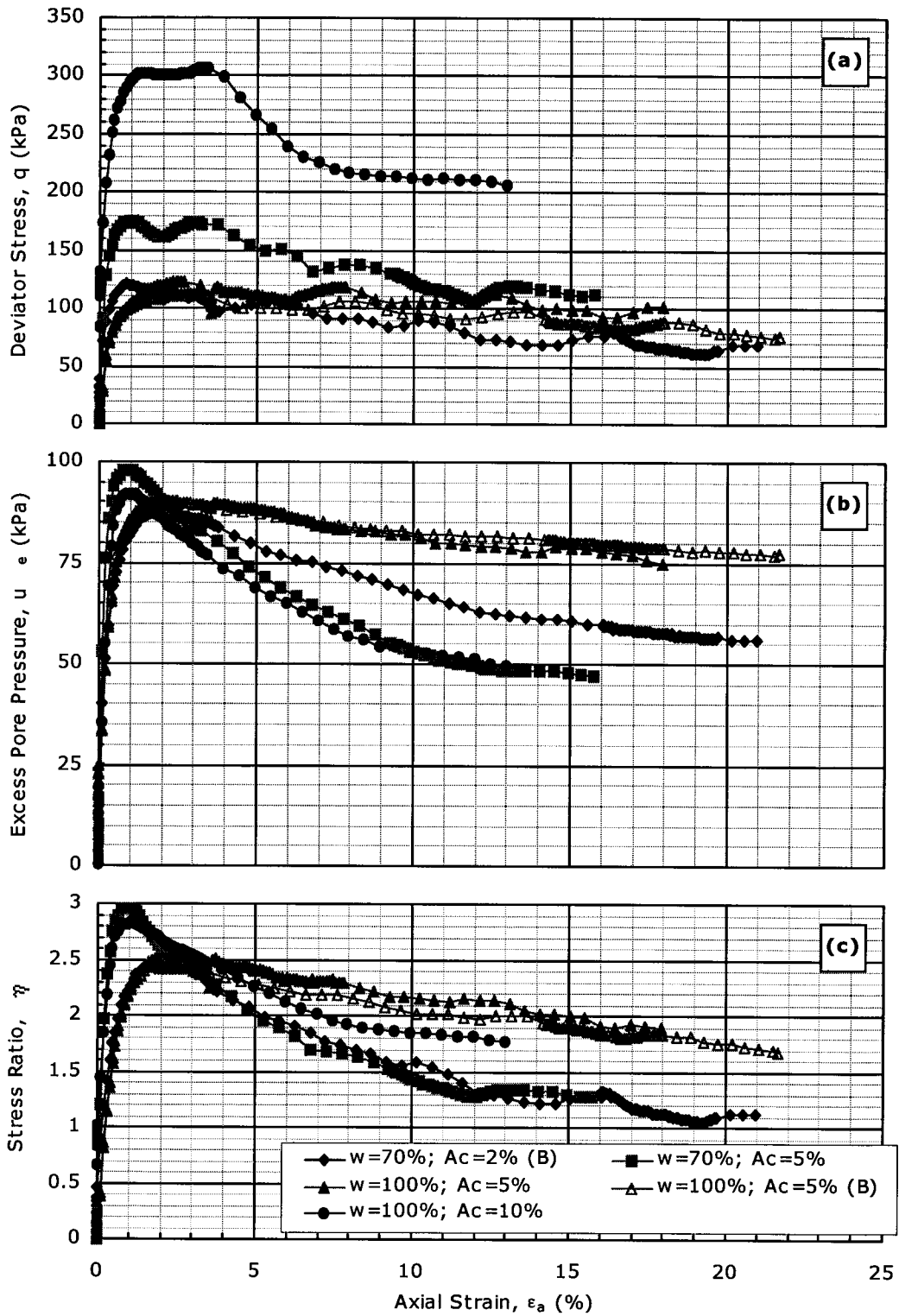
Figure B.11. CIU data for $T_c = 28$ days & $p_o' = 100$ kPa. (a) q vs. ε_a; (b) u_e vs. ε_a; (c) η vs. ε_a.
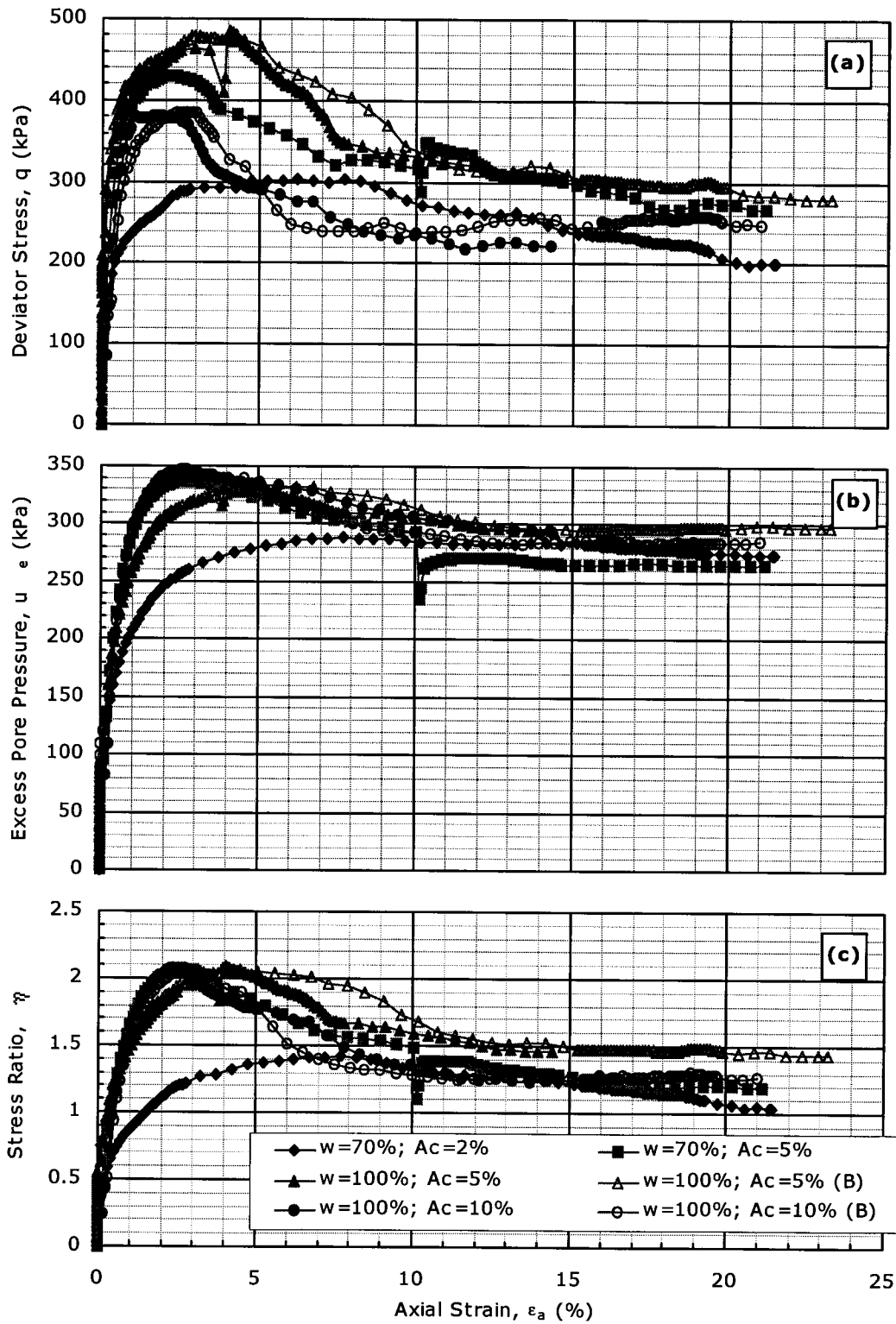
Figure B.12. CIU data for T_c=28 days & $p_o{}'$=400 kPa. (a) q vs. ε_a; (b) u_e vs. ε_a; (c) η vs. ε_a.

Mechanical Characteristics of Kaolin-Cement Mixture   237
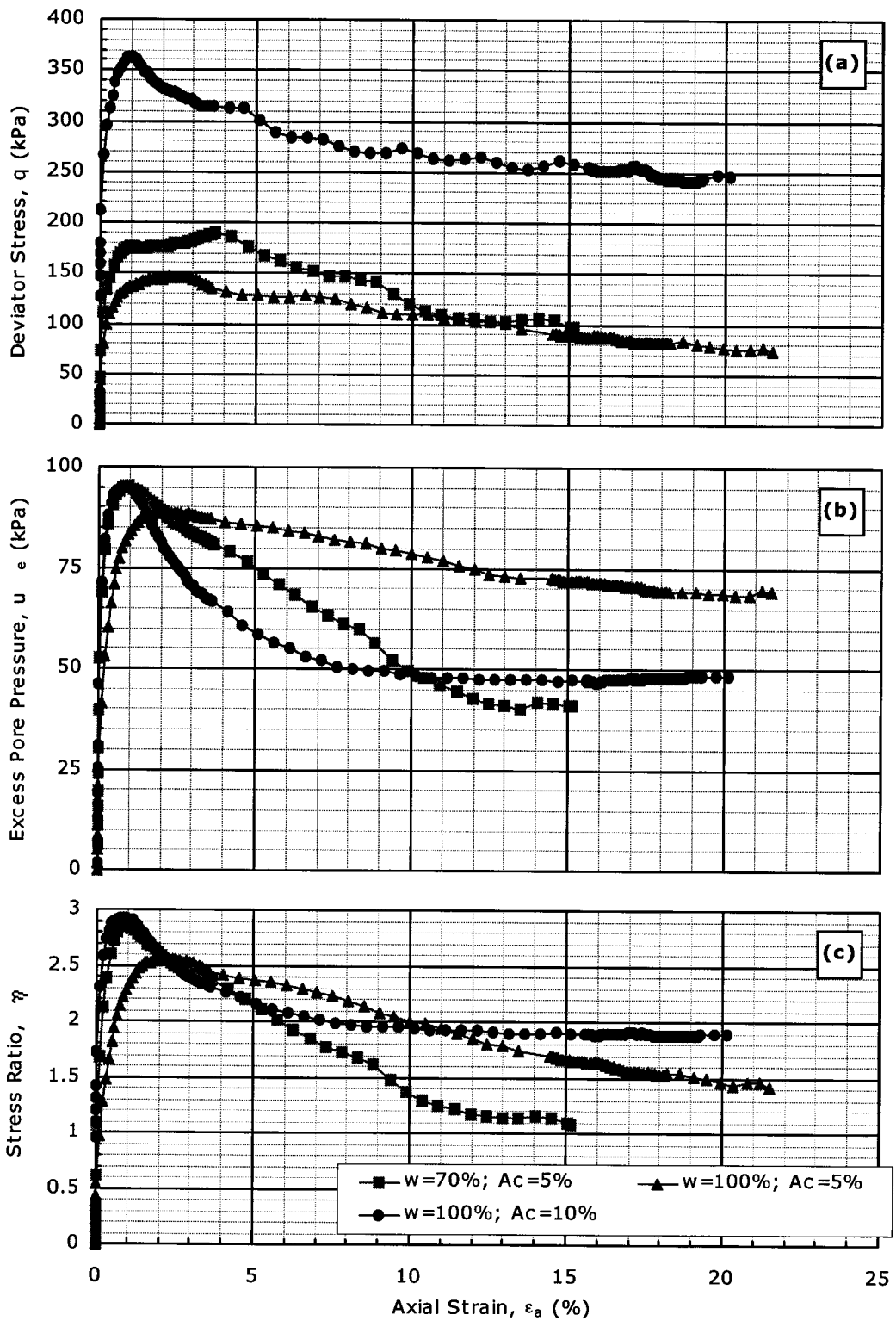
Figure B.13. CIU data for T_c=56 days & $p_o{}'$=100 kPa. (a) q vs. ε_a; (b) u_e vs. ε_a; (c) η vs. ε_a.
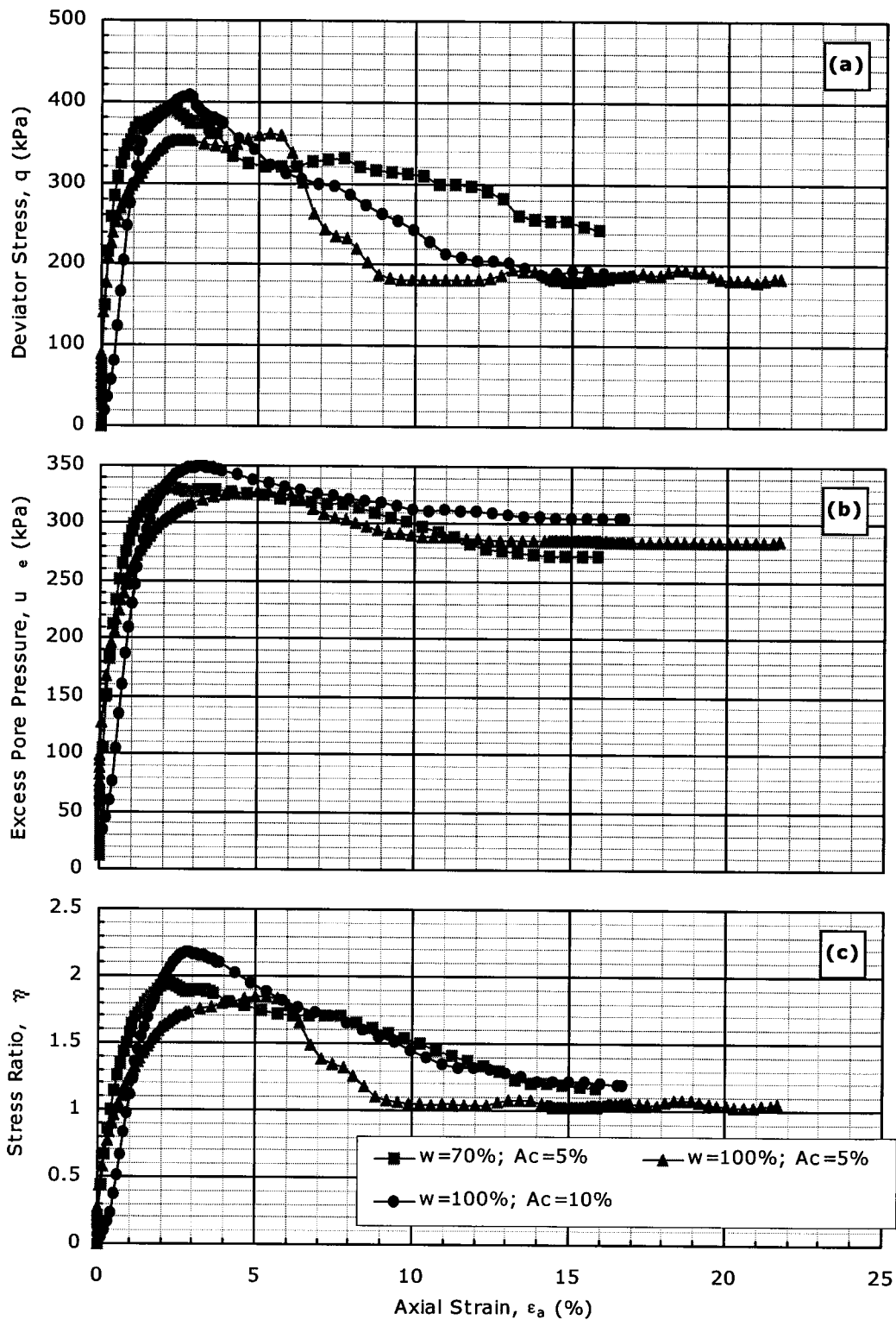
Figure B.14. CIU data for $T_c=56$ days & $p_o{}'=400$ kPa. (a) q vs. ε_a; (b) u_e vs. ε_a; (c) η vs. ε_a.

Mechanical Characteristics of Kaolin-Cement Mixture
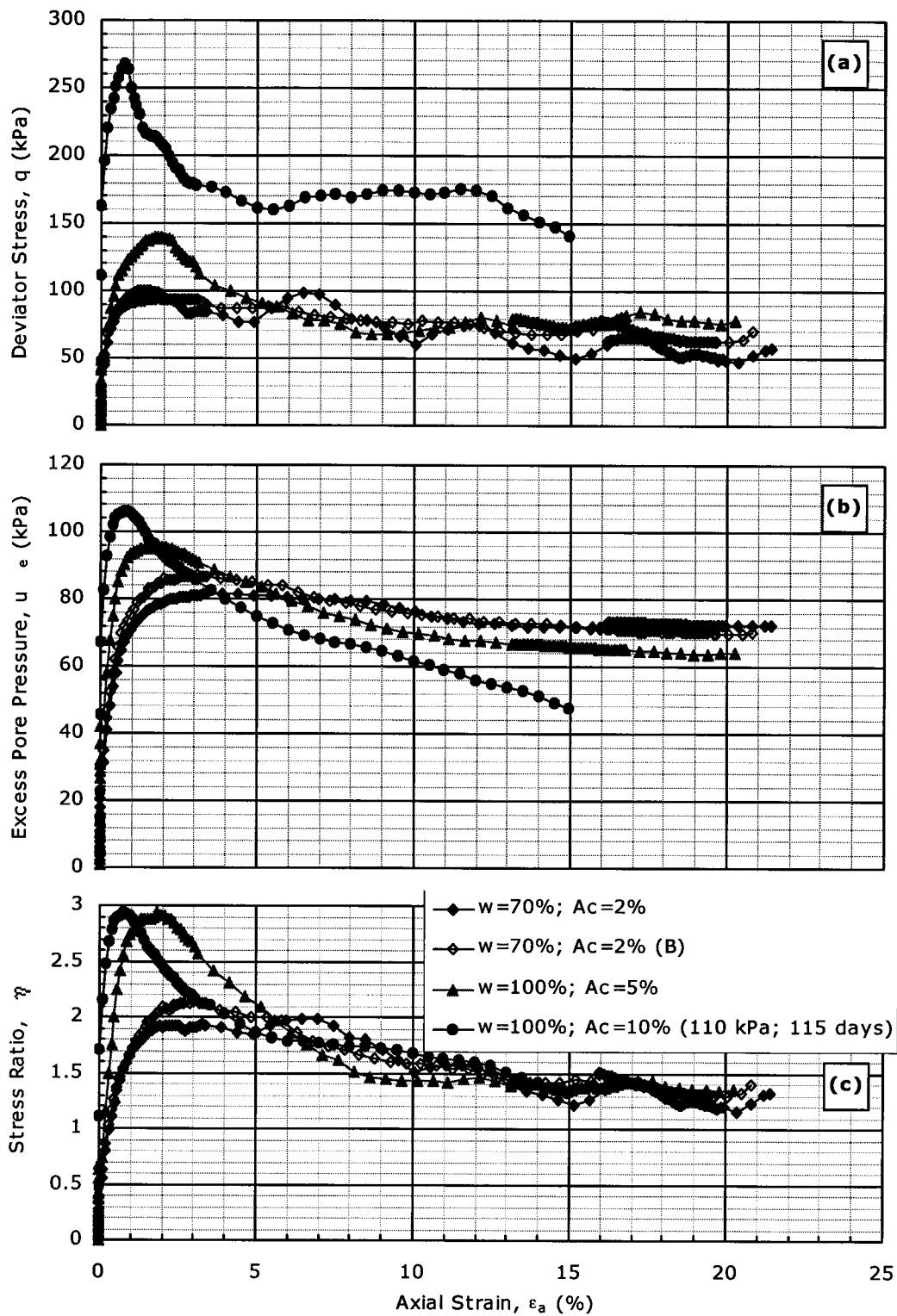
Figure B.15.   CIU data for T_c=112 days & p_o'=100 kPa.   (a) q vs. ε_a; (b) u_e vs. ε_a; (c) η vs. ε_a.
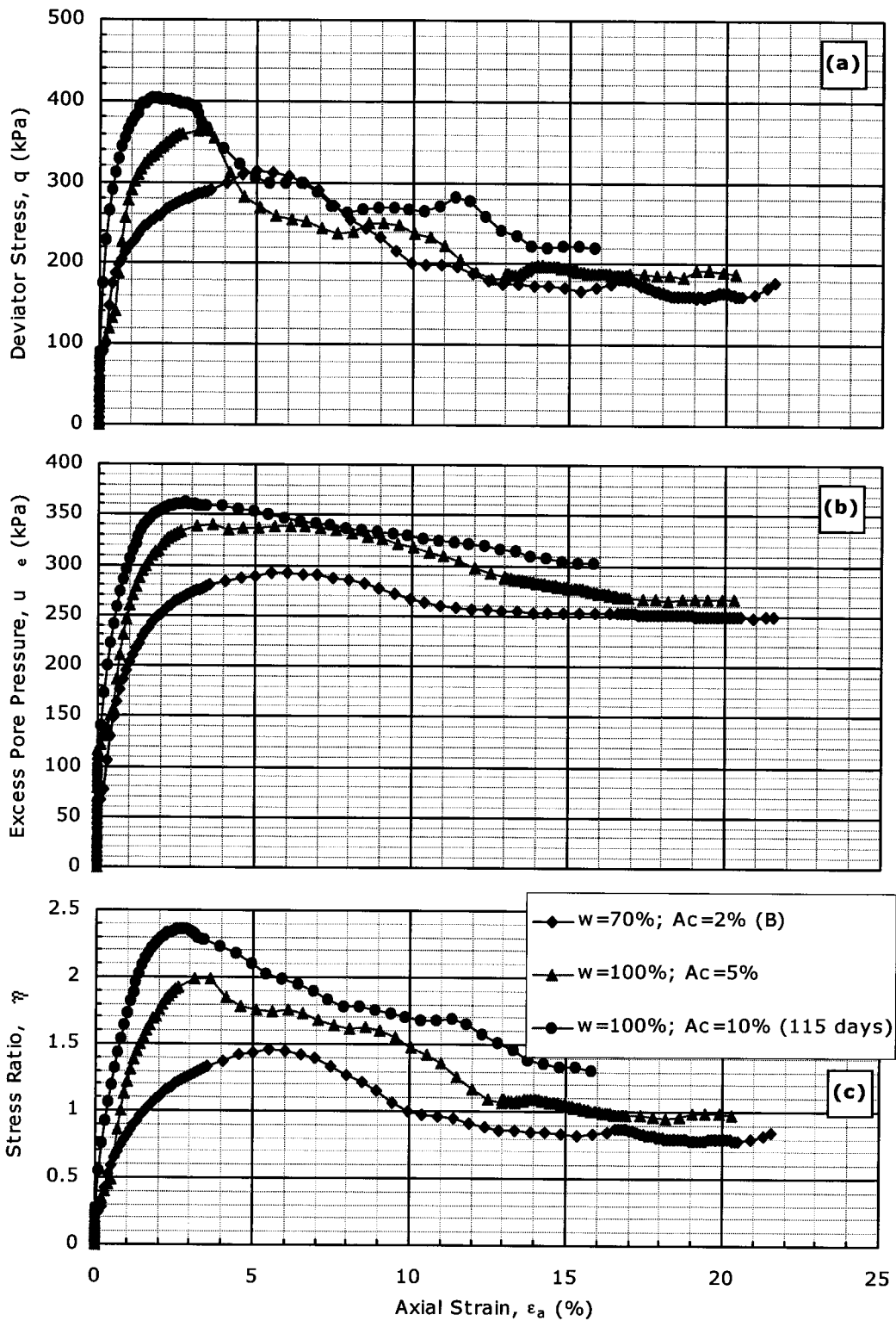
Figure B.16. CIU data for $T_c=112$ days & $p_o{'}=400$ kPa. (a) q vs. ε_a; (b) u_e vs. ε_a; (c) η vs. ε_a.

Mechanical Characteristics of Kaolin-Cement Mixture 241
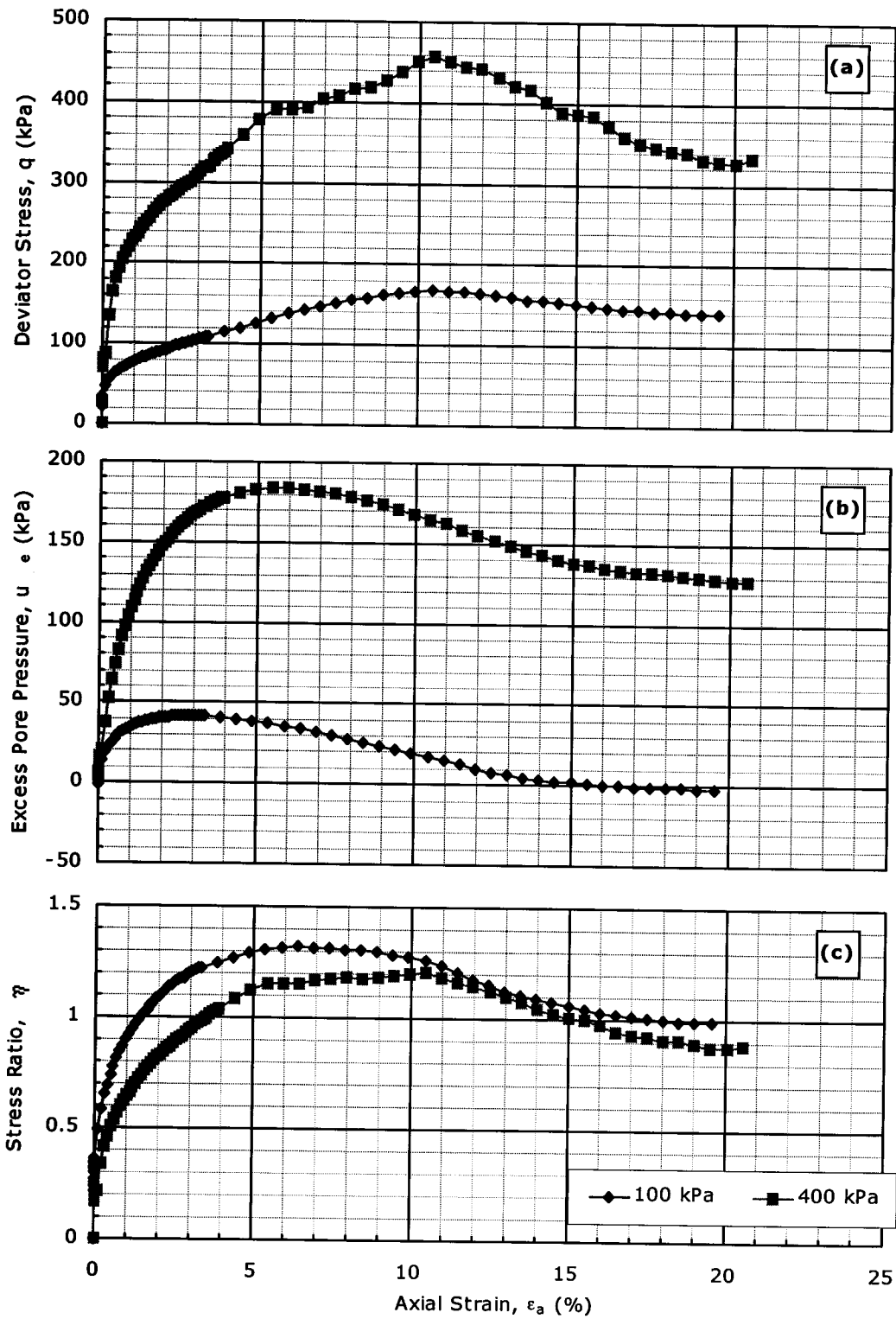
Figure B.17. CIU data for w=40% & A_c=0%. (a) q vs. ε_a; (b) u_e vs. ε_a; (c) η vs. ε_a.
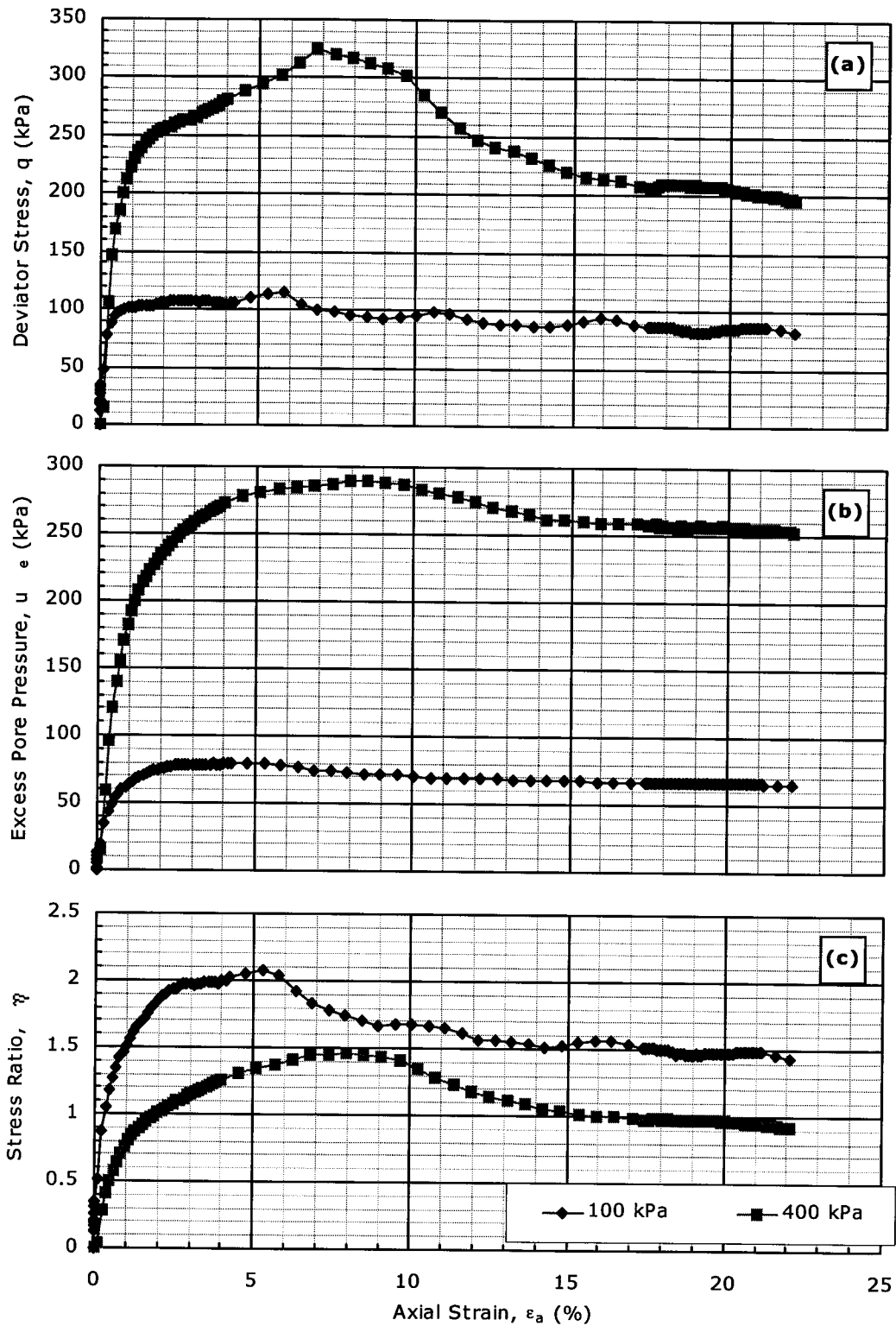
Figure B.18. CIU data for w=70%; A_c=2% & T_c=7 days. (a) q vs. ε_a; (b) u_e vs. ε_a; (c) η vs. ε_a.

Mechanical Characteristics of Kaolin-Cement Mixture 243
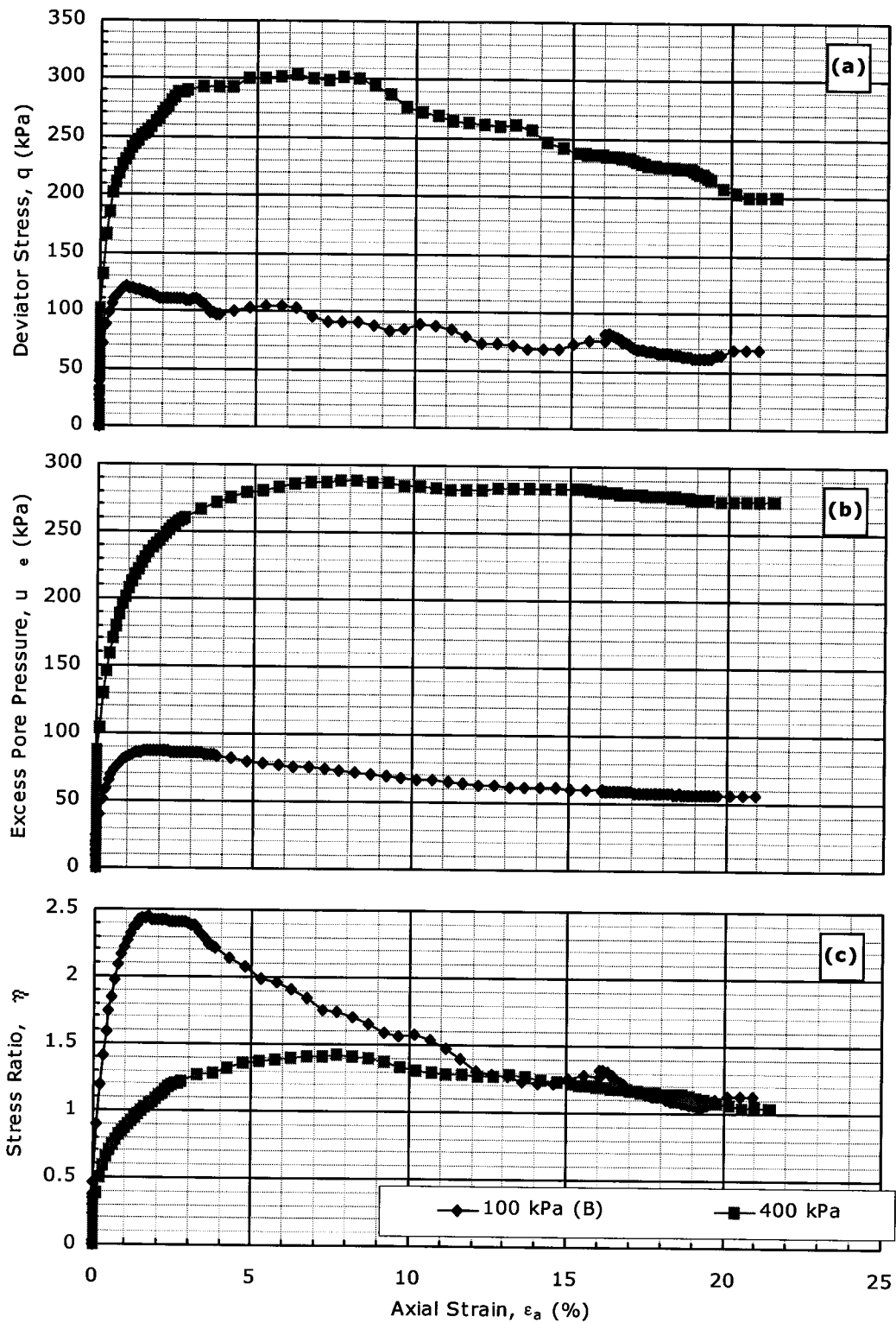
Figure B.19. CIU data for w=70%; A_c=2% & T_c=28 days. (a) q vs. ε_a; (b) u_e vs. ε_a; (c) η vs. ε_a.

Mechanical Characteristics of Kaolin-Cement Mixture
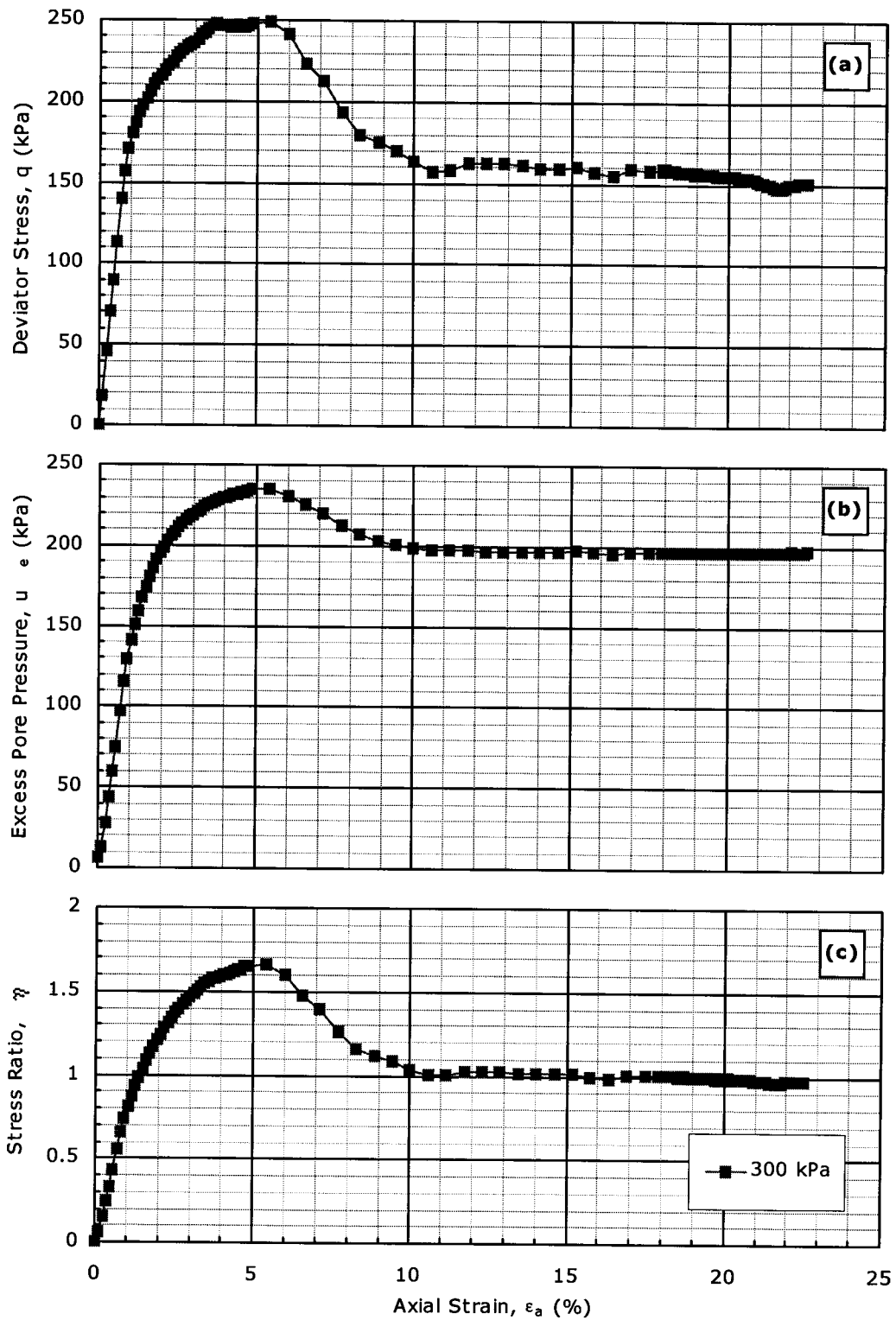
Figure B.20. CIU data for w=70%; A_c=2% & T_c=56 days. (a) q vs. ε_a; (b) u_e vs. ε_a; (c) η vs. ε_a.

Mechanical Characteristics of Kaolin-Cement Mixture
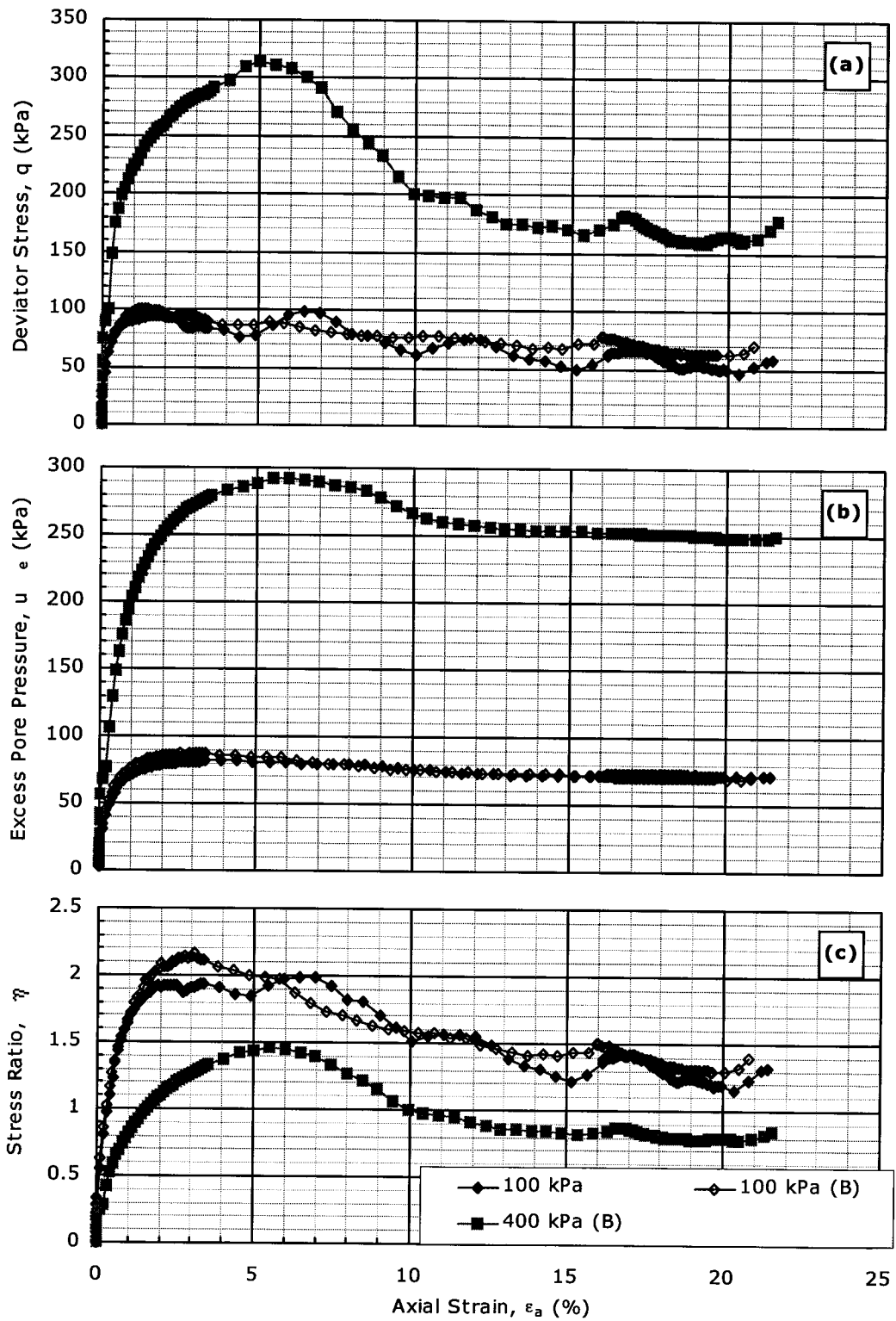
Figure B.21. CIU data for w=70%; A_c=2% & T_c=112 days. (a) q vs. ε_a; (b) u_e vs. ε_a; (c) η vs. ε_a.

Mechanical Characteristics of Kaolin-Cement Mixture
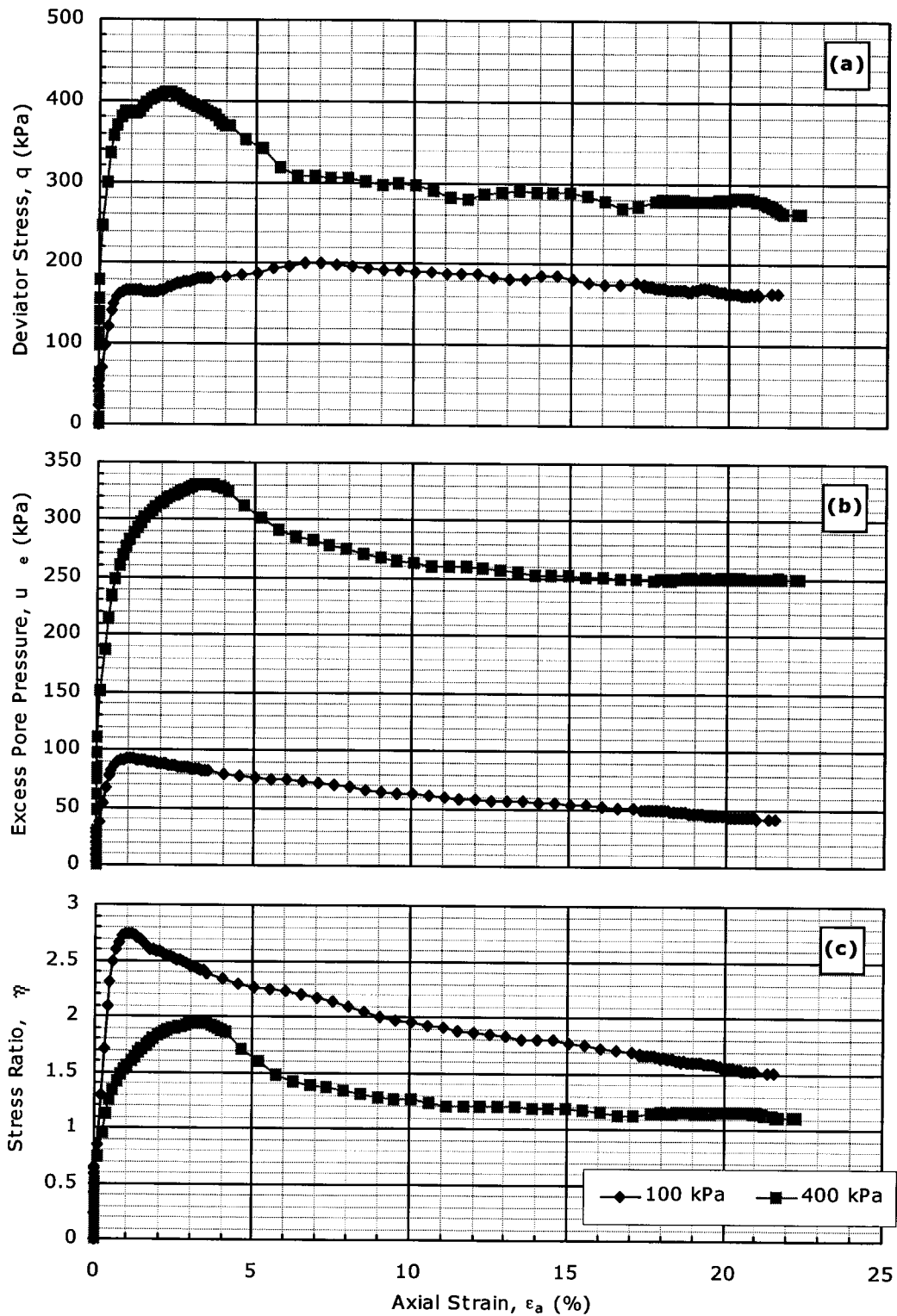
Figure B.22. CIU data for w=70%; A_c=5% & T_c=7 days. (a) q vs. ε_a; (b) u_e vs. ε_a; (c) η vs. ε_a.

Mechanical Characteristics of Kaolin-Cement Mixture   247
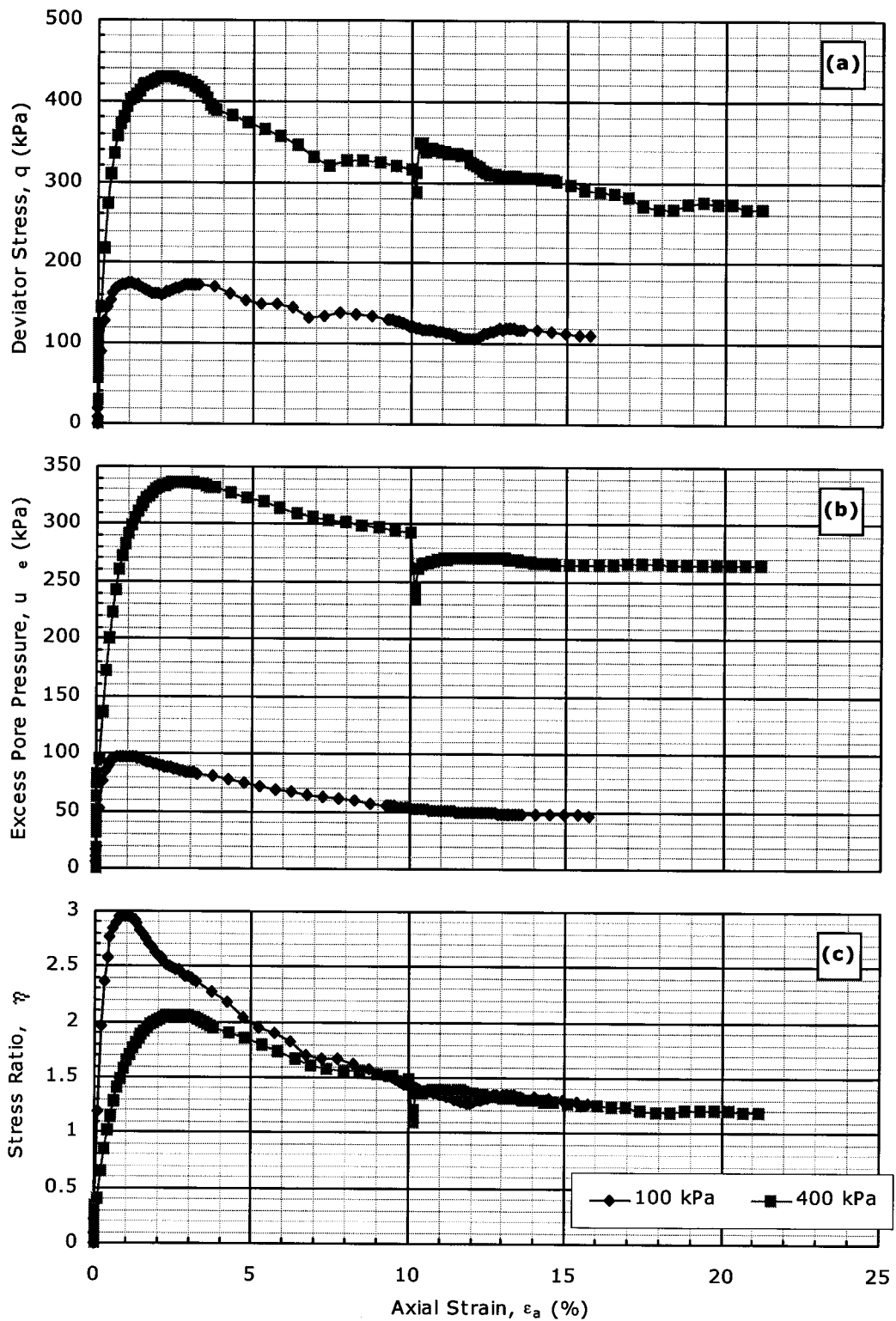
Figure B.23. CIU data for w=70%; A_c=5% & T_c=28 days. (a) q vs. ε_a; (b) u_e vs. ε_a; (c) η vs. ε_a.

Mechanical Characteristics of Kaolin-Cement Mixture
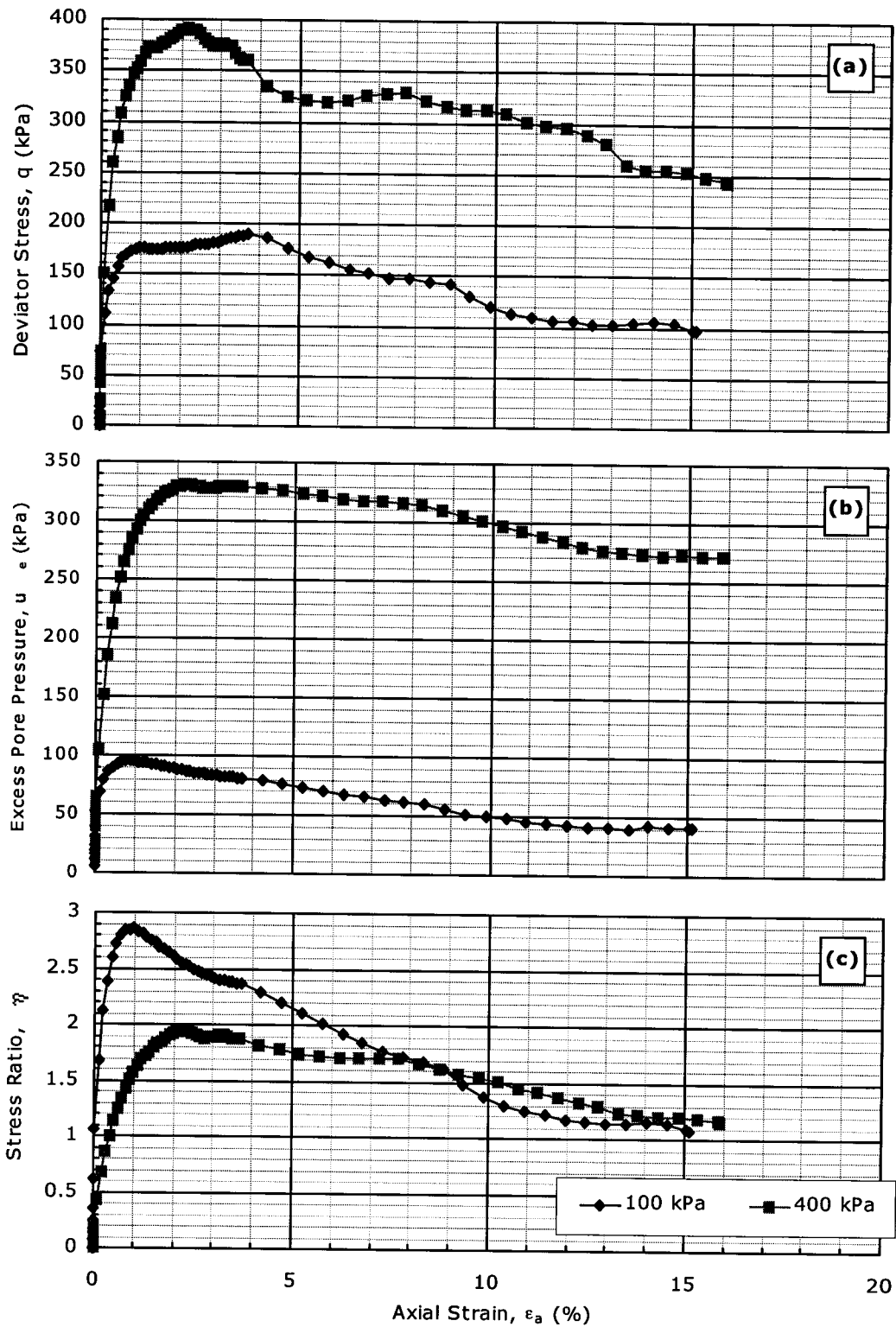
Figure B.24. CIU data for w=70%; A_c=5% & T_c=56 days. (a) q vs. ε_a; (b) u_e vs. ε_a; (c) η vs. ε_a.
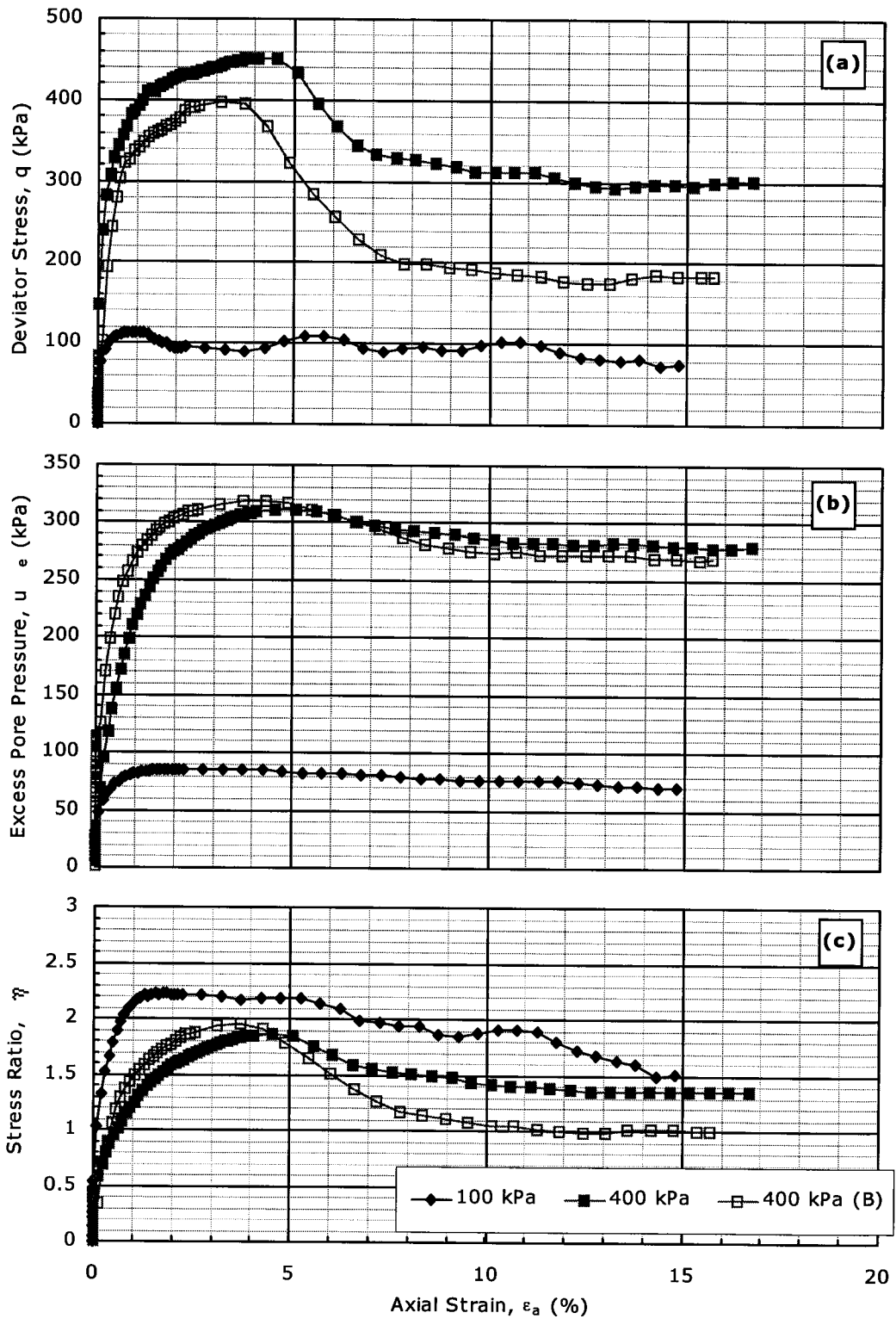
Figure B.25. CIU data for w=100%; A_c=5% & T_c=7 days. (a) q vs. ε_a; (b) u_e vs. ε_a; (c) η vs. ε_a.
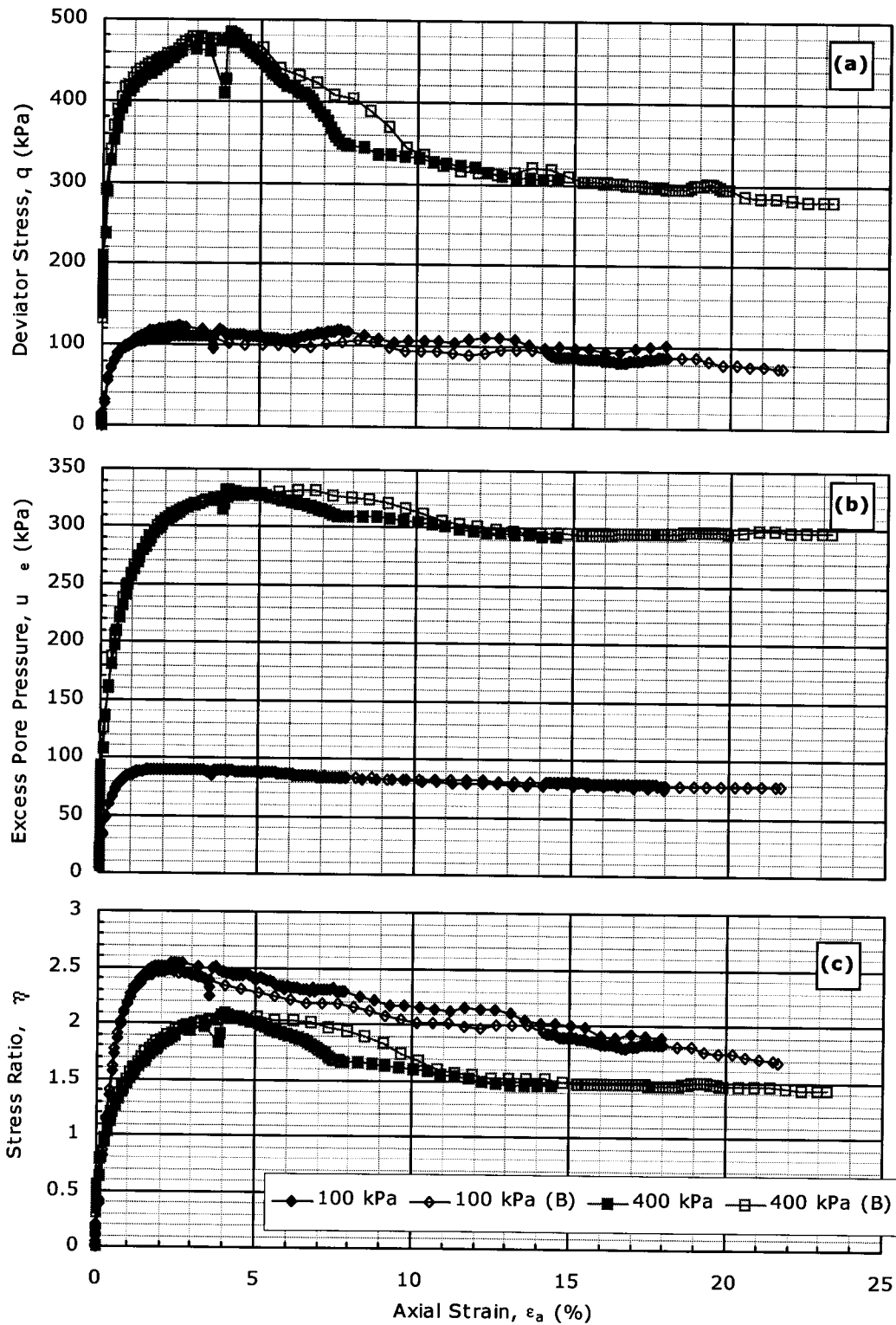
Figure B.26. CIU data for w=100%; A_c=5% & T_c=28 days. (a) q vs. ε_a; (b) u_e vs. ε_a; (c) η vs. ε_a.
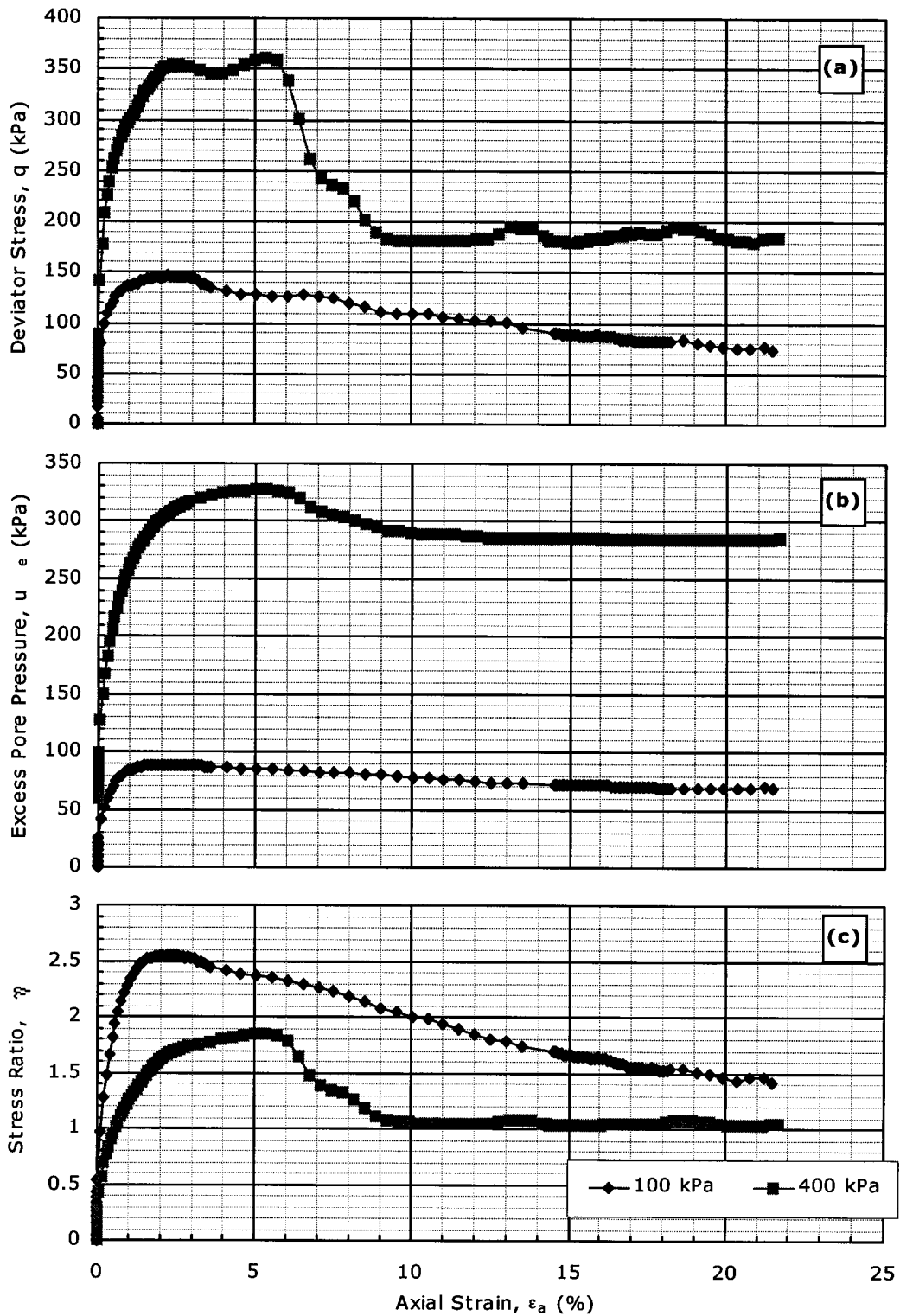
Figure B.27. CIU data for w=100%; A_c=5% & T_c=56 days. (a) q vs. ε_a; (b) u_e vs. ε_a; (c) η vs. ε_a.
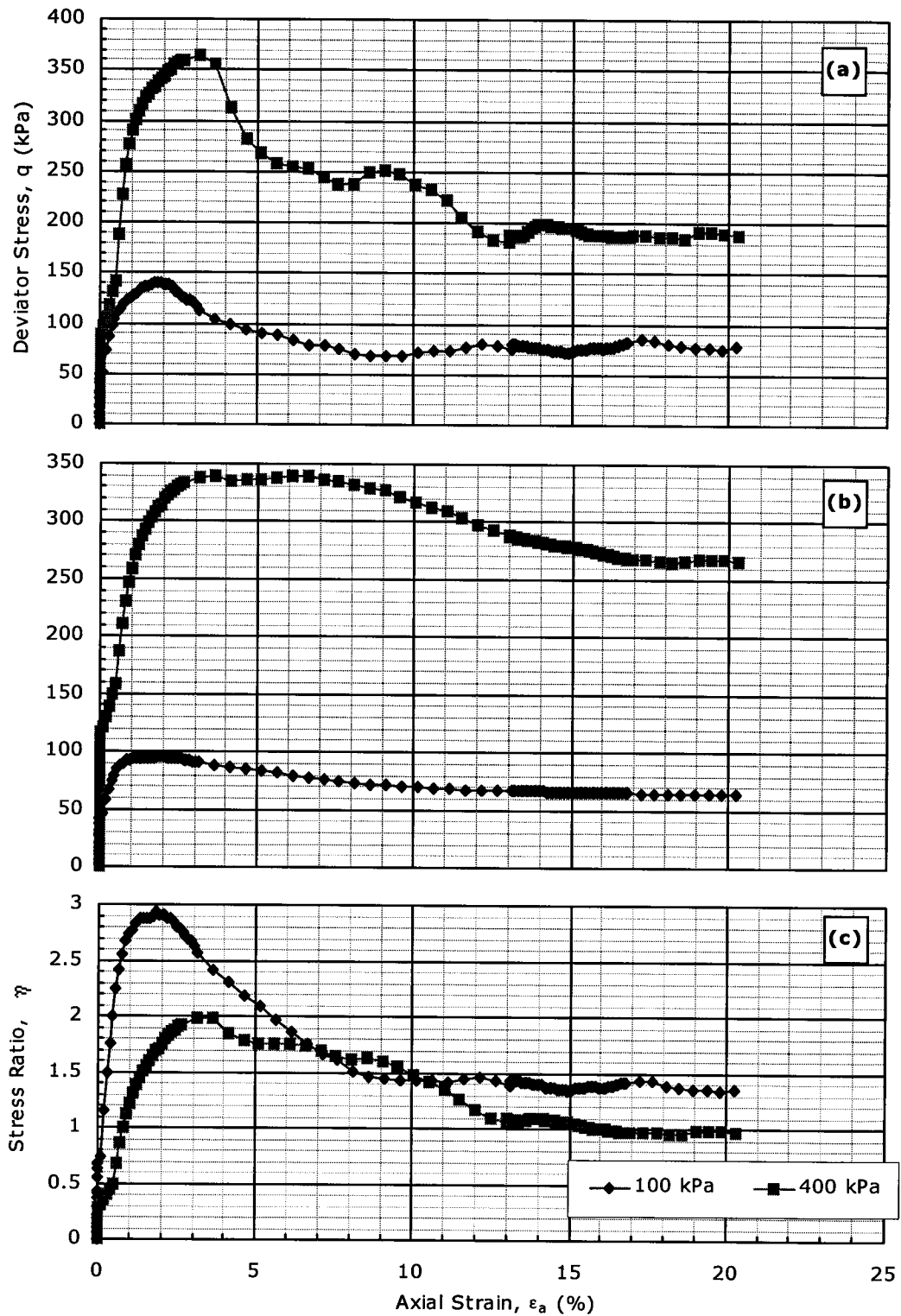
Figure B.28.   CIU data for w=100%; A_c=5% & T_c=112 days. (a) q vs. ε_a; (b) u_e vs. ε_a; (c) η vs. ε_a.

Mechanical Characteristics of Kaolin-Cement Mixture   253
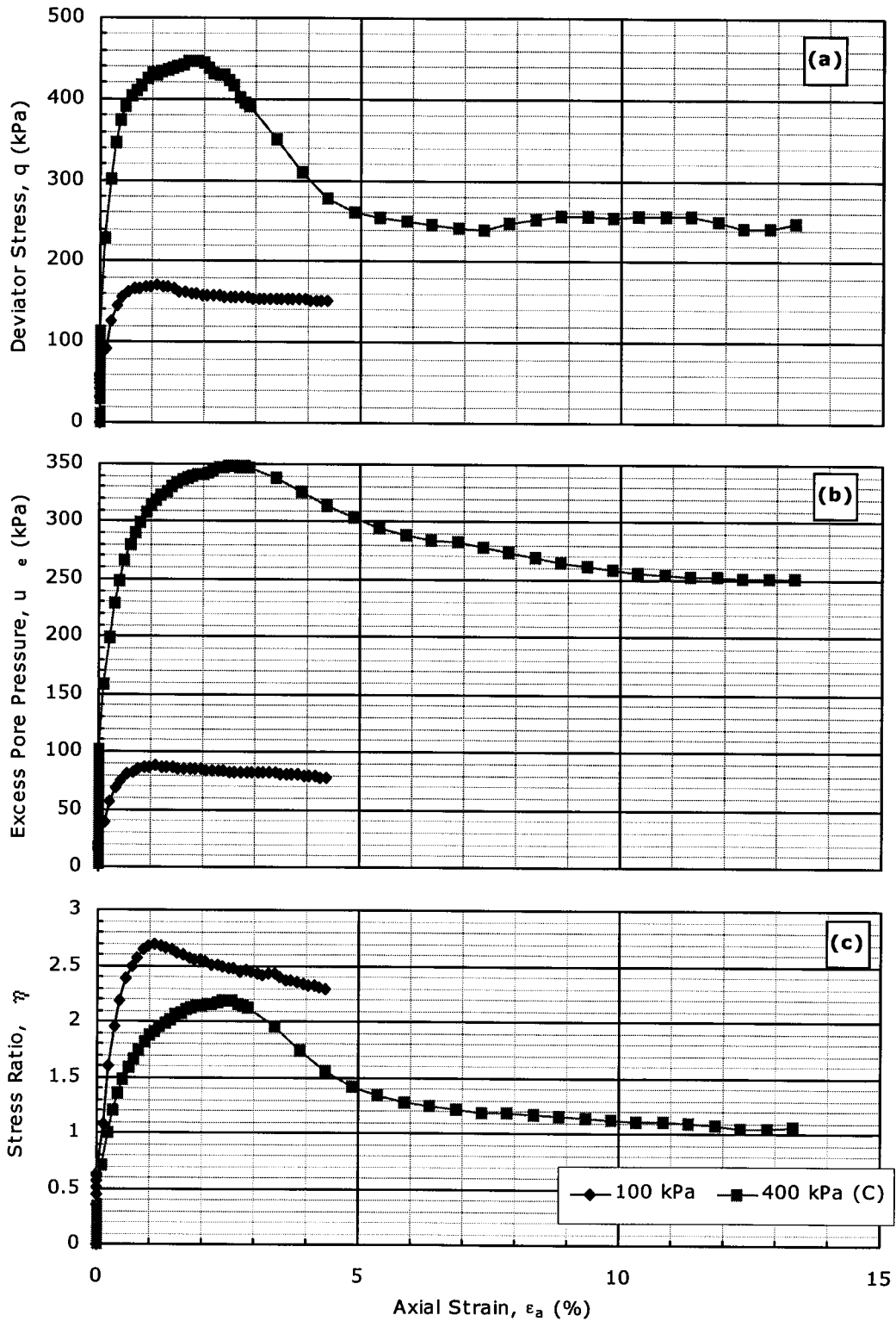
Figure B.29. CIU data for w=100%; A_c=10% & T_c=7 days. (a) q vs. ε_a; (b) u_e vs. ε_a; (c) η vs. ε_a.
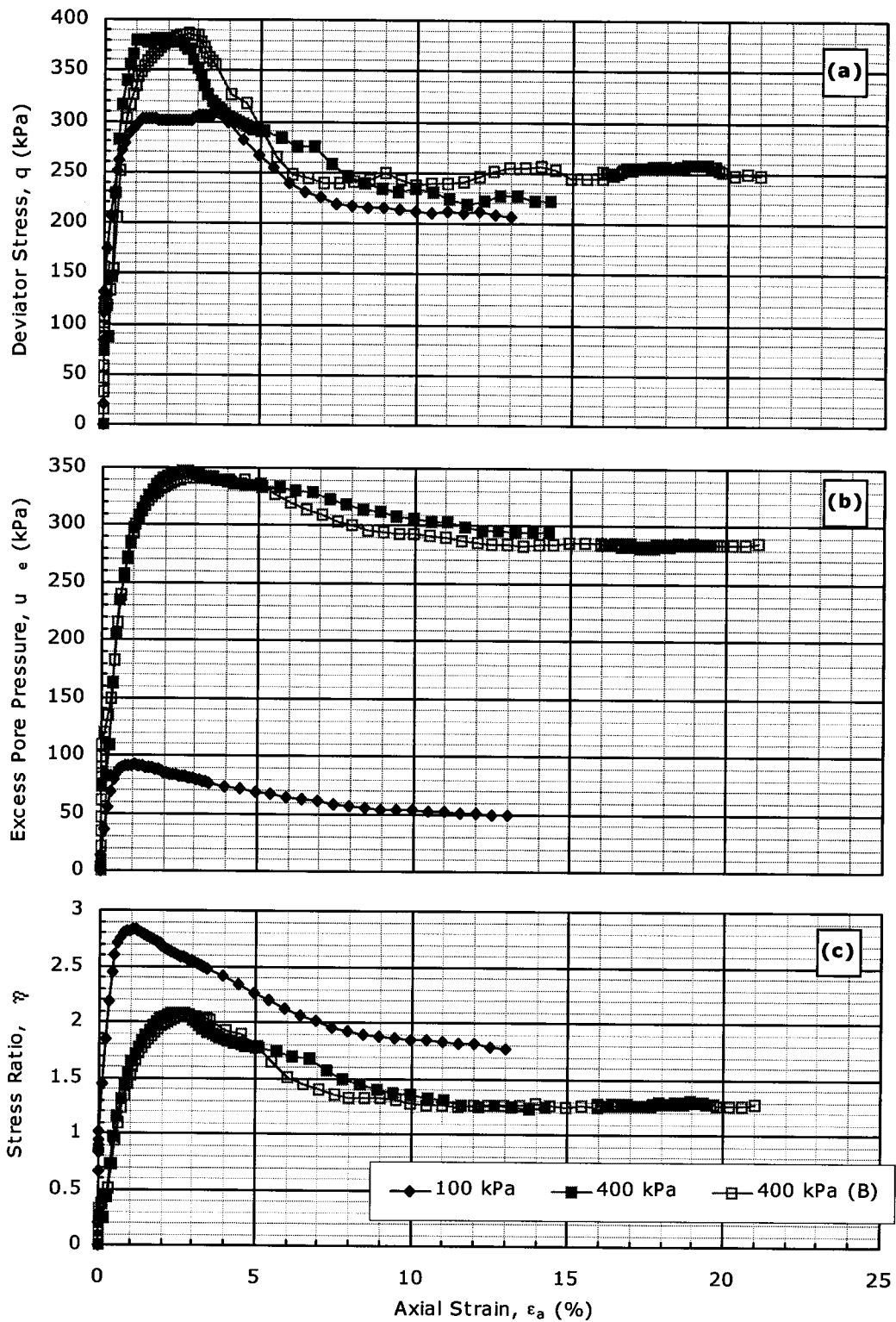
Figure B.30. CIU data for w=100%; A_c=10% & T_c=28 days. (a) q vs. ε_a; (b) u_e vs. ε_a; (c) η vs. ε_a.

Mechanical Characteristics of Kaolin-Cement Mixture   255
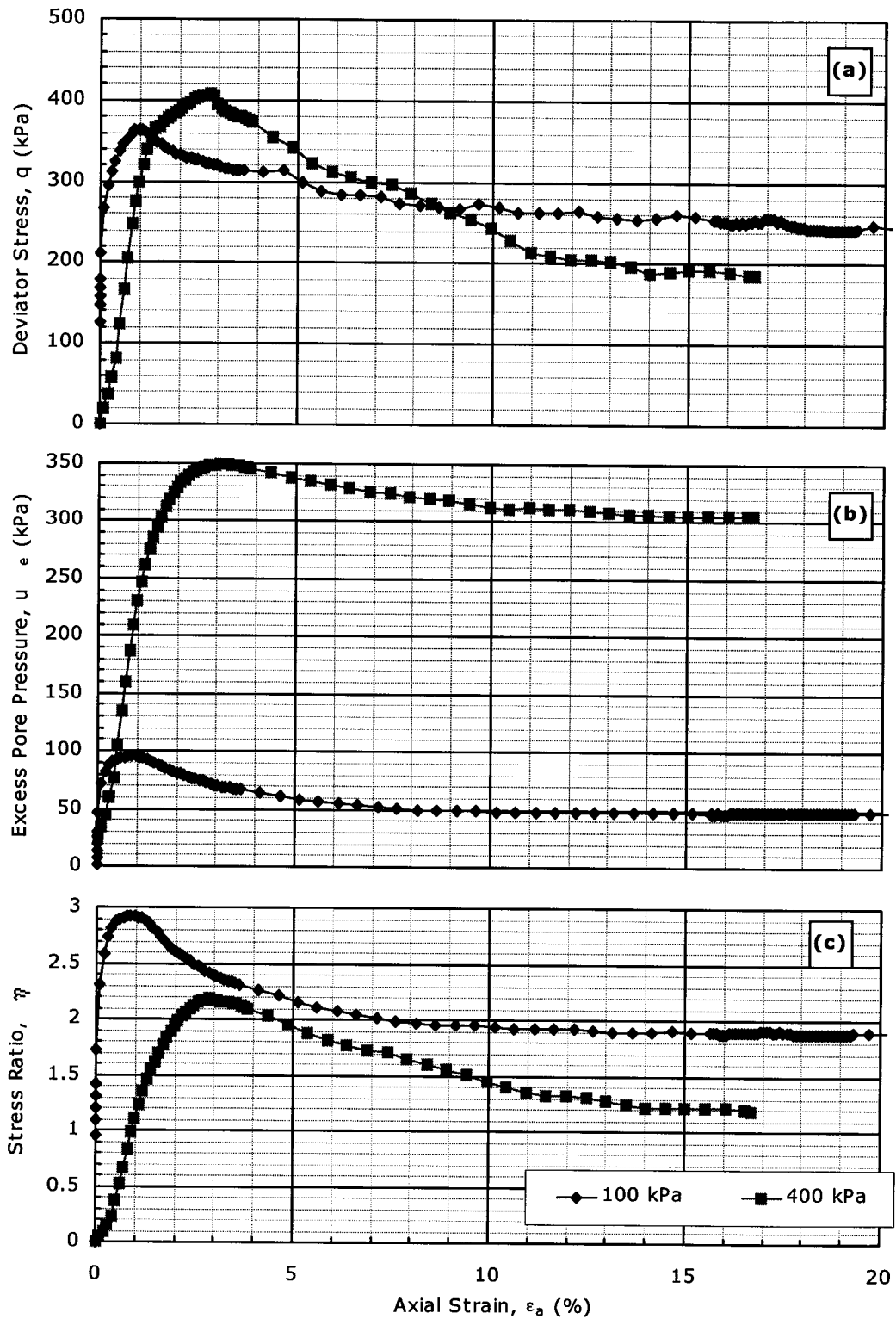
Figure B.31. CIU data for w=100%; A_c=10% & T_c=56 days. (a) q vs. ε_a; (b) u_e vs. ε_a; (c) η vs. ε_a.

Mechanical Characteristics of Kaolin-Cement Mixture
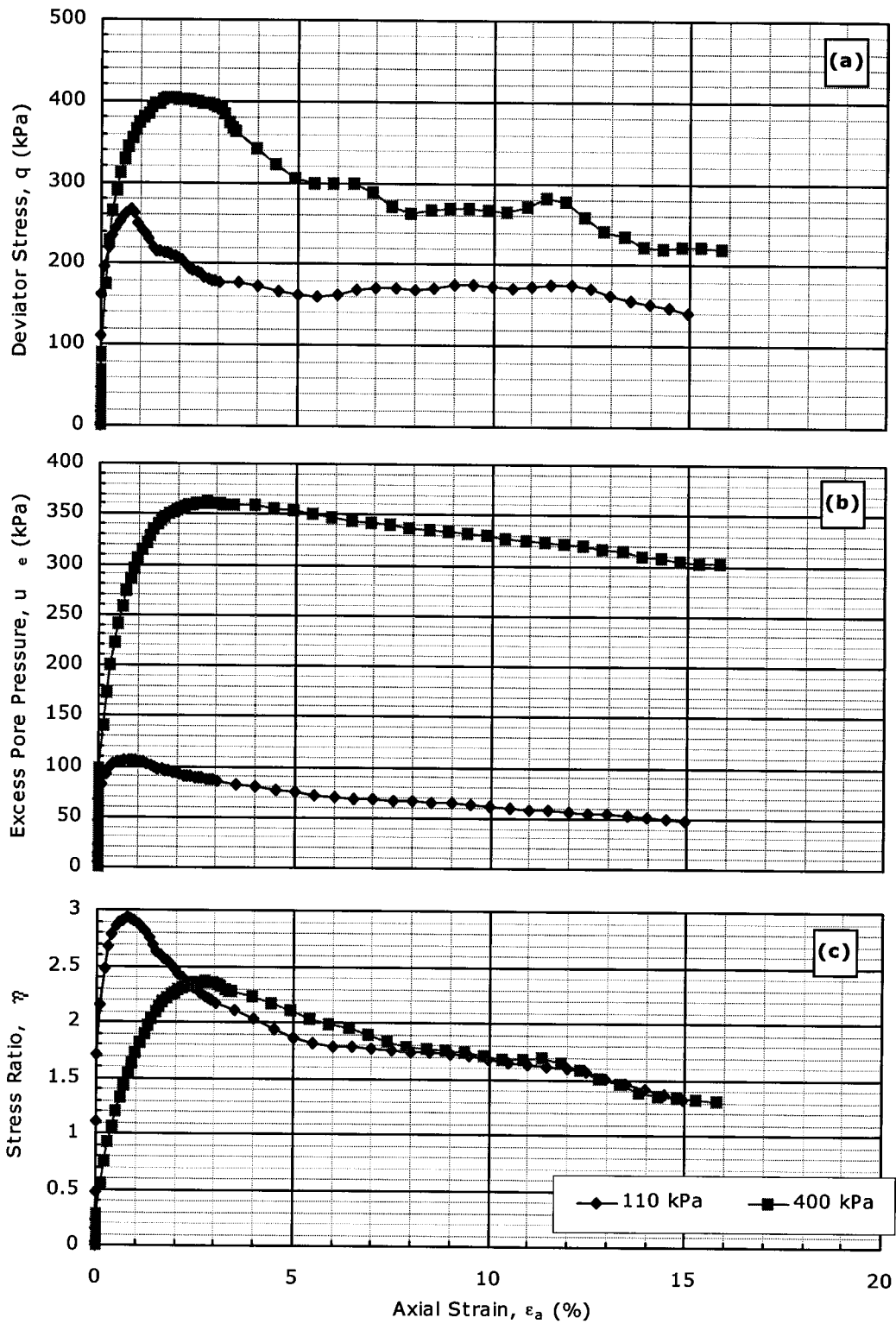
Figure B.32. CIU data for w=100%; A_c=10% & T_c=112 days. (a) q vs. ε_a; (b) u_e vs. ε_a; (c) η vs. ε_a.

Mechanical Characteristics of Kaolin-Cement Mixture 257

APPENDIX C: UNCONFINED COMPRESSION TEST DATA

Unconfined compression (UC) tests were conducted at the City University of Hong Kong between June 2000 and July 2001. Similar to the triaxial tests, UC tests were conducted on samples at 70 percent moisture content with 2 and 5 percent cement and samples at 100 percent moisture content with 5 and 10 percent cement. Samples were cured in distilled water at 20°C for 7, 28, 56 and 112 days. Tests were also done on samples at 100 percent moisture content and 2 percent cement and cured for only 7 days and on samples of pure kaolin at 40 percent moisture content. Chapter 5 describes and interprets the results of the UC tests.

Graphs of the stress-strain data from the UC tests are included in this appendix. Plots appear in groups so that the effects of curing time and cement and moisture content can be interpretted. Therefore, data for each test appear more than once. Typically, at least 3 tests were conducted for each mix and curing time considered; only the tests yielding the highest strength within each group are included here. Tables C.1 and C.2 summarize the figures provided in this appendix.

Unconfined compression tests were also conducted on humid-cured samples to examine the effects of curing environment. These plots are not included here.

Table C.1. Plots illustrating the effects of curing time.

w (%)	A_c(%)	Curing Time, T_c (days)			
		7	28	56	112
70	2	C.1			
	5	C.2			
100	5	C.3			
	10	C.4			

Table C.2. Plots illustrating the effects of cement and moisture content

T_c (days)	w=40%; A_c=0%*	w=100%; A_c=2%	w=70%; A_c=2%	w=70%; A_c=5%	w=100%; A_c=5%	w=100%; A_c=10%
7	C.5					
28		C.6				
56		C.7				
112		C.8				

*samples tested immediately following casting; T_c=0 days.
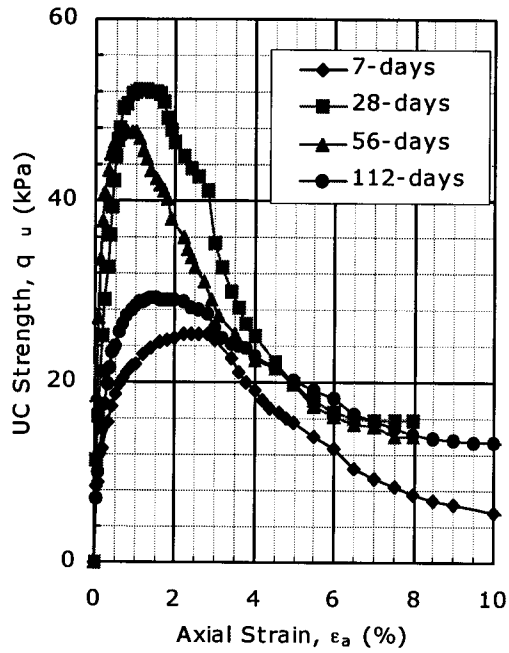
Figure C.1. Stress-strain plot for w=70% and A_c=2% (UC).
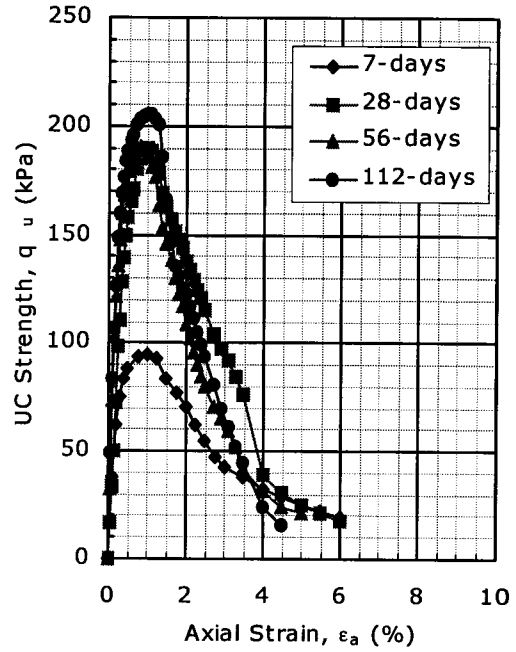
Figure C.2. Stress-strain plot for w=70% and A_c=5% (UC).
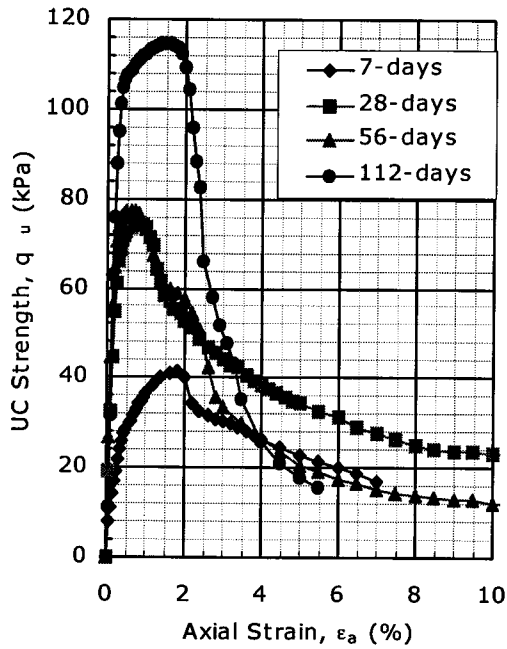
Figure C.3. Stress-strain plot for w=100% and A_c=5% (UC).
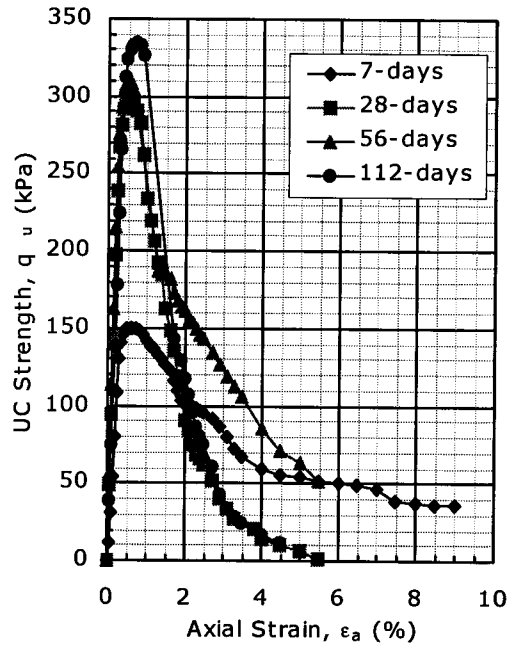
Figure C.4. Stress-strain plot for w=100% and A_c=10% (UC).
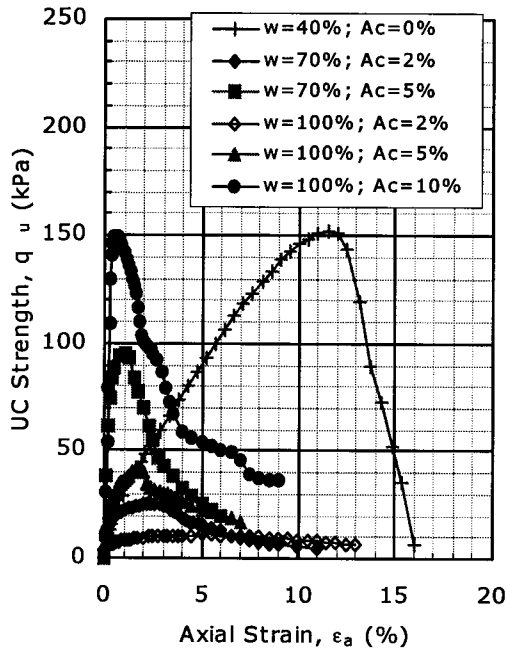
Figure C.5. Stress-strain plot for T_c=7 days (UC).
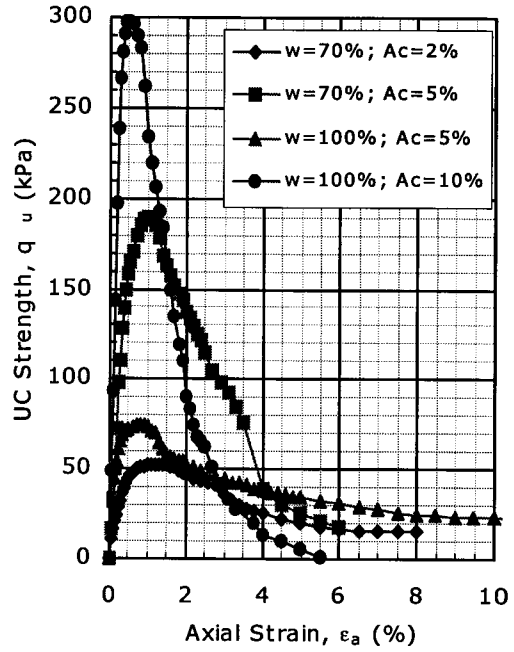
Figure C.6. Stress-strain plot for T_c=28 days (UC).
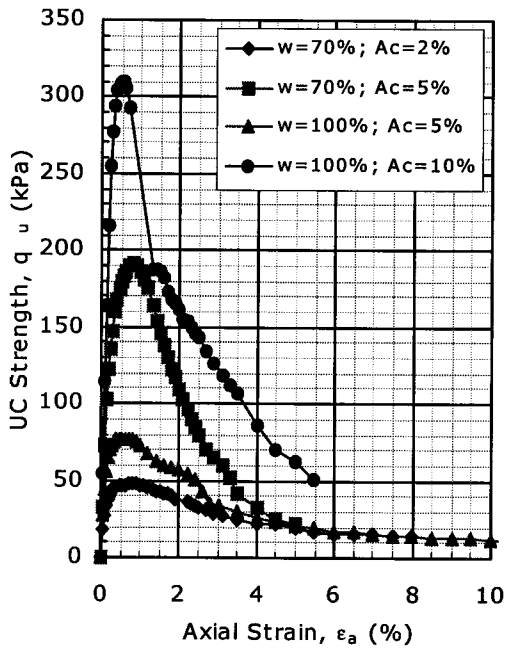
Figure C.7. Stress-strain plot for T_c=56 days (UC).
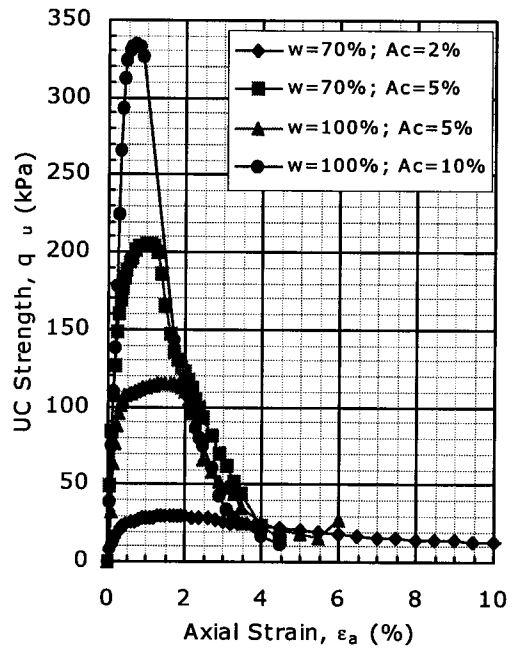
Figure C.8. Stress-strain plot for T_c=112 days (UC).

APPENDIX D: CONSOLIDATION DATA (ISOTROPIC CONSOLIDATION, OEDOMETER AND TRIAXIAL TESTS)

Chapter 6 describes the results of the consolidation tests. Isotropic consolidation and oedometer (one-dimensional consolidation) tests were done at City University of Hong Kong between June 2000 and July 2001. Tests were performed on all mixes considered for the triaxial tests. This includes cement contents of 2 and 5 percent for moisture contents of 70 percent and cement contents of 5 and 10 percent for moisture contents of 100 percent. Samples were cured in distilled water at 20°C for 7, 28, 56 and 112 days. Tests were also conducted on samples of pure kaolin at 40 percent moisture content. Isotropic consolidation tests were loaded up to 400 kPa, in the following sequence: 50, 100, 200, 400, 200, 100, 50, 10 kPa. Each test took place over a period of 6 days, with each stage lasting 10 to 14 hours. Oedometer tests were loaded up to 3200 kPa, in the following sequence: 50, 100, 200, 400, 800, 1600, 3200, 800, 200, 50 and 10 kPa. Each test took place over a period of 2 weeks, with each stage lasting approximately 24 hours.

The following appendix includes all consolidation curves (log p_c' vs. v) as well as plots of the coefficient of consolidation (c_v and c_{vi}) and coefficient of volume compressibility (m_v and m_{vi}) vs. log pressure. Data extracted from the consolidation stage of the triaxial tests is also included. Because the maximum load is greater for the oedometer tests, often this data provides better information on the deformation properties. Therefore, when interpreting the effects of curing time and cement and moisture content, only the oedometer data is plotted.

The methods for determining c_v are graphical and based on judgement which may differ between users and between types of tests. Therefore, the values provided for c_v are not intended to be exact. For the oedometer tests, two methods established by Casagrande and Taylor were used to calculate the coefficient of consolidation. This makes for a lot of data and even greater amounts of scatter. Therefore, to simplify the presentation of the results, only Taylor's method using the displacement vs. root time data has been plotted. In general, this method provided more consistent plots and the trends in the data are easier to determine, particularly for the unloading

stages. Furthermore, Taylor's method most closely resembles the method used to establish c_{vi} for the isotropic consolidation test results, allowing the values obtained for each test to be better compared.

During the initial oedometer load of 50 kPa, primary consolidation was nearly instantaneous and the displacement vs. log time plot was often linear, showing only secondary consolidation. Often during unloading, the displacement vs. log time and displacement vs. root time plots were impossible to interpret for both the oedometer and isotropic consolidation tests; therefore, the coefficient of consolidation (c_v) and the coefficient of volume compressibility (m_v) could often not be calculated for the unloading stages.

Tables D.1 to D.5 summarize the figures included in this appendix. The test results from samples of each mixture are plotted individually and test results of samples of the same mixture at different curing times are plotted together to better distinguish the effects of aging on the consolidation characteristics. The consolidation yield stress is also indicated on each consolidation curve.

Table D.1. Comparison of oedometer data vs. IC data vs. triaxial data. (a) v vs. $p_c{'}$; (b) c_v & c_{vi} vs. $p_c{'}$; (c) m_v & m_{vi} vs. $p_c{'}$.

w (%)	A_c(%)	Curing Time, T_c (days)			
		7	28	56	112
40	0*	D.1			
70	2	D.2	D.3	D.4	D.5
	5	D.6	D.7	D.8	D.9
100	5	D.10	D.11	D.12	D.13
	10	D.14	D.15	D.16	D.17

*samples tested immediately following casting; T_c=0 days.

Table D.2. Plots of oedometer data illustrating the effects of curing time. (a) v vs. p_C'; (b) c_v vs. p_C'; (c) m_v vs. p_C'.

w (%)	A_c(%)	Curing Time, T_c (days)			
		7	28	56	112
70	2	D.18			
	5	D.19			
100	5	D.20			
	10	D.21			

Table D.3. Plots of oedometer data illustrating the effects of cement and moisture content. (a) v vs. p_C'; (b) c_v vs. p_C'; (c) m_v vs. p_C'.

T_c (days)	w=40%; A_c=0%*	w=70%; A_c=2%	w=70%; A_c=5%	w=100%; A_c=5%	w=100%; A_c=10%
7	D.22				
28	■	D.23			
56	■	D.24			
112	■	D.25			

*samples tested immediately following casting; T_c=0 days.
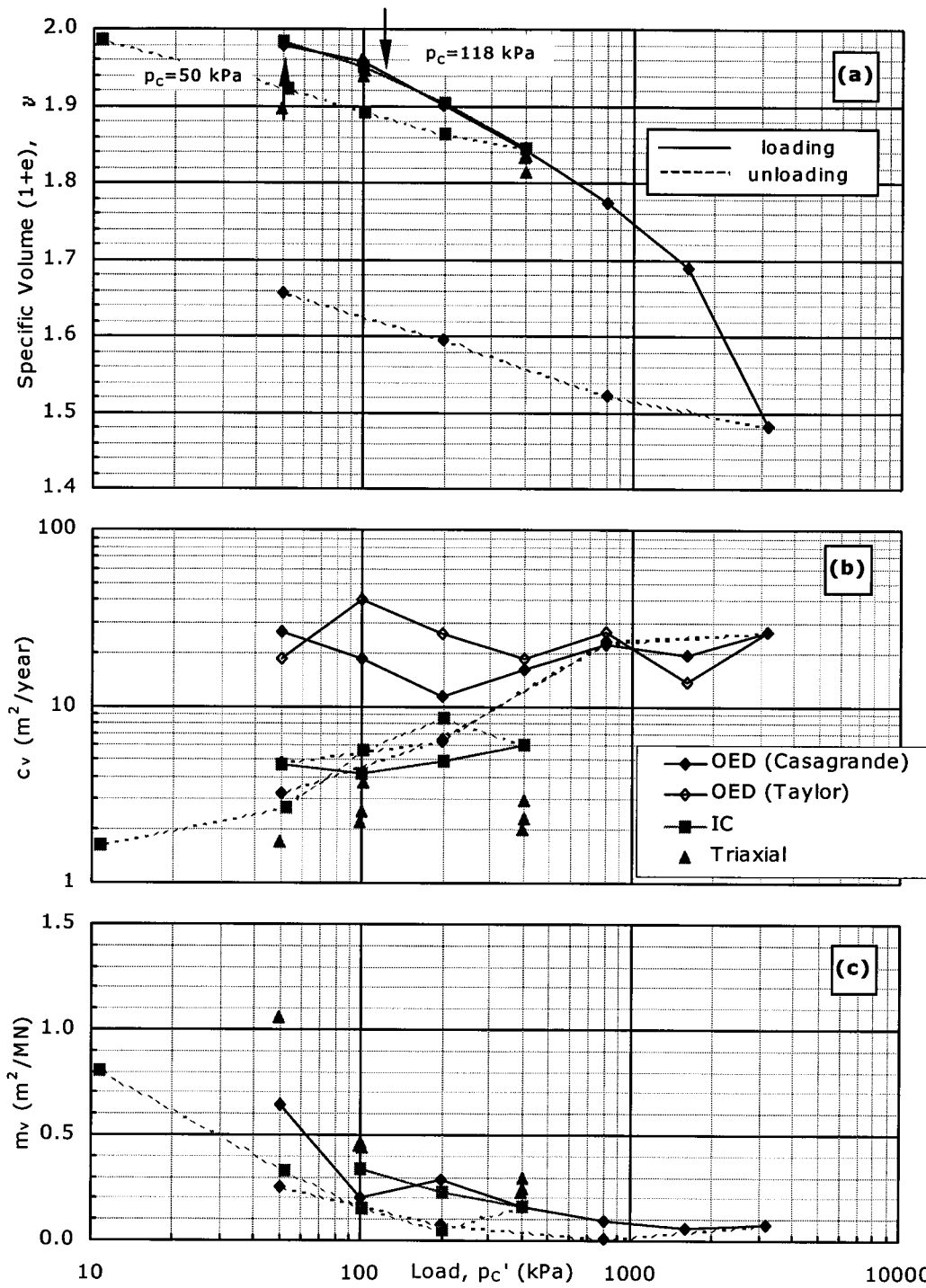
Figure D.1. Oedometer, IC and triaxial consolidation data for w=40% & A_c=0%. (a) υ vs. $p_C{}'$; (b) c_v & c_{vi} vs. $p_C{}'$; (c) m_v & m_{vi} vs. $p_C{}'$.
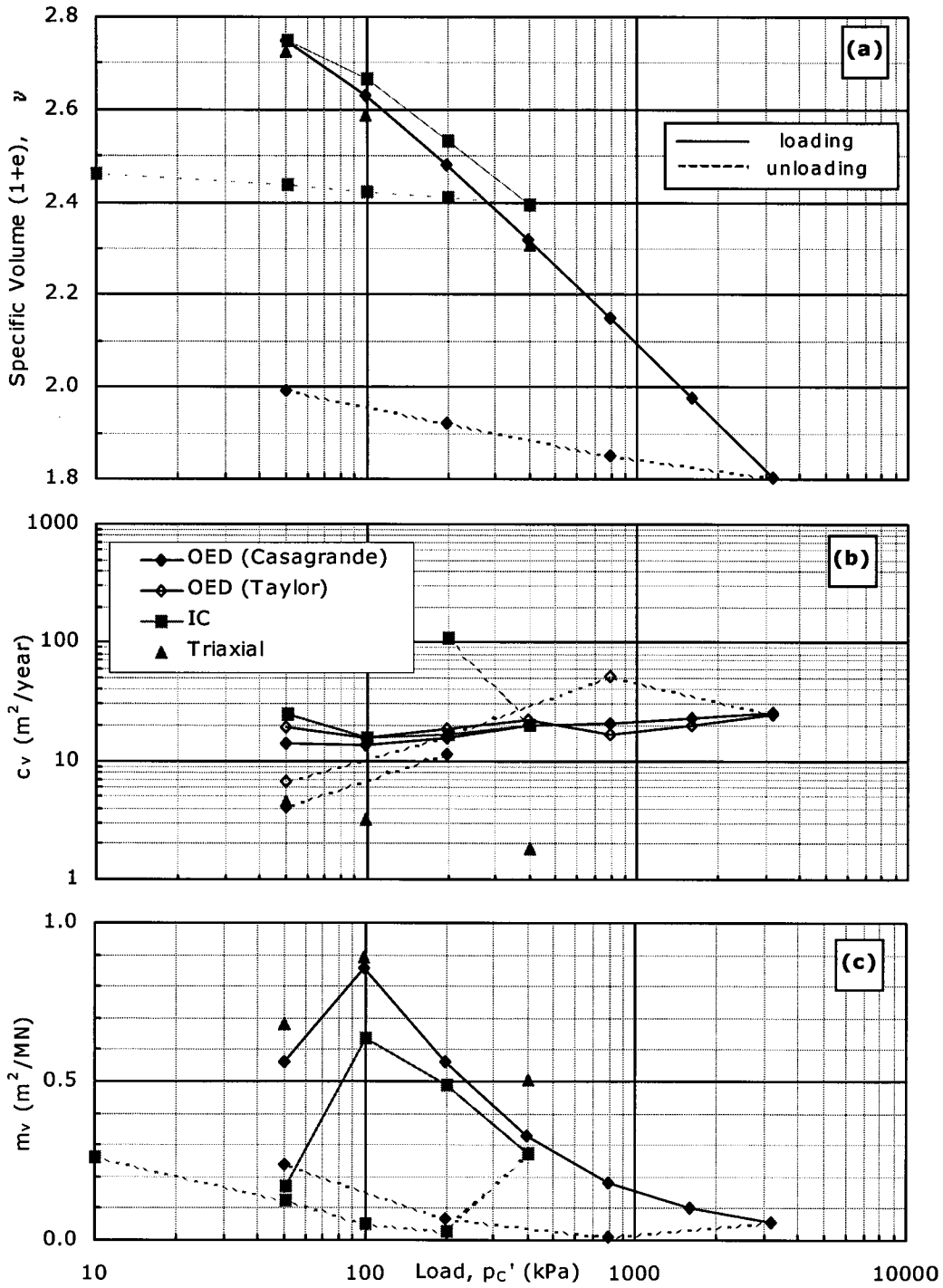
Figure D.2. Oedometer, IC and triaxial consolidation data for w=70%, A_c=2% & T_c=7 days. (a) υ vs. $p_c{'}$; (b) c_v & c_{vi} vs. $p_c{'}$; (c) m_v & m_{vi} vs. $p_c{'}$.

Mechanical Characteristics of Kaolin-Cement Mixture   267
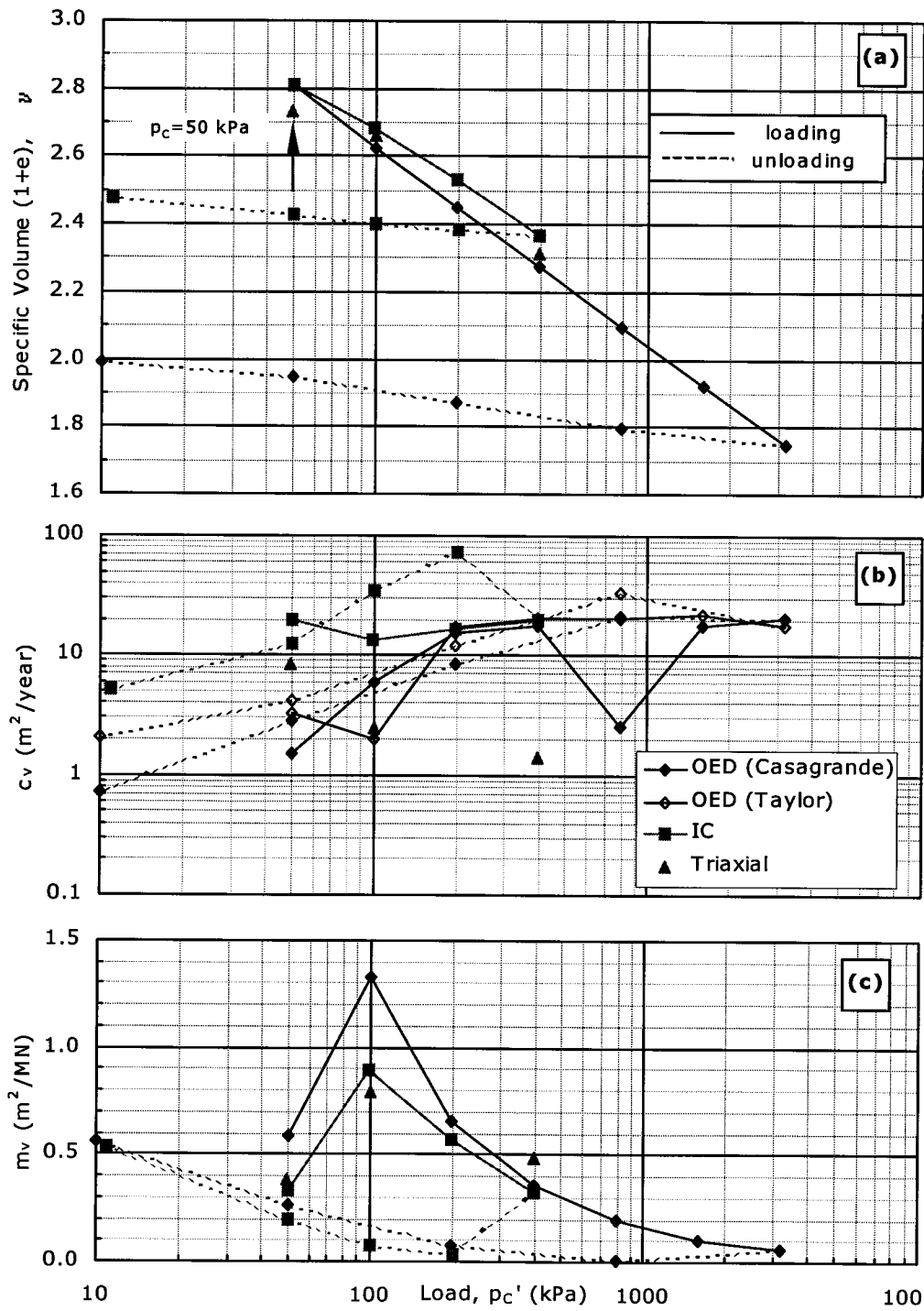
Figure D.3. Oedometer, IC and triaxial consolidation data for w=70%, A_c=2% & T_c=28 days. (a) v vs. $p_C{}'$; (b) c_v & c_{vi} vs. $p_C{}'$; (c) m_v & m_{vi} vs. $p_C{}'$.
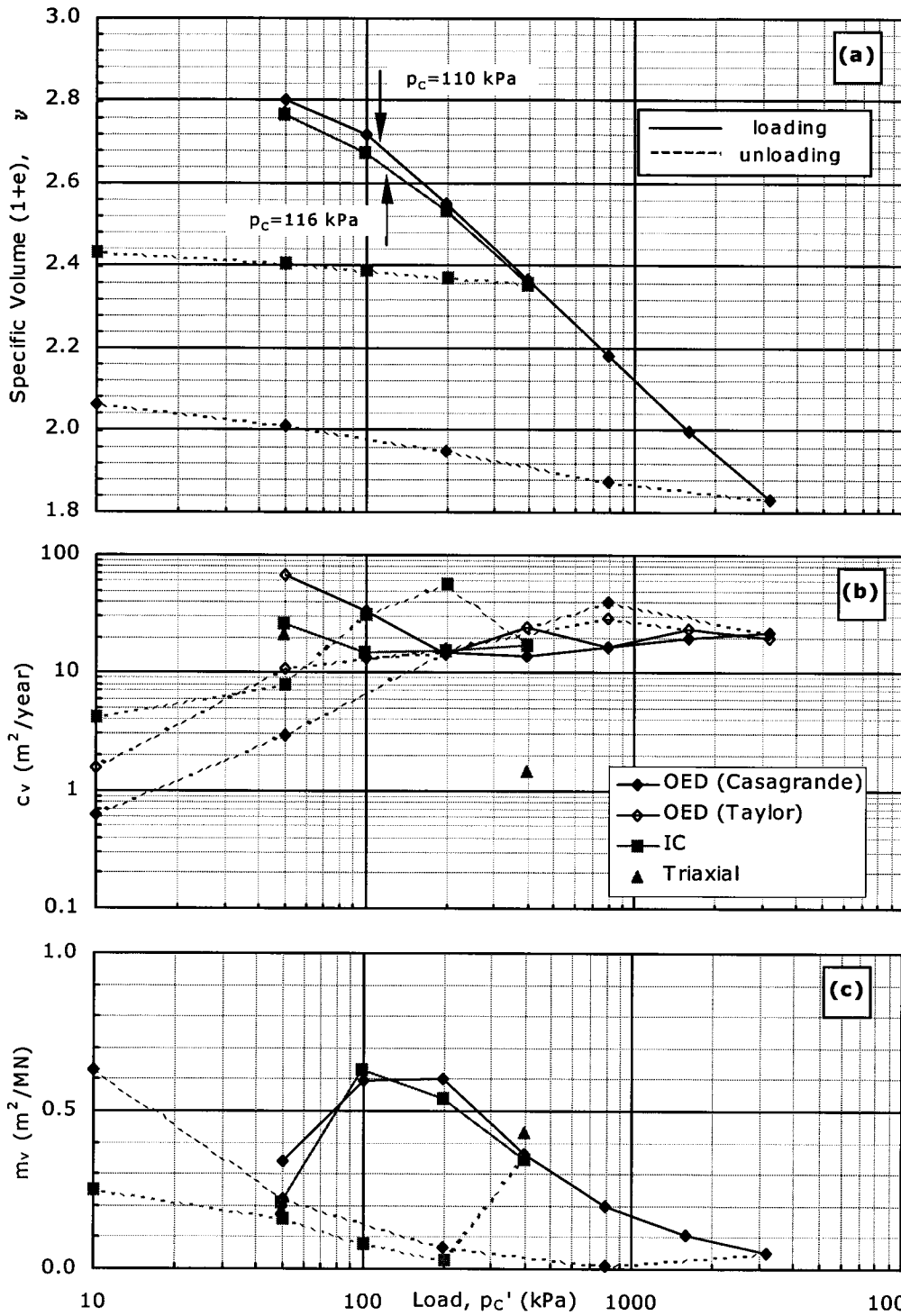
Figure D.4. Oedometer, IC and triaxial consolidation data for w=70%, A_c=2% & T_c=56 days. (a) v vs. $p_c{}'$; (b) c_v & c_{vi} vs. $p_c{}'$; (c) m_v & m_{vi} vs. $p_c{}'$.

Mechanical Characteristics of Kaolin-Cement Mixture   269
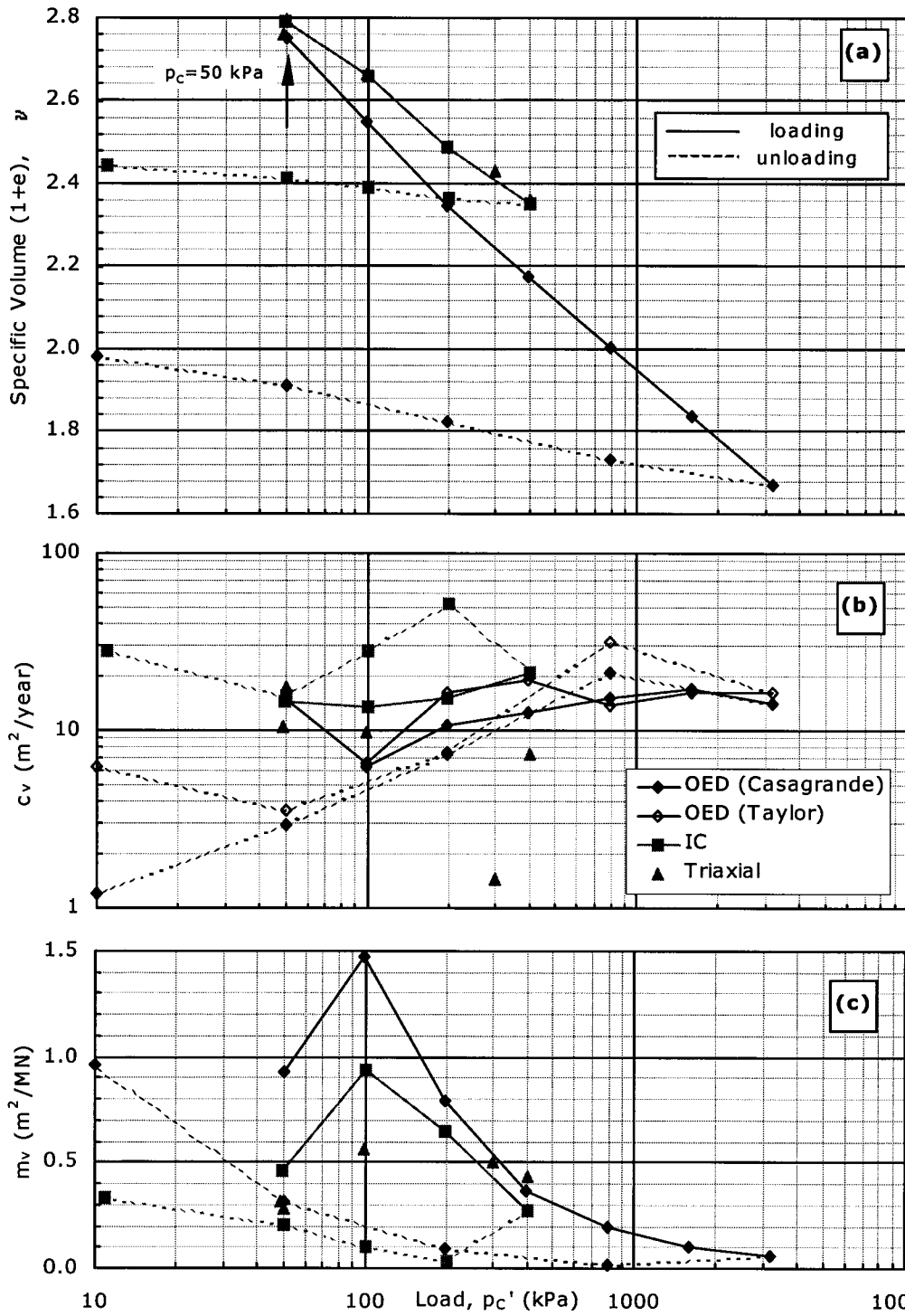
Figure D.5. Oedometer, IC and triaxial consolidation data for w=70%, A_c=2% & T_c=112 days. (a) υ vs. $p_C{}'$; (b) c_v & c_{vi} vs. $p_C{}'$; (c) m_v & m_{vi} vs. $p_C{}'$.
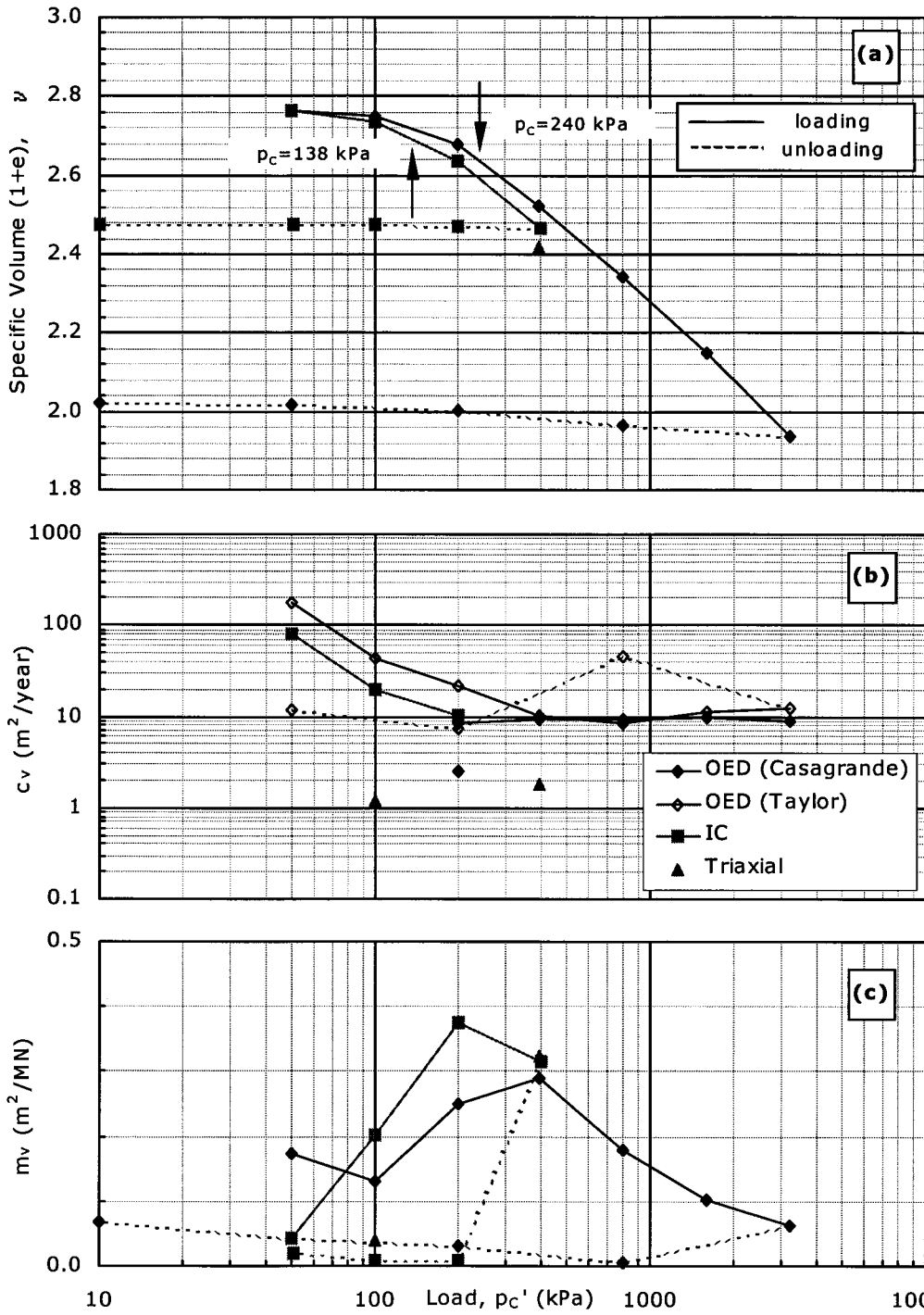
Figure D.6. Oedometer, IC and triaxial consolidation data for w=70%, A_c=5% & T_c=7 days. (a) υ vs. $p_C{}'$; (b) c_v & c_{vi} vs. $p_C{}'$; (c) m_v & m_{vi} vs. $p_C{}'$.

Mechanical Characteristics of Kaolin-Cement Mixture

271
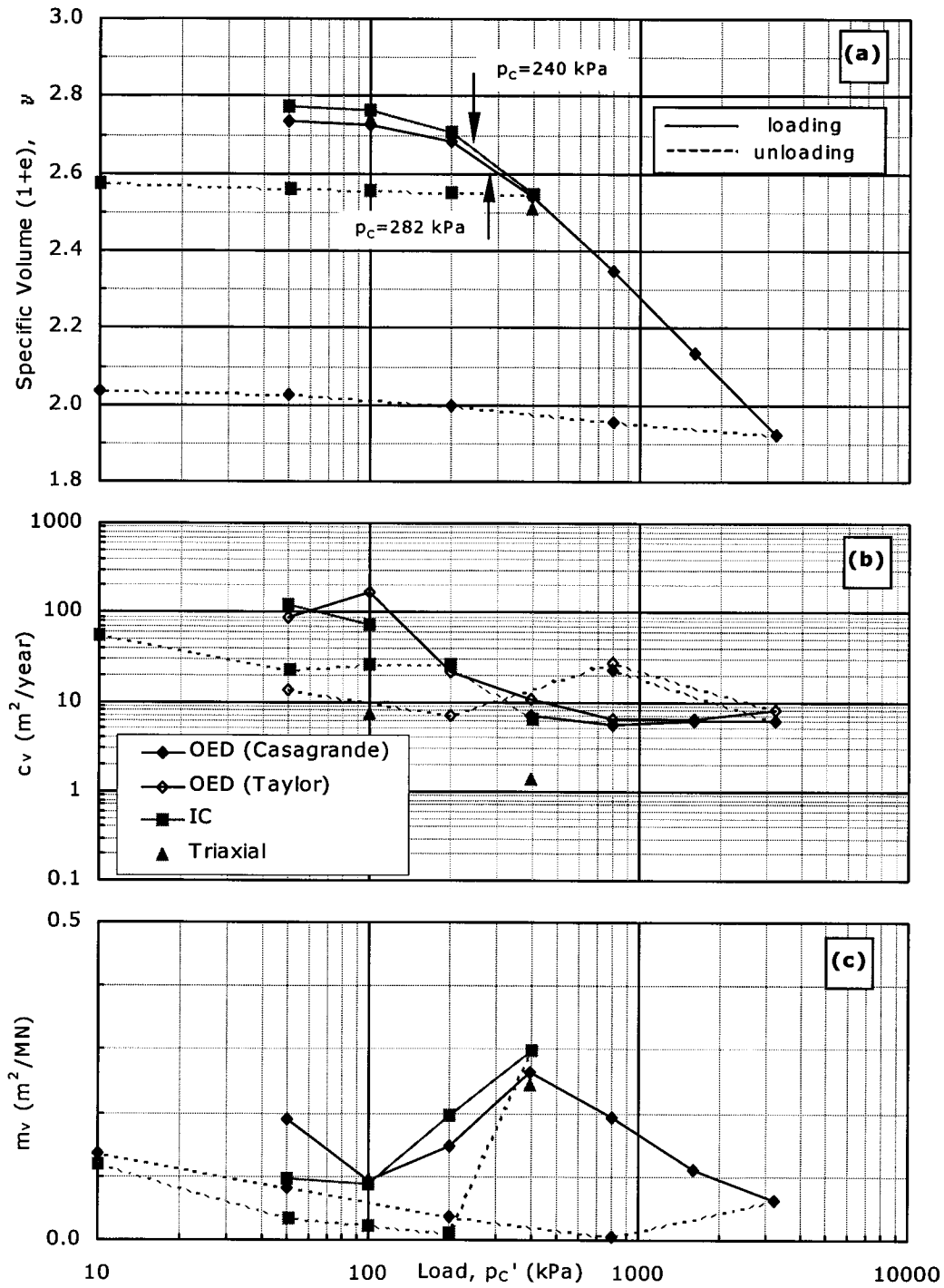
Figure D.7. Oedometer, IC and triaxial consolidation data for w=70%, A_c=5% & T_c=28 days. (a) υ vs. p_C'; (b) c_v & c_{vi} vs. p_C'; (c) m_v & m_{vi} vs. p_C'.
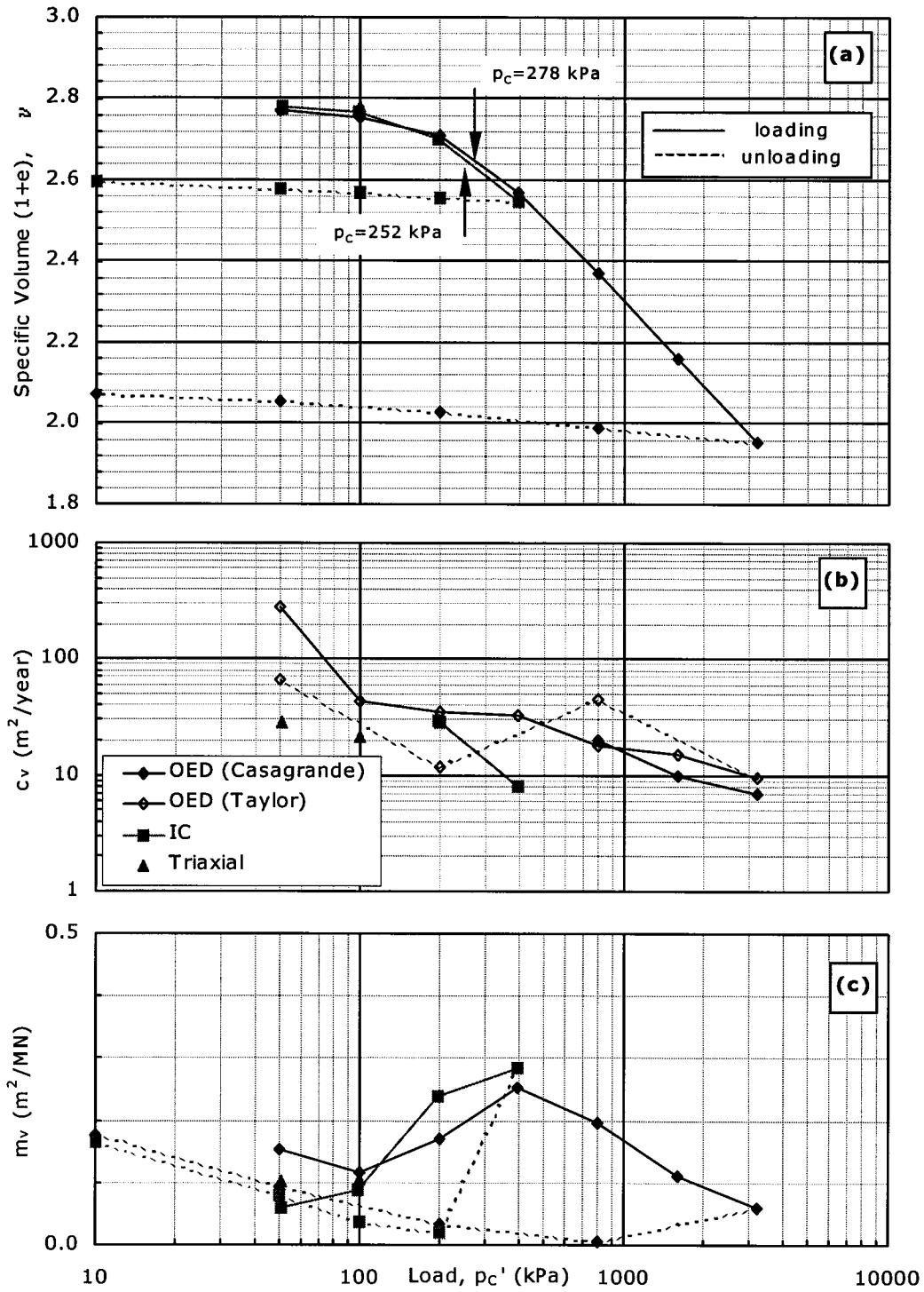
Figure D.8. Oedometer, IC and triaxial consolidation data for w=70%, A_c=5% & T_c=56 days. (a) v vs. $p_c{'}$; (b) c_v & c_{vi} vs. $p_c{'}$; (c) m_v & m_{vi} vs. $p_c{'}$.

Mechanical Characteristics of Kaolin-Cement Mixture 273
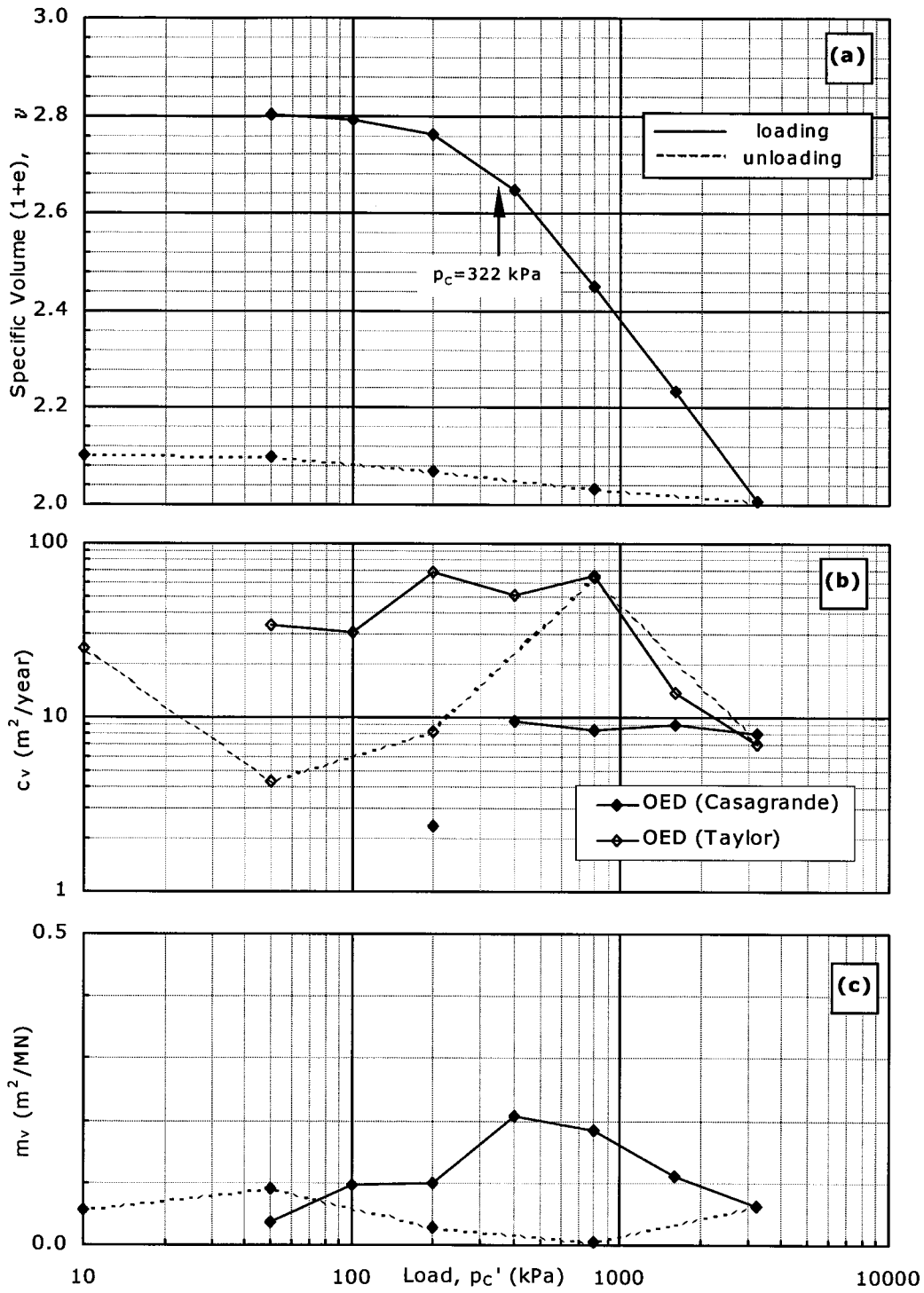
Figure D.9. Oedometer data for w=70%, A_c=5% & T_c=112 days. (a) υ vs. $p_c{}'$; (b) c_v & c_{vi} vs. $p_c{}'$; (c) m_v & m_{vi} vs. $p_c{}'$.

Figure D.10. Oedometer, IC and triaxial consolidation data for w=100%, A_c=5% & T_c=7 days. (a) υ vs. $p_C{}'$; (b) c_v & c_{vi} vs. $p_C{}'$; (c) m_v & m_{vi} vs. $p_C{}'$.

Mechanical Characteristics of Kaolin-Cement Mixture   275
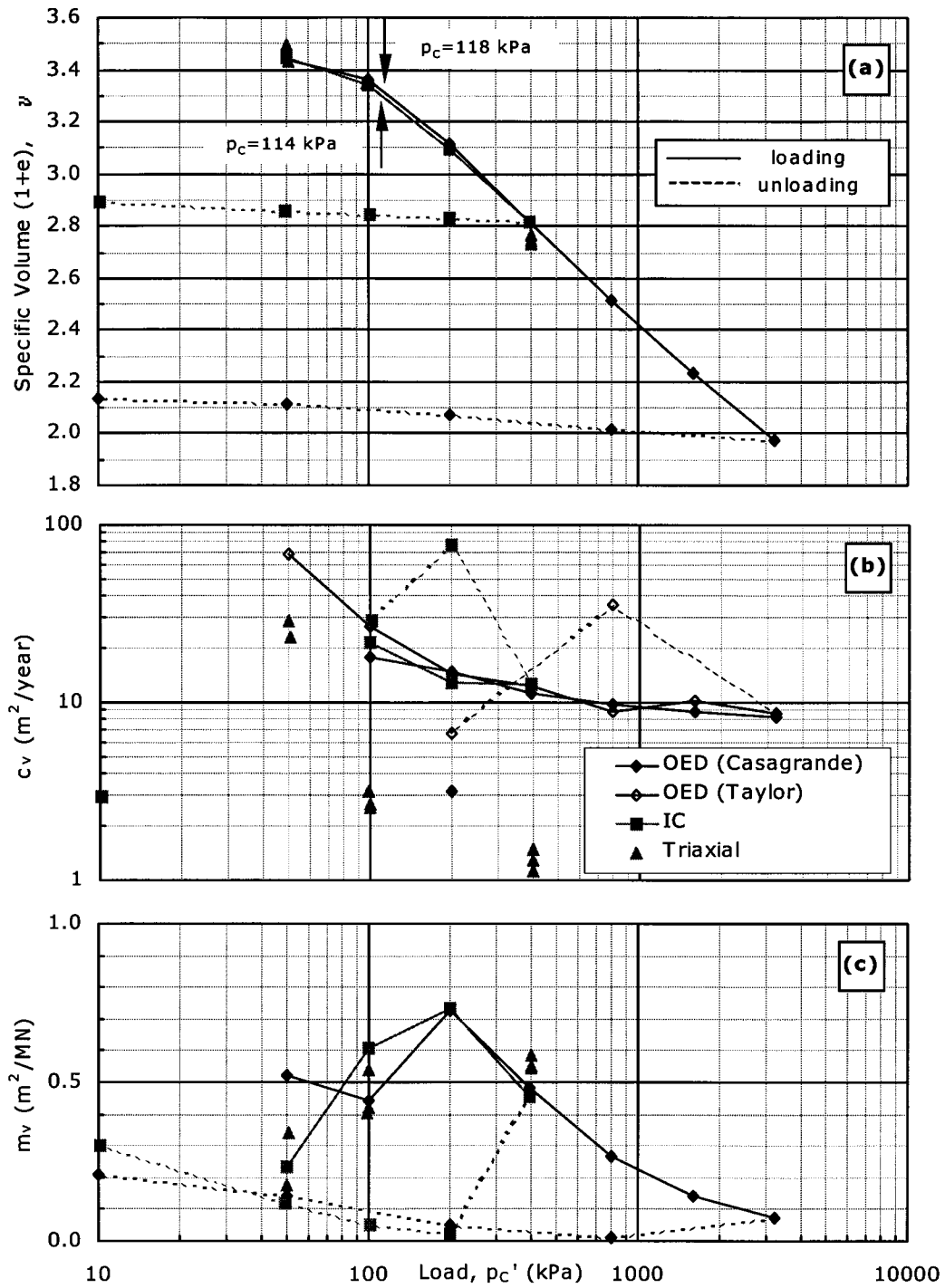
Figure D.11. Oedometer, IC and triaxial consolidation data for w=100%, A_c=5% & T_c=28 days. (a) υ vs. $p_c{}'$; (b) c_v & c_{vi} vs. $p_c{}'$; (c) m_v & m_{vi} vs. $p_c{}'$.
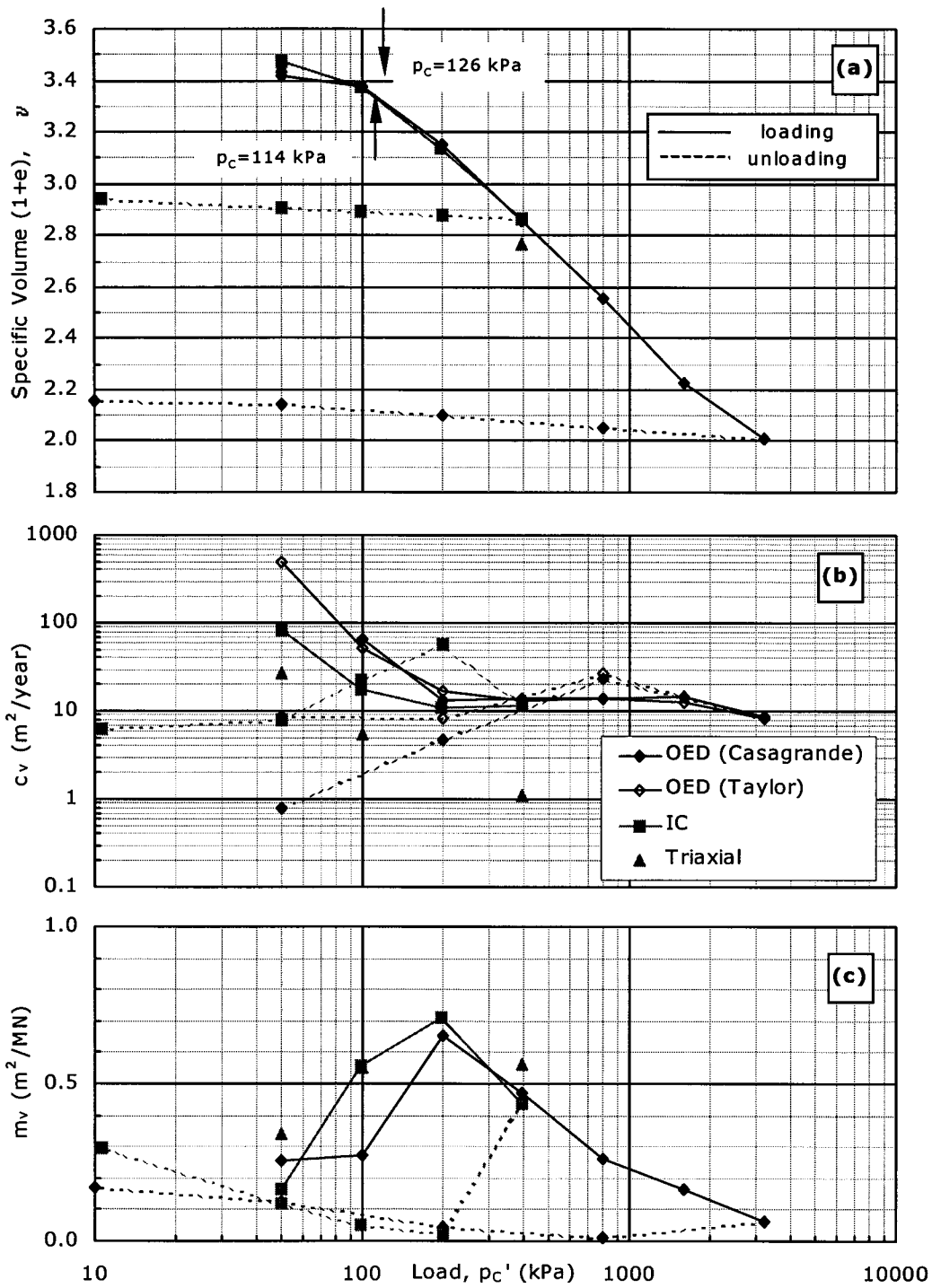
Figure D.12. Oedometer, IC and triaxial consolidation data for w=100%, A_c=5% & T_c=56 days. (a) v vs. p_C'; (b) c_v & c_{vi} vs. p_C'; (c) m_v & m_{vi} vs. p_C'.
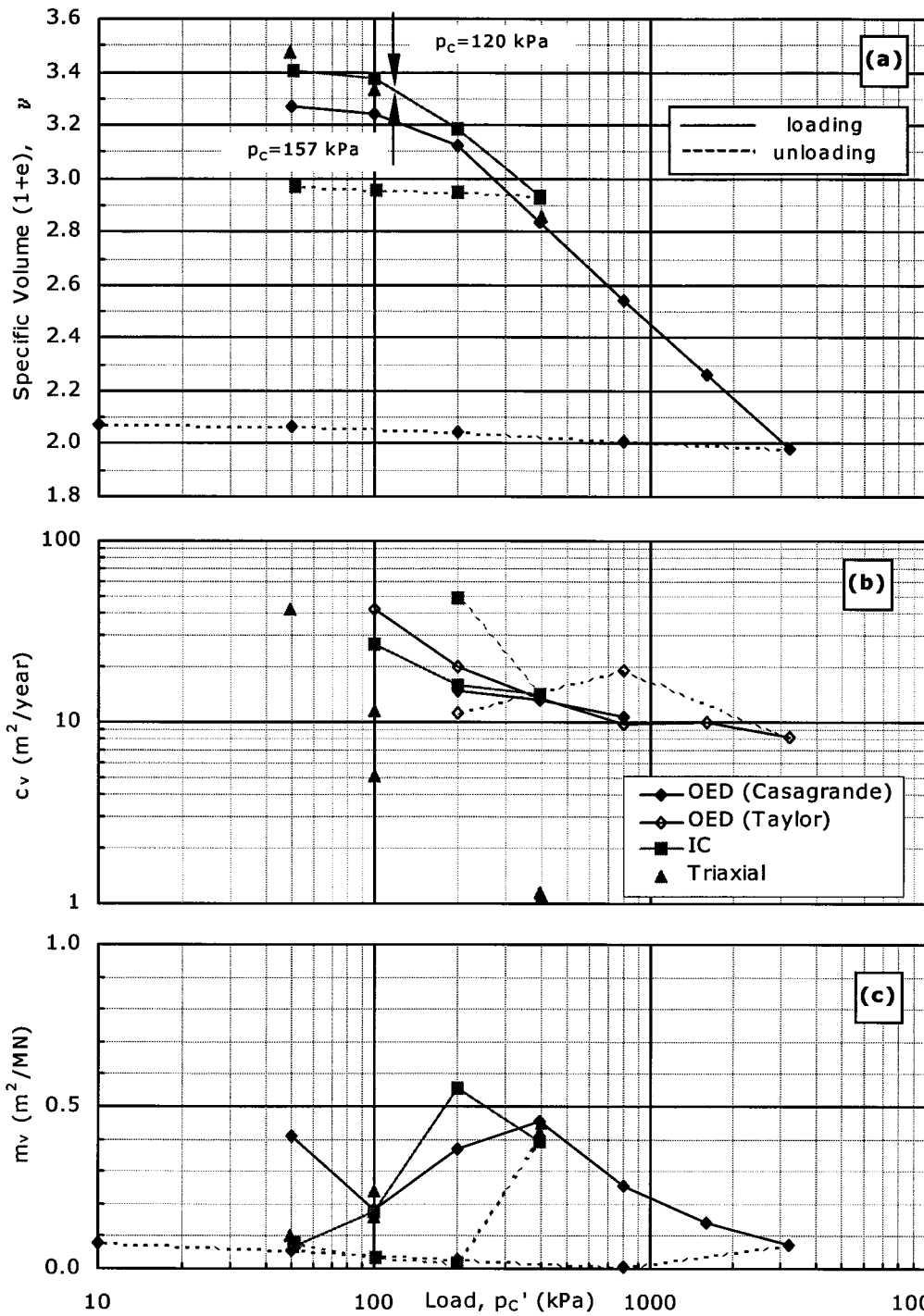
Figure D.13. Oedometer, IC and triaxial consolidation data for w=100%, A_c=5% & T_c=112 days. (a) v vs. $p_C{}'$; (b) c_v & c_{vi} vs. $p_C{}'$; (c) m_v & m_{vi} vs. $p_C{}'$.
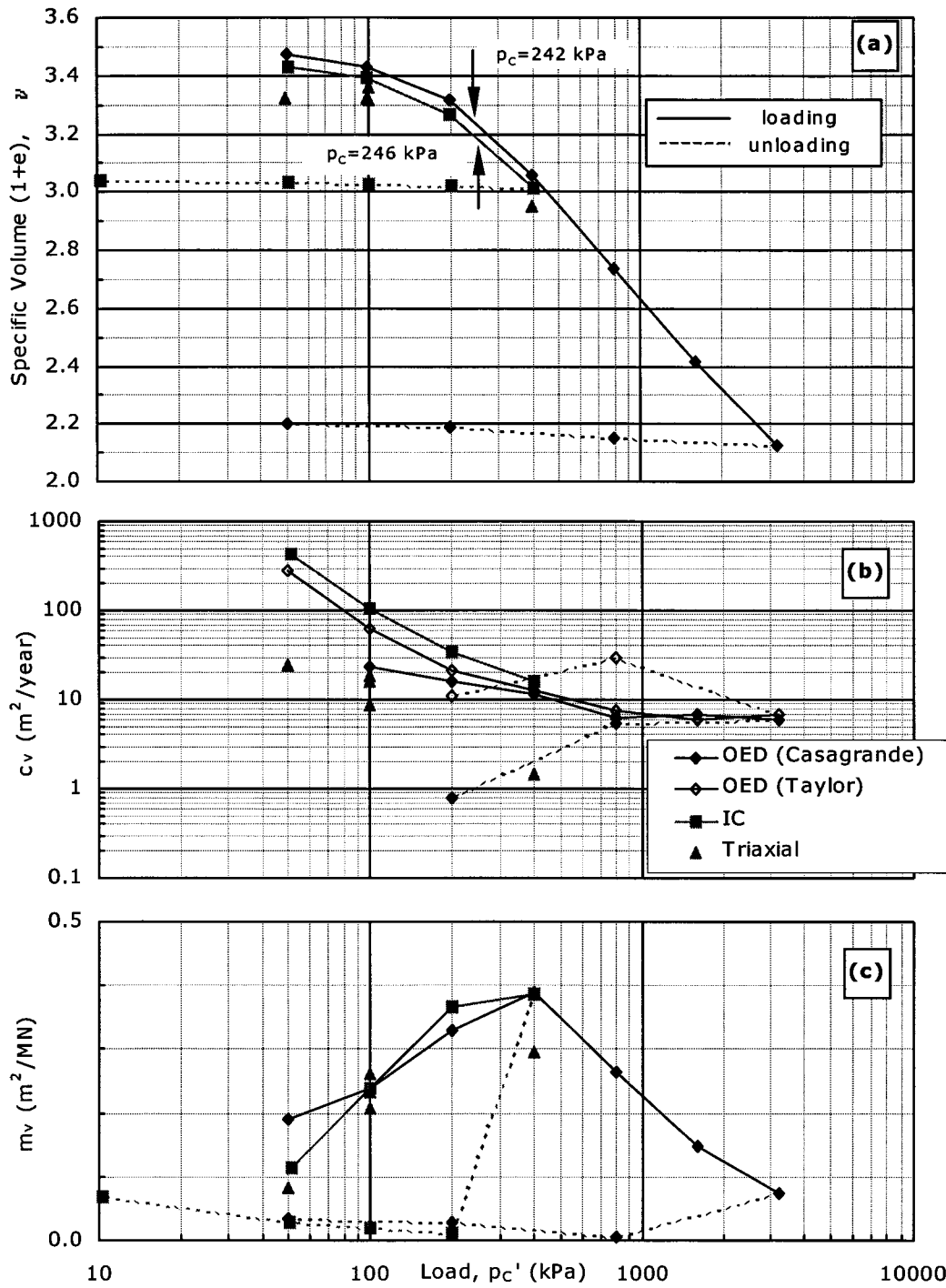
Figure D.14. Oedometer, IC and triaxial consolidation data for w=100%, A_c=10% & T_c=7 days. (a) υ vs. p_C'; (b) c_v & c_{vi} vs. p_C'; (c) m_v & m_{vi} vs. p_C'.
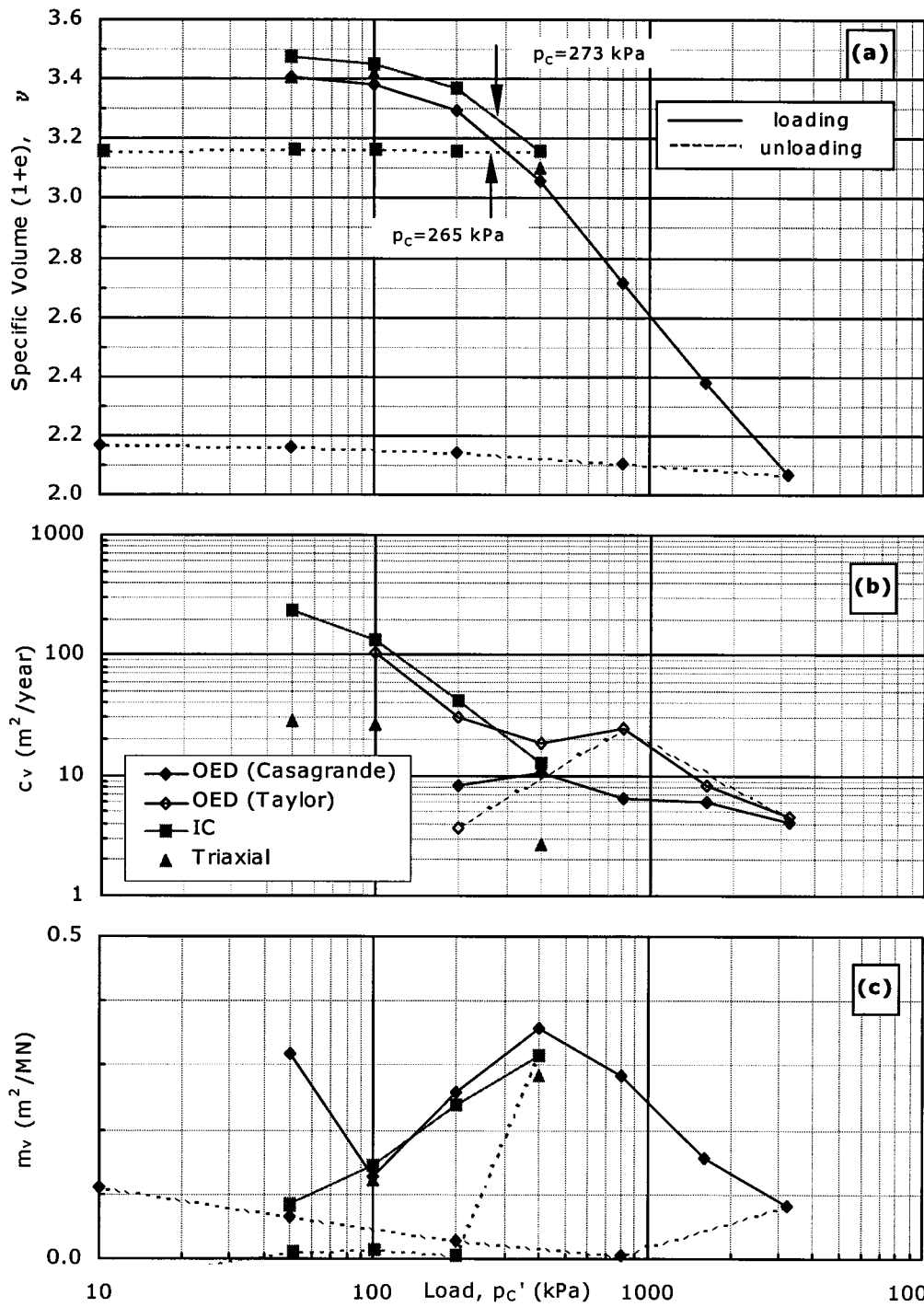
Figure D.15.   Oedometer, IC and triaxial consolidation data for w=100%, A_c=10% & T_c=28 days.   (a) v vs. $p_C{}'$; (b) c_v & c_{vi} vs. $p_C{}'$; (c) m_v & m_{vi} vs. $p_C{}'$.
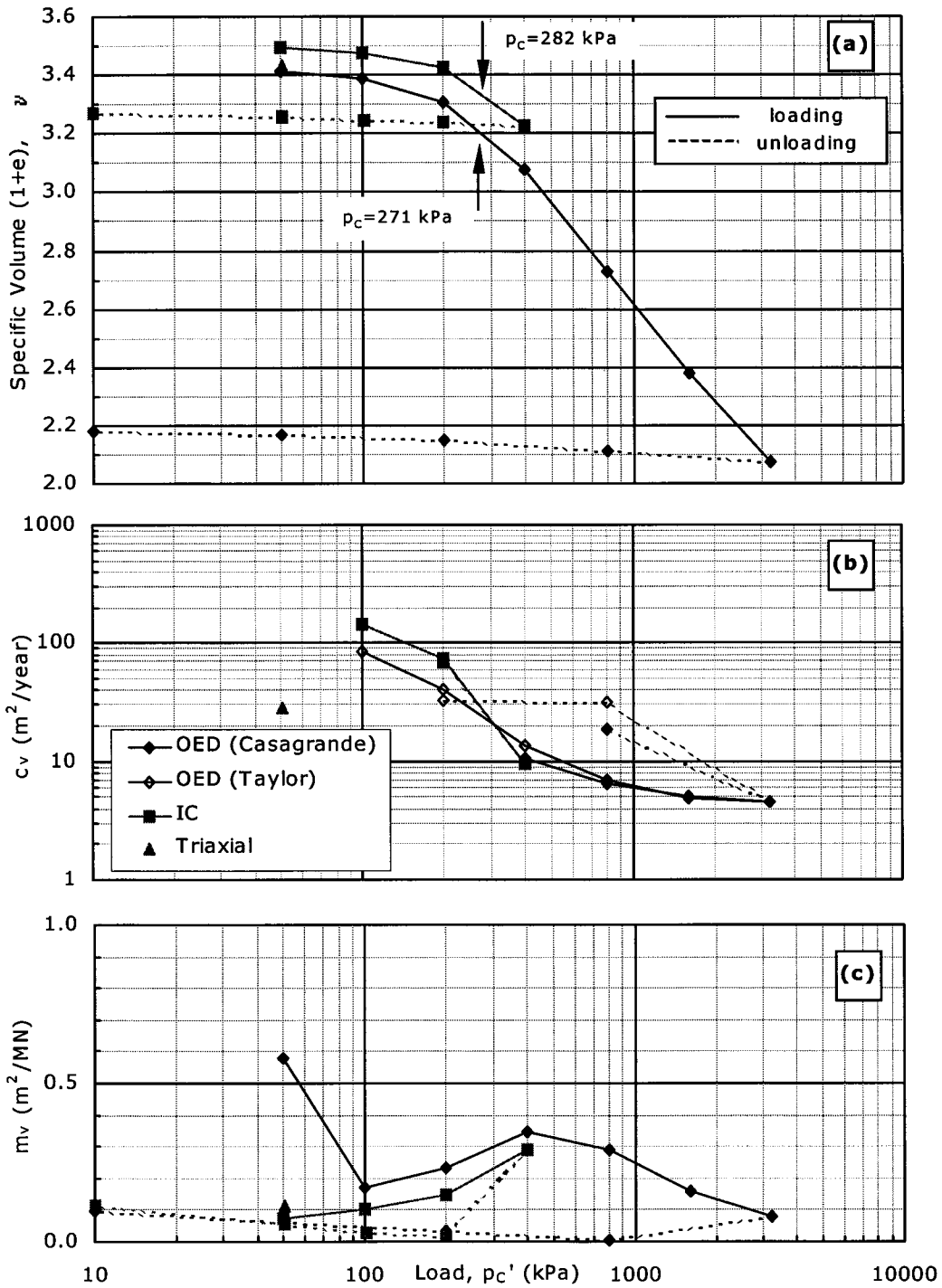
Figure D.16. Oedometer, IC and triaxial consolidation data for w=100%, A_c=10% & T_c=56 days. (a) v vs. $p_c{'}$; (b) c_v & c_{vi} vs. $p_c{'}$; (c) m_v & m_{vi} vs. $p_c{'}$.

Mechanical Characteristics of Kaolin-Cement Mixture   281
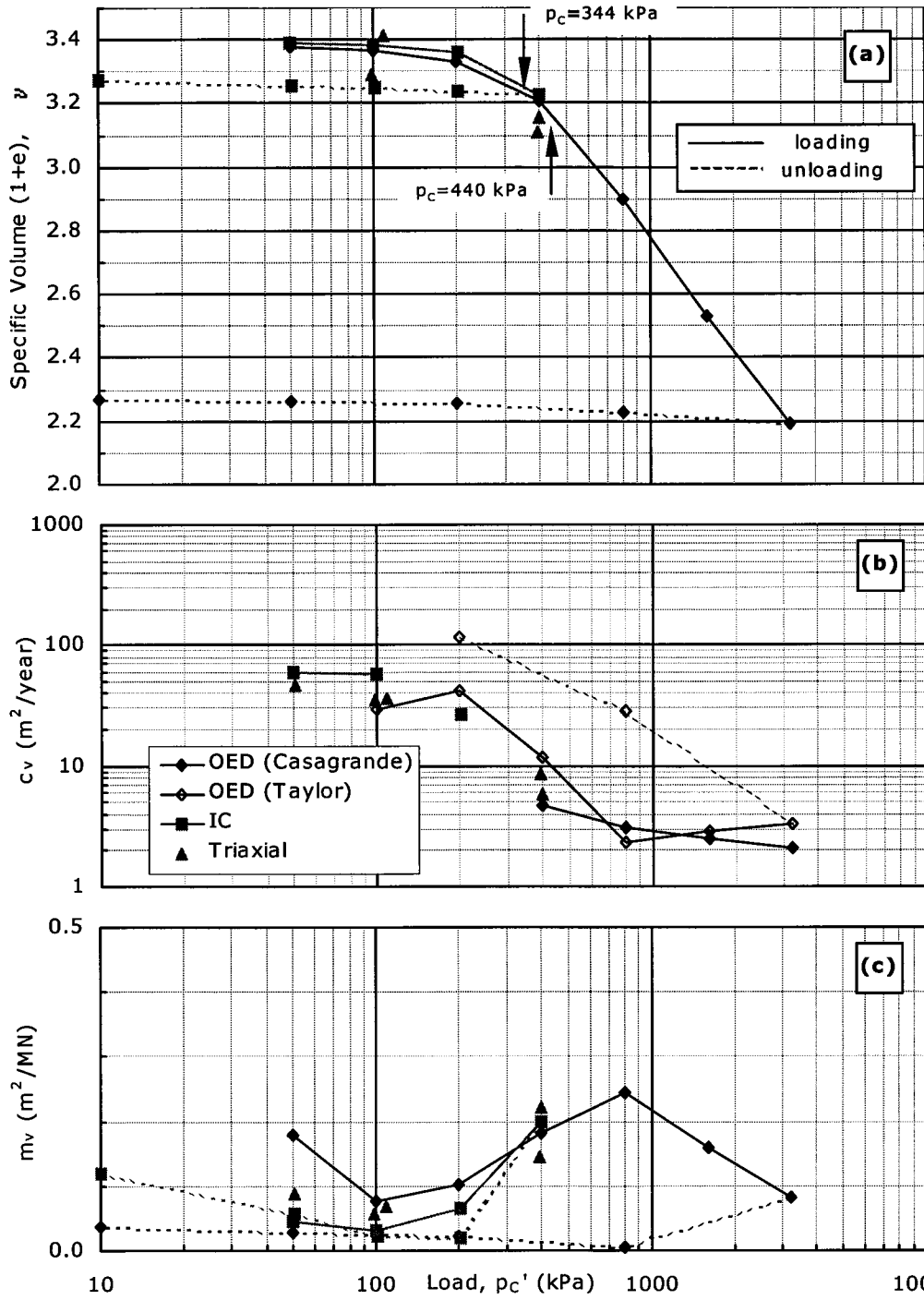
Figure D.17. Oedometer, IC and triaxial consolidation data for w=100%, A_c=10% & T_c=112 days. (a) υ vs. $p_C{}'$; (b) c_v & c_{vi} vs. $p_C{}'$; (c) m_v & m_{vi} vs. $p_C{}'$.
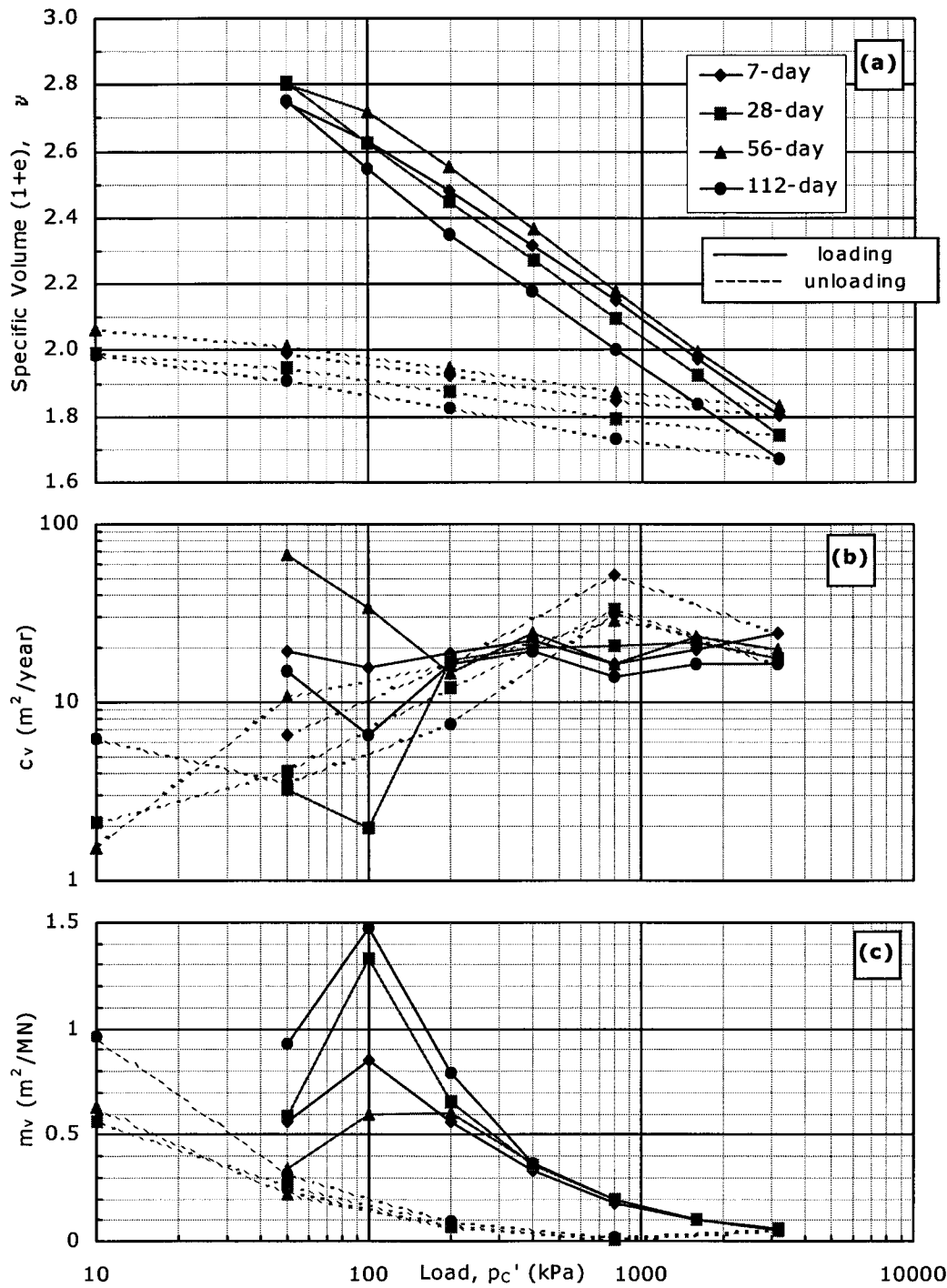
Figure D.18. Oedometer consolidation data for w=70% & A_c=2%. (a) υ vs. p_C'; (b) c_v vs. p_C'; (c) m_v vs. p_C'.
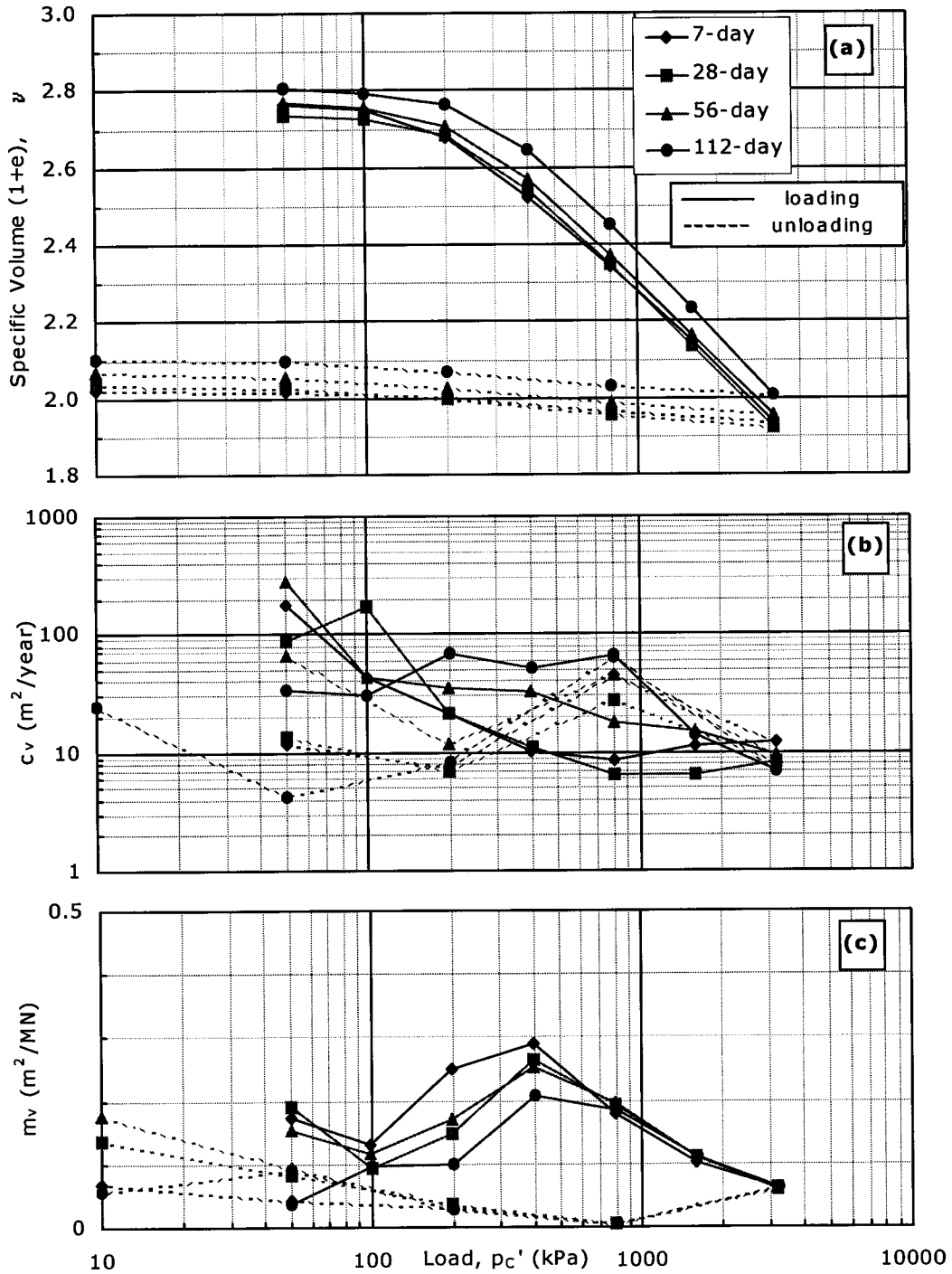
Figure D.19. Oedometer consolidation data for w=70% & A_c=5%. (a) υ vs. $p_c{}'$; (b) c_v vs. $p_c{}'$; (c) m_v vs. $p_c{}'$.
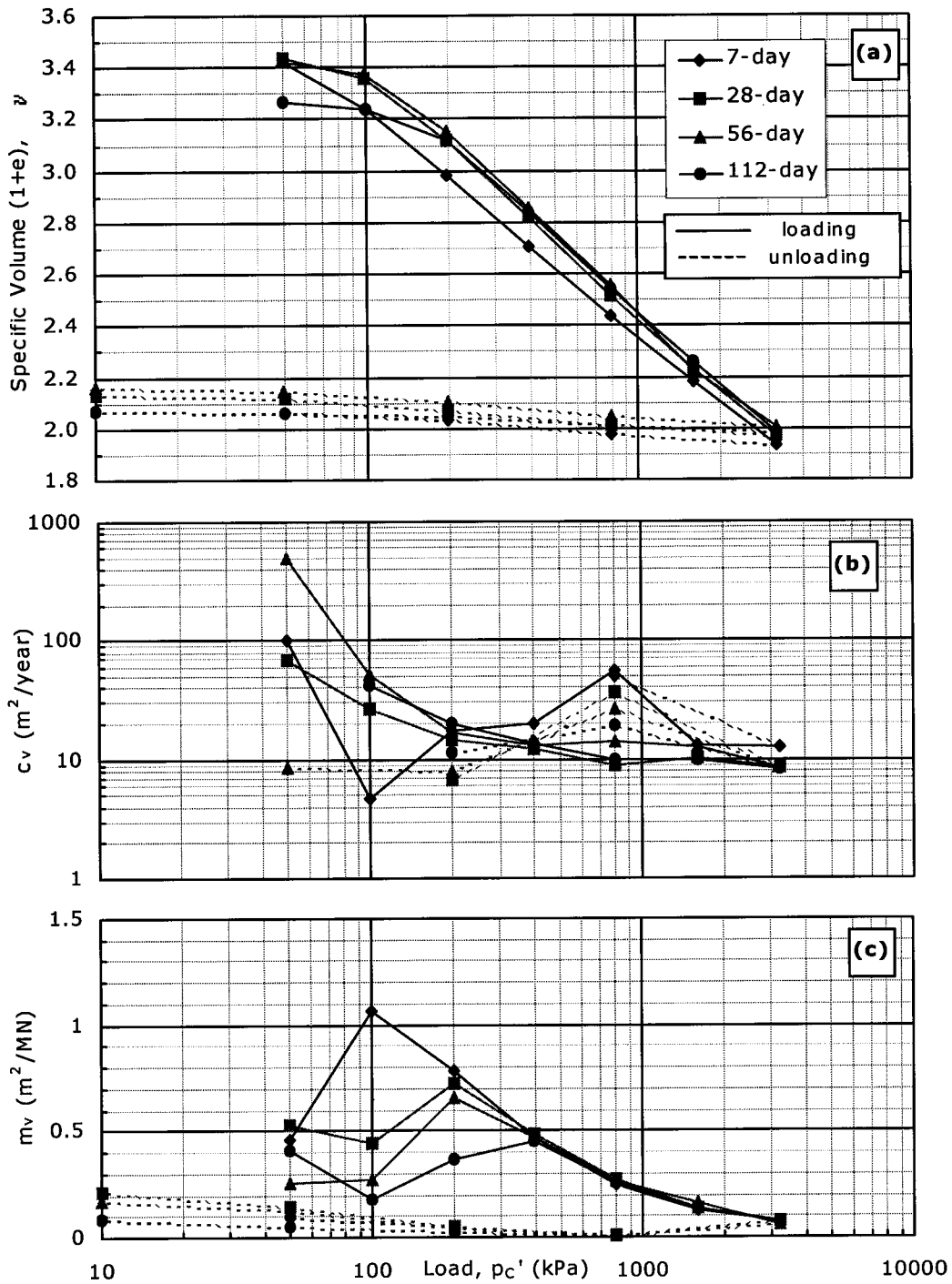
Figure D.20. Oedometer consolidation data for w=100% & A_c=5%. (a) v vs. $p_c{}'$; (b) c_v vs. $p_c{}'$; (c) m_v vs. $p_c{}'$.
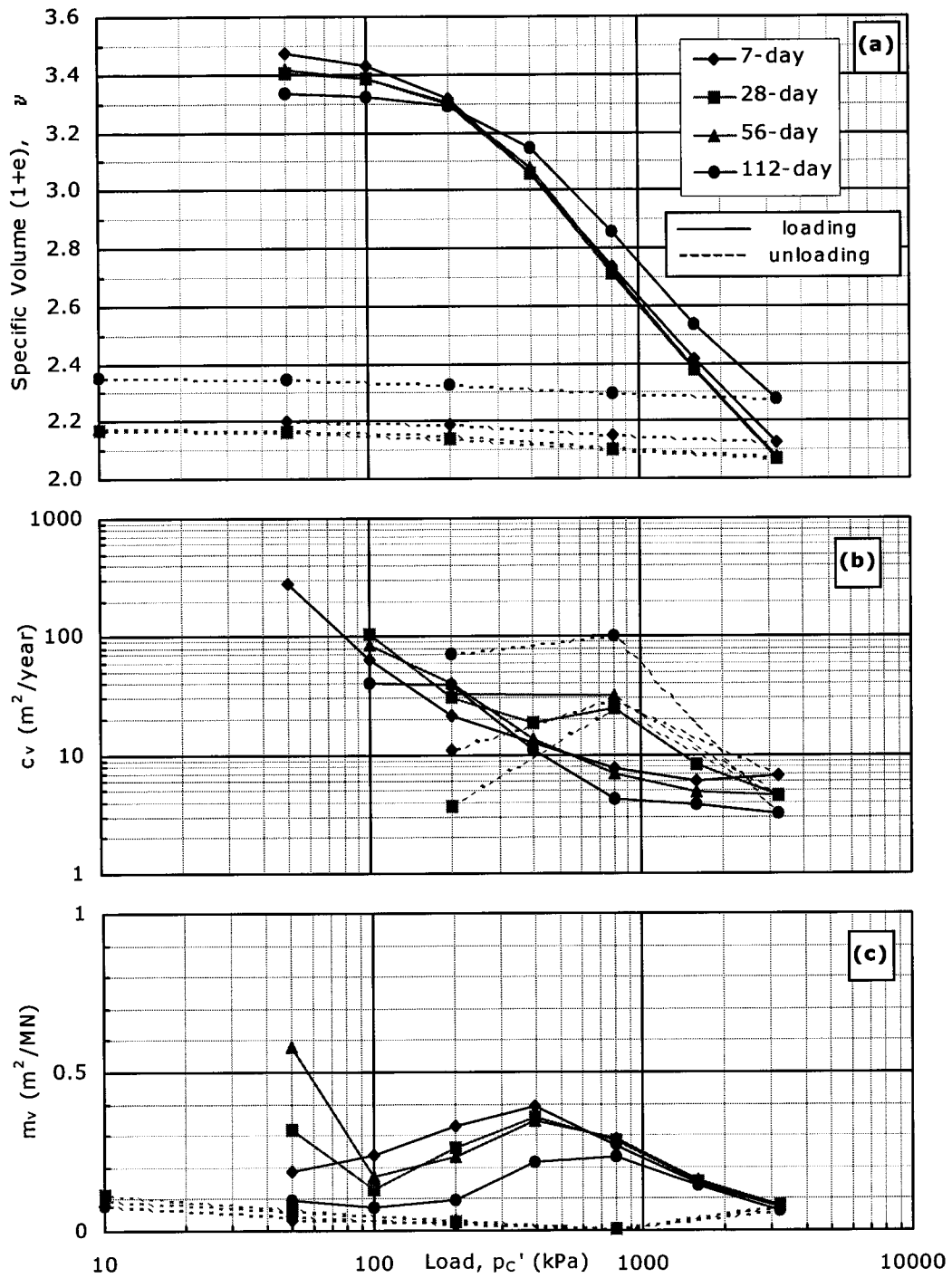
Figure D.21. Oedometer consolidation data for w=100% & A_c=10%. (a) υ vs. p_c'; (b) c_v vs. p_c'; (c) m_v vs. p_c'.
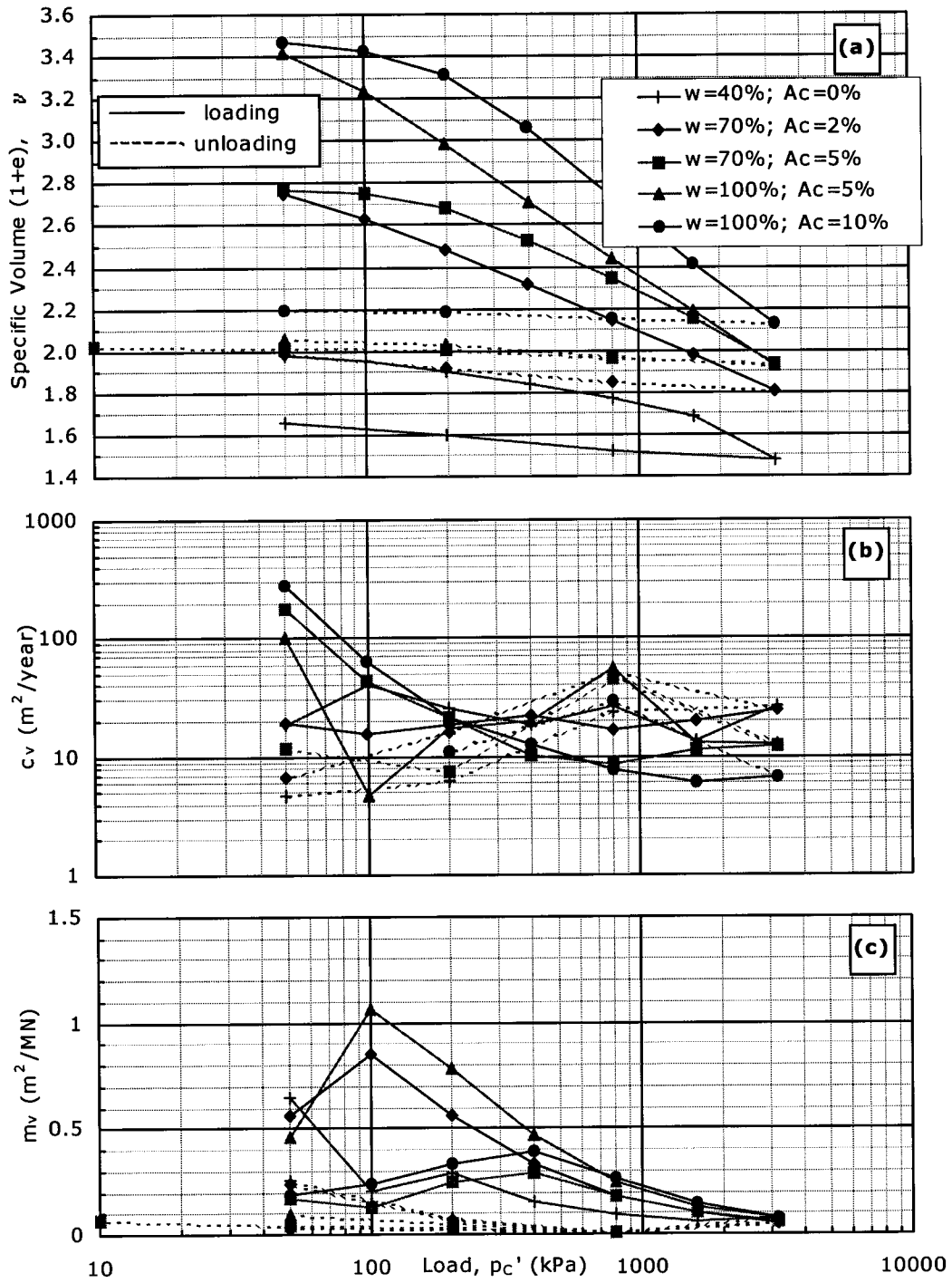
Figure D.22. Oedometer consolidation data for $T_c=7$ days. (a) υ vs. p_c'; (b) c_v vs. p_c'; (c) m_v vs. p_c'.

Mechanical Characteristics of Kaolin-Cement Mixture 287
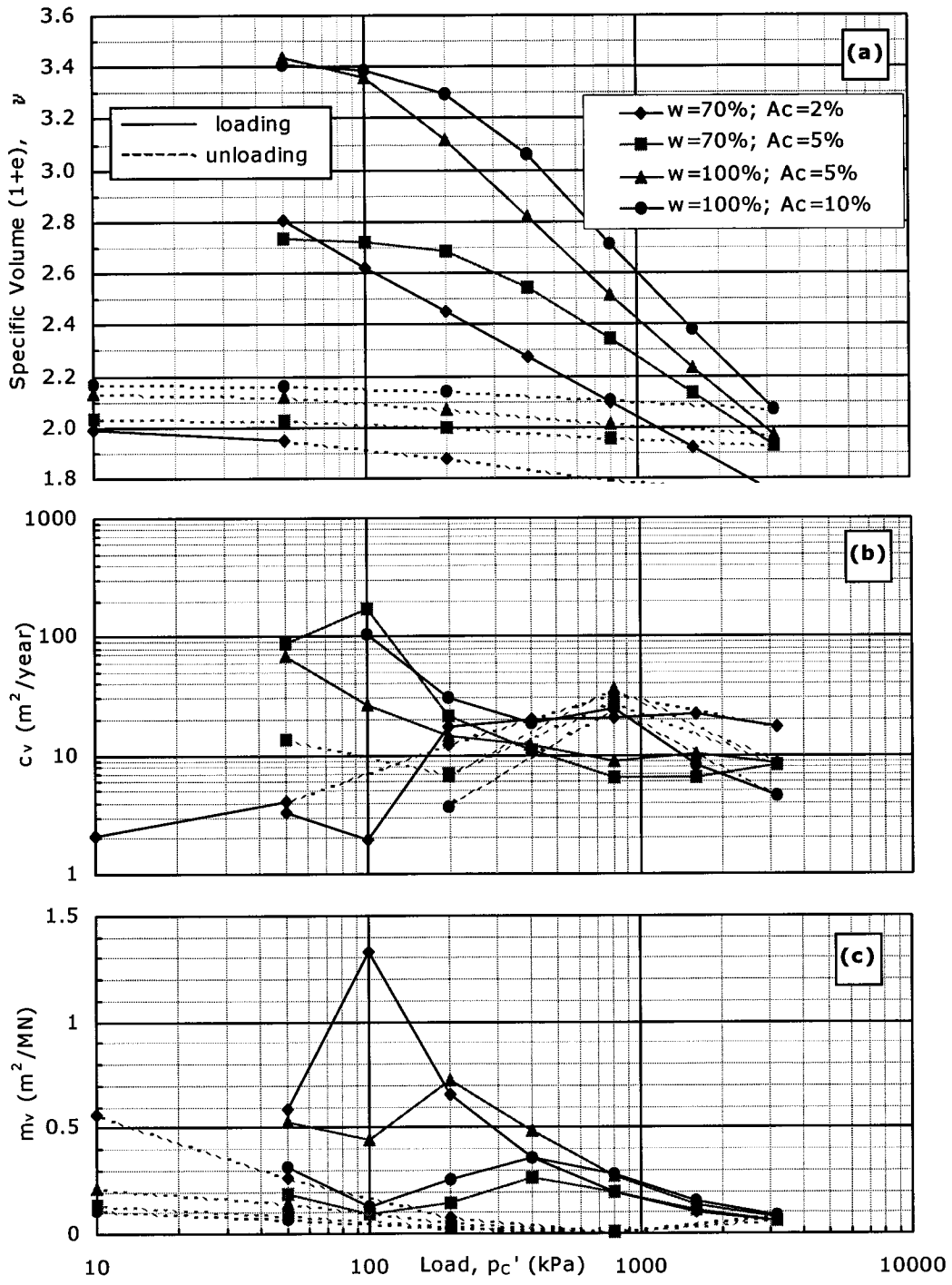
Figure D.23. Oedometer consolidation data for T_c=28 days. (a) v vs. $p_C{}'$; (b) c_v vs. $p_C{}'$; (c) m_v vs. $p_C{}'$.
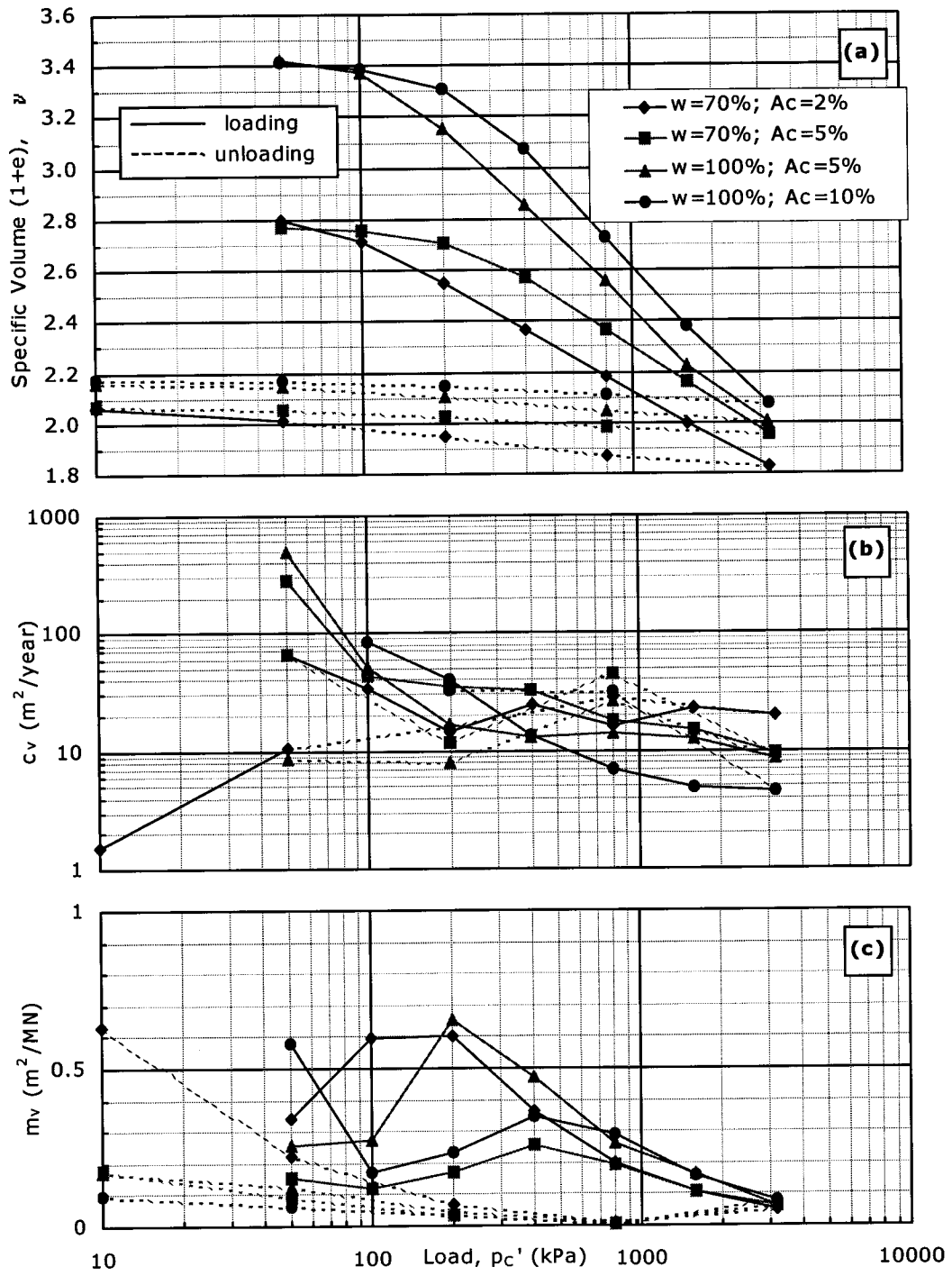
Figure D.24. Oedometer consolidation data for $T_c=56$ days. (a) υ vs. $p_c{}'$; (b) c_v vs. $p_c{}'$; (c) m_v vs. $p_c{}'$.
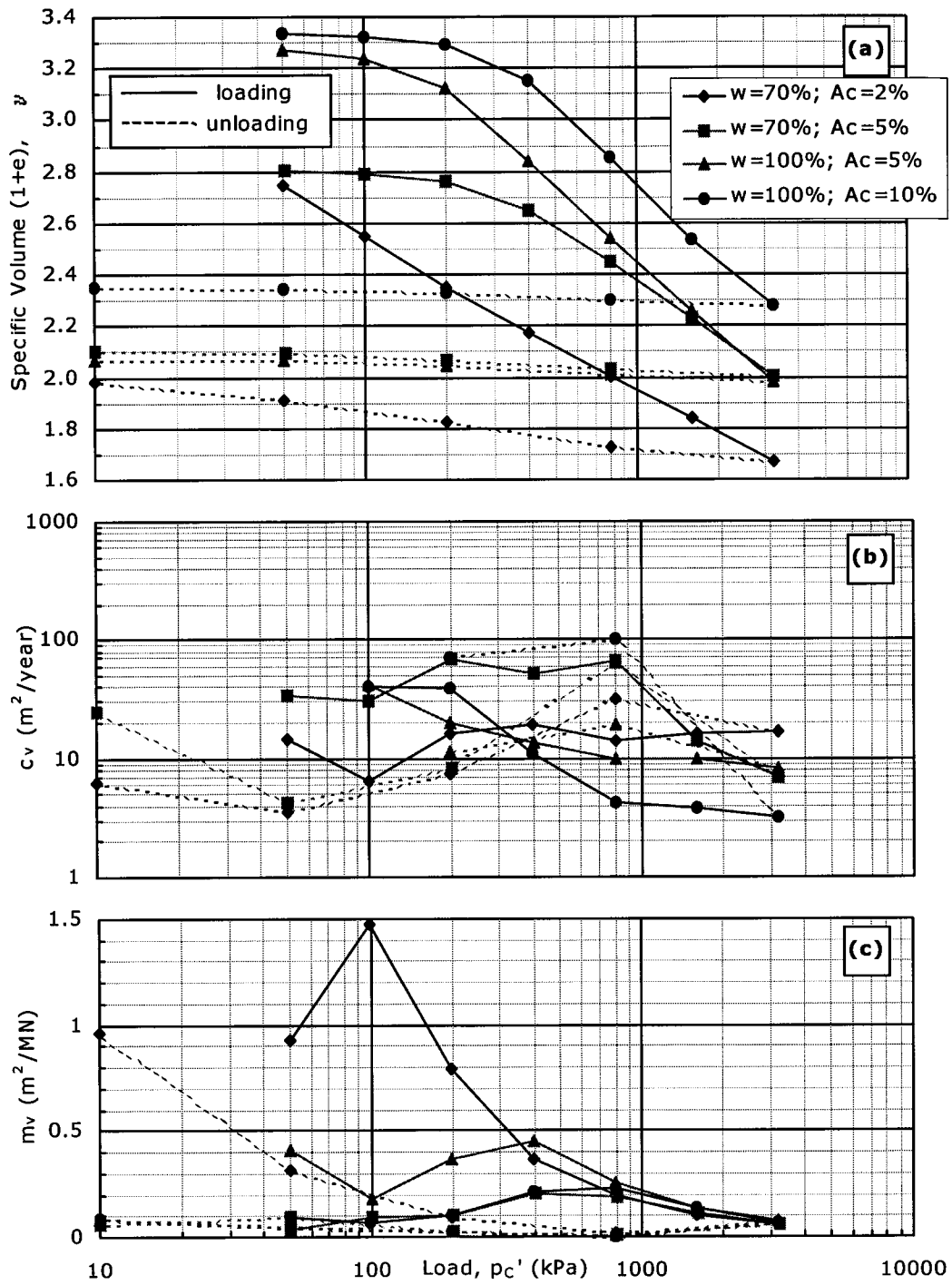
Figure D.25. Oedometer consolidation data for T_c=112 days. (a) υ vs. $p_C{}'$; (b) c_v vs. $p_C{}'$; (c) m_v vs. $p_C{}'$.

APPENDIX E: PHOTOMICROGRAPHS OF OVEN-DRIED KAOLIN AND KAOLIN-CEMENT

Chapter 7 describes the microstructure of kaolin and kaolin-cement and details the results of the Scanning Electron Microscope (SEM) analysis. Photomicrographs were taken with a traditional SEM on May 2 and May 10, 2001 at the University of Alberta.

To prepare samples for scanning, sub-samples were dried in a low temperature oven and then broken to expose a fresh and clean fracture surface. Silver paint was used as glue to paste the sub-sample onto the sample stub and to coat all exposed surfaces of the sub-sample that did not require scanning. A line of silver paint was also painted across the top of the sample. The use of silver paint improves the conductivity of otherwise poor samples, such as porous soil. Samples were left to dry at least overnight, and then covered with 1 or 2 coats of gold, following the "sputter" method. Scanning was done immediately, while the gold was still fresh.

An acceleration voltage of 2 kV was selected. This is relatively low but necessary in order to minimize undesirable charging during scanning; charging was a problem for the porous kaolin and kaolin-cement samples, particularly when the cement content was low or zero. Charging causes bright areas or streaks across the image, but was reduced in areas near the conductive silver paint. Therefore, images were captured near the line of silver paint across the top of the sample so that the best image possible could be obtained. However, areas of charging are still visible.

Images were captured at three separate magnifications: 1000X, 3000X and 10,000X; images were then reduced for presentation purposes to magnifications of approximately 750X, 2250X and 7500X, respectively.

All mixtures considered in the laboratory program were sub-sampled and prepared for SEM analysis, with the exception of two. In addition, samples of pure kaolin at moisture contents of 40 and 70 percent were scanned. The following is a summary of the photomicrographs included in Appendix E.

Table E.1. Summary of SEM Photomicrographs.

w (%)	A_c(%)	Curing Time, T_c (days)			
		7	28	56	112
40	0*	E.1			
70	0*	E.2			
70	2	E.3	E.4	■	E.5
	5	E.6	E.7	E.8	■
100	5	E.9	E.10	E.11	E.12
	10	E.13	E.14	E.15	E.16

*samples tested immediately following casting; T_c=0 days.
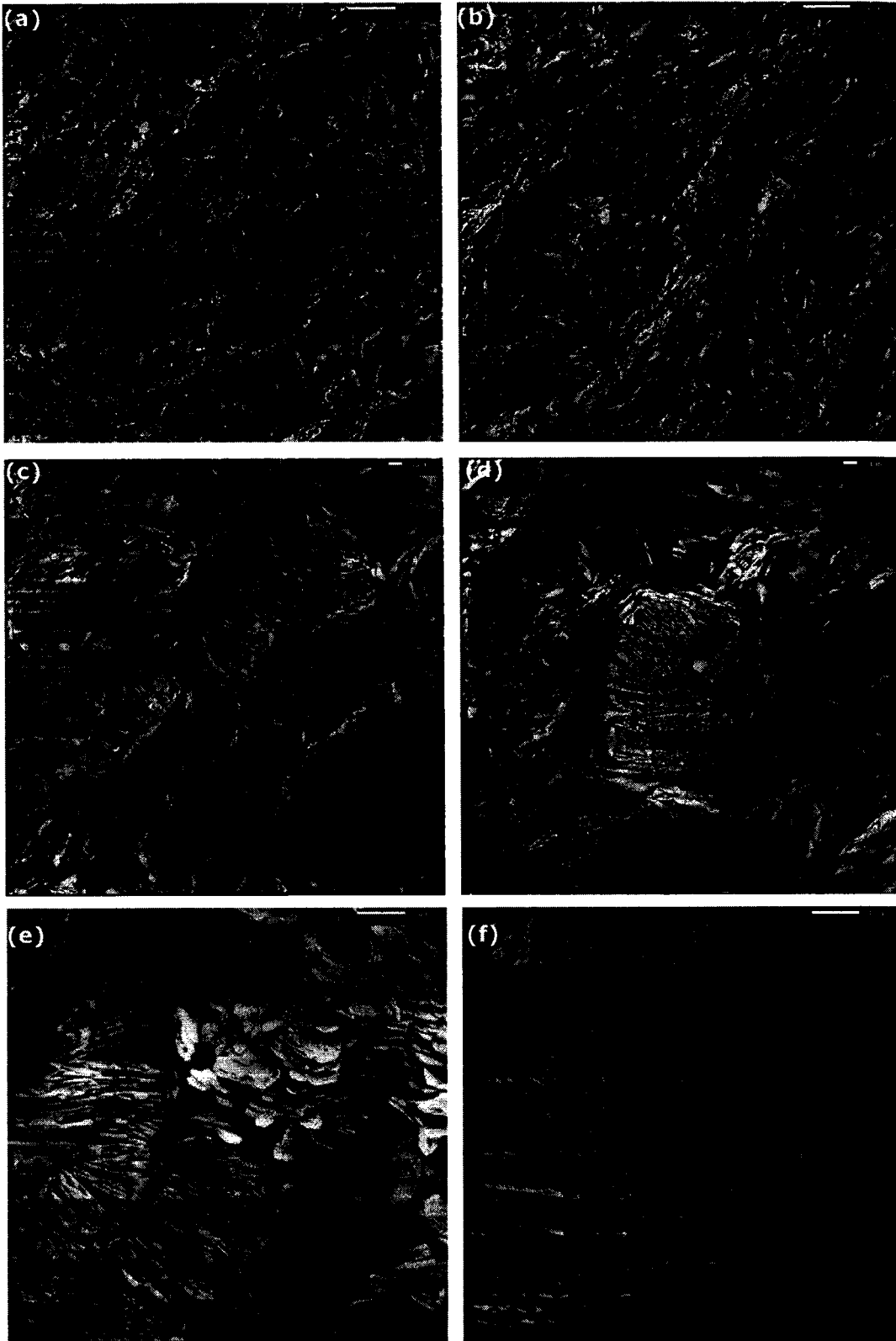
Figure E.1. Photomicrographs of oven-dried kaolin at w=40%. (a) & (b) M≈750X; (c) & (d) M≈2250X; (e) & (f) M≈7500X.
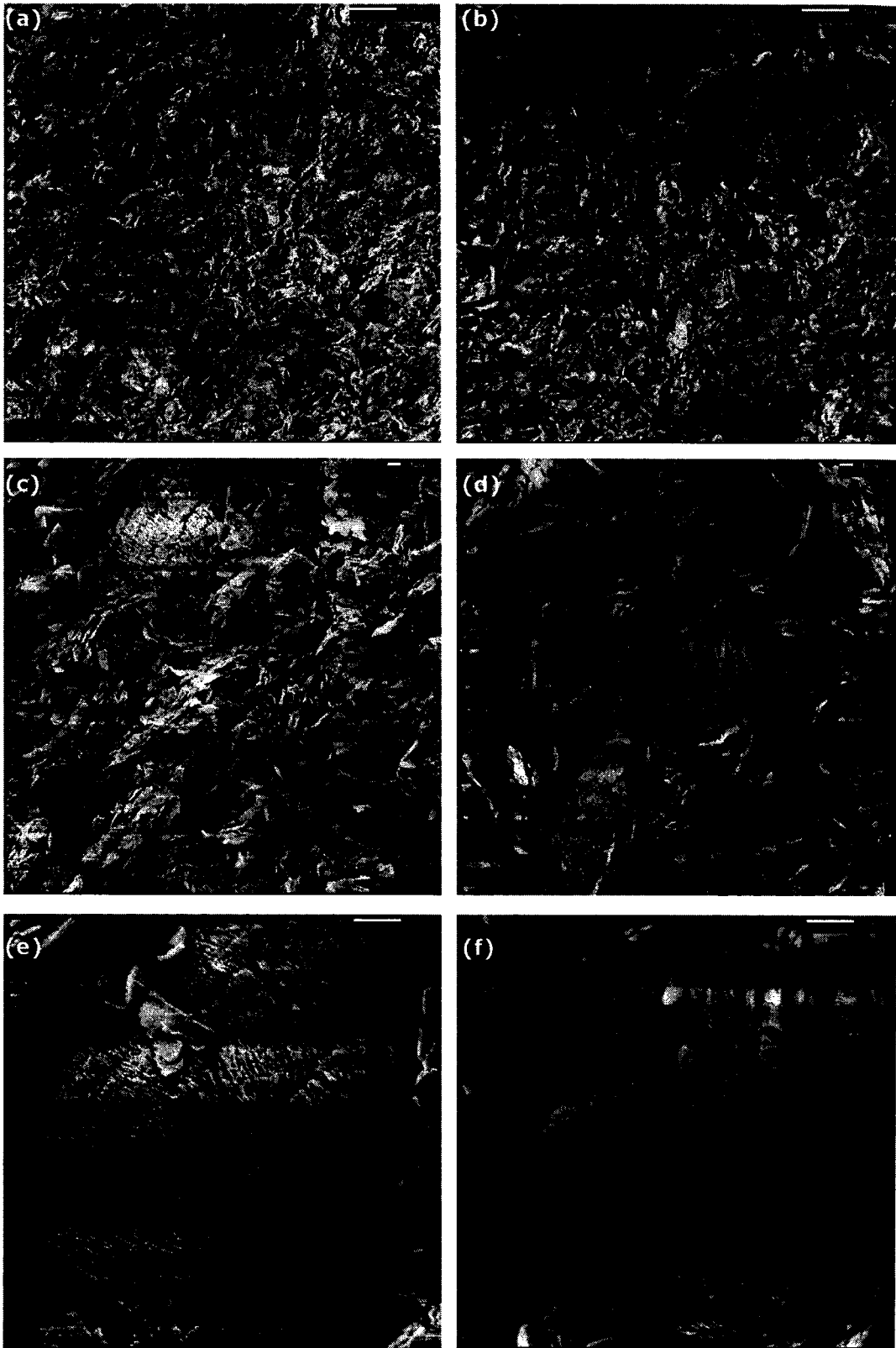
Figure E.2. Photomicrographs of oven-dried kaolin at w=70%. (a) & (b) M≈750X; (c) & (d) M≈2250X; (e) & (f) M≈7500X.
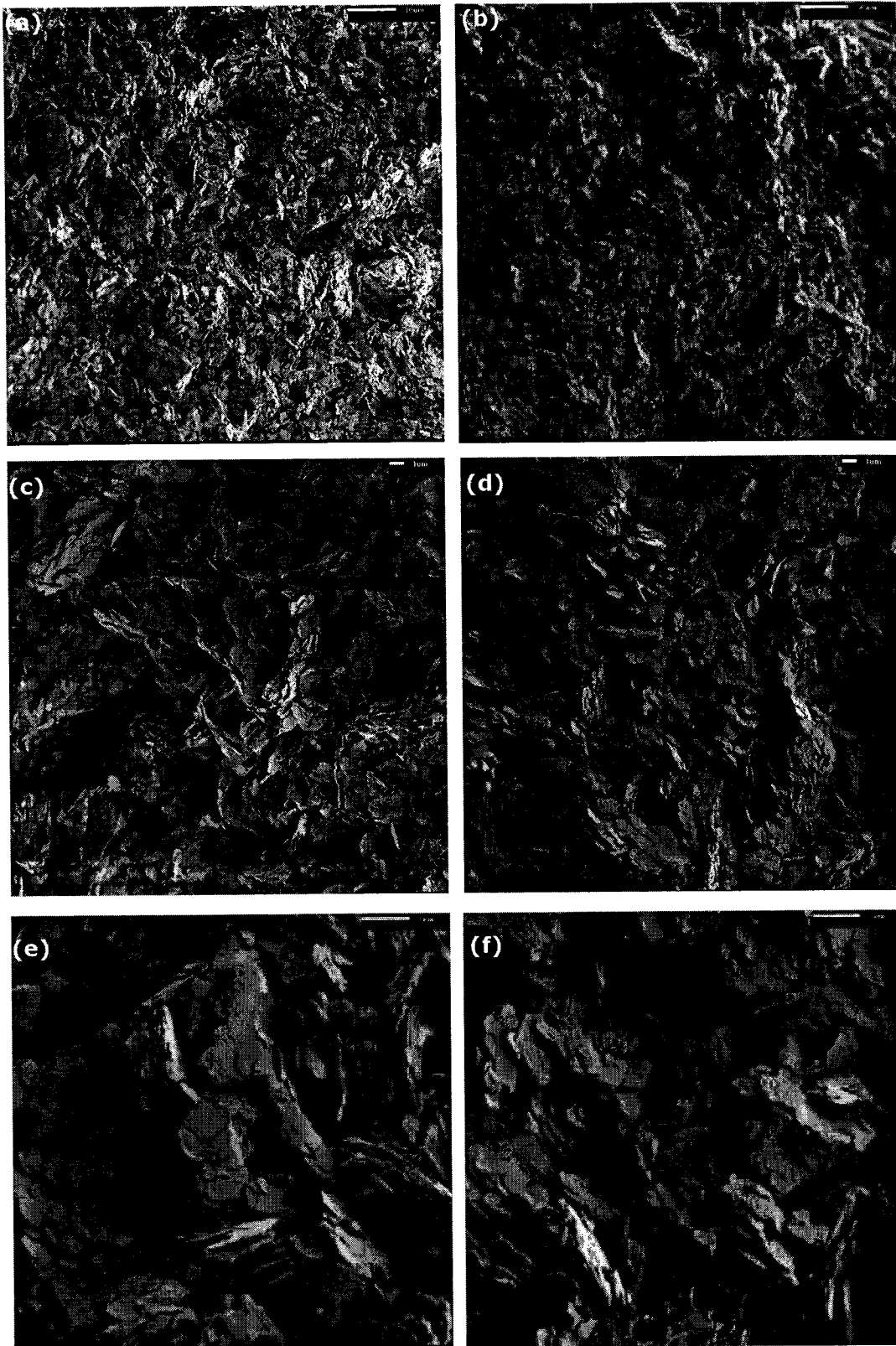
Figure E.3. Photomicrographs of oven-dried kaolin-cement at w=70%, A_c=2% and T=7 days. (a) & (b) M≈750X; (c) & (d) M≈2250X; (e) & (f) M≈7500X.
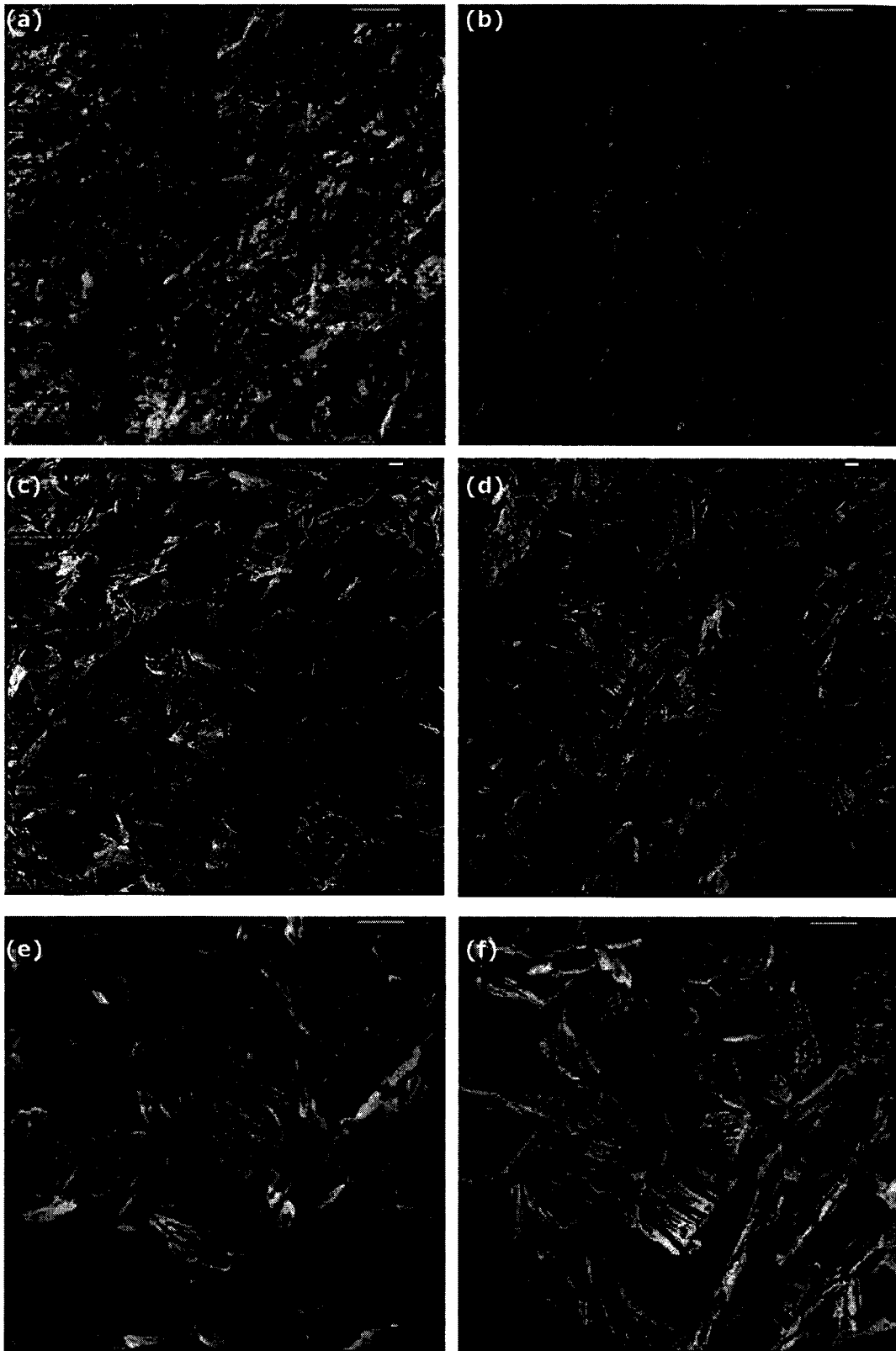
Figure E.4. Photomicrographs of oven-dried kaolin-cement at w=70%, A_c=2% and T_c =28 days. (a) & (b) M$\approx$750X; (c) & (d) M$\approx$2250X; (e) & (f) M$\approx$7500X.
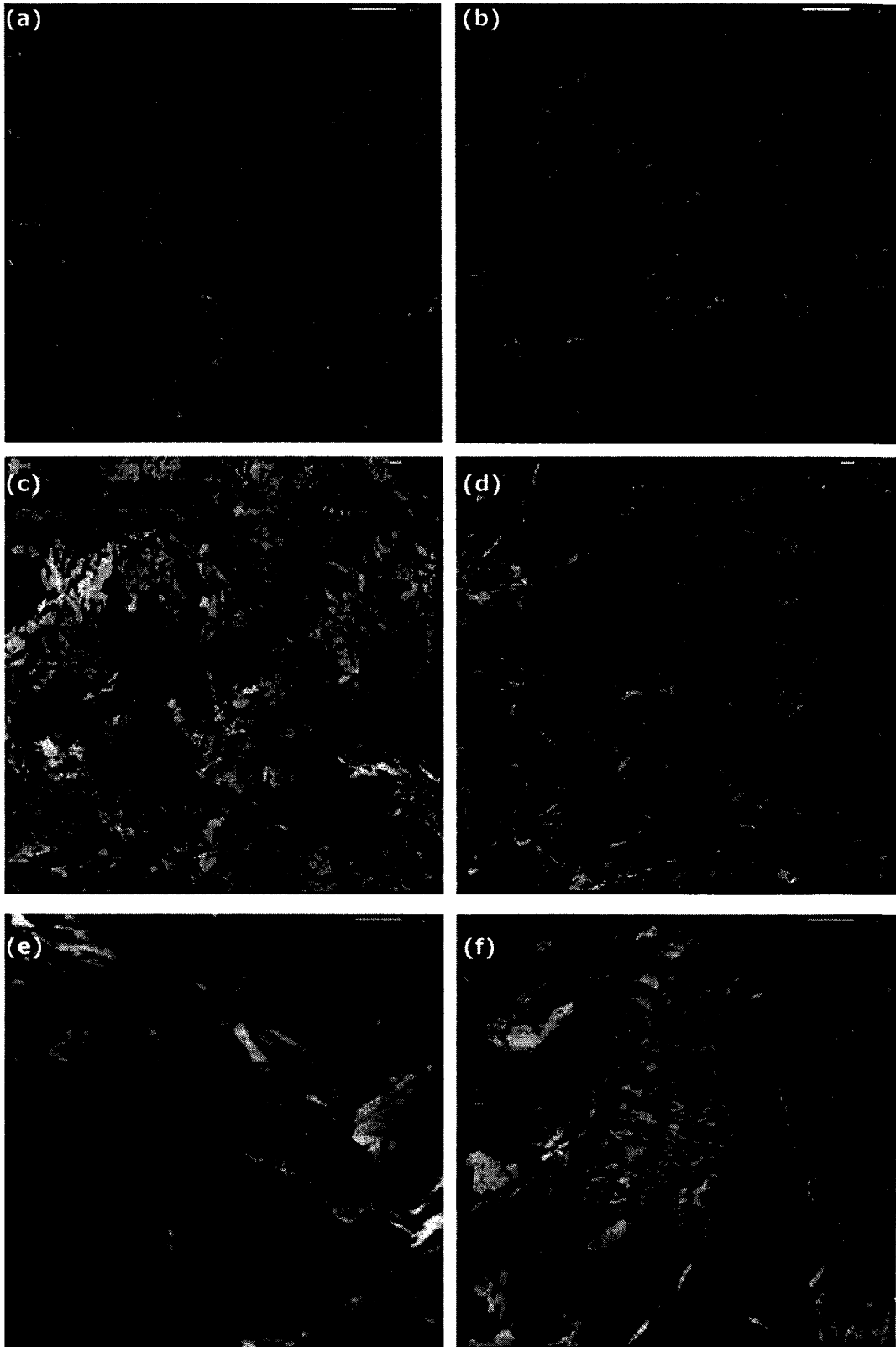
Figure E.5. Photomicrographs of oven-dried kaolin-cement at w=70%, A_c=2% and T_c =112 days. (a) & (b) M≈750X; (c) & (d) M≈2250X; (e) & (f) M≈7500X.
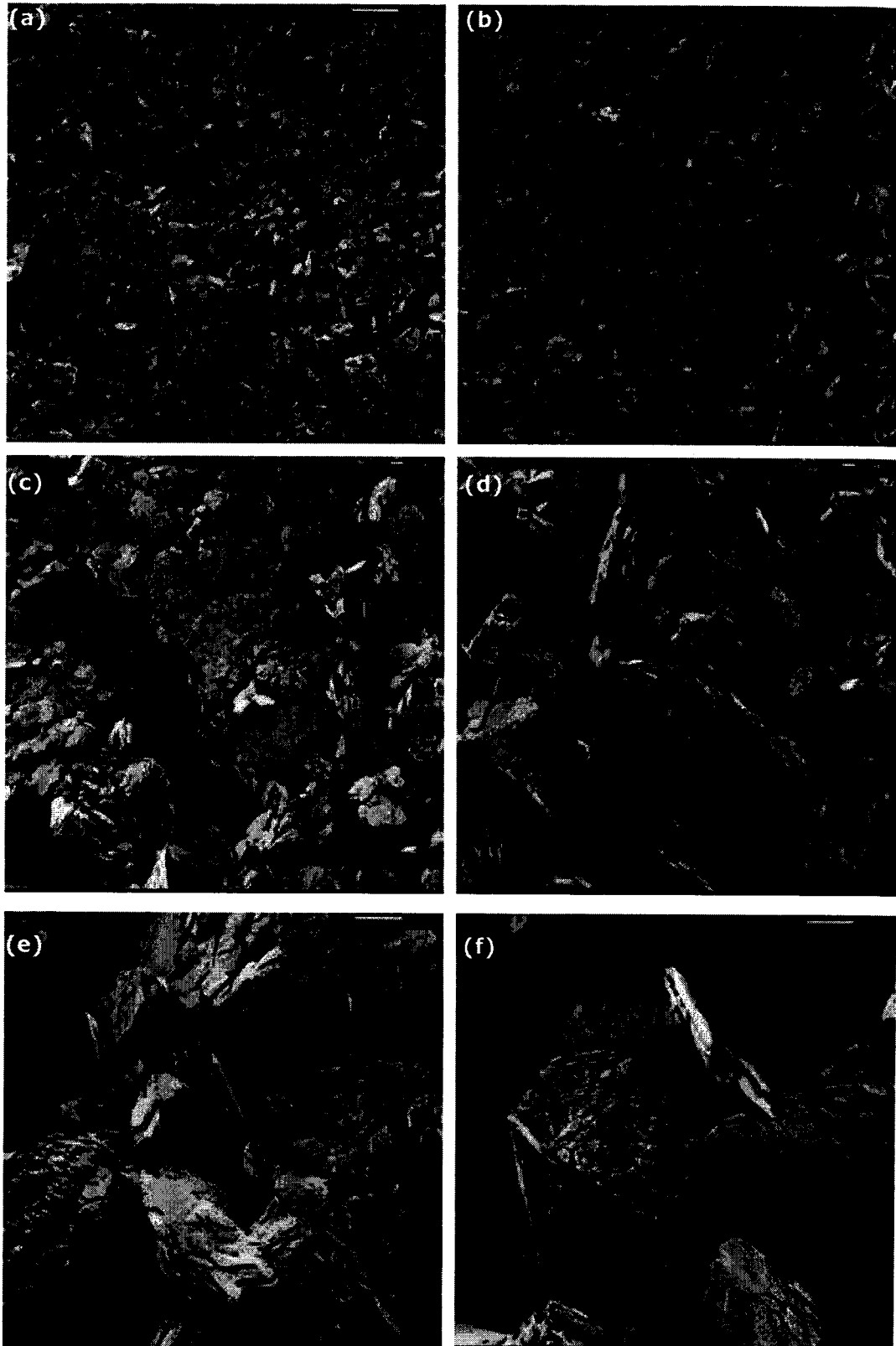
Figure E.6. Photomicrographs of oven-dried kaolin-cement at w=70%, A_c=5% and T_c =7 days. (a) & (b) M≈750X; (c) & (d) M≈2250X; (e) & (f) M≈7500X.

Mechanical Characteristics of Kaolin-Cement Mixture
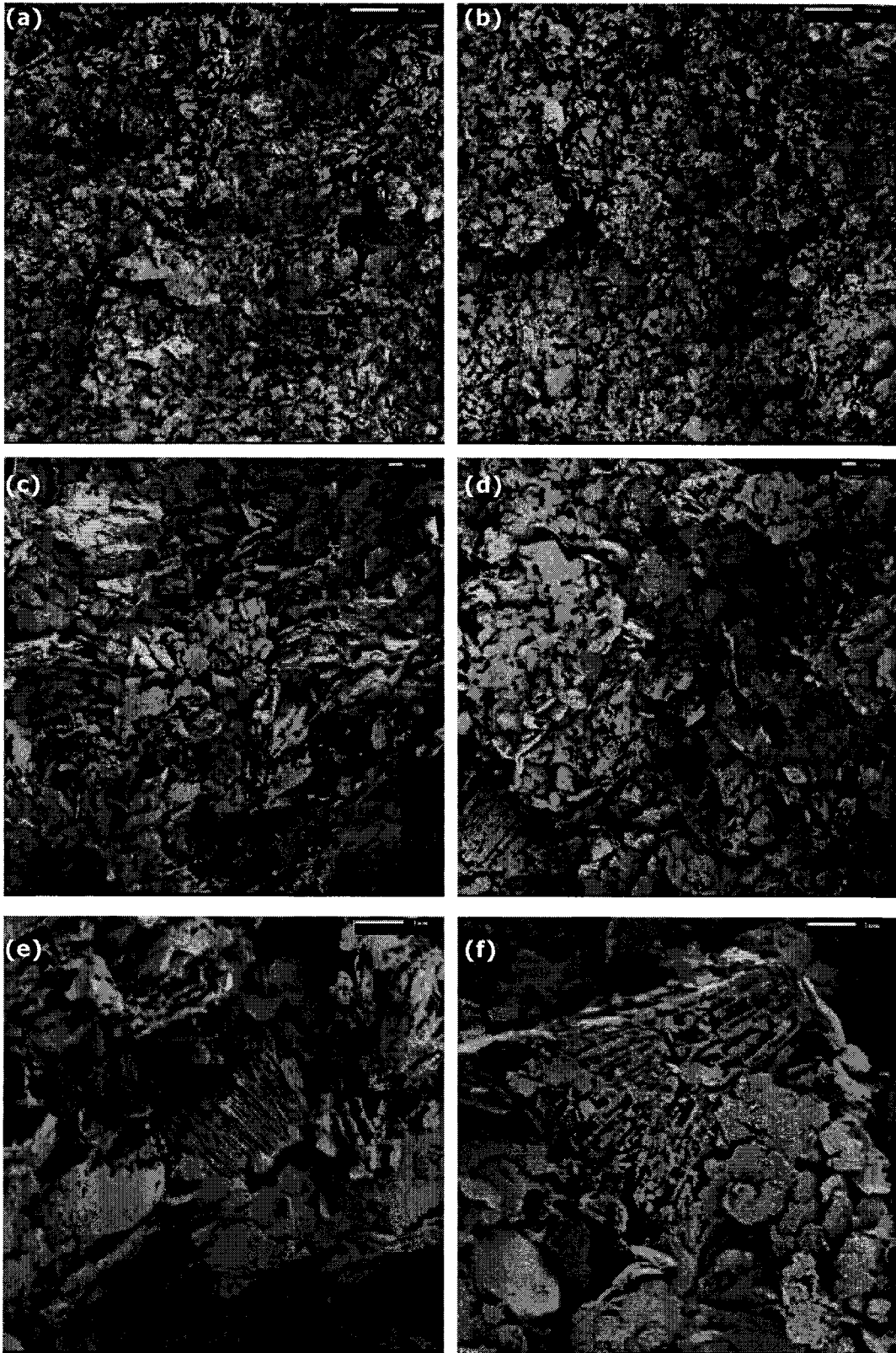
Figure E.7. Photomicrographs of oven-dried kaolin-cement at w=70%, A_c=5% and T_c =28 days. (a) & (b) M≈750X; (c) & (d) M≈2250X; (e) & (f) M≈7500X.
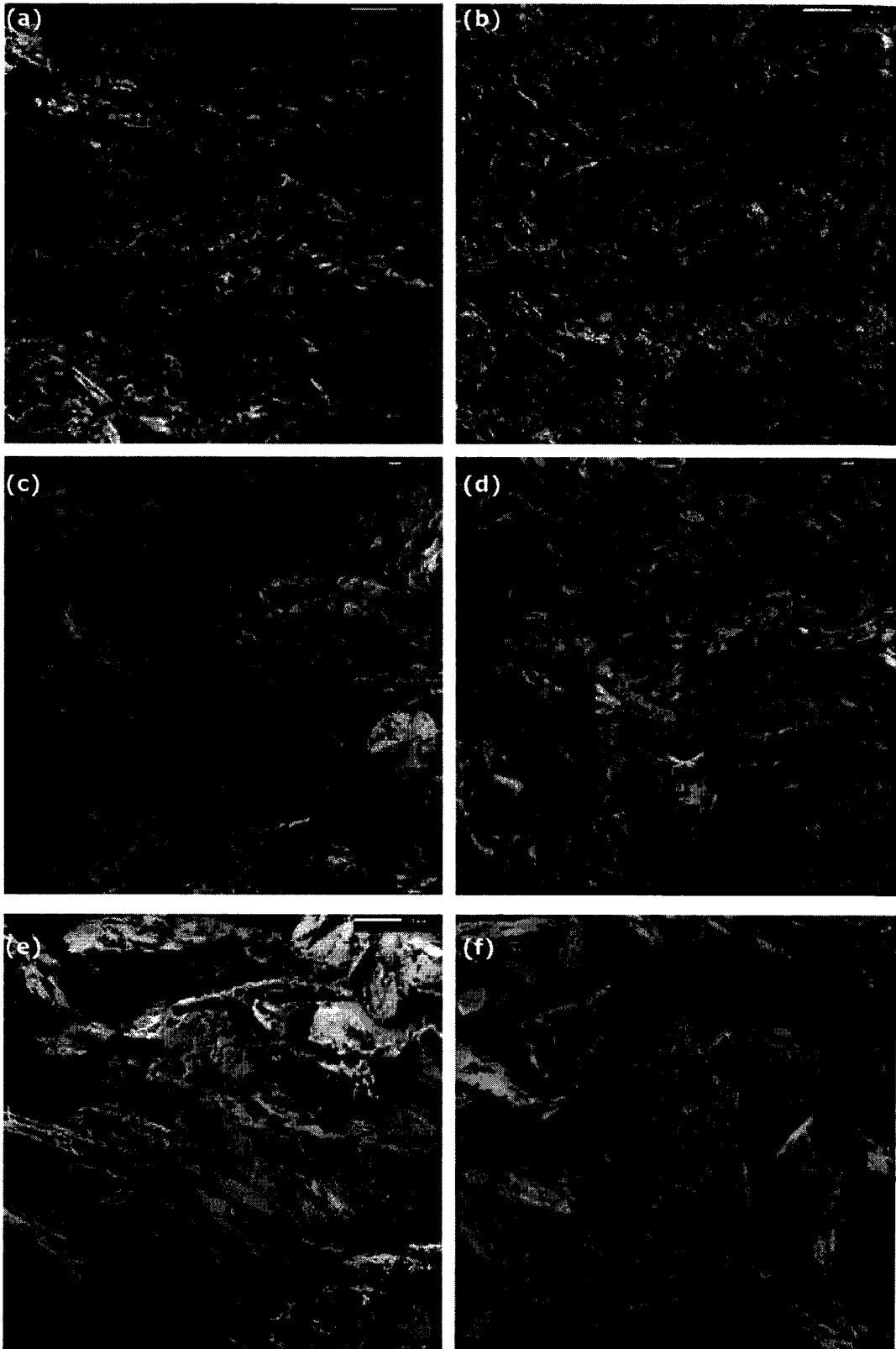
Figure E.8. Photomicrographs of oven-dried kaolin-cement at w=70%, A_c=5% and T_c =56 days. (a) & (b) M≈750X; (c) & (d) M≈2250X; (e) & (f) M≈7500X.
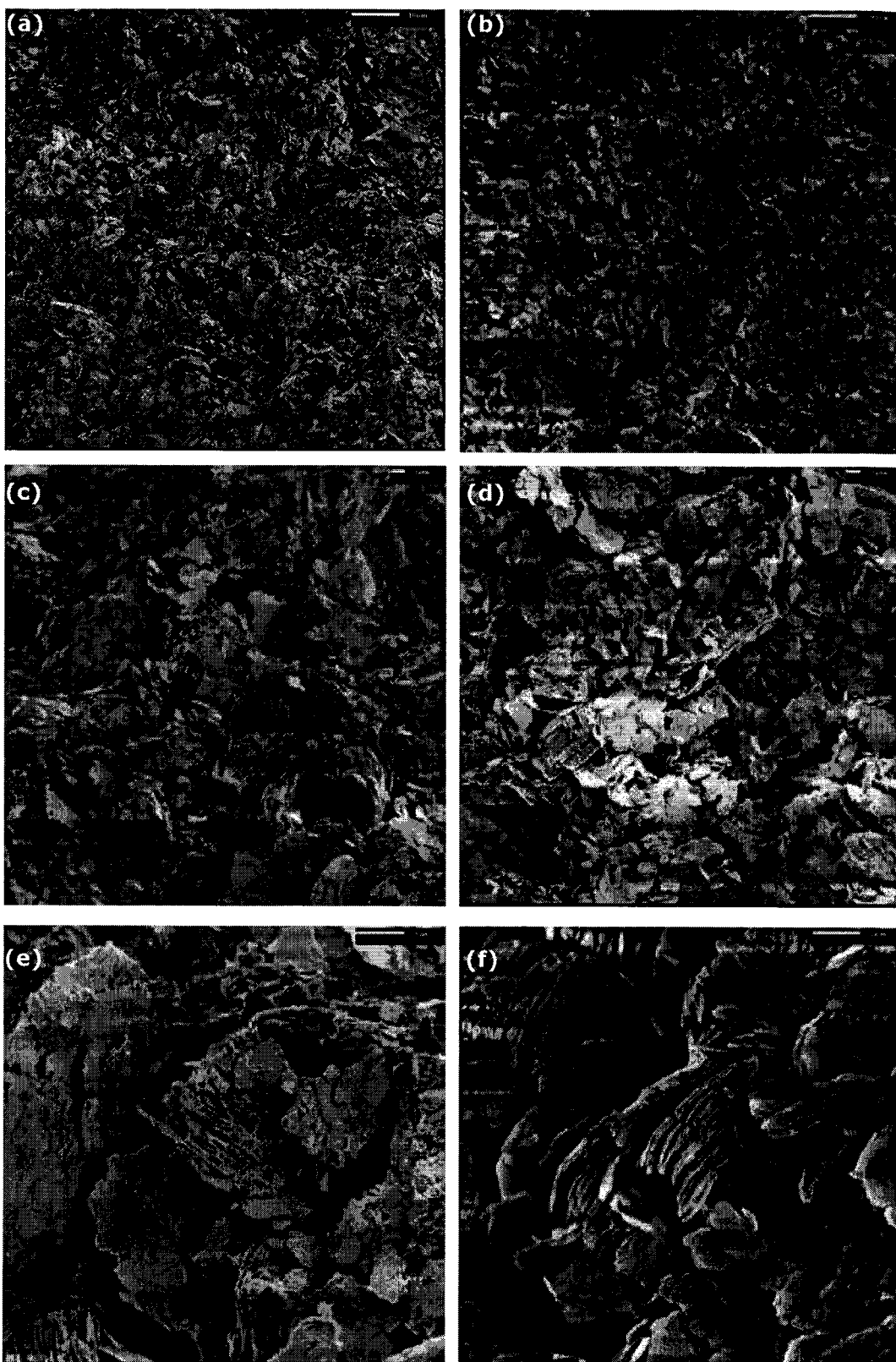
Figure E.9. Photomicrographs of oven-dried kaolin-cement at w=100%, A_c=5% and T_c =7 days. (a) & (b) M≈750X; (c) & (d) M≈2250X; (e) & (f) M≈7500X.
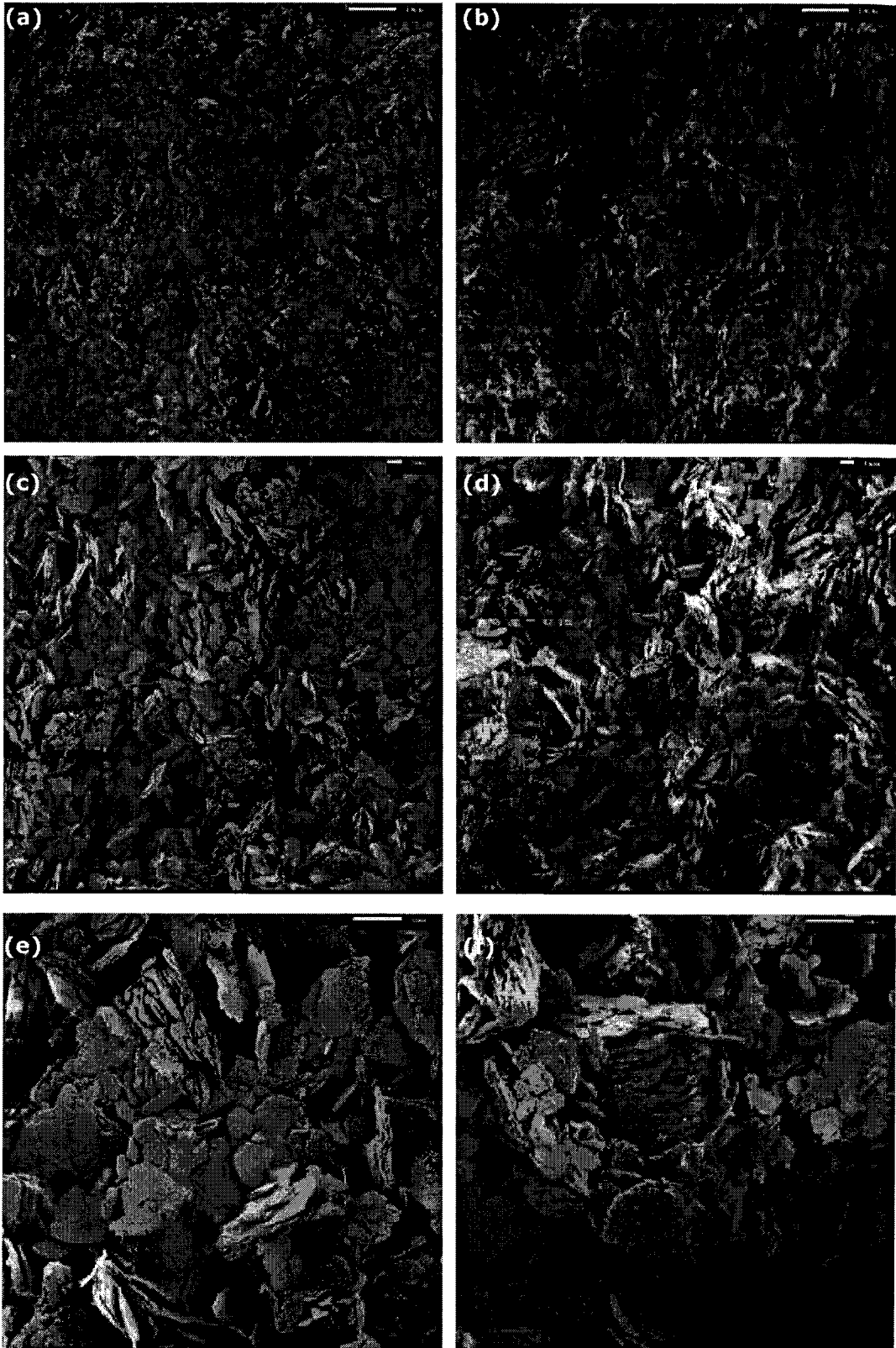
Figure E.10. Photomicrographs of oven-dried kaolin-cement at w=100%, A_c=5% and T_c =28 days. (a) & (b) M≈750X; (c) & (d) M≈2250X; (e) & (f) M≈7500X.
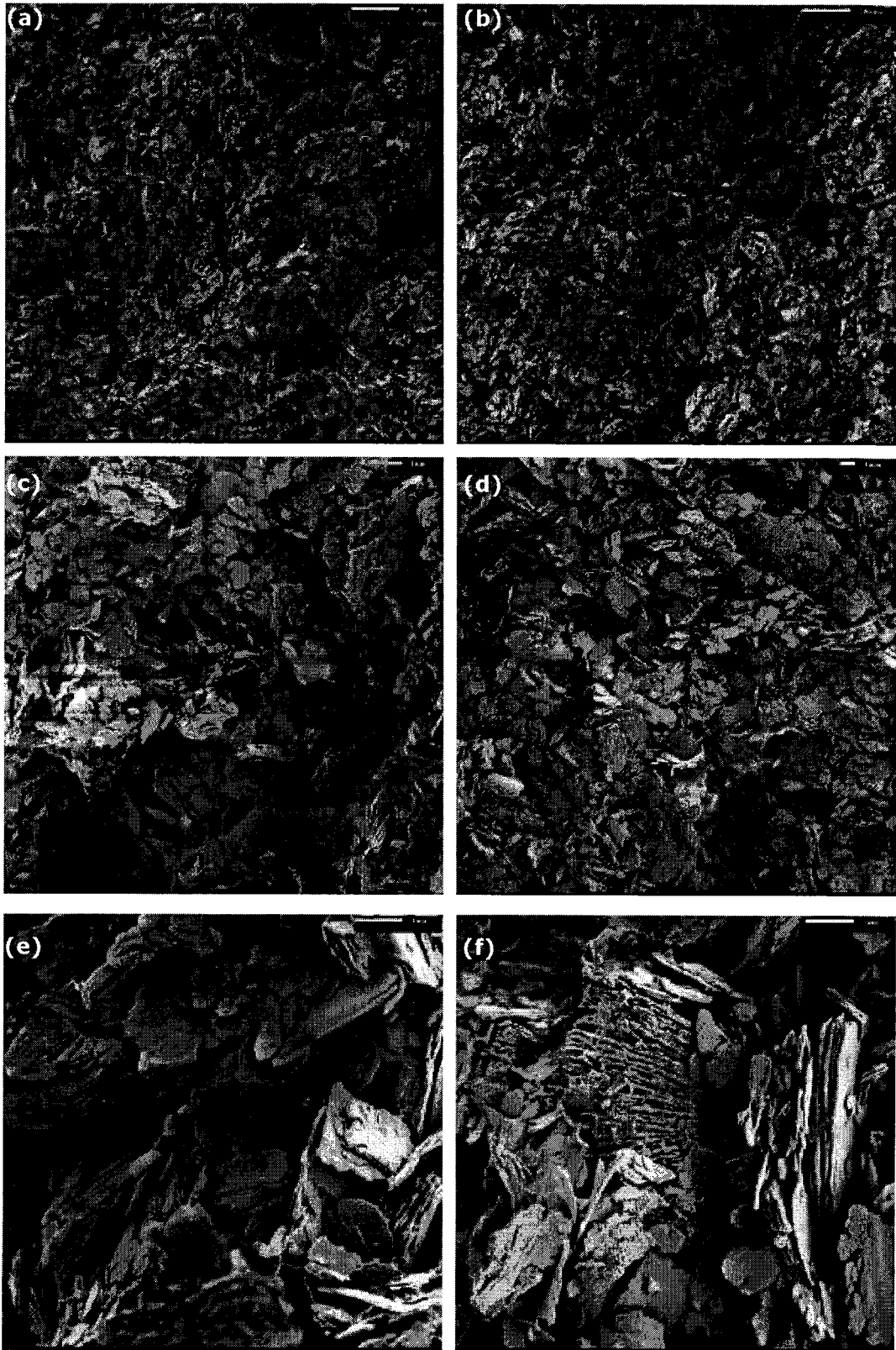
Figure E.11.   Photomicrographs of oven-dried kaolin-cement at w=100%, A_c=5% and T_c =56 days.   (a) & (b) M≈750X; (c) & (d) M≈2250X; (e) & (f) M≈7500X.

Figure E.12. Photomicrographs of oven-dried kaolin-cement at w=100%, A_c=5% and T_c =112 days. (a) & (b) M≈750X; (c) & (d) M≈2250X; (e) & (f) M≈7500X.
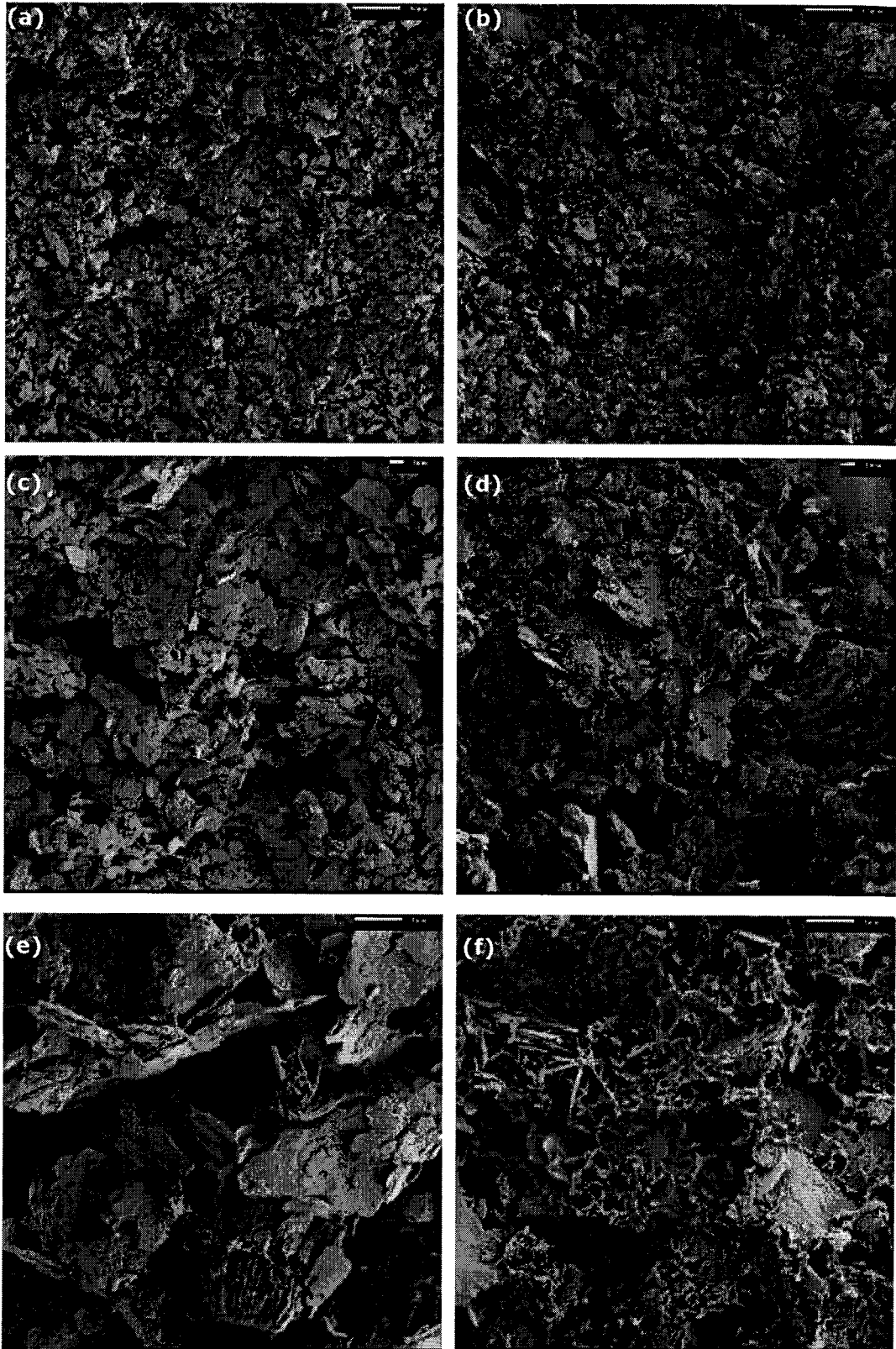
Figure E.13. Photomicrographs of oven-dried kaolin-cement at w=100%, A_c=10% and T_c =7 days. (a) & (b) M≈750X; (c) & (d) M≈2250X; (e) & (f) M≈7500X.
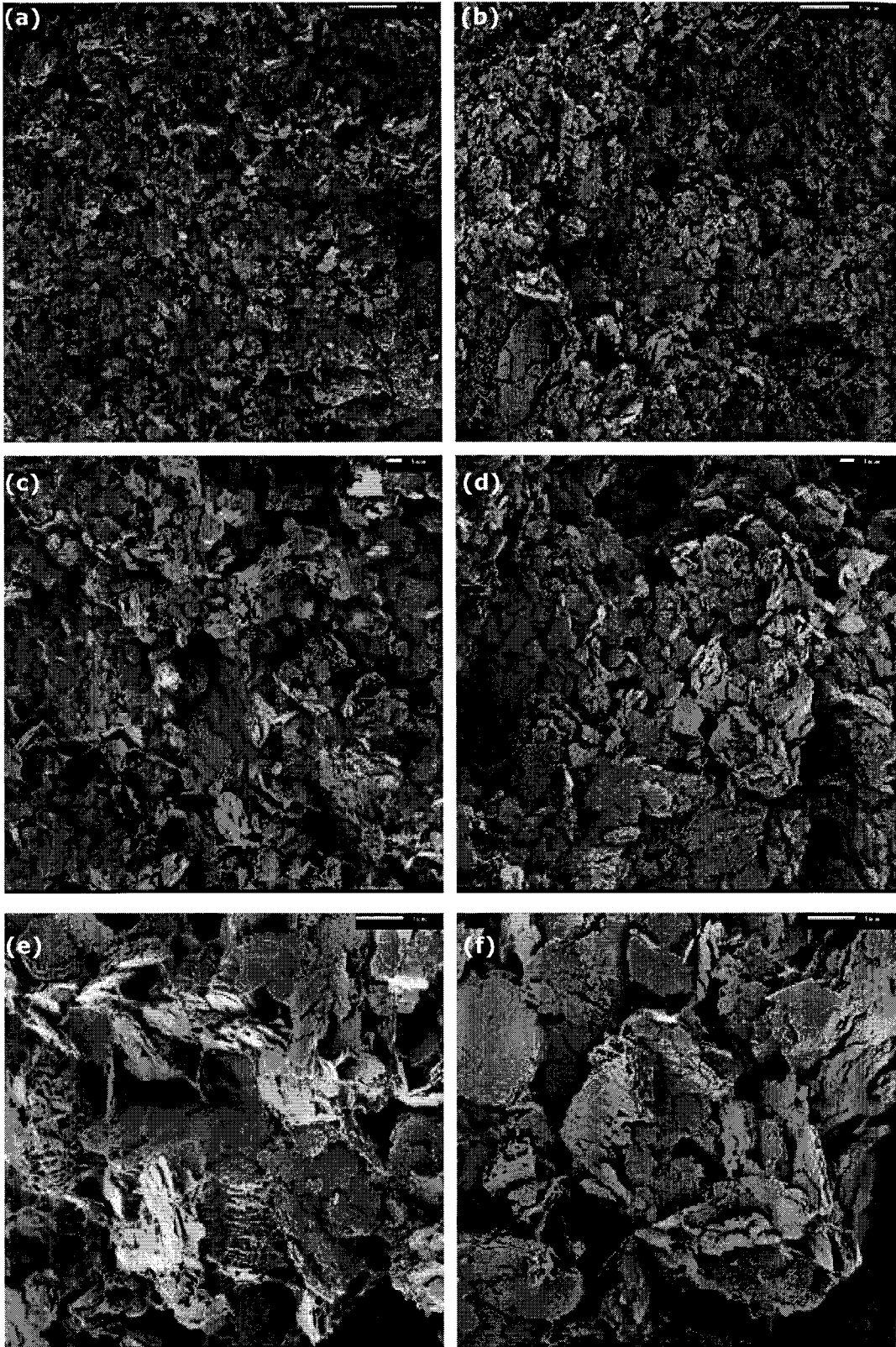
Figure E.14. Photomicrographs of oven-dried kaolin-cement at w=100%, A_c=10% and T_c =28 days. (a) & (b) M≈750X; (c) & (d) M≈2250X; (e) & (f) M≈7500X.
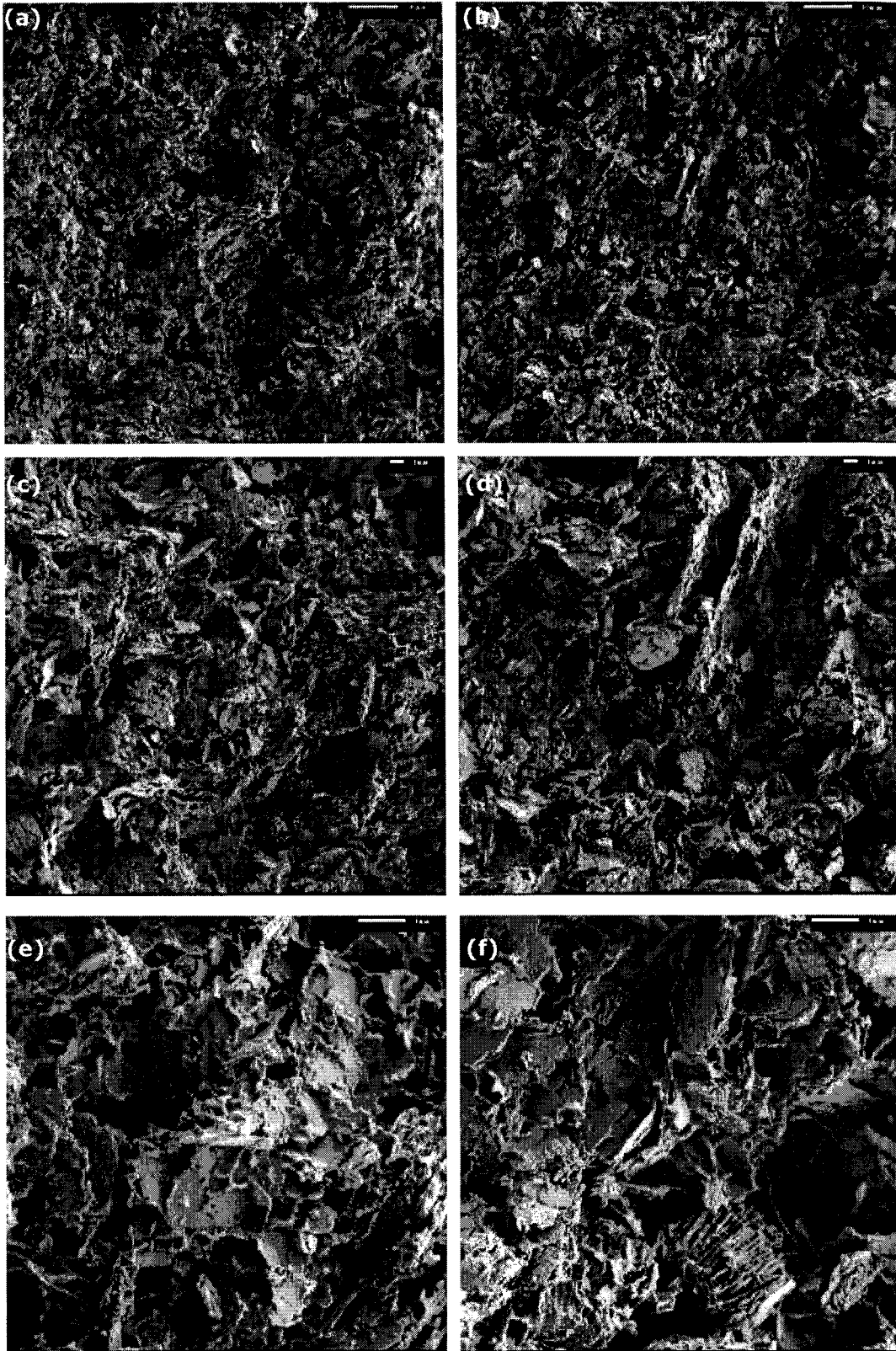
Figure E.15. Photomicrographs of oven-dried kaolin-cement at w=100%, A_c=10% and T_c =56 days. (a) & (b) M$\approx$750X; (c) & (d) M$\approx$2250X; (e) & (f) M$\approx$7500X.
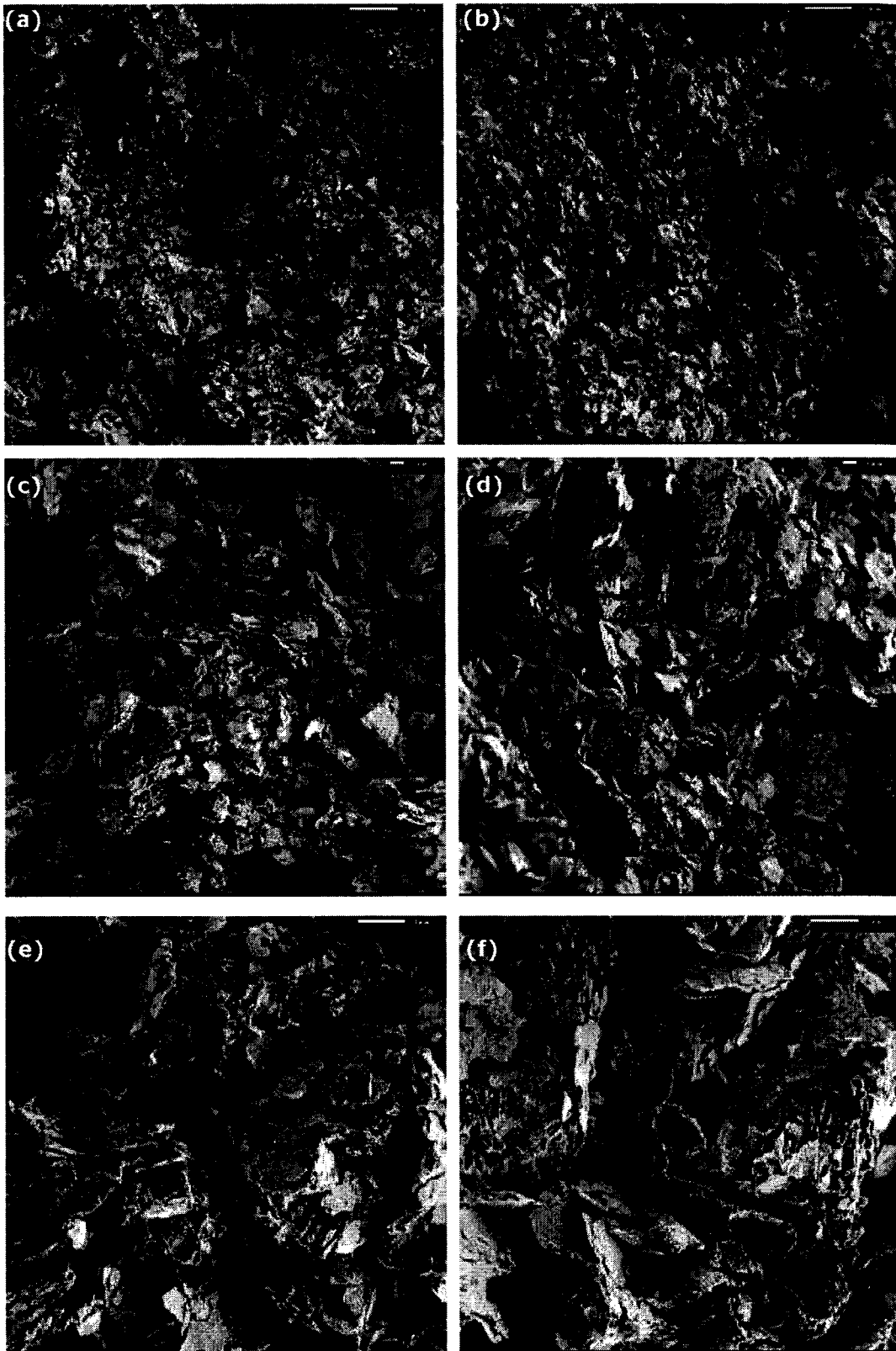
Figure E.16. Photomicrographs of oven-dried kaolin-cement at w=100%, A_c=10% and T_c =112 days. (a) & (b) M≈750X; (c) & (d) M≈2250X; (e) & (f) M≈7500X.

APPENDIX F: EFFECTIVE STRESS PATH PLOTS FROM TRIAXIAL TESTS IN A CRITICAL STATE FRAMEWORK

Chapter 5 describes the results of the drained and undrained triaxial compression tests; the results of these tests are provided in Appendices A and B. Chapter 8 briefly discusses the triaxial results in a critical state framework for the purposes of a proposed constitutive elastic-plastic model of clay-cement. Effective stress path plots in v-p'-q space as well as accompanying plots of both the isotropic consolidation line (ICL) and critical state line (CSL) are provided here to accompany the discussion in Chapter 8. Note that the critical state was not actually achieved for the majority of the triaxial tests; however, the results were interpretted so that the CSL could be drawn as best as possible.

Table F.1 below summarizes the figures in this appendix.

Table F.1. Effective stress path plots with respect to critical state soil mechanics in v-p'-q space.

w (%)	A_c(%)	Curing Time, T_c (days)			
		7	28	56	112
70	2	F.1	F.2	F.3	F.4
	5	F.5	F.6	F.7	■
100	5	F.8	F.9	F.10	F.11
	10	F.12	F.13	F.14	F.15
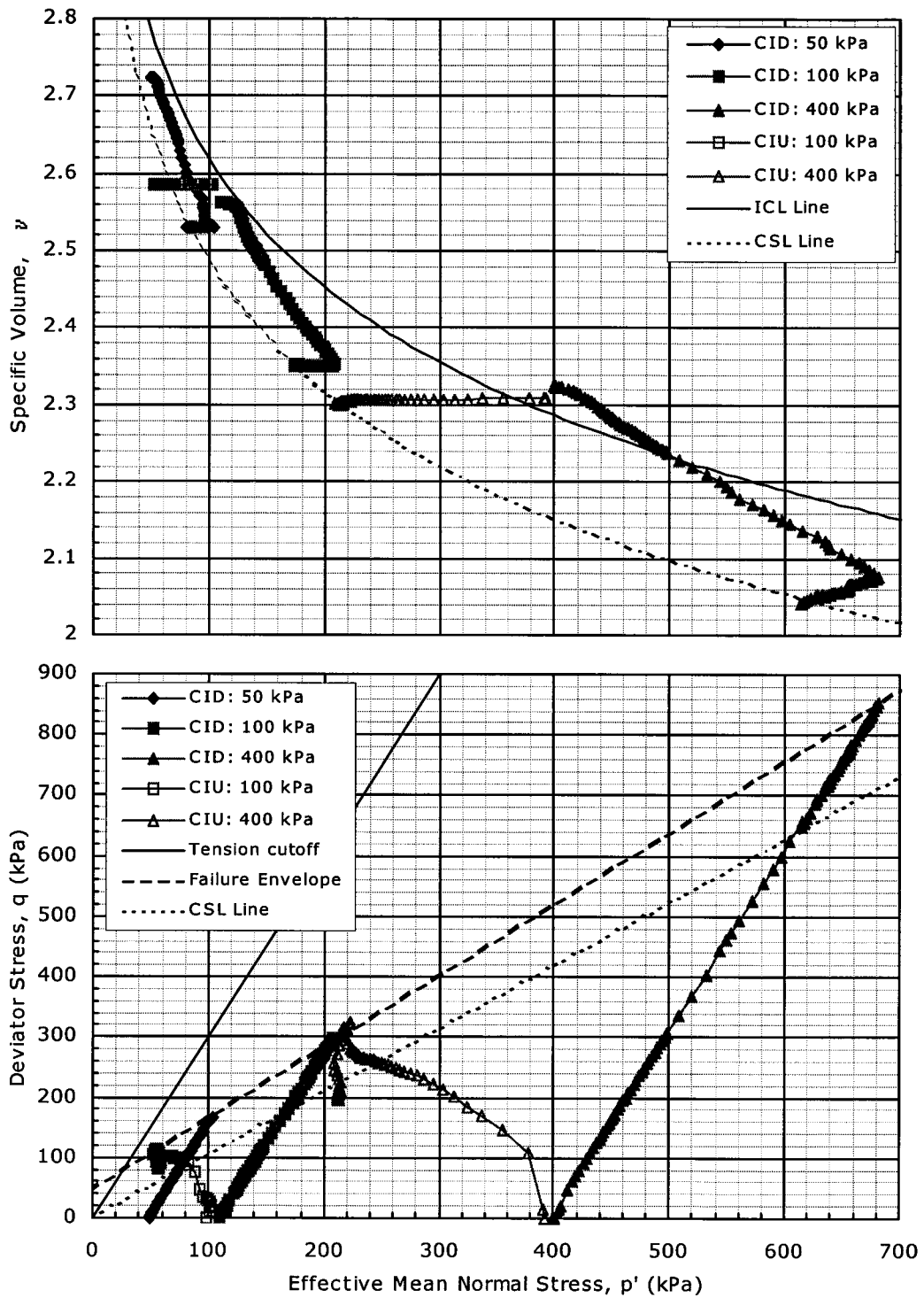
Figure F.1. Effective stress path plots for w=70%, A_c=2% and T_c=7 days.
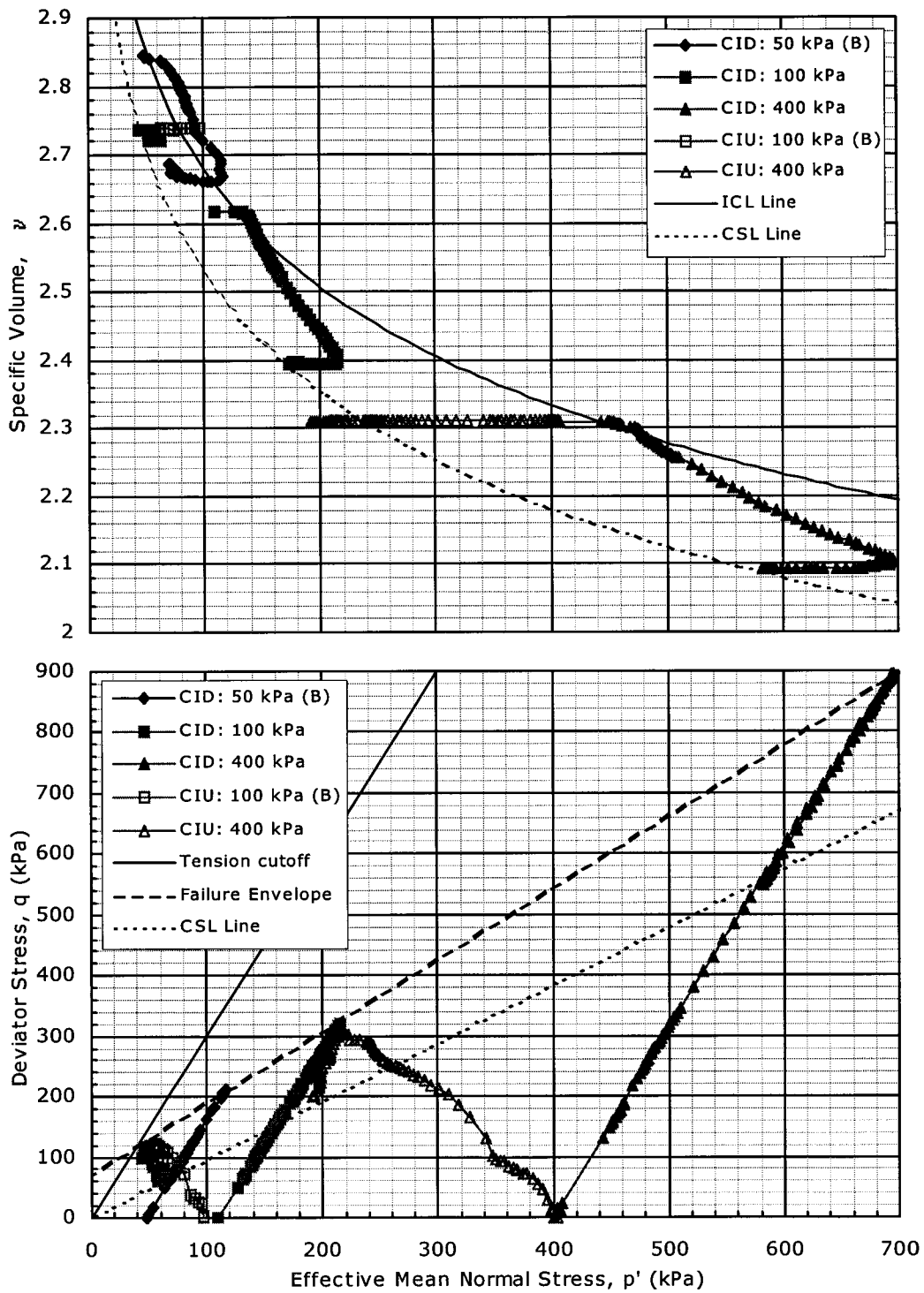
Figure F.2. Effective stress path plots for w=70%, A_c=2% and T_c=28 days.
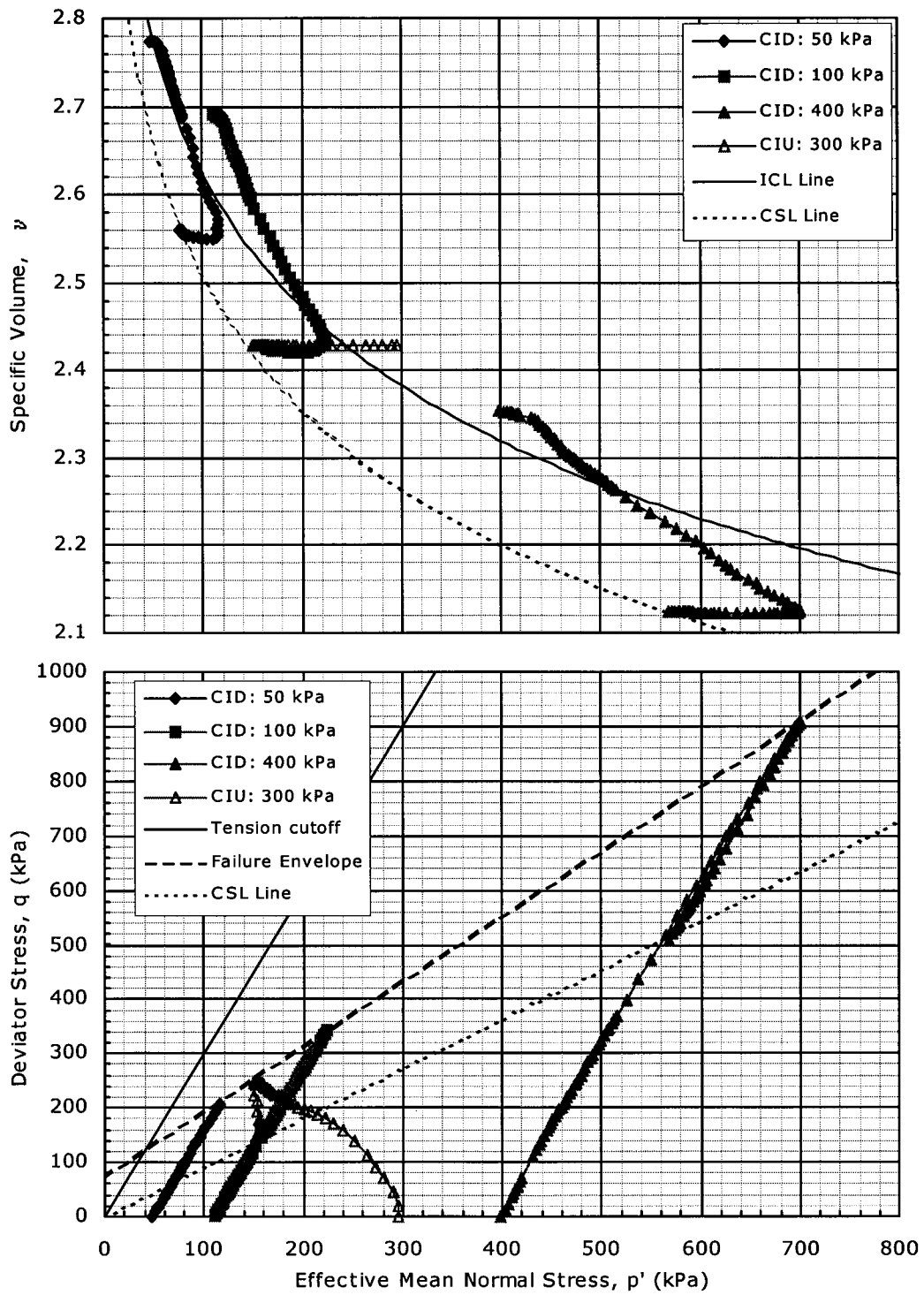
Figure F.3. Effective stress path plots for w=70%, A_c=2% and T_c=56 days.
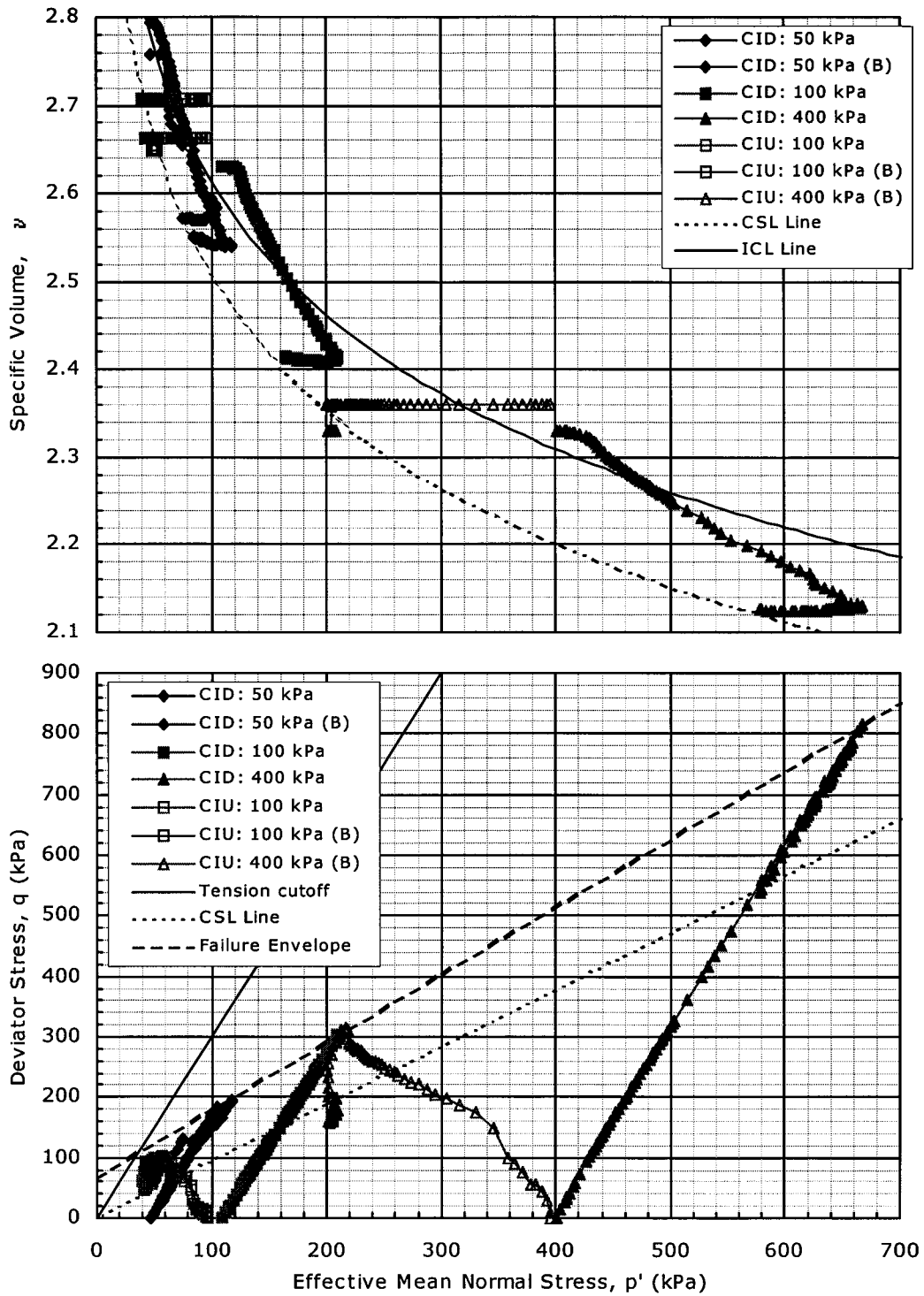
Figure F.4. Effective stress path plots for w=70%, A_c=2% and T_c=112 days.
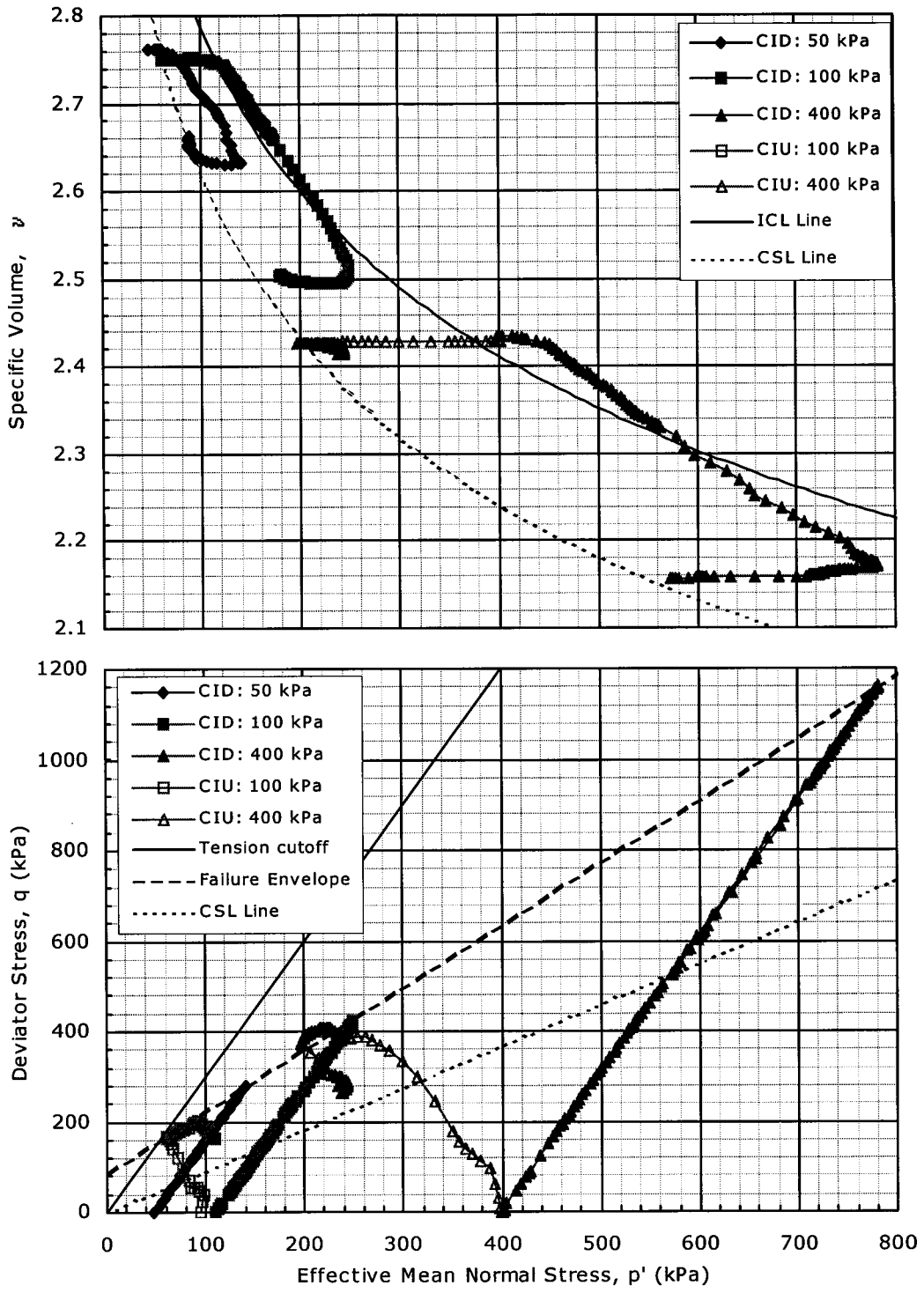
Figure F.5. Effective stress path plots for w=70%, A_c=5% and T_c=7 days.
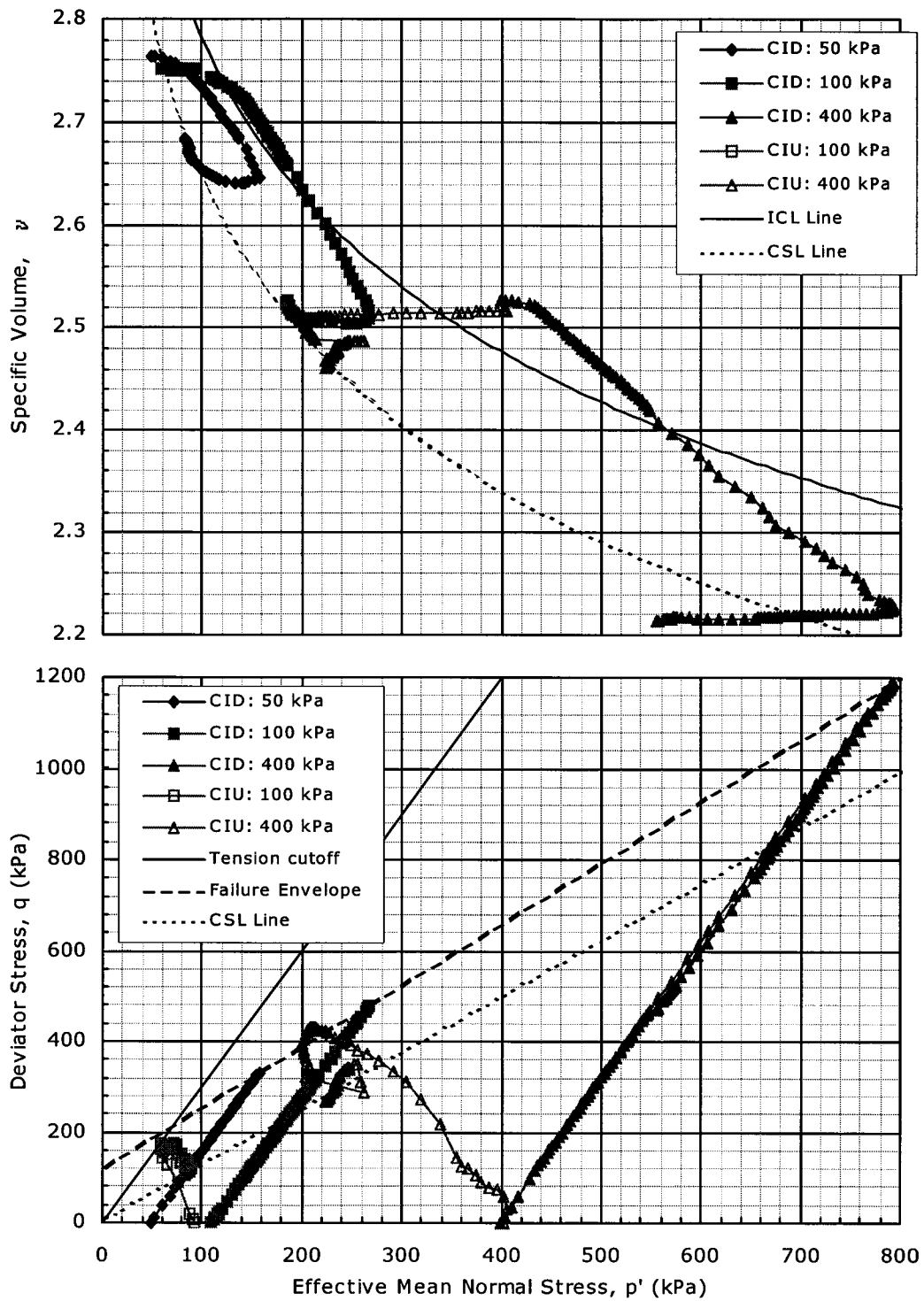
Figure F.6. Effective stress path plots for w=70%, A_c=5% and T_c=28 days.
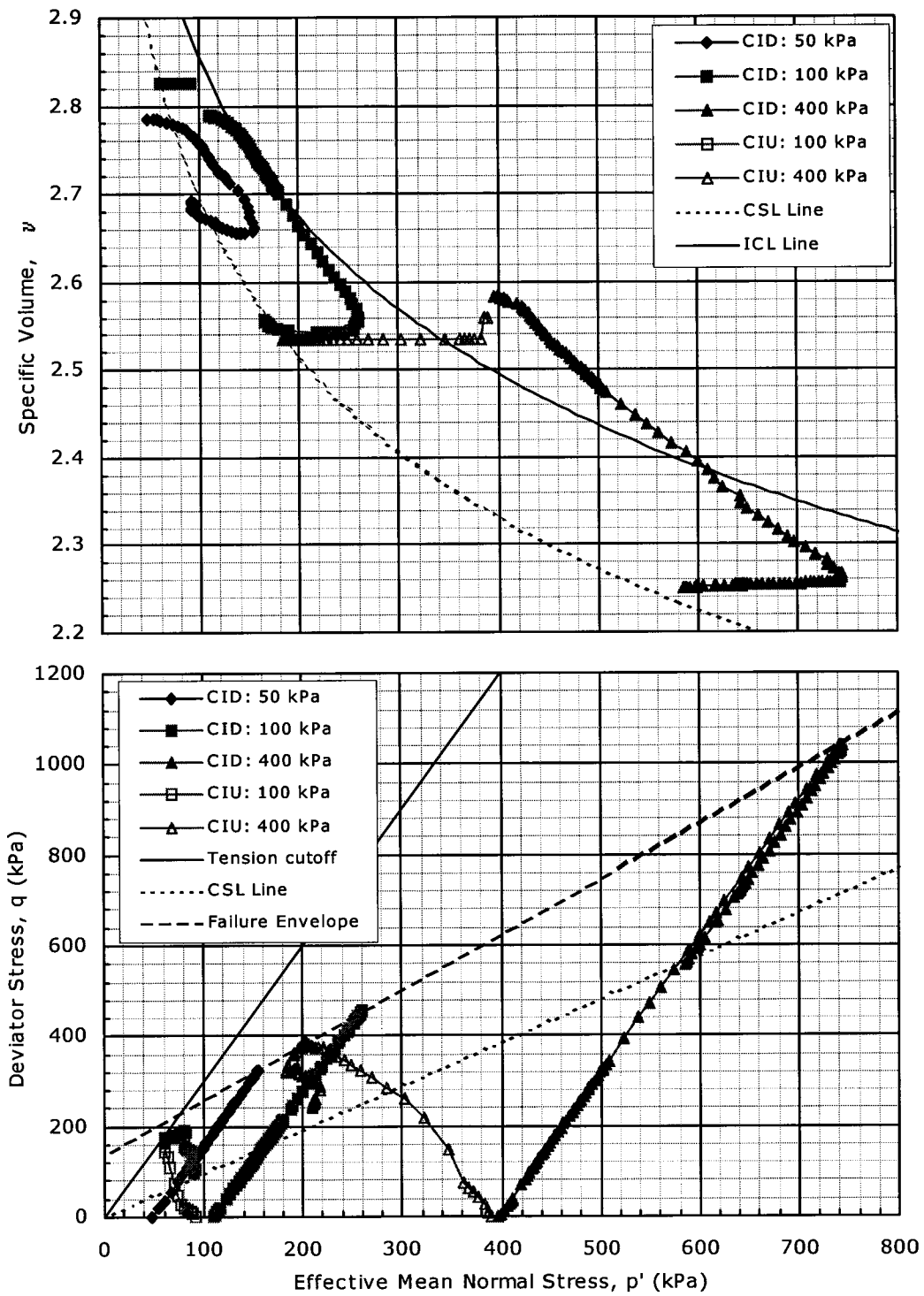
Figure F.7. Effective stress path plots for w=70%, A_c=5% and T_c=56 days.
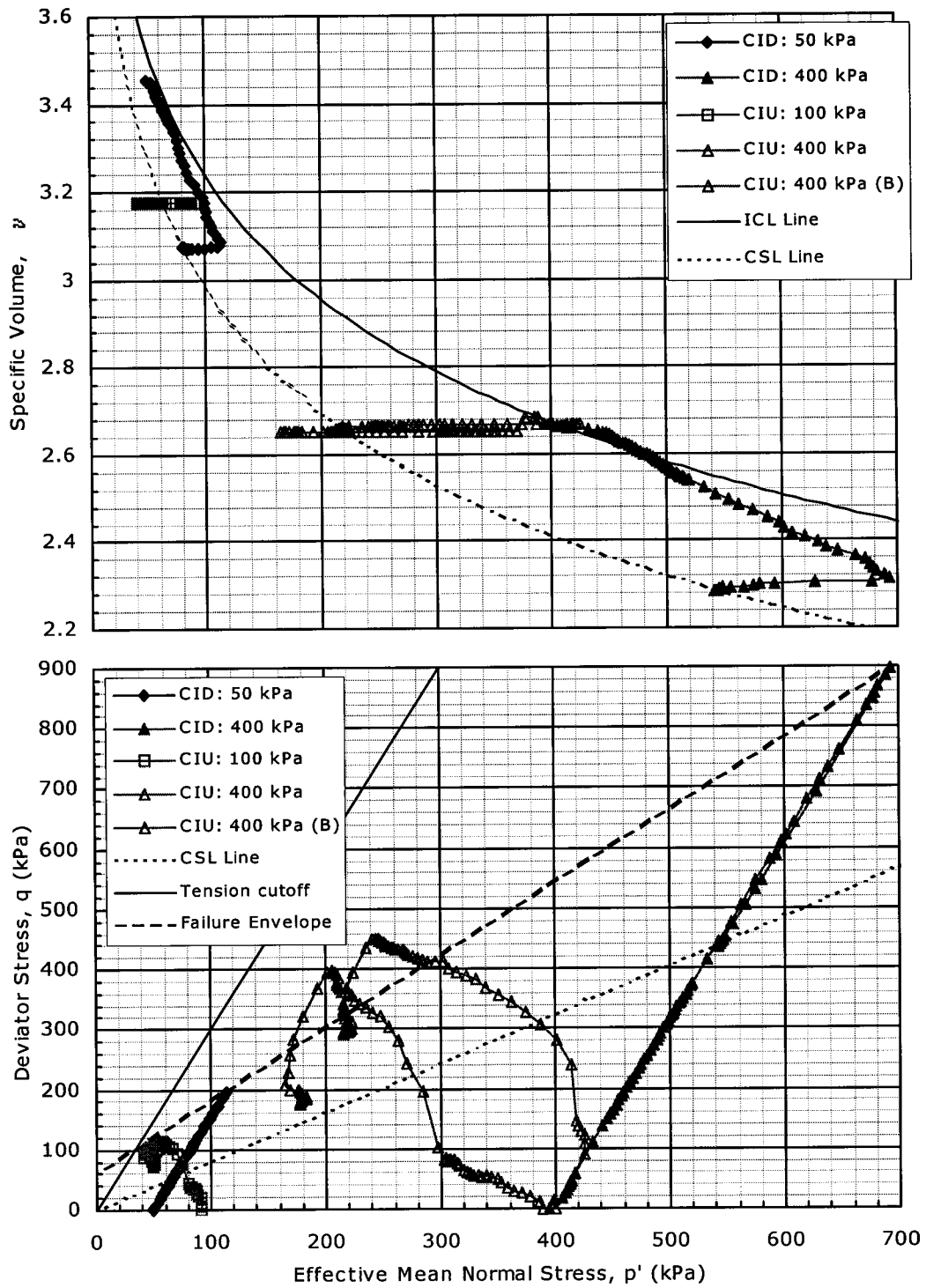
Figure F.8. Effective stress path plots for w=100%, A_c=5% and T_c=7 days.
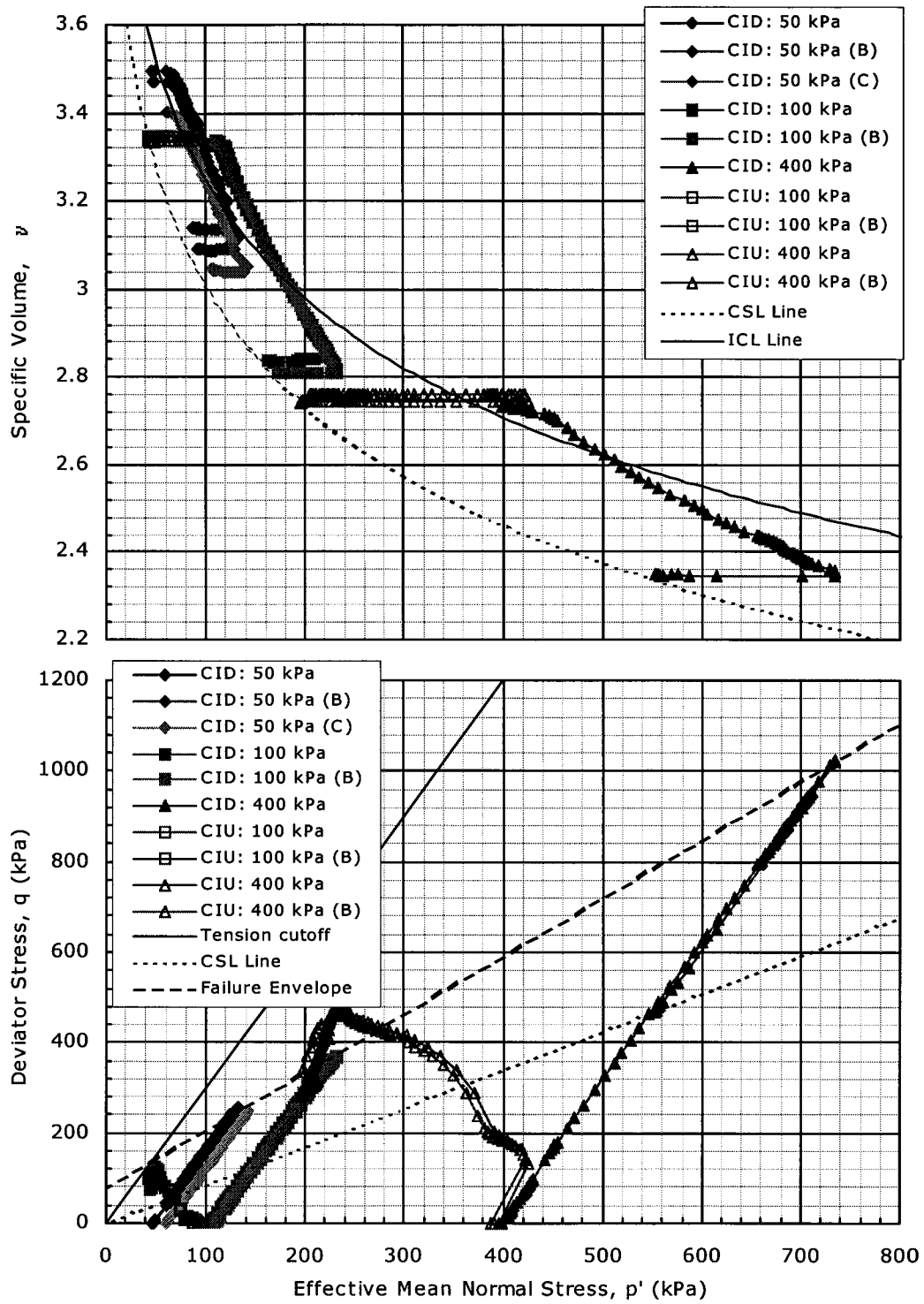
Figure F.9. Effective stress path plots for w=100%, A_c=5% and T_c=28 days.
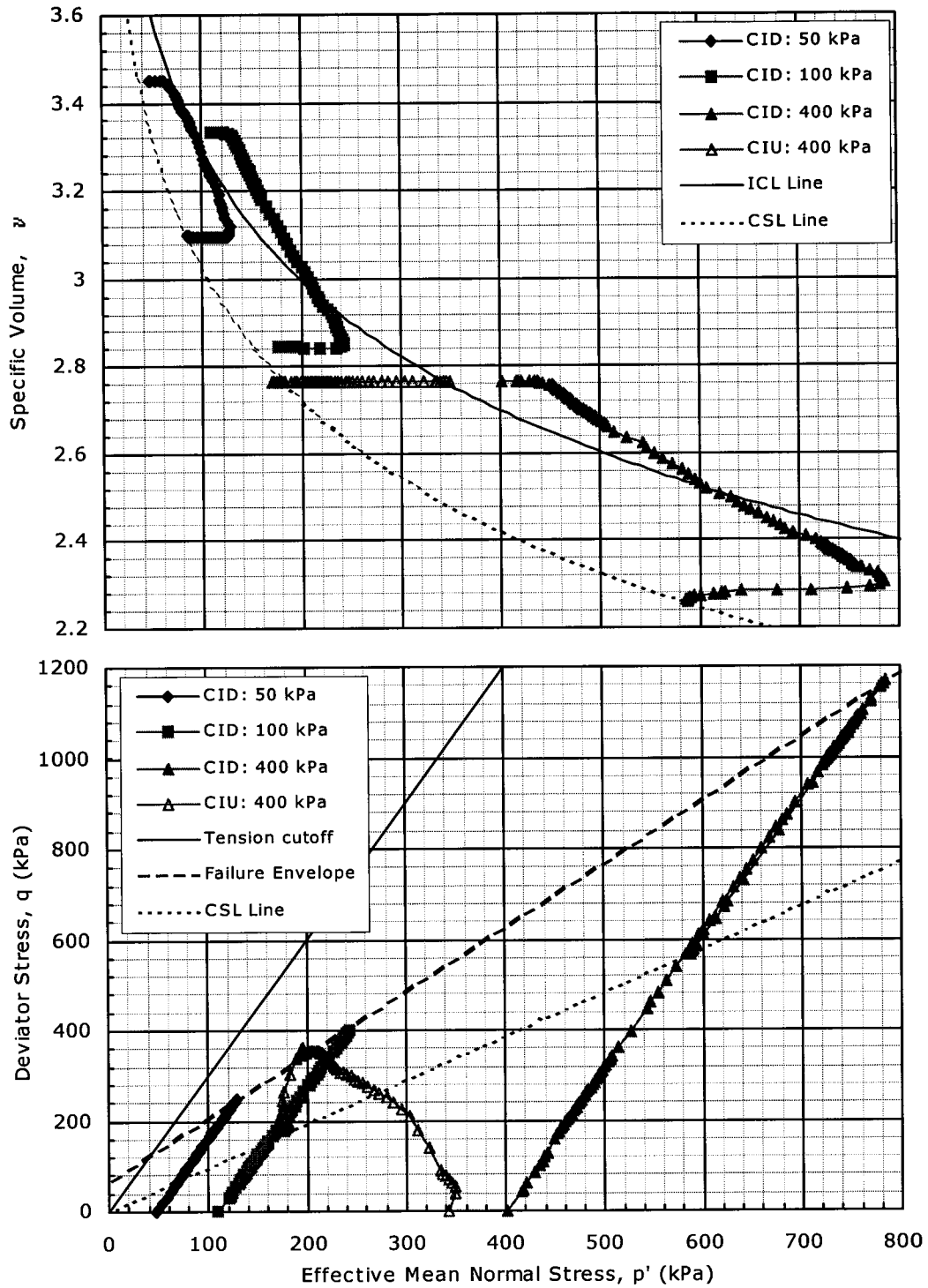
Figure F.10. Effective stress path plots for w=100%, A_c=5% and T_c=56 days.
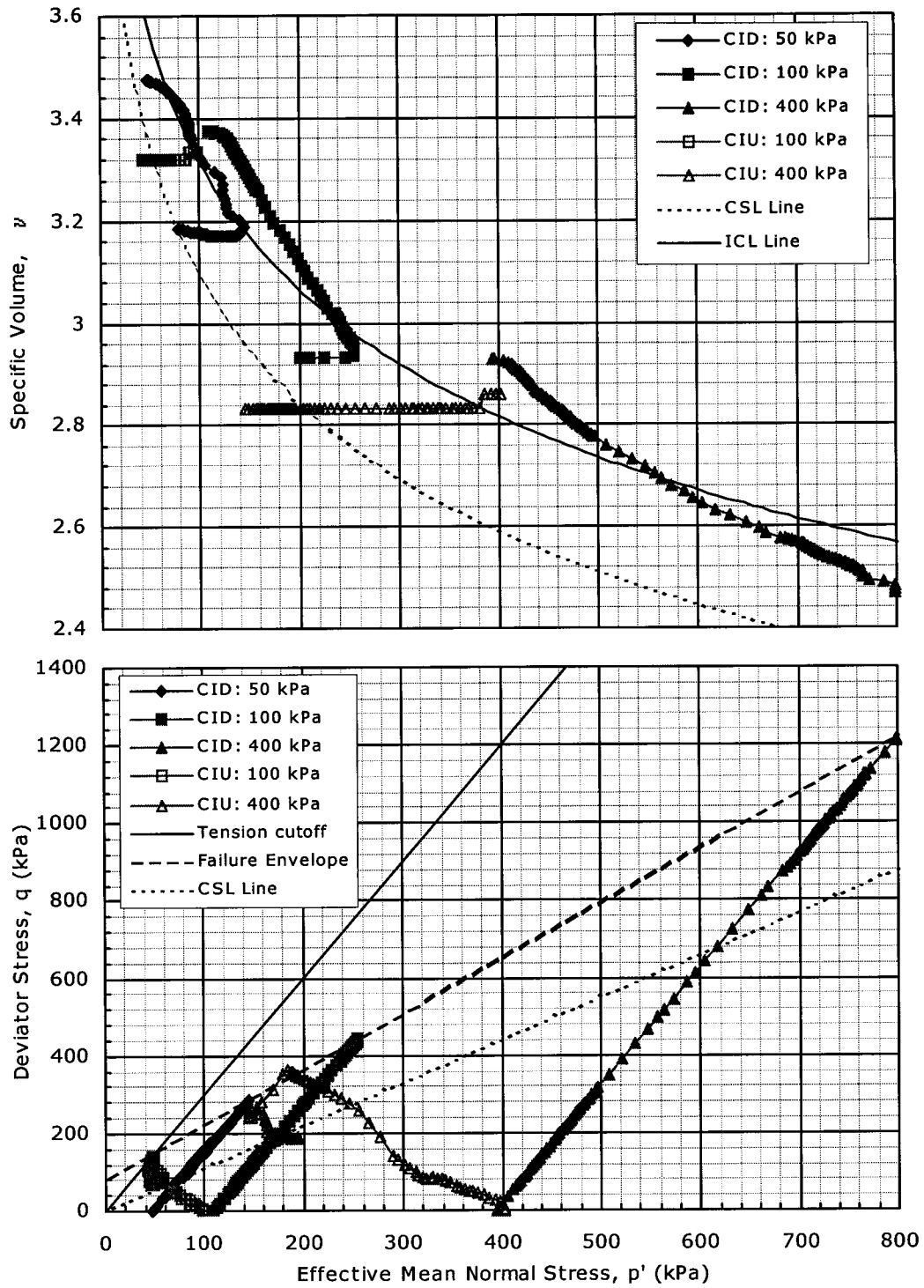
Figure F.11. Effective stress path plots for w=100%, A_c=5% and T_c=112 days.
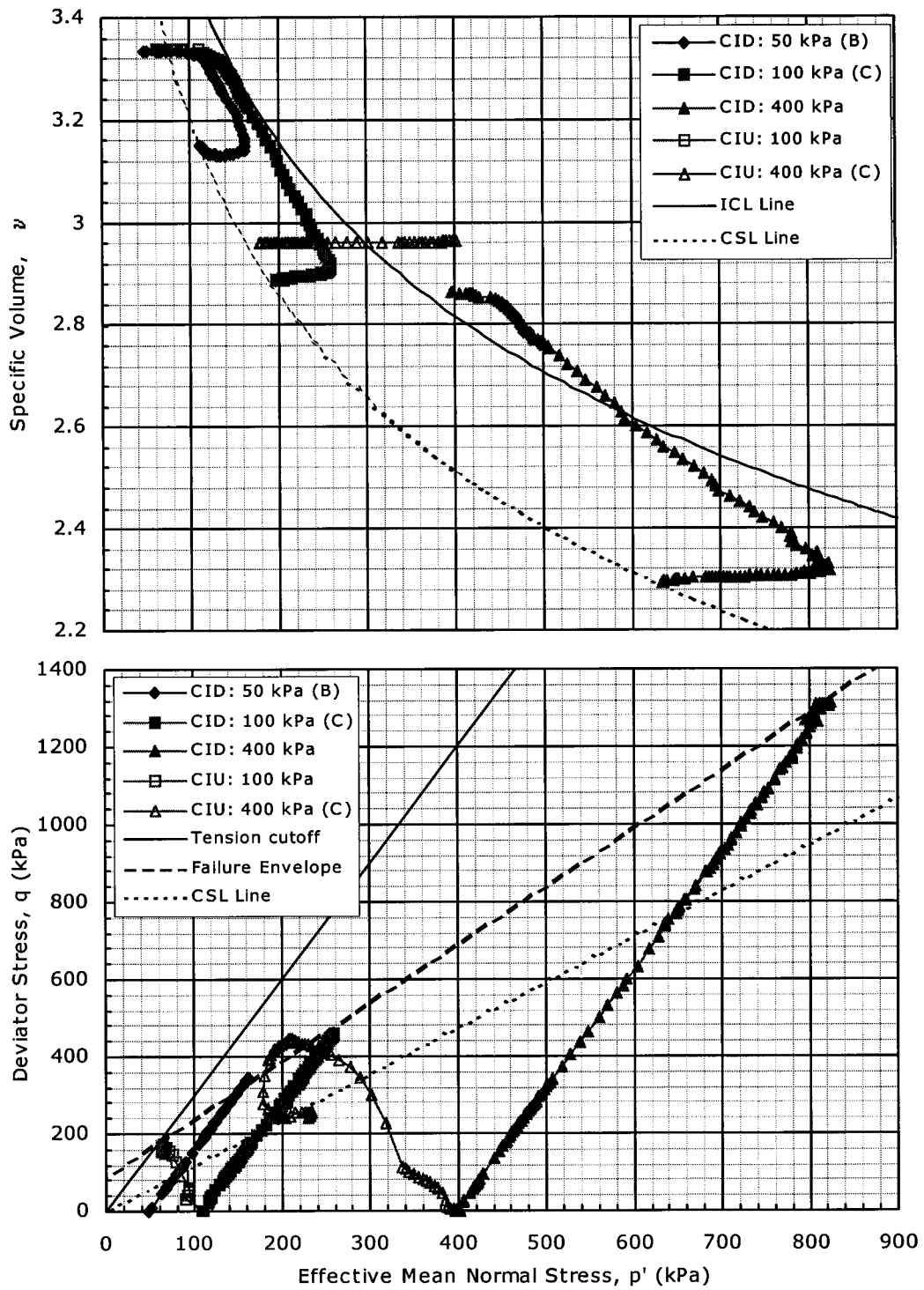
Figure F.12. Effective stress path plots for w=100%, A_c=10% and T_c=7 days.
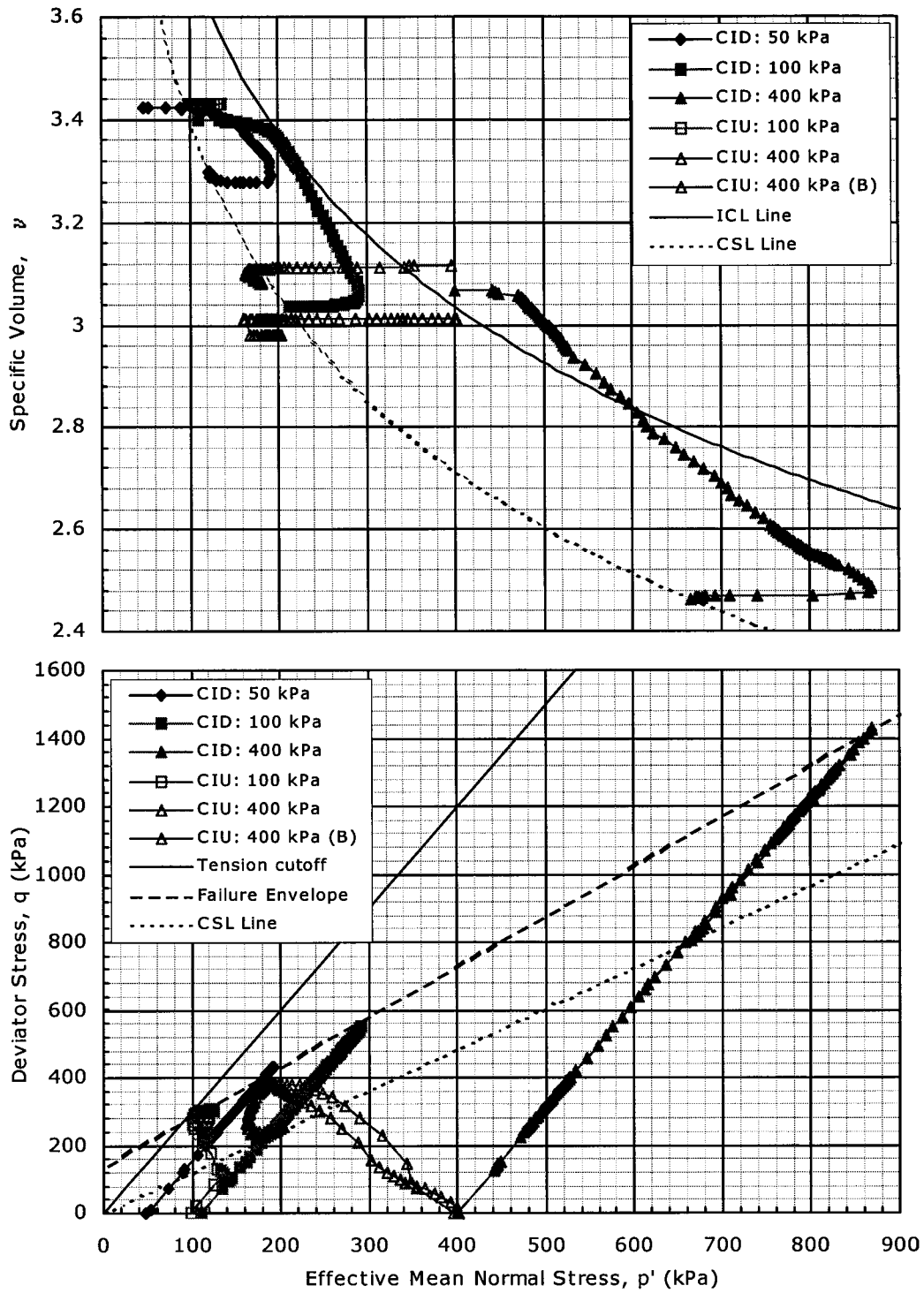
Figure F.13. Effective stress path plots for w=100%, A_c=10% and T_c=28 days.
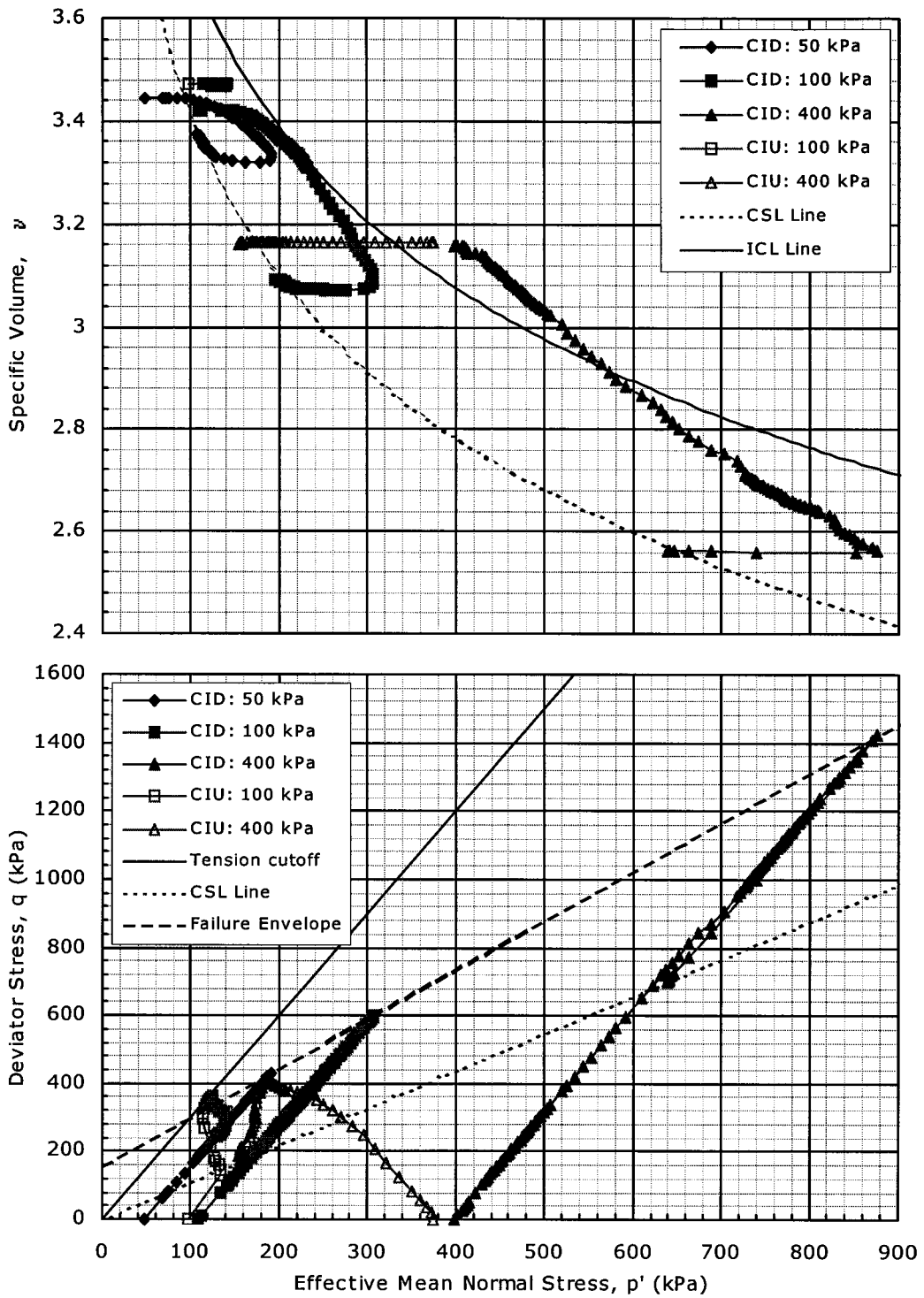
Figure F.14. Effective stress path plots for w=100%, A$_c$=10% and T$_c$=56 days.
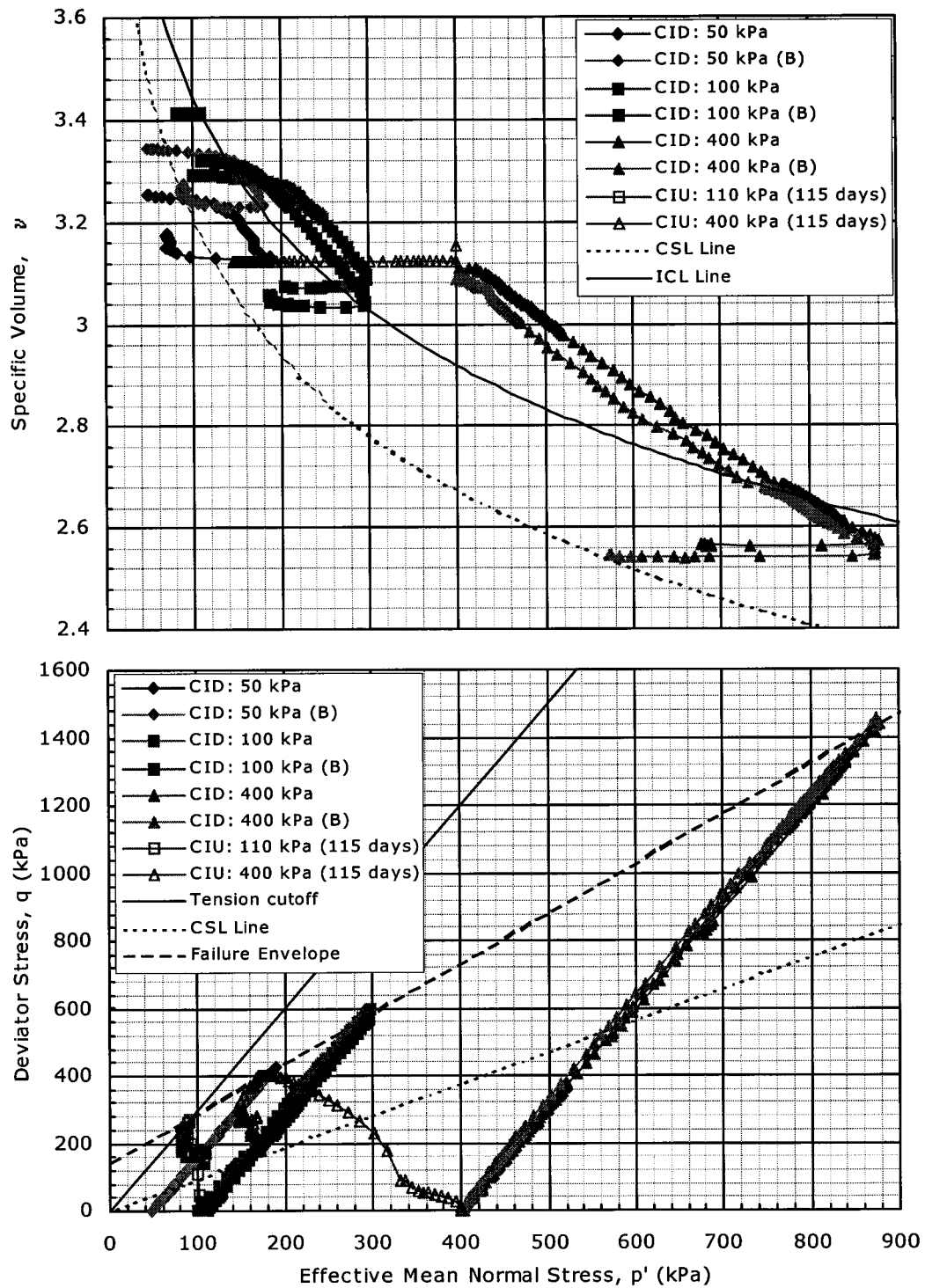
Figure F.15. Effective stress path plots for w=100%, A_c=10% and T_c=112 days.

APPENDIX G: PHOTOGRAPHS OF SAMPLES FROM LABORATORY PROGRAM ON KAOLIN AND KAOLIN-CEMENT

Digital photographs were taken of all triaxial (CID and CIU) and unconfined compression (UC) samples before and after tests to document the sample quality and the failure behaviour. Photographs were also taken of all isotropic consolidation (IC) samples. In some cases, photographs are missing; only photographs of successful tests are included here. Unfortunately, some images are not well-focused, however, the sample quality and orientation of failure planes can still be seen.

For the triaxial tests, a clear failure plane at roughly 30° from the vertical axis of the sample was usually formed during shear. In most cases, failure was by plastic shear for the triaxial tests. with some tensile cracking after peak conditions. For the UC tests, failure was normally by crushing and often tension cracks, that were nearly vertical, formed during shear.

The following tables summarize the photographs included in this appendix.

Table 1. Photographs of CID tests.

w (%)	A_c(%)	Curing Time, T_c (days)			
		7	28	56	112
40	0	1.1 to 1.5			
70	2	2.1 to 2.3	2.4 to 2.6	2.7 to 2.9	2.10 to 2.13
	5	3.1 to 3.3	3.4 to 3.6	3.7 to 3.9	███████
100	5	4.1 to 4.2	4.3 to 4.8	4.9 to 4.11	4.12 to 4.14
	10	5.1 to 5.3	5.4 to 5.6	5.7 to 5.9	5.10 to 5.15

Table 2. Photographs of CIU tests.

w (%)	A_c(%)	Curing Time, T_c (days)			
		7	28	56	112
40	0	6.1 to 6.2			
70	2	7.1 to 7.2	7.3 to 7.4	7.5	7.6 to 7.8
	5	8.1 to 8.2	8.3 to 8.4	8.5 to 8.6	■■■
100	5	9.1 to 9.3	9.4 to 9.7	9.8 to 9.9	9.10 to 9.11
	10	10.1 to 10.2	10.3 to 10.5	10.6 to 10.7	10.8 to 10.9*

*115-day samples.

Table 3. Photographs of UC tests.

w (%)	A_c(%)	Curing Time, T_c (days)			
		7	28	56	112
40	0	11.1			
70	2	12.1	12.2	12.3	12.4
	5	13.1	13.2	13.3	13.4
100	2	14.1	■■■		
	5	15.1	15.2	15.3	15.4
	10	16.1	16.2	16.3	16.4

Table 4. Photographs of IC tests.

w (%)	A_c(%)	Curing Time, T_c (days)			
		7	28	56	112
40	0	17.1			
70	2	18.1	18.2	18.3	18.4
	5	19.1	19.2	19.3	■■■
100	5	20.1	20.2	20.3	20.4
	10	21.1	21.2	21.3	21.4
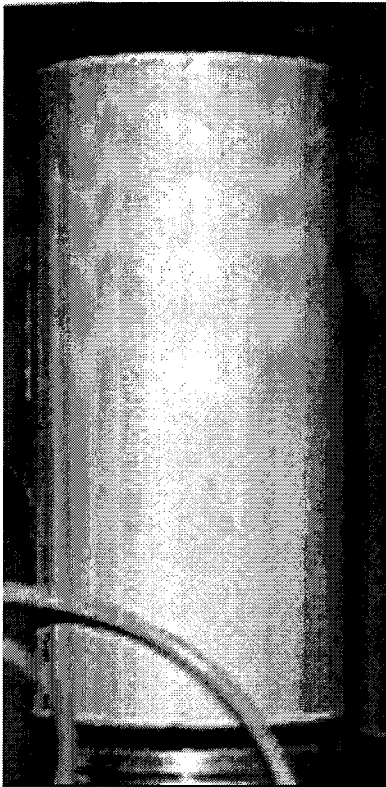
Figure 1.1. CID triaxial sample at w=40%, A_c=0% & $p_o{'}$=50 kPa.
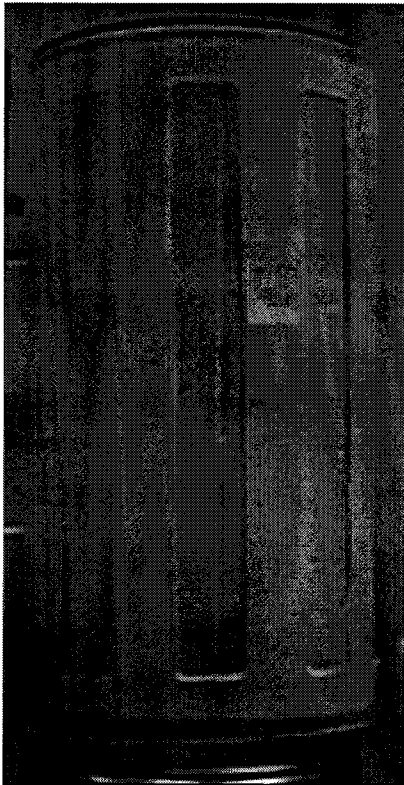
Figure 1.2. CID triaxial sample at w=40%, A_c=0% & $p_o{'}$=100 kPa.
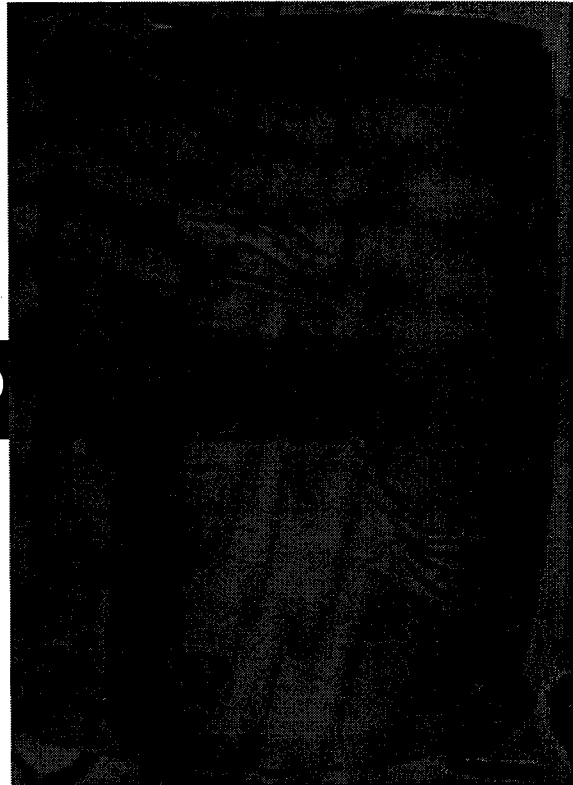
Figure 1.3. CID triaxial sample at w=40%, A_c=0% & $p_o{}'$=100 kPa (test B).
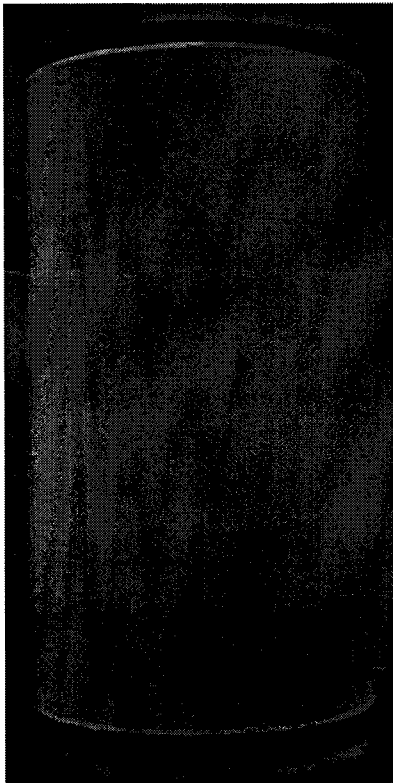
Figure 1.4. CID triaxial sample at w=40%, A_c=0% & $p_o{}'$=400 kPa.
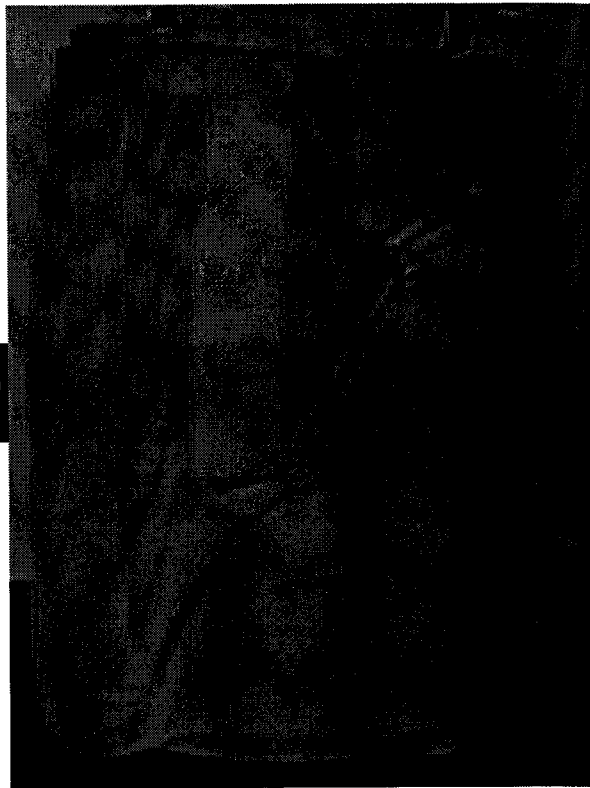
Figure 1.5. CID triaxial sample at w=40%, A_c=0% & $p_o{}'$=400 kPa (test B).
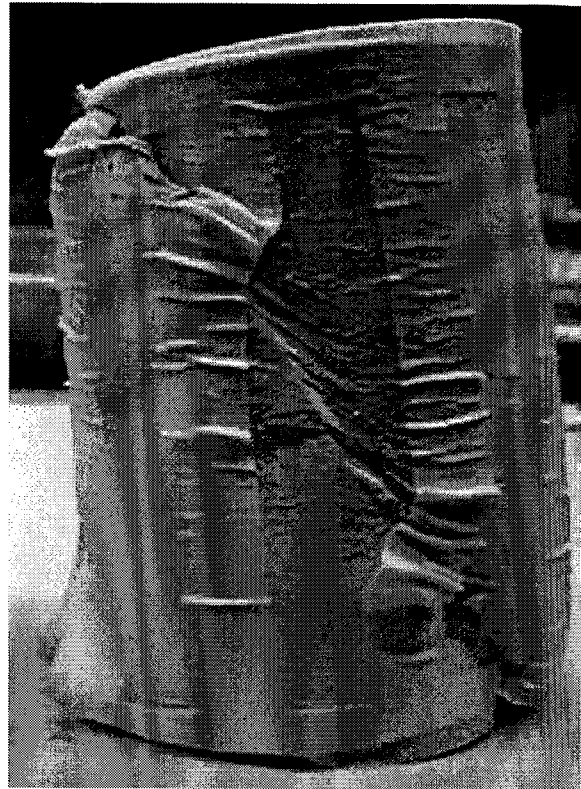
Figure 2.1. CID triaxial sample at w=70%, A_c=2%, p_o'=50 kPa & T_c=7 days.
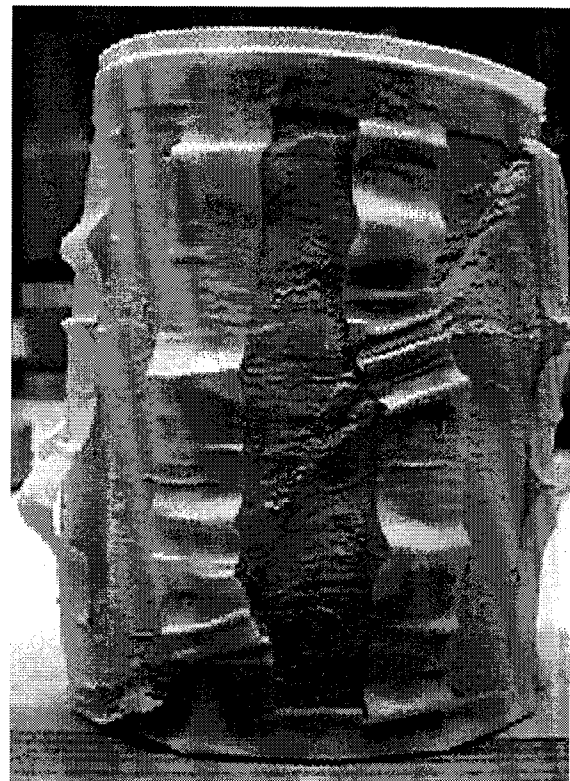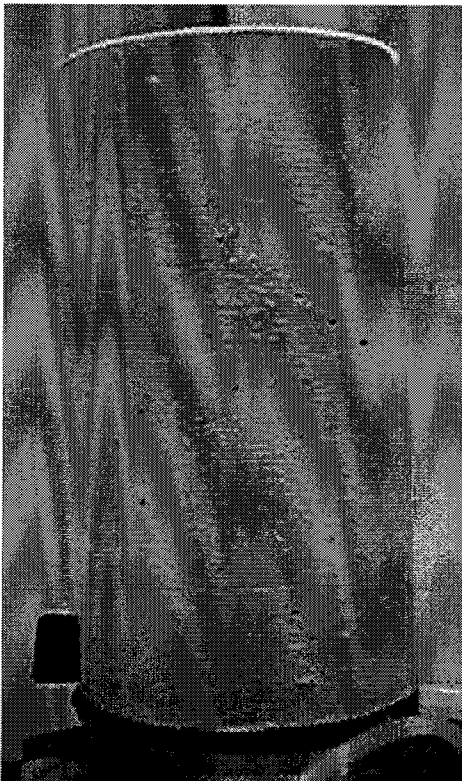
Figure 2.2. CID triaxial sample at w=70%, A_c=2%, p_o'=100 kPa & T_c=7 days.

Figure 2.3. CID triaxial sample at w=70%, A_c=2%, $p_o{}'$=400 kPa & T_c=7 days.

Figure 2.4. CID triaxial sample at w=70%, A_c=2%, $p_o{}'$=50 kPa & T_c=28 days (test B).
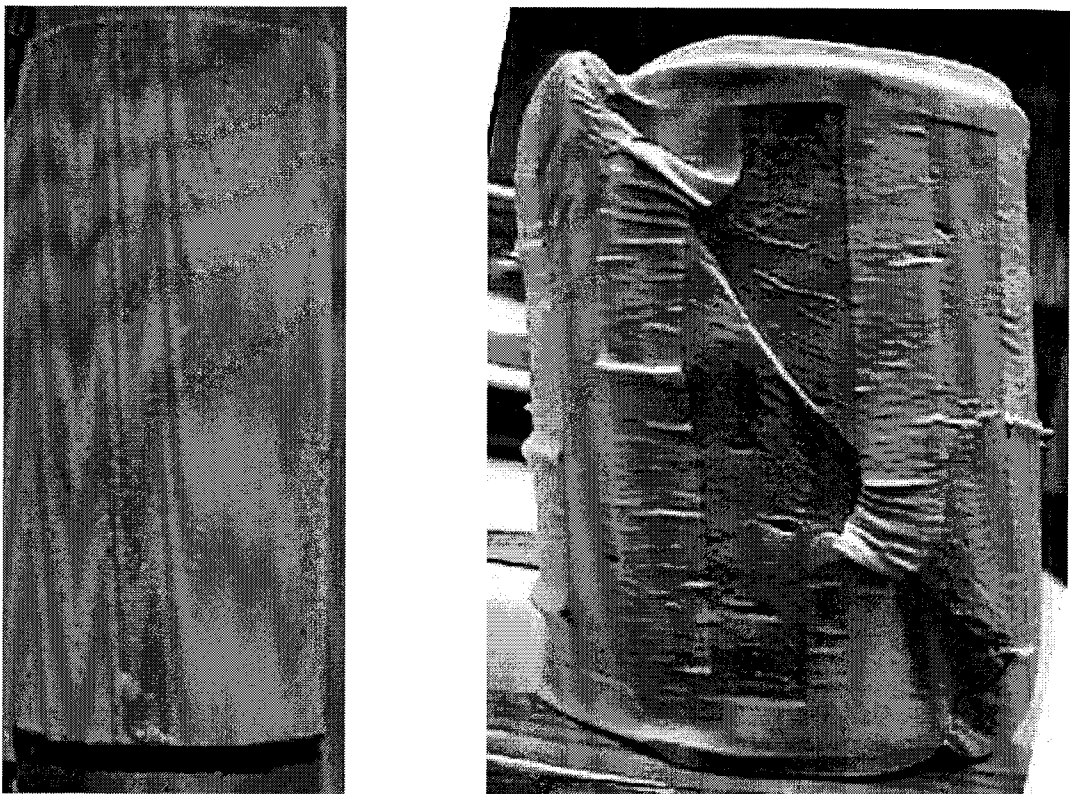
Figure 2.5. CID triaxial sample at w=70%, A_c=2%, $p_o{}'$=100 kPa & T_c=28 days.
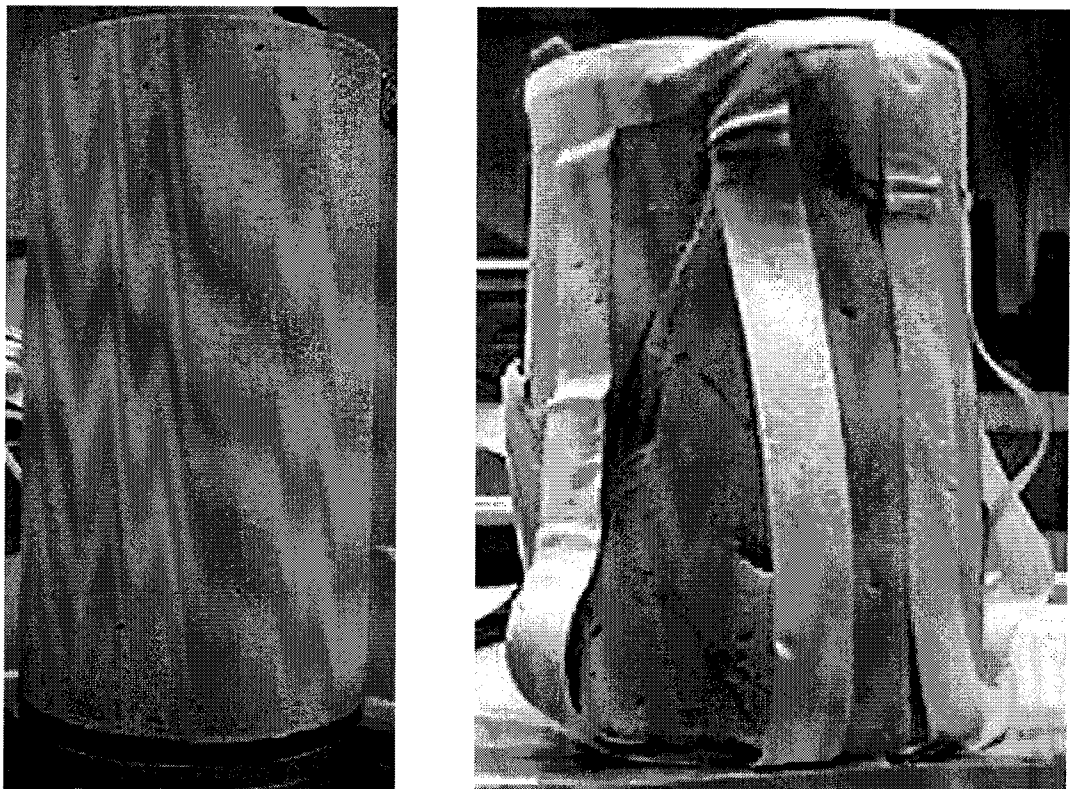
Figure 2.6. CID triaxial sample at w=70%, A_c=2%, $p_o{}'$=400 kPa & T_c=28 days.

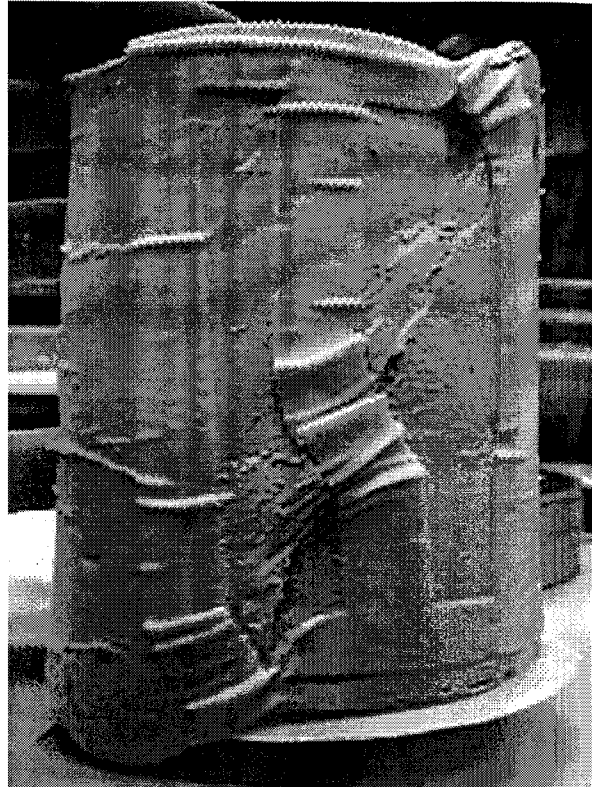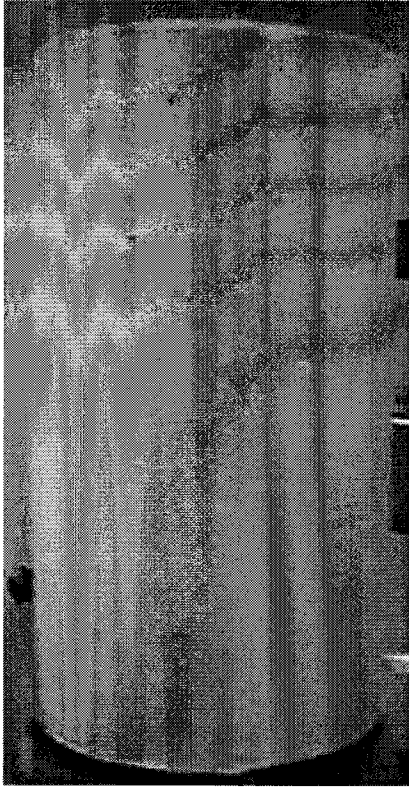Figure 2.7. CID triaxial sample at w=70%, A_c=2%, p_o'=50 kPa & T_c=56 days.
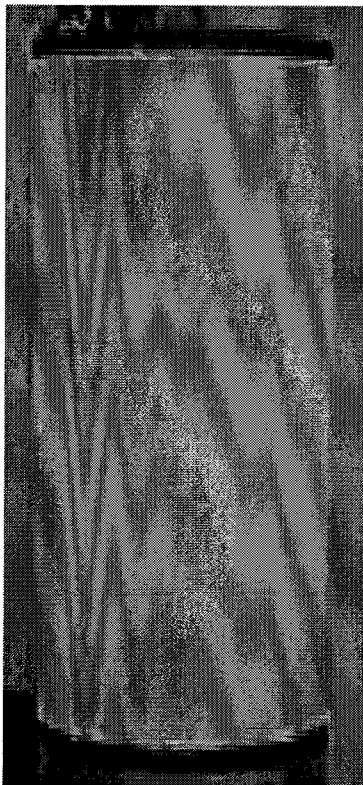
Figure 2.8. CID triaxial sample at w=70%, A_c=2%, p_o'=100 kPa & T_c=56 days.
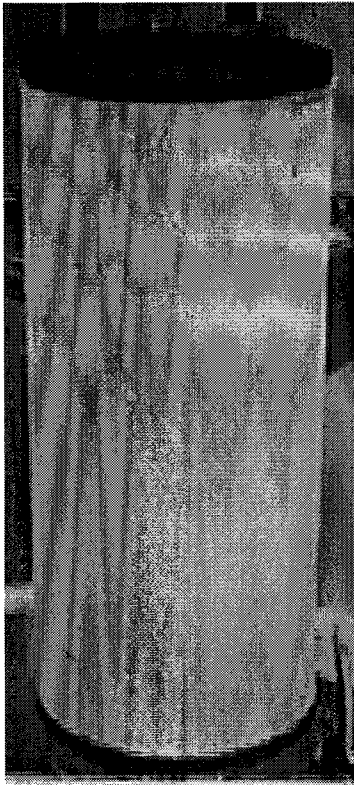
Figure 2.9. CID triaxial sample at w=70%, A_c=2%, p_o'=400 kPa & T_c=56 days.
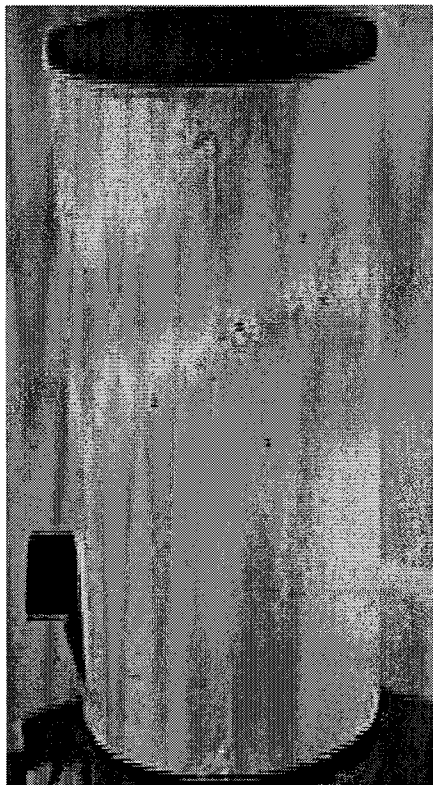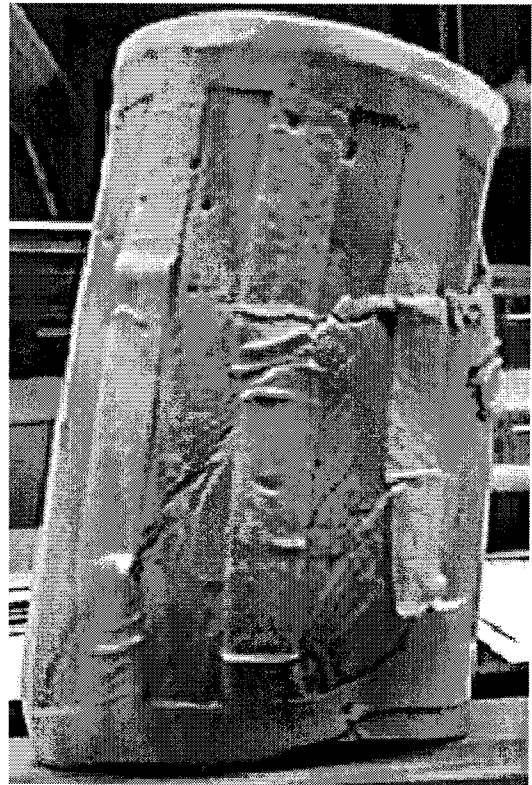

Figure 2.10. CID triaxial sample at w=70%, A_c=2%, p_o'=50 kPa & T_c=112 days.

MISSING PHOTOS

Figure 2.11. CID triaxial sample at w=70%, A_c=2%, $p_o{'}$=50 kPa & T_c=112 days (test B).
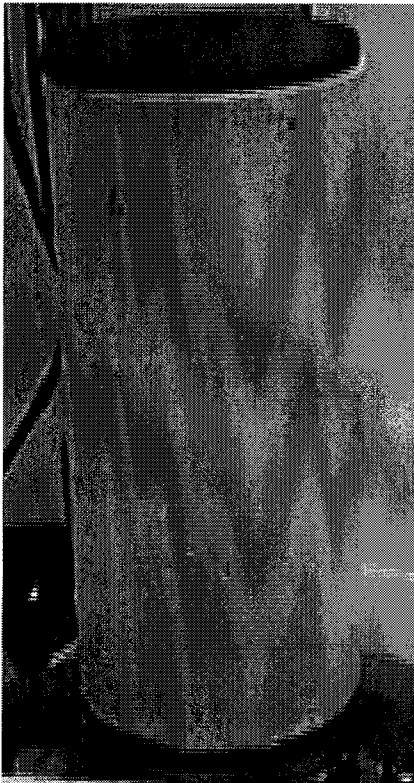
Figure 2.12. CID triaxial sample at w=70%, A_c=2%, $p_o{'}$=100 kPa & T_c=112 days.

Figure 2.13. CID triaxial sample at w=70%, A_c=2%, $p_o{'}$=400 kPa & T_c=112 days.

Figure 3.1. CID triaxial sample at w=70%, A_c=5%, $p_o{}'$=50 kPa & T_c=7 days.
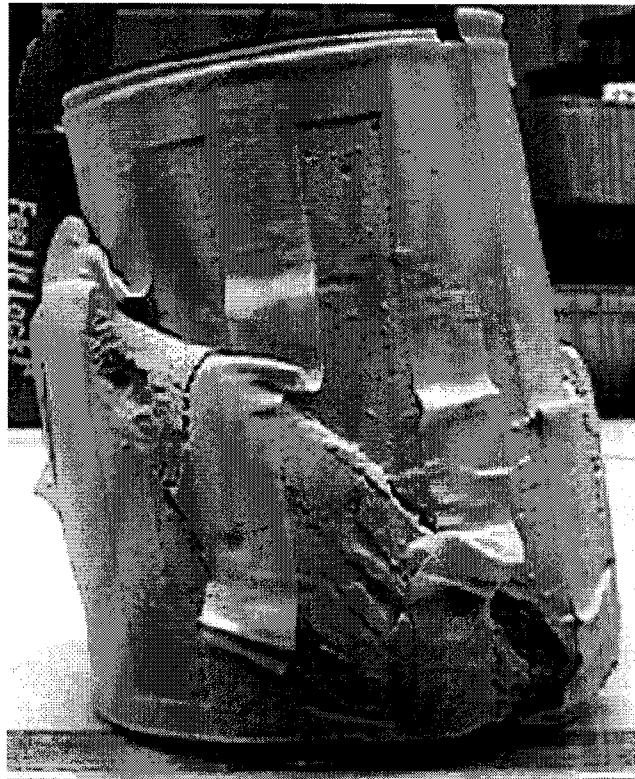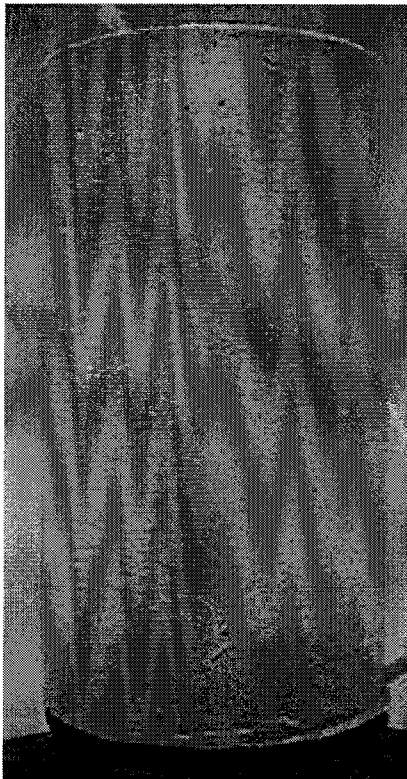
Figure 3.2. CID triaxial sample at w=70%, A_c=5%, $p_o{}'$=100 kPa & T_c=7 days.

Figure 3.3. CID triaxial sample at w=70%, A_c=5%, $p_o{}'$=400 kPa & T_c=7 days.
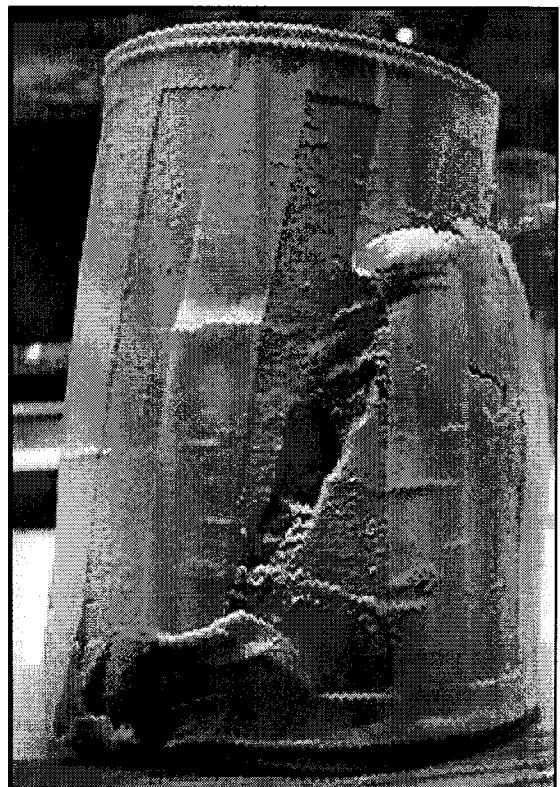
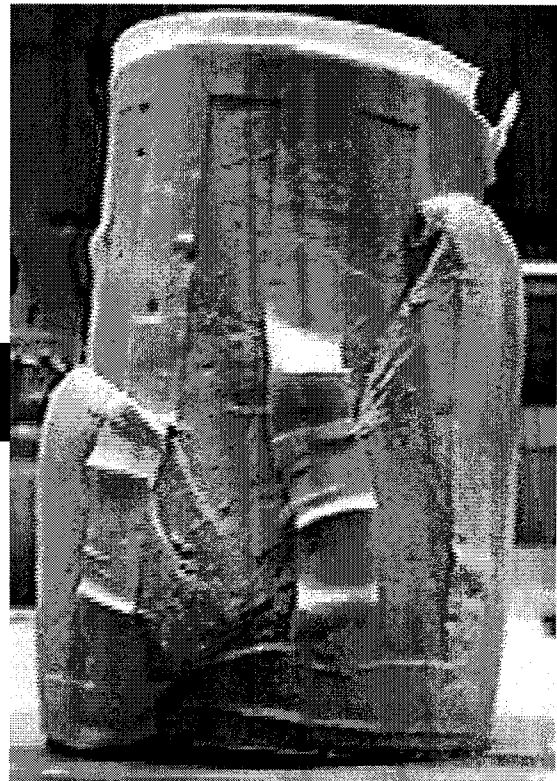Figure 3.4. CID triaxial sample at w=70%, A_c=5%, $p_o{}'$=50 kPa & T_c=28 days.
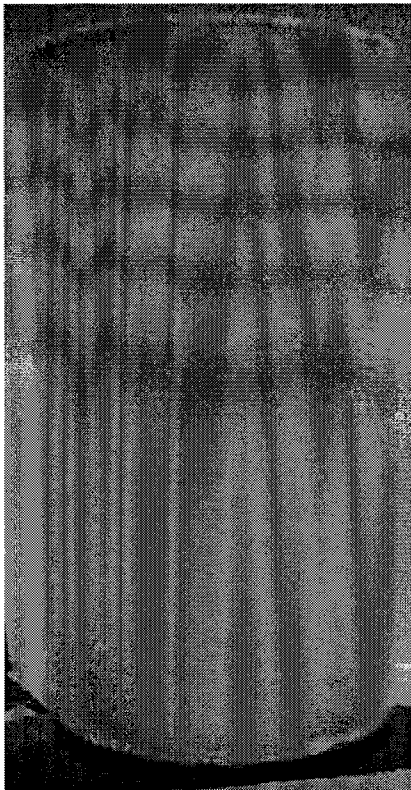
Figure 3.5. CID triaxial sample at w=70%, A_c=5%, $p_o{'}$ =100 kPa & T_c=28 days.
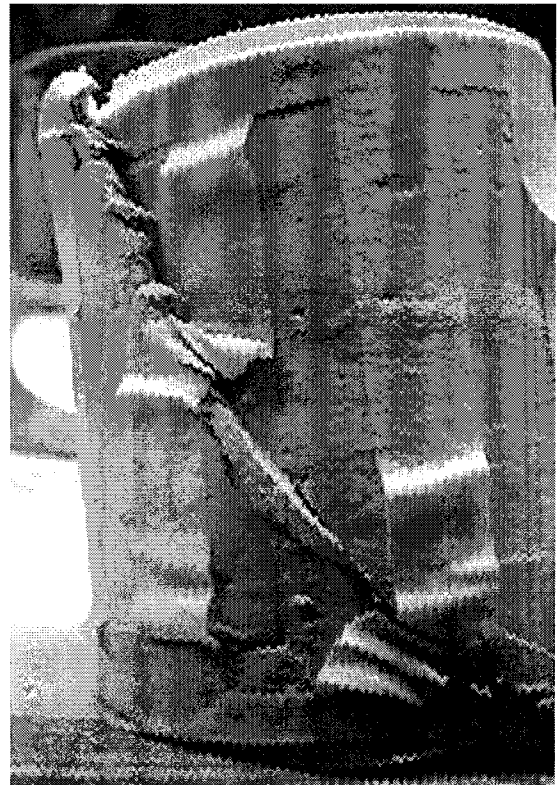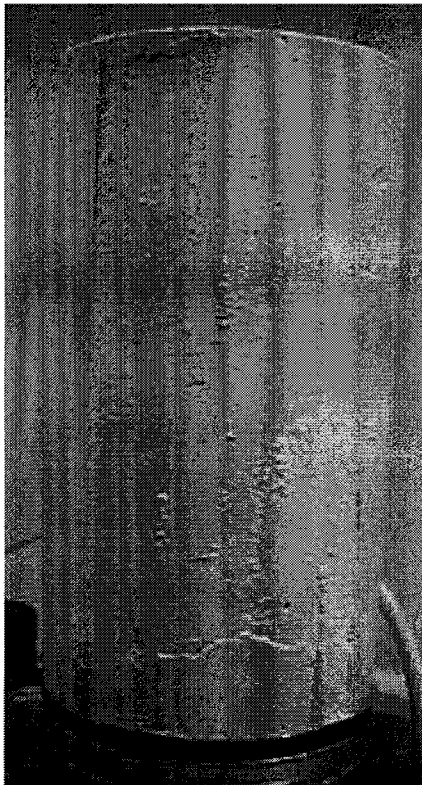
Figure 3.6. CID triaxial sample at w=70%, A_c=5%, $p_o{'}$ =400 kPa & T_c=28 days.
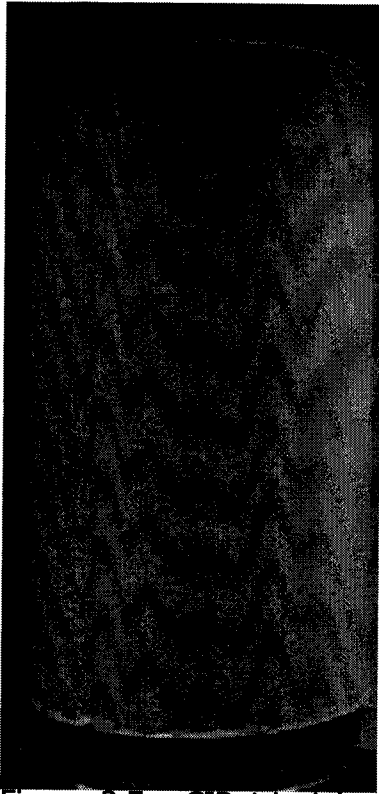
Figure 3.7. CID triaxial sample at w=70%, A_c=5%, $p_o{}'$=50 kPa & T_c=56 days.
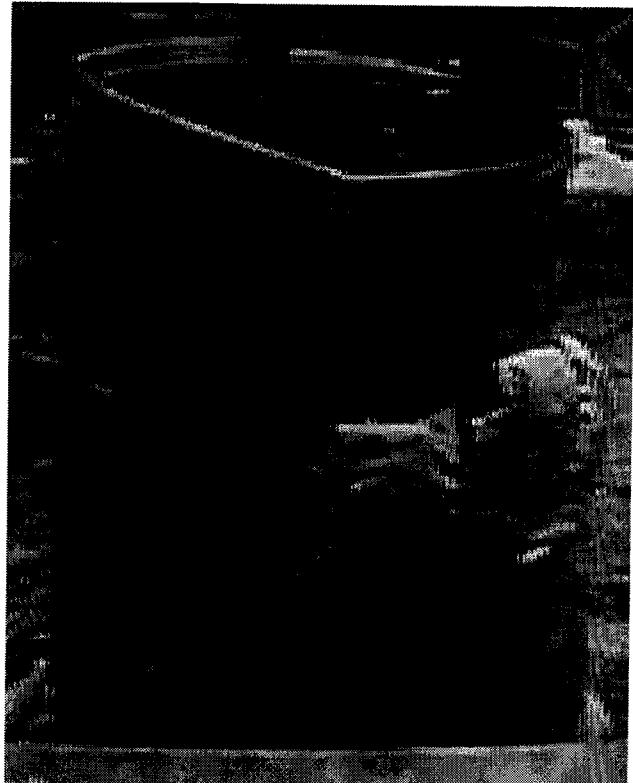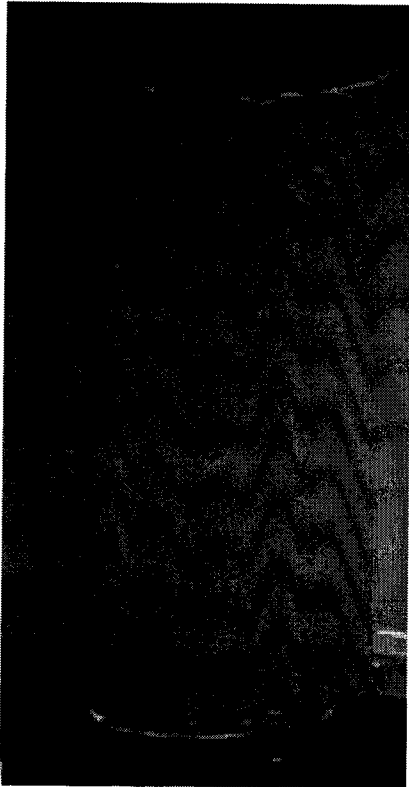
Figure 3.8. CID triaxial sample at w=70%, A_c=5%, $p_o{}'$=100 kPa & T_c=56 days.
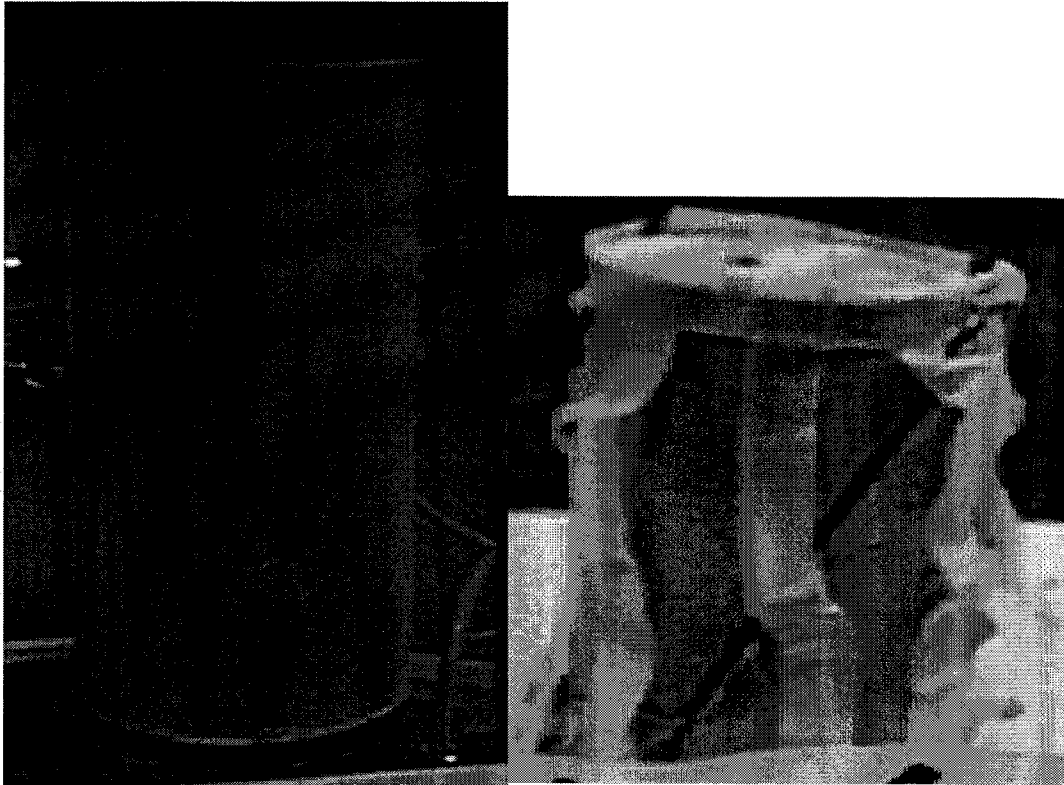
Figure 3.9. CID triaxial sample at w=70%, A_c=5%, $p_o{'}$=400 kPa & T_c=56 days.
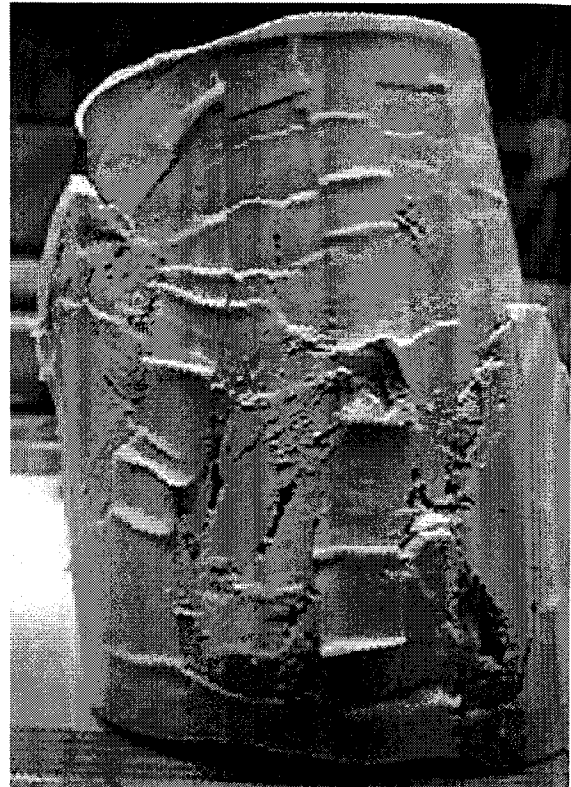
Figure 4.1. CID triaxial sample at w=100%, A_c=5%, p_o'=50 kPa & T_c=7 days.
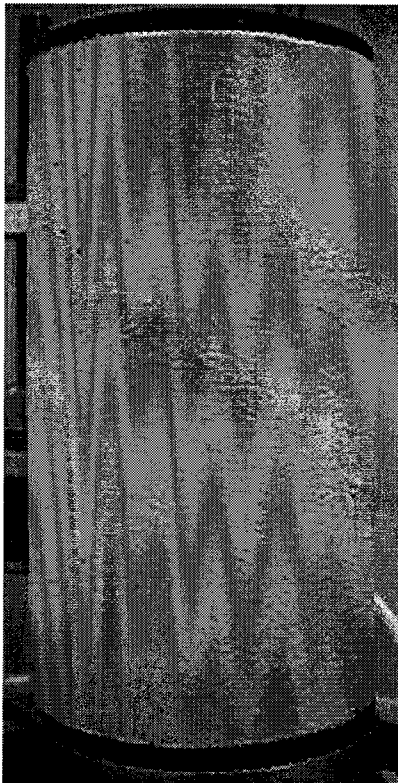
Figure 4.2. CID triaxial sample at w=100%, A_c=5%, p_o'=400 kPa & T_c=7 days.
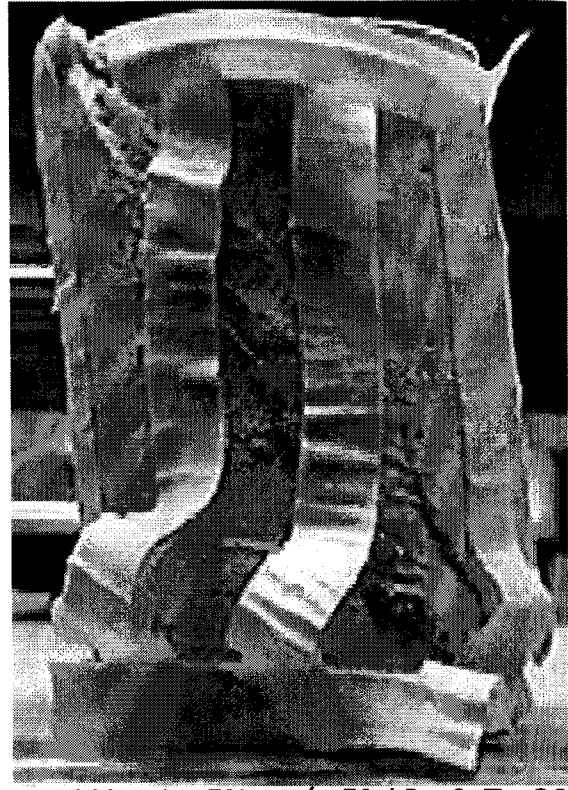
Figure 4.3.   CID triaxial sample at w=100%, A_c=5%, p_o'=50 kPa & T_c=28 days.

Figure 4.4.   CID triaxial sample at w=100%, A_c=5%, p_o'=50 kPa & T_c=28 days (test B).
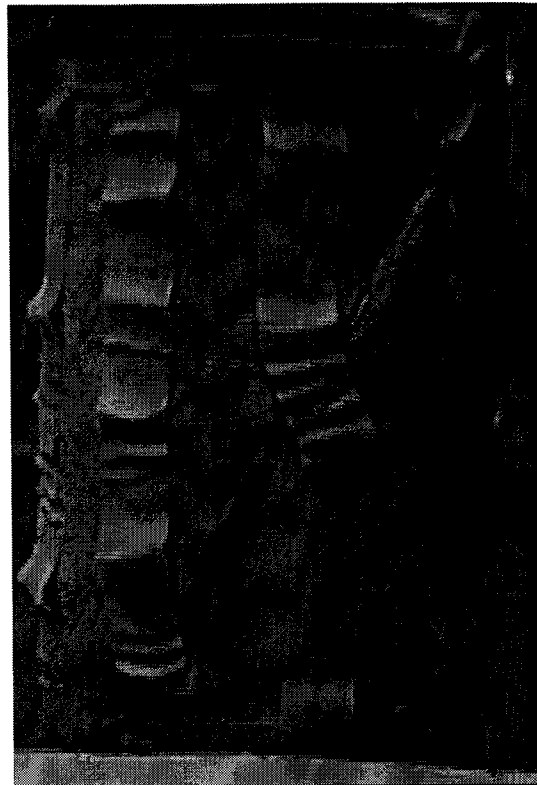
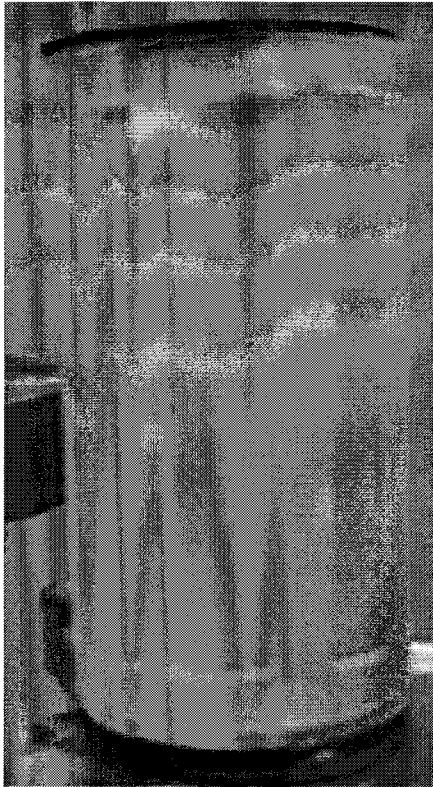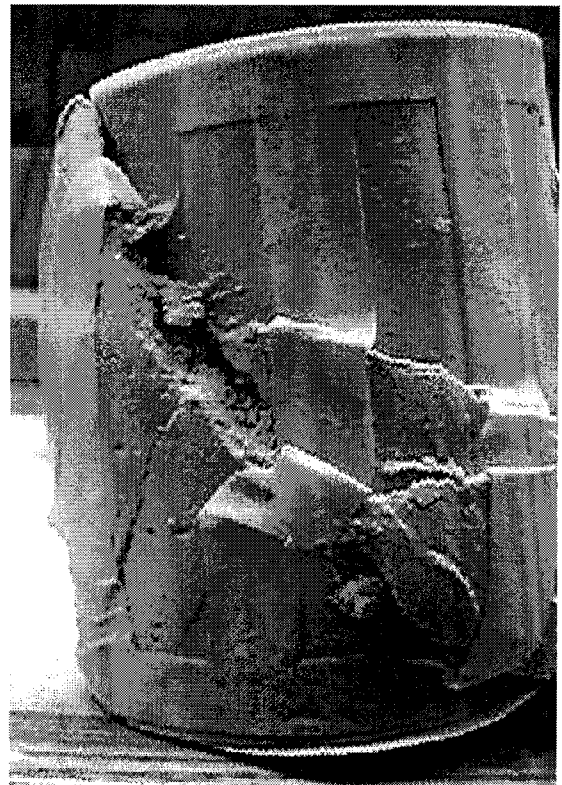Figure 4.5. CID triaxial sample at w=100%, A_c=5%, p_o'=50 kPa & T_c=28 days (test C).
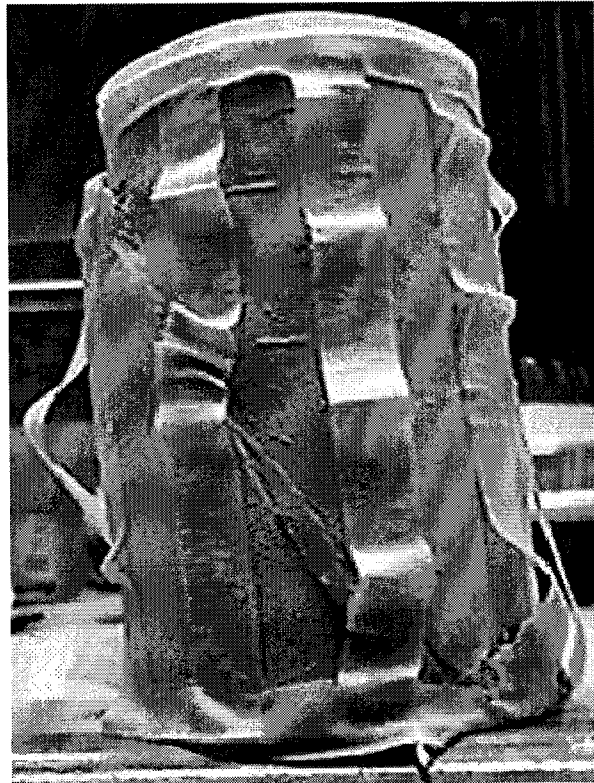
Figure 4.6. CID triaxial sample at w=100%, A_c=5%, p_o'=100 kPa & T_c=28 days.
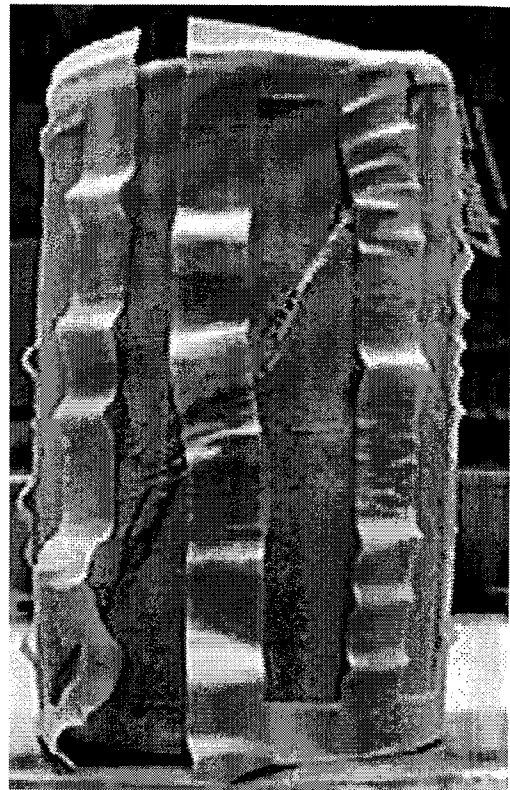
Figure 4.7. CID triaxial sample at w=100%, A_c=5%, $p_o{'}$=100 kPa & T_c=28 days (test B).
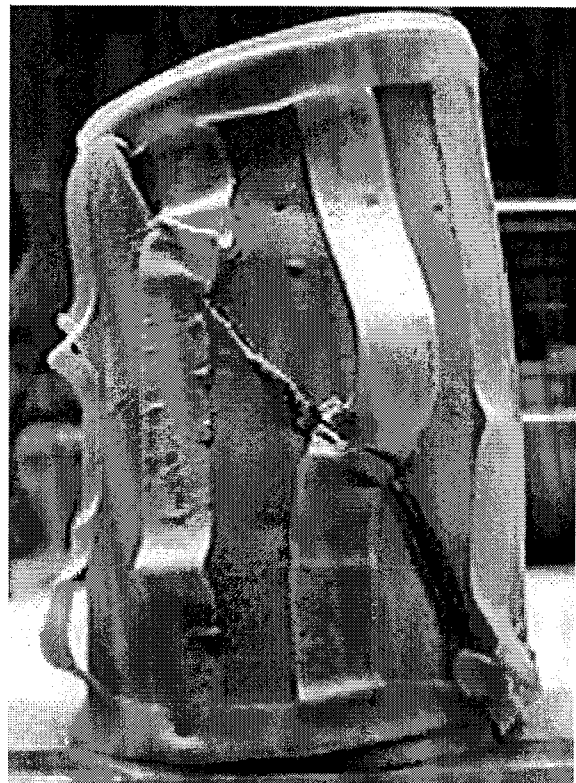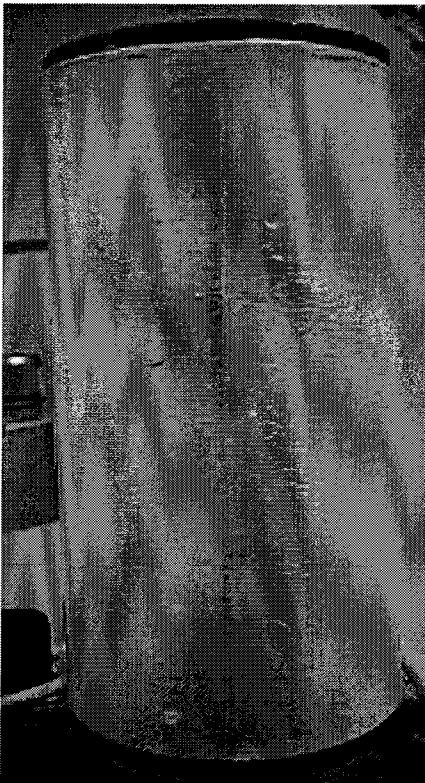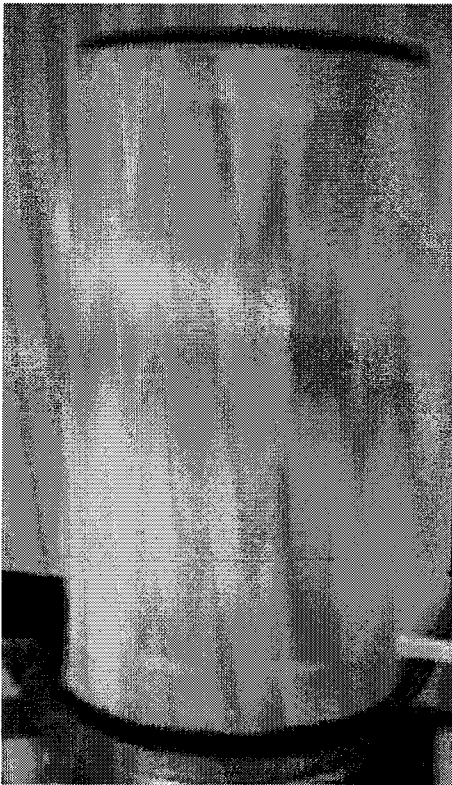

Figure 4.8. CID triaxial sample at w=100%, A_c=5%, $p_o{'}$=400 kPa & T_c=28 days.
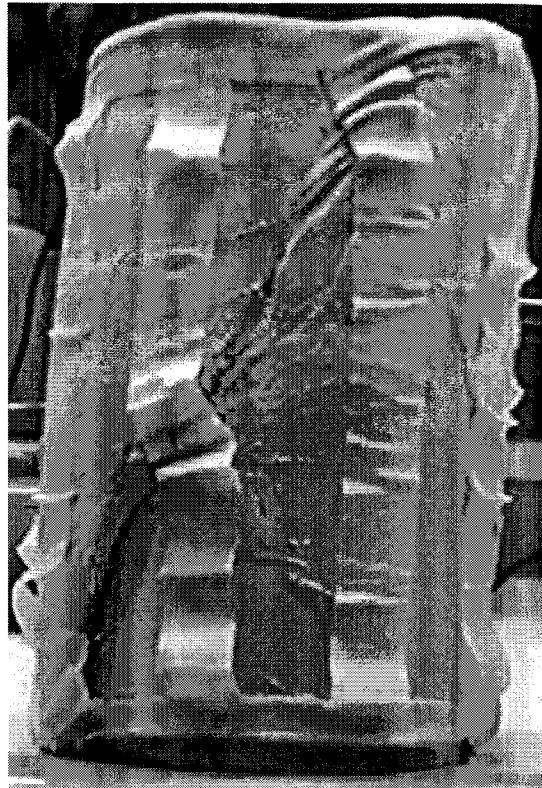
Figure 4.9. CID triaxial sample at w=100%, A_c=5%, $p_o{'}$=50 kPa & T_c=56 days.
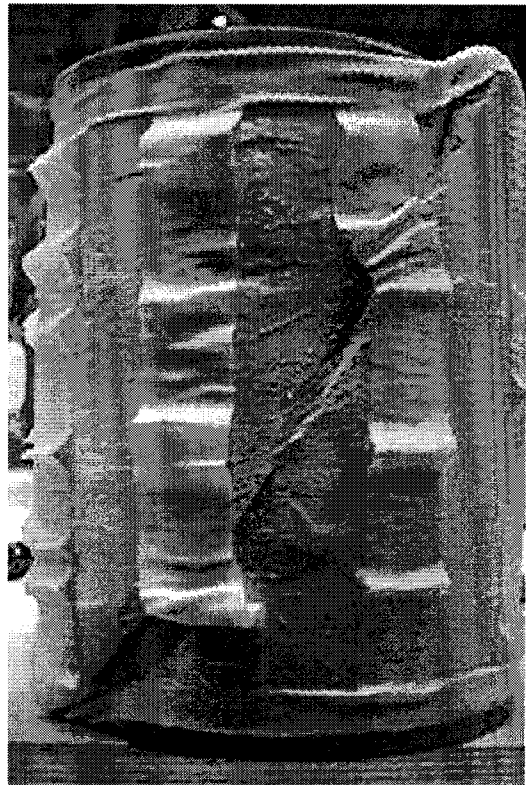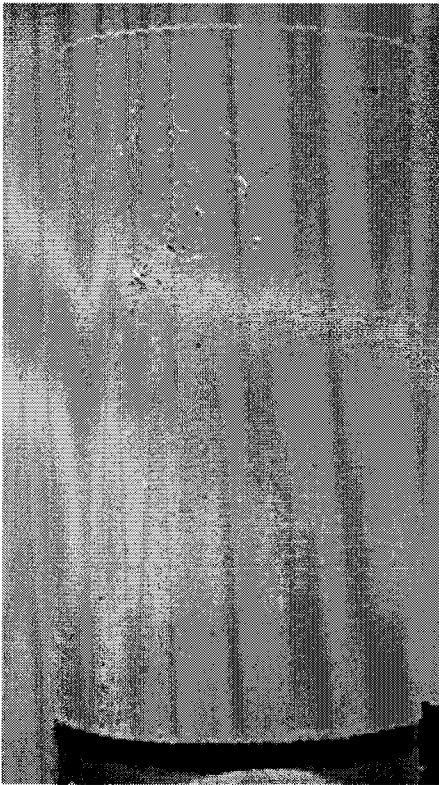
Figure 4.10. CID triaxial sample at w=100%, A_c=5%, $p_o{'}$=100 kPa & T_c=56 days.
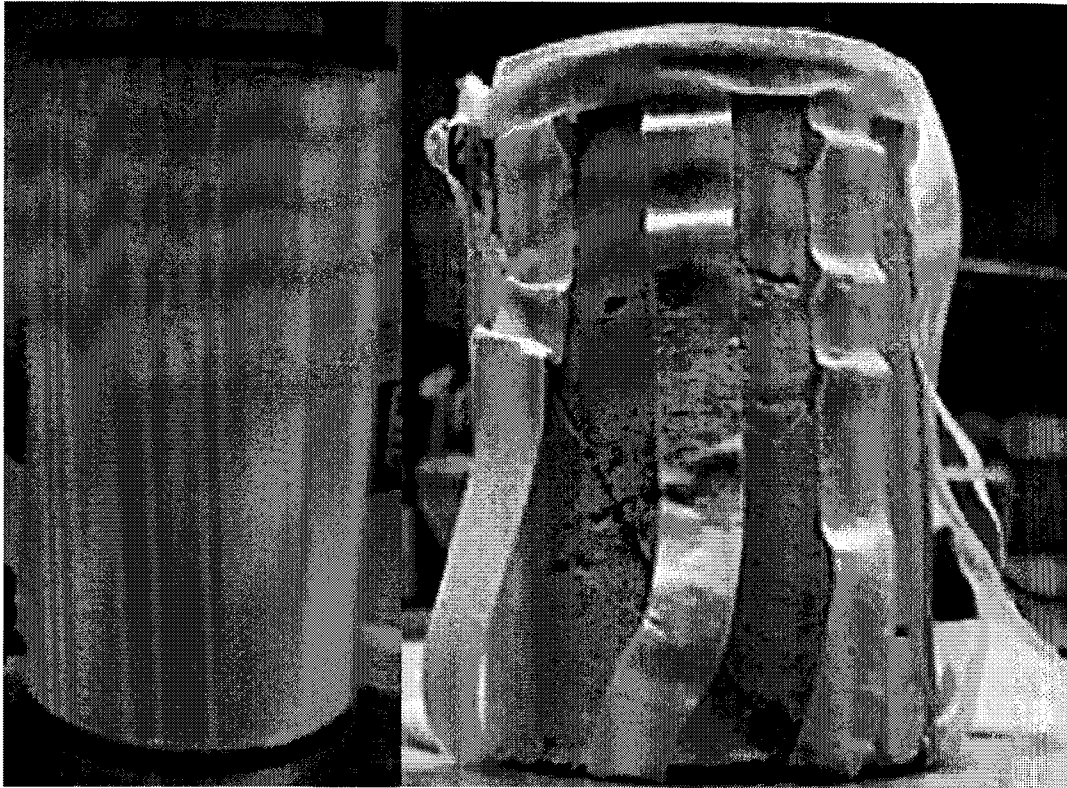
Figure 4.11. CID triaxial sample at w=100%, A_c=5%, $p_o{'}$=400 kPa & T_c=56 days.
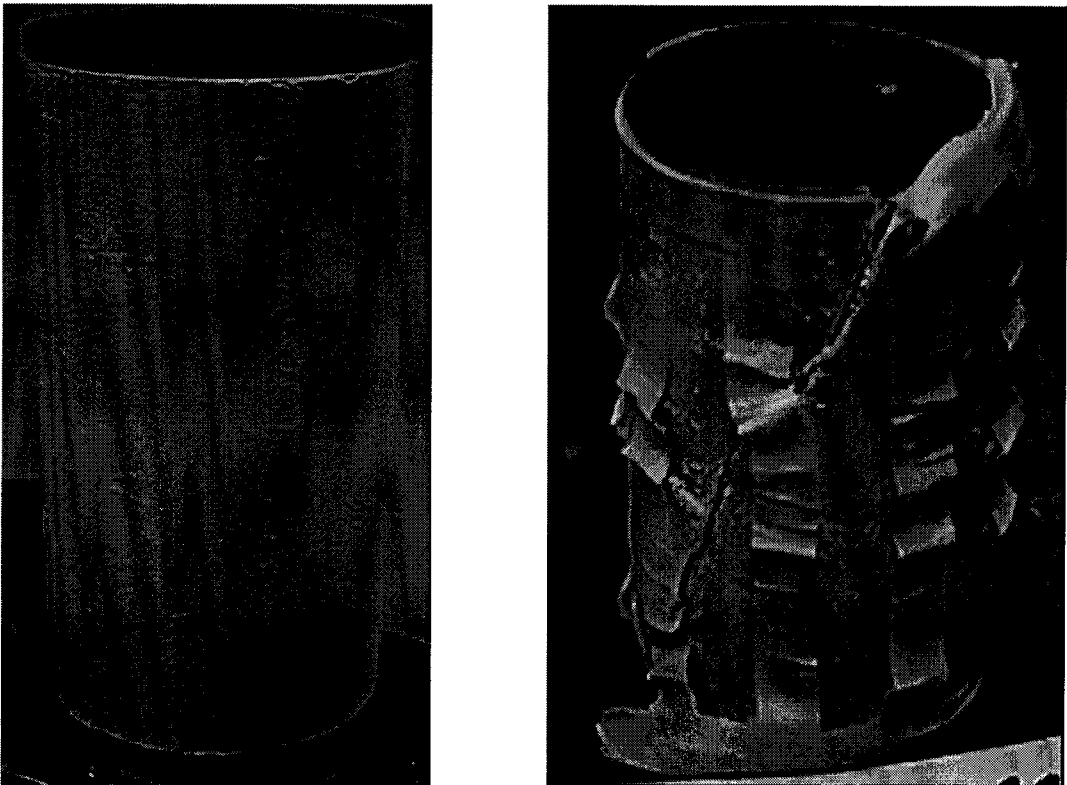

Figure 4.12. CID triaxial sample at w=100%, A_c=5%, $p_o{'}$=50 kPa & T_c=112 days.
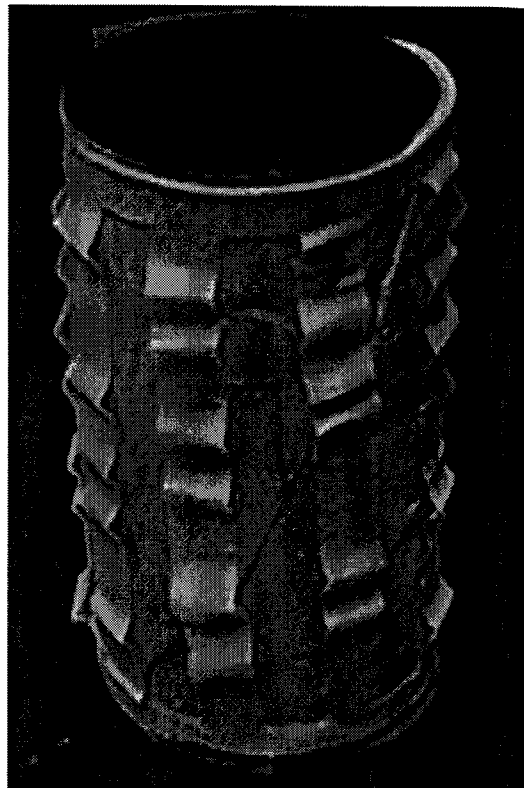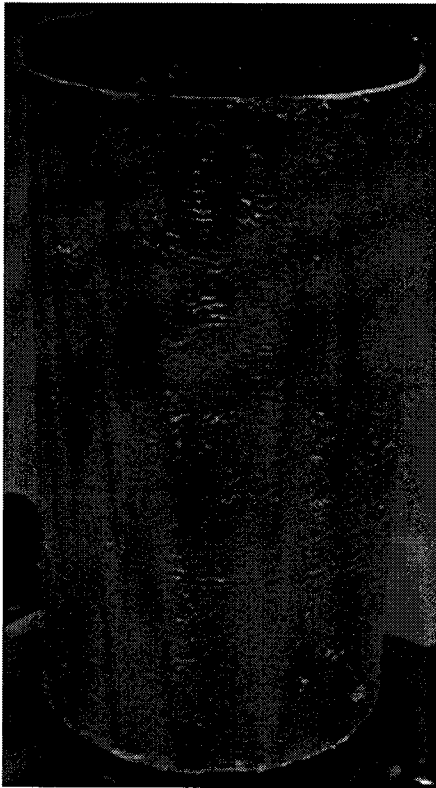
Figure 4.13. CID triaxial sample at w=100%, A_c=5%, $p_o{'}$=100 kPa & T_c=112 days.
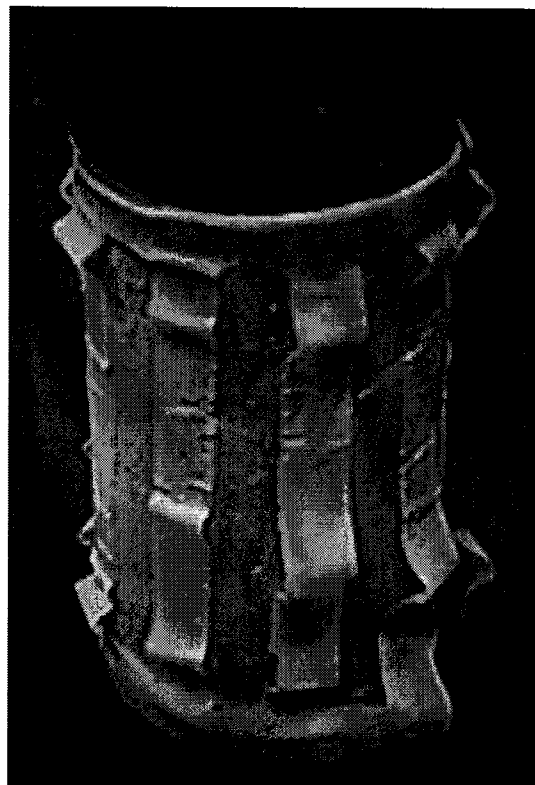
Figure 4.14. CID triaxial sample at w=100%, A_c=5%, $p_o{'}$=400 kPa & T_c=112 days.
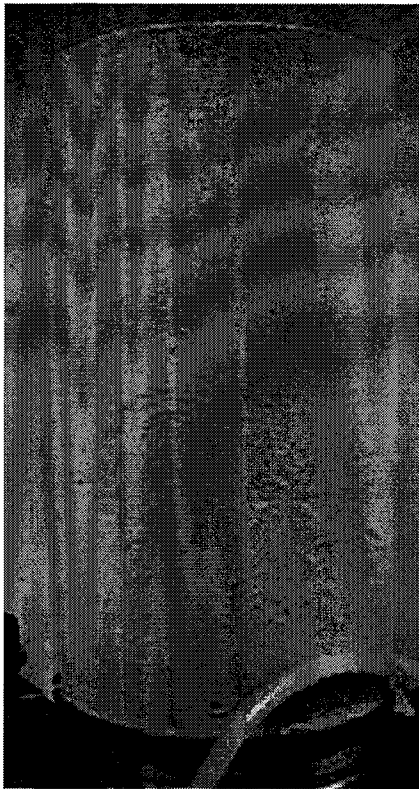
Figure 5.1. CID triaxial sample at w=100%, A_c=10%, p_o'=50 kPa & T_c=7 days (test B).
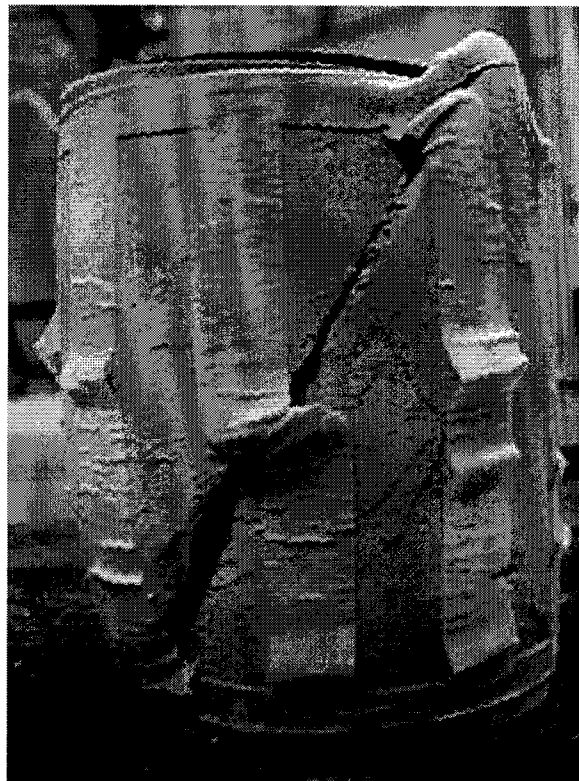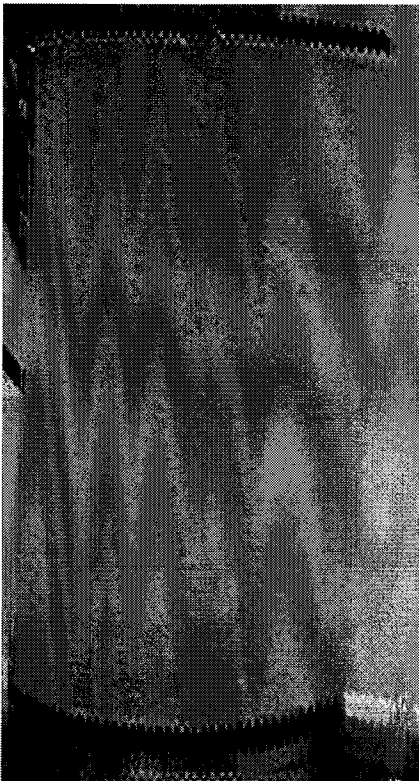
Figure 5.2. CID triaxial sample at w=100%, A_c=10%, p_o'=100 kPa & T_c=7 days (test C).
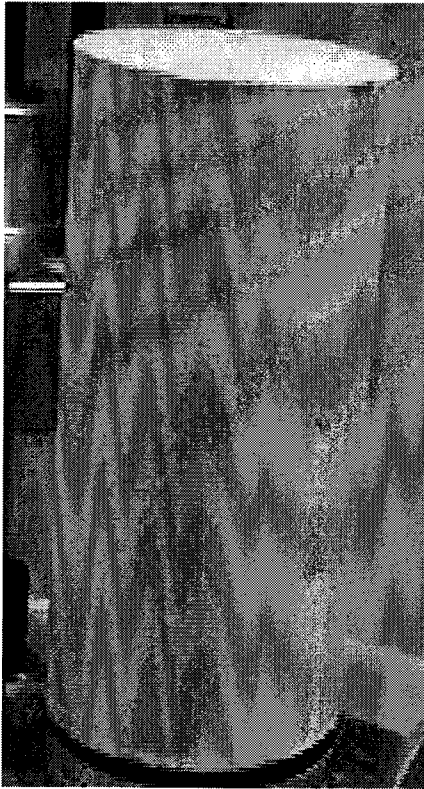
Figure 5.3. CID triaxial sample at w=100%, A_c=10%, p_o'=400 kPa & T_c=7 days.
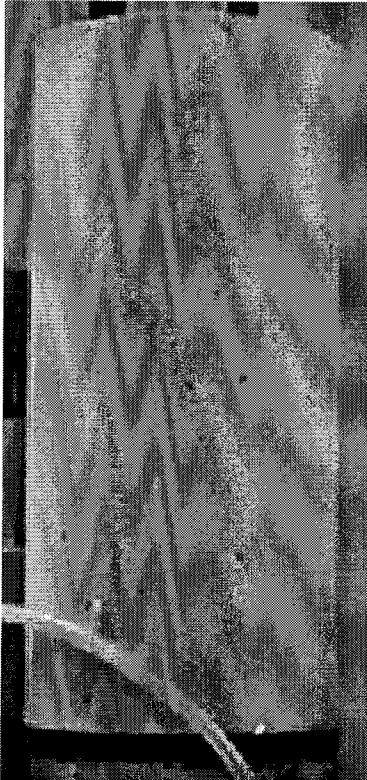
Figure 5.4. CID triaxial sample at w=100%, A_c=10%, p_o'=50 kPa & T_c=28 days.
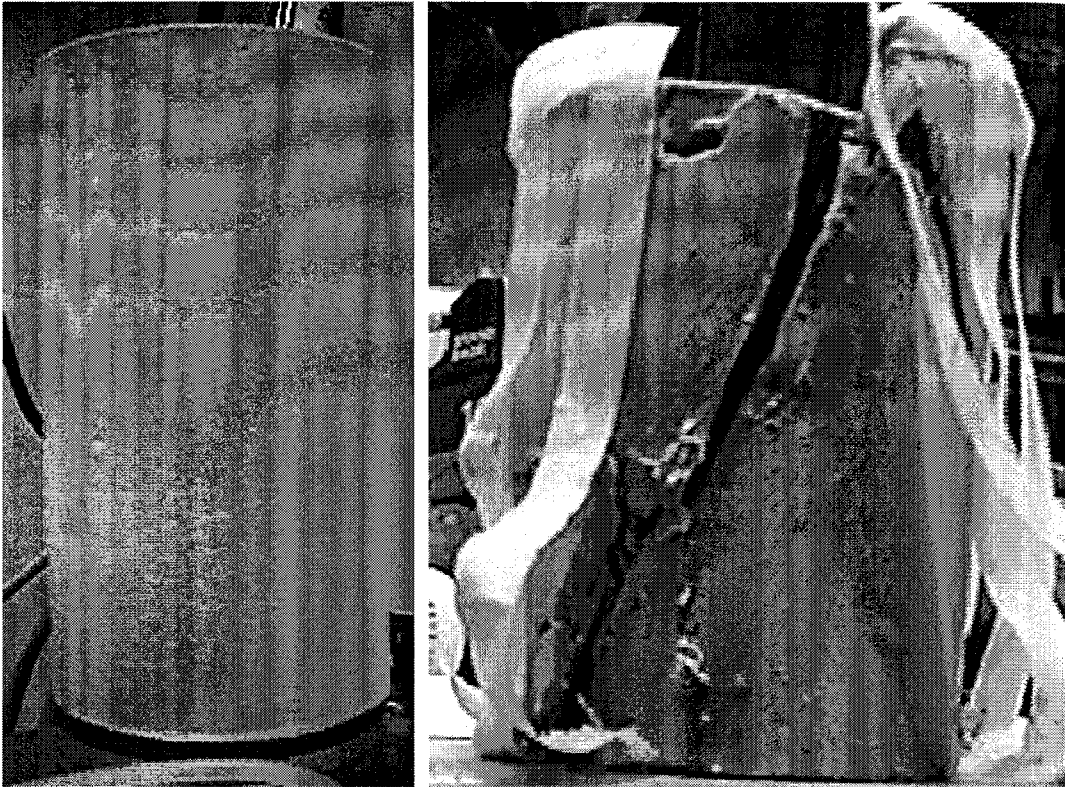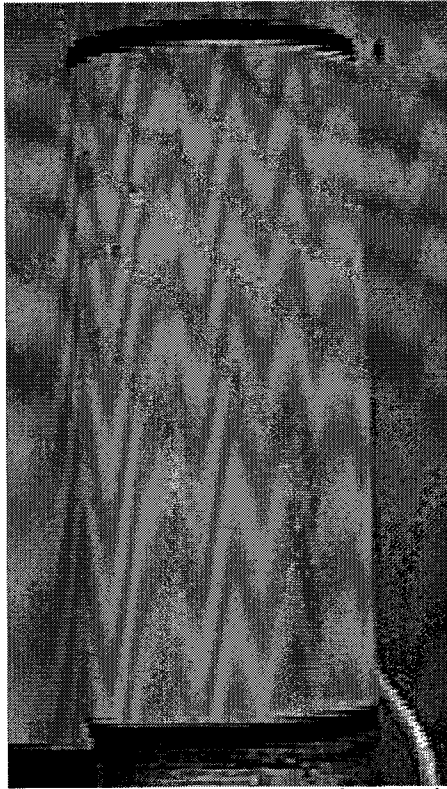
Figure 5.5. CID triaxial sample at w=100%, A_c=10%, $p_o{}'$=100 kPa & T_c=28 days.
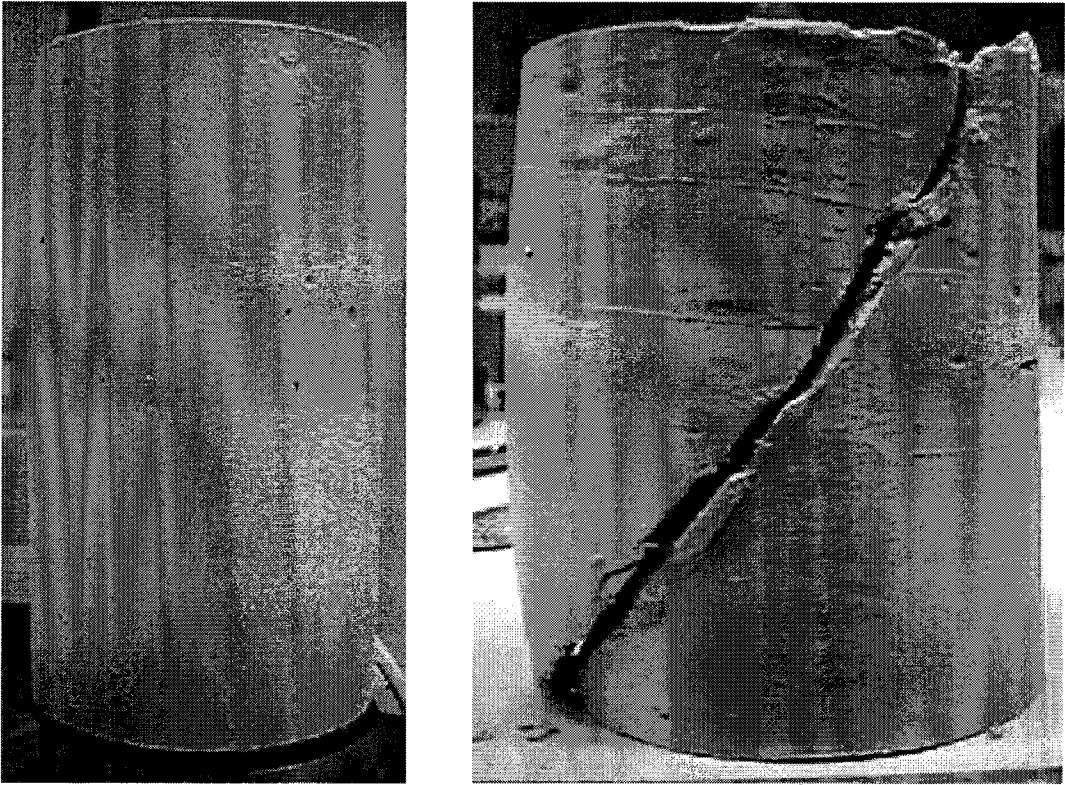
Figure 5.6. CID triaxial sample at w=100%, A_c=10%, $p_o{}'$=400 kPa & T_c=28 days.

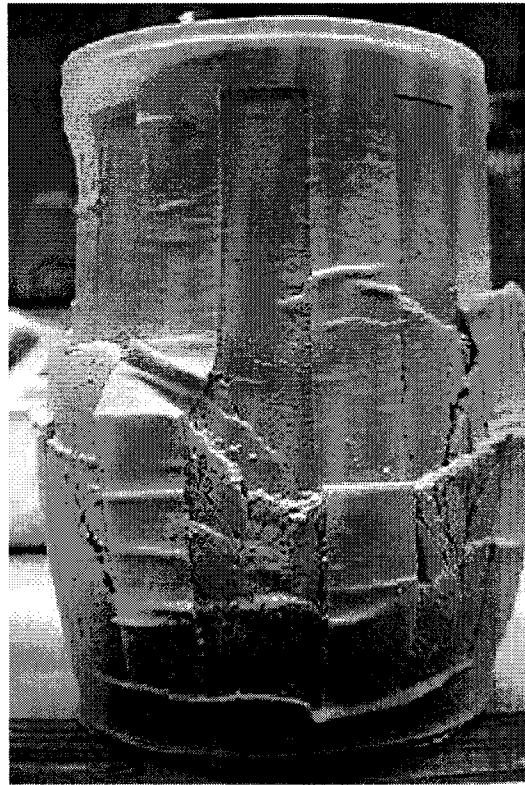Figure 5.7. CID triaxial sample at w=100%, A_c=10%, $p_o{}'$=50 kPa & T_c=56 days.
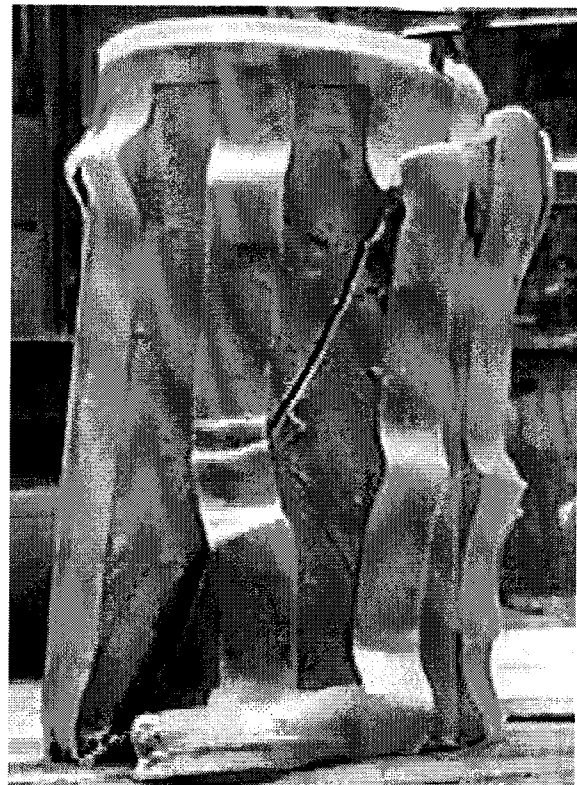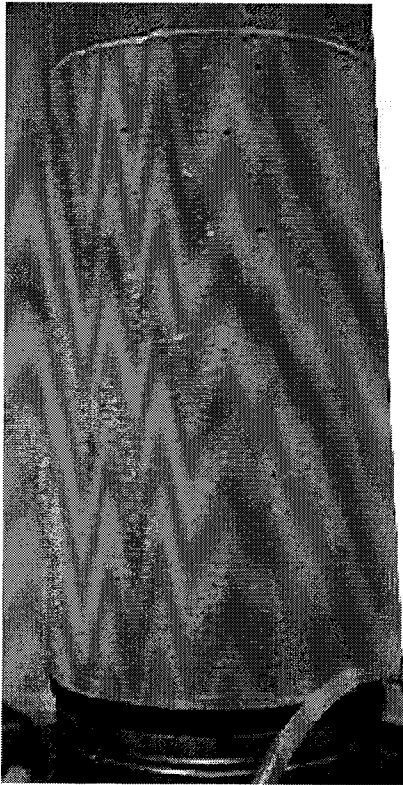
Figure 5.8. CID triaxial sample at w=100%, A_c=10%, $p_o{}'$=100 kPa & T_c=56 days.
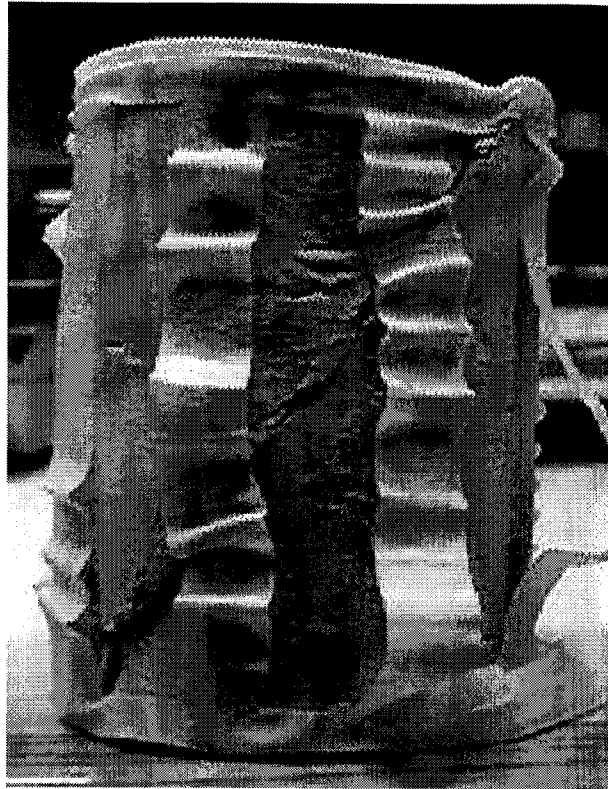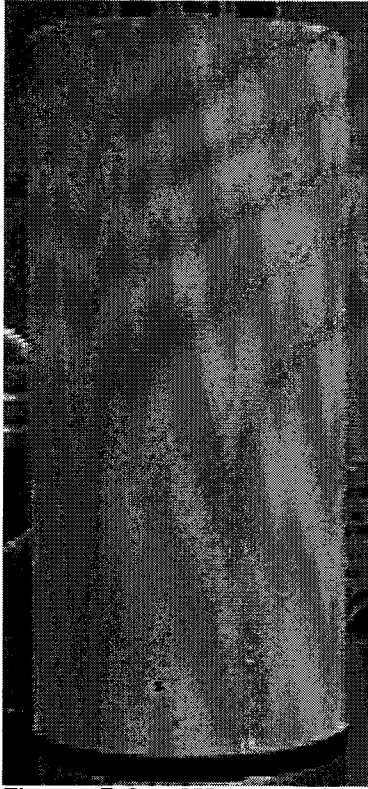
Figure 5.9. CID triaxial sample at w=100%, A_c=10%, $p_o{'}$=400 kPa & T_c=56 days.
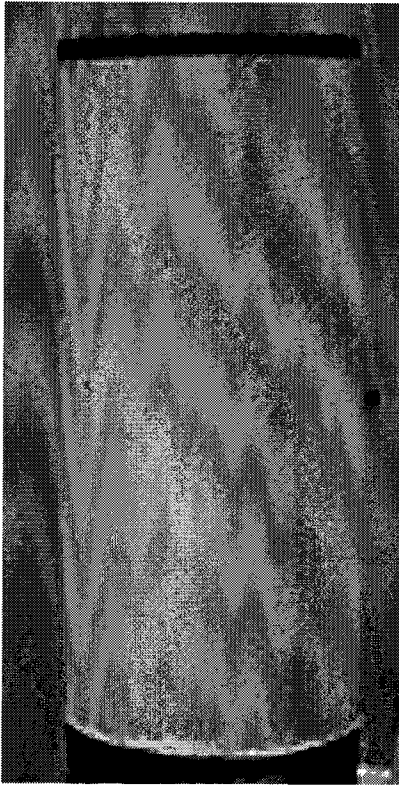
Figure 5.10. CID triaxial sample at w=100%, A_c=10%, $p_o{'}$=50 kPa & T_c=112 days.

MISSING PHOTOS

Figure 5.11. CID triaxial sample at w=100%, A_c=10%, $p_o{'}$=50 kPa & T_c=112 days (test B).

Figure 5.12. CID triaxial sample at w=100%, A_c=10%, $p_o{'}$=100 kPa & T_c=112 days.

MISSING PHOTOS

Figure 5.13. CID triaxial sample at w=100%, A_c=10%, $p_o{'}$=100 kPa & T_c=112 days (test B).
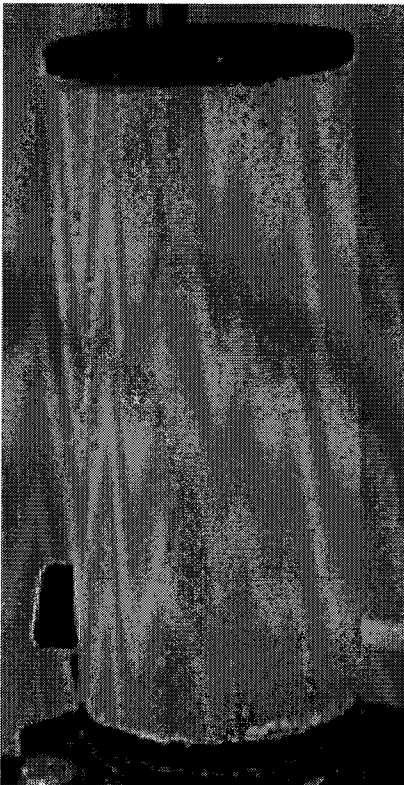
Figure 5.14. CID triaxial sample at w=100%, A_c=10%, $p_o{'}$=400 kPa & T_c=112 days.
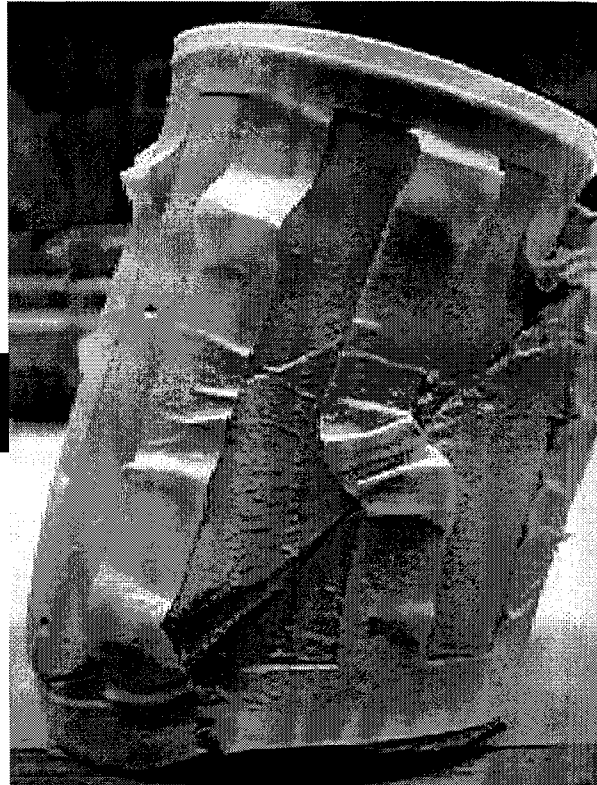
MISSING PHOTOS

Figure 5.15. CID triaxial sample at w=100%, A_c=10%, $p_o{'}$=400 kPa & T_c=112 days (test B).

Figure 6.1. CIU triaxial sample at w=40%, A_c=0% & $p_o{}'$ =100 kPa.
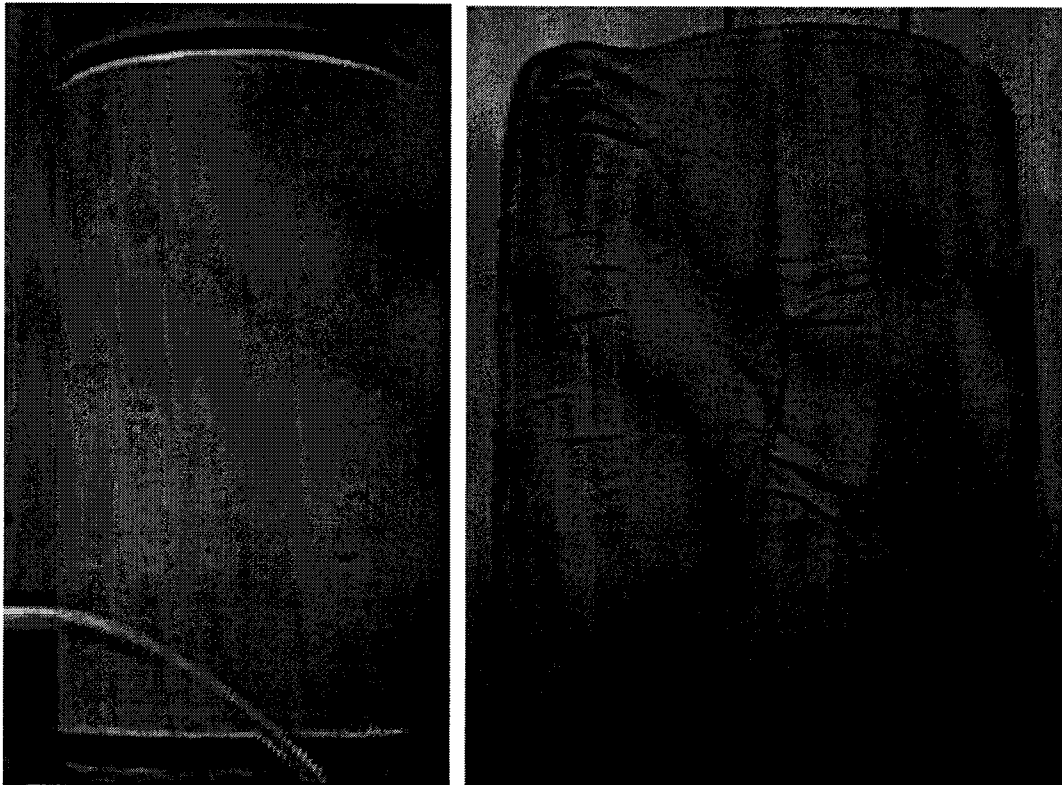
Figure 6.2. CIU triaxial sample at w=40%, A_c=0% & $p_o{}'$ =400 kPa.

Figure 7.1. CIU triaxial sample at w=70%, A_c=2%, p_o' =100 kPa & T_c=7 days.

Figure 7.2. CIU triaxial sample at w=70%, A_c=2%, p_o' =400 kPa & T_c=7 days.

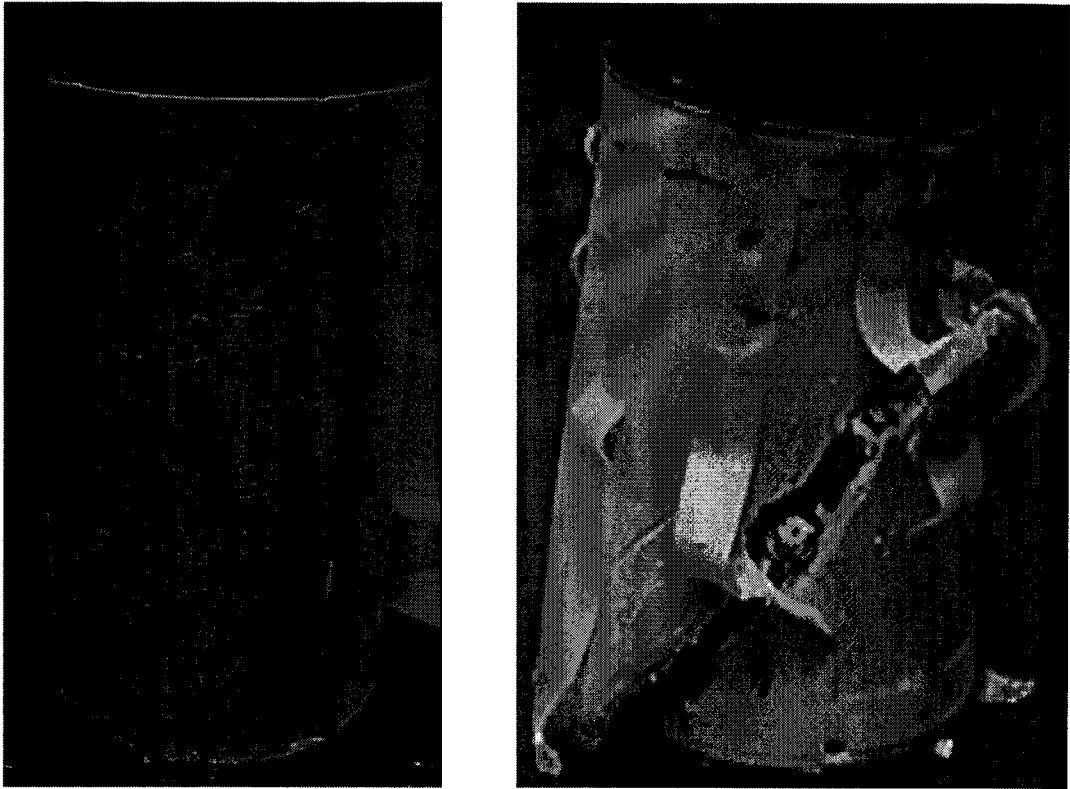Figure 7.3. CIU triaxial sample at w=70%, A_c=2%, $p_o{}'$=100 kPa & T_c=28 days (test B).

Figure 7.4. CIU triaxial sample at w=70%, A_c=2%, $p_o{}'$=400 kPa & T_c=28 days.

Figure 7.5. CIU triaxial sample at w=70%, A_c=2%, $p_o{'}$=300 kPa & T_c=56 days.
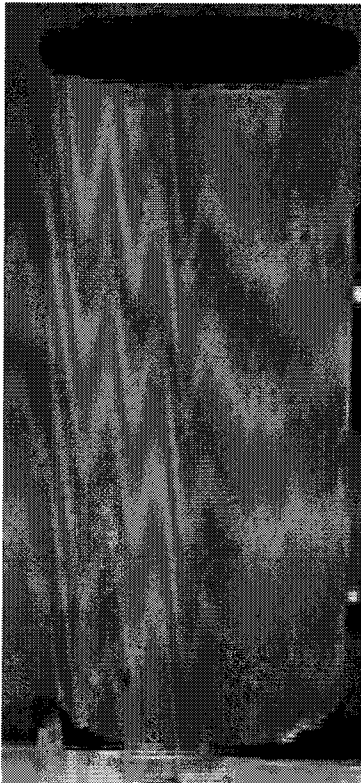
Figure 7.6. CIU triaxial sample at w=70%, A_c=2%, $p_o{'}$=100 kPa & T_c=112 days.

MISSING PHOTOS

Figure 7.7. CIU triaxial sample at w=70%, A_c=2%, p_o'=100 kPa & T_c=112 days (test B).

MISSING PHOTOS

Figure 7.8. CIU triaxial sample at w=70%, A_c=2%, p_o'=400 kPa & T_c=112 days (test B).

Figure 8.1. CIU triaxial sample at w=70%, A_c=5%, p_o'=100 kPa & T_c=7 days.
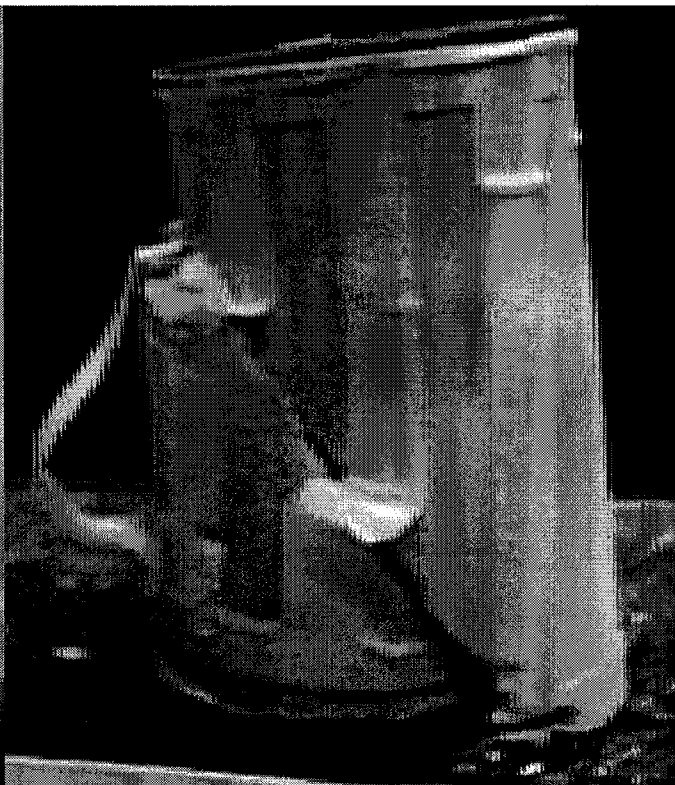

Figure 8.2. CIU triaxial sample at w=70%, A_c=5%, p_o'=400 kPa & T_c=7 days.
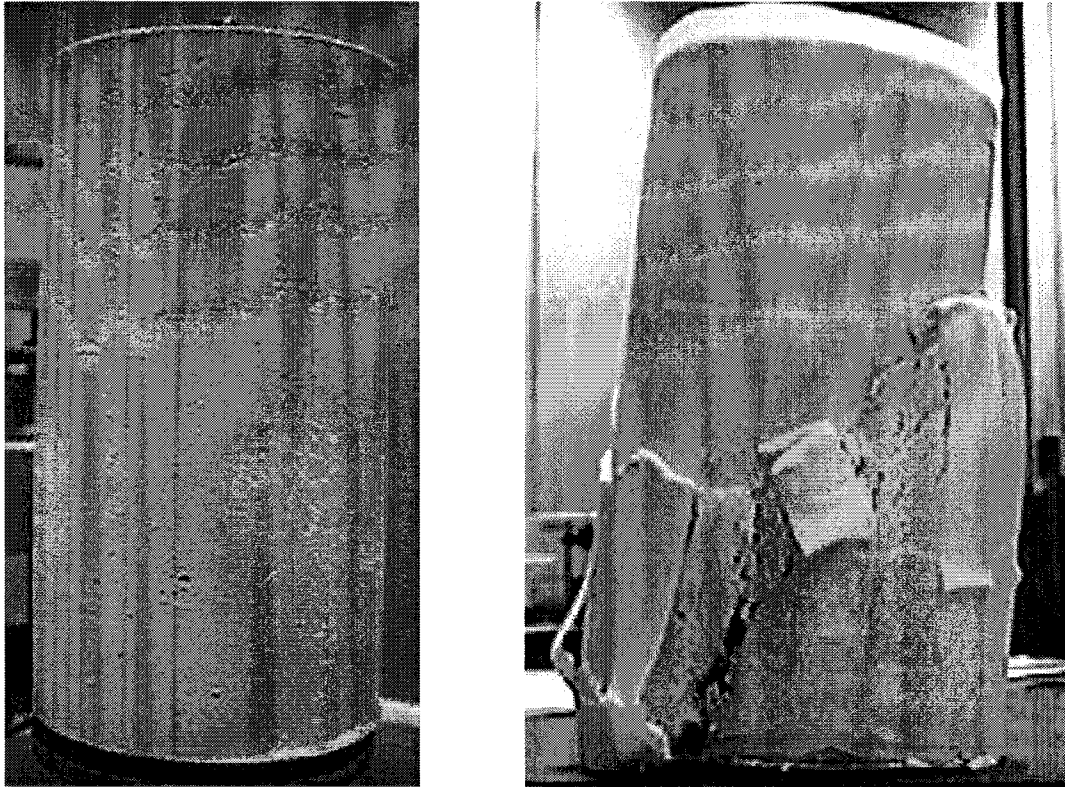
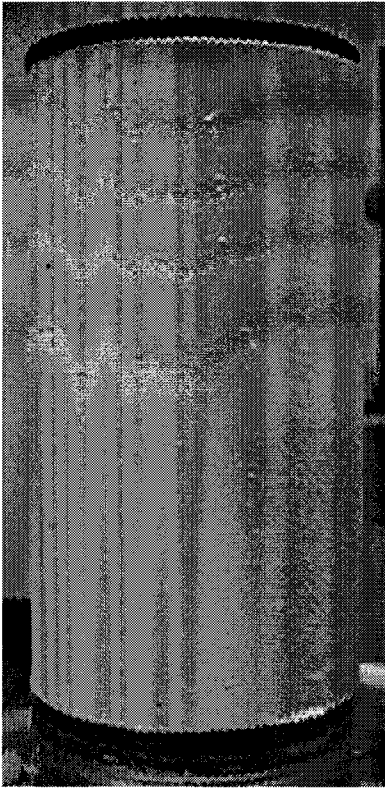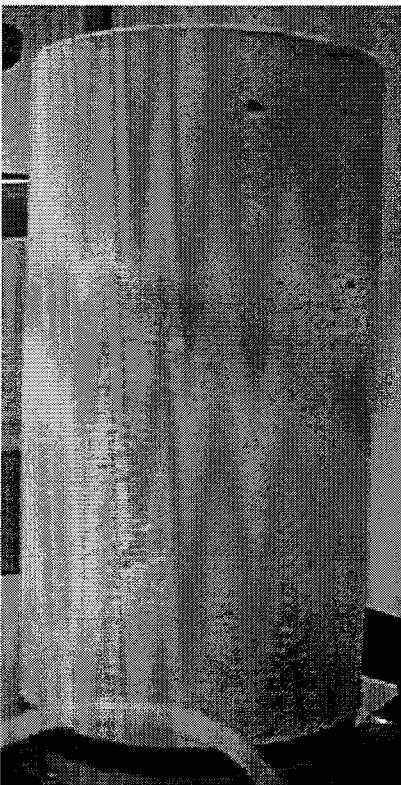Figure 8.3. CIU triaxial sample at w=70%, A_c=5%, p_o'=100 kPa & T_c=28 days.
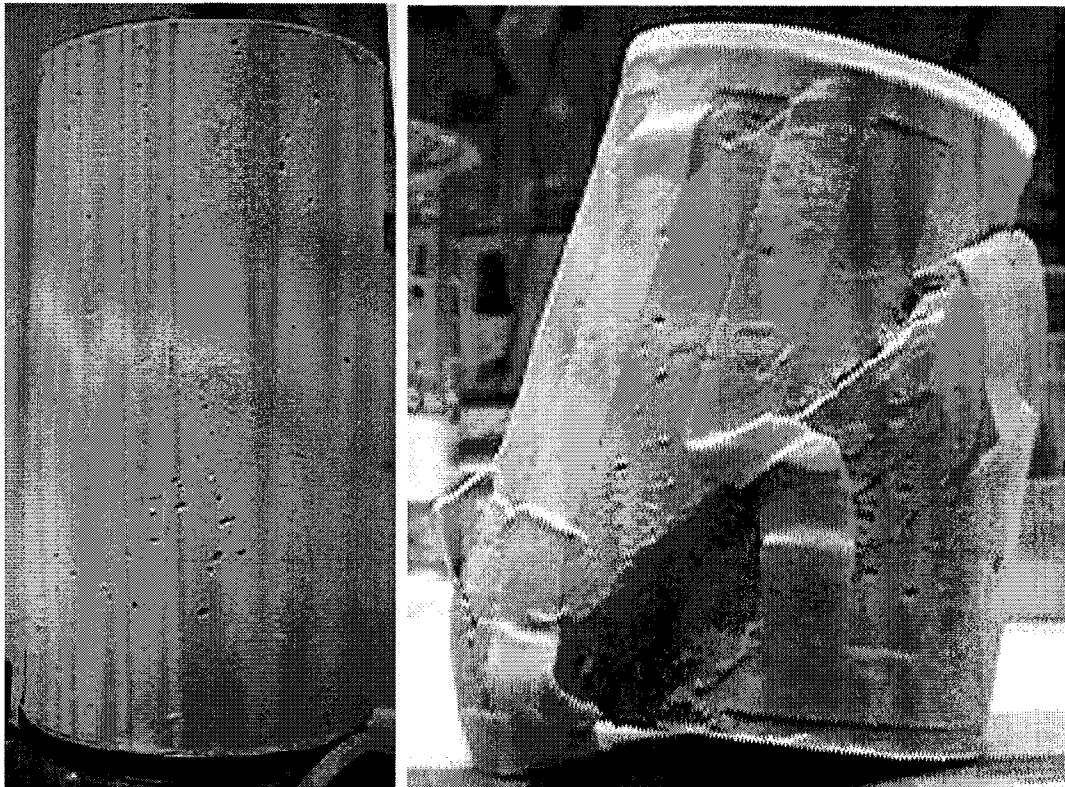
Figure 8.4. CIU triaxial sample at w=70%, A_c=5%, p_o'=400 kPa & T_c=28 days.

MISSING PHOTOS

Figure 8.5. CIU triaxial sample at w=70%, A_c=5%, p_o'=100 kPa & T_c=56 days.
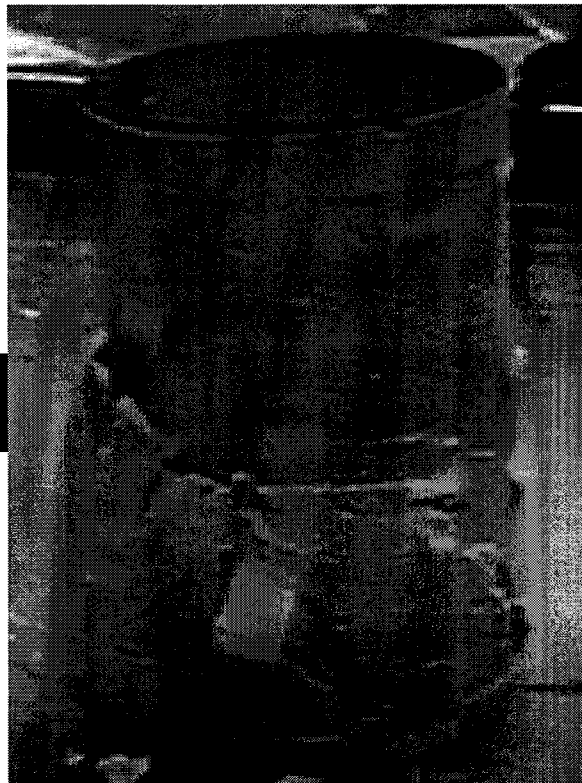
MISSING PHOTO

Figure 8.6. CIU triaxial sample at w=70%, A_c=5%, p_o'=400 kPa & T_c=56 days.

Figure 9.1. CIU triaxial sample at w=100%, A_c=5%, $p_o{'}$=100 kPa & T_c=7 days.

Figure 9.2. CIU triaxial sample at w=100%, A_c=5%, $p_o{'}$=400 kPa & T_c=7 days.

Figure 9.3. CIU triaxial sample at w=100%, A_c=5%, p_o'=400 kPa & T_c=7 days (test B).

Figure 9.4. CIU triaxial sample at w=100%, A_c=5%, p_o'=100 kPa & T_c=28 days.

Figure 9.5.   CIU triaxial sample at w=100%, A_c=5%, $p_o{'}$=100 kPa & T_c=28 days (test B).

MISSING PHOTO

Figure 9.6.   CIU triaxial sample at w=100%, A_c=5%, $p_o{'}$=400 kPa & T_c=28 days.

Figure 9.7. CIU triaxial sample at w=100%, A_c=5%, p_o'=400 kPa & T_c=28 days (test B).

Figure 9.8. CIU triaxial sample at w=100%, A_c=5%, p_o'=100 kPa & T_c=56 days.

Figure 9.9. CIU triaxial sample at w=100%, A_c=5%, $p_o{}'$=400 kPa & T_c=56 days.

Figure 9.10. CIU triaxial sample at w=100%, A_c=5%, $p_o{}'$=100 kPa & T_c=112 days.

Figure 9.11. CIU triaxial sample at w=100%, A_c=5%, $p_o{}'$=400 kPa & T_c=112 days.
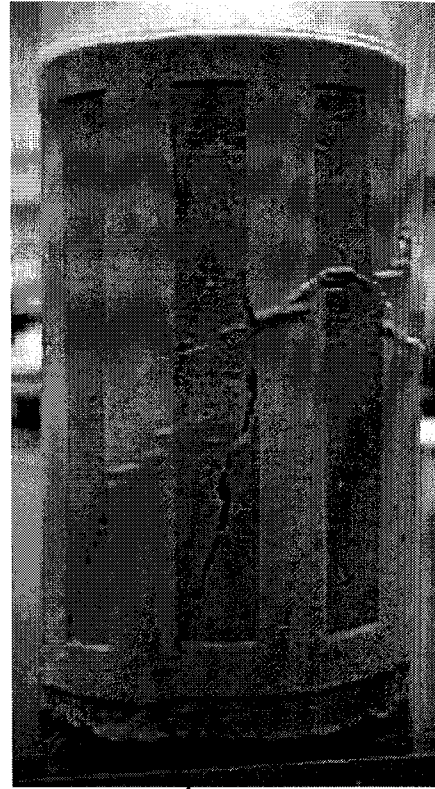
Figure 10.1. CIU triaxial sample at w=100%, A_c=10%, $p_o{}'$=100 kPa & T_c=7 days.

Figure 10.2. CIU triaxial sample at w=100%, A_c=10%, $p_o{}'$=400 kPa & T_c=7 days (test C).

Figure 10.3. CIU triaxial sample at w=100%, A_c=10%, p_o'=100 kPa & T_c=28 days.

Figure 10.4. CIU triaxial sample at w=100%, A_c=10%, p_o'=400 kPa & T_c=28 days.

Figure 10.5. CIU triaxial sample at w=100%, A_c=10%, p_o'=400 kPa & T_c=28 days (test B).

Figure 10.6. CIU triaxial sample at w=100%, A_c=10%, p_o'=100 kPa & T_c=56 days.

Figure 10.7. CIU triaxial sample at w=100%, A_c=10%, p_o'=400 kPa & T_c=56 days.

Figure 10.8. CIU triaxial sample at w=100%, A_c=10%, p_o'=110 kPa & T_c=115 days.

Figure 10.9. CIU triaxial sample at w=100%, A_c=10%, $p_o{}'$=400 kPa & T_c=115 days.
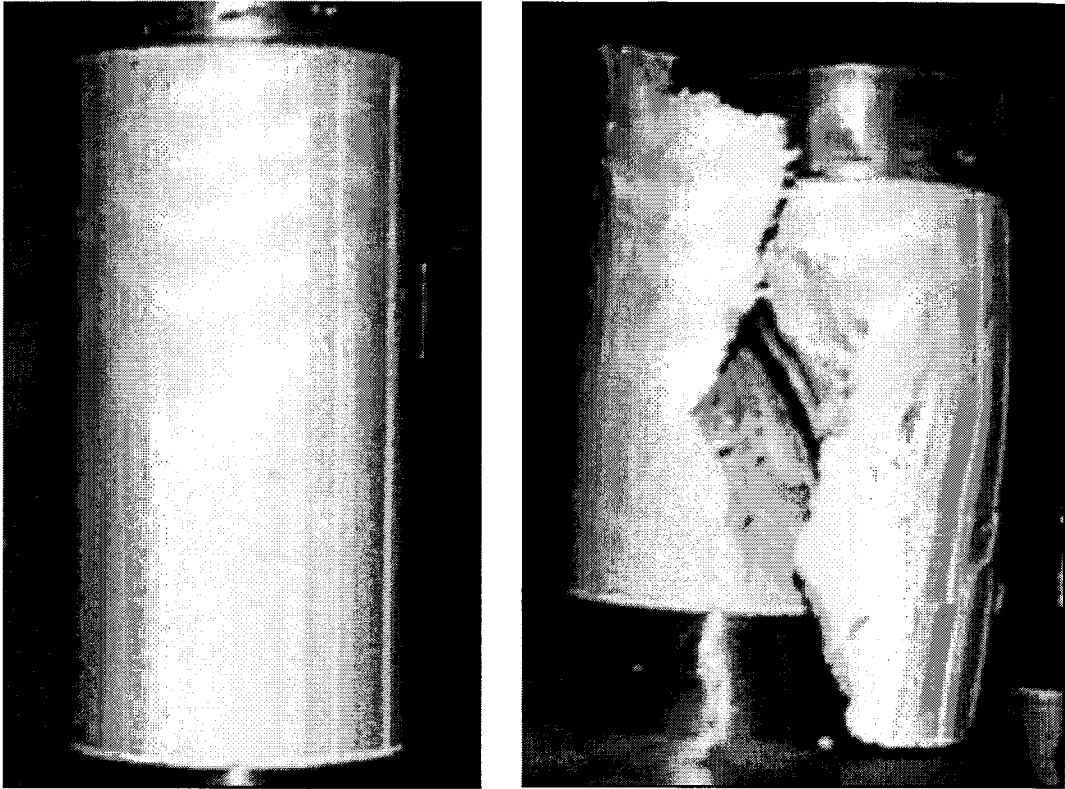
Figure 11.1. UC sample at w=40% & A_c=0% (test B).
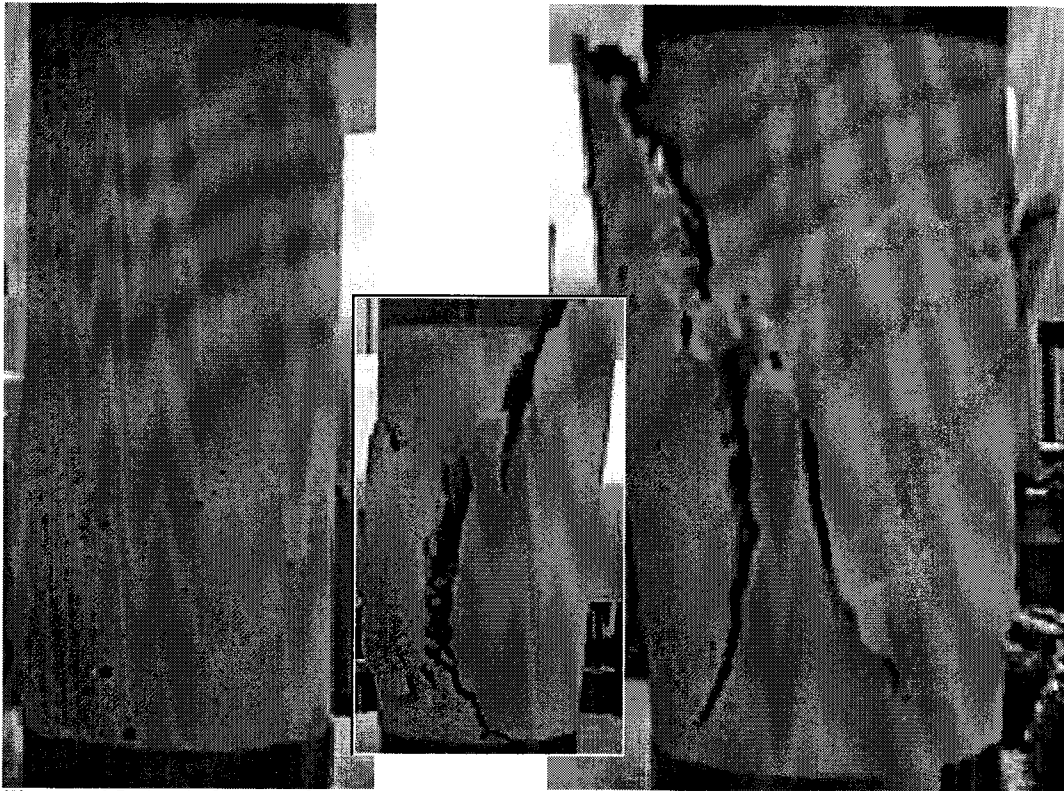
Figure 12.1. UC sample at w=70%, A_c=2% & T_c=7 days (test A).

MISSING PHOTOS

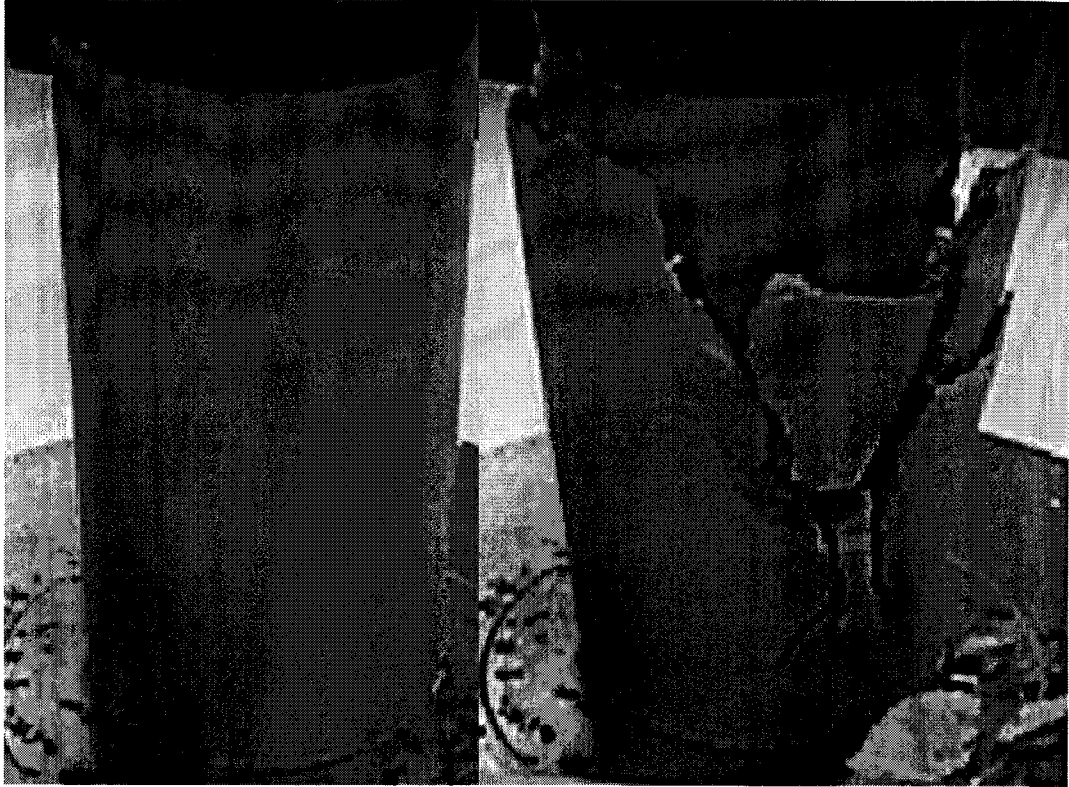Figure 12.2. UC sample at w=70%, A_c=2% & T_c=28 days (test E).
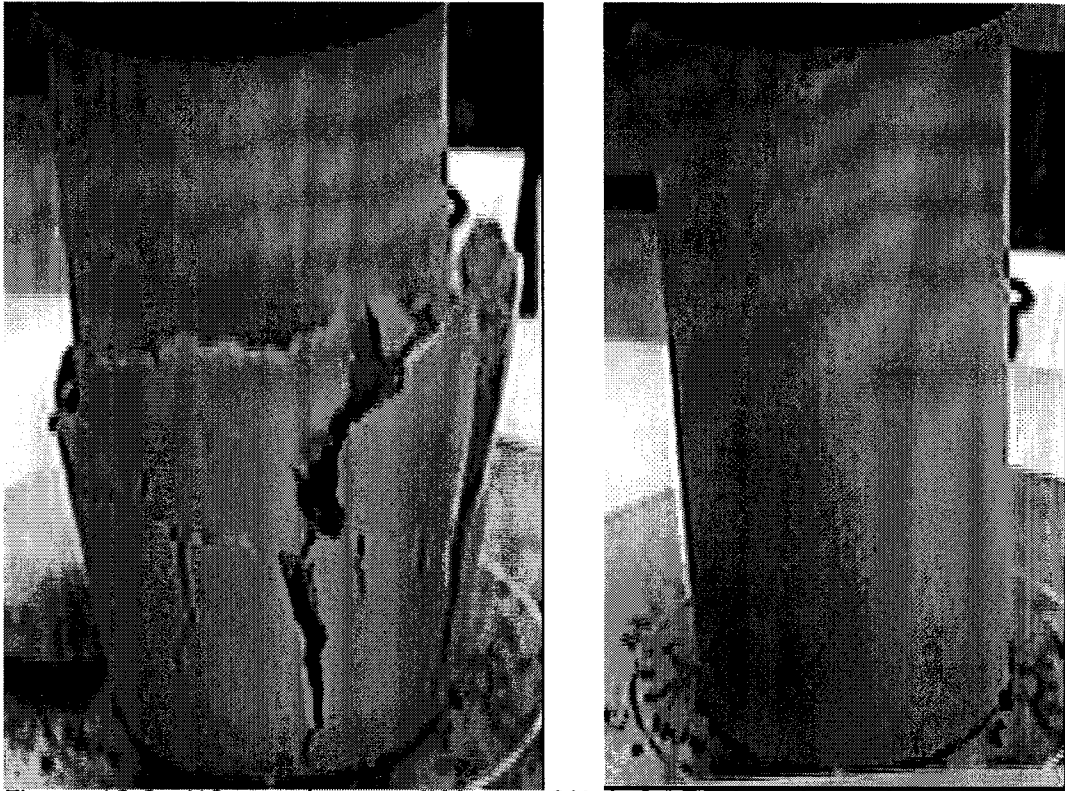
Figure 12.3. UC sample at w=70%, A_c=2% & T_c=56 days (test A).
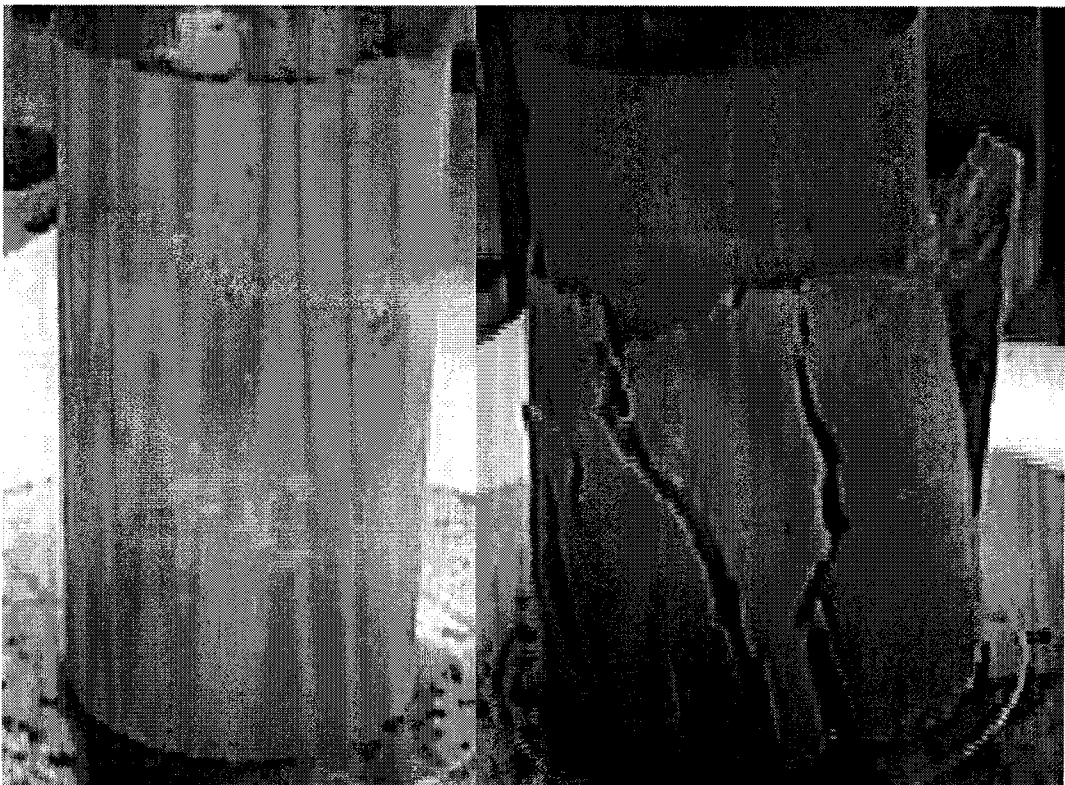
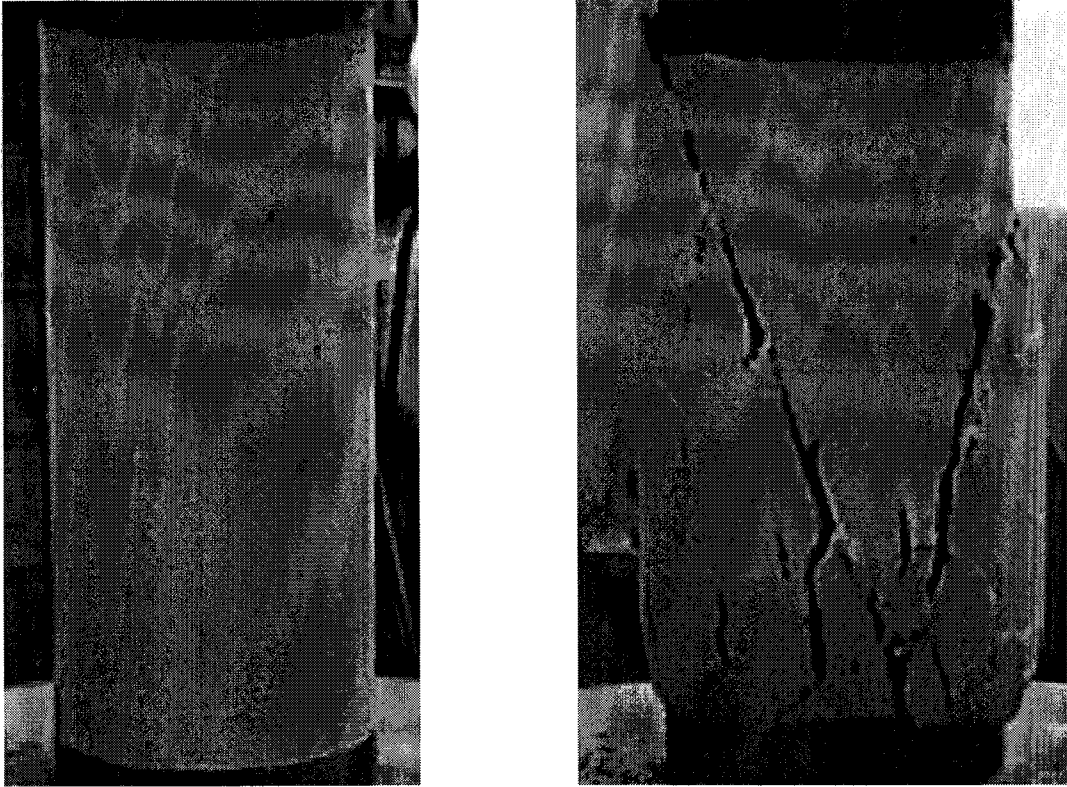Figure 12.4. UC sample at w=70%, A_c=2% & T_c=112 days (test A).

Figure 13.1. UC sample at w=70%, A_c=5% & T_c=7 days (test A).
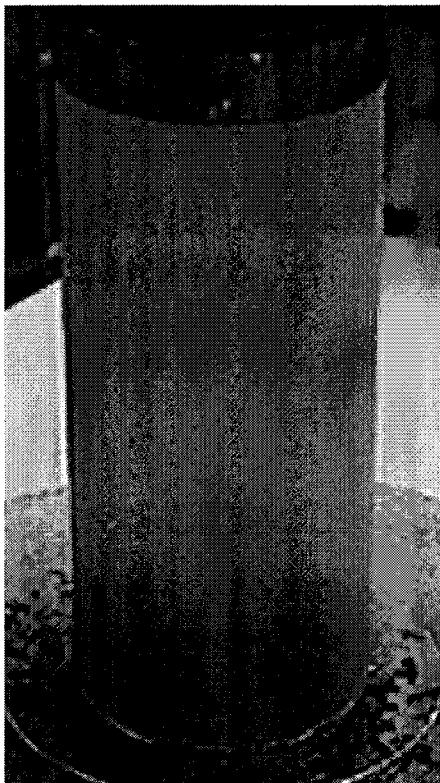
Figure 13.2. UC sample at w=70%, A_c=5% & T_c=28 days (test E).

Figure 13.3. UC sample at w=70%, A_c=5% & T_c=56 days (test D).

Figure 13.4. UC sample at w=70%, A_c=5% & T_c=112 days (test A).

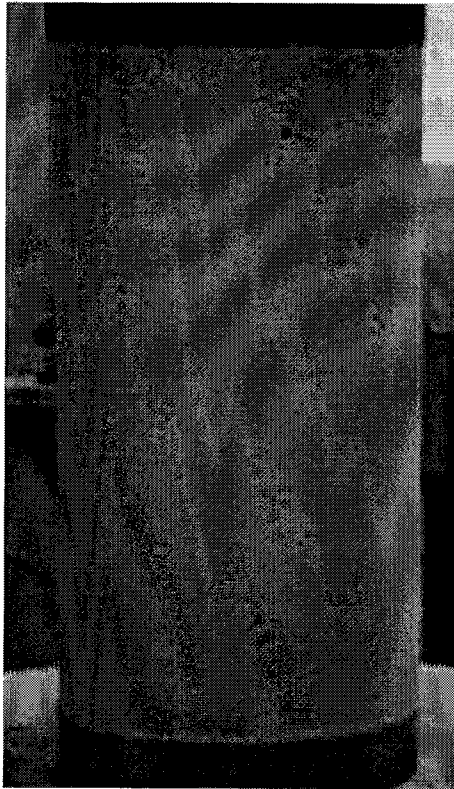Figure 14.1. UC sample at w=100%, A_c=2% & T_c=7 days (test A).

Figure 15.1. UC sample at w=100%, A_c=5% & T_c=7 days (test C).

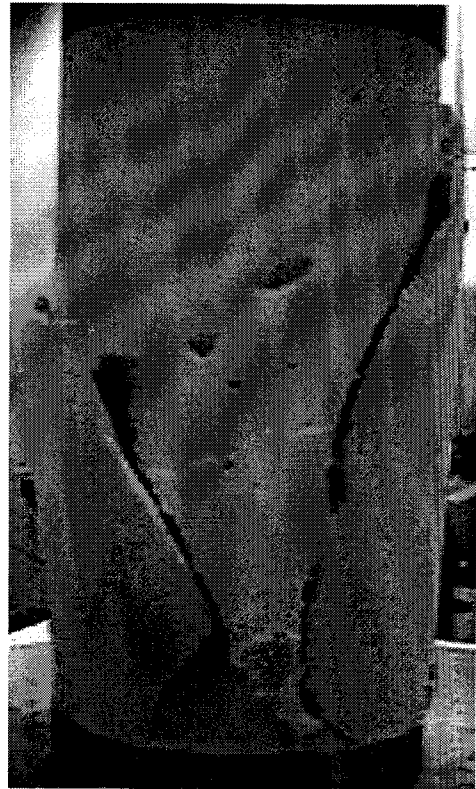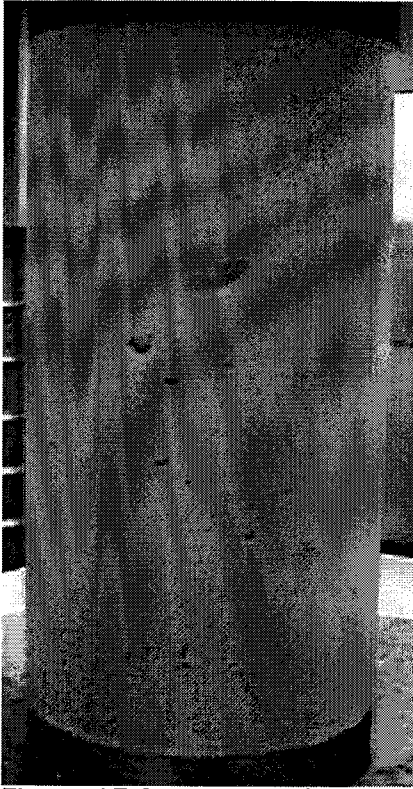Figure 15.2. UC sample at w=100%, A_c=5% & T_c=28 days (test B).

Figure 15.3. UC sample at w=100%, A_c=5% & T_c=56 days (test B).

Figure 15.4 UC sample at w=100%, A_c=5% & T_c=112 days (test A).

Mechanical Characteristics of Kaolin-Cement Mixture 383
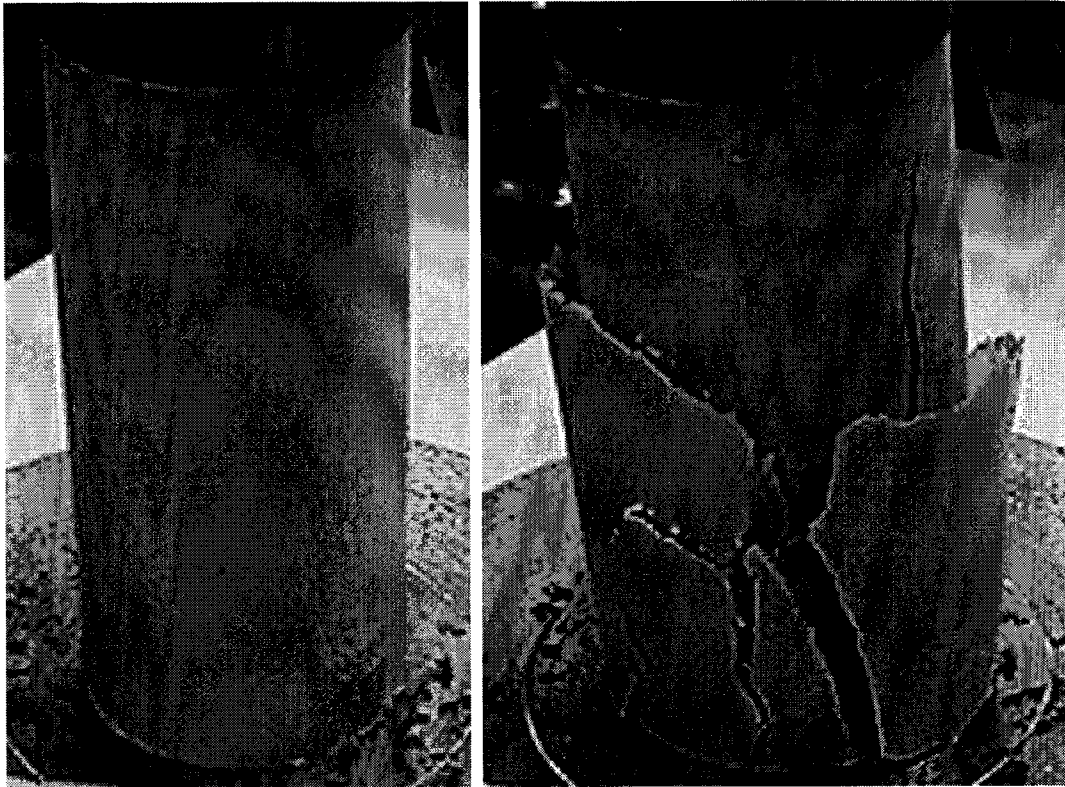
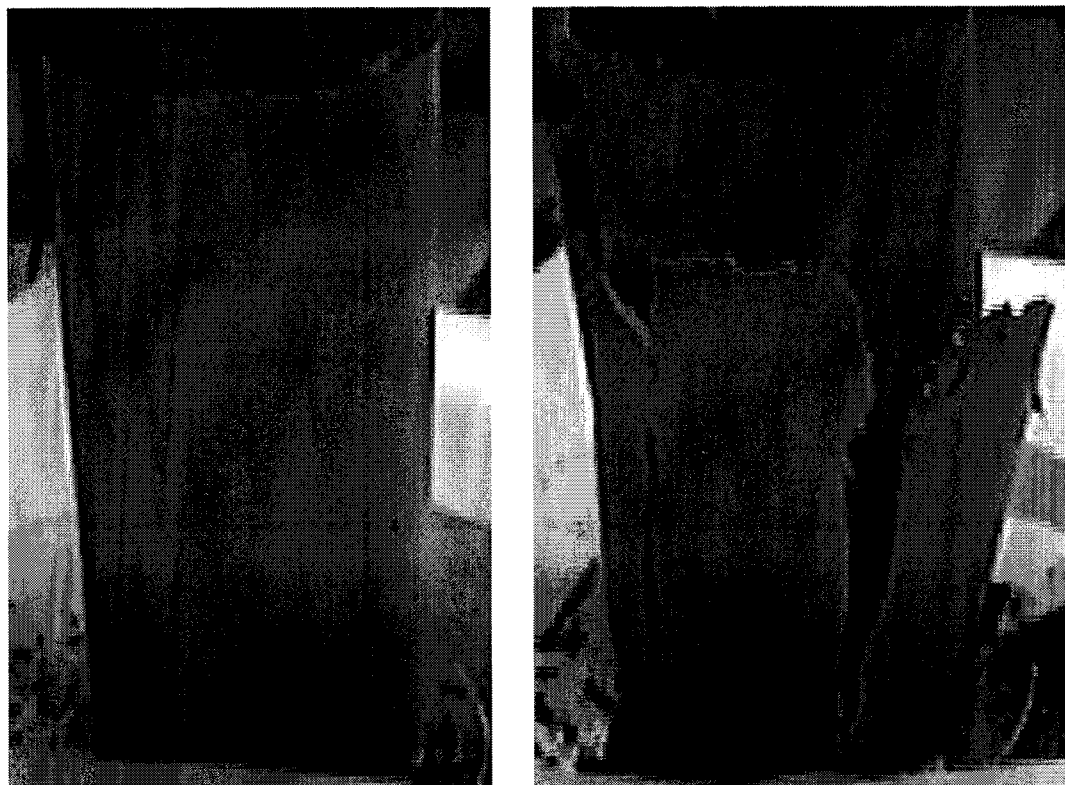Figure 16.1. UC sample at w=100%, A_c=10% & T_c=7 days (test C).

Figure 16.2. UC sample at w=100%, A_c=10% & T_c=28 days (test B).

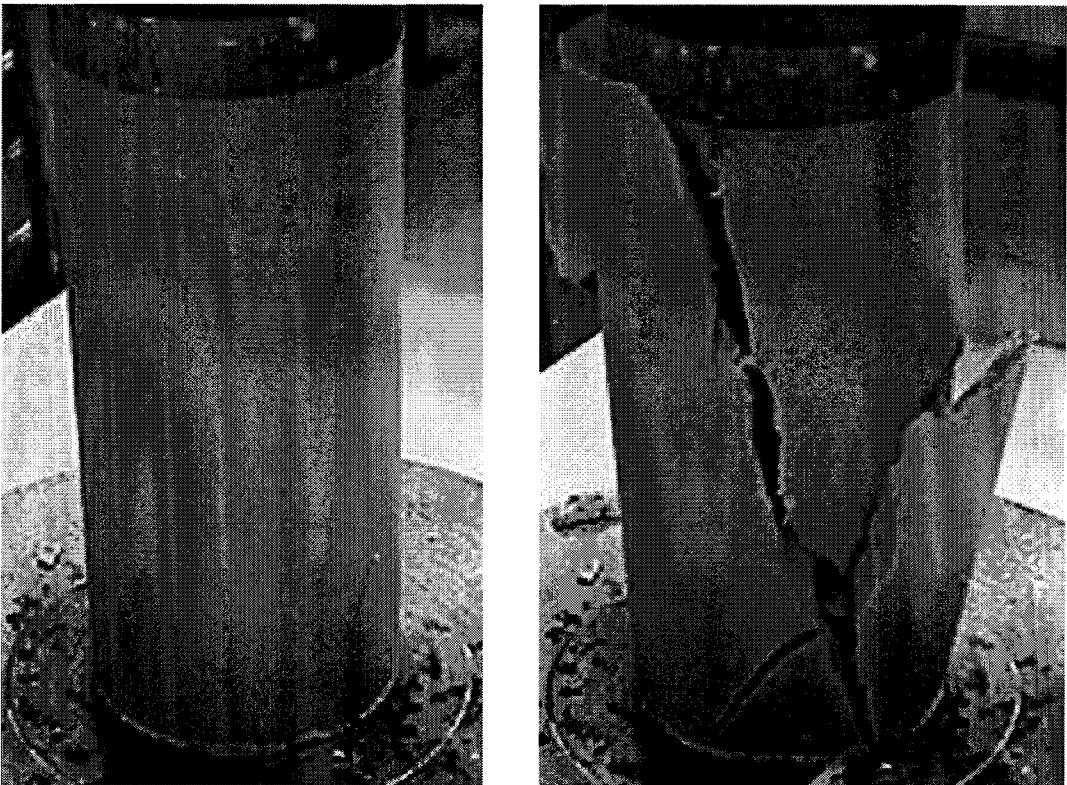Figure 16.3. UC sample at w=100%, A_c=10% & T_c=56 days (test A).

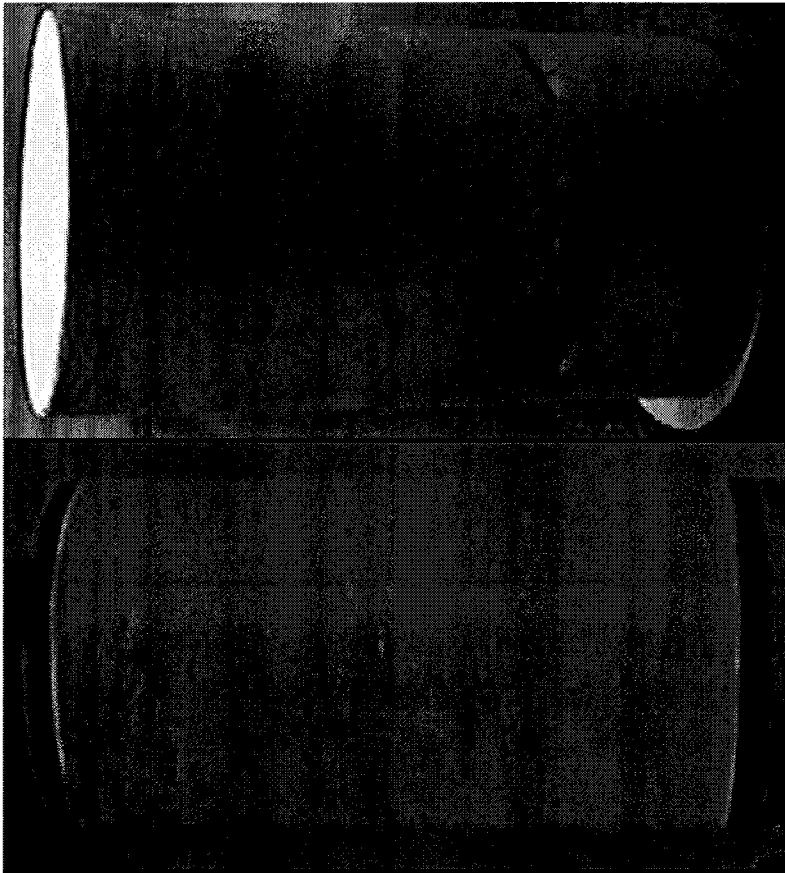Figure 16.4. UC sample at w=100%, A_c=10% & T_c=112 days (test A).

Figure 17.1. IC sample at w=40% & A_c=0%.

Mechanical Characteristics of Kaolin-Cement Mixture

Figure 18.2. IC sample at w=70%, A_c=2% & T_c=28 days.

Figure 18.4. IC sample at w=70%, A_c=2% & T_c=112 days.

Figure 18.1. IC sample at w=70%, A_c=2% & T_c=7 days.

Figure 18.3. IC sample at w=70%, A_c=2% & T_c=56 days.

Mechanical Characteristics of Kaolin-Cement Mixture 387

Figure 19.2. IC sample at w=70%, A_c=5% & T_c=28 days.
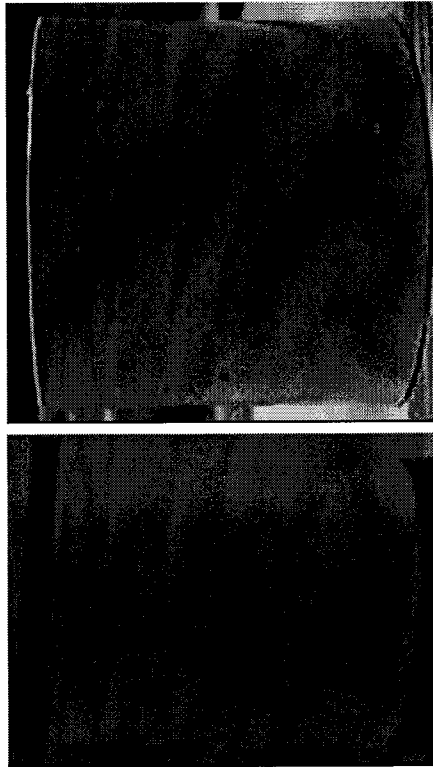
Figure 19.1. IC sample at w=70%, A_c=5% & T_c=7 days.

MISSING PHOTO

Figure 19.3. IC sample at w=70%, A_c=5% & T_c=56 days.

Figure 20.2. IC sample at w=100%, A_c=5% & T_{ic}=28 days.

Figure 20.1. IC sample at w=100%, A_c=5% & T_c=7 days.

MISSING PHOTO

Figure 20.4. IC sample at w=100%, A_c=5% & T_c=112 days.

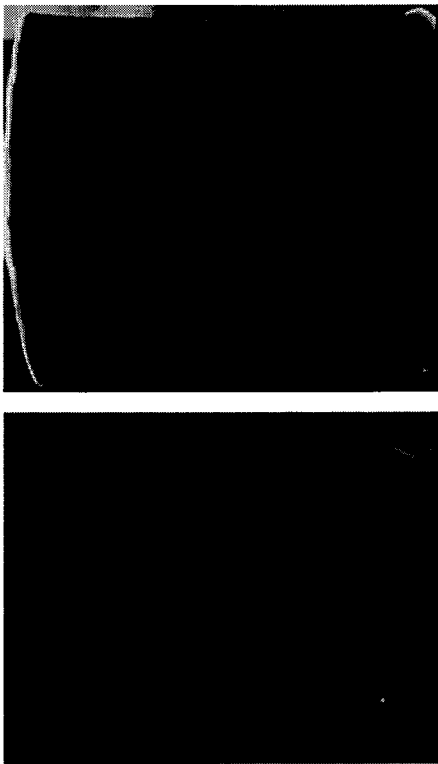Figure 20.3. IC sample at w=100%, A_c=5% & T_c=56 days.

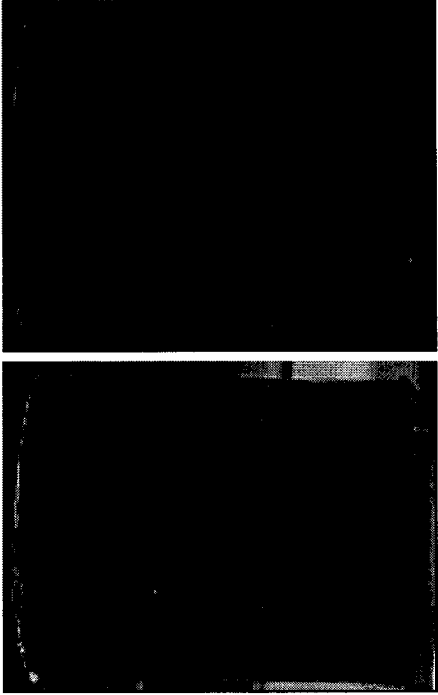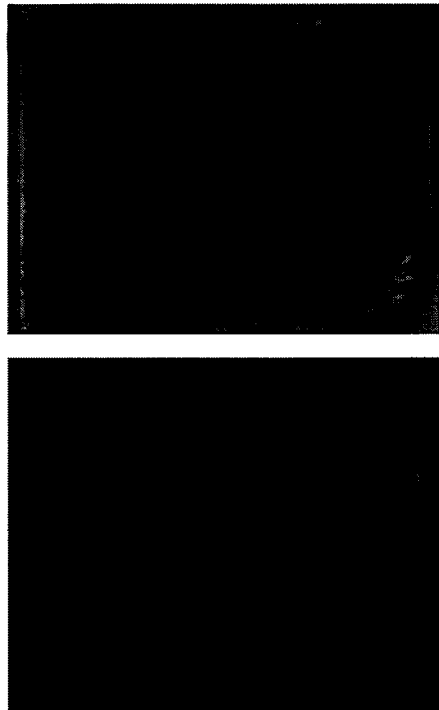Figure 21.1. IC sample at w=100%, A_c=10% & T_c=7 days.

Figure 21.2. IC sample at w=100%, A_c=10% & T_c=28 days.

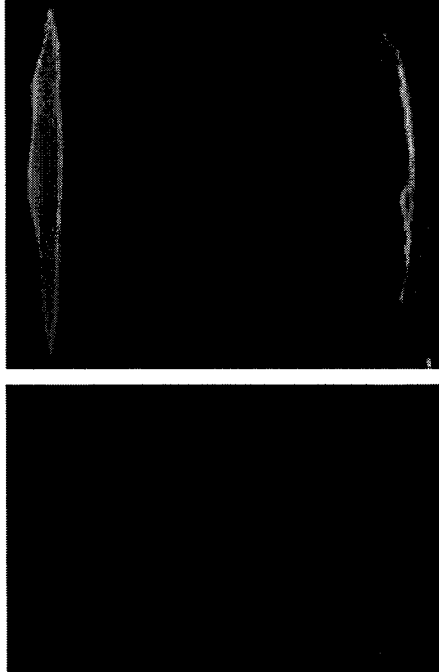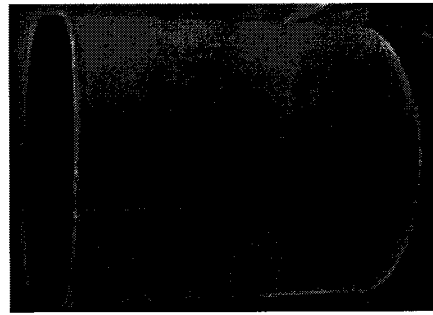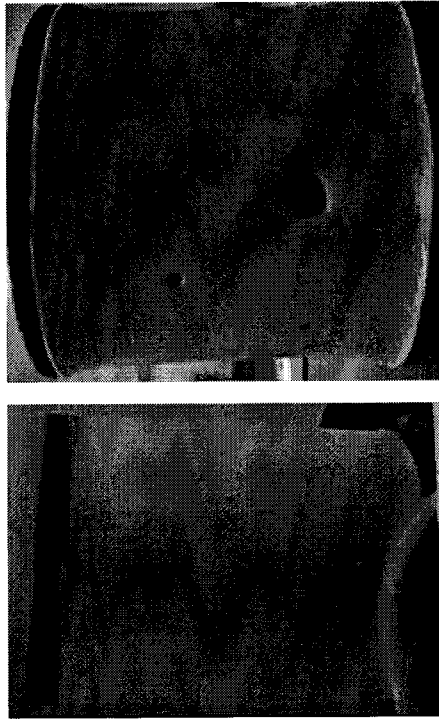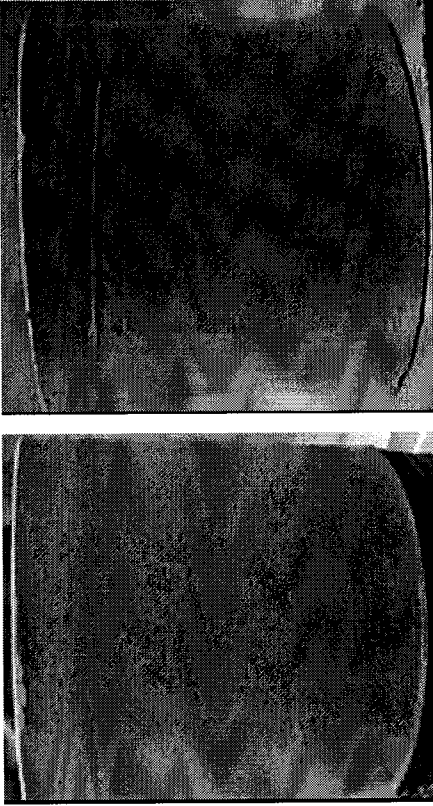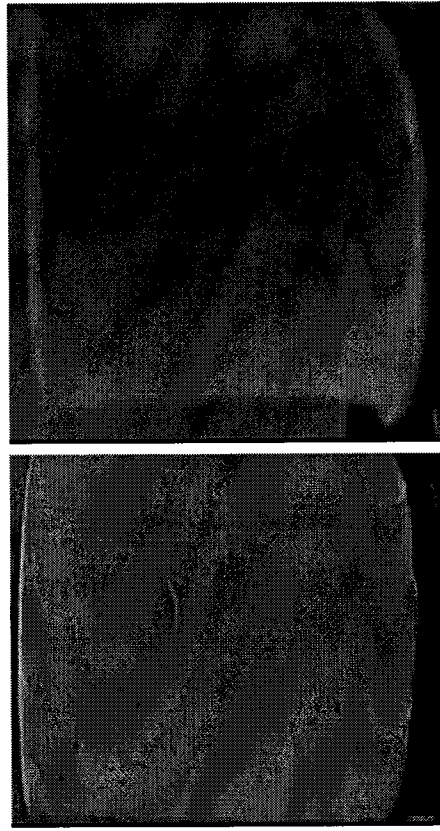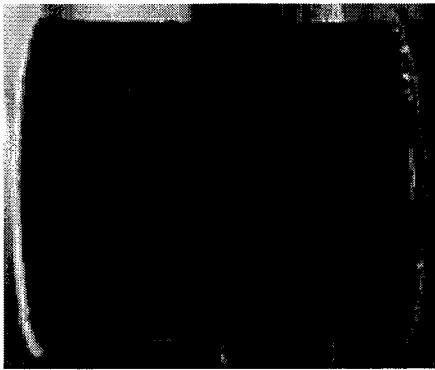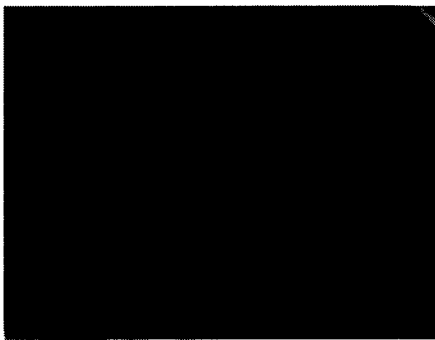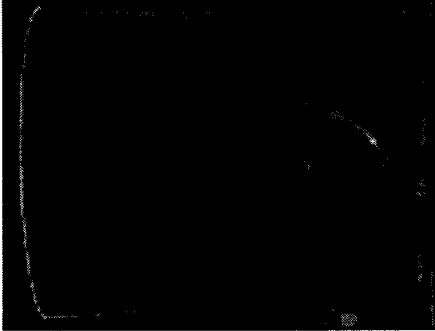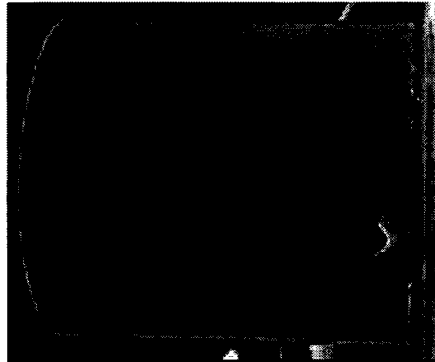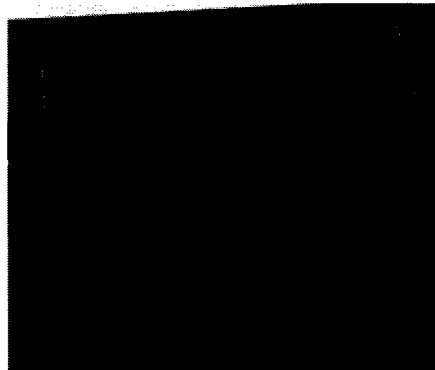Figure 21.3. IC sample at w=100%, A_c=10% & T_c=56 days.

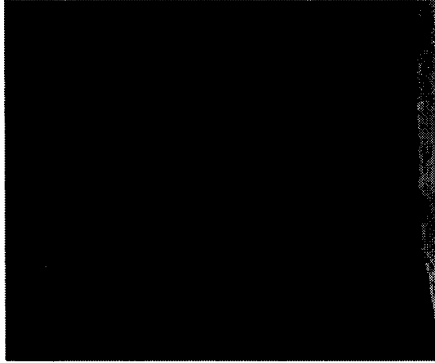Figure 21.4. IC sample at w=100%, A_c=10% & T_c=112 days.

Mechanical Characteristics of Kaolin-Cement Mixture

APPENDIX H: EFFECTS OF CURING TIME AND CURING METHOD ON THE MECHANICAL PROPERTIES OF KAOLIN-CEMENT

The current general practice in design of DM projects is to consider the mechanical properties of the stabilized soil after 28 days of curing (Kohata *et al.*, 1997). Typically, unconfined compression tests are conducted in the laboratory to evaluate various proposed mixes; occasionally, advanced tests such as consolidated triaxial tests and oedometer tests are also performed. The common theory expressed in literature is that soil-cement will continue to gain strength with time (i.e. Mitchell, 1981; Bergado *et al.*, 1996; Porbaha *et al.*, 2000) and that the strength at 28 days is a representative and relatively conservative value for design purposes. This theory is adapted from that of concrete. However, depending on the cement content, soil type and curing method, some literature and the present research suggests that soil-cement does not necessarily continue to gain strength with time. In fact, under some circumstances, which include water curing and low cement contents, the strength and deformation properties of cement stabilized soil will actually deteriorate with time. When the strength does increase with curing time, it is usually in exchange for an increase in stiffness and more brittle failure.

Uddin (1995) observed that when Bangkok clay is stabilized with 5 percent cement or less and cured in a humid environment, the mechanical properties generally do not improve with time.

Azman *et al.* (1995) studied the undrained shear response of cement-treated soil and the effects of initial consolidation. Black soil from Malaysia, containing less than 20 percent clay and silt size particles, was used for the study. Cement contents considered were 2, 5 and 7 percent. Curing was done by submerging the samples in water for periods of 7, 28 and 60 days. Results show that the samples having a moisture content of 70 percent and a cement content of only 2 percent decreased in strength between 28 and 60 days of curing. The conclusion was drawn that the small amount of cement behaved as a separating agent rather than a binding agent so that softening occurred.

Babasaki *et al.* (1997) reviewed a decade of research in Japan and found evidence to indicate that cement stabilized soil will deteriorate over time when exposed to water. This suggests that the curing environment and

moisture content may significantly influence the effectiveness of DM, depending on the soil type and amount of cement added. Furthermore, Kézdi (1979) reported that the UC strength of samples cured in water was 20 to 30 percent less than that of the same material cured in a humid environment. A study of the effects of curing environment on the strength of kaolin-cement is currently taking place at the City University of Hong Kong; preliminary results suggest that at low cement contents (i.e. 2 percent), the unconfined compressive strength of water cured samples may be as little as one-third of the UC strength of humid cured samples.

Bergado *et al.* (1996) indicate that the pozzolanic reactions which lead to an increase in material strength with time last longer in basic environments. Furthermore, when the pH is less than 12.6, the reactions that lead to an increase in strength produce CSH instead of the stronger $C_3S_2H_x$. The pH of kaolin when stabilized with 2 to 10 percent cement ranged from 12.3 to 12.9, respectively, and decreased with curing time.

The observations in this study and by others suggest that the effects of curing time and curing environment on the mechanical behaviour of soil-cement are not well understood. The following sections examine the effects of curing time on the kaolin-cement samples considered in the current study. Some discussion on the effects of curing method is also presented. Much of what is discussed here has already been discussed in Chapters 5 and 6. It is clear that more research would be useful on the topic of aging following different curing methods in cement-stabilized soil.

Figures to support the conclusions made on the effect of curing time can be found in the Appendices. Figures A.1 to A.12 illustrate the findings of the drained triaxial tests, Figures B.1 to B.8 illustrate the findings of the undrained triaxial tests. Figures C.1 to C.4 illustrate the findings of the unconfined compression tests. Figures D.17 to D.20 illustrate the findings of the oedometer tests.

H.1   Physical Properties

As discussed in Chapter 7, the pozzolanic reactions that occur when cement is added to wet clay cause changes in both the chemical and physical properties

of the soil. Cement increases the pH of the pore water so that it becomes highly basic, causing flocculation of clay particles. As curing proceeds, however, the pH decreases (Fig. H.1), typical of aging soils (Mitchell, 1993), and the degree of flocculation may be reduced, causing a very small increase in the void ratio up to at least 56 days (Fig. H.2). The increase is greatest at 10 percent cement. After 56 days of curing, however, there is a small *reduction* in the void ratio for both mixtures with 100 percent moisture content. If significant, this may indicate a change in the degree of flocculation and/or shrinkage.

The moisture content after curing (Fig. H.3) and the bulk and dry density (Figs. H.4 and H.5) were also compared for each curing time. For all mixes, the average moisture content increases with curing time up to 56 days by up to 3 percent. After 56 days, the moisture content decreases when the initial moisture content is 100 percent. At an initial moisture content of 70 percent, there is very little to no change in moisture content between 56 and 112 days of curing. When cured in a humid environment, the moisture content *decreases* with curing time (Uddin, 1995). Therefore, the current data suggests that when cured in water, the material absorbs moisture up to around 56 days. This phenomenon is expected under field conditions when the stabilized soil is below the water table. The trend of increasing average moisture content corresponds to the increasing average initial void ratio; as moisture content increases, so does void ratio. The bulk density consistently increased slightly or stayed the same with curing time. The increase may be a result of sample consolidation but is contrary to the increasing void ratio. The dry density, which is a function of the moisture content, showed a very slight increase or decrease with curing time but more or less did not change.

H.2   Effect of Curing Environment: Humid Curing vs. Water Curing

Some preliminary tests have been conducted at the City University of Hong Kong as part of a related study to examine the difference in the unconfined compressive strength of samples cured in a humid environment vs. samples cured in water. Samples were prepared at 70 percent moisture content with 2, 5 and 10 percent cement. Tests were conducted after 7, 14, 28 and 56

days of curing. Samples with no cement were also prepared and "cured" for 7 days to see the effects of the curing environment, independent of the cementation effects. The results of these tests are provided in Figure H.6.
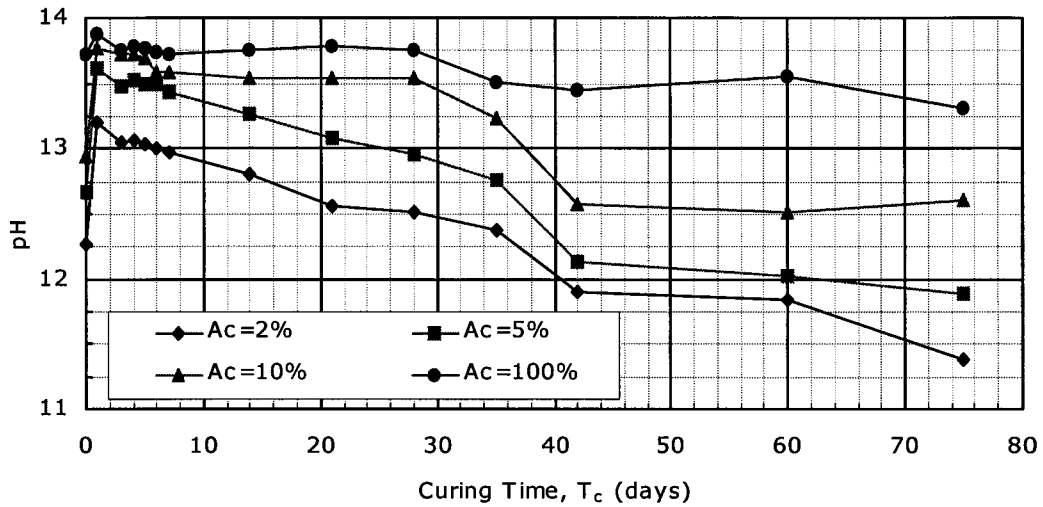
Figure H.1. pH vs. curing time.
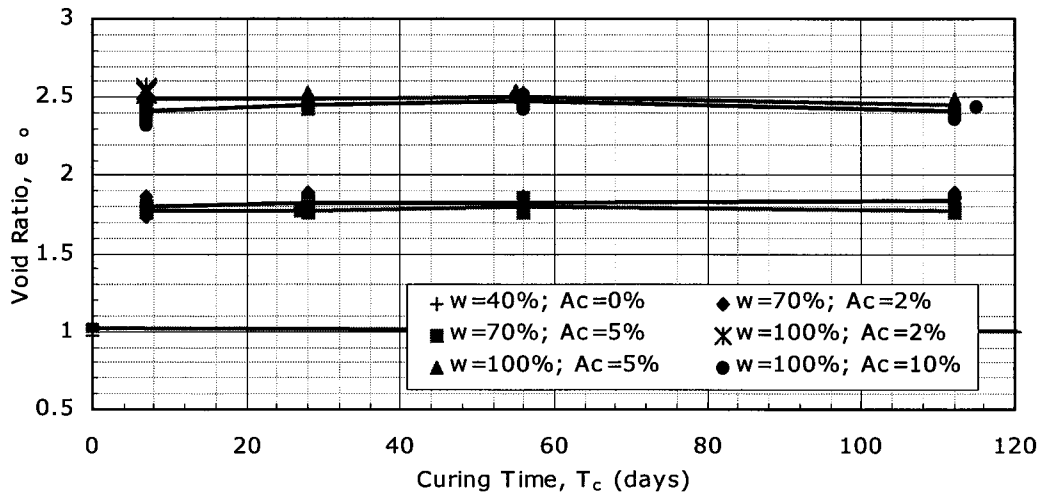
Figure H.2. Average void ratio vs. curing time (results include all successful laboratory tests).
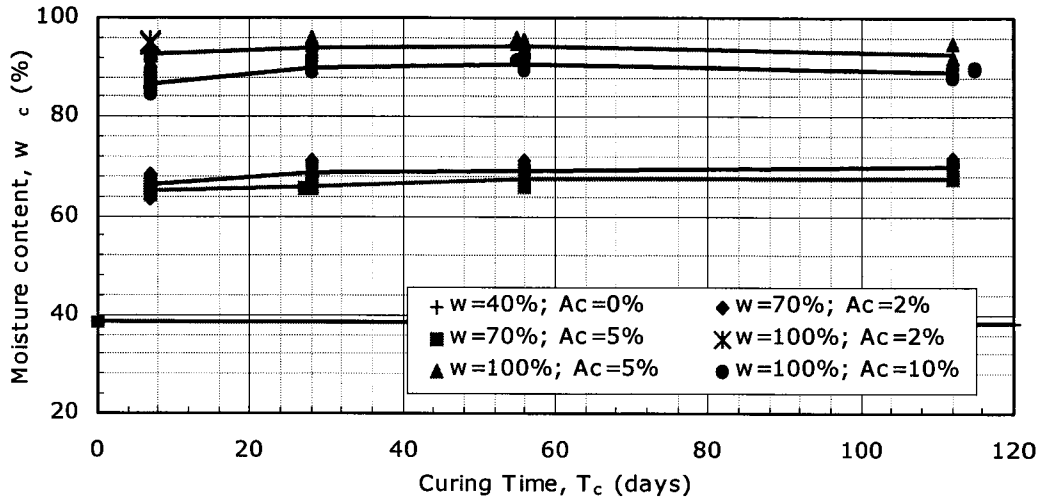
Figure H.3. Average moisture content after curing vs. curing time (results include all successful laboratory tests).
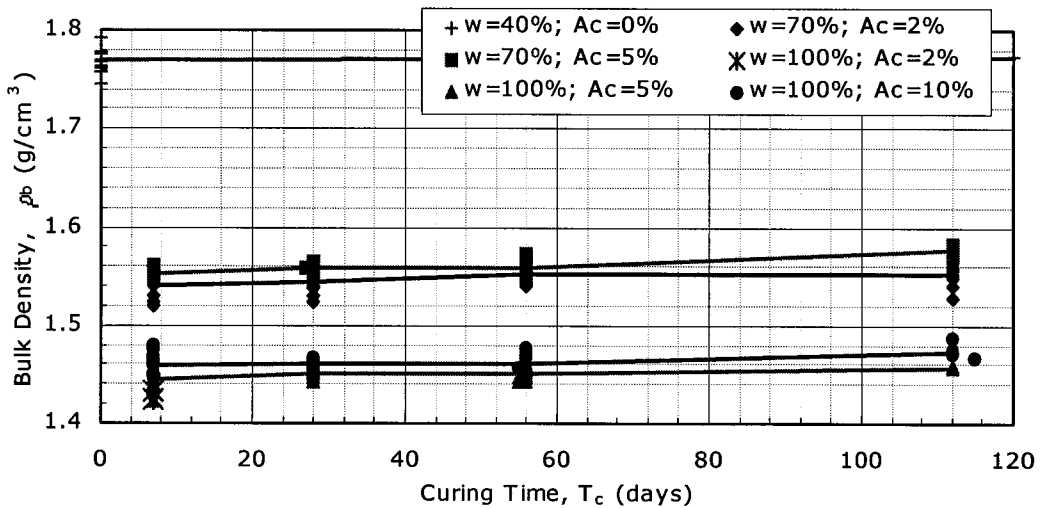
Figure H.4. Average bulk density vs. curing time (results include all successful laboratory tests).

For all mixes, the strength increased with age, at a decreasing rate. The peak strength following humid curing was far greater than that following water curing. At 2 percent cement, the strength following humid curing was up to 3 times that following water curing. At 10 percent cement, the difference was as much as double.
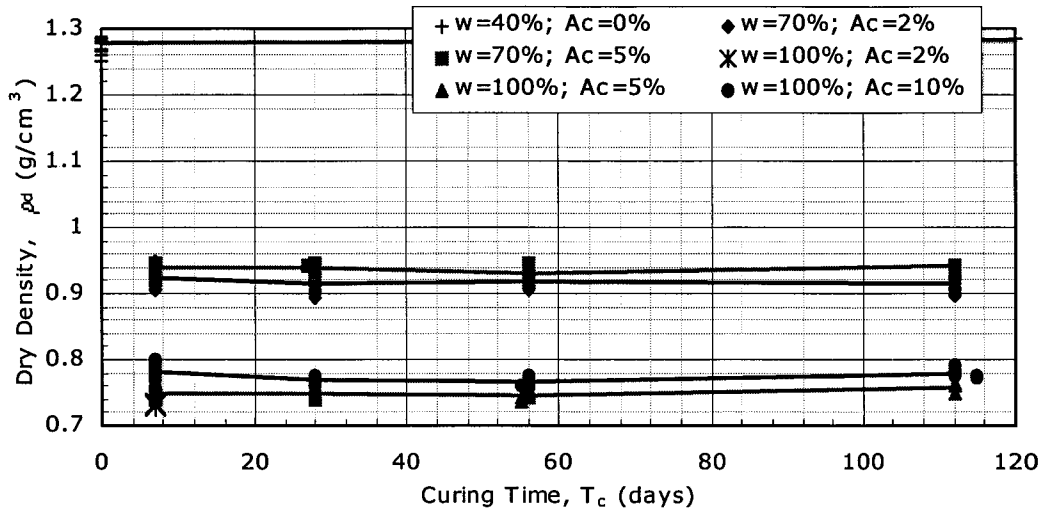
Figure H.5. Average dry density vs. curing time (results include all successful laboratory tests).

The moisture content following curing was determined for each sample. Results show that the moisture content following humid curing is significantly less than that following water curing. Furthermore, the humid cured samples continued to lose moisture with time, whereas the moisture content of the water cured samples dropped initially and then increased after 28 days. After 28 days of curing, the humid cured samples lost so much moisture that many of the samples cracked as a result and could not be tested. Table H.1 summarizes the moisture contents of the water cured and humid cured samples, all having an initial moisture content (prior to addition of cement) of 70 percent. Considering the data from samples with no cement, it can be seen that there is a larger difference in moisture content between water "cured" and humid "cured" samples. This indicates that either cement reduces the capacity of the kaolin to absorb moisture during water curing, or reduces the capacity of the kaolin to lose moisture during humid curing.
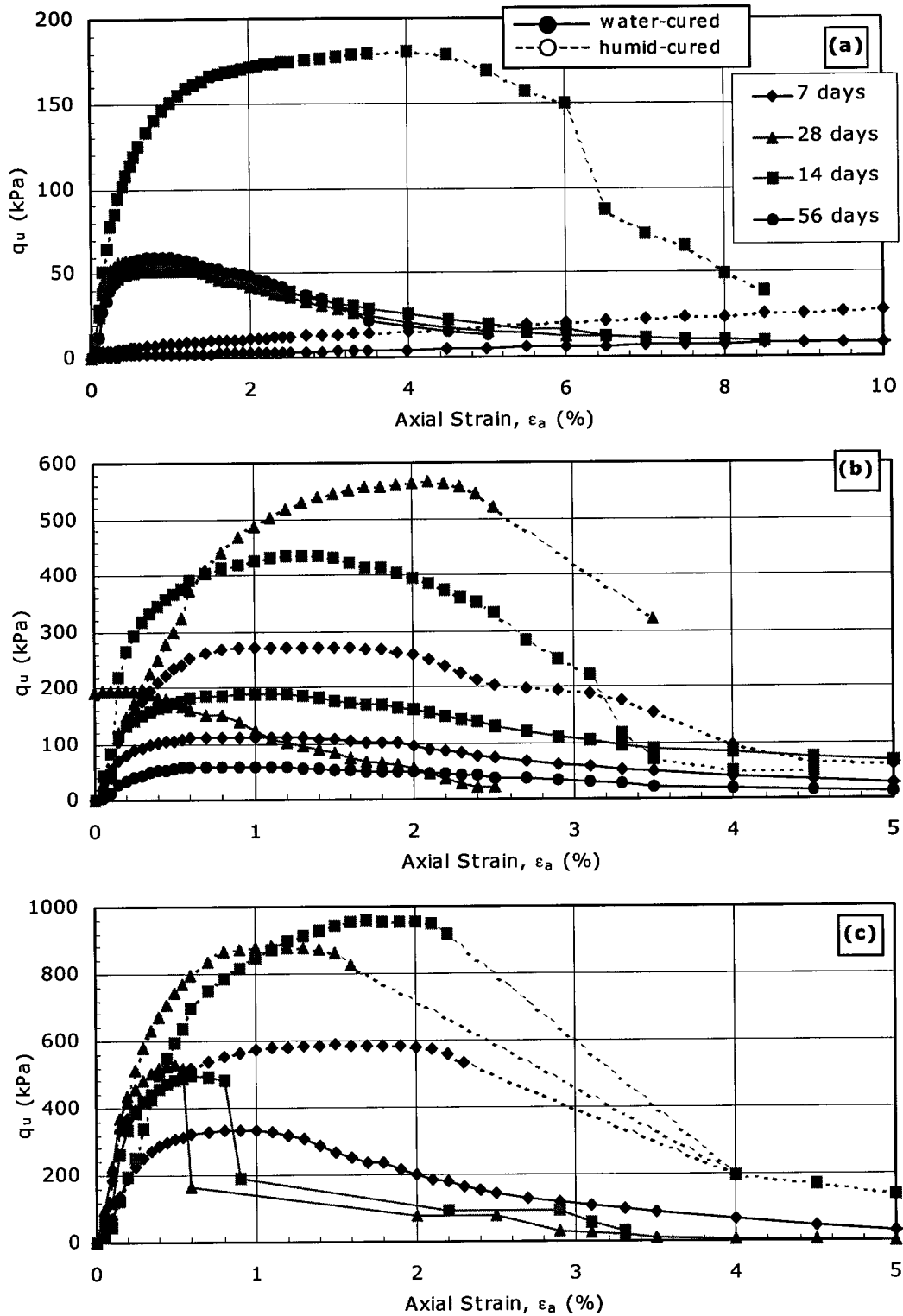
Figure H.6. Stress-strain plots for UC tests on water-cured samples vs. humid-cured samples at w=70%. (a) A_c=2%; (b) A_c=5%; (c) A_c=10%.

Table H.1. Moisture content following curing for samples with an initial moisture content of 70 percent.

Cement content, A_c (%)	Curing time, T_c (days)	Moisture content after curing, w_c (%)		Δw_c (%)
		water curing	humid curing	
0	7	71.9	60.6	11.3
2	7	68.1	61.9	6.2
	14	65.5	56.2	9.3
	28	66.9	*	-
	56	65.9	*	-
5	7	65.3	60.0	5.3
	14	61.7	56.2	5.5
	28	64.7	52.2	12.5
10	7	65.0	57.1	7.9
	14	57.6	49.0	8.6
	28	59.2	50.3	8.9

*For humid cured samples after 28 or 56 days of curing, samples were found to be cracked and broken upon extrusion so UC tests were not performed.

H.3   Deviator Stress and Stress Ratio

The peak deviator stress and peak stress ratio for the triaxial tests are expected to increase with curing time, at a decreasing rate. However, based on the results of the current study, this was not always found to be the case, particularly for the undrained tests. Significant excess pore water pressure generated for the undrained tests makes it necessary to consider the stress ratio instead of the deviator stress, as the excess pore water pressure is inherent in the calculation of the stress ratio.

Figures H.7 and H.8 illustrate the peak deviator stress and peak stress ratio vs. curing time, for the drained and undrained tests, respectively. Frequently, the peak strength was found to decrease following 28 days or 56 days of curing. This reduction in strength was most common at low cement contents and/or low moisture contents (i.e. 70 percent). For the samples with 70 percent moisture content, compacting the samples in lifts, which was

not the case for the samples with 100 percent moisture content, may be an influencing factor. At high cement contents, there was typically no further gain in strength following 56 days of curing. It is suggested that this deterioration in strength is due to softening caused by curing the samples in water. Similar observations and conclusions were made by Azman *et al.* (1995), who studied the undrained shear response of cement-treated soil and the effects of initial consolidation. Black soil from Malaysia, containing less than 20 percent clay and silt size particles, was used for the study. Cement contents considered were 2, 5 and 7 percent. Curing was done by submerging the samples in water for periods of 7, 28 and 60 days. Results show that the samples having a moisture content of 70 percent and a cement content of only 2 percent decreased in strength between 28 and 60 days of curing. The conclusion was drawn that the small amount of cement behaved as a separating agent rather than a binding agent so that softening occurred.

At fully-softened stress conditions, axial strain was high and therefore, lateral deformation was great so that it was difficult to accurately calculate fully-softened values. However, for both drained and undrained triaxial tests, the stress-strain curves seemed to approach a common value (Fig. H.9), regardless of curing time, when all other factors such as cement and moisture content and confining pressure were equal. So while the fully-softened values extracted from the test results may not be the same for all curing times, it is suggested that if shear had continued to greater strains and stress at these strains could be more accurately calculated, the fully-softened stress would be the same at all curing times.
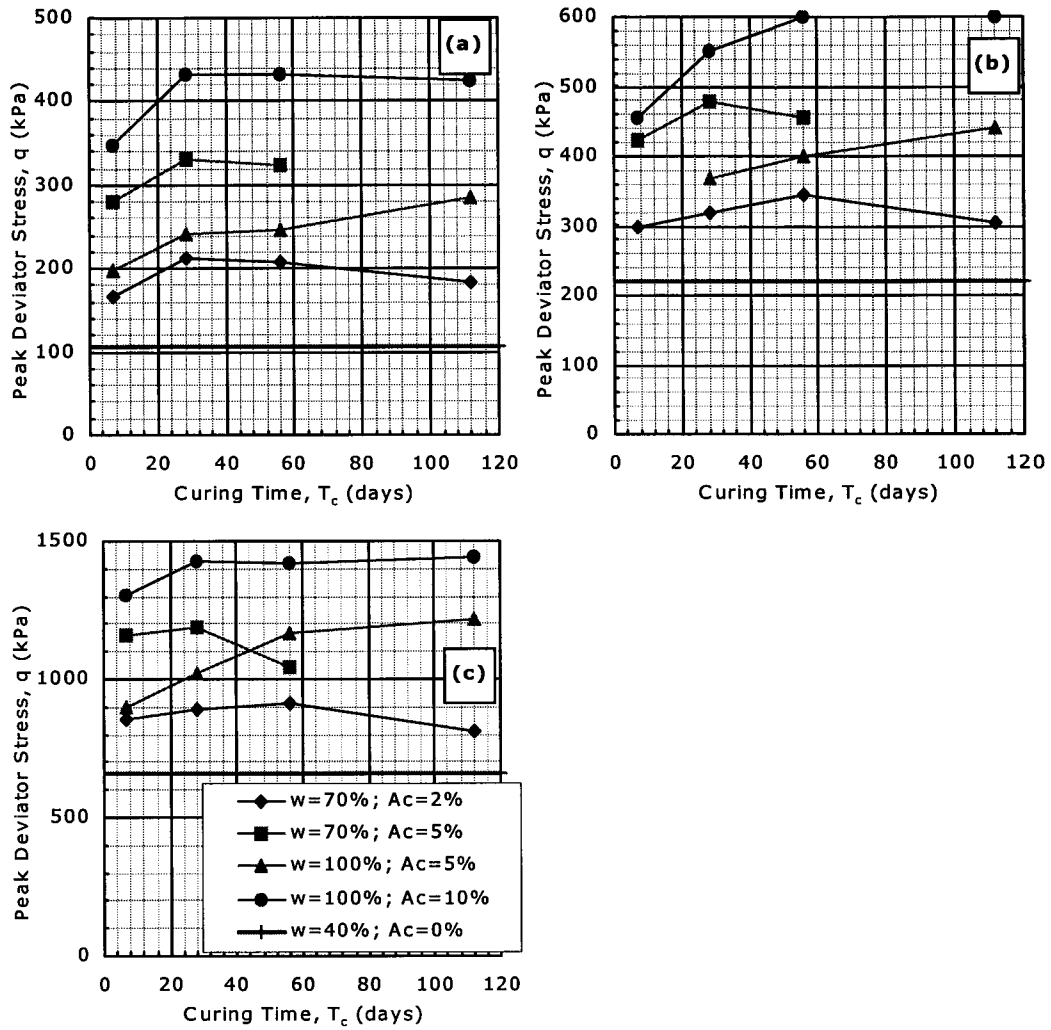
Figure H.7. Peak deviator stress vs. curing time for CID triaxial tests, at confining pressures of (a) 50 kPa; (b) 100 kPa; (c) 400 kPa.
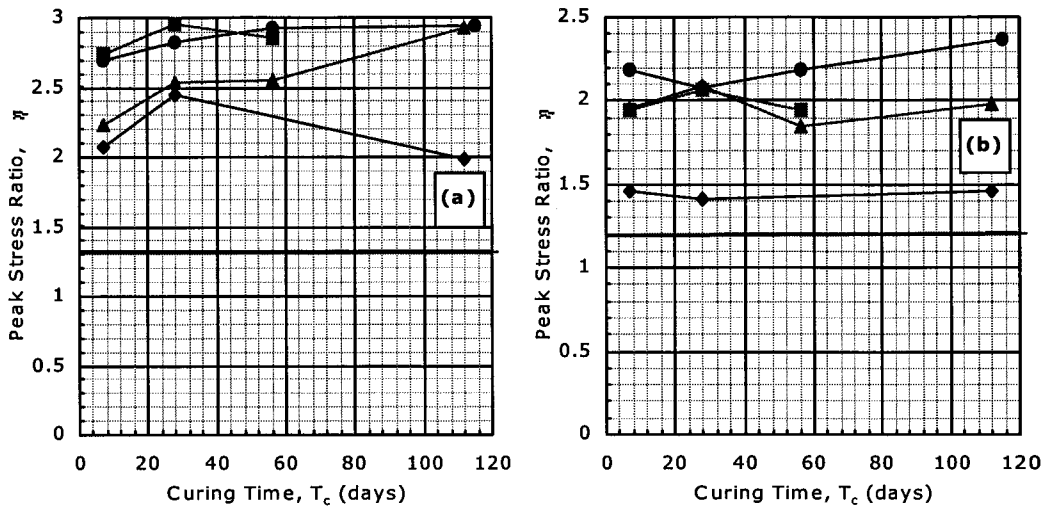
Figure H.8. Peak stress ratio vs. curing time for CIU triaxial tests, at confining pressures of (a) 100 kPa; (b) 400 kPa.
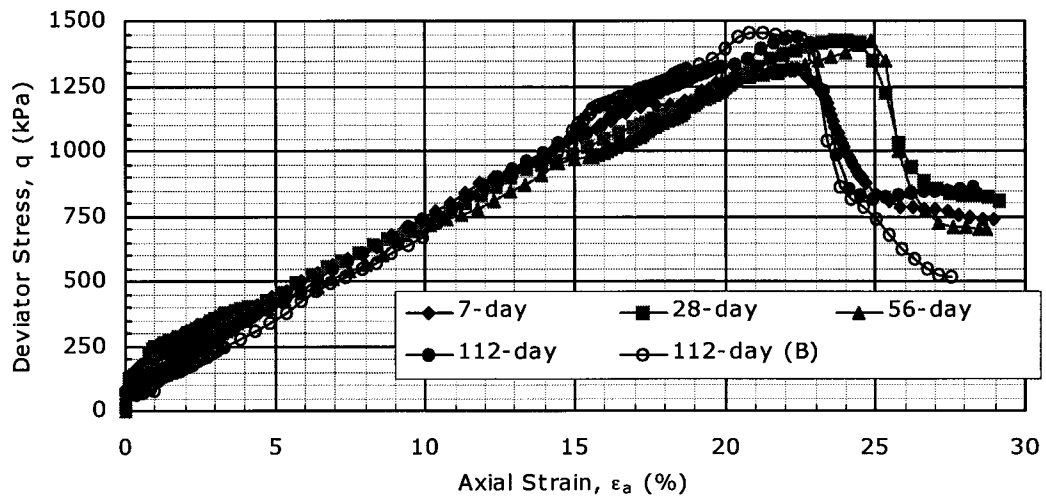
Figure H.9. q vs. ε_a for CID triaxial tests at w=100%, A_c=10% & $p_o{}'$=400 kPa.

H.4 Axial Strain At Peak Stress Conditions and Material Consistency

The effect of curing time on the axial strain at peak conditions is a function of confining pressure and drainage conditions. For drained tests at low confining pressures (i.e. 50 and 100 kPa), the axial strain corresponding to peak conditions decreased with an increase in curing time (Fig. H.10). The same is

true for undrained test up to a confining pressure of at least 400 kPa. However, the opposite is true for drained tests at high confining pressures (i.e. 400 kPa), when the axial strain corresponding to peak conditions *increases* with curing time, up to at least 56 days (Fig. H.9).

The first observation is an indication of an increase in the material stiffness with curing time. However, at higher confining pressures and drained conditions, the material stiffness is governed by the confining pressure and is independent of curing time. Therefore, the axial strain is directly related to the material strength, which sometimes deteriorates with curing time. Furthermore, the axial strain at peak stress conditions is directly related to the corresponding volumetric strain during drained tests, and the volumetric strain during drained shear is a function of the volume change during consolidation. At high confining pressures, cement bonds can fail during consolidation. Therefore, as the cement bonds strengthen with curing time, the volume change during consolidation under high pressures decreases and the capacity of the material to strain during drained shear increases. For undrained tests, often the axial strain is roughly the same for all curing times, particularly at lower confining pressures.

Failure for drained triaxial tests becomes more brittle as the strength increases. This is a trade-off; while the strength improves, failure occurs sooner and is more catastrophic.
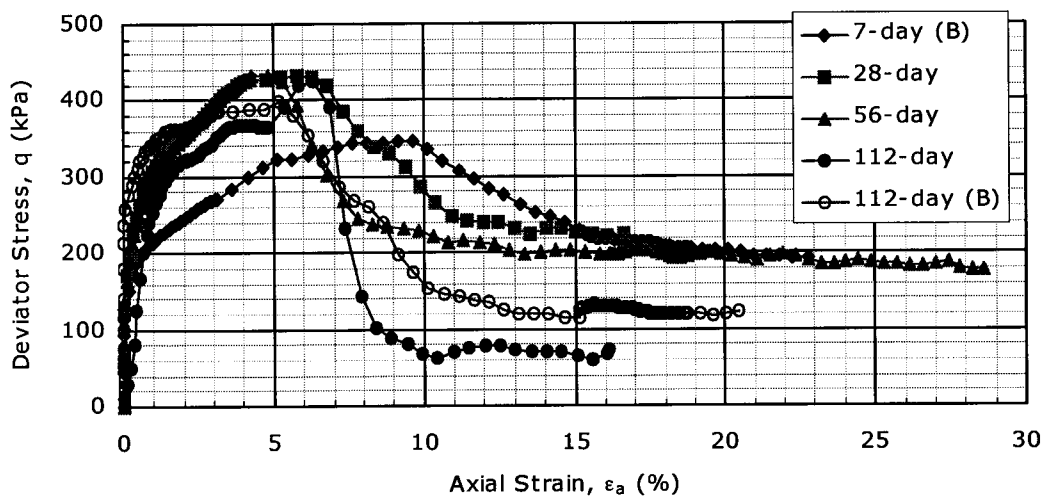

Figure H.10. q vs. ε_a for CID triaxial tests at w=100%, A_c=10% & p_o'=50 kPa.

H.5   Volumetric Strain During Drained Shear

Volume change during shear is largely influenced by confining pressure and therefore, curing time does not have a great influence. Generally, as curing time increases, the volume change during shear decreases, at a decreasing rate. This pattern is most clear at 100 percent moisture content and a confining pressure of only 50 kPa   (Fig. H.11). Occasionally the trend is somewhat reversed and the volume change is greatest after at least 56 days of curing; this phenomenon is likely due to a weakening of the cementation effects after a particular curing time. When this was observed, greater volume change is often, but not always, associated with a reduction in strength.

Most samples dilated slightly following peak stress conditions; samples cured for greater curing times tended to dilate more. This is because as the strength of the cement bonds increases, the material is able to dilate instead of crush during shear (Wissa and Ladd, 1964). Occasionally, when the curing time was only 7 days, some samples continued to contract following peak but at a slower rate than prior to peak, while samples of the same mixture but greater curing times dilated once peak had occurred. Contraction also continued following peak stress conditions for the occasional sample with a curing time greater than 7 days; in these cases, premature brittle failure may have occurred.

Figure H.11. ε_v vs. ε_a for CID triaxial tests at w=100%, A_c=10% & $p_o{}'$=50 kPa.

H.6   Excess Pore Pressure During Undrained Shear

The maximum excess pore pressure generally increased with curing time (Fig. H.12). However, for roughly half of the cases, the maximum excess pore water pressure decreased slightly between 28 and 56 days of curing. This often corresponded to a peak strength that also decreased during the same time.

Following peak stress conditions, dilation occurred and the excess pore water pressure is approximately the same for all curing times when fully-softened stress conditions are achieved.
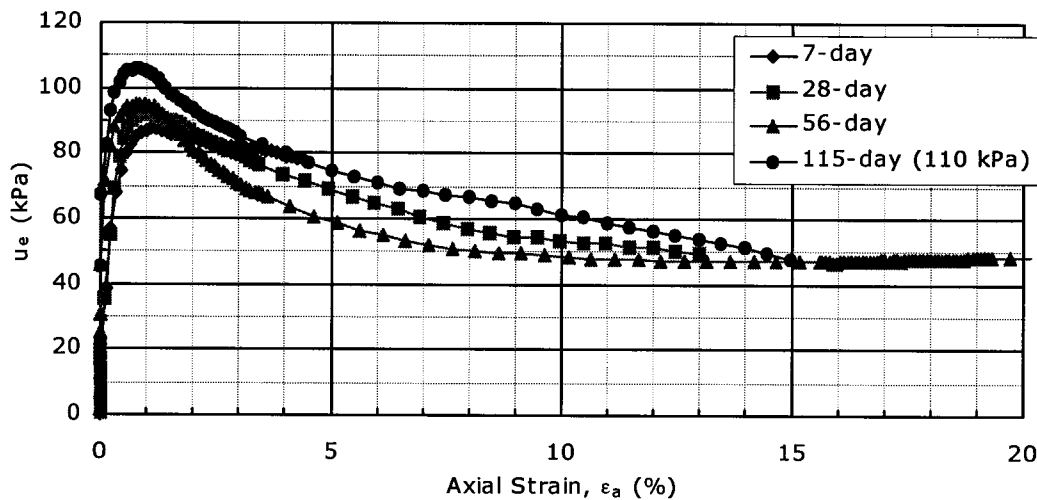
Figure H.12. u_e vs. ε_a for CIU triaxial tests at w=100%, A_c=10% & $p_o{}'$=100 kPa.

H.7   Mohr-Coulomb Strength Parameters

H.7.1 Cohesion

Cohesion in clay-cement has two components which include cohesion from clay particles and cohesion from the cement bonding effects. Any change in cohesion with curing time is due to the cement bonding effects.

The peak cohesion increased between 7 and 28 days for all mixes considered (Fig. H.13a). The rate of increase increased with cement to moisture content ratio and was almost negligible when the cement content

404   *Mechanical Characteristics of Kaolin-Cement Mixture*

was 2 percent. Following 28 days of curing, the peak cohesion for the two samples with an intermediate cement to moisture content ratio continued to increase, at a reduced rate, up to 56 days. For the case of 10 percent cement, the peak cohesion decreased between 56 and 112 days so that the peak cohesion after 112 days is similar to that after 28 days.

When the cement to moisture content ratio is low, however, the trend in peak cohesion with curing time is less predictable. At 2 percent cement, the effects of cementation are very small so the peak cohesion, which is a function of cementation, is not expected to improve significantly with curing time. At 100 percent moisture content and 5 percent cement, an initial increase in peak cohesion is followed by a decrease which is followed by another increase up to 112 days of curing. However, for all cases when the cement content is at least 5 percent and the curing time at least 28 days, peak cohesion and peak friction angle influence one another. That is, a drop in peak cohesion is associated with a rise in peak friction angle, and vice versa. While the failure envelope was found to be linear up to a confining pressure of 400 kPa, it is suggested that a curved failure envelope would be more appropriate over a wider range of confining pressures. Uddin (1995) concluded that a curved failure envelope was appropriate for cement stabilized Bangkok clay, when considering confining pressures up to 2000 kPa. At low confining pressures, a curved failure envelope results in changing peak cohesion and peak friction angle; one increases at the expense of the other. This trade-off was observed in the current data.

The fully-softened cohesion increased initially for all cases, and then decreased after 28 days of curing, so that the fully-softened values were approximately the same after 56 days as they were after 7 days. It is concluded that curing time does not influence the fully-softened cohesion.

H.7.2 Friction Angle

To interpret the change in peak friction angle with curing time, the peak cohesion must also be considered. As discussed in the previous sub-section, it is suggested that the two parameters are inversely related due to the initial curved portion of the failure envelope. At high cement to moisture content ratios, the peak friction angle decreases with curing time, up to 56 days (Fig.

H.13b); this is associated with an increase in peak cohesion. At low cement to moisture content ratios, the trend is the opposite and the peak friction angle *increases* with curing time, up to 56 days. This increase is usually, but not always, associated with a decrease in peak cohesion. Beyond 56 days, the trend usually reverses for both all cases. Based on the results of triaxial tests, it is suggested that the sample strength may deteriorate following 28 or 56 days of curing in water.

Authors such as Uddin (1995) expect the friction angle to increase with curing time when samples are cured in a humid environment. However, Wissa and Ladd (1964) concluded that when the cement content was low, the effective friction angle is independent of curing time. Sivapullaiah *et al.* (2000) found the peak friction angle and degree of flocculation to be directly related. As discussed in Chapter 7, the degree of flocculation decreases with curing time and therefore, one can expect the friction angle to also decrease with curing time, as seen at intermediate cement to moisture content ratios.

Almost no trend could be identified with curing time for the fully-softened friction angle. It is suggested that, similar to cohesion, the fully-softened friction angle is independent of curing time. Fully-softened values may not be accurate due to significant lateral deformation at high strains.

H.8 Unconfined Compressive Strength

Similar to the peak deviator stress and peak cohesion, the unconfined compressive (UC) strength generally increases with curing time, at a decreasing rate (Fig. H.14). For all cases, the UC strength roughly doubles between 7 and 28 days of curing. When the cement content is at least 5 percent, the UC strength continues to increase slightly up to at least 112 days. With only 2 percent cement, however, the UC strength is approximately constant between 28 and 56 days of curing, and after 112 days, the UC strength is very near its 7-day value.

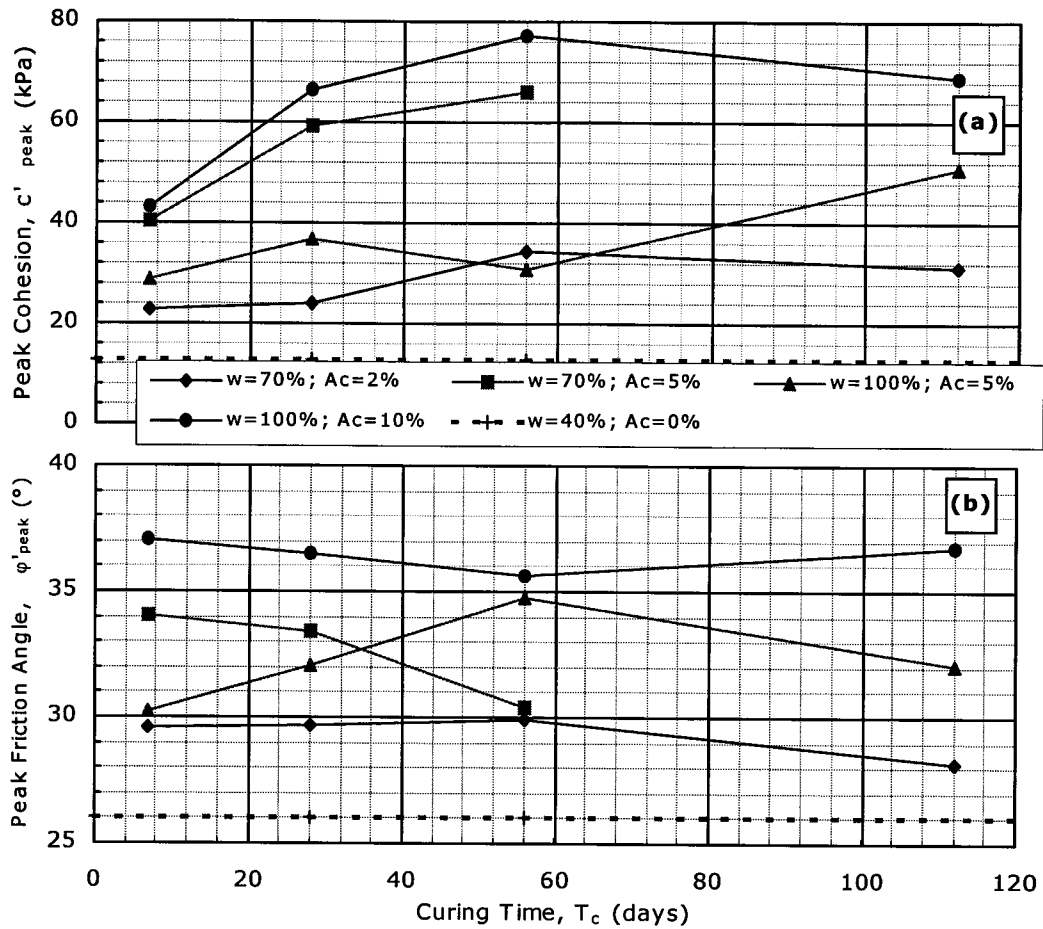The fully-softened UC strength is independent of curing time.

Figure H.13. Effective Mohr-Coulomb parameters vs. curing time (from CID test results). (a) peak cohesion; (b) peak friction angle.
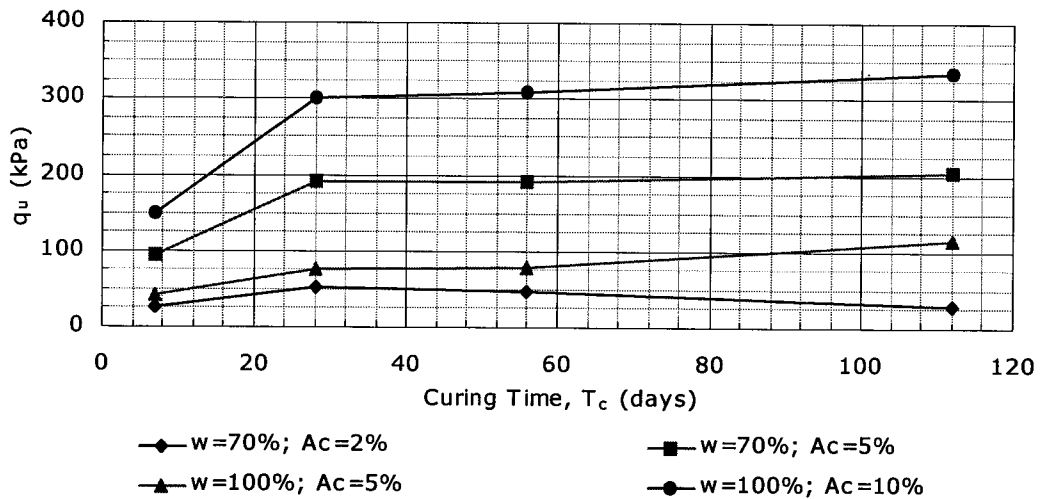

Figure H.14. Unconfined compressive strength vs. curing time.

H.9 Consolidation Properties

According to some authors (i.e. Kohata *et al.*, 1997), the deformation characteristics of cement-treated soils are similar to those of over-consolidated clay. Furthermore, due to the bonding caused by cementation, the consolidation characteristics of clay-cement can be compared to those of natural clays with soil structure.

The current study defines apparent consolidation properties, since consolidation does not actually occur during cementation and therefore, the derived consolidation properties do not yield information about the soil's stress history, as is the case with consolidated clay. Results of both oedometer and isotropic consolidation tests are discussed. Figure H.15 provides consolidation curves for isotropic consolidation tests on samples with a moisture content of 100 percent and cement content of 10 percent. Appendix D includes consolidation curves for all tests.
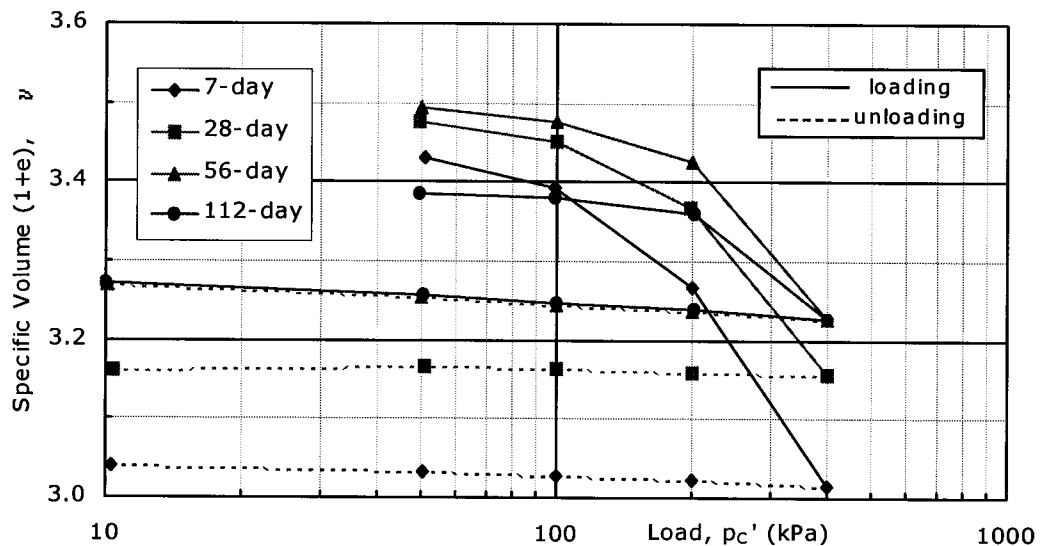

Figure H.15. Consolidation curves from IC tests for w=100% and A$_c$=10%.

H.9.1 Apparent Consolidation Yield Stress

The apparent consolidation yield stress and therefore, the apparent over-consolidation ratio, increased with curing time up to at least 56 days, as determined from both the oedometer and IC tests (Fig. H.16). When the

cement content is only 2 percent, however, the apparent consolidation yield stress decreased after 56 days of curing so that after 112 days, the apparent consolidation yield stress was roughly the same as after only 7 days of curing. The same deterioration was seen in the results of the strength tests; with so little cement and curing in water, softening may have occurred during curing.

Similar to the trends observed for the strength tests, the change in the apparent consolidation yield stress is generally greatest between 7 and 28 days of curing. This indicates that the increase in strength with curing time is directly linked to the apparent consolidation that progresses with curing.
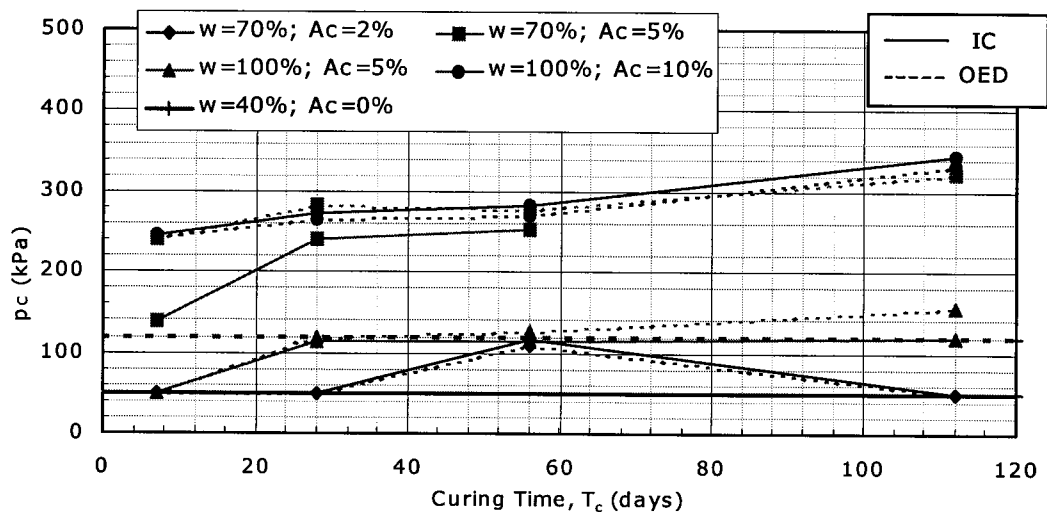
Figure H.16. Apparent consolidation yield stress vs. curing time.

H.9.2 Compression Index

For the oedometer tests, the compression index increased slightly with curing time (Fig. H.17); often the rate was roughly constant. Typically, the opposite trend was observed in the IC test results; the compression index *decreased* with curing time. Furthermore, the compression index was almost always greater for the oedometer tests than for the IC tests.

For a bonded material, an increase in sample deformation with curing time, as seen in the oedometer test results, suggests an increase in void ratio with curing time and failure of cement bonds during consolidation. As already discussed, void ratio increases slightly up to 56 days of curing. A maximum load of 3200 kPa for the oedometer tests would be sufficient to break the

cement bonds for the cement contents considered, therefore, an increase in compression with curing time is expected for these tests.

The pattern in the IC test results is different because a maximum load of only 400 kPa was not great enough to cause failure of cement bonds, except when the cement content was very low at 2 percent. Therefore, a *reduction* in compression with curing time is seen. The same trend was observed by Uddin (1995) from oedometer tests on stabilized Bangkok clay with 5 to 10 percent cement. Uddin cured samples in a humid environment and some coarse-grained material was present in the stabilized material. Therefore, the cement bonds did not fail during consolidation as was the case for the current study. Uddin did not observe any significant changes in the consolidation properties with curing time at cement contents less than 5 percent.
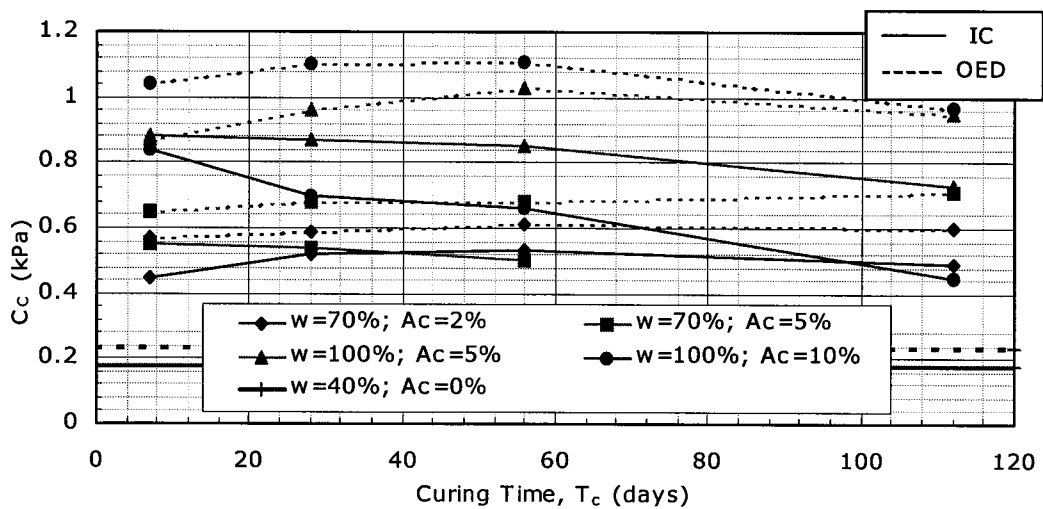
Figure H.17. Compression index vs. curing time.

H.9.3 Swelling Index

A general increase in the swelling index with curing time was observed (Fig. H.18) and corresponds to the trend in the compression index with curing time. All changes in the swelling index due to curing time were very small. At only 2 percent cement, the change in the swelling index is very erratic for both the oedometer and IC tests. This material is very weakly bonded and the bonds fail during consolidation; this may influence the swelling in an unpredictable manner.

410   *Mechanical Characteristics of Kaolin-Cement Mixture*

Figure H.18. Swelling index vs. curing time.

H.9.4 Coefficient of Consolidation

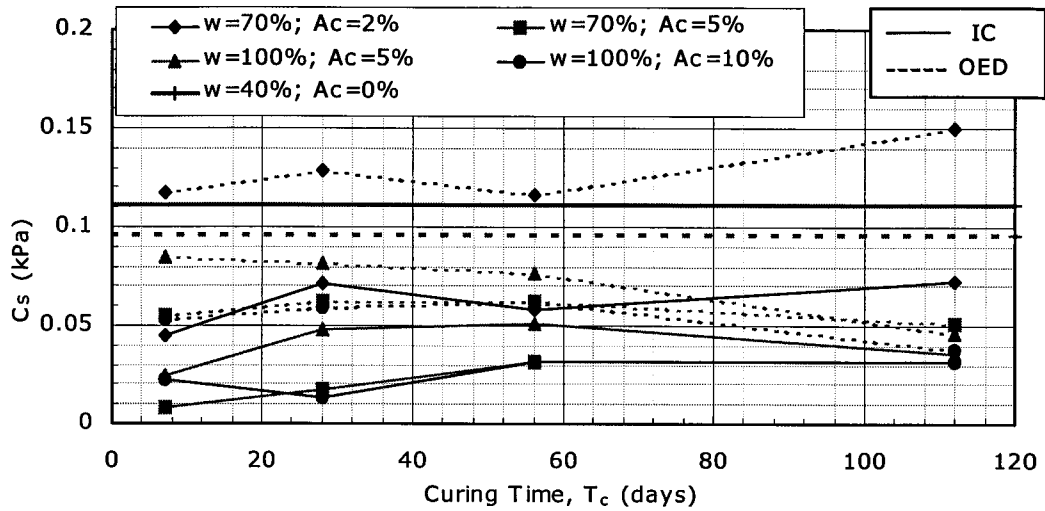While it is difficult to see this trend, up to a given consolidation pressure, which depends on the sample mixture, the coefficient of consolidation generally increased with curing time (Fig. H.19). This is the desired effect and the same observation was made by Uddin (1995) at all pressures. However, at high consolidation pressures for the current study, the coefficient of consolidation actually *decreased* with curing time. It is suggested that this reversal occurs at approximately the apparent consolidation yield stress and is due to failure of cement bonds and subsequent collapse of structure during consolidation. Patterns observed in the apparent consolidation yield stress and compression index also support this theory.
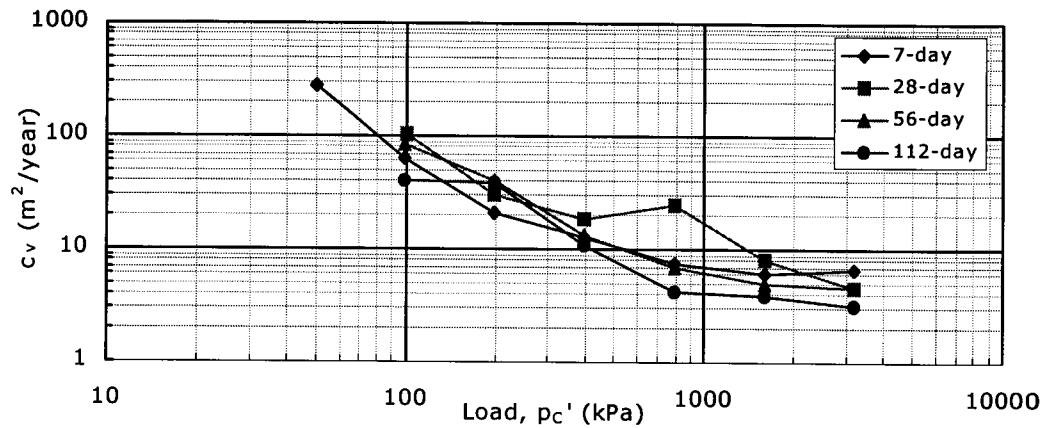
Figure H.19. Coefficient of consolidation vs. load for w=100% & A_c=10% (oedometer tests, loading only).

H.9.5 Coefficient of Volume Compressibility

An increase in curing time, up to at least 56 days, generally leads to a decrease in the coefficient of volume compressibility during both loading and unloading (Fig. H.20), except when the cement content is 2 percent or occasionally during the initial loading stage for the oedometer tests. This indicates that as curing proceeds, the material becomes more stiff and consolidation takes more time. At high loads, the change in the coefficient of volume compressibility with curing time was small to negligible. At 2 percent cement and in some cases, beyond approximately 56 days of curing, softening may be occurring with curing time due to insufficient cementation.
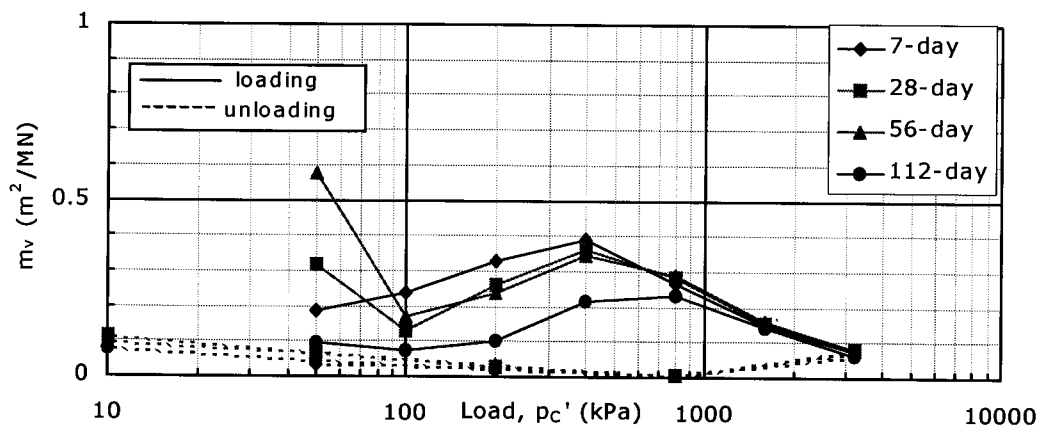

Figure H.20. Coefficient of volume compressibility vs. load for w=100% & A_c=10% (oedometer tests).

H.10 Conclusions

Here the physical changes in kaolin-cement with curing time come together with both the strength and deformation properties in an attempt to provide an overall picture as to what happens to kaolin-cement when cured in water. By no means does this study cover all bases as there are still many questions that remain unanswered. Below is a summary of some of the key changes in kaolin-cement due to curing in water and overall conclusions from the results of this study.

H.10.1 General

- When cured in water, both the void ratio and moisture content increase slightly up to 56 days of curing, indicating that the kaolin-cement is absorbing moisture from the water bath. Furthermore, the pH and hence the electrolytic concentration of the pore water in kaolin-cement decreases with curing time up to at least 75 days of curing. This reduction in pH causes a reduction in the degree of flocculation of the cement particles, which corresponds to an increase in void ratio. When cured in a humid environment, the moisture content will decrease with curing time; Uddin (1995) concludes that this leads to an increase in the degree of flocculation.

- Curing environment has a very large influence on the strength properties of cement stabilized soil. The strength of cement stabilized clay cured in water is less than when cured in a humid environment, particularly when the cement content is low.

- When cured in water, both the strength and deformation properties of kaolin-cement improved up to at least 28 days of curing. The only exception to this was seen occasionally during undrained triaxial tests. After 28 days of curing, the rate of improvement decreased significantly and typically following 28 or 56 days of curing, further improvement was very small to negligible or deterioration of the kaolin-cement was observed. Deterioration usually occurred when the cement content was only 2 percent and/or the moisture content 70 percent. Samples with a moisture content of 70 percent were compacted in lifts which may lead to greater softening effects during curing.

- Further testing at greater cement contents and greater confining pressures would be useful.

H.10.2 Strength Properties

- An improvement in strength corresponds to an increase in material stiffness and failure at reduced axial strains at low confining pressures (i.e. 50 and 100 kPa) for drained conditions or at confining pressures up to at least 400 kPa during undrained conditions. This is a trade-off with cement stabilized material; while the strength improves, failure will occur after smaller amounts of strain and will also be more brittle.

- Volumetric strain during drained shear decreased as curing time increased. When this is not true, it is usually associated with a reduction in strength. Most samples dilated following peak stress conditions; an increase in curing time increases the dilation tendency.

- Excess pore water pressure generated during undrained shear increased with curing time. When this is not true, it is usually associated with a reduction in strength.

- At intermediate cement to moisture content ratios, peak cohesion increased with curing time up to 56 days of curing. This is associated with a reduction in peak friction angle. At low cement to moisture content ratios, however, the trend is not so clear. At 100 percent moisture content and 5 percent cement content, peak cohesion increases initially up to 28 days of curing but then decreases after 56 days and increases after 112 days. After 28 days, the peak friction angle is inversely related to peak cohesion. It is suggested that the failure envelope may be curved for the low confining pressures considered so that cohesion increases at the expense of friction angle, and vice versa. However, peak friction angle and degree of flocculation are directly related (Sivapullaiah et al., 2000) so based on the reduction in pH, it is expected that friction angle will decrease with curing time.

- At only 2 percent cement content, the change in peak cohesion with curing time is rather unpredictable and the peak friction angle is almost constant until it decreases after 112 days of curing. With so little cementation, the Mohr-Coulomb properties are not expected to change significantly with curing time.

- The unconfined compressive (UC) strength increases with curing time up to 112 days when the cement content is at least 5 percent. The increase is roughly double between 7 and 28 days of curing, and then is very small following 28 days of curing. For the material with only 2 percent cement, the trends are similar to the other cases except the UC strength decreases following 56 days of curing so that the UC strength after 112 days is near that after only 7 days of curing.

- Based on the results of all strength tests, curing time does not affect the fully-softened strength of kaolin-cement.

H.10.3 Consolidation Properties

- Cement-stabilization causes soil-cement to have an apparent consolidation yield stress, which does not reflect its stress history. The consolidation yield stress is related to the soil strength, and also increases with curing time up to at least 56 days.

- When the apparent consolidation yield stress is exceeded, cement bonds will begin to fail causing an increase in volume change during consolidation. This volume change will affect the subsequent volumetric and axial strain during drained shear. Curing time affects the degree of cementation and therefore, must be considered with confining (consolidation) pressure when interpreting the volume change and axial strain of the drained triaxial test results.

- When the maximum consolidation pressure was sufficiently high to cause the cement bonds to fail, the compression index increased with curing time due to the increase in void ratio with curing time. However, at low consolidation pressures, the opposite is true since cement bonds do not fail and therefore, compression is reduced with an increase in strength.

- The coefficient of consolidation generally increased with curing time up to a consolidation pressure sufficiently great enough to cause failure of cement bonds. The trend was reversed once the structure began to collapse at higher consolidation pressures.

- At low consolidation pressures, the coefficient of volume compressibility decreases with curing time, up to at least 56 days. That is to say that as curing proceeds and the material becomes more stiff, consolidation takes

more time. However, at high consolidation pressures, which likely correspond to failure of the cement bonds, the coefficient of volume compressibility is independent of curing time.